STRATEGIES FOR MODULATING T CELL RESPONSES IN AUTOIMMUNITY AND INFECTION

EDITED BY: Maria Florencia Quiroga, María Fernanda Pascutti and Gustavo Javier Martinez

PUBLISHED IN: Frontiers in Immunology

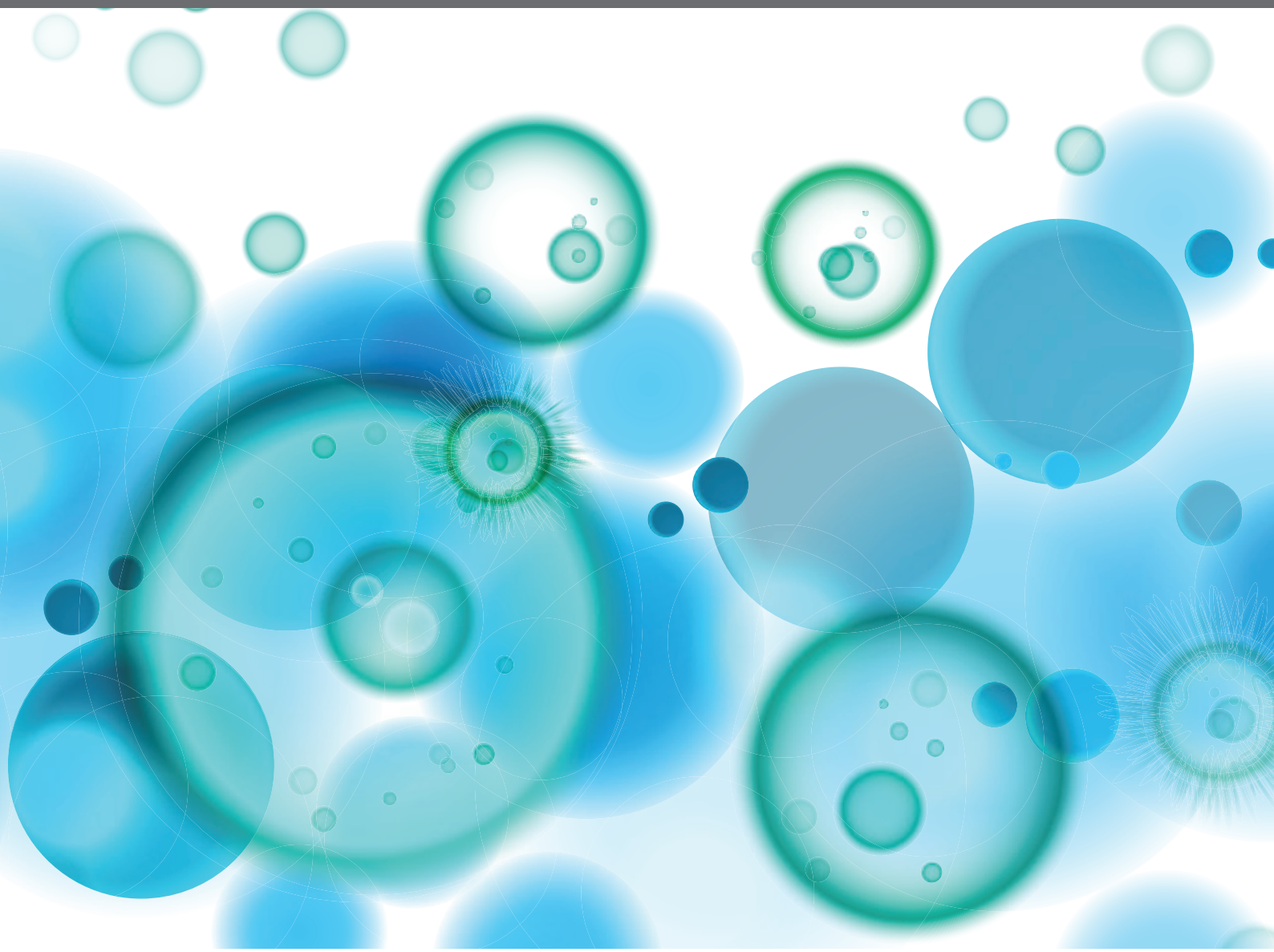

frontiers Research Topics

Frontiers eBook Copyright Statement

The copyright in the text of individual articles in this eBook is the property of their respective authors or their respective institutions or funders. The copyright in graphics and images within each article may be subject to copyright of other parties. In both cases this is subject to a license granted to Frontiers.

The compilation of articles constituting this eBook is the property of Frontiers.

Each article within this eBook, and the eBook itself, are published under the most recent version of the Creative Commons CC-BY licence. The version current at the date of publication of this eBook is CC-BY 4.0. If the CC-BY licence is updated, the licence granted by Frontiers is automatically updated to the new version.

When exercising any right under the CC-BY licence, Frontiers must be attributed as the original publisher of the article or eBook, as applicable.

Authors have the responsibility of ensuring that any graphics or other materials which are the property of others may be included in the CC-BY licence, but this should be checked before relying on the CC-BY licence to reproduce those materials. Any copyright notices relating to those materials must be complied with.

Copyright and source acknowledgement notices may not be removed and must be displayed in any copy, derivative work or partial copy which includes the elements in question.

All copyright, and all rights therein, are protected by national and international copyright laws. The above represents a summary only. For further information please read Frontiers' Conditions for Website Use and Copyright Statement, and the applicable CC-BY licence.

ISSN 1664-8714
ISBN 978-2-88963-609-9
DOI 10.3389/978-2-88963-609-9

About Frontiers

Frontiers is more than just an open-access publisher of scholarly articles: it is a pioneering approach to the world of academia, radically improving the way scholarly research is managed. The grand vision of Frontiers is a world where all people have an equal opportunity to seek, share and generate knowledge. Frontiers provides immediate and permanent online open access to all its publications, but this alone is not enough to realize our grand goals.

Frontiers Journal Series

The Frontiers Journal Series is a multi-tier and interdisciplinary set of open-access, online journals, promising a paradigm shift from the current review, selection and dissemination processes in academic publishing. All Frontiers journals are driven by researchers for researchers; therefore, they constitute a service to the scholarly community. At the same time, the Frontiers Journal Series operates on a revolutionary invention, the tiered publishing system, initially addressing specific communities of scholars, and gradually climbing up to broader public understanding, thus serving the interests of the lay society, too.

Dedication to Quality

Each Frontiers article is a landmark of the highest quality, thanks to genuinely collaborative interactions between authors and review editors, who include some of the world's best academicians. Research must be certified by peers before entering a stream of knowledge that may eventually reach the public - and shape society; therefore, Frontiers only applies the most rigorous and unbiased reviews.
Frontiers revolutionizes research publishing by freely delivering the most outstanding research, evaluated with no bias from both the academic and social point of view. By applying the most advanced information technologies, Frontiers is catapulting scholarly publishing into a new generation.

What are Frontiers Research Topics?

Frontiers Research Topics are very popular trademarks of the Frontiers Journals Series: they are collections of at least ten articles, all centered on a particular subject. With their unique mix of varied contributions from Original Research to Review Articles, Frontiers Research Topics unify the most influential researchers, the latest key findings and historical advances in a hot research area! Find out more on how to host your own Frontiers Research Topic or contribute to one as an author by contacting the Frontiers Editorial Office: researchtopics@frontiersin.org

STRATEGIES FOR MODULATING T CELL RESPONSES IN AUTOIMMUNITY AND INFECTION

Topic Editors:
Maria Florencia Quiroga, National Council for Scientific and Technical Research (CONICET), Argentina
María Fernanda Pascutti, Sanquin Diagnostic Services, Netherlands
Gustavo Javier Martinez, Rosalind Franklin University of Medicine and Science, United States

Citation: Quiroga, M. F., Pascutti, M. F., Martinez, G. J., eds. (2020). Strategies for Modulating T cell Responses in Autoimmunity and Infection.
Lausanne: Frontiers Media SA. doi: 10.3389/978-2-88963-609-9

Table of Contents

05 ***Editorial: Strategies for Modulating T Cell Responses in Autoimmunity and Infection***
María Fernanda Pascutti, Gustavo Javier Martinez and Maria Florencia Quiroga

08 ***Features of Effective T Cell-Inducing Vaccines Against Chronic Viral Infections***
Eleni Panagioti, Paul Klenerman, Lian N. Lee, Sjoerd H. van der Burg and Ramon Arens

19 ***Inducible Costimulator Expressing T Cells Promote Parasitic Growth During Blood Stage* Plasmodium berghei *ANKA Infection***
Gajendra M. Jogdand, Soumya Sengupta, Gargee Bhattacharya, Santosh Kumar Singh, Prakash Kumar Barik and Satish Devadas

33 ***Therapies to Suppress ß Cell Autoimmunity in Type 1 Diabetes***
Charles J. Kroger, Matthew Clark, Qi Ke and Roland M. Tisch

47 ***A Type I Interferon and IL-10 Induced by* Orientia tsutsugamushi *Infection Suppresses Antigen-Specific T Cells and Their Memory Responses***
Chan-Ki Min, Hong-Il Kim, Na-Young Ha, Yuri Kim, Eun-Kyung Kwon, Nguyen Thi Hai Yen, Je-In Youn, Yoon Kyung Jeon, Kyung-Soo Inn, Myung-Sik Choi and Nam-Hyuk Cho

62 ***Deficient O-GlcNAc Glycosylation Impairs Regulatory T Cell Differentiation and Notch Signaling in Autoimmune Hepatitis***
Xiaohua Hao, Yufeng Li, Jianwen Wang, Jiali Ma, Shuli Zhao, Xiaohui Ye, Lingling He, Junru Yang, Meixin Gao, Fan Xiao and Hongshan Wei

73 ***IL-17RA-Signaling Modulates CD8+ T Cell Survival and Exhaustion During* Trypanosoma cruzi *Infection***
Jimena Tosello Boari, Cintia L. Araujo Furlan, Facundo Fiocca Vernengo, Constanza Rodriguez, María C. Ramello, María C. Amezcua Vesely, Melisa Gorosito Serrán, Nicolás G. Nuñez, Wilfrid Richer, Eliane Piaggio, Carolina L. Montes, Adriana Gruppi and Eva V. Acosta Rodríguez

91 ***Alpha2beta1 Integrin (VLA-2) Protects Activated Human Effector T Cells From Methotrexate-Induced Apoptosis***
Amna Abderrazak, Mohammed-Amine El Azreq, Dalila Naci, Paul R. Fortin and Fawzi Aoudjit

103 ***γδ T Lymphocytes: An Effector Cell in Autoimmunity and Infection***
Carolina Maiumi Shiromizu and Carolina Cristina Jancic

111 ***Phenotype, Polyfunctionality, and Antiviral Activity of* in vitro *Stimulated CD8⁺ T-Cells From HIV⁺ Subjects Who Initiated cART at Different Time-Points After Acute Infection***
Jimena Salido, María Julia Ruiz, César Trifone, María Inés Figueroa, María Paula Caruso, María Magdalena Gherardi, Omar Sued, Horacio Salomón, Natalia Laufer, Yanina Ghiglione and Gabriela Turk

132 ***Harnessing the Induction of CD8⁺ T-Cell Responses Through Metabolic Regulation by Pathogen-Recognition-Receptor Triggering in Antigen Presenting Cells***
Francesco Nicoli, Stéphane Paul and Victor Appay

140 ***Limited Foxp3⁺ Regulatory T Cells Response During Acute* Trypanosoma cruzi *Infection is Required to Allow the Emergence of Robust Parasite-Specific CD8⁺ T Cell Immunity***
Cintia L. Araujo Furlan, Jimena Tosello Boari, Constanza Rodriguez, Fernando P. Canale, Facundo Fiocca Vernengo, Santiago Boccardo, Cristian G. Beccaria, Véronique Adoue, Olivier Joffre, Adriana Gruppi, Carolina L. Montes and Eva V. Acosta Rodriguez

157 ***CCL22-Producing Resident Macrophages Enhance T Cell Response in Sjögren's Syndrome***
Aya Ushio, Rieko Arakaki, Kunihiro Otsuka, Akiko Yamada, Takaaki Tsunematsu, Yasusei Kudo, Keiko Aota, Masayuki Azuma and Naozumi Ishimaru

172 ***Sulforaphane Inhibits Inflammatory Responses of Primary Human T-Cells by Increasing ROS and Depleting Glutathione***
Jie Liang, Beate Jahraus, Emre Balta, Jacqueline D. Ziegler, Katrin Hübner, Norbert Blank, Beate Niesler, Guido H. Wabnitz and Yvonne Samstag

189 ***CD32 Ligation Promotes the Activation of CD4⁺ T Cells***
María Pía Holgado, Inés Sananez, Silvina Raiden, Jorge R. Geffner and Lourdes Arruvito

201 ***Modulating T Cell Responses via Autophagy: The Intrinsic Influence Controlling the Function of Both Antigen-Presenting Cells and T Cells***
Seth D. Merkley, Cameron J. Chock, Xuexian O. Yang, James Harris and Eliseo F. Castillo

220 ***Differential Regulation of Human Treg and Th17 Cells by Fatty Acid Synthesis and Glycolysis***
Deborah Cluxton, Andreea Petrasca, Barry Moran and Jean M. Fletcher

frontiers in Immunology

EDITORIAL
published: 20 February 2020
doi: 10.3389/fimmu.2020.00208

Editorial: Strategies for Modulating T Cell Responses in Autoimmunity and Infection

María Fernanda Pascutti[1], *Gustavo Javier Martinez*[2] *and Maria Florencia Quiroga*[3]*

[1] Department of Immunohematology and Blood Transfusion, Leiden University Medical Center, Leiden, Netherlands, [2] Center for Cancer Cell Biology, Immunology and Infection, Discipline of Microbiology and Immunology, Rosalind Franklin University of Medicine and Science, North Chicago, IL, United States, [3] Consejo Nacional de Investigaciones Científicas y Técnicas, Instituto de Investigaciones Biomédicas en Retrovirus y Sida, Universidad de Buenos Aires, Buenos Aires, Argentina

Keywords: T cells, animal studies, human studies, immunemodulation, health, disease

Editorial on the Research Topic

Strategies for Modulating T Cell Responses in Autoimmunity and Infection

T-cell differentiation and effector functions are shaped by the integration of different signals from the environment. The process initiated when the T-cell receptor is engaged is then modulated by activating (costimulatory molecules and cytokines) and inhibitory (checkpoint receptors and cytokines) signals, which have a direct impact on the development or function of effector and/or regulatory T (Treg) cells (1, 2). In pre-clinical human or animal studies, the manipulation of T-cell function has been attempted via numerous different approaches, including (i) manipulation of metabolism (3), (ii) modulation of autophagy, (iii) regulation of epigenetic processes (4), (iv) agonistic or antagonistic therapies engaging cellular receptors (5), (v) the use of cytokines/chemokines to skew immune response profiles, (vi) the expansion/depletion of certain cell type (i.e., depletion of Tregs or expansion of effector T cells specific for a certain pathogen) (6), and (vii) the use of diverse immunomodulating natural or synthetic compounds that could regulate any of the above mentioned aspects of the immune response (7), among others. The goal of the current Research Topic is to highlight some of these approaches and to focus on the diverse ways of modulating T-cell function or frequency in health and disease.

Within this eBook, some authors addressed the potential of diverse strategies, such as manipulating metabolic pathways, autophagy processes, and/or modification of the redox cellular milieu with an impact on T-cell function. Cluxton et al. proposed that the fundamental difference in metabolic requirements of human Tregs and Th17 cells could be used in order to modulate inflammatory responses in human diseases. Similarly, Liang et al. work focused on the effect of sulforaphane (SFN), a compound derived from certain vegetables, as a modulator of the extracellular redox milieu. They observed that SFN induced a pro-oxidative state, consequently inhibiting Th17-related cytokines via targeting of STAT3. They finally stated that SFN could be a novel option for treatment of inflammatory/autoimmune diseases, such as rheumatoid arthritis. Continuing with the importance of metabolism in mediating T-cell function, Nicoli et al. suggested in their review that antigen-presenting cells could be metabolically manipulated through TLR4, TLR9, or STING to induce metabolic and/or autophagy changes in order to subsequently impact on CD8+ T cell responses, while Merkley et al. revisited the influence of autophagy over T-cell responses by modulating several aspects of antigen-presenting cells' function and the impact of this modulation over T-cell signaling, survival, cytokine production, and metabolism.

The impact of post-transcriptional modifications on T-cell responses was explored in a very nice study by Hao et al.. They unraveled, in a rat model of autoimmune hepatitis, the major role of

OPEN ACCESS

Edited and reviewed by:
Wanjun Chen,
National Institutes of Health (NIH), United States

***Correspondence:**
Maria Florencia Quiroga
florenciaquiroga@gmail.com

Specialty section:
This article was submitted to T Cell Biology, a section of the journal Frontiers in Immunology

Received: *08 January 2020*
Accepted: *27 January 2020*
Published: *20 February 2020*

Citation:
Pascutti MF, Martinez GJ and Quiroga MF (2020) Editorial: Strategies for Modulating T Cell Responses in Autoimmunity and Infection. Front. Immunol. 11:208. doi: 10.3389/fimmu.2020.00208

glycosylation on Treg differentiation and the impact of this deficiency on disease development. They demonstrated that deficiency in O-GlcNAc glycosylation affects the Notch function, a signaling pathway previously reported to promote the differentiation and survival of Tregs. As a result, impaired Treg differentiation allowed for increasing CD4+ T cell infiltration in the liver, indicating that modulation of O-GlcNAc glycosylation in this model could be a target for immunotherapy. In a related disease model, Kroger et al. enumerated the various immunotherapies aimed at controlling autoimmunity in type I diabetes, including among other modulation of regulatory T cells and cytokines.

A more traditional approach used by several authors within this eBook consists of underscoring how signaling through various receptors modifies cellular functions in T cells. For instance, Holgado et al. have described for the first time the role of CD32, a low-affinity Fc-gamma receptor, as promoter of human CD4+ T-cell responses that consequently increases cell proliferation and creates a wide pattern of cytokines triggered by polyclonal stimulation, thus enhancing inflammatory responses. Additionally, the work of Jogdand et al. explored the relevance of ICOS signaling in the context of the blood stage of *Plasmodium berghei* ANKA infection. In this setting, they observed that depletion of ICOS+ cells from infected mice induced longer survival and lower parasitemia. Also, they observed that ICOS+ T cells also expressed IFN-γ and the transcription factor Tbet; both positively correlated with ICOS expression, therefore suggesting a positive regulation loop between ICOS expression and T-cell function. Abderrazak et al. observed in their manuscript that VLA-2 integrin signaling protected T cells from methotrexate-induced apoptosis (a drug used for rheumatoid arthritis treatment), and "rescued" cells producing IL-17 and IFN-γ contributing to the perpetuation of inflammation and the development of methotrexate resistance seen in rheumatoid arthritis. Finally, Tosello Boari et al. demonstrated the importance of IL-17 cytokines and their receptor IL-17RA in a model of chronic infection with *Trypanosoma cruzi*. In their work, the authors demonstrated that signaling through IL-17RA is required for the maintenance of effector function in CD8+ T cells in a cell-intrinsic manner. In fact, deficiency in IL-17RA rendered CD8+ T cells more dysfunctional, and blockade of PD-L1, a checkpoint inhibitor currently targeted in many cancer models, partially restored the effector function of these cells. In line with this topic, Panagioti et al. discussed in their review article the various T-cell inducing vaccines used in protection against chronic infections, particularly in viral infections.

Chemokines and/or cytokines themselves could serve as therapeutic targets. In their work, Ushio et al. used a murine model for Sjögren's syndrome as a way to understand the role of CCL22 in this autoimmune disease. They observed that CCL22-producing tissue-resident macrophages may control autoimmune lesions by enhancing the migratory capacity of CD4+ T cells to the affected tissue as well as by inducing IFN-γ production of T cells. Another example of how cytokines and their downstream effects could be used as targets for immunotherapy is addressed in the work of Min et al.. The authors clearly showed the relevance of the Type I IFN/IL-10 axis in the induction of antigen-specific T-cell function and the generation of T-cell memory in a mouse model for scrub typhus, an infectious disease caused by the intracellular bacteria *Orientia tsutsugamushi*. Their work contributes to a better understanding of the mechanisms behind the short longevity of antigen-specific adaptive immunity observed during this human infection (8).

A different approach proposed by some authors consists of expanding effector cells or limiting the function of regulatory cells with the aim to improve immune responses against pathogens. Salido et al. expanded *in vitro* CD8+ T cells from HIV+ subjects on combination antiretroviral therapy (cART). Their ultimate goal was to explore new strategies aimed at modulating CD8+ T lymphocytes to achieve functional cure of HIV infections. They observed that expanded cells were polyfunctional, skewed toward an effector phenotype, and that PD-1 expression was clustered in HIV-specific effector memory CD8+ T cells, which had the highest cytokine-producing capacity. Antiviral activity was also enhanced in these cells, indicating that, despite being dampened in subjects on cART, the HIV-specific CD8+ T-cell response could be selectively stimulated and expanded *in vitro*. On the other hand, the work of Araujo Furlan et al. explored the role of Tregs during *Trypanosoma cruzi* infection and the impact of Treg frequency over pathology. They observed that massive accumulation of effector immune cells resulted in a diminished frequency of Tregs and inversely correlated with the magnitude of the immune response as well as with emergence of acute immunopathology. After transfer of Tregs, CD8+ T-cell function was affected and parasite control in blood and tissues was diminished, highlighting the relevance of Tregs over cytotoxic immunity against the parasite. Another important population of T cells that was reviewed by Shiromizu et al. consists of γδ T cells, whose role during autoimmunity and infection has been analyzed in depth in their work. They have also revised concepts about the mechanisms that modulate γδ T-cell function, giving the framework to consider the modulation of these cells as a tool to control pathological immune responses.

Collectively, the wide spectrum of original papers and reviews presented in this eBook have provided a comprehensive overview of potential strategies aiming to convert a pathological immune response into a protective one through the control or reprogramming of specific T-cell subsets. The insights outlined here will hopefully help shape future therapeutics for the treatment of infectious and autoimmune diseases.

AUTHOR CONTRIBUTIONS

MQ wrote the first draft of the present Editorial article. MP and GM revised it and provided their valuable and precious comments, remarks, and suggestions. The final Editorial's draft and the current Editorial's text were entirely agreed and approved by all three Guest co-Editors of the present Research Topic, and it details the Strategies for Modulating T cell Responses in Autoimmunity and Infection.

REFERENCES

1. Raffin C, Vo LT, Bluestone JA. Treg cell-based therapies: challenges and perspectives. *Nat Rev Immunol*. (2019). doi: 10.1038/s41577-019-0232-6. [Epub ahead of print].
2. Boer MC, Joosten SA, Ottenhoff THM. Regulatory T-cells at the interface between human host and pathogens in infectious diseases and vaccination. *Front Immunol*. (2015) 6:217. doi: 10.3389/fimmu.2015.00217
3. Teijeira A, Garasa S, Etxeberria I, Gato-Canas M, Melero I, Delgoffe GM. Metabolic consequences of T-cell costimulation in anticancer immunity. *Cancer Immunol Res*. (2019) 7:1564–9. doi: 10.1158/2326-6066.CIR-19-0115
4. Topper MJ, Vaz M, Marrone KA, Brahmer JR, Baylin SB. The emerging role of epigenetic therapeutics in immuno-oncology. *Nat Rev Clin Oncol*. (2019) 17:75–90. doi: 10.1038/s41571-019-0266-5
5. Nakajima M, Tamada K. Cancer immunotherapy targeting co-signal molecules. *Adv Exp Med Biol*. (2019) 1189:313–26. doi: 10.1007/978-981-32-9717-3_11
6. Grant ML, Bollard CM. Cell therapies for hematological malignancies: don't forget non-gene-modified t cells! *Blood Rev*. (2018) 32:203–24. doi: 10.1016/j.blre.2017.11.004
7. Ketelhuth DFJ, Gistera A, Johansson DK, Hansson GK. T cell-based therapies for atherosclerosis. *Curr Pharm Des*. (2013) 19:5850–8. doi: 10.2174/1381612811319330003
8. Ha N-Y, Kim Y, Min C-K, Kim H-I, Yen NTH, Choi M-S, et al. Longevity of antibody and T-cell responses against outer membrane antigens of Orientia tsutsugamushi in scrub typhus patients. *Emerg Microbes Infect*. (2017) 6:1–8. doi: 10.1038/emi.2017.106

Conflict of Interest: The authors declare that the research was conducted in the absence of any commercial or financial relationships that could be construed as a potential conflict of interest.

Copyright © 2020 Pascutti, Martinez and Quiroga. This is an open-access article distributed under the terms of the Creative Commons Attribution License (CC BY). The use, distribution or reproduction in other forums is permitted, provided the original author(s) and the copyright owner(s) are credited and that the original publication in this journal is cited, in accordance with accepted academic practice. No use, distribution or reproduction is permitted which does not comply with these terms.

frontiers in Immunology

REVIEW
published: 16 February 2018
doi: 10.3389/fimmu.2018.00276

Features of Effective T Cell-Inducing Vaccines against Chronic Viral Infections

*Eleni Panagioti[1,2], Paul Klenerman[3], Lian N. Lee[3], Sjoerd H. van der Burg[1] and Ramon Arens[2]**

[1] Department of Medical Oncology, Leiden University Medical Center, Leiden, Netherlands, [2] Department of Immunohematology and Blood Transfusion, Leiden University Medical Center, Leiden, Netherlands, [3] Nuffield Department of Medicine, University of Oxford, Oxford, United Kingdom

For many years, the focus of prophylactic vaccines was to elicit neutralizing antibodies, but it has become increasingly evident that T cell-mediated immunity plays a central role in controlling persistent viral infections such as with human immunodeficiency virus, cytomegalovirus, and hepatitis C virus. Currently, various promising prophylactic vaccines, capable of inducing substantial vaccine-specific T cell responses, are investigated in preclinical and clinical studies. There is compelling evidence that protection by T cells is related to the magnitude and breadth of the T cell response, the type and homing properties of the memory T cell subsets, and their cytokine polyfunctionality and metabolic fitness. In this review, we evaluated these key factors that determine the qualitative and quantitative properties of $CD4^+$ and $CD8^+$ T cell responses in the context of chronic viral disease and prophylactic vaccine development. Elucidation of the mechanisms underlying T cell-mediated protection against chronic viral pathogens will facilitate the development of more potent, durable and safe prophylactic T cell-based vaccines.

Keywords: T cells, quality, vaccine, prophylaxis, chronic infection, virus

OPEN ACCESS

Edited by:
Maria Florencia Quiroga, Universidad de Buenos Aires, Argentina

Reviewed by:
John J. Miles, James Cook University, Australia
Maria Magdalena Gherardi, Consejo Nacional de Investigaciones Científicas y Técnicas (CONICET), Argentina

****Correspondence:***
Ramon Arens
r.arens@lumc.nl

Specialty section:
This article was submitted to T Cell Biology, a section of the journal Frontiers in Immunology

Received: *21 November 2017*
Accepted: *31 January 2018*
Published: *16 February 2018*

Citation:
Panagioti E, Klenerman P, Lee LN, van der Burg SH and Arens R (2018) Features of Effective T Cell-Inducing Vaccines against Chronic Viral Infections. Front. Immunol. 9:276. doi: 10.3389/fimmu.2018.00276

INTRODUCTION

Our bodies are persistently exposed to various pathogens present in the environment. The immune system is fortified with physical barriers and with diverse immune cell populations that play an integral role in protection against disease. Long-term immune responses are mediated by antigen-specific lymphocytes and antibodies that are formed upon pathogen entry. Memory B and T cells are numerically and functionally superior to their naïve precursors cells that are present before infection, and upon encounter with the same pathogen memory immune cells are able to induce a more rapid and powerful recall response (i.e., immunological memory) (1, 2).

The majority of prophylactic vaccines against viral infections have focused on the induction of neutralizing antibodies. Indeed, potent antibody inducing vaccines against virally induced diseases are available. Nevertheless, they fail to provide long-term efficacy and protection against a number of chronic viral infections. Studies in mice, non-human primates, and humans provide evidence that effective prophylactic vaccines against chronic (low level and high level) replicating viruses [i.e., herpesviruses, human immunodeficiency virus (HIV), and hepatitis C virus (HCV)] should engage strong cellular T cell immunity (3–5). The development of T cell-eliciting prophylactic vaccines has gained increasing attention, although such vaccines are not always able to provide

sterilizing immunity. Despite various promising vaccines that are capable of stimulating robust T cell responses, the critical factors of T cell-mediated immune protection against these chronic infections have not been clearly defined. Often, the memory response provoked by vaccines is not sustained and frequently diminishes over time (6, 7). Thus, more knowledge is required to tailor the vaccine's capacity to induce durable $CD4^+$ and/or $CD8^+$ T cell responses of appropriate magnitude and quality to effectively contribute to pathogen clearance. Elucidating the mechanisms through which antigen-specific T cell populations mediate long-term protection against viruses at body surfaces and (lymphoid) tissues remains an important goal, and will facilitate the development of more effective and safe prophylactic T cell-eliciting vaccines. Here, we review determinants and mechanistic factors of effective T cell populations implicated in the vaccine efficacy against chronic viral infections, and discuss how this knowledge can be utilized to maximize the possibility of creating effective vaccine platforms for persistent viral infections.

THE COMPLEXITY OF THE ANTIGEN-SPECIFIC T CELL RESPONSE DURING INFECTION

The antigen-specific interactions between T cells and DCs resulting in activation may initially be short lived, before stabilizing and may last up to 12 h. During this period, T cells receive their necessary activating signals (8, 9). For proper activation of naïve $CD4^+$ and $CD8^+$ T cells, cognate antigenic signals through the TCR (signal 1), costimulatory signals (signal 2) and signals provided by inflammatory cytokines (signal 3) are required (10, 11). Expression of particular chemokine receptors such as CCL19 and CCL21 enhance immune responses by stimulating the interactions between T cells and DCs during antigen presentation (12–15). In addition, the secretion of chemokines by activated DCs and $CD4^+$ T cells enhances $CD8^+$ T cell accumulation and help attract rare antigen-specific T cells (16, 17). The activation of T cells results in alteration of the expression of various molecules including integrins, selectins, and chemokine receptors, leading to the modulation of key intracellular signaling events that promote proliferation, differentiation, and migration of T cells to inflamed tissues (18–20).

After resolution of the infection, the majority (90–95%) of the effector T cells are eliminated due to programmed cell death and only a small, yet diverse pool of memory cells remains (21, 22). Traditionally, memory T cells were classified into two major categories based on their proliferation capacity, phenotypic features, and migration potential (23). Effector-memory T (T_{EM}) cells are identified based on combined expression and/or lack of certain cell surface markers including $KLRG1^{hi}/CD44^{hi}/CD127^{lo}/CD62L^{lo}$. These cells have limited proliferation capacity upon TCR triggering but rapidly produce effector molecules and cytokines such as IFN-γ and TNF (24, 25). Central-memory T (T_{CM}) cells are distinguished by the expression of $KLRG1^{lo}/CD44^{hi}/CD127^{hi}/CD62L^{hi}$ surface markers, exhibit a superior proliferation capacity and produce cytokines that are directly associated with better secondary expansion such as interleukin (IL)-2. Secondary lymphoid organs are the main homing sites of T_{CM} cells whereas T_{EM} cells are more dominantly present in (non-lymphoid) tissues (26–29). Both T_{CM} and T_{EM} cells can circulate, whereas a recently discovered new category of T cells present in tissues lacks migratory capacity. These cells, named tissue-resident memory T (T_{RM}) cells, permanently reside in peripheral tissues, even after the infection is cleared. T_{RM} cells are present in most organs and tissues and can be defined based on the expression of $CD69^{hi}/CD62L^{lo}/CD44^{hi}$ and other surface markers (e.g., CD11a, CD38, CD49a, CD103, and CXCR3) (30–33). However, the composition of these markers depends on tissue-specific cues, and expression levels vary in different tissues. Besides these three main memory T cell subsets, a small subset of memory T cells exists that exhibit advanced stem cell like qualities and proliferation capacities compared with other T cell subsets (34). These memory T cells, which were designated stem cell memory T cells (T_{SCM} cells), display a phenotype highly similar to naïve T cells (T_N cells), being $KLRG1^{lo}/CD44^{lo}/CD127^{hi}/CD62L^{hi}/CD69^{lo}$, but also co-express stem cell antigen (Sca-1), the β chain of the IL-2 and IL-15 receptor (CD122 and IL-2Rβ), and the chemokine receptor CXCR3 (34–39). Some studies reported that T cells with an early stage of differentiation can be induced by vaccines (40, 41) but whether this induction is important for vaccine efficacy is unclear. Thus, whether sufficient amounts of T_{SCM}-like T cells able to elicit protection can be generated by vaccines needs further exploration. Notably, humans and mice have broadly analogous T cell biology, and the above described subsets (i.e., T_{CM}, T_{EM}, T_{RM}, and T_{SCM} cells) have been described in both species and share similar characteristics.

Live attenuated as well as synthetic or subunit vaccines are able to elicit T_{CM}, T_{EM}, and T_{RM} cells (30, 32). With respect to live attenuated vaccines, the vaccine-induced T cell subsets can be highly similar to those subsets that develop upon infection (42). However, live vaccines have disadvantages (e.g., transformation to a virulent form and requires refrigeration), which prompts the development of inactivated, synthetic, or subunit vaccines. T cell subsets that develop upon immunization with those vaccines are highly dependent on the addition of adjuvants and on the route of administration (43).

THE MAGNITUDE OF THE T CELL RESPONSE IS IMPORTANT FOR OPTIMAL PROTECTION

The magnitude of viral-specific T cell responses is highly dictated by the infectious dose and route of infection (44). Higher infectious dosages lead generally to higher peak values of effector T cells, and correspondingly larger amounts of memory T cells in the circulation are found. However, if the immune system is overwhelmed and virus replication remains at a high level, this eventually leads to exhaustion of T cells and poor memory formation (45).

Given the frequently observed correlation between the magnitude of T cell responses and establishment of immunity during infections, simply determining the magnitude of the vaccine-elicited T cell response may already serve as a predictor of efficacy

in vaccination settings. A number of studies have shown a direct association between the vaccine-elicited T cell response size and the ability for virus control (5, 46–48). Several parameters directly impact the magnitude of the vaccine-induced T cell response. In the case of live (attenuated) viruses, the size of the initial dose of the inoculum correlates to the magnitude of the vaccine-specific T cell response until a threshold is reached (49). To reach similar levels as that elicited by virulent virus, inoculum sizes are generally higher for replication-deficient or single-cycle viral vectors. For synthetic vaccines, however, the saturation threshold may not be reached because of lack of sufficient inflammatory signals. However, recent discoveries in adjuvant development and synthetic (nano)particles provide promising approaches to augment T cell responses (50–52). Besides the initial inoculum dosage, booster vaccine regimens increase the magnitude of the T cell response (43, 53, 54) and are likely essential for the majority of vaccine platforms including live vaccines (55). In this regard, vaccines that prime with DNA or adenoviral vectors and boost with modified vaccinia Ankara are excellent demonstrations that underline the supremacy of prime-boost vaccination regimens (4, 56–64).

MEMORY T CELL INFLATION PROVOKED BY RECOMBINANT VACCINES

An alternative mechanism leading to a durable increased magnitude of memory T cells, described as memory "inflation" (65, 66), is observed for certain viral-specific responses following infection by cytomegalovirus (CMV). Here, antigen-specific T cells specific to a subset of viral peptides show an unusual response, whereby they expand gradually over time and are maintained at high frequencies as T_{EM}-like populations—as opposed to the standard expansion and contraction kinetic of conventional memory cells. Critically, and unlike exhausted CD8 T cells that develop during other persistent infections these inflationary responses maintain their effector functions, tissue homing ability and can provide protection against pathogen rechallenge. Memory inflation has also been observed for CMV-specific antibodies, whose levels gradually increase over time (67). Although the rules that determine the onset of memory inflation have not been fully defined, it is clear that for inflation to occur viral antigen must persist long term, a criterion fulfilled by CMV infection through periodic episodes of reactivation from its latent state. Memory T cell inflation appears to require T cell costimulation (68, 69), yet is less dependent on the immunoproteasome (70). Modifying the context of the peptide can convert a classical response to an inflationary one (71).

Recombinant CMVs may provide important vectors for vaccines, although they are highly complex viruses containing multiple immune evasion genes. Nevertheless, in experimental models engineered mouse cytomegalovirus (MCMV)-based vaccine vectors containing foreign viral sequences (e.g., derived from influenza virus, lymphocytic choriomeningitis virus, Ebola virus, herpes simplex virus, and respiratory syncytial virus) provide long-lasting protection (42, 71–73). In rhesus macaques, a recombinant CMV vector expressing simian immunodeficiency virus (SIV) antigens induced in addition to MHC class I-restricted $CD8^+$ T cell responses also MHC class II-restricted and HLA-E-restricted $CD8^+$ T cell responses (74, 75). These unconventional responses are likely to arise because of the restrictions placed on normal antigen presentation by the attenuated CMV vectors used. More work is needed to identify which of these populations is critical for protection, and whether this protection correlates to magnitude, breadth, or effector mechanism.

Memory inflation is not exclusively induced by CMV. Similar phenomena have been observed with other viruses, e.g., Epstein–Barr virus (EBV), herpes simplex virus-1, parvovirus B19, murine polyoma virus, and adenoviral vectors (66, 76). The latter is of interest with respect to vaccine-induced responses. In mouse models, adenovirus-based vectors can lead to induction of inflationary responses, which closely resemble those induced by natural CMV infections (77, 78). Moreover, in this vaccine platform, it is possible to generate inflationary responses against otherwise non-inflationary epitopes by constructing "minigenes," in which only the CD8 T cell epitope of interest is inserted into the vector and expressed, thus bypassing antigen processing requirements (79). Adenoviral vectored vaccines have been developed against many pathogens, including EBV, HCV, HIV, malaria, and Ebola (4, 64, 80–82), and the responses elicited by these vectors in human volunteers are sustained over time. The HCV-specific responses induced in healthy CMV^+ volunteers after immunization with a chimpanzee adenovectored-HCV vaccine shared similar phenotype and functionality to their CMV-specific memory populations as well as to inflating memory cells induced after AdHu5 and MCMV infection in mice (78).

THE BREADTH OF THE INDUCED T CELL RESPONSE IMPACTS ON PROTECTION

An increased breadth of the vaccine-induced T cell response has been found beneficial against many chronic viral pathogens (5, 54, 83–86). Induction of T cells with multiple antigen-specificities correlates with advanced killing capacity for control of HCV or even complete eradication during primary infection with HCV and superior protection upon reinfection (80, 86, 87). Analysis of $CD8^+$ T cell responses in untreated HIV-infected individuals showed that an increasing breadth of Gag-specific responses is associated with decreased viremia (88).

Successful induction of potent and broad T cell responses has been reported for DNA plasmid vaccines (89, 90) and adenovirus serotype 26 vector-based vaccines (91). The latter approach incorporated a combination of subdominant and dominant epitopes of rhesus macaques SIV in prime-boost vaccination schedules. In parallel with these findings, the efficacy of synthetic long peptide (SLP)-based vaccines to protect against MCMV was significantly improved by combinations of SLPs that increased the breadth of the antigen-specific T cell response (5). These findings indicate that cytotoxic $CD8^+$ T cell populations consisting of a broad repertoire of specificities are better capable to effectively kill virus-infected cells compared with T cell pools with a single specificity. Possible explanations are that T cells of diverse specificity results in enhanced killing of virus-infected

cells (compared with T cells with one specificity) or that viral escape mechanisms become restricted. Moreover, an increase in recognition of multiple epitopes may also contribute to protection against infection with heterologous viruses *via* cross-reactive responses (92). Vaccine efficacy is expected to be also dictated by the TCR clonotypes within a polyclonal antigen-specific T cell population, since immune escape during viral infection is linked to conserved TCR motifs while diverse clonotypic repertoires without discernible motifs are not associated with viral escape (93, 94). Hence, the importance of the diversity in the antigen-specific T cell repertoire (with respect to recognition of multiple antigens and diversity in clonotypes specific for the same epitope) should be taken into account while designing prophylactic T cell-based vaccines.

As discussed earlier, both the magnitude and breadth of the T cell response is of importance. However, it should be noted that simply determining the magnitude in the blood is not always valuable, as vaccine efficacy depends also on the type of memory T cell and its location. For example, a direct association between protection and the frequency of the T cells in the circulation does not always exist (95). Actually, depending on the route of infection, T cells present in the mucosal surfaces or in the tissues (T_{EM} and/or T_{RM}) play a dominant role in controlling the infection, and sufficient numbers in these areas rather than in the circulation are likely required to form a robust frontline defense against, e.g., HIV-1 (30, 96). Competition between antigens (e.g., the cellular processing and presentation machinery) is also an important consideration (5), highlighting that antigen selection is not simply a case of "the more the better." Furthermore, not all antigen-specific T cell populations have the same efficacy on a per-cell basis. For example, T cell populations specific for CMV antigens that invoke inflationary responses show superior protective capacity (5). Selection of the correct but also the appropriate quantity of antigens will ultimately steer the immune response and is thus a very critical step of the vaccine development process. Especially, antigens provoking antigen-specific T cell populations with enhanced magnitude, breadth, and diversity in the clonotypic repertoire should be tested and subsequently selected for inclusion when designing vaccine vectors or synthetic vaccines. Furthermore, there is evidence that, besides the quantity and breadth, specific features of antigen-specific T cell populations such as their cytokine polyfunctionality and metabolic properties are also of crucial importance for vaccine efficacy, and this will be further discussed in the next sections.

CYTOKINE POLYFUNCTIONALITY OF T CELLS AS PARAMETER OF VACCINE EFFICACY

Cytokine production is an important effector mechanism of T cell-mediated immunity. Upon most viral and bacterial infections protective T cell immunity consists of $CD4^+$ and $CD8^+$ T cells with a "Th1" cytokine profile that is characterized by (co-) production of IFN-γ, TNF, and IL-2 (97).

The frequency of IFN-γ-producing T cells has been widely used as a parameter to assess vaccine-induced responses. In terms of effector function, IFN-γ has been shown to play a role in the clearance of various viral infections (98). However, there are many examples showing that the magnitude of the IFN-γ secreting T cell response is not a sufficient immune correlate of protection. Single positive IFN-γ-producing T cells can comprise a relatively large fraction of the total cytokine-producing $CD4^+$ and $CD8^+$ T cell population after immunization. However, such T cells have a limited capacity to be sustained as memory T cells (99). Hence, prophylactic vaccines that elicit a high proportion of single IFN-γ-producing T cells would likely not be protective and provide a clear example for why the quality of the response is far more useful in assessing long-term protection than just measuring the frequency of IFN-γ-producing T cells. Instead, studies characterizing (vaccine-elicited) T cell responses against HIV, HBV, HCV, CMV, influenza, and *Leishmania* revealed a strong correlation between the protection level and the induction of high frequencies of polyfunctional T cells [e.g., coproducing IFN-γ, TNF, and IL-2 (4, 80, 100–107)]. Importantly, some of these studies showed that measuring the magnitude of IFN-γ-producing $CD4^+$ and $CD8^+$ T cells alone was not sufficient to predict protection, and provided evidence that measuring the quality of the $CD4^+$ and $CD8^+$ T cell response, *vis-à-vis* polyfunctional T cells, is required.

The supremacy of the polyfunctional T cells may relate to the superior survival properties of these cells (81, 99, 108) and to a higher level of target killing (109). This may be related to a higher IFN-γ production on a per-cell basis by polyfunctional cells compared with monofunctional cells (110), and to the capacity of TNF that is like IFN-γ also capable of mediating the killing of virus-infected cells (111–113). Moreover, reciprocal production of IFN-γ and TNF leads to synergistic actions (114).

Furthermore, the other cytokine in the panel, IL-2, is decisive as well. Studies analyzing the production of IL-2 and IFN-γ by $CD4^+$ and $CD8^+$ T cells from individuals infected with HIV showed that long-term non-progressors, or individuals on anti-retroviral treatment, had increased frequencies of T cells expressing IL-2 only or both IL-2 and IFN-γ, whereas individuals with high viral loads (progressors) have increased frequencies of T cells producing IFN-γ only (95). Although IL-2 has no direct antiviral function, it promotes proliferation and secondary expansion of antigen-specific T cells (115–120). In addition, IL-2 increases expression of the effector molecules perforin and granzyme, which mediate cytolytic function (121, 122). IL-2 signals may also enhance NK cell activity that could contribute to the early control of infection following challenge (99, 123–126). Taken together, we conclude that cytokine polyfunctionality is of major importance for the efficacy of T cell-based vaccines (**Figure 1**), hence dissecting how cytokine polyfunctionality is regulated during the programming of T cells is of interest and may reveal potential strategies to improve vaccine-mounted T cell responses.

IMPROVING VACCINATION BY TARGETING T CELL METABOLISM?

The transition of naïve T cells to active effector cells and memory T cells involves dynamic and coordinated metabolic modifications (129). This reprogramming of the cellular metabolism is

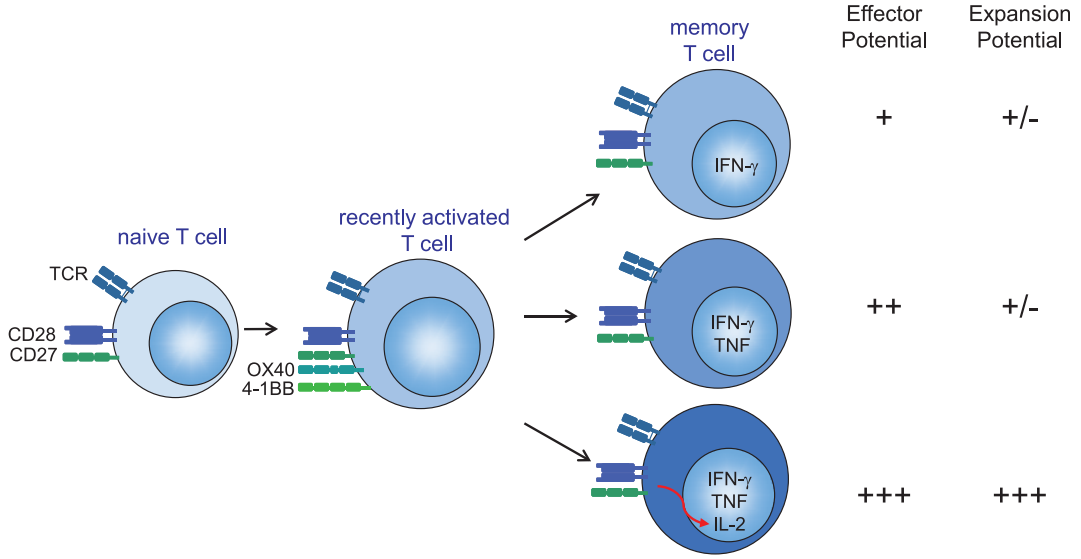

FIGURE 1 | Several mechanisms account for the optimal protection of (vaccine-elicited) polyfunctional cytokine-producing CD4+ and CD8+ T cells. (1) Secretion of more IFN-γ on a per-cell basis. (2) T cells secreting both IFN-γ and TNF have enhanced effector activity compared with T cells that secrete IFN-γ alone. (3) Autocrine interleukin (IL)-2 production promotes the secondary expansion of memory T cells. Hence, IL-2, TNF, and IFN-γ provide a relatively simple set of cytokines that can be used to define a vaccine-elicited response against specific infections that require T cells for protection. CD28 signals are required for sufficient T cell priming during the primary phase of an infection, while OX40 (CD134) and 4-1BB (CD137) gain importance during the late effector and memory stages of antigen-specific T cells either by providing pro-survival signals or by enhancing the quality of the memory T cells (127, 128). CD27 stimulation is important during both early and late phases after infection (68). T cell costimulation *via* CD28 and tumor necrosis factor receptor family members (CD27, OX40, and 4-1BB) can provide signals to enhance autocrine IL-2 production.

not a consequence of activation but is linked to the differentiation and activation processes and reflects the fuel and substrates necessary to support the differentiation stages of a T cell (130, 131). Both naïve T cells and memory T cells rely primarily on oxidative phosphorylation (OXPHOS) and fatty acid oxidation (FAO) for fuel. This reflects the low level yet persistent need for energy as such cells are generally long-lived. Effector T cells on the other hand have particularly high energetic and synthesis demands. These cells have enhanced glycolysis and employ the mitochondrial tricarboxylic acid cycle to support their demand for *de novo* proteins, lipids, and nucleic acids synthesis. It is becoming increasingly clear that metabolic reprogramming plays a critical role in T cell activation, differentiation, and function. The distinct metabolic demands of different T cell subsets make them exquisitely sensitive to pharmacologic inhibitors of metabolism (132). These different metabolic requirements of T cell subsets provide us with a promising therapeutic opportunity to selectively tailor (vaccine-induced) immune responses. Thus, targeting T cell metabolism affords the opportunity to additionally regulate vaccine-induced responses.

Metabolic reprogramming occurs simultaneously with T cell activation and is facilitated by mTOR (mammalian target of rapamycin) (133). mTOR activation promotes glycolysis, fatty acid synthesis, and mitochondrial biogenesis. As such, targets upstream and downstream of the mTOR signaling pathway are potential therapeutic targets. Rapamycin, although known as an "immunosuppressive" drug due to its ability to slow down T cell proliferation, promote robust responses to vaccination by enhancing CD8+ T cell memory formation (134). Correspondingly, deletion of the mTORC1 inhibitory protein TSC2 leads to enhanced mTORC1 activity and increased effector function (135). Targeting of TSC2 or other molecules in the mTOR pathway might accordingly enhance immunity.

Targeting of glycolysis to inhibit immune responses in the setting of autoimmune disease and transplantation rejection is evolving, and this strategy is also used to enhance antitumor immunity by promoting long-lived memory cells *ex vivo* (136). Whether this can be used in vaccination strategies remains to be examined. Although most studies have focused on the critical role of glycolysis in promoting effector T cell generation and function, it has become clear that mitochondrial-directed metabolism also plays an important role. Memory T cells rely for their energy upon OXPHOS and FAO. Because these metabolic pathways are dependent on mitochondria, the abundance and the organization of the mitochondria are instrumental for development of fit memory cells (137). Alterations in the mitochondrial biogenesis can influence the differentiation of T cells, thereby providing opportunity to augment T cell-mediated immunity (138, 139). The transcription factor PGC1α promotes mitochondrial biogenesis and function (140). Hence, pharmacologically or genetically enhancing PGC1α represents a potential strategy for improving vaccine-induced T cell responses. In *ex vivo* systems, it has already been shown that enforced overexpression of PGC1α, leads to improved metabolic fitness and effector cytokine function of CD8+ T cells (141). Finally, the immediate uptake of amino acids such as glutamine and leucine is critical for proper

metabolic reprogramming of T cells. This is accompanied with the upregulation of amino acid transporters involved in glutamine (SLC1A5) and leucine (SLC7A5/SLC3A2 heterodimer) (142, 143). Whether *in vivo* targeting of the above described metabolic processes is possible remains to be examined and may depend on the specificity of metabolic inhibitors/enhancers as they could affect many cells of the body. The future will tell if indeed metabolic targeting is possible to enhance vaccines. Nevertheless, the metabolic profiles of (vaccine-induced) T cells are surely of interest and correlate to vaccine-mediated immunity (144).

COSTIMULATION EMPOWERS T CELL-ELICITING VACCINES

Targeting costimulatory and inhibitory receptors on the cell surface of T cells has shown efficacy in various preventive and therapeutic preclinical vaccination settings. Costimulatory signals transduced *via* the CD28 family members CD28 and ICOS and *via* the tumor necrosis factor receptor (TNFR) family members CD27, 4-1BB, and OX40 play dominant roles in orchestrating the required "signal 2" for optimal T cell proliferation and survival (127). While CD28 and CD27 are constitutively expressed on naïve T cells, ICOS, 4-1BB, and OX40 are upregulated upon T cell activation (127, 145). Collaboration between costimulatory molecules was expected (127, 146) and confirmed in experimental models (147).

Enforced engagement of costimulatory molecules results in enhanced T cell activation, expansion, survival, and establishment of long-term memory (148–154), and has thus the potential to serve as effective immunomodulatory components of prophylactic vaccines against chronic viruses (127, 151, 155). Indeed, this has already been observed for DNA and adenovirus-based vector vaccines in which enforced expression of costimulatory ligands stimulating CD27, 4-1BB, and OX40 leads to increased T cell expansion, enhanced cytotoxic activity and antibody responses (156, 157). Strikingly, agonistic antibodies to OX40 combined with synthetic peptide vaccines prompt robust effector and memory $CD4^+$ and $CD8^+$ antiviral T cell responses, thereby enhancing the prophylactic vaccine efficacy against lytic MCMV infection (153). Chronic viral infections are characterized by accumulation of functionally impaired antigen-specific $CD8^+$ T cells. Studies have shown that activation *via* 4-1BBL alone or in combination with CD80 can enhance the generation of primary $CD8^+$ T cell responses and induce expansion of the antigen-specific $CD8^+$ T cells from this pool of impaired T cells (145, 158). Similarly, 4-1BB stimulation has been shown to enhance the generation of primary $CD8^+$ T cell responses (148, 159, 160) and synergizes with attenuated vaccinia virus vectors to augment $CD8^+$ T cell responses (148).

Targeting of inhibitory molecules on T cells, such as PD-1 and CTLA-4, has been shown to restore the effector function of (over) activated T cells in settings of chronic viral infections and cancer (161–164). Inhibitor blockade with monoclonal antibodies in combination with therapeutic vaccines synergizes in reinvigorating antitumor and antiviral T cell responses (165, 166). Targeting of inhibitory pathways during primary immunization with prophylactic vaccines may advance the vaccine efficacy as well (167, 168).

Although the use of antibodies targeting costimulatory and inhibitory molecules as immunostimulatory modalities in vaccine approaches can facilitate antigen-specific T cell responses, the use of such Abs, however, is associated with toxicity as demonstrated in rodents and in clinical settings (164, 169–171). Nevertheless, given the potential benefit to significantly increase the effectiveness of vaccines, both the efficacy and safety of targeting costimulation is currently extensively examined in various immunotherapeutic approaches against persistent viral infections. Examining the timing and/or the dosing is in this respect an important aspect, not only to prevent unwanted side effects but also to improve effectiveness. However, mass deployment of antibodies to improve vaccines may be too expensive, hence alternative methods able to target costimulatory and inhibitory molecules are desired.

CD28-mediated costimulation modulates T cell metabolism *via* activation of PI3K pathways, and this is essential to control effector cytokine production (172, 173). Moreover, CD28 signaling leads to PI3K-dependent upregulation of surface GLUT1 to facilitate enhanced glucose influx (172). This upregulation of GLUT1 is critical for T cell function, as genetic deletion of GLUT1 markedly inhibits effector T cells (174). Concomitant with increased expression of glucose transporters is the upregulation of key glycolytic enzymes (175). The inhibitory receptor PD-1 also regulates metabolic activity including glycolytic and mitochondrial processes (139, 176). TNFR family members are also able to metabolically program T cells (177, 178). Another important property of T cell costimulation is its effect on improving the T cell cytokine polyfunctionality. For example CD28 but also the TNFR family members are able to promote IL-2 production (153, 179–181), thereby directly improving the cytokine polyfunctionality (**Figure 1**). The TCR affinity also impacts polyfunctionality (182), and likely the collective signals of the TCR and costimulatory receptors are programming the polyfunctional status of T cells. In conclusion, targeting of T cell costimulation can impact the important quantitative (magnitude, breadth) and qualitative (cytokine polyfunctionality and metabolic fitness) determinants of vaccine-induced T cells, and provides thus major opportunities for further exploration in future vaccine designs.

CONCLUSION AND PERSPECTIVES FOR VACCINE DESIGN

The design of vaccines that imprint T cells with the ability to protect against persistent viral pathogens has gained remarkable progress. An understanding of the appropriate initial programming signals is a key step, as is how the route of priming or boosting influences the development of effective memory T cells. A combination of several metrics such as the type of the memory T cell, breadth, polyfunctional quality, and metabolic characteristics demonstrate a valid toolbox to define when a vaccine-elicited T cell response is protective. Information about the anatomic location, activation, and differentiation of memory T cells in lymphoid compared with non-lymphoid organs could

be very valuable as well. Costimulatory signaling pathways mediate important T cell memory properties (e.g., programming of cytokine polyfunctionality and metabolism) and may serve as interesting targets for vaccine improvement. Insight into these pathways may identify the requisite pathways and potentially other targets to improve T cell-based immunotherapy. Coupling this to the identification of the best correlates of protection for persistent viral pathogens will foster the development of more effective vaccination regimes.

AUTHOR CONTRIBUTIONS

All authors contributed to the writing of this review.

FUNDING

This work was funded by a grant from the European Commission [FP7 Marie Curie Action, Grant number: 316655, VacTrain (SB and RA)].

REFERENCES

1. Ahmed R, Gray D. Immunological memory and protective immunity: understanding their relation. *Science* (1996) 272:54–60. doi:10.1126/science.272.5258.54
2. Berard M, Tough DF. Qualitative differences between naive and memory T cells. *Immunology* (2002) 106:127–38. doi:10.1046/j.1365-2567.2002.01447.x
3. Hansen SG, Ford JC, Lewis MS, Ventura AB, Hughes CM, Coyne-Johnson L, et al. Profound early control of highly pathogenic SIV by an effector memory T-cell vaccine. *Nature* (2011) 473:523–7. doi:10.1038/nature10003
4. Swadling L, Capone S, Antrobus RD, Brown A, Richardson R, Newell EW, et al. A human vaccine strategy based on chimpanzee adenoviral and MVA vectors that primes, boosts, and sustains functional HCV-specific T cell memory. *Sci Transl Med* (2014) 6:261ra153. doi:10.1126/scitranslmed.3009185
5. Panagioti E, Redeker A, van Duikeren S, Franken KL, Drijfhout JW, van der Burg SH, et al. The breadth of synthetic long peptide vaccine-induced CD8+ T cell responses determines the efficacy against mouse cytomegalovirus infection. *PLoS Pathog* (2016) 12:e1005895. doi:10.1371/journal.ppat.1005895
6. Plotkin SA. Vaccines: correlates of vaccine-induced immunity. *Clin Infect Dis* (2008) 47:401–9. doi:10.1086/589862
7. Goronzy JJ, Weyand CM. Successful and maladaptive T cell aging. *Immunity* (2017) 46:364–78. doi:10.1016/j.immuni.2017.03.010
8. Fooksman DR, Vardhana S, Vasiliver-Shamis G, Liese J, Blair DA, Waite J, et al. Functional anatomy of T cell activation and synapse formation. *Annu Rev Immunol* (2010) 28:79–105. doi:10.1146/annurev-immunol-030409-101308
9. Mempel TR, Henrickson SE, Von Andrian UH. T-cell priming by dendritic cells in lymph nodes occurs in three distinct phases. *Nature* (2004) 427:154–9. doi:10.1038/nature02238
10. Arens R, Schoenberger SP. Plasticity in programming of effector and memory CD8 T-cell formation. *Immunol Rev* (2010) 235:190–205. doi:10.1111/j.0105-2896.2010.00899.x
11. Curtsinger JM, Mescher MF. Inflammatory cytokines as a third signal for T cell activation. *Curr Opin Immunol* (2010) 22:333–40. doi:10.1016/j.coi.2010.02.013
12. Friedman RS, Jacobelli J, Krummel MF. Surface-bound chemokines capture and prime T cells for synapse formation. *Nat Immunol* (2006) 7:1101–8. doi:10.1038/ni1106-1234a
13. Marsland BJ, Battig P, Bauer M, Ruedl C, Lassing U, Beerli RR, et al. CCL19 and CCL21 induce a potent proinflammatory differentiation program in licensed dendritic cells. *Immunity* (2005) 22:493–505. doi:10.1016/j.immuni.2005.02.010
14. Forster R, Davalos-Misslitz AC, Rot A. CCR7 and its ligands: balancing immunity and tolerance. *Nat Rev Immunol* (2008) 8:362–71. doi:10.1038/nri2297
15. Kaiser A, Donnadieu E, Abastado JP, Trautmann A, Nardin A. CC chemokine ligand 19 secreted by mature dendritic cells increases naive T cell scanning behavior and their response to rare cognate antigen. *J Immunol* (2005) 175:2349–56. doi:10.4049/jimmunol.175.4.2349
16. Castellino F, Huang AY, Altan-Bonnet G, Stoll S, Scheinecker C, Germain RN. Chemokines enhance immunity by guiding naive CD8+ T cells to sites of CD4+ T cell-dendritic cell interaction. *Nature* (2006) 440:890–5. doi:10.1038/nature04651
17. Hickman HD, Li L, Reynoso GV, Rubin EJ, Skon CN, Mays JW, et al. Chemokines control naive CD8+ T cell selection of optimal lymph node antigen presenting cells. *J Exp Med* (2011) 208:2511–24. doi:10.1084/jem.20102545
18. Nolz JC, Starbeck-Miller GR, Harty JT. Naive, effector and memory CD8 T-cell trafficking: parallels and distinctions. *Immunotherapy* (2011) 3:1223–33. doi:10.2217/imt.11.100
19. Denucci CC, Mitchell JS, Shimizu Y. Integrin function in T-cell homing to lymphoid and nonlymphoid sites: getting there and staying there. *Crit Rev Immunol* (2009) 29:87–109. doi:10.1615/CritRevImmunol.v29.i2.10
20. Murdoch C, Finn A. Chemokine receptors and their role in inflammation and infectious diseases. *Blood* (2000) 95:3032–43.
21. Zhang M, Byrne S, Liu N, Wang Y, Oxenius A, Ashton-Rickardt PG. Differential survival of cytotoxic T cells and memory cell precursors. *J Immunol* (2007) 178:3483–91. doi:10.4049/jimmunol.178.6.3483
22. Gerlach C, van Heijst JW, Schumacher TN. The descent of memory T cells. *Ann N Y Acad Sci* (2011) 1217:139–53. doi:10.1111/j.1749-6632.2010.05830.x
23. Sallusto F, Lenig D, Forster R, Lipp M, Lanzavecchia A. Two subsets of memory T lymphocytes with distinct homing potentials and effector functions. *Nature* (1999) 401:708–12. doi:10.1038/44385
24. Lefrancois L, Marzo AL. The descent of memory T-cell subsets. *Nat Rev Immunol* (2006) 6:618–23. doi:10.1038/nri1866
25. Mahnke YD, Brodie TM, Sallusto F, Roederer M, Lugli E. The who's who of T-cell differentiation: human memory T-cell subsets. *Eur J Immunol* (2013) 43:2797–809. doi:10.1002/eji.201343751
26. Rosenblum MD, Way SS, Abbas AK. Regulatory T cell memory. *Nat Rev Immunol* (2016) 16:90–101. doi:10.1038/nri.2015.1
27. Pepper M, Jenkins MK. Origins of CD4(+) effector and central memory T cells. *Nat Immunol* (2011) 12:467–71. doi:10.1038/ni.2038
28. Chang JT, Wherry EJ, Goldrath AW. Molecular regulation of effector and memory T cell differentiation. *Nat Immunol* (2014) 15:1104–15. doi:10.1038/ni.3031
29. Masopust D, Schenkel JM. The integration of T cell migration, differentiation and function. *Nat Rev Immunol* (2013) 13:309–20. doi:10.1038/nri3442
30. Mueller SN, Gebhardt T, Carbone FR, Heath WR. Memory T cell subsets, migration patterns, and tissue residence. *Annu Rev Immunol* (2013) 31:137–61. doi:10.1146/annurev-immunol-032712-095954
31. Mueller SN, Mackay LK. Tissue-resident memory T cells: local specialists in immune defence. *Nat Rev Immunol* (2016) 16:79–89. doi:10.1038/nri.2015.3
32. Rosato PC, Beura LK, Masopust D. Tissue resident memory T cells and viral immunity. *Curr Opin Virol* (2017) 22:44–50. doi:10.1016/j.coviro.2016.11.011
33. Carbone FR. Tissue-resident memory T cells and fixed immune surveillance in nonlymphoid organs. *J Immunol* (2015) 195:17–22. doi:10.4049/jimmunol.1500515
34. Gattinoni L, Lugli E, Ji Y, Pos Z, Paulos CM, Quigley MF, et al. A human memory T cell subset with stem cell-like properties. *Nat Med* (2011) 17:1290–7. doi:10.1038/nm.2446
35. Zhang Y, Joe G, Hexner E, Zhu J, Emerson SG. Host-reactive CD8+ memory stem cells in graft-versus-host disease. *Nat Med* (2005) 11:1299–305. doi:10.1038/nm1326
36. Gattinoni L, Zhong XS, Palmer DC, Ji Y, Hinrichs CS, Yu Z, et al. Wnt signaling arrests effector T cell differentiation and generates CD8+ memory stem cells. *Nat Med* (2009) 15:808–13. doi:10.1038/nm.1982
37. Neuenhahn M, Busch DH. The quest for CD8+ memory stem cells. *Immunity* (2009) 31:702–4. doi:10.1016/j.immuni.2009.10.002
38. Ahmed R, Roger L, Costa Del Amo P, Miners KL, Jones RE, Boelen L, et al. Human stem cell-like memory T cells are maintained in a state of dynamic flux. *Cell Rep* (2016) 17:2811–8. doi:10.1016/j.celrep.2016.11.037
39. Gattinoni L, Speiser DE, Lichterfeld M, Bonini C. T memory stem cells in health and disease. *Nat Med* (2017) 23:18–27. doi:10.1038/nm.4241

40. Freel SA, Lamoreaux L, Chattopadhyay PK, Saunders K, Zarkowsky D, Overman RG, et al. Phenotypic and functional profile of HIV-inhibitory CD8 T cells elicited by natural infection and heterologous prime/boost vaccination. *J Virol* (2010) 84:4998–5006. doi:10.1128/JVI.00138-10
41. Maeto C, Rodriguez AM, Holgado MP, Falivene J, Gherardi MM. Novel mucosal DNA-MVA HIV vaccination in which DNA-IL-12 plus cholera toxin B subunit (CTB) cooperates to enhance cellular systemic and mucosal genital tract immunity. *PLoS One* (2014) 9:e107524. doi:10.1371/journal.pone.0107524
42. Karrer U, Wagner M, Sierro S, Oxenius A, Hengel H, Dumrese T, et al. Expansion of protective CD8+ T-cell responses driven by recombinant cytomegaloviruses. *J Virol* (2004) 78:2255–64. doi:10.1128/JVI.78.5.2255-2264.2004
43. van Duikeren S, Fransen MF, Redeker A, Wieles B, Platenburg G, Krebber WJ, et al. Vaccine-induced effector-memory CD8+ T cell responses predict therapeutic efficacy against tumors. *J Immunol* (2012) 189:3397–403. doi:10.4049/jimmunol.1201540
44. Hu Z, Molloy MJ, Usherwood EJ. CD4(+) T-cell dependence of primary CD8(+) T-cell response against Vaccinia virus depends upon route of infection and viral dose. *Cell Mol Immunol* (2016) 13:82–93. doi:10.1038/cmi.2014.128
45. Wherry EJ. T cell exhaustion. *Nat Immunol* (2011) 12:492–9. doi:10.1038/ni.2035
46. Ogg GS, Jin X, Bonhoeffer S, Dunbar PR, Nowak MA, Monard S, et al. Quantitation of HIV-1-specific cytotoxic T lymphocytes and plasma load of viral RNA. *Science* (1998) 279:2103–6. doi:10.1126/science.279.5359.2103
47. Davenport MP, Zhang L, Bagchi A, Fridman A, Fu TM, Schleif W, et al. High-potency human immunodeficiency virus vaccination leads to delayed and reduced CD8+ T-cell expansion but improved virus control. *J Virol* (2005) 79:10059–62. doi:10.1128/JVI.79.15.10059-10062.2005
48. Mudd PA, Martins MA, Ericsen AJ, Tully DC, Power KA, Bean AT, et al. Vaccine-induced CD8+ T cells control AIDS virus replication. *Nature* (2012) 491:129–33. doi:10.1038/nature11443
49. Akondy RS, Johnson PL, Nakaya HI, Edupuganti S, Mulligan MJ, Lawson B, et al. Initial viral load determines the magnitude of the human CD8 T cell response to yellow fever vaccination. *Proc Natl Acad Sci U S A* (2015) 112:3050–5. doi:10.1073/pnas.1500475112
50. Stano A, Nembrini C, Swartz MA, Hubbell JA, Simeoni E. Nanoparticle size influences the magnitude and quality of mucosal immune responses after intranasal immunization. *Vaccine* (2012) 30:7541–6. doi:10.1016/j.vaccine.2012.10.050
51. Swaminathan G, Thoryk EA, Cox KS, Meschino S, Dubey SA, Vora KA, et al. A novel lipid nanoparticle adjuvant significantly enhances B cell and T cell responses to sub-unit vaccine antigens. *Vaccine* (2016) 34:110–9. doi:10.1016/j.vaccine.2015.10.132
52. Billeskov R, Wang Y, Solaymani-Mohammadi S, Frey B, Kulkarni S, Andersen P, et al. Low antigen dose in adjuvant-based vaccination selectively induces CD4 T cells with enhanced functional avidity and protective efficacy. *J Immunol* (2017) 198:3494–506. doi:10.4049/jimmunol.1600965
53. Penaloza-MacMaster P, Teigler JE, Obeng RC, Kang ZH, Provine NM, Parenteau L, et al. Augmented replicative capacity of the boosting antigen improves the protective efficacy of heterologous prime-boost vaccine regimens. *J Virol* (2014) 88:6243–54. doi:10.1128/JVI.00406-14
54. Wu L, Kong WP, Nabel GJ. Enhanced breadth of CD4 T-cell immunity by DNA prime and adenovirus boost immunization to human immunodeficiency virus Env and Gag immunogens. *J Virol* (2005) 79:8024–31. doi:10.1128/JVI.79.13.8024-8031.2005
55. Amanna IJ, Slifka MK. Wanted, dead or alive: new viral vaccines. *Antiviral Res* (2009) 84:119–30. doi:10.1016/j.antiviral.2009.08.008
56. Hanke T, Blanchard TJ, Schneider J, Hannan CM, Becker M, Gilbert SC, et al. Enhancement of MHC class I-restricted peptide-specific T cell induction by a DNA prime/MVA boost vaccination regime. *Vaccine* (1998) 16:439–45. doi:10.1016/S0264-410X(97)00226-0
57. Brave A, Boberg A, Gudmundsdotter L, Rollman E, Hallermalm K, Ljungberg K, et al. A new multi-clade DNA prime/recombinant MVA boost vaccine induces broad and high levels of HIV-1-specific CD8(+) T-cell and humoral responses in mice. *Mol Ther* (2007) 15:1724–33. doi:10.1038/sj.mt.6300235
58. Amara RR, Villinger F, Altman JD, Lydy SL, O'Neil SP, Staprans SI, et al. Control of a mucosal challenge and prevention of AIDS by a multiprotein DNA/MVA vaccine. *Science* (2001) 292:69–74. doi:10.1126/science.1058915
59. Barouch DH, Liu J, Li H, Maxfield LF, Abbink P, Lynch DM, et al. Vaccine protection against acquisition of neutralization-resistant SIV challenges in rhesus monkeys. *Nature* (2012) 482:89–93. doi:10.1038/nature10766
60. Goonetilleke N, Moore S, Dally L, Winstone N, Cebere I, Mahmoud A, et al. Induction of multifunctional human immunodeficiency virus type 1 (HIV-1)-specific T cells capable of proliferation in healthy subjects by using a prime-boost regimen of DNA- and modified Vaccinia virus Ankara-vectored vaccines expressing HIV-1 Gag coupled to CD8+ T-cell epitopes. *J Virol* (2006) 80:4717–28.
61. Chea LS, Amara RR. Immunogenicity and efficacy of DNA/MVA HIV vaccines in rhesus macaque models. *Expert Rev Vaccines* (2017) 16:973–85. doi:10.1080/14760584.2017.1371594
62. Borducchi EN, Cabral C, Stephenson KE, Liu J, Abbink P, Ng'ang'a D, et al. Ad26/MVA therapeutic vaccination with TLR7 stimulation in SIV-infected rhesus monkeys. *Nature* (2016) 540:284–7. doi:10.1038/nature20583
63. Joachim A, Munseri PJ, Nilsson C, Bakari M, Aboud S, Lyamuya EF, et al. Three-year durability of immune responses induced by HIV-DNA and HIV-modified vaccinia virus Ankara and effect of a late HIV-modified vaccinia virus Ankara boost in Tanzanian volunteers. *AIDS Res Hum Retroviruses* (2017) 33:880–8. doi:10.1089/AID.2016.0251
64. Ewer KJ, O'Hara GA, Duncan CJ, Collins KA, Sheehy SH, Reyes-Sandoval A, et al. Protective CD8+ T-cell immunity to human malaria induced by chimpanzee adenovirus-MVA immunisation. *Nat Commun* (2013) 4:2836. doi:10.1038/ncomms3836
65. Karrer U, Sierro S, Wagner M, Oxenius A, Hengel H, Koszinowski UH, et al. Memory inflation: continuous accumulation of antiviral CD8+ T cells over time. *J Immunol* (2003) 170:2022–9. doi:10.4049/jimmunol.170.4.2022
66. O'Hara GA, Welten SP, Klenerman P, Arens R. Memory T cell inflation: understanding cause and effect. *Trends Immunol* (2012) 33:84–90. doi:10.1016/j.it.2011.11.005
67. Welten SP, Redeker A, Toes RE, Arens R. Viral persistence induces antibody inflation without altering antibody avidity. *J Virol* (2016) 90:4402–11. doi:10.1128/JVI.03177-15
68. Welten SP, Redeker A, Franken KL, Benedict CA, Yagita H, Wensveen FM, et al. CD27-CD70 costimulation controls T cell immunity during acute and persistent cytomegalovirus infection. *J Virol* (2013) 87:6851–65. doi:10.1128/JVI.03305-12
69. Humphreys IR, Loewendorf A, De TC, Schneider K, Benedict CA, Munks MW, et al. OX40 costimulation promotes persistence of cytomegalovirus-specific CD8 T Cells: a CD4-dependent mechanism. *J Immunol* (2007) 179:2195–202. doi:10.4049/jimmunol.179.4.2195
70. Hutchinson S, Sims S, O'Hara G, Silk J, Gileadi U, Cerundolo V, et al. A dominant role for the immunoproteasome in CD8+ T cell responses to murine cytomegalovirus. *PLoS One* (2011) 6:e14646. doi:10.1371/journal.pone.0014646
71. Dekhtiarenko I, Jarvis MA, Ruzsics Z, Cicin-Sain L. The context of gene expression defines the immunodominance hierarchy of cytomegalovirus antigens. *J Immunol* (2013) 190:3399–409. doi:10.4049/jimmunol.1203173
72. Tsuda Y, Caposio P, Parkins CJ, Botto S, Messaoudi I, Cicin-Sain L, et al. A replicating cytomegalovirus-based vaccine encoding a single Ebola virus nucleoprotein CTL epitope confers protection against Ebola virus. *PLoS Negl Trop Dis* (2011) 5:e1275. doi:10.1371/journal.pntd.0001275
73. Morabito KM, Ruckwardt TR, Redwood AJ, Moin SM, Price DA, Graham BS. Intranasal administration of RSV antigen-expressing MCMV elicits robust tissue-resident effector and effector memory CD8+ T cells in the lung. *Mucosal Immunol* (2017) 10:545–54. doi:10.1038/mi.2016.48
74. Hansen SG, Sacha JB, Hughes CM, Ford JC, Burwitz BJ, Scholz I, et al. Cytomegalovirus vectors violate CD8+ T cell epitope recognition paradigms. *Science* (2013) 340:1237874. doi:10.1126/science.1237874
75. Hansen SG, Wu HL, Burwitz BJ, Hughes CM, Hammond KB, Ventura AB, et al. Broadly targeted CD8(+) T cell responses restricted by major histocompatibility complex E. *Science* (2016) 351:714–20. doi:10.1126/science.aac9475
76. Klarenbeek PL, Remmerswaal EB, ten Berge IJ, Doorenspleet ME, van Schaik BD, Esveldt RE, et al. Deep sequencing of antiviral T-cell responses to HCMV and EBV in humans reveals a stable repertoire that is maintained for many years. *PLoS Pathog* (2012) 8:e1002889. doi:10.1371/journal.ppat.1002889
77. Bolinger B, Sims S, O'Hara G, de Lara C, Tchilian E, Firner S, et al. A new model for CD8+ T cell memory inflation based upon a recombinant adenoviral vector. *J Immunol* (2013) 190:4162–74. doi:10.4049/jimmunol.1202665

78. Bolinger B, Sims S, Swadling L, O'Hara G, de Lara C, Baban D, et al. Adenoviral vector vaccination induces a conserved program of CD8(+) T cell memory differentiation in mouse and man. *Cell Rep* (2015) 13:1578–88. doi:10.1016/j.celrep.2015.10.034
79. Colston JM, Bolinger B, Cottingham MG, Gilbert S, Klenerman P. Modification of antigen impacts on memory quality after adenovirus vaccination. *J Immunol* (2016) 196:3354–63. doi:10.4049/jimmunol.1502687
80. Barnes E, Folgori A, Capone S, Swadling L, Aston S, Kurioka A, et al. Novel adenovirus-based vaccines induce broad and sustained T cell responses to HCV in man. *Sci Transl Med* (2012) 4:3003155. doi:10.1126/scitranslmed.3003155
81. Moyo N, Borthwick NJ, Wee EG, Capucci S, Crook A, Dorrell L, et al. Long-term follow up of human T-cell responses to conserved HIV-1 regions elicited by DNA/simian adenovirus/MVA vaccine regimens. *PLoS One* (2017) 12:e0181382. doi:10.1371/journal.pone.0181382
82. Smith C, Tsang J, Beagley L, Chua D, Lee V, Li V, et al. Effective treatment of metastatic forms of Epstein-Barr virus-associated nasopharyngeal carcinoma with a novel adenovirus-based adoptive immunotherapy. *Cancer Res* (2012) 72:1116–25. doi:10.1158/0008-5472.CAN-11-3399
83. Andersson AC, Holst PJ. Increased T cell breadth and antibody response elicited in prime-boost regimen by viral vector encoded homologous SIV Gag/Env in outbred CD1 mice. *J Transl Med* (2016) 14:343. doi:10.1186/s12967-016-1102-7
84. Martins MA, Wilson NA, Reed JS, Ahn CD, Klimentidis YC, Allison DB, et al. T-cell correlates of vaccine efficacy after a heterologous simian immunodeficiency virus challenge. *J Virol* (2010) 84:4352–65. doi:10.1128/JVI.02365-09
85. Ragonnaud E, Pedersen AG, Holst PJ. Breadth of T cell responses after immunization with adenovirus vectors encoding ancestral antigens or polyvalent papillomavirus antigens. *Scand J Immunol* (2017) 85:182–90. doi:10.1111/sji.12522
86. Filskov J, Mikkelsen M, Hansen PR, Christensen JP, Thomsen AR, Andersen P, et al. Broadening CD4+ and CD8+ T cell responses against hepatitis C virus by vaccination with NS3 overlapping peptide panels in cross-priming liposomes. *J Virol* (2017) 91:e00130-17. doi:10.1128/JVI.00130-17
87. Abdel-Hakeem MS, Bedard N, Murphy D, Bruneau J, Shoukry NH. Signatures of protective memory immune responses during hepatitis C virus reinfection. *Gastroenterology* (2014) 147:870–81.e8. doi:10.1053/j.gastro.2014.07.005
88. Radebe M, Gounder K, Mokgoro M, Ndhlovu ZM, Mncube Z, Mkhize L, et al. Broad and persistent Gag-specific CD8+ T-cell responses are associated with viral control but rarely drive viral escape during primary HIV-1 infection. *AIDS* (2015) 29:23–33. doi:10.1097/QAD.0000000000000508
89. Hu X, Valentin A, Dayton F, Kulkarni V, Alicea C, Rosati M, et al. DNA prime-boost vaccine regimen to increase breadth, magnitude, and cytotoxicity of the cellular immune responses to subdominant Gag epitopes of simian immunodeficiency virus and HIV. *J Immunol* (2016) 197:3999–4013. doi:10.4049/jimmunol.1600697
90. Santra S, Liao HX, Zhang R, Muldoon M, Watson S, Fischer W, et al. Mosaic vaccines elicit CD8+ T lymphocyte responses that confer enhanced immune coverage of diverse HIV strains in monkeys. *Nat Med* (2010) 16:324–8. doi:10.1038/nm.2108
91. Barouch DH, O'Brien KL, Simmons NL, King SL, Abbink P, Maxfield LF, et al. Mosaic HIV-1 vaccines expand the breadth and depth of cellular immune responses in rhesus monkeys. *Nat Med* (2010) 16:319–23. doi:10.1038/nm.2089
92. Che JW, Daniels KA, Selin LK, Welsh RM. Heterologous immunity and persistent murine cytomegalovirus infection. *J Virol* (2017) 91:e1386–1316. doi:10.1128/JVI.01386-16
93. Price DA, Asher TE, Wilson NA, Nason MC, Brenchley JM, Metzler IS, et al. Public clonotype usage identifies protective Gag-specific CD8+ T cell responses in SIV infection. *J Exp Med* (2009) 206:923–36. doi:10.1084/jem.20081127
94. Price DA, West SM, Betts MR, Ruff LE, Brenchley JM, Ambrozak DR, et al. T cell receptor recognition motifs govern immune escape patterns in acute SIV infection. *Immunity* (2004) 21:793–803. doi:10.1016/j.immuni.2004.10.010
95. Betts MR, Nason MC, West SM, De Rosa SC, Migueles SA, Abraham J, et al. HIV nonprogressors preferentially maintain highly functional HIV-specific CD8+ T cells. *Blood* (2006) 107:4781–9. doi:10.1182/blood-2005-12-4818
96. Wijesundara DK, Ranasinghe C, Grubor-Bauk B, Gowans EJ. Emerging targets for developing T cell-mediated vaccines for human immunodeficiency virus (HIV)-1. *Front Microbiol* (2017) 8:2091. doi:10.3389/fmicb.2017.02091
97. Zhu J, Yamane H, Paul WE. Differentiation of effector CD4 T cell populations (*). *Annu Rev Immunol* (2010) 28:445–89. doi:10.1146/annurev-immunol-030409-101212
98. Stark GR, Kerr IM, Williams BR, Silverman RH, Schreiber RD. How cells respond to interferons. *Annu Rev Biochem* (1998) 67:227–64. doi:10.1146/annurev.biochem.67.1.227
99. Seder RA, Darrah PA, Roederer M. T-cell quality in memory and protection: implications for vaccine design. *Nat Rev Immunol* (2008) 8:247–58. doi:10.1038/nri2274
100. Duvall MG, Precopio ML, Ambrozak DA, Jaye A, McMichael AJ, Whittle HC, et al. Polyfunctional T cell responses are a hallmark of HIV-2 infection. *Eur J Immunol* (2008) 38:350–63. doi:10.1002/eji.200737768
101. Van Braeckel E, Desombere I, Clement F, Vandekerckhove L, Verhofstede C, Vogelaers D, et al. Polyfunctional CD4(+) T cell responses in HIV-1-infected viral controllers compared with those in healthy recipients of an adjuvanted polyprotein HIV-1 vaccine. *Vaccine* (2013) 31:3739–46. doi:10.1016/j.vaccine.2013.05.021
102. Kannanganat S, Ibegbu C, Chennareddi L, Robinson HL, Amara RR. Multiple-cytokine-producing antiviral CD4 T cells are functionally superior to single-cytokine-producing cells. *J Virol* (2007) 81:8468–76. doi:10.1128/JVI.00228-07
103. Schmidt J, Blum HE, Thimme R. T-cell responses in hepatitis B and C virus infection: similarities and differences. *Emerg Microbes Infect* (2013) 2:e15. doi:10.1038/emi.2013.14
104. Darrah PA, Patel DT, De Luca PM, Lindsay RW, Davey DF, Flynn BJ, et al. Multifunctional TH1 cells define a correlate of vaccine-mediated protection against *Leishmania major*. *Nat Med* (2007) 13:843–50. doi:10.1038/nm1592
105. Sridhar S, Begom S, Bermingham A, Hoschler K, Adamson W, Carman W, et al. Cellular immune correlates of protection against symptomatic pandemic influenza. *Nat Med* (2013) 19:1305–12. doi:10.1038/nm.3350
106. Snyder LD, Chan C, Kwon D, Yi JS, Martissa JA, Copeland CA, et al. Polyfunctional T-cell signatures to predict protection from cytomegalovirus after lung transplantation. *Am J Respir Crit Care Med* (2016) 193:78–85. doi:10.1164/rccm.201504-0733OC
107. Park SH, Shin EC, Capone S, Caggiari L, De Re V, Nicosia A, et al. Successful vaccination induces multifunctional memory T-cell precursors associated with early control of hepatitis C virus. *Gastroenterology* (2012) 143:1048–60.e4. doi:10.1053/j.gastro.2012.06.005
108. Kim MT, Harty JT. Impact of inflammatory cytokines on effector and memory CD8+ T cells. *Front Immunol* (2014) 5:295. doi:10.3389/fimmu.2014.00295
109. Almeida JR, Sauce D, Price DA, Papagno L, Shin SY, Moris A, et al. Antigen sensitivity is a major determinant of CD8+ T-cell polyfunctionality and HIV-suppressive activity. *Blood* (2009) 113:6351–60. doi:10.1182/blood-2009-02-206557
110. Precopio ML, Betts MR, Parrino J, Price DA, Gostick E, Ambrozak DR, et al. Immunization with Vaccinia virus induces polyfunctional and phenotypically distinctive CD8(+) T cell responses. *J Exp Med* (2007) 204:1405–16. doi:10.1084/jem.20062363
111. Ruby J, Bluethmann H, Peschon JJ. Antiviral activity of tumor necrosis factor (TNF) is mediated via p55 and p75 TNF receptors. *J Exp Med* (1997) 186:1591–6. doi:10.1084/jem.186.9.1591
112. Sedger LM, McDermott MF. TNF and TNF-receptors: from mediators of cell death and inflammation to therapeutic giants – past, present and future. *Cytokine Growth Factor Rev* (2014) 25:453–72. doi:10.1016/j.cytogfr.2014.07.016
113. Wohlleber D, Kashkar H, Gartner K, Frings MK, Odenthal M, Hegenbarth S, et al. TNF-induced target cell killing by CTL activated through cross-presentation. *Cell Rep* (2012) 2:478–87. doi:10.1016/j.celrep.2012.08.001
114. Paludan SR. Synergistic action of pro-inflammatory agents: cellular and molecular aspects. *J Leukoc Biol* (2000) 67:18–25. doi:10.1002/jlb.67.1.18
115. Williams MA, Tyznik AJ, Bevan MJ. Interleukin-2 signals during priming are required for secondary expansion of CD8+ memory T cells. *Nature* (2006) 441:890–3. doi:10.1038/nature04790
116. Liao W, Lin JX, Leonard WJ. Interleukin-2 at the crossroads of effector responses, tolerance, and immunotherapy. *Immunity* (2013) 38:13–25. doi:10.1016/j.immuni.2013.01.004
117. Feau S, Arens R, Togher S, Schoenberger SP. Autocrine IL-2 is required for secondary population expansion of CD8(+) memory T cells. *Nat Immunol* (2011) 12:908–13. doi:10.1038/ni.2079

118. Bachmann MF, Wolint P, Walton S, Schwarz K, Oxenius A. Differential role of IL-2R signaling for CD8+ T cell responses in acute and chronic viral infections. *Eur J Immunol* (2007) 37:1502–12. doi:10.1002/eji.200637023
119. Cox MA, Harrington LE, Zajac AJ. Cytokines and the inception of CD8 T cell responses. *Trends Immunol* (2011) 32:180–6. doi:10.1016/j.it.2011.01.004
120. Redeker A, Welten SP, Baert MR, Vloemans SA, Tiemessen MM, Staal FJ, et al. The quantity of autocrine IL-2 governs the expansion potential of CD8+ T cells. *J Immunol* (2015) 195:4792–801. doi:10.4049/jimmunol.1501083
121. Janas ML, Groves P, Kienzle N, Kelso A. IL-2 regulates perforin and granzyme gene expression in CD8+ T cells independently of its effects on survival and proliferation. *J Immunol* (2005) 175:8003–10. doi:10.4049/jimmunol.175.12.8003
122. Pipkin ME, Rao A, Lichtenheld MG. The transcriptional control of the perforin locus. *Immunol Rev* (2010) 235:55–72. doi:10.1111/j.0105-2896.2010.00905.x
123. Kalia V, Sarkar S, Subramaniam S, Haining WN, Smith KA, Ahmed R. Prolonged interleukin-2Ralpha expression on virus-specific CD8+ T cells favors terminal-effector differentiation in vivo. *Immunity* (2010) 32:91–103. doi:10.1016/j.immuni.2009.11.010
124. Kehrl JH, Dukovich M, Whalen G, Katz P, Fauci AS, Greene WC. Novel interleukin 2 (IL-2) receptor appears to mediate IL-2-induced activation of natural killer cells. *J Clin Invest* (1988) 81:200–5. doi:10.1172/JCI113295
125. Lee SH, Fragoso MF, Biron CA. Cutting edge: a novel mechanism bridging innate and adaptive immunity: IL-12 induction of CD25 to form high-affinity IL-2 receptors on NK cells. *J Immunol* (2012) 189:2712–6. doi:10.4049/jimmunol.1201528
126. Wu Z, Frascaroli G, Bayer C, Schmal T, Mertens T. Interleukin-2 from adaptive T cells enhances natural killer cell activity against human cytomegalovirus-infected macrophages. *J Virol* (2015) 89:6435–41. doi:10.1128/JVI.00435-15
127. Croft M. Co-stimulatory members of the TNFR family: keys to effective T-cell immunity? *Nat Rev Immunol* (2003) 3:609–20. doi:10.1038/nri1148
128. Welten SP, Melief CJ, Arens R. The distinct role of T cell costimulation in antiviral immunity. *Curr Opin Virol* (2013) 3:475–82. doi:10.1016/j.coviro.2013.06.012
129. van der Windt GJ, Pearce EL. Metabolic switching and fuel choice during T-cell differentiation and memory development. *Immunol Rev* (2012) 249:27–42. doi:10.1111/j.1600-065X.2012.01150.x
130. Buck MD, O'Sullivan D, Pearce EL. T cell metabolism drives immunity. *J Exp Med* (2015) 212:1345–60. doi:10.1084/jem.20151159
131. MacIver NJ, Michalek RD, Rathmell JC. Metabolic regulation of T lymphocytes. *Annu Rev Immunol* (2013) 31:259–83. doi:10.1146/annurev-immunol-032712-095956
132. Patel CH, Powell JD. Targeting T cell metabolism to regulate T cell activation, differentiation and function in disease. *Curr Opin Immunol* (2017) 46:82–8. doi:10.1016/j.coi.2017.04.006
133. Pollizzi KN, Powell JD. Regulation of T cells by mTOR: the known knowns and the known unknowns. *Trends Immunol* (2015) 36:13–20. doi:10.1016/j.it.2014.11.005
134. Araki K, Turner AP, Shaffer VO, Gangappa S, Keller SA, Bachmann MF, et al. mTOR regulates memory CD8 T-cell differentiation. *Nature* (2009) 460:108–12. doi:10.1038/nature08155
135. Pollizzi KN, Patel CH, Sun IH, Oh MH, Waickman AT, Wen J, et al. mTORC1 and mTORC2 selectively regulate CD8(+) T cell differentiation. *J Clin Invest* (2015) 125:2090–108. doi:10.1172/JCI77746
136. Sukumar M, Liu J, Ji Y, Subramanian M, Crompton JG, Yu Z, et al. Inhibiting glycolytic metabolism enhances CD8+ T cell memory and antitumor function. *J Clin Invest* (2013) 123:4479–88. doi:10.1172/JCI69589
137. van der Windt GJ, O'Sullivan D, Everts B, Huang SC, Buck MD, Curtis JD, et al. CD8 memory T cells have a bioenergetic advantage that underlies their rapid recall ability. *Proc Natl Acad Sci U S A* (2013) 110:14336–41. doi:10.1073/pnas.1221740110
138. Buck MD, O'Sullivan D, Klein Geltink RI, Curtis JD, Chang CH, Sanin DE, et al. Mitochondrial dynamics controls T cell fate through metabolic programming. *Cell* (2016) 166:63–76. doi:10.1016/j.cell.2016.05.035
139. Bengsch B, Johnson AL, Kurachi M, Odorizzi PM, Pauken KE, Attanasio J, et al. Bioenergetic insufficiencies due to metabolic alterations regulated by the inhibitory receptor PD-1 are an early driver of CD8(+) T cell exhaustion. *Immunity* (2016) 45:358–73. doi:10.1016/j.immuni.2016.07.008
140. Austin S, St-Pierre J. PGC1alpha and mitochondrial metabolism – emerging concepts and relevance in ageing and neurodegenerative disorders. *J Cell Sci* (2012) 125:4963–71. doi:10.1242/jcs.113662
141. Scharping NE, Menk AV, Moreci RS, Whetstone RD, Dadey RE, Watkins SC, et al. The tumor microenvironment represses T cell mitochondrial biogenesis to drive intratumoral T cell metabolic insufficiency and dysfunction. *Immunity* (2016) 45:374–88. doi:10.1016/j.immuni.2016.07.009
142. Nakaya M, Xiao Y, Zhou X, Chang JH, Chang M, Cheng X, et al. Inflammatory T cell responses rely on amino acid transporter ASCT2 facilitation of glutamine uptake and mTORC1 kinase activation. *Immunity* (2014) 40:692–705. doi:10.1016/j.immuni.2014.04.007
143. Sinclair LV, Rolf J, Emslie E, Shi YB, Taylor PM, Cantrell DA. Control of amino-acid transport by antigen receptors coordinates the metabolic reprogramming essential for T cell differentiation. *Nat Immunol* (2013) 14:500–8. doi:10.1038/ni.2556
144. Li S, Sullivan NL, Rouphael N, Yu T, Banton S, Maddur MS, et al. Metabolic phenotypes of response to vaccination in humans. *Cell* (2017) 169:862–77. doi:10.1016/j.cell.2017.04.026
145. Duttagupta PA, Boesteanu AC, Katsikis PD. Costimulation signals for memory CD8+ T cells during viral infections. *Crit Rev Immunol* (2009) 29:469–86. doi:10.1615/CritRevImmunol.v29.i6.20
146. Chen L, Flies DB. Molecular mechanisms of T cell co-stimulation and co-inhibition. *Nat Rev Immunol* (2013) 13:227–42. doi:10.1038/nri3405
147. Welten SP, Redeker A, Franken KL, Oduro JD, Ossendorp F, Cicin-Sain L, et al. The viral context instructs the redundancy of costimulatory pathways in driving CD8(+) T cell expansion. *Elife* (2015) 4:e07486. doi:10.7554/eLife.07486
148. Zhao Y, Tahiliani V, Salek-Ardakani S, Croft M. Targeting 4-1BB (CD137) to enhance CD8 T cell responses with poxviruses and viral antigens. *Front Immunol* (2012) 3:332. doi:10.3389/fimmu.2012.00332
149. Vezys V, Penaloza-MacMaster P, Barber DL, Ha SJ, Konieczny B, Freeman GJ, et al. 4-1BB signaling synergizes with programmed death ligand 1 blockade to augment CD8 T cell responses during chronic viral infection. *J Immunol* (2011) 187:1634–42. doi:10.4049/jimmunol.1100077
150. Kim YH, Seo SK, Choi BK, Kang WJ, Kim CH, Lee SK, et al. 4-1BB costimulation enhances HSV-1-specific CD8+ T cell responses by the induction of CD11c+CD8+ T cells. *Cell Immunol* (2005) 238:76–86. doi:10.1016/j.cellimm.2006.01.004
151. Croft M. The role of TNF superfamily members in T-cell function and diseases. *Nat Rev Immunol* (2009) 9:271–85. doi:10.1038/nri2526
152. Waller EC, McKinney N, Hicks R, Carmichael AJ, Sissons JG, Wills MR. Differential costimulation through CD137 (4-1BB) restores proliferation of human virus-specific "effector memory" (CD28(-) CD45RA(HI)) CD8(+) T cells. *Blood* (2007) 110:4360–6. doi:10.1182/blood-2007-07-104604
153. Panagioti E, Boon L, Arens R, van der Burg SH. Enforced OX40 stimulation empowers booster vaccines to induce effective CD4+ and CD8+ T cell responses against mouse cytomegalovirus infection. *Front Immunol* (2017) 8:144. doi:10.3389/fimmu.2017.00144
154. Bartholdy C, Kauffmann SO, Christensen JP, Thomsen AR. Agonistic anti-CD40 antibody profoundly suppresses the immune response to infection with lymphocytic choriomeningitis virus. *J Immunol* (2007) 178:1662–70. doi:10.4049/jimmunol.178.3.1662
155. Watts TH. TNF/TNFR family members in costimulation of T cell responses. *Annu Rev Immunol* (2005) 23:23–68. doi:10.1146/annurev.immunol.23.021704.115839
156. Kanagavelu S, Termini JM, Gupta S, Raffa FN, Fuller KA, Rivas Y, et al. HIV-1 adenoviral vector vaccines expressing multi-trimeric BAFF and 4-1BBL enhance T cell mediated anti-viral immunity. *PLoS One* (2014) 9:e90100. doi:10.1371/journal.pone.0090100
157. Ahlers JD, Belyakov IM. Memories that last forever: strategies for optimizing vaccine T-cell memory. *Blood* (2010) 115:1678–89. doi:10.1182/blood-2009-06-227546
158. Bukczynski J, Wen T, Wang C, Christie N, Routy JP, Boulassel MR, et al. Enhancement of HIV-specific CD8 T cell responses by dual costimulation with CD80 and CD137L. *J Immunol* (2005) 175:6378–89. doi:10.4049/jimmunol.175.10.6378
159. Laderach D, Movassagh M, Johnson A, Mittler RS, Galy A. 4-1BB co-stimulation enhances human CD8(+) T cell priming by augmenting the

proliferation and survival of effector CD8(+) T cells. *Int Immunol* (2002) 14:1155–67. doi:10.1093/intimm/dxf080
160. Halstead ES, Mueller YM, Altman JD, Katsikis PD. In vivo stimulation of CD137 broadens primary antiviral CD8+ T cell responses. *Nat Immunol* (2002) 3:536–41. doi:10.1038/ni798
161. Barber DL, Wherry EJ, Masopust D, Zhu B, Allison JP, Sharpe AH, et al. Restoring function in exhausted CD8 T cells during chronic viral infection. *Nature* (2006) 439:682–7. doi:10.1038/nature04444
162. Velu V, Titanji K, Zhu B, Husain S, Pladevega A, Lai L, et al. Enhancing SIV-specific immunity in vivo by PD-1 blockade. *Nature* (2009) 458:206–10. doi:10.1038/nature07662
163. Fuller MJ, Callendret B, Zhu B, Freeman GJ, Hasselschwert DL, Satterfield W, et al. Immunotherapy of chronic hepatitis C virus infection with antibodies against programmed cell death-1 (PD-1). *Proc Natl Acad Sci U S A* (2013) 110:15001–6. doi:10.1073/pnas.1312772110
164. Larkin J, Chiarion-Sileni V, Gonzalez R, Grob JJ, Cowey CL, Lao CD, et al. Combined nivolumab and ipilimumab or monotherapy in untreated melanoma. *N Engl J Med* (2015) 373:23–34. doi:10.1056/NEJMoa1504030
165. Karaki S, Anson M, Tran T, Giusti D, Blanc C, Oudard S, et al. Is there still room for cancer vaccines at the era of checkpoint inhibitors. *Vaccines (Basel)* (2016) 4:37. doi:10.3390/vaccines4040037
166. Liu J, Zhang E, Ma Z, Wu W, Kosinska A, Zhang X, et al. Enhancing virus-specific immunity in vivo by combining therapeutic vaccination and PD-L1 blockade in chronic hepadnaviral infection. *PLoS Pathog* (2014) 10:e1003856. doi:10.1371/journal.ppat.1003856
167. Finnefrock AC, Tang A, Li F, Freed DC, Feng M, Cox KS, et al. PD-1 blockade in rhesus macaques: impact on chronic infection and prophylactic vaccination. *J Immunol* (2009) 182:980–7. doi:10.4049/jimmunol.182.2.980
168. Yuan J, Ginsberg B, Page D, Li Y, Rasalan T, Gallardo HF, et al. CTLA-4 blockade increases antigen-specific CD8(+) T cells in prevaccinated patients with melanoma: three cases. *Cancer Immunol Immunother* (2011) 60:1137–46. doi:10.1007/s00262-011-1011-9
169. Hixon JA, Blazar BR, Anver MR, Wiltrout RH, Murphy WJ. Antibodies to CD40 induce a lethal cytokine cascade after syngeneic bone marrow transplantation. *Biol Blood Marrow Transplant* (2001) 7:136–43. doi:10.1053/bbmt.2001.v7.pm11302547
170. Niu L, Strahotin S, Hewes B, Zhang B, Zhang Y, Archer D, et al. Cytokine-mediated disruption of lymphocyte trafficking, hemopoiesis, and induction of lymphopenia, anemia, and thrombocytopenia in anti-CD137-treated mice. *J Immunol* (2007) 178:4194–213. doi:10.4049/jimmunol.178.7.4194
171. Khan U, Ali F, Khurram MS, Zaka A, Hadid T. Immunotherapy-associated autoimmune hemolytic anemia. *J Immunother Cancer* (2017) 5:15. doi:10.1186/s40425-017-0214-9
172. Frauwirth KA, Riley JL, Harris MH, Parry RV, Rathmell JC, Plas DR, et al. The CD28 signaling pathway regulates glucose metabolism. *Immunity* (2002) 16:769–77. doi:10.1016/S1074-7613(02)00323-0
173. Chang CH, Curtis JD, Maggi LB Jr, Faubert B, Villarino AV, O'Sullivan D, et al. Posttranscriptional control of T cell effector function by aerobic glycolysis. *Cell* (2013) 153:1239–51. doi:10.1016/j.cell.2013.05.016
174. Macintyre AN, Gerriets VA, Nichols AG, Michalek RD, Rudolph MC, Deoliveira D, et al. The glucose transporter Glut1 is selectively essential for CD4 T cell activation and effector function. *Cell Metab* (2014) 20:61–72. doi:10.1016/j.cmet.2014.05.004
175. Wang R, Dillon CP, Shi LZ, Milasta S, Carter R, Finkelstein D, et al. The transcription factor Myc controls metabolic reprogramming upon T lymphocyte activation. *Immunity* (2011) 35:871–82. doi:10.1016/j.immuni.2011.09.021
176. Patsoukis N, Bardhan K, Chatterjee P, Sari D, Liu B, Bell LN, et al. PD-1 alters T-cell metabolic reprogramming by inhibiting glycolysis and promoting lipolysis and fatty acid oxidation. *Nat Commun* (2015) 6:6692. doi:10.1038/ncomms7692
177. Kawalekar OU, O'Connor RS, Fraietta JA, Guo L, McGettigan SE, Posey AD Jr, et al. Distinct signaling of coreceptors regulates specific metabolism pathways and impacts memory development in CAR T cells. *Immunity* (2016) 44:380–90. doi:10.1016/j.immuni.2016.01.021
178. Choi BK, Lee DY, Lee DG, Kim YH, Kim SH, Oh HS, et al. 4-1BB signaling activates glucose and fatty acid metabolism to enhance CD8+ T cell proliferation. *Cell Mol Immunol* (2017) 14:748–57. doi:10.1038/cmi.2016.02
179. June CH, Ledbetter JA, Gillespie MM, Lindsten T, Thompson CB. T-cell proliferation involving the CD28 pathway is associated with cyclosporine-resistant interleukin 2 gene expression. *Mol Cell Biol* (1987) 7:4472–81. doi:10.1128/MCB.7.12.4472
180. Peperzak V, Xiao Y, Veraar EA, Borst J. CD27 sustains survival of CTLs in virus-infected nonlymphoid tissue in mice by inducing autocrine IL-2 production. *J Clin Invest* (2010) 120:168–78. doi:10.1172/JCI40178
181. Oh HS, Choi BK, Kim YH, Lee DG, Hwang S, Lee MJ, et al. 4-1BB signaling enhances primary and secondary population expansion of CD8+ T cells by maximizing autocrine IL-2/IL-2 receptor signaling. *PLoS One* (2015) 10:e0126765. doi:10.1371/journal.pone.0126765
182. Tan MP, Gerry AB, Brewer JE, Melchiori L, Bridgeman JS, Bennett AD, et al. T cell receptor binding affinity governs the functional profile of cancer-specific CD8+ T cells. *Clin Exp Immunol* (2015) 180:255–70. doi:10.1111/cei.12570

Conflict of Interest Statement: The authors declare that the research was conducted in the absence of any commercial or financial relationships that could be construed as a potential conflict of interest.

Copyright © 2018 Panagioti, Klenerman, Lee, van der Burg and Arens. This is an open-access article distributed under the terms of the Creative Commons Attribution License (CC BY). The use, distribution or reproduction in other forums is permitted, provided the original author(s) and the copyright owner are credited and that the original publication in this journal is cited, in accordance with accepted academic practice. No use, distribution or reproduction is permitted which does not comply with these terms.

frontiers in Immunology

ORIGINAL RESEARCH
published: 28 May 2018
doi: 10.3389/fimmu.2018.01041

Inducible Costimulator Expressing T Cells Promote Parasitic Growth During Blood Stage *Plasmodium berghei* ANKA Infection

*Gajendra M. Jogdand, Soumya Sengupta, Gargee Bhattacharya, Santosh Kumar Singh, Prakash Kumar Barik and Satish Devadas**

Infectious Disease Biology, Institute of Life Sciences, Bhubaneswar, India

The lethality of blood stage *Plasmodium berghei ANKA* (PbA) infection is associated with the expression of T-bet and production of cytokine IFN-γ. Expression of inducible costimulator (ICOS) and its downstream signaling has been shown to play a critical role in the T-bet expression and IFN-γ production. Although earlier studies have examined the role of ICOS in the control of acute blood-stage infection of *Plasmodium chabaudi chabaudi* AS (a non-lethal model of malaria infection), its significance in the lethal blood-stage of PbA infection remains unclear. Thus, to address the seminal role of ICOS in lethal blood-stage of PbA infection, we treated PbA-infected mice with anti-ICOS antibody and observed that these mice survived longer than their infected counterparts with significantly lower parasitemia. Anti-ICOS treatment notably depleted ICOS expressing $CD4^+$ and $CD8^+$ T cells with a concurrent reduction in plasma IFN-γ, which strongly indicated that ICOS expressing T cells are major IFN-γ producers. Interestingly, we observed that while ICOS expressing $CD4^+$ and $CD8^+$ T cells produced IFN-γ, $ICOS^-CD8^+$ T cells were also found to be producers of IFN-γ. However, we report that $ICOS^+CD8^+$ T cells were higher producers of IFN-γ than $ICOS^-CD8^+$ T cells. Moreover, correlation of ICOS expression with IFN-γ production in $ICOS^+IFN\text{-}\gamma^+$ T cell population ($CD4^+$ and $CD8^+$ T cells) suggested that ICOS and IFN-γ could positively regulate each other. Further, master transcription factor T-bet importantly involved in regulating IFN-γ production was also found to be expressed by ICOS expressing $CD4^+$ and $CD8^+$ T cells during PbA infection. As noted above with IFN-γ and ICOS, a positive correlation of expression of ICOS with the transcription factor T-bet suggested that both of them could regulate each other. Taken together, our results depicted the importance of ICOS expressing $CD4^+$ and $CD8^+$ T cells in malaria parasite growth and lethality through IFN-γ production and T-bet expression.

Keywords: malaria, inducible costimulator, T cells, IFN-γ, T-bet, CD4, CD8

OPEN ACCESS

Edited by:
Maria Florencia Quiroga, Universidad de Buenos Aires, Argentina

Reviewed by:
Jason Scott Stumhofer, University of Arkansas for Medical Sciences, United States
Shahram Salek-Ardakani, Pfizer, United States

****Correspondence:***
Satish Devadas
satdevs@ils.res.in

Specialty section:
This article was submitted to T Cell Biology, a section of the journal Frontiers in Immunology

Received: *18 January 2018*
Accepted: *26 April 2018*
Published: *28 May 2018*

Citation:
Jogdand GM, Sengupta S, Bhattacharya G, Singh SK, Barik PK and Devadas S (2018) Inducible Costimulator Expressing T Cells Promote Parasitic Growth During Blood Stage Plasmodium berghei ANKA Infection. Front. Immunol. 9:1041. doi: 10.3389/fimmu.2018.01041

INTRODUCTION

Malaria is a major cause of mortality in millions of infected individuals every year, especially children from developing countries. Among all human Plasmodium strains, infection with *Plasmodium falciparum* is the leading cause of death involving severity, cerebral manifestation, and multi-organ dysfunction. To some extent, murine infection of *Plasmodium berghei ANKA* (PbA) can be correlated

to human *P. falciparum* infection corresponding to parasite growth, lethality, or severity and immune response (1). As human malaria studies are restricted to only clinical observations, modulation of T cell immune response in murine models can provide a better insight to ameliorate malaria pathology and vaccine design (2, 3). The role of T cells in malaria infection, however, has been controversial as studies have shown both its critical role in protection from the malaria parasite and its direct role exacerbating malaria pathogenesis. As an example, $CD4^+$ T cells play a major role in the clearance of parasite *Plasmodium chabaudi chabaudi* blood stage infection (4). However, during lethal PbA infection, both $CD4^+$ and $CD8^+$ T cells are involved in cerebral manifestation. Moreover, depletion of both the T cells by antibodies before or during infection ameliorated pathology (5). Thus, these studies among others suggested that T cells play both protective as well as pathological roles during malaria infection.

In both human and murine malaria, $CD4^+$ and $CD8^+$ T cells are producers of IFN-γ, which have been shown to play crucial protective and pathological roles (6, 7). During lethal malaria infection, extraneous administration of IFN-γ led to the dose-dependent protection of BALB/c mice (8). In contrast, another study suggested that IFN-γ produced by $CD4^+$ T cells enhanced $CD8^+$ T cell accumulation in the brain leading to augmented cerebral malaria (9). Moreover, suppressing IFN-γ production from T-bet positive $CD4^+$ T cells efficiently hampered parasite clearance (10). Also, studies with T-bet knockout mice have demonstrated the role of T-bet in regulating parasite burden as well as its role in pathogenesis during experimental cerebral malaria (11). Taken together, these studies indicated that both IFN-γ and T-bet play a role in malaria parasite growth and lethality.

Along with antigenic stimulation, signaling through CD28 plays a critical role in T cell-mediated immunity in clearance of acute blood-stage *P. chabaudi* infection (12). Inhibiting CD28 signaling by blocking CD86 with anti-CD86 antibody preferentially differentiated T cells toward IFN-γ producing Th1 cells and inhibited the Th2 cytokine IL-4. This Th1 cytokine IFN-γ controlled acute parasite infection but did not play a role in limiting chronic malaria infection. Thus, blockade of CD28 signaling suggested that IL-4 production during malaria infection required CD28 signaling whereas augmentation of IFN-γ illustrated the involvement of other co-stimulatory molecules (13). Moreover, *P. chabaudi* infection in the CD28 knock out mice also demonstrated that redundant CD28 signaling pathway with other costimulatory molecules might play a role in IFN-γ production (14). Thus, these studies suggested that IFN-γ production during malarial infection could involve other co-stimulatory molecules.

Inducible costimulator (ICOS), a CD28 homolog, plays a critical role in T cell proliferation, differentiation, cytokine secretion, cell–cell interaction, and B cell maturation (15–21). Depending on the nature of antigen and chronicity of infection, ICOS signaling mediates differential effector $CD4^+$ T cell response. As an example, during *Schistosome mansoni* infection, Th2 and Tfh response were observed whereas, during *Toxoplasma gondii* and *Mycobacterium tuberculosis* infection (Mtb), it was a Th1 response (22–24). In contrast, during non-lethal blood stage *P. chabaudi chabaudi* infection, in the absence of ICOS, enhanced Th1 response led to reduced peak parasitemia (20). In case of $CD8^+$ T cells, ICOS signaling played a role in its activation, expansion, and enhanced secondary response (21, 25). A substantial defect in antigen-specific $CD8^+$ T cells along with hampered $CD4^+$ T cells response was observed during Salmonella infection in ICOS knockout mice (26). Moreover, during late stage of Mtb, ICOS deficiency was associated with reduced Mtb-specific $CD8^+$ T cell response (27). Taken together, these studies strongly suggest that ICOS plays a critical role in $CD4^+$ and $CD8^+$ T cell response in both intra and extracellular infection. However, during lethal intracellular blood-stage of PbA infection, the role of ICOS in T cell response ($CD4^+$ and $CD8^+$) remains unclear.

In this study, we examined the role of ICOS in parasite growth and lethality during lethal PbA infection in BALB/c mice. We characterized ICOS expression and found that both $CD4^+$ and $CD8^+$ T cells express higher ICOS in the PbA-infected mice. Upon depletion of ICOS-expressing T cells by anti-ICOS antibody treatment, we observed prolonged survival of mice with lower parasitemia, suggesting a positive role for ICOS expressing T cells in PbA parasite growth. Further, we report that these T cells are major producers of IFN-γ as correlated with reduced plasma IFN-γ cytokine level and depleted percentage of ICOS expressing T cells upon anti-ICOS treatment. We found both $CD4^+$ and $CD8^+$ T cells expressed transcription factor, T-bet, which is already known to be involved in malaria pathogenesis. Collectively, our study demonstrates that ICOS expressing $CD4^+$ and $CD8^+$ T cells are involved in malarial parasite growth and lethality through IFN-γ production and T-bet expression.

MATERIALS AND METHODS

Ethics Statement

The use of animals and animal procedures were approved by the Institutional Animal Ethics Committee, Institute of Life Sciences, Bhubaneswar, India in accordance with the "Committee for the Purpose of Control and Supervision of Experiments on Animals (CPCSEA)."

Mice, Antibodies, Kits, Reagents, and Malaria Parasite

Male BALB/c mice (6–8 weeks old) used for this study were maintained under pathogen-free condition at institutional animal house facility. Anti-mouse antibodies Alexa Fluor 700-CD8 (Clone 53-6.7), APC-cy7-CD19 (Clone 1D3), APC-cy7-CD45R/B220 (Clone RA3-6B2), were procured from BD Biosciences (San Jose, CA, USA), FITC-CD4 (clone GK 1.5), FITC CD278 (7E.17G9), APC-CD278 (Clone-C398.4A), PerCP-Cy 5.5-CD4 (clone RM4-5), PE-Cy7-IFN-γ (clone XMG 1.2), PE-T-bet (clone eBio 4B10), Alexa Fluor 700-CD8 (53-6.7) were from eBioscience (San Diego, CA, USA), Brilliant violet 605 TCR Vb (clone H57-597), APC-CD278 (clone C398.4A), Anti-CD49b (clone DX5) were from BioLegend (San Diego, CA, USA). Purified antibodies Anti-mouse CD278 ICOS (clone 7E.17G9), Anti-Rat IgG2b isotype control, and anti-CD16/32 were procured from BioXcell (West Lebanon, USA). Dynabeads untouched mouse $CD4^+$ T cell isolation kit was procured from Life Technologies AS (Oslo, Norway) and $CD8^+$ T cell negative selection kit was from Stem cell

technologies (Vancouver, BC, Canada). Phorbol 12-myristate 13-acetate (PMA), Ionomycin, Brefeldin A was procured from Sigma-Aldrich (St. Louis, MO, USA). Malarial parasite *P. berghei ANKA* (MRA-671, MR4, ATCC, Manassas, VA, USA) was obtained from MR4 repository, ATCC, Manassas, VA, USA.

Parasite Infection

Plasmodium berghei ANKA parasitized red blood cells were stored in liquid nitrogen. The parasitic infection was initiated by thawing *P. berghei* ANKA parasite stabilate and intraperitoneally (i.p.) injecting into a donor mouse. After initial expansion of parasites in the donor mouse, blood was collected from tail vein bleed and serially diluted in PBS. Infection was then induced in experimental mice by intravenous (i.v.) injection of 1×10^4 *P. berghei* ANKA parasitic RBCs. After 3 days of infection, percent parasitemia was enumerated by thin blood films stained with modified Giemsa stain (Sigma-Aldrich, St. Louis, MO, USA).

In Vivo Depletion of ICOS-Positive T Cells

On day 1 of PbA infection, ICOS positive T cells were depleted by administering a single dose of anti-CD278 monoclonal antibody (clone 7E.17G9) and its isotype control (rat IgG2b) at 0.2 mg dose, *via* intraperitoneal (i.p.) injection in 200 µl DPBS. Specific depletion of ICOS positive T cells was analyzed by flow cytometry as shown in figure (**Figure 3H**).

Determination of Plasma Cytokines

On day 3, day 5, and day 7, day of PbA infection, murine blood was collected in 15% acid citrate dextrose anticoagulant and centrifuged at 1,000 *g* for 10 min. The collected plasma was stored in −80°C until assayed for cytokines. Cytokine from stored plasma was quantified using the Milliplex mag mouse cytokine/chemokine kit as per the manufacturer's protocol (Millipore, Billerica, MA, USA). The samples were acquired in Bio-plex200 system, and the concentration of cytokines was calculated using Bio-Plex manager software with a five-parameter curve-fitting algorithm applied for standard curve calculation.

Intracellular Cytokine Staining

For measuring T cell secreted cytokines, the negatively selected splenic $CD4^+$ T cells (purity was >93%) and splenocyte (for $CD8^+$ T cell analysis) from uninfected and PbA-infected mice were cultured in RPMI 1640 complete medium [RPMI 1640 (# P04-16500), PAN-Biotech GmbH, Germany] supplemented with 10% FBS US origin (#1302-P100402, PAN-Biotech GmbH, Germany), 50 µM 2-ME, 100 U/ml penicillin and 100 µg/ml streptomycin (# P4333-100 ml, Sigma-Aldrich, USA) and stimulated by 20 ng/ml PMA/1 µg ionomycin for 5 h after with Brefeldin A added in the last 2.5 h of stimulation. Stimulated cells were stained with dead cell discrimination dye for 20 min on the ice and then washed and stained for surface markers. Surface stained cells were fixed with Fixation/permeabilization buffer of BD Biosciences for 20 min at room temperature.

Intracellular Transcription Factor Staining

FoxP3 transcription factor staining kit protocol (eBiosciences, San Diego, CA, USA) was used for intracellular transcription factor staining. In brief, T cells were stained for desired surface markers after dead cell discrimination and blocking with CD16/32 (2.4 G) antibody. After 20 min of incubation, the cells were washed twice and then fixed and permeabilized at room temperature for 20 min as recommended by the manufacturer. The cells were then washed twice with permeabilization buffer and then stained with transcription factor antibody cocktail for 20–30 min at room temperature.

Statistical Analysis

Non-parametric Mann–Whitney test was used for comparisons between two groups. One-way ANOVA with Bonferroni's Multiple Comparison Test was used for multiple comparisons having three or more groups. Two-way ANOVA with Bonferroni posttest was used for comparing weight lost. A log-rank (Mantel–Cox) test was used to determine the significance of survival of PbA-infected mice with or without anti-ratIgG2b and anti-ICOS treatment. Graphs depict mean values ± SEM. p-value < 0.05 ($^*p < 0.05$; $^{**}p < 0.01$; $^{***}p < 0.001$) was considered significant. All graphs were prepared with Prism 5.0 (GraphPad, La Jolla, CA, USA) software.

RESULTS

Anti-ICOS Administration Slows *P. berghei* ANKA Growth and Prolonged Mice Survival

To understand the possible involvement of ICOS in the lethality of blood stage *PbA* infection, we first established parasite infection in BALB/c mice by intravenous injection of 1×10^4 parasitic RBCs. To one group of PbA-infected mice, a single dose of anti-ICOS was given while to another group, rat-anti-IgG2b antibody was injected. On every alternate day starting from day 3, percent parasitemia was ascertained from Giemsa-stained thin blood smear prepared from tail vein blood. On Day 3, the mean parasitemia in untreated (0.0875 ± 0.025%), anti-ICOS (0.1%), and anti-rat IgG2b (0.1%) treated mice were found to be similar, indicating that infection in all the groups started equally. On Day 5 of infection, we observed lowered percent parasitemia albeit non-significant in anti-ICOS treated mice (2.125 ± 0.478%) when compared to untreated (3.62 ± 0.643%) and rat IgG2b-treated (3.5 ± 0.408%) mice. Statistically significant lower parasitemia in anti-ICOS treated (4.16 ± 0.372, p-value < 0.001) as compared to untreated PbA group (10.916 ± 1.067) (**Figure 1A**) was established on day 7. Lowered parasitemia in anti-ICOS-treated mice suggested that ICOS indeed played a significant role in parasite growth. Further, analyzing for the survival of the mice, anti-ICOS treated mice survived significantly longer than the rat IgG2b treated and rat IgG2b treated mice survived longer than the non-treated one (**Figure 1B**). Eventually, anti-ICOS treated mice died with hyperparasitemia. Next, we analyzed percent weight loss; a pathological marker in anti-ICOS treated and untreated mice during PbA infection. On day 5 and day 7 of PbA infection, significantly reduced percent weight loss was observed in anti-ICOS treated mice as compared to PbA-infected mice (**Figure 1C**). The above results indicated that ICOS plays a significant role in PbA parasite growth and pathogenesis.

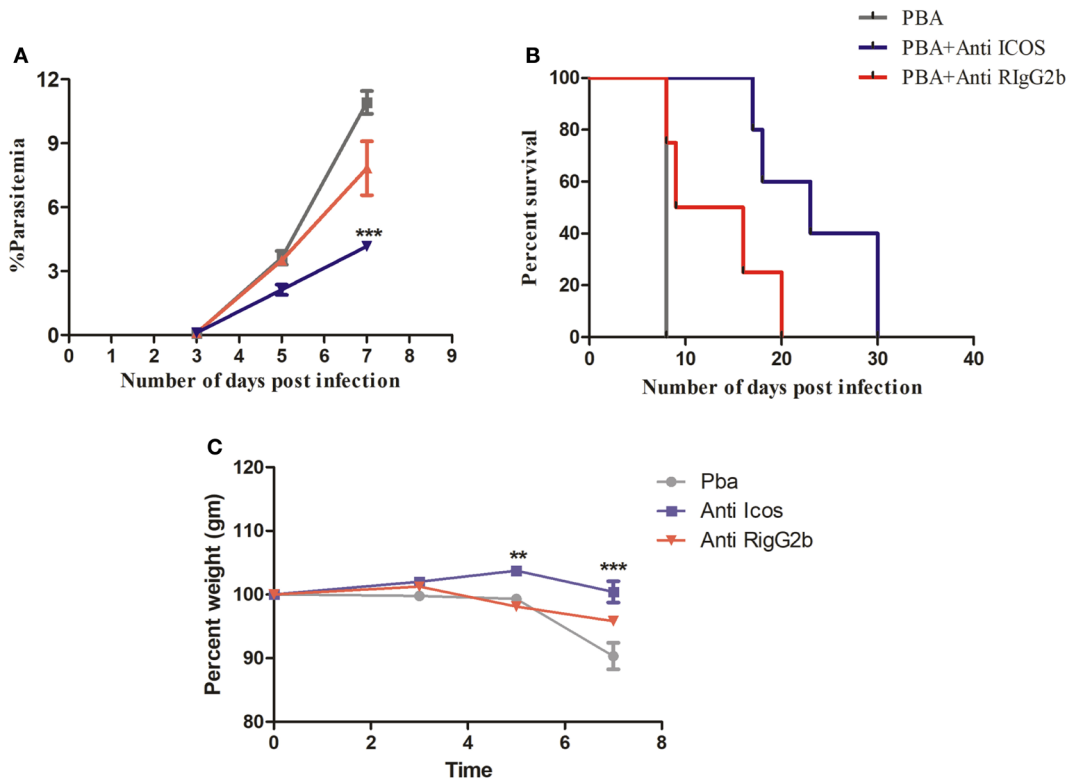

FIGURE 1 | Inducible costimulator (ICOS) positively regulates *Plasmodium berghei* ANKA parasite growth and pathogenesis. BALB/c mice (n = 6/group) were infected with i.v. injection of 1×10^4 *P. berghei* ANKA and on day 1 of infection treated with a single dose of anti-ICOS (200 μg) or isotype control (200 μg). **(A)** Percent parasitemia calculated from Geimsa-stained tail vein blood. **(B)** Percent survival of mice from *Plasmodium berghei* ANKA infection with anti-ICOS treatment and isotype control. **(C)** Percent weight loss a marker of immunopathology. Data represent one of the two independent experiments. Bar represent mean ± SEM. Statistics: Mann–Whitney test, two-way ANOVA with Bonferroni posttest was used for comparing weight loss. Log-rank (Mantel-Cox) test applied for significance of percent survival, p-value <0.05 (*$p < 0.05$; **$p < 0.01$; ***$p < 0.001$) considered significant.

It is well known that regulation of pro-inflammatory (IFN-γ, TNF-α, IL-6, IL-17) and anti-inflammatory (IL-10, IL-4) cytokines play a pivotal role in malaria parasite growth, protection, and/or pathogenesis (28–32). Moreover, previous studies in blood stage infection of PbA have determined the crucial role of IFN-γ in immunopathology and death. However, during acute non-lethal blood-stage malaria infection, IL-27-mediated IL-10 production from IFN-γ-producing $CD4^+$ T cells has been shown to play an essential role in protection from immune pathology (33). Thus, we scored for plasma cytokine IFN-γ, IL-4, IL-10, IL-17, IL-6, IL-27, and TNF-α during PbA infection in BALB/c mice with and without anti-ICOS treatment. In plasma samples of PbA-infected mice, significantly higher IFN-γ levels were observed as compared to other tested cytokines (**Figure 2A**). The ratio of cytokines in infected to uninfected samples (fold change) also suggested that IFN-γ production was higher than other tested cytokines between the groups (**Figure 2B**). Moreover, significantly higher IFN-γ was observed on day 5 and 7 of PbA infection as compared to day 3 (**Figure 2C**). Interestingly, significantly reduced plasma IFN-γ level was found after anti-ICOS treatment (**Figure 2D**). Also, non-significant changes in the levels of cytokine IL-10 (**Figure 2E**), IL-4 (**Figure 2F**), and no difference in the levels of other tested cytokines were observed (data not shown). Altogether, this suggested the critical involvement of ICOS in malaria parasite growth and lethality might be through IFN-γ production.

ICOS Expression During Blood Stage *P. berghei* ANKA Infection

To investigate the role of ICOS and cells associated with its expression for *PbA* lethality, we scored ICOS expression on lymphocytes. On day 3 and day 6 of *PbA* infection, mice were sacrificed and their spleens analyzed for surface markers to identify ICOS expression on $CD4^+$, $CD8^+$, NK, NKT, and B cells by flow cytometry. After gating out doublets and dead cells (**Figure 3A**), we observed higher ICOS expression on $CD4^+$ and $CD8^+$ T cells (**Figure 3B**). Minimal ICOS expression was found on B cells, NK cells, and NKT cells in PbA infected and uninfected mice (data not shown) that did not vary with progressive infection. On day 6 of infection, however, we observed an increased percentage of ICOS-positive $CD4^+$ and $CD8^+$ T cells as compared to uninfected mice (**Figures 3C–E**). A significant increase in mean fluorescent intensity for ICOS on $CD4^+$ and $CD8^+$ T cells suggested that expression of ICOS at protein level per cell was also higher on day 6 of PbA infection (**Figures 3F,G**). Anti-ICOS treatment significantly reduced the percentage of ICOS-positive

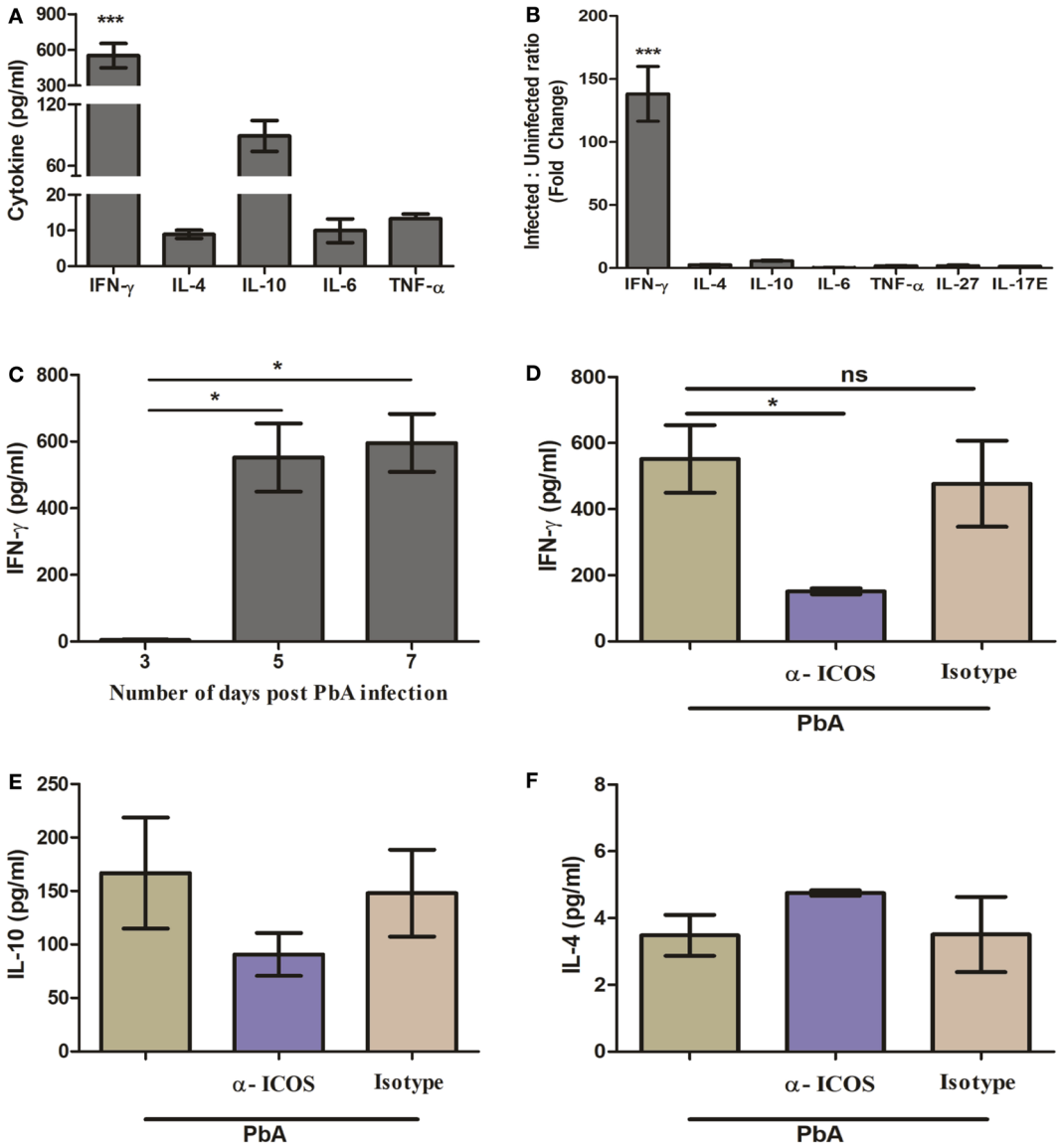

FIGURE 2 | Th1 cytokine IFN-γ is highly produced during PbA infection. Plasma was collected on indicated days from anti-inducible costimulator (ICOS), anti-ratIgG2b, untreated PbA infected and uninfected (control) mice (N = 3/group). The collected plasma was analyzed for cytokine IFN-γ, IL-4, IL-10, IL-6, TNF-α, IL-27, and IL-17E with bioplex ELISA. **(A)** Th1 cytokine IFN-γ is significantly increased as compared to Th2 (IL-4), Treg (IL-10), TNF-α, and IL-6 in *Plasmodium berghei* ANKA (PbA)-infected mice. **(B)** Percent cytokine change as compared to uninfected mice. **(C)** Kinetics of IFN-γ during PbA infection. **(D)** Reduction in plasma IFN-γ production by anti-ICOS treatment. **(E)** Plasma level of IL-10 **(F)** plasma level of IL-4. Data represent one of the two independent experiments. Bar represent mean ± SEM. Statistics: Mann–Whitney test, one-way ANOVA with Bonferroni's Multiple Comparison Test, p-value <0.05 (*$p < 0.05$; **$p < 0.01$; ***$p < 0.001$) considered significant.

CD4$^+$ and CD8$^+$ T cells (**Figures 3H–J**) while ICOS MFI on non-depleted T cells from anti-ICOS treated mice was significantly lower (**Figures 3K,L**) than untreated and RatIgG-treated mice. Moreover, we observed significant depletion in percent activated (CD44^{hi}CD62L^{lo}) as well as total ICOS expressing CD44^{hi}CD62L^{lo} CD4$^+$ T cells upon anti-ICOS treatment (**Figures 3M,N**). Further, we observed non-significant depletion in percent activated (CD44^{hi}CD62L^{lo}) CD8$^+$ T cells and a significant depletion in ICOS expressing CD44^{hi}CD62L^{lo} CD8$^+$ T cells (**Figures 3O,P**). However, anti-Rat IgG2b administration non-significantly reduced ICOS expressing CD4$^+$ and CD8$^+$ T cells (**Figures 3I,K,N,P**). Collectively, the above data indicated that PbA growth and lethality might be associated with ICOS expressing CD4$^+$ and CD8$^+$ T cells.

IFN-γ-Producing CD4$^+$ T Cells Are Highly ICOS Positive at Protein Level

Higher ICOS expression on T cells and increased plasma IFN-γ production suggested that ICOS expressing T cells may be the source and major producers of IFN-γ. Thus, to quantify IFN-γ

production by ICOS expressing CD4$^+$ T cells, on day 6, we negatively isolated CD4$^+$ T cells from uninfected and *PbA* infected BALB/c mice and stimulated them with PMA/ionomycin. The stimulated cells were analyzed for ICOS and IFN-γ co-expression by staining cells with anti-ICOS, anti-IFN-γ antibodies after dead cell discrimination and Fc blocking (**Figure 4A**). As expected, we found a significant increase in the percentage of ICOS$^+$IFN-γ$^+$ CD4$^+$ T cells from *PbA*-infected mice as compared to uninfected mice (**Figure 4B**). Increased integrated mean fluorescent intensity for IFN-γ depicted that IFN-γ production was significantly higher in CD4$^+$ T cell from infected mice than in uninfected mice at the protein level (**Figure 4C**). We further analyzed ICOS expression on IFN-γ positive and IFN-γ negative CD4$^+$ T cells from PbA-infected mice. We found that ICOS expression per cell

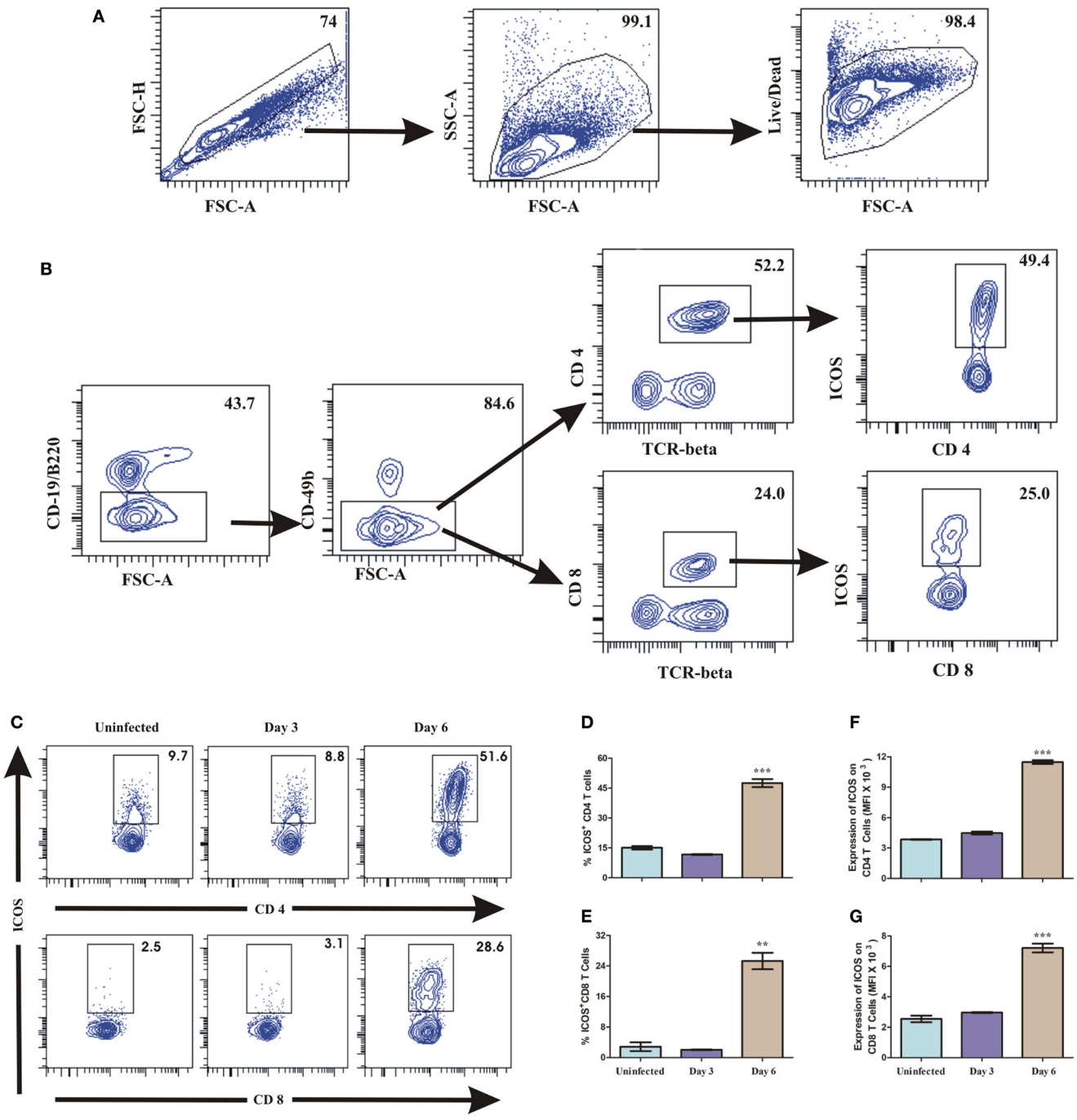

FIGURE 3 | Continued

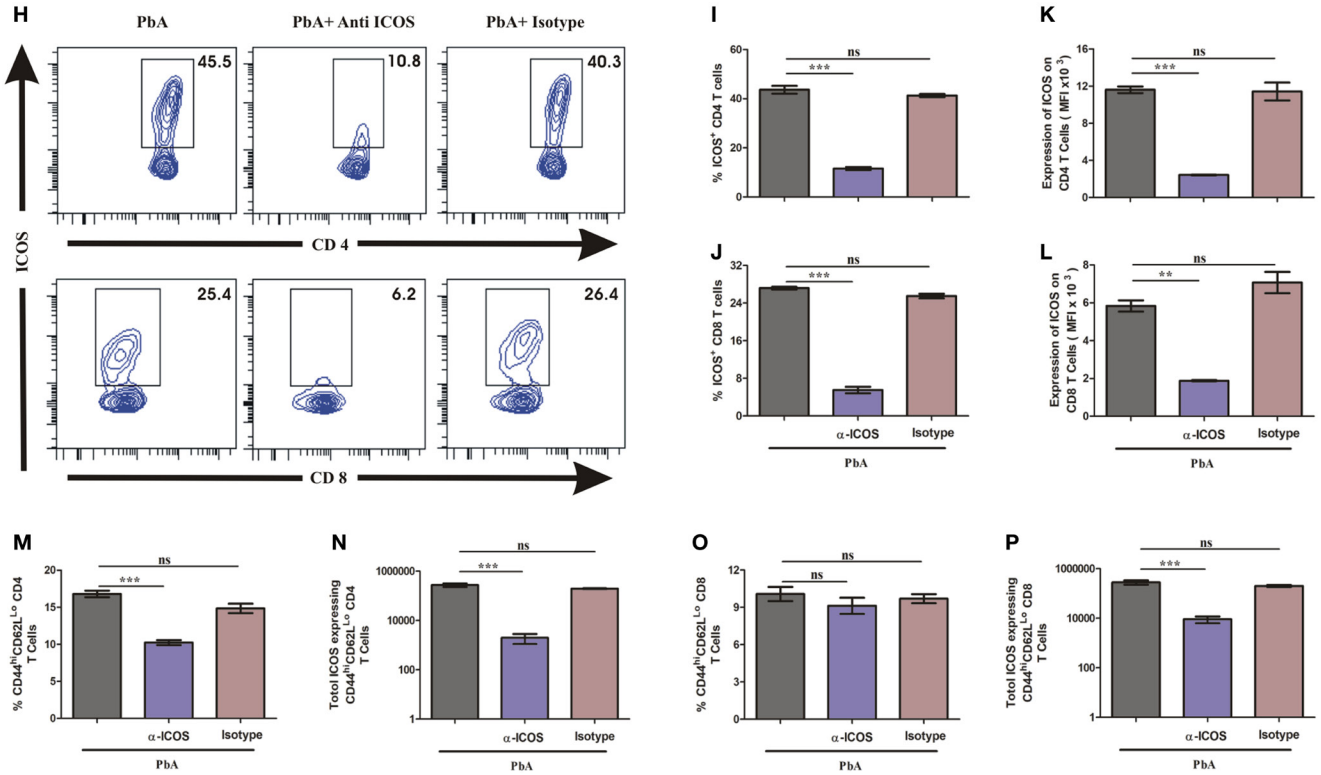

FIGURE 3 | Both CD4$^+$ and CD8$^+$ T cells express inducible costimulator (ICOS) during *Plasmodium berghei* ANKA (PbA). A single cell suspension of splenic cells from uninfected and PbA infected (N = 3/group) were stained with surface staining with antibodies to anti-TCR-vb, anti-CD4, anti-CD8a, CD19/B220, CD278 (ICOS) after dead cell staining with fixable blue dead cell stain. **(A)** Gating strategy for selection of live cells after doublet and dead cell discrimination. This gating strategy was used for all flow cytometry analysis. **(B)** Representative gating strategy for selecting CD4$^+$ and CD8$^+$ T cells and ICOS expression. **(C)** Representative counter plot showed ICOS expression by CD4$^+$ and CD8$^+$ T cells on day 3 and day 6 of PbA infection. **(D)** Percentage ICOS expressing CD4$^+$ T cells. **(E)** Percentage ICOS expressing CD8$^+$ T cells. **(F)** Expression of ICOS on CD4$^+$ T cells. **(G)** Expression of ICOS on CD8$^+$ T cells. **(H)** Representative counter plot showed depletion of ICOS expressing CD4$^+$ and CD8$^+$ T cells upon anti-ICOS treatment. **(I)** Percentage depletion of ICOS expressing CD4$^+$ T cells. **(J)** Percentage depletion of ICOS expressing CD8$^+$ T cells. **(K)** ICOS expression on non-depleted CD4$^+$ T cells. **(L)** ICOS expression on non-depleted CD8$^+$ T cells. **(M)** Percentage activated (CD44^{hi}CD62L^{Lo}) CD4$^+$ T cells. **(N)** Total number of ICOS expressing activated (CD44^{hi}CD62L^{Lo}) CD4$^+$ T cells. **(O)** Percentage activated (CD44^{hi}CD62L^{Lo}) CD8$^+$ T cells. **(P)** Total number of ICOS expressing activated (CD44^{hi}CD62L^{Lo}) CD8$^+$ T cells. Data represent one of the three independent experiments. Bar represent mean ± SEM. Statistics: Mann–Whitney test, one-way ANOVA with Bonferroni's Multiple Comparison Test, p-value <0.05 (*p < 0.05; **p < 0.01; ***p < 0.001) considered significant.

(as scored with mean fluorescent intensity) was significantly higher on IFN-γ$^+$ cells than the negative ones (**Figure 4D**). Moreover, anti-ICOS treatment significantly reduced percentage as well as total ICOS$^+$IFN-γ$^+$ CD4$^+$ T cells (**Figures 4E,F**). Taken together, our data for CD4$^+$ T cells suggest that ICOS may play a role in IFN-γ production based on correlation of ICOS expression and IFN-γ production. It also clearly indicated that all IFN-γ-producing CD4$^+$ T cells were ICOS positive but all ICOS-positive CD4$^+$ T cells were not IFN-γ producers.

ICOS Expressing CD8$^+$ T Cells Are Higher IFN-γ Producers

To ascertain the role of ICOS in the production of IFN-γ by CD8$^+$ T cells during PbA infection, we stimulated single cell splenocyte with PMA/ionomycin. The stimulated cells were stained with anti-TCR-Vb, anti-CD8a, anti-ICOS, and anti-IFN-γ antibodies. After gating TCR-Vb and CD8$^+$, we observed four populations including ICOS$^+$IFN-γ$^-$, ICOS$^+$IFN-γ$^+$, ICOS$^-$IFN-γ$^+$, and ICOS$^-$IFN-γ$^-$ CD8$^+$ T cells (**Figure 4G**). We observed that all ICOS-expressing CD8$^+$ T cells were not IFN-γ producers and all IFN-γ producers were not ICOS expressing (**Figure 4G**). Additionally, we found a significant increase in percent ICOS$^+$IFN-γ$^+$ CD8$^+$ T cells in PbA-infected mice as compared to both the CD8$^+$ T cell populations (ICOS$^-$IFN-γ$^+$, ICOS$^+$IFN-γ$^+$) of uninfected mice (4H). Moreover, in PbA-infected mice, the percentage of ICOS$^+$IFN-γ$^+$ CD8$^+$ T cells was significantly higher than the ICOS$^-$IFN-γ$^+$ population (**Figure 4H**). Increased mean fluorescence intensity of IFN-γ in ICOS$^+$ CD8$^+$ T cells than ICOS$^-$ depicted that ICOS expressing CD8$^+$ T cells were higher IFN-γ producers (**Figure 4I**). Moreover, ICOS expression in PbA-infected mice was higher on ICOS$^+$IFN-γ$^+$ CD8$^+$ T cells than ICOS$^+$IFN-γ$^-$ CD8$^+$ T cells as determined by the increased mean fluorescent intensity (**Figure 4J**). In addition, we found anti-ICOS treatment significantly reduced percentage as well as total ICOS$^+$IFN-γ$^+$ CD8$^+$ T cells (**Figures 4K,L**). Taken together, the above results suggested that during PbA infection, IFN-γ was produced by

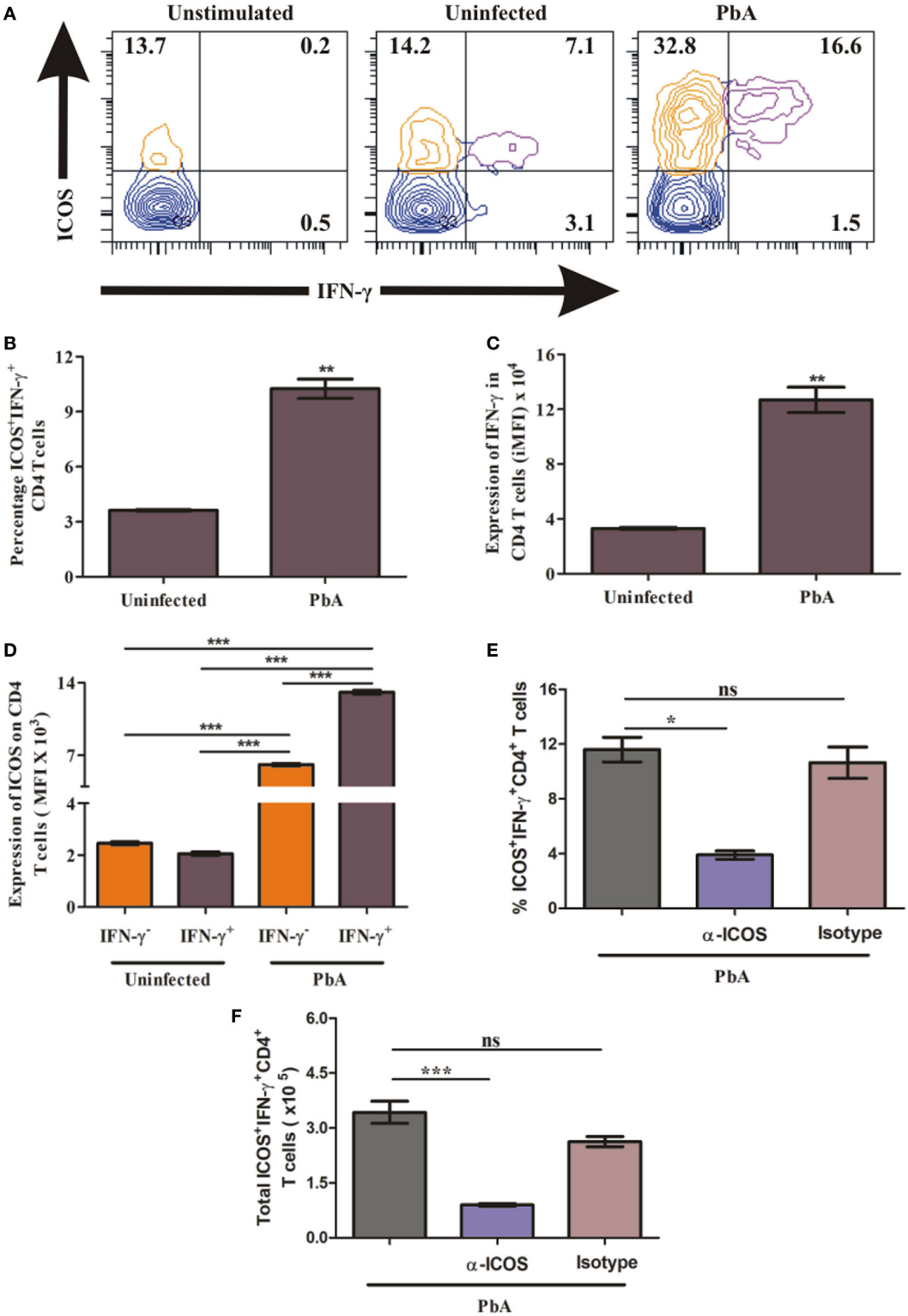

FIGURE 4 | Continued

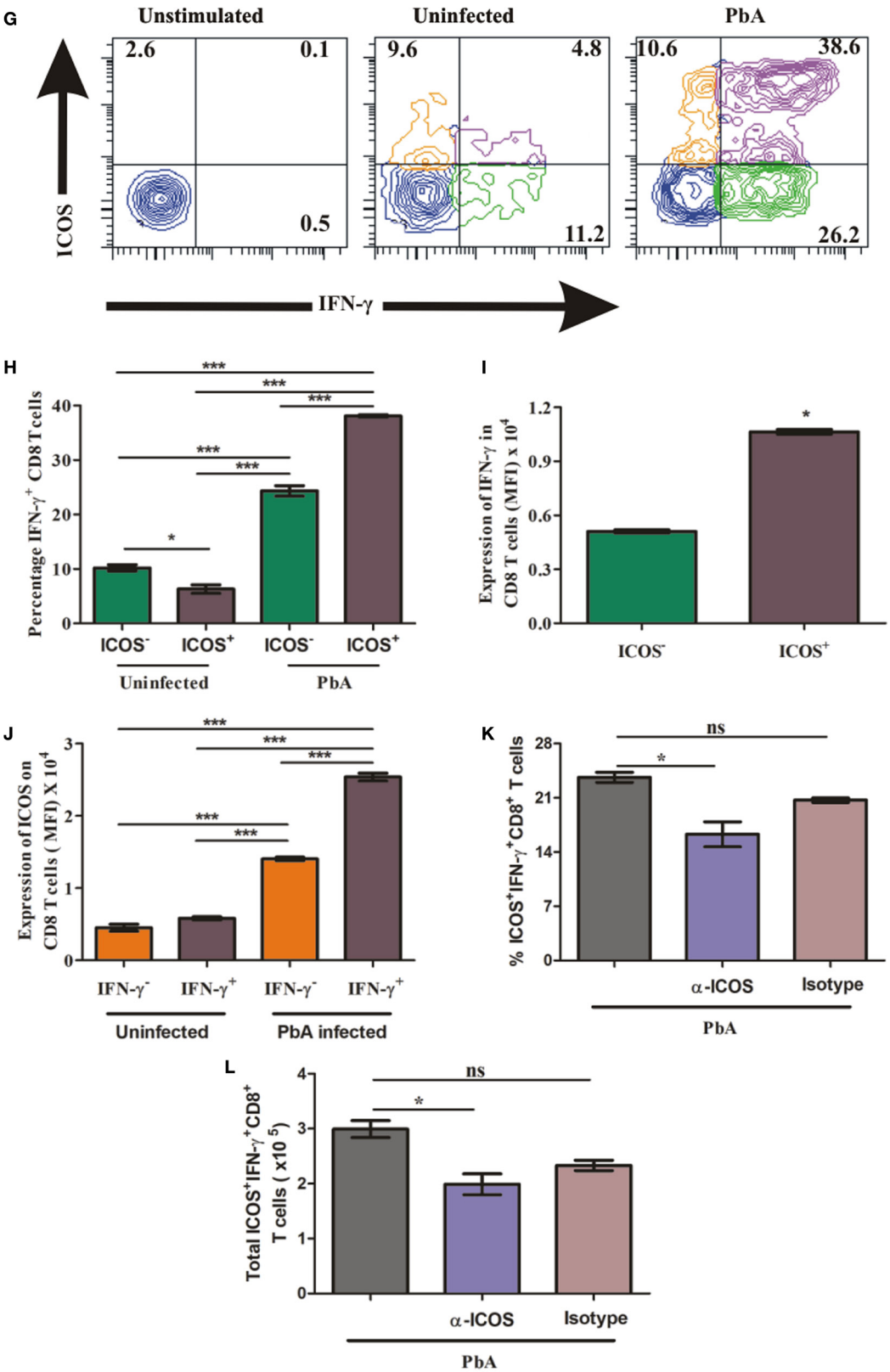

FIGURE 4 | Continued

FIGURE 4 | Higher inducible costimulator (ICOS) expression on IFN-γ producing T cells. Negatively isolated CD4$^+$ T cells and single cell splenocyte from *Plasmodium berghei* ANKA infected and uninfected mice (N = 5/group) were stimulated by Phorbol 12-myristate 13-acetate/Ionomycin for 5 h with Brefeldin A at last 2.5 h. Stimulated CD4$^+$ T cells were stained with anti-ICOS and anti-IFN-γ after dead cell discriminator staining and Fc blocking. The stimulated single cell splenocytes were stained with anti-TCR-vb, anti-CD8a, anti-ICOS, and IFN-γ. **(A)** Representative counter plot show co-expression of ICOS and IFN-γ by CD4$^+$ T cells. **(B)** Percentage increase in ICOS$^+$IFN-γ$^+$ CD4$^+$ T cells. **(C)** Increased expression of IFN-γ in CD4$^+$ T cells. **(D)** ICOS expression on IFN-γ$^+$ and IFN-γ$^-$ CD4$^+$ T cells. **(E)** Anti-ICOS treatment reduced percentage ICOS$^+$IFN-γ$^+$ CD4$^+$ T cells. **(F)** Anti-ICOS treatment depleted total number of ICOS$^+$IFN-γ$^+$ CD4$^+$ T cells after anti-ICOS treatment. **(G)** Representative counter plot show expression of ICOS and IFN-γ in CD8$^+$ T cells. **(H)** Percentage IFN-γ positive CD8$^+$ T cells in ICOS$^+$ and ICOS$^-$ population. **(I)** Expression of IFN-γ by ICOS$^+$ and ICOS$^-$ CD8$^+$ T cells. **(J)** ICOS expression on IFN-γ$^+$ and IFN-γ$^-$ CD8$^+$ T cells. **(K)** Anti-ICOS treatment reduced percentage ICOS$^+$IFN-γ$^+$ CD8$^+$ T cells. **(L)** Anti-ICOS treatment depleted total number of ICOS$^+$IFN-γ$^+$ CD8$^+$ T cells. Data represent one of the two independent experiments. Bar represent mean ± SEM. Statistics: Mann–Whitney test, one-way ANOVA with Bonferroni's multiple comparison test, p-value <0.05 ($^*p < 0.05$; $^{**}p < 0.01$; $^{***}p < 0.001$) considered significant.

ICOS$^+$ and ICOS$^-$ CD8$^+$ T cells; however, ICOS$^+$ CD8$^+$ T cells were higher producers of IFN-γ than the ICOS$^-$ ones.

T-Bet Expressing CD4$^+$ and CD8$^+$ T Cells Have Higher ICOS

The master transcription factor T-bet importantly involved in regulating IFN-γ has been shown to play a paradoxical role during blood-stage malaria infection. As an example, in non-lethal blood stage infection, transcription factor T-bet plays a role in parasite growth wherein T-bet knock out mice infected with *Plasmodium yoelii yoelii* exhibited lower parasitemia (34). Conversely, during PbA infection, while T-bet regulated parasite burden, it also promoted ECM pathology (11). Moreover, T-bet expression critically depends on ICOS expression and its downstream signaling (35). Therefore, we hypothesized that ICOS expressing CD4$^+$ and CD8$^+$ T cells promote PbA parasite growth through T-bet expression. Thus, we analyzed co-expression of ICOS and T-bet by CD4$^+$ and CD8$^+$ T cells during blood stage PbA infection. To ascertain ICOS and T-bet co-expression, we negatively isolated CD4$^+$ T cells and stimulated with PMA/ionomycin for 5 h. The stimulated CD4$^+$ T cells were stained with anti-ICOS and anti-T-bet antibody. We observed low (Lo), intermediate (Int), and high (Hi) ICOS$^+$T-bet$^+$ and ICOS$^+$T-bet$^-$ CD4$^+$ T cell population (**Figure 5A**) in *PbA*-infected mice. Percent ICOS$^+$T-bet$^+$ (Lo), ICOS$^+$T-bet$^+$ (Int) CD4$^+$ T cells were significantly higher than ICOS$^+$T-bet$^+$(Hi) in uninfected mice. Whereas in PbA infected mice, percent ICOS$^+$T-bet$^+$(Hi) and ICOS$^+$T-bet$^+$(Int) were significantly higher than ICOS$^+$T-bet$^+$(Lo) of *PbA*. Percent ICOS$^+$T-bet$^{+\,(Hi,Int,Lo)}$ CD4$^+$ T cells of infected mice was higher than ICOS$^+$T-bet$^{+\,(Hi,Int,Lo)}$ of the uninfected (**Figure 5B**). We observed significantly higher T-bet expression in CD4$^+$ T cells from PbA-infected mice as compared to the uninfected (**Figure 5C**). Also, we analyzed ICOS expression on T-bet-positive CD4$^+$ T cells from infected and uninfected mice. We observed significantly higher ICOS expression on T-bet$^{(Int,\,Hi)}$ positive CD4$^+$ T cells of PbA-infected mice as compared to T-bet$^{+\,(Hi,Int,Lo)}$ of uninfected and T-bet (low) of infected mice (**Figure 5D**). ICOS expression was significantly higher in T-bet$^+$ (Hi) than T-bet$^-$ CD4$^+$ T cells of PbA-infected mice (**Figure 5E**). Thus, our data suggested that all T-bet expressing CD4$^+$ T cells were ICOS positive, but all ICOS-positive CD4$^+$ T cells were not expressing T-bet.

Similar to CD4$^+$ T cells, we determined the role of ICOS for T-bet expression in CD8$^+$ T cells during PbA infection. The splenocytes were stimulated as described earlier and stained with TCR-Vb, CD8a, ICOS, and T-bet antibodies. After gating TCR-vb and CD8$^+$, we observed four populations; ICOS$^+$T-bet$^{+\,(Hi)}$, ICOS$^+$T-bet$^{+\,(Lo)}$, ICOS$^+$T-bet$^{-\,(Hi)}$, and ICOS$^+$T-bet$^{-\,(Lo)}$ of CD8$^+$ T cells (**Figure 5F**). A significant increase in percent ICOS$^+$T-bet$^{+(Hi)}$ CD8$^+$ T cells was observed as compared to ICOS$^+$T-bet$^{+\,(Lo)}$ of infected mice. Also, it was higher than the uninfected (ICOS$^+$T-bet$^{+\,(Hi,\,Lo)}$) CD8$^+$ T cell population (**Figure 5G**). Expression of T-bet at protein level per cell was significantly higher in ICOS$^+$T-bet$^{+\,(Hi)}$ than ICOS$^+$T-bet$^{+\,(Lo)}$ in PbA infected mice and ICOS$^+$T-bet$^{+\,(Hi)}$, ICOS$^+$T-bet$^{+\,(Lo)}$ CD8$^+$ T cells in uninfected mice (**Figure 5H**). Also, we analyzed ICOS expression on T-bet positive cells from uninfected and PbA infected mice and found that ICOS expression was higher on ICOS$^+$T-bet$^{+\,(Hi)}$ (**Figure 5I**). Moreover, ICOS expression on T-bet positive CD8$^+$ T cells was higher than T-bet negative cells in infected mice (**Figure 5J**). Thus, our data suggested that all T-bet expressing CD8$^+$ T cells were ICOS positive, but all ICOS positive CD8$^+$ T cells were not expressing T-bet. Taken together, our data indicated that the transcription factor T-bet was expressed by ICOS positive CD4$^+$ as well as CD8$^+$ T cells during PbA infection.

DISCUSSION

Most symptoms such as fever, anemia, and cerebral manifestations occur during the asexual erythrocytic or blood-stage malaria parasite infection and have been shown to be strongly associated with IFN-γ production by various cells. The produced IFN-γ is involved in modulation of parasite growth leading to protection as well as pathology (7, 8, 29, 36–38). In experimental allergic encephalomyelitis, IFN-γ-mediated immunopathology is associated with ICOS expression and its signaling (39). Further, impaired IFN-γ production and reduced CD4$^+$ and CD8$^+$ T cell response was observed in ICOS-deficient patients leading to immunodeficiency and autoimmunity (40, 41). Moreover, during non-lethal blood-stage malaria infection, ICOS plays an essential role as a regulator of IFN-γ production and also in distributing parasite-specific CD4$^+$ T cells to both lymphoid and non-lymphoid organs (20, 42). Thus, these studies suggested that ICOS could play a role in IFN-γ production during infectious and autoimmune diseases (43). ICOS signaling regulate transcription factor T-bet, which is also involved in regulation of malaria parasite growth and pathogenesis (11, 34, 35). Taking these studies into consideration, we tried to demonstrate the role of ICOS in parasite growth and lethality through T-bet expression and IFN-γ production,

during lethal blood stage of PbA infection. Thus, in our initial experiment, the depletion of ICOS-expressing cells resulted in significantly lowered parasitemia and prolonged mice survival, suggesting that ICOS positive cells are required for PbA growth. Lowered parasitemia due to substantial slowing of parasite maturation, was observed during intraerythrocytic *P. berghei* ANKA infection in Rag$^{(-/-)}$ (lacks T and B cells and mount weak inflammatory response) mice (44). Thus, in our study, we speculate that impaired T cell response leading to diminished parasitemia might be associated with parasite maturation.

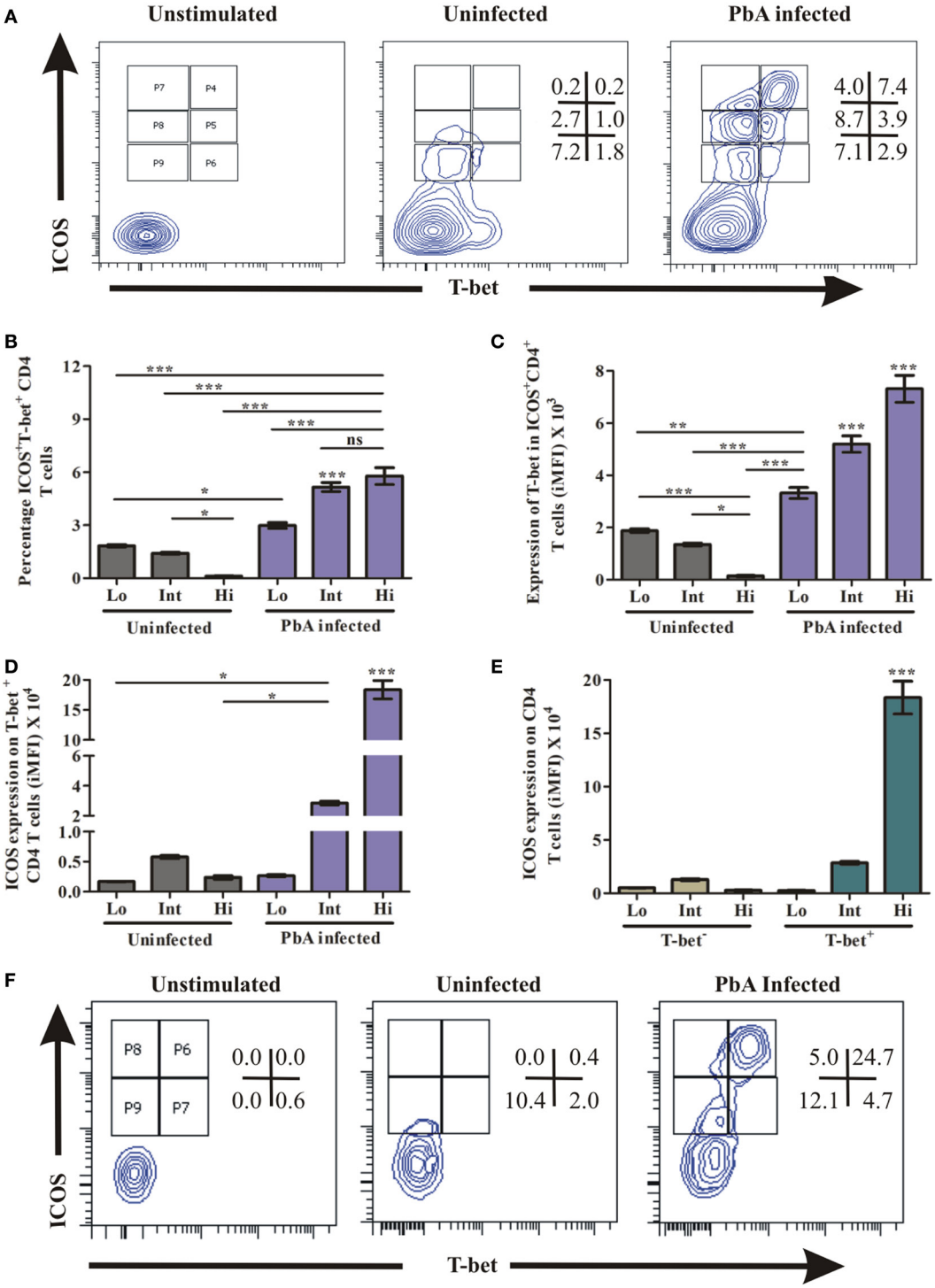

FIGURE 5 | Continued

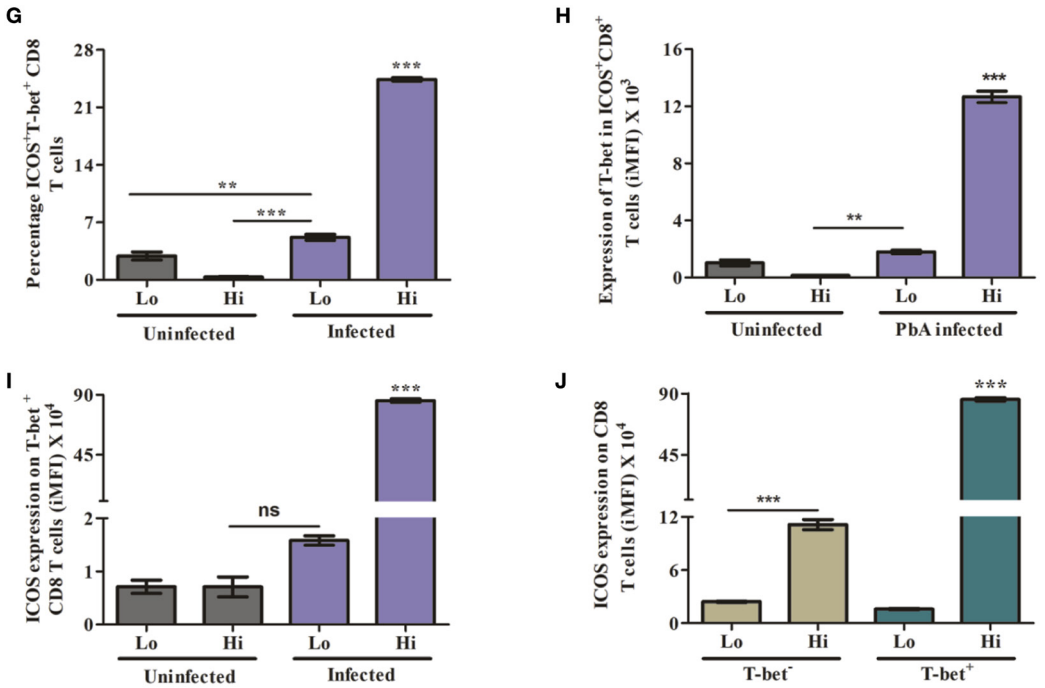

FIGURE 5 | Higher inducible costimulator (ICOS) expression on T-bet-positive T cells. Negatively isolated CD4+ T cells and single cell splenocyte from *Plasmodium berghei* ANKA infected and uninfected mice (N = 3/group) were stimulated by Phorbol 12-myristate 13-acetate/ionomycin for 5 h. Stimulated CD4+ T cells were stained with anti-ICOS and anti-T-bet antibodies after dead cell staining and Fc blocking. The stimulated single cell splenocytes were stained with anti-TCR-vb, anti-CD8a, anti-ICOS, and T-bet. **(A)** Representative counter plot show co-expression of ICOS and T-bet by CD4+ T cells. **(B)** Percentage increase in ICOS+T-bet+ CD4+ T cells. **(C)** Increased expression of T-bet in ICOS+CD4+ T cells. **(D)** Increased ICOS expression on T-bet positive CD4+ T cells. **(E)** ICOS expression on T-bet+ and T-bet− CD4+ T cells. **(F)** Representative counter plot show expression of ICOS and T-bet in CD8+ T cells. **(G)** Percentage T-bet positive CD8+ T cells in ICOS+ and ICOS− population. **(H)** Expression of T-bet by ICOS+CD8+ T cells. **(I)** ICOS Expression on T-bet expressing CD8+ T cells. **(J)** ICOS expression on T-bet+ and T-bet− CD8+ T cells. Data represent one of the two independent experiments. Bar represent mean ± SEM. Statistics: Mann–Whitney test, one-way ANOVA with Bonferroni's multiple comparison test, p-value < 0.05 (*p < 0.05; **p < 0.01; ***p < 0.001) considered significant.

Further, reduced percent weight loss (a marker of pathology) in anti-ICOS treated mice as compared to untreated suggested that ICOS expressing cells are also involved in PbA pathology. The role of ICOS in parasite growth and pathology, thus, led us to further characterize its expression during PbA infection.

During blood-stage malarial infection, helper CD4+ and cytotoxic CD8+ T cells contribute to both protection and pathology (45–48). For activation of both T cells, ICOS expression, and its downstream signaling is critical (21, 40, 41, 49, 50). Consistent with this, in our experiment during blood stage PbA infection, ICOS may be involved in the activation of splenic CD4+ and CD8+ T cells as both these cells express significantly higher ICOS. A study involving depletion of these T cells with antibodies prevented pathology of experimental cerebral malaria (5). Similarly, in this study, upon anti-ICOS administration, depletion of ICOS expressing CD4+ and CD8+ T cells led to lower parasitemia, longer survival, and ameliorated pathology. Thus our study suggested that depletion of ICOS expressing CD4+ and CD8+ T cell was sufficient to control parasite growth and lethality as compared to total T cell depletion.

IFN-γ has been known to play a critical role in lethality during *P. berghei* ANKA infection (9) and consistent with these earlier findings, increased plasma IFN-γ production in our study may be correlated with its role in PbA pathogenesis. Lowered parasitemia, reduced IFN-γ, and increased survival upon anti-ICOS treatment suggest that ICOS plays a role in PbA growth and lethality through IFN-γ production. Further, characterization of CD4+ and CD8+ T cells for IFN-γ production showed that both these cells were indeed IFN-γ producers. Moreover, depletion of ICOS-expressing CD4+ and CD8+ T cells and reduction of plasma IFN-γ upon anti-ICOS treatment suggested that in blood stage of PbA infection, ICOS expressing CD4+ and CD8+ T cells were the major producers of IFN-γ. Further, earlier studies also demonstrated the role of ICOS in modulating cytokines of naïve and activated T cells. Moreover, during *Mycobacterium tuberculosis*, ICOS signaling controlled antigen-specific protective IFN-γ production and the produced IFN-γ, in turn, regulated ICOS expression (24). Similarly, in our study, higher ICOS expression on IFN-γ producing T cells and higher IFN-γ production in ICOS expressing T cells suggested that both ICOS and IFN-γ could regulate each other.

On similar line master transcription factor T-bet has shown to be involved in malaria parasite growth and pathogenesis. For example, lower parasite burden was observed in T-bet knock out ($Tbx21^{-/-}$) mice than T-bet wild-type mice suggesting that T-bet promotes malaria parasite growth (34). In another study, T-bet regulated PbA growth but has also been shown to promote the pathogenesis of ECM (11). Interestingly, ICOS expression and its downstream signaling have been shown to be critical for T-bet expression (35). In our study, ICOS expressing CD4+ and CD8+

T cells, which were involved in PbA growth has also been shown to co-express T-bet. Our results also demonstrated that ICOS and T-bet might regulate each other's expression as correlated with higher ICOS expression on T-bet positive cells and *vice versa*.

The malaria parasite has evolved with multiple mechanisms such as changing shapes, motility, metabolic requirement, and immune evasion strategies to survive inside the host (51). In correlation with this, we demonstrated that malaria parasite utilizes ICOS-expressing T cells for their growth through T-bet expression and IFN-γ production. Other studies have depicted that altering ICOS signaling leads to modulated T cell response, which in turn is involved in infection clearance, tumor regression, and ameliorated pathology (52–54). Thus, modulation of ICOS expression and its signaling might be helpful in altering parasite growth and lethality, which might be valuable in preventing severe malaria in humans.

ETHICS STATEMENT

The use of animals and animal procedures were approved by the Institutional Animal Ethics Committee, Institute of Life Sciences, Bhubaneswar, India in accordance with the "Committee for the Purpose of Control and Supervision of Experiments on Animals (CPCSEA)."

AUTHOR CONTRIBUTIONS

GJ conceived the study and discussed with SD. GJ planned and performed experiments, analyzed data, and drafted manuscript. SS, GB, SS, and PB helped to perform components of some of the experiments. SD arranged the grants for the study and edited manuscript. All authors contributed intellectual content and approved it for publication.

ACKNOWLEDGMENTS

We thank MR4 for providing us with malaria parasite *P. berghei ANKA* contributed by Mark Weiser M. Hollingdale. We thank Dr. Brian deSouza (London School of Hygiene and Tropical Medicine London) and Dr. Suchitra Mohanty for their critical suggestions. We also thank Dr. Ajay Parida (Director), Dr. B. Ravindran (Former Director), Dr. Durg V. Singh, Dr. Vivek Rai, and Dr. Madhumita Panda from Institute of Life Sciences, Bhubaneswar, for their kind support. We are thankful to the ILS animal facility Staff for supplying mice as required.

FUNDING

This work was supported in part by core funds from the Institute of Life Sciences and from the Basic Research in Modern Biology Task Force, Department of Biotechnology, Govt. of India (Grant number-BT/PR11259/BRB/10/646/2008 and BT/PR14425/BRB/10/839/2010). GJ was supported with Senior Research Fellowship of Council of Scientific and Industrial Research (CSIR).

REFERENCES

1. Craig AG, Grau GE, Janse C, Kazura JW, Milner D, Barnwell JW, et al. The role of animal models for research on severe malaria. *PLoS Pathog* (2012) 8(2):e1002401. doi:10.1371/journal.ppat.1002401
2. de Souza JB, Riley EM. Cerebral malaria: the contribution of studies in animal models to our understanding of immunopathogenesis. *Microbes Infect* (2002) 4(3):291–300. doi:10.1016/S1286-4579(02)01541-1
3. Langhorne J. The immune response to the blood stages of *Plasmodium* in animal models. *Immunol Lett* (1994) 41(2–3):99–102. doi:10.1016/0165-2478(94)90115-5
4. Suss G, Eichmann K, Kury E, Linke A, Langhorne J. Roles of CD4- and CD8-bearing T lymphocytes in the immune response to the erythrocytic stages of *Plasmodium chabaudi*. *Infect Immun* (1988) 56(12):3081–8.
5. Hermsen C, van de Wiel T, Mommers E, Sauerwein R, Eling W. Depletion of CD4+ or CD8+ T-cells prevents *Plasmodium berghei* induced cerebral malaria in end-stage disease. *Parasitology* (1997) 114(Pt 1):7–12. doi:10.1017/S0031182096008293
6. King T, Lamb T. Interferon-gamma: the Jekyll and Hyde of malaria. *PLoS Pathog* (2015) 11(10):e1005118. doi:10.1371/journal.ppat.1005118
7. McCall MB, Sauerwein RW. Interferon-gamma – central mediator of protective immune responses against the pre-erythrocytic and blood stage of malaria. *J Leukoc Biol* (2010) 88(6):1131–43. doi:10.1189/jlb.0310137
8. Shear HL, Srinivasan R, Nolan T, Ng C. Role of IFN-gamma in lethal and nonlethal malaria in susceptible and resistant murine hosts. *J Immunol* (1989) 143(6):2038–44.
9. Villegas-Mendez A, Greig R, Shaw TN, de Souza JB, Gwyer Findlay E, Stumhofer JS, et al. IFN-gamma-producing CD4+ T cells promote experimental cerebral malaria by modulating CD8+ T cell accumulation within the brain. *J Immunol* (2012) 189(2):968–79. doi:10.4049/jimmunol.1200688
10. Haque A, Best SE, Ammerdorffer A, Desbarrieres L, de Oca MM, Amante FH, et al. Type I interferons suppress CD4(+) T-cell-dependent parasite control during blood-stage *Plasmodium* infection. *Eur J Immunol* (2011) 41(9):2688–98. doi:10.1002/eji.201141539
11. Oakley MS, Sahu BR, Lotspeich-Cole L, Solanki NR, Majam V, Pham PT, et al. The transcription factor T-bet regulates parasitemia and promotes pathogenesis during *Plasmodium berghei* ANKA murine malaria. *J Immunol* (2013) 191(9):4699–708. doi:10.4049/jimmunol.1300396
12. Rummel T, Batchelder J, Flaherty P, LaFleur G, Nanavati P, Burns JM, et al. CD28 costimulation is required for the expression of T-cell-dependent cell-mediated immunity against blood-stage *Plasmodium chabaudi* malaria parasites. *Infect Immun* (2004) 72(10):5768–74. doi:10.1128/IAI.72.10.5768-5774.2004
13. Taylor-Robinson AW, Smith EC. Modulation of experimental blood stage malaria through blockade of the B7/CD28 T-cell costimulatory pathway. *Immunology* (1999) 96(3):498–504. doi:10.1046/j.1365-2567.1999.00718.x
14. Elias RM, Sardinha LR, Bastos KR, Zago CA, da Silva AP, Alvarez JM, et al. Role of CD28 in polyclonal and specific T and B cell responses required for protection against blood stage malaria. *J Immunol* (2005) 174(2):790–9. doi:10.4049/jimmunol.174.2.790
15. Dong C, Juedes AE, Temann UA, Shresta S, Allison JP, Ruddle NH, et al. ICOS co-stimulatory receptor is essential for T-cell activation and function. *Nature* (2001) 409(6816):97–101. doi:10.1038/35051100
16. Dong C, Temann UA, Flavell RA. Cutting edge: critical role of inducible costimulator in germinal center reactions. *J Immunol* (2001) 166(6):3659–62. doi:10.4049/jimmunol.166.6.3659
17. Hutloff A, Dittrich AM, Beier KC, Eljaschewitsch B, Kraft R, Anagnostopoulos I, et al. ICOS is an inducible T-cell co-stimulator structurally and functionally related to CD28. *Nature* (1999) 397(6716):263–6. doi:10.1038/16717
18. Jogdand GM, Mohanty S, Devadas S. Regulators of Tfh cell differentiation. *Front Immunol* (2016) 7:520. doi:10.3389/fimmu.2016.00520
19. Kopf M, Coyle AJ, Schmitz N, Barner M, Oxenius A, Gallimore A, et al. Inducible costimulator protein (ICOS) controls T helper cell subset

polarization after virus and parasite infection. *J Exp Med* (2000) 192(1):53–61. doi:10.1084/jem.192.1.53
20. Wikenheiser DJ, Ghosh D, Kennedy B, Stumhofer JS. The costimulatory molecule ICOS regulates host Th1 and follicular Th cell differentiation in response to *Plasmodium chabaudi chabaudi* AS infection. *J Immunol* (2016) 196(2):778–91. doi:10.4049/jimmunol.1403206
21. Wallin JJ, Liang L, Bakardjiev A, Sha WC. Enhancement of CD8+ T cell responses by ICOS/B7h costimulation. *J Immunol* (2001) 167(1):132–9. doi:10.4049/jimmunol.167.1.132
22. Bonhagen K, Liesenfeld O, Stadecker MJ, Hutloff A, Erb K, Coyle AJ, et al. ICOS+ Th cells produce distinct cytokines in different mucosal immune responses. *Eur J Immunol* (2003) 33(2):392–401. doi:10.1002/immu.200310013
23. de Jong YP, Rietdijk ST, Faubion WA, Abadia-Molina AC, Clarke K, Mizoguchi E, et al. Blocking inducible co-stimulator in the absence of CD28 impairs Th1 and CD25+ regulatory T cells in murine colitis. *Int Immunol* (2004) 16(2):205–13. doi:10.1093/intimm/dxh019
24. Quiroga MF, Pasquinelli V, Martinez GJ, Jurado JO, Zorrilla LC, Musella RM, et al. Inducible costimulator: a modulator of IFN-gamma production in human tuberculosis. *J Immunol* (2006) 176(10):5965–74. doi:10.4049/jimmunol.176.10.5965
25. Liu X, Bai XF, Wen J, Gao JX, Liu J, Lu P, et al. B7H costimulates clonal expansion of, and cognate destruction of tumor cells by, CD8(+) T lymphocytes in vivo. *J Exp Med* (2001) 194(9):1339–48. doi:10.1084/jem.194.9.1339
26. Vidric M, Bladt AT, Dianzani U, Watts TH. Role for inducible costimulator in control of *Salmonella enterica* serovar Typhimurium infection in mice. *Infect Immun* (2006) 74(2):1050–61. doi:10.1128/IAI.74.2.1050-1061.2006
27. Nouailles G, Day TA, Kuhlmann S, Loewe D, Dorhoi A, Gamradt P, et al. Impact of inducible co-stimulatory molecule (ICOS) on T-cell responses and protection against *Mycobacterium tuberculosis* infection. *Eur J Immunol* (2011) 41(4):981–91. doi:10.1002/eji.201040608
28. Xu L, Zheng X, Berzins K, Chaudhuri A. Cytokine dysregulation associated with malarial anemia in *Plasmodium yoelii* infected mice. *Am J Transl Res* (2013) 5(2):235–45.
29. da Silva HB, de Salles EM, Panatieri RH, Boscardin SB, Rodriguez-Malaga SM, Alvarez JM, et al. IFN-gamma-induced priming maintains long-term strain-transcending immunity against blood-stage *Plasmodium chabaudi* malaria. *J Immunol* (2013) 191(10):5160–9. doi:10.4049/jimmunol.1300462
30. Day NP, Hien TT, Schollaardt T, Loc PP, Chuong LV, Chau TT, et al. The prognostic and pathophysiologic role of pro- and antiinflammatory cytokines in severe malaria. *J Infect Dis* (1999) 180(4):1288–97. doi:10.1086/315016
31. Herbert F, Tchitchek N, Bansal D, Jacques J, Pathak S, Becavin C, et al. Evidence of IL-17, IP-10, and IL-10 involvement in multiple-organ dysfunction and IL-17 pathway in acute renal failure associated to *Plasmodium falciparum* malaria. *J Transl Med* (2015) 13:369. doi:10.1186/s12967-015-0731-6
32. Lyke KE, Burges R, Cissoko Y, Sangare L, Dao M, Diarra I, et al. Serum levels of the proinflammatory cytokines interleukin-1 beta (IL-1beta), IL-6, IL-8, IL-10, tumor necrosis factor alpha, and IL-12(p70) in Malian children with severe *Plasmodium falciparum* malaria and matched uncomplicated malaria or healthy controls. *Infect Immun* (2004) 72(10):5630–7. doi:10.1128/IAI.72.10.5630-5637.2004
33. Freitas do Rosario AP, Lamb T, Spence P, Stephens R, Lang A, Roers A, et al. IL-27 promotes IL-10 production by effector Th1 CD4+ T cells: a critical mechanism for protection from severe immunopathology during malaria infection. *J Immunol* (2011) 188(3):1178–90. doi:10.4049/jimmunol.1102755
34. Oakley MS, Sahu BR, Lotspeich-Cole L, Majam V, Thao Pham P, Sengupta Banerjee A, et al. T-bet modulates the antibody response and immune protection during murine malaria. *Eur J Immunol* (2014) 44(9):2680–91. doi:10.1002/eji.201344437
35. Chen H, Fu T, Suh WK, Tsavachidou D, Wen S, Gao J, et al. CD4 T cells require ICOS-mediated PI3K signaling to increase T-Bet expression in the setting of anti-CTLA-4 therapy. *Cancer Immunol Res* (2014) 2(2):167–76. doi:10.1158/2326-6066.CIR-13-0155
36. Doe HT, Kimura D, Miyakoda M, Kimura K, Akbari M, Yui K. Expression of PD-1/LAG-3 and cytokine production by CD4(+) T cells during infection with *Plasmodium* parasites. *Microbiol Immunol* (2015) 60(2):121–31. doi:10.1111/1348-0421.12354
37. Jagannathan P, Nankya F, Stoyanov C, Eccles-James I, Sikyomu E, Naluwu K, et al. IFNgamma responses to pre-erythrocytic and blood-stage malaria antigens exhibit differential associations with past exposure and subsequent protection. *J Infect Dis* (2014) 211(12):1987–96. doi:10.1093/infdis/jiu814
38. Inoue S, Niikura M, Mineo S, Kobayashi F. Roles of IFN-gamma and gammadelta T cells in protective immunity against blood-stage malaria. *Front Immunol* (2013) 4:258. doi:10.3389/fimmu.2013.00258
39. Rottman JB, Smith T, Tonra JR, Ganley K, Bloom T, Silva R, et al. The costimulatory molecule ICOS plays an important role in the immunopathogenesis of EAE. *Nat Immunol* (2001) 2(7):605–11. doi:10.1038/89750
40. Takahashi N, Matsumoto K, Saito H, Nanki T, Miyasaka N, Kobata T, et al. Impaired CD4 and CD8 effector function and decreased memory T cell populations in ICOS-deficient patients. *J Immunol* (2009) 182(9):5515–27. doi:10.4049/jimmunol.0803256
41. Bossaller L, Burger J, Draeger R, Grimbacher B, Knoth R, Plebani A, et al. ICOS deficiency is associated with a severe reduction of CXCR5+CD4 germinal center Th cells. *J Immunol* (2006) 177(7):4927–32. doi:10.4049/jimmunol.177.7.4927
42. Villegas-Mendez A, Shaw TN, Inkson CA, Strangward P, de Souza JB, Couper KN. Parasite-specific CD4+ IFN-gamma+ IL-10+ T cells distribute within both lymphoid and nonlymphoid compartments and are controlled systemically by interleukin-27 and ICOS during blood-stage malaria infection. *Infect Immun* (2015) 84(1):34–46. doi:10.1128/IAI.01100-15
43. Wikenheiser DJ, Stumhofer JS. ICOS co-stimulation: friend or foe? *Front Immunol* (2016) 7:304. doi:10.3389/fimmu.2016.00304
44. Khoury DS, Cromer D, Akter J, Sebina I, Elliott T, Thomas BS, et al. Host-mediated impairment of parasite maturation during blood-stage *Plasmodium* infection. *Proc Natl Acad Sci U S A* (2017) 114(29):7701–6. doi:10.1073/pnas.1618939114
45. Chandele A, Mukerjee P, Das G, Ahmed R, Chauhan VS. Phenotypic and functional profiling of malaria-induced CD8 and CD4 T cells during blood-stage infection with *Plasmodium yoelii*. *Immunology* (2011) 132(2):273–86. doi:10.1111/j.1365-2567.2010.03363.x
46. Podoba JE, Stevenson MM. CD4+ and CD8+ T lymphocytes both contribute to acquired immunity to blood-stage *Plasmodium chabaudi* AS. *Infect Immun* (1991) 59(1):51–8.
47. Good MF, Miller LH. Involvement of T cells in malaria immunity: implications for vaccine development. *Vaccine* (1989) 7(1):3–9. doi:10.1016/0264-410X(89)90002-9
48. Nitcheu J, Bonduelle O, Combadiere C, Tefit M, Seilhean D, Mazier D, et al. Perforin-dependent brain-infiltrating cytotoxic CD8+ T lymphocytes mediate experimental cerebral malaria pathogenesis. *J Immunol* (2003) 170(4):2221–8. doi:10.4049/jimmunol.170.4.2221
49. Wilson EH, Zaph C, Mohrs M, Welcher A, Siu J, Artis D, et al. B7RP-1-ICOS interactions are required for optimal infection-induced expansion of CD4+ Th1 and Th2 responses. *J Immunol* (2006) 177(4):2365–72. doi:10.4049/jimmunol.177.4.2365
50. Watanabe M, Hara Y, Tanabe K, Toma H, Abe R. A distinct role for ICOS-mediated co-stimulatory signaling in CD4+ and CD8+ T cell subsets. *Int Immunol* (2005) 17(3):269–78. doi:10.1093/intimm/dxh206
51. Renia L, Goh YS. Malaria parasites: the great escape. *Front Immunol* (2016) 7:463. doi:10.3389/fimmu.2016.00463
52. Zamarin D, Holmgaard RB, Ricca J, Plitt T, Palese P, Sharma P, et al. Intratumoral modulation of the inducible co-stimulator ICOS by recombinant oncolytic virus promotes systemic anti-tumour immunity. *Nat Commun* (2017) 8:14340. doi:10.1038/ncomms14340
53. Sakthivel P, Gereke M, Breithaupt A, Fuchs D, Gigliotti L, Gruber AD, et al. Attenuation of immune-mediated influenza pneumonia by targeting the inducible co-stimulator (ICOS) molecule on T cells. *PLoS One* (2014) 9(7):e100970. doi:10.1371/journal.pone.0100970
54. Fan X, Quezada SA, Sepulveda MA, Sharma P, Allison JP. Engagement of the ICOS pathway markedly enhances efficacy of CTLA-4 blockade in cancer immunotherapy. *J Exp Med* (2014) 211(4):715–25. doi:10.1084/jem.20130590

Conflict of Interest Statement: The authors declare that the research conducted have no commercial or financial involvement that could be considered as potential conflict of interest.

Copyright © 2018 Jogdand, Sengupta, Bhattacharya, Singh, Barik and Devadas. This is an open-access article distributed under the terms of the Creative Commons Attribution License (CC BY). The use, distribution or reproduction in other forums is permitted, provided the original author(s) and the copyright owner are credited and that the original publication in this journal is cited, in accordance with accepted academic practice. No use, distribution or reproduction is permitted which does not comply with these terms.

frontiers in Immunology

REVIEW
published: 16 August 2018
doi: 10.3389/fimmu.2018.01891

Therapies to Suppress β Cell Autoimmunity in Type 1 Diabetes

*Charles J. Kroger[1,2], Matthew Clark[1,2], Qi Ke[1,2] and Roland M. Tisch[1,2]**

[1] *Department of Microbiology and Immunology, University of North Carolina at Chapel Hill, Chapel Hill, NC, United States,*
[2] *Lineberger Comprehensive Cancer Center, University of North Carolina at Chapel Hill, Chapel Hill, NC, United States*

Type 1 diabetes (T1D) is an autoimmune disease that is generally considered to be T cell-driven. Accordingly, most strategies of immunotherapy for T1D prevention and treatment in the clinic have targeted the T cell compartment. To date, however, immunotherapy has had only limited clinical success. Although certain immunotherapies have promoted a protective effect, efficacy is often short-term and acquired immunity may be impacted. This has led to the consideration of combining different approaches with the goal of achieving a synergistic therapeutic response. In this review, we will discuss the status of various T1D therapeutic strategies tested in the clinic, as well as possible combinatorial approaches to restore β cell tolerance.

Keywords: autoimmunity, diabetes, immunoregulation, immunotherapy

OPEN ACCESS

Edited by:
Gustavo Javier Martinez, Rosalind Franklin University of Medicine and Science, United States

Reviewed by:
Abdel Rahim A. Hamad, Johns Hopkins University, United States
Maja Wallberg, University of Cambridge, United Kingdom
Rachel Friedman, National Jewish Health, United States

****Correspondence:***
Roland M. Tisch
rmtisch@med.unc.edu

Specialty section:
This article was submitted to Autoimmune and Autoinflammatory Disorders, a section of the journal Frontiers in Immunology

Received: *14 June 2018*
Accepted: *31 July 2018*
Published: *16 August 2018*

Citation:
Kroger CJ, Clark M, Ke Q and Tisch RM (2018) Therapies to Suppress β Cell Autoimmunity in Type 1 Diabetes. Front. Immunol. 9:1891. doi: 10.3389/fimmu.2018.01891

INTRODUCTION

Type 1 diabetes (T1D) is an autoimmune disease marked by the dysfunction and/or destruction of the insulin-producing β cells found in the pancreatic islets of Langerhans (1–4). T1D most often arises in children but also develops in adults. To compensate for impaired β cell function, T1D individuals require daily insulin therapy. Despite insulin administration, however, establishing optimal glycemic control long-term is often problematic resulting in a number of complications, including retinopathy, nephropathy, vasculopathy, and neuropathy. This morbidity coupled with an increasing incidence of T1D world-wide, underscores an urgent need for effective immunotherapies for T1D prevention and treatment.

The goal of an immunotherapy is threefold: (1) selectively suppress ongoing autoimmunity, (2) reestablish self-tolerance long-term, and (3) preserve acquired immunity. This review will focus on the different strategies of immunotherapy being tested experimentally and in the clinic to suppress β cell autoimmunity, and prevent clinical onset and/or treat T1D.

IMMUNOPATHOLOGY OF T1D

The loss of β cell tolerance involves both genetic and ill-defined environmental factors (5–16). A strong genetic association with specific human leukocyte antigen haplotypes, coupled with several variants of genes expressed by β cells, T cells, and other immune effectors underscore the complexity of the autoimmune response of T1D (17–23). β cell autoimmunity is typically viewed as a chronic inflammatory response characterized by the progressive infiltration of the pancreatic islets with various immune effectors (24). In the nonobese diabetic (NOD) mouse, a spontaneous model of T1D, islet infiltration is initiated at an early age by macrophages and dendritic cells (DC), $CD4^+$ and $CD8^+$ T cells, and B cells. This insulitis initially exhibits benign properties with little effect on β cell viability or function. However, at a late preclinical stage, an ill-defined qualitative change occurs within the islet infiltrate, which promotes efficient β cell destruction leading to the onset of overt diabetes.

In NOD mice and other rodent models of T1D, pathogenic β cell-specific $CD4^+$ and $CD8^+$ effector T cells (Teff) are essential drivers of autoimmunity. Diabetogenic $CD4^+$ and $CD8^+$ T cells target several β cell autoantigens and related peptide epitopes, including proinsulin/insulin, glutamic acid decarboxylase 65 (GAD65), chromogranin A (ChgA), zinc transporter 8 (ZnT8), glucose-6-phosphatase catalytic subunit-related protein (IGRP), and hybrid insulin peptides (HIPs) among others (25–34). It is thought that early in the disease process only few β cell autoantigens and epitopes are targeted by T cells. However, over time additional epitopes within a given autoantigen as well as new autoantigens are recognized. Furthermore, chronic inflammation negatively affects β cells in part by generating neo-autoantigens, such as HIPs, *via* post-translational modification events (32–39). These neo-autoantigens further diversify the diabetogenic response. Together this epitope spread effectively amplifies the β cell-specific T cell response (28, 40–42).

Analyses of human cadaveric T1D pancreases have also demonstrated islet infiltrates consisting of $CD8^+$ T cells and macrophages, and to a lesser extent $CD4^+$ T cells, and B cells (29, 31, 43–52). However, T1D pancreases have been reported that lack T cell infiltrates suggesting that the immunopathology of human T1D is heterogeneous (53, 54). The prevalence of T cell-independent subsets of T1D is unclear, and thought to be primarily associated with adult T1D onset. On the other hand, evidence indicates that the rapid and severe T1D that develops in children and adolescents is T cell-mediated (44). For instance, recent reports show that childhood onset is marked by a broader and more aggressive β cell-specific T cell response compared to adult T1D (29, 31, 43–52, 55–57). Multiple β cell autoantigens are recognized by human $CD4^+$ and $CD8^+$ T cells found in peripheral blood, as well as the islets of T1D subjects; many of which are also targeted in the NOD mouse diabetogenic response (e.g., insulin, GAD65, IGRP, and ZnT8) (4, 25, 28, 57).

Pathogenic β cell-specific $CD4^+$ and $CD8^+$ Teff in NOD and human T1D typically exhibit a type 1 or T helper 1 (Th1) phenotype marked by IFNγ production (47, 58, 59). IL-17-producing $CD4^+$ Th17 cells have also been implicated in mediating β cell destruction (60–62). Differentiation and expansion of pathogenic Teff are in part attributed to aberrant peripheral immunoregulation (63–68). An impaired pool of thymic-derived FoxP3-expressing immunoregulatory T cells ($Foxp3^+$Treg) has been linked to T1D (68–70). In general, $Foxp3^+$Treg play an essential role in maintaining peripheral self-tolerance through cytokine and contact-dependent mechanisms of suppression (71). Decreased survival of islet-resident $Foxp3^+$Treg is thought to be a key factor in promoting the progression from benign to pathogenic insulitis in NOD mice (69). Failure to maintain islet $Foxp3^+$Treg numbers in NOD mice is due to insufficient local levels of IL-2, a critical cytokine needed for $Foxp3^+$Treg survival, fitness, and function (69, 72–74). $FOXP3^+$Treg from T1D subjects have defective IL-2 receptor (R) signaling which limits fitness and function of $FOXP3^+$Treg (66, 75). Additionally, production of the proinflammatory cytokine IL-21, which is critical for T1D development, can inhibit IL-2 expression by T cells which negatively impacts $Foxp3^+$Treg viability and function (76). Human T1D is also marked by deficiencies in non-FoxP3-expressing adaptive (a) Treg. For example, the frequency of β cell-specific IL-10-secreting Tr1 cells is reduced in T1D versus healthy subjects (77–79). In both NOD and human T1D, Teff exhibit a reduced sensitivity to Treg-mediated suppression, which further permits expansion of the diabetogenic Teff pool (63, 64).

Dysregulation among antigen-presenting cells (APC), such as DC, macrophages, and B cells, has also been reported to contribute to T1D (80–85). Although detection of autoantibodies is a key indicator of β cell autoimmunity, B cells are thought to play a critical role in the development of T1D by functioning primarily as an APC (86–88). APC exhibiting proinflammatory properties also skew differentiation of naïve β cell-specific T cells toward pathogenic Teff, as well as amplify islet inflammation and β cell destruction. For instance cytokines, such as IFNγ, TNFα, and IL-1β secreted by islet APC are cytotoxic to β cells *in vitro* (89). The culmination of the adaptive and innate effector immune response within the islets results in β cell destruction/dysfunction and elevated blood glucose levels (**Figure 1**).

Aberrant peripheral immunoregulation has been the focus of most T1D immunotherapies. Different strategies have attempted to selectively suppress the pathogenic proinflammatory events that affect β cells, while reestablishing protective immunoregulation that persists long-term without altering acquired immunity (**Figure 1**). Achieving these goals in the clinic, however, has proven to be highly challenging.

IMMUNOTHERAPY OF T1D

The progression of T1D affords three windows of therapeutic intervention to alter disease outcome (90, 91). The first is during the prodromal stage of T1D, which may persist for a number of years. At-risk individuals with ongoing β cell autoimmunity, identified by serum autoantibodies specific for various β cell autoantigens, are candidates for prevention of clinical onset of T1D (90–92). The second window of intervention is at the time of clinical onset. The goal here is to suppress β cell autoimmunity, rescue residual β cell mass, and ideally reverse clinical diabetes. Early studies provided proof of principle that sufficient β cell mass exists at the time of diagnosis to reverse diabetes (93, 94). Administration of the immunosuppressive drug cyclosporine A (CsA) induces remission in new onset children. However, CsA results in severe kidney toxicity, and once therapy is halted, patients develop recurrent diabetes (95, 96). The third window of intervention is in long-standing T1D patients to protect residual β cell function. Evidence indicates that after T1D onset low but sustained C-peptide levels are observed (93, 94). Therefore, maintenance of a small amount of functional β mass may aid in the control of glycemia as well as limit morbidity.

Two general approaches of immunotherapy have been tested experimentally and in the clinic for the prevention and treatment of T1D. The first approach entails manipulating the autoimmune response independent of β cell specificity. Typically, antibodies (Ab) targeting specific immune effectors or effector molecules have been employed for this approach. The second approach makes use of β cell antigen-specific strategies. Here, β cell autoantigens or corresponding peptides are administered under various conditions. In the following sections, we will discuss

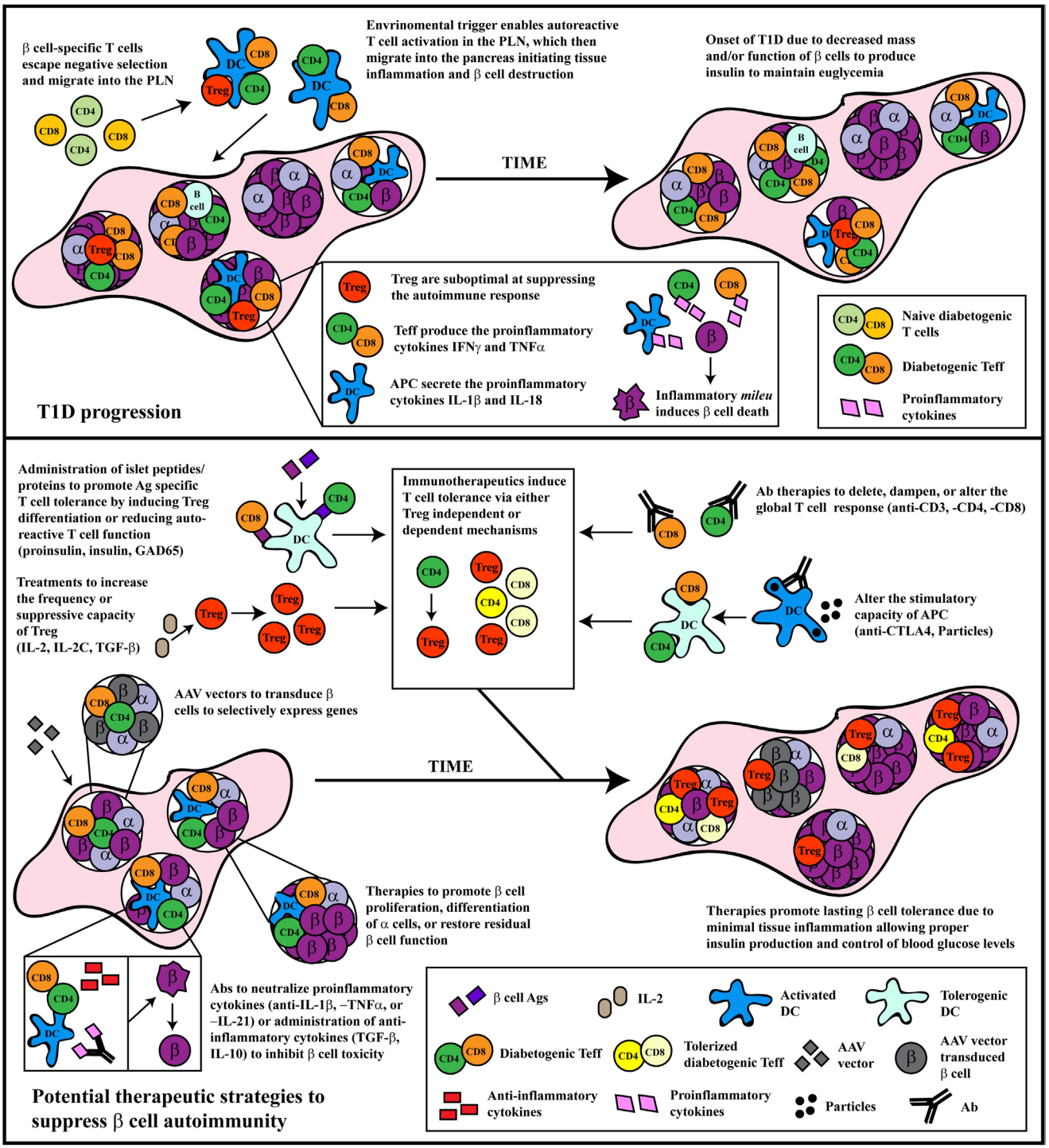

FIGURE 1 | The progression and treatment of β cell autoimmunity. *Top panel*: In general, overt diabetes results from the gradual loss of functional insulin-producing β cells due to the inflammatory environment driven by infiltrating self-reactive T cells and antigen-presenting cells (APC). Although β cell-specific T cell clones are detected in both healthy and type 1 diabetes (T1D) susceptible individuals, a number of factors promote T1D development in the latter population. Decreased efficiency of negative selection in the thymus allows for the increased escape of β cell-specific T cell clones into the periphery. In the periphery, β cell-specific T cells are stimulated in the pancreatic lymph nodes (PLN) by APC derived from the islets, leading to effector T cells (Teff) differentiation due to suboptimal Foxp3$^+$Treg suppression. These pathogenic Teff then infiltrate the islets and drive inflammation leading to reduced β cell function and/or survival. *Bottom panel:* Several distinct therapeutic interventions have been tested for the prevention or treatment of T1D. The major approaches have included: administration of β cell autoantigens, expansion of Foxp3$^+$Treg, Ab therapies that alter T cell responses, therapeutic reagents that tolerize APC function, neutralization of proinflammatory molecules, or treatments that expand or enhance β cell function and/or survival. Some of these approaches have had clinical, albeit limited, success. Future therapeutic interventions should look toward refinement in the specificity of these treatments, and the development of combinatorial therapies targeting multiple arms of the immune system, as T1D is a multi-pronged autoimmune disease.

different strategies of immunotherapy that are included in these two general approaches, highlighting related strengths and weaknesses (**Figure 1**).

ANTIGEN-INDEPENDENT IMMUNOTHERAPIES

Ab and cytokines have been administered to modulate or block the function of immune effector cells and/or molecules. The general approach is advantageous, since pathogenic effectors can be targeted *en masse*, often resulting in rapid and robust outcomes in experimental settings. However, the limited specificity of these therapeutics can lead to unwanted systemic effects impacting acquired immunity for instance. Nevertheless, a sizable body of work has demonstrated clinical efficacy for certain Ab therapies, whereas promising early results are being seen with cytokine- and cell-based strategies.

Antibody-Based Therapies

Arguably, the most effective strategy to clinically alter T1D progression has been to target diabetogenic Teff with anti-CD3 monoclonal Ab (mAb) (97, 98). In new onset NOD mice anti-CD3 mAb therapy reverses diabetes in part by driving apoptosis of islet-infiltrating Teff. Engulfment of the apoptotic T cells induces TGF-β secretion by APC that promotes differentiation of Foxp3$^+$Treg. Once established this pool of induced (i) Foxp3$^+$Treg mediate long-lasting β cell tolerance (99–101). In addition, peripheral Teff exhibit reduced IFNγ production, and increased markers of exhaustion and anergy (102). Interestingly, anti-CD3 mAb therapy given at a preclinical stage fails to prevent diabetes onset in NOD mice (98, 103). This indicates that a given immunotherapy may be effective only at particular stages of T1D progression.

For clinical trials, humanized anti-CD3 mAb hOKT3γ1 (Ala-Ala) (teplizumab) or CCHAglyCD3 (otelixizumab) have been engineered to prevent binding to Fc receptor, and minimize proinflammatory cytokine release by APC (97, 100, 104–112). Anti-CD3 mAb therapy administered to new onset T1D patients reduces the rate of loss of β cell function in the majority of individuals (113). The mechanism of protection is ill-defined, although expansion of CD8$^+$ Treg and CD8$^+$ Teff exhibiting an exhausted phenotype has been reported (109). Despite this efficacy, diabetes reversal is not achieved, and protection of residual β cell mass is short-term, lasting up to 4 years in some individuals (113). Furthermore, anti-CD3 mAb binding can activate T cells resulting in cytokine release and unwanted inflammation, albeit transient. Moreover, the transient depletion of T cells systemically by anti-CD3 mAb is linked to recurrent viral infections (100, 104). Nevertheless, these findings provide direct evidence that progression of β cell autoimmunity can be modulated by targeting T cells. However, further refinement of the approach is required to enhance β cell protection while minimizing effects on acquired immunity. This may in part be achieved by using anti-CD3 mAb in combination with other therapeutics (114–116). For instance, treatment of NOD mice with anti-CD3 mAb and the β cell trophic growth factor prolactin, increases both diabetes reversal and β cell proliferation relative to anti-CD3 mAb alone (116).

The aim of Ab-based combinatorial strategies is to establish a synergistic or additive effect to enhance both efficacy and safety. An increased tolerogenic response may permit reduced dosing and, therefore, minimize unwanted complications with a given therapeutic. One combinatorial strategy being tested in the clinic is the application of antithymocyte globulin (ATG) and granulocyte colony stimulating factor (G-CSF). Low dose ATG induces apoptosis and transiently depletes T cells, whereas G-CSF promotes mobilization of aTreg and induction of tolerogenic DC. In preclinical studies, ATG alone induces ~30% remission in newly diabetic NOD mice, whereas the combination of ATG and G-CSF increases diabetes reversal >twofold (117). Initial phase I clinical results for low dose ATG plus G-CSF therapy given to recent onset T1D patients indicate that β cell function can be maintained up to 2 years in a group of responders (118). This protective effect correlates with quantitative and qualitative changes in the conventional T cell pool, coupled with an increase in the frequency of FOXP3$^+$Treg (118).

Although most T1D immunotherapies have targeted T cells, success has also been demonstrated by altering the B cell response in various autoimmune diseases including T1D, both in mice and humans (88, 119, 120). As previously mentioned, serum autoantibodies indicate B cells also target β cell antigens, including GAD65 and insulin, which serve as a biomarker for individuals with an increased risk for developing T1D (90–92). NOD mice lacking B cells are protected from insulitis and diabetes onset (86, 87). Several molecules, such as CD20, CD22, BAFF, and BCMA have been targeted to modulate the B cell pool (121–125). In different murine models of T1D, anti-CD20 mAb suppresses the progression of β cell autoimmunity as well as reverses diabetes onset, by promoting Foxp3$^+$Treg and regulatory B cell populations (121, 122). In recent onset T1D patients, anti-CD20 mAb (Rituximab), which has also been used in the treatment of rheumatoid arthritis (RA), transiently depleted B cells and prolonged β cell function (126, 127). However, this protective effect was only transient, diminishing after 1 year, suggesting brief deletion of B cells alone is not sufficient to restore β cell tolerance.

The depleting effects of a given Ab make dosing problematic, as well as limit the frequency of treatments. On the other hand, nondepleting (ND) Ab provide a strategy to modulate the function of Teff and other immune cells without systemic cell depletion. Human IgG4 is intrinsically ND due to a decreased capacity to fix complement and bind to Fc receptor, and, therefore, is well suited for this purpose. Other IgG isotypes can be engineered accordingly to establish a ND property. A striking example of altering the activity of β cell-specific Teff is observed with the application of ND anti-CD4 and -CD8α Ab. A short-course of ND anti-CD4 and -CD8α Ab induces remission in the majority of new onset diabetic NOD mice without affecting systemic T cell numbers (128–131). Induction of remission is due to Ab-mediated crosslinking of the CD4 and CD8 molecules, which reduces TCR signaling as well as upregulates additional signaling pathways (128, 131–133). The result is suppressed expression of proinflammatory cytokines by Teff combined with the induction of a promigratory phenotype that drives pancreatic egress of Teff (128, 133).

ND Ab and immunoglobulin (Ig) fusion molecules can also serve to block the function of key surface effector molecules. For instance, CTLA-4-Ig (Abatacept)-mediated blockade of the CD80 and CD86 co-stimulatory molecules inhibits APC function and alters the Teff pool in recent onset T1D patients. Abatacept therapy administered monthly for 24 months extends β cell function up to 30 months (134, 135). Examination of peripheral blood shows a decrease in the central memory $CD4^+$ T cell population with a concomitant increase in naïve T cells in Abatacept-treated individuals, supporting the notion that Teff expansion is limited (135).

Inhibiting cytotoxic pathways with ND blocking Ab offer another option to protect β cell viability. NOD mice deficient in Fas lack islet-infiltrating effector cells and fail to develop T1D (136, 137). Ab blockade of FasL between 2 and 4 weeks of age prevents T1D in NOD mice. Interestingly, FasL blockade results in the presence of protective IL-10-producing B cells in the pancreas of NOD mice after treatment (138). These results suggest the targeting the Fas–FasL pathway may be a viable therapeutic avenue for the treatment of clinical T1D.

In addition to directly targeting immune effector cells, Ab or Ig-fusion molecules have been used to neutralize secreted effector molecules, such as proinflammatory cytokines. Neutralization of TNFα with several antagonists including mAb (infliximab, adalimumab) and a recombinant TNFα receptor fusion protein, etanercept, have been widely used to treat the autoimmunity driving RA (139). Although TNFα is directly cytotoxic to β cells, its role in the pathogenesis of T1D is controversial. In NOD mice, for instance, TNFα accelerates the progression of β cell autoimmunity when given at a young but not older age (140, 141). In a 24-week clinical study, anti-TNFα therapy in human T1D patients was seen to reduce levels of glycated hemoglobin A1C (HbA1c), a marker indicative of blood glucose values over a 3-month period, as well as increase C-peptide levels suggesting preservation of β cell function (142). In a case report, treatment with infliximab was also found to reduce HbA1c levels, increase insulin secretion, and alleviate insulin resistance in a T1D patient also diagnosed with Crohn's disease (143). Anti-TNFα therapy, however, fails to prevent the development of T1D in at-risk patients, and may in fact accelerate disease progression (144). These results further underscore how efficacy (or lack of) is dependent on the stage of disease progression at which a given therapeutic is administered.

IL-21 is an appealing cytokine to target and suppress β cell autoimmunity. IL-21 is chiefly produced by T follicular helper cells (Tfh) and Th17 cells, and has diverse roles that include regulating B cell and $CD8^+$ Teff function (145–147). The emerging role for both Tfh and Th17 cells in the progression of T1D, and the protective phenotype seen in NOD mice deficient of IL-21 suggests that neutralizing human IL-21 is a promising approach (60, 148–152). Indeed, neutralization of IL-21 with an IL-21R-Ig prevents diabetes in NOD mice (153).

Cytokine-Based Immunotherapies

Administration of cytokines offers an approach to reestablish peripheral immunoregulation and β cell tolerance. One such strategy currently being investigated is administration of low dose IL-2 (65, 154–156). Conventional $CD4^+$ and $CD8^+$ T cells but not $Foxp3^+$Treg are producers of IL-2, which plays a central role in driving both pro- and anti-inflammatory responses (157, 158). IL-2 for instance is needed for conventional T cell activation and expansion, and IL-2 drives proinflammatory responses by other immune effectors (158). IL-2 also plays an essential role in $Foxp3^+$ Treg survival, expansion, and suppressor function (159–161). Constitutive expression of the high affinity IL-2R (CD25) allows $Foxp3^+$Treg to out-compete conventional T cells for limiting amounts of IL-2. The latter provides rationale for using low dose IL-2 to preferentially affect $Foxp3^+$Treg versus conventional T cells (154). Indeed, low dose IL-2 has been effective in the clinic for the treatment of graft-versus-host disease, and systemic vasculitis (162, 163). In NOD mice, low-dose IL-2 prevents clinical onset and reverses diabetes *via* an expanded pool of $Foxp3^+$ Treg in the islets and draining pancreatic lymph nodes (69, 164, 165). Similarly, low-dose IL-2 in combination with rapamycin in recent onset T1D patients increases the frequency of $Foxp3^+$Treg in blood (166). However, these patients also exhibit an accelerated rate of β cell loss (166), suggesting an enhanced pathogenic response, and highlighting the key problem of administering a cytokine with pleiotropic effects (167, 168).

Different strategies are being developed to enhance the efficacy of IL-2 (and other cytokines), while avoiding unwanted systemic effects (169, 170). One approach is to promote selective binding of IL-2 to $Foxp3^+$Treg *via* IL-2-Ab complexes (IL-2C) (170–172). Targeting particular epitopes on IL-2 with anti-IL-2 Ab can favor binding to the high affinity IL-2R constitutively expressed by $Foxp3^+$Treg (173). Administration of IL-2C readily expands $Foxp3^+$Treg in mice and prevents autoimmunity (170–172). While promising, polyclonal expansion of $Foxp3^+$Treg by IL-2C may compromise protective immunity against pathogens.

An additional strategy to minimize the systemic effects of IL-2 while expanding β cell-specific $Foxp3^+$Treg is to target cytokine expression to β cells *in vivo*. Adeno-associated virus (AAV) vectors have been used to deliver and target expression of an insulin promoter-driven IL-2 transgene (AAViP-IL2) to β cells *in vivo* (72–74, 174). In general, AAV vectors are appealing for *in vivo* gene delivery due to limited immunogenicity, lack of integration into the genome, and efficient transduction of non-proliferating cells (175). Notably, treatment of NOD mice at a late preclinical T1D stage with AAViP-IL2 results in the expansion of islet-resident $Foxp3^+$Treg, suppression of β cell-specific Teff, and prevention of diabetes onset (72–74). AAV vectors can be further exploited by co-delivering genes encoding other anti-inflammatory cytokines (e.g., IL-10, TGFβ1, and IL-35) and/or pro-survival proteins to enhance both the tolerogenic effect and maintenance of β cell mass *in vivo* (72, 174, 176–179).

$Foxp3^+$Treg-Mediated Therapy

An alternative strategy to manipulate the $Foxp3^+$Treg population *in vivo* is to transfer $Foxp3^+$Treg that have been expanded *in vitro* (180–182). The approach is effective in preventing diabetes onset in NOD mice (183). However, *in vitro* expansion of a homogeneous and stable pool of $Foxp3^+$Treg, particularly when starting from relatively few cells, has been technically difficult. Expansion protocols are being devised using drugs such as rapamycin to prevent outgrowth of Teff, as well as DNA methyltransferase and histone deacetylase inhibitors to enhance $Foxp3^+$Treg stability

(184, 185). Despite these hurdles, clinical studies have shown Foxp3$^+$Treg therapy is well tolerated and therapeutic efficacy is observed for various diseases (180, 181). Furthermore, a phase I trial has demonstrated that *in vitro*-expanded Foxp3$^+$Treg persist long-term and exhibit a stable phenotype when transferred back into T1D subjects (180). Notably, loss of C peptide is also limited in some patients. These results provide justification for additional clinical studies to directly assess the efficacy of Foxp3$^+$Treg transfer for T1D treatment.

Microbiome Interventions in T1D

In recent years, the importance of the gut microbiota in maintaining the normal function of the immune system has emerged (186). Reports have documented that changes in gut microbiota can markedly influence T1D development, and that differences in the colonizing microflora contributes to variations in T1D onset among NOD mouse colonies (187, 188). Toll-like receptors (TLRs) play a crucial role in the innate immune system's recognition of common bacterial and viral components. TLR signaling triggers APC maturation and production of proinflammatory mediators (189). One of the major TLR signaling adaptor molecules driving APC maturation is MyD88, which activates several downstream signaling pathways (190). NOD mice lacking MyD88 expression and housed under normal specific-pathogen-free conditions exhibit a reduced T1D incidence. In contrast, MyD88-deficient NOD mice housed in germ-free conditions develop robust diabetes (16). Interestingly sex differences in the gut microbiota also influence T1D susceptibility. For example, young female NOD mice receiving gut microbiota from male NOD mice exhibit a reduced T1D incidence (191). These results demonstrate that the gut microbiota can have a protective role against autoimmunity, and specifically T1D. Furthermore, differences in the biodiversity of the gut microbiome are seen between T1D patients and healthy individuals (192–196). Similarly, the microbiome within the gut of T1D infants fails to diversify during development in comparison to healthy individuals, potentially due to hyperglycemia (197). Here, changes in the production of microbial metabolites such as short-chain fatty acids found in the colonic lumen and peripheral blood are thought to impact immunoregulatory networks. Indeed, a recent study showed that diets that enhance production of acetate and butyrate by the gut microbiome, effectively prevent diabetes in NOD mice (198). Increased acetate is seen to reduce β cell-specific Teff, whereas elevated butyrate expands Foxp3$^+$Treg. Together these results indicate an association between modified gut microbiota and compromised self-tolerance. Manipulating the gut microbiota may prove to be an effective adjuvant therapy to limit the progression of β cell autoimmunity in at-risk individuals.

ANTIGEN-DEPENDENT IMMUNOTHERAPIES

The goal of antigen-based therapies is to selectively tolerize the autoreactive Teff pool and induce or expand autoantigen-specific Treg (199–202). The approach is appealing, since β cell antigen vaccination is expected to have no effect on acquired immunity. Teff are tolerized *via* whole antigen or peptide by various mechanisms, including: (i) clonal anergy, (ii) clonal deletion, or (iii) exhaustion. This has classically been achieved by administration of high doses of soluble antigen or peptide. On the other hand, antigen vaccination has been used to induce differentiation of naïve β cell-specific T cells into aTreg, including iFoxp3$^+$Treg. Depending on the conditions of antigen vaccination, distinct subsets of aTreg can be induced. Expanding the aTreg pool is advantageous, since local cytokine-mediated suppression is independent of Teff antigen-specificity; this bystander-mediated suppression also can downregulate the activity of proinflammatory APC. Success of either tolerizing Teff or inducing/expanding Treg is dictated by multiple factors including dose, the frequency, and route of antigen vaccination. Also important is the context in which the antigen is delivered. Antigen administration in the context of an adjuvant, microparticles, or DC can significantly alter the nature of the T cell response. The most critical factor determining efficacy, however, is the identity of the autoantigen (or peptide) used for vaccination. To effectively block the progression of β cell autoimmunity, prevalent, or immunodominant Teff clonotypes need to be targeted. Ongoing efforts defining the specificity of islet-resident Teff are expected to identify immunodominant Teff clonotypes (31). Furthermore, promising antigen-based immunotherapies are exploiting advancements in targeted drug delivery systems to effectively tolerize Teff and promote Treg-mediated suppression.

β Cell-Autoantigen Vaccination

Early clinical studies have highlighted the difficulty in establishing a protective, β cell-specific T cell response *via* autoantigen vaccination (203). The Diabetes Prevention Trial-type 1 tested parenteral insulin delivery *via* intravenous (i.v.), subcutaneous (s.c.), and oral routes in at-risk individuals (202, 204–206). No significant difference, however, was detected in the frequency and onset of diabetes in the treatment and control cohorts. Similarly, phase II and III studies of s.c. vaccination of aluminum hydroxide (alum)-formulated GAD65 to new onset T1D patients had no marked effect on C-peptide secretion over time (207, 208). Alum as an adjuvant is included due to a potent capacity to induce IL-4-secreting Th2 cells, which in turn can block the differentiation of pathogenic IFNγ-producing Teff (209, 210).

Additional studies have tested insulin and proinsulin peptides to restore β cell tolerance in human T1D patients. An altered-peptide ligand of the insulin B chain 9–23 epitope administered s.c. to recent onset T1D subjects reduces peptide-specific IFNγ-secreting Teff, while elevating Th2-like aTreg (211, 212). Nevertheless, no clinical benefit was detected, suggesting that altering insulin B chain-specific Teff reactivity alone is insufficient to induce robust β cell tolerance. Clinical trials assessing intradermal vaccination of a natural peptide derived from proinsulin (C19-A3) have also been carried out (213, 214). Vaccination with low (30ug) versus high (300 μg) doses of C19-A3 increases the frequency of peptide-specific CD4$^+$ Tr1 cells in long-standing T1D subjects (213). A similar increase in CD4$^+$ Tr1 cells is detected in newly diagnosed T1D subjects vaccinated with C19-A3 (214). Notably, FOXP3$^+$ Treg are also increased, and evidence suggests that residual β cell function is preserved in some individuals (214). Treatment with a pool of peptides derived from additional β cell autoantigens

may promote a more robust tolerogenic effect on Teff, as well as enhance induction and/or expansion of the aTreg pool.

Strategies to Enhance the Efficacy of β Cell-Autoantigen Vaccination

As noted above the context of autoantigen vaccination is critical for determining the nature and magnitude of the induced T cell response, and in turn therapeutic efficacy. Various strategies are being developed to better "tailor" the antigen-specific T cell response. One such approach has been the application of plasmid DNA (pDNA) vaccination. Injection of soluble pDNA or *via* gene gun delivered pDNA-coated particles results in significant levels of transgene expression lasting several weeks *in vivo* (215, 216). Co-vaccination of pDNA encoding β cell autoantigens and anti-inflammatory cytokines both induces protective β cell-specific aTreg, and prevents diabetes onset in NOD mice (174, 217–220). In a T1D clinical trial, patients received intramuscular injections of pDNA encoding proinsulin over a 12-week period. C-peptide levels were maintained up to 3 months after treatment, which corresponded with a reduced frequency of proinsulin-specific $CD8^+$ T cells in peripheral blood (221). Notably, the frequency of $CD8^+$ T cells specific for foreign antigen remained unperturbed, illustrating a key strength of β cell-autoantigen vaccination.

An additional approach to enhance the efficacy of β cell-autoantigen vaccines is the use of small molecule particles (222, 223). Typically, injected β cell antigens and other soluble reagents have a short half-life *in vivo*, which can be greatly enhanced by encapsulation into a particle. Particles are generated using different compounds, including poly(lactide-co-glycolide) and acetalated dextran (222, 224). The particle size and composition can be readily manipulated to determine cellular uptake and cargo release *in vivo* (225). Some studies have included cell-specific Ab or ligands to target particles to a desired cell population, and avoid off-target effects (222, 226–228). However, most treatments utilize the natural phagocytic function of DC and macrophages to engulf the injected particles. In this way, a tolerogenic APC phenotype can also be established *in vivo* by encapsulating various immunomodulatory agents such as the aryl hydrocarbon receptor ligand 2-(1′H-indole-3′-carbonyl)-thiazole-4-carboxylic acid methyl ester, rapamycin, dexamethasone, cytokines, and/or antisense oligodeoxynucleotides (222, 223, 229–232). These APC upon presenting the loaded antigen more readily tolerize Teff and/or induce aTreg (229–232).

As opposed to delivering a cargo to APC, nanoparticles have also been used as surrogate APC (233, 234). Here the surface of nanoparticles is complexed with MHC class II (MHCII) molecules tethered to a β cell-derived peptide (234). These MHCII-peptide-coated nanoparticles promote differentiation of $CD4^+$ Teff into Tr1 cells that are readily expanded, and in turn drive diabetes remission in NOD mice (234). Another approach has exploited the tolerogenic properties of apoptotic cells. Uptake of apoptotic bodies by immature DC and macrophages blocks subsequent APC maturation and promotes upregulation of TGFβ1 (235). Accordingly, i.v. injection of 1-ethyl-3-(3 dimethylaminopropyl) carbodiimide (ECDI) fixed splenocytes loaded with autoantigen suppresses experimental autoimmune encephalomyelitis, a murine model of multiple sclerosis (MS) (236). Currently, this approach is being tested in clinical trials in which MS patients receive an i.v. transfusion of ECDI-fixed peripheral blood mononuclear cells loaded with MS-relevant peptides recognized by $CD4^+$ T cells (237, 238).

SUMMARY

Type 1 diabetes is a complex disease driven by pathogenic adaptive and innate responses leading to the dysfunction and destruction of β cells (1–4). Although disease immunopathology is heterogeneous, T cells are considered to be the key mediators of β cell destruction/dysfunction for the majority of cases of human T1D (57). Consequently, T cells have been the focus of most strategies of immunotherapy. Suppression of pathogenic β cell-specific T cell reactivity in the islets long-term, while preserving acquired immunity is the ultimate goal for a given immunotherapy (**Figure 1**). Achieving this goal in the clinic, however, has been elusive. To date, the most effective strategies have been broadly acting on the majority if not all T cells although protection has also been demonstrated by targeting B cells (88, 100, 119, 120, 239). Efficacy, however, is short-lived. Furthermore, systemic depletion and unwanted effects on protective immunity seen with anti-CD3 mAb therapy for instance, limit dosing and repeated application for efforts to extend β cell protection. On the other hand, antigen-based immunotherapy, such as β cell protein/peptide or particle vaccination, must contend with what is likely to be a high degree of diversity in the β cell-specific T cell response among T1D individuals and T1D subsets (199–201). Therefore, the ability to tolerize a sufficient number of disease-driving self-reactive T cell clones residing in the islets will be challenging. The most effective approach may reside in combining strategies functioning *via* distinct mechanisms. ND Ab specific for CD4 and CD8, for example, can be used to purge pathogenic Teff residing in the islets (128, 133). This would then be followed by an antigen-based strategy in which the need to establish a sufficiently sized pool of aTreg becomes less stringent. A novel combinatorial approach recently described utilizes IL-2C and MHC class II-peptide tetramers. This combination expands the frequency of $Foxp3^+$Treg in a peptide-specific manner that results in prevention of diabetes in NOD mice (240).

Further studies defining common biomarkers of T1D will be critical in designing treatment protocols for individual patients, as well as for monitoring the effects of a given immunotherapy. Current advancements in large-scale genomic and proteomic analyses are making identification of these types of markers a reality, in addition to "matching" at risk or T1D patients with the most appropriate immunotherapy.

AUTHOR CONTRIBUTIONS

CJK, MC, QK, and RMT contributed to the preparation of the review article.

FUNDING

This work was supported by National Institutes of Health grants R01DK100256 and R01DK1035486 (RMT) and T32AI007273 (MC).

REFERENCES

1. Bach JF. Insulin-dependent diabetes mellitus as an autoimmune disease. *Endocr Rev* (1994) 15(4):516–42. doi:10.1210/edrv-15-4-516
2. Tisch R, McDevitt H. Insulin-dependent diabetes mellitus. *Cell* (1996) 85(3):291–7. doi:10.1016/S0092-8674(00)81106-X
3. Eisenbarth GS. Type 1 diabetes: molecular, cellular and clinical immunology. *Adv Exp Med Biol* (2004) 552:306–10.
4. Anderson MS, Bluestone JA. The NOD mouse: a model of immune dysregulation. *Annu Rev Immunol* (2005) 23:447–85. doi:10.1146/annurev.immunol.23.021704.115643
5. Barrett JC, Clayton DG, Concannon P, Akolkar B, Cooper JD, Erlich HA, et al. Genome-wide association study and meta-analysis find that over 40 loci affect risk of type 1 diabetes. *Nat Genet* (2009) 41(6):703–7. doi:10.1038/ng.381
6. Pociot F, Akolkar B, Concannon P, Erlich HA, Julier C, Morahan G, et al. Genetics of type 1 diabetes: what's next? *Diabetes* (2010) 59(7):1561–71. doi:10.2337/db10-0076
7. Noble JA, Erlich HA. Genetics of type 1 diabetes. *Cold Spring Harb Perspect Med* (2012) 2(1):a007732. doi:10.1101/cshperspect.a007732
8. Onengut-Gumuscu S, Chen WM, Burren O, Cooper NJ, Quinlan AR, Mychaleckyj JC, et al. Fine mapping of type 1 diabetes susceptibility loci and evidence for colocalization of causal variants with lymphoid gene enhancers. *Nat Genet* (2015) 47(4):381–6. doi:10.1038/ng.3245
9. Op de Beeck A, Eizirik DL. Viral infections in type 1 diabetes mellitus – why the beta cells? *Nat Rev Endocrinol* (2016) 12(5):263–73. doi:10.1038/nrendo.2016.30
10. Laitinen OH, Honkanen H, Pakkanen O, Oikarinen S, Hankaniemi MM, Huhtala H, et al. Coxsackievirus B1 is associated with induction of beta-cell autoimmunity that portends type 1 diabetes. *Diabetes* (2014) 63(2):446–55. doi:10.2337/db13-0619
11. Oikarinen S, Tauriainen S, Hober D, Lucas B, Vazeou A, Sioofy-Khojine A, et al. Virus antibody survey in different European populations indicates risk association between coxsackievirus B1 and type 1 diabetes. *Diabetes* (2014) 63(2):655–62. doi:10.2337/db13-0620
12. Atkinson MA. The pathogenesis and natural history of type 1 diabetes. *Cold Spring Harb Perspect Med* (2012) 2(11). doi:10.1101/cshperspect.a007641
13. Katsarou A, Gudbjornsdottir S, Rawshani A, Dabelea D, Bonifacio E, Anderson BJ, et al. Type 1 diabetes mellitus. *Nat Rev Dis Primers* (2017) 3:17016. doi:10.1038/nrdp.2017.16
14. Knip M, Siljander H. The role of the intestinal microbiota in type 1 diabetes mellitus. *Nat Rev Endocrinol* (2016) 12(3):154–67. doi:10.1038/nrendo.2015.218
15. Vaarala O, Atkinson MA, Neu J. The "perfect storm" for type 1 diabetes: the complex interplay between intestinal microbiota, gut permeability, and mucosal immunity. *Diabetes* (2008) 57(10):2555–62. doi:10.2337/db08-0331
16. Wen L, Ley RE, Volchkov PY, Stranges PB, Avanesyan L, Stonebraker AC, et al. Innate immunity and intestinal microbiota in the development of type 1 diabetes. *Nature* (2008) 455(7216):1109–13. doi:10.1038/nature07336
17. Nerup J, Platz P, Andersen OO, Christy M, Lyngsoe J, Poulsen JE, et al. HL-A antigens and diabetes mellitus. *Lancet* (1974) 2(7885):864–6. doi:10.1016/S0140-6736(74)91201-X
18. Bottini N, Musumeci L, Alonso A, Rahmouni S, Nika K, Rostamkhani M, et al. A functional variant of lymphoid tyrosine phosphatase is associated with type I diabetes. *Nat Genet* (2004) 36(4):337–8. doi:10.1038/ng1323
19. Smyth D, Cooper JD, Collins JE, Heward JM, Franklyn JA, Howson JM, et al. Replication of an association between the lymphoid tyrosine phosphatase locus (LYP/PTPN22) with type 1 diabetes, and evidence for its role as a general autoimmunity locus. *Diabetes* (2004) 53(11):3020–3. doi:10.2337/diabetes.53.11.3020
20. Nistico L, Buzzetti R, Pritchard LE, Van der Auwera B, Giovannini C, Bosi E, et al. The CTLA-4 gene region of chromosome 2q33 is linked to, and associated with, type 1 diabetes. Belgian Diabetes Registry. *Hum Mol Genet* (1996) 5(7):1075–80. doi:10.1093/hmg/5.7.1075
21. Ueda H, Howson JM, Esposito L, Heward J, Snook H, Chamberlain G, et al. Association of the T-cell regulatory gene CTLA4 with susceptibility to autoimmune disease. *Nature* (2003) 423(6939):506–11. doi:10.1038/nature01621
22. Field LL, Larsen Z, Pociot F, Nerup J, Tobias R, Bonnevie-Nielsen V. Evidence for a locus (IDDM16) in the immunoglobulin heavy chain region on chromosome 14q32.3 producing susceptibility to type 1 diabetes. *Genes Immun* (2002) 3(6):338–44. doi:10.1038/sj.gene.6363857
23. Morahan G, Huang D, Ymer SI, Cancilla MR, Stephen K, Dabadghao P, et al. Linkage disequilibrium of a type 1 diabetes susceptibility locus with a regulatory IL12B allele. *Nat Genet* (2001) 27(2):218–21. doi:10.1038/84872
24. Clark M, Kroger CJ, Tisch RM. Type 1 diabetes: a chronic anti-self-inflammatory response. *Front Immunol* (2017) 8:1898. doi:10.3389/fimmu.2017.01898
25. Mallone R, Brezar V, Boitard C. T cell recognition of autoantigens in human type 1 diabetes: clinical perspectives. *Clin Dev Immunol* (2011) 2011:513210. doi:10.1155/2011/513210
26. Enee E, Kratzer R, Arnoux JB, Barilleau E, Hamel Y, Marchi C, et al. ZnT8 is a major CD8+ T cell-recognized autoantigen in pediatric type 1 diabetes. *Diabetes* (2012) 61(7):1779–84. doi:10.2337/db12-0071
27. Han S, Donelan W, Wang H, Reeves W, Yang LJ. Novel autoantigens in type 1 diabetes. *Am J Transl Res* (2013) 5(4):379–92.
28. Roep BO, Peakman M. Antigen targets of type 1 diabetes autoimmunity. *Cold Spring Harb Perspect Med* (2012) 2(4):a007781. doi:10.1101/cshperspect.a007781
29. Michels AW, Landry LG, McDaniel KA, Yu L, Campbell-Thompson M, Kwok WW, et al. Islet-derived CD4 T cells targeting proinsulin in human autoimmune diabetes. *Diabetes* (2017) 66(3):722–34. doi:10.2337/db16-1025
30. Delong T, Baker RL, He J, Barbour G, Bradley B, Haskins K. Diabetogenic T-cell clones recognize an altered peptide of chromogranin A. *Diabetes* (2012) 61(12):3239–46. doi:10.2337/db12-0112
31. Babon JA, DeNicola ME, Blodgett DM, Crevecoeur I, Buttrick TS, Maehr R, et al. Analysis of self-antigen specificity of islet-infiltrating T cells from human donors with type 1 diabetes. *Nat Med* (2016) 22(12):1482–7. doi:10.1038/nm.4203
32. Delong T, Wiles TA, Baker RL, Bradley B, Barbour G, Reisdorph R, et al. Pathogenic CD4 T cells in type 1 diabetes recognize epitopes formed by peptide fusion. *Science* (2016) 351(6274):711–4. doi:10.1126/science.aad2791
33. Baker RL, Jamison BL, Wiles TA, Lindsay RS, Barbour G, Bradley B, et al. CD4 T cells reactive to hybrid insulin peptides are indicators of disease activity in the NOD mouse. *Diabetes* (2018) 67(8):db180200. doi:10.2337/db18-0200
34. Wiles TA, Delong T, Baker RL, Bradley B, Barbour G, Powell RL, et al. An insulin-IAPP hybrid peptide is an endogenous antigen for CD4 T cells in the non-obese diabetic mouse. *J Autoimmun* (2017) 78:11–8. doi:10.1016/j.jaut.2016.10.007
35. Roep BO, Kracht MJ, van Lummel M, Zaldumbide A. A roadmap of the generation of neoantigens as targets of the immune system in type 1 diabetes. *Curr Opin Immunol* (2016) 43:67–73. doi:10.1016/j.coi.2016.09.007
36. Kracht MJ, van Lummel M, Nikolic T, Joosten AM, Laban S, van der Slik AR, et al. Autoimmunity against a defective ribosomal insulin gene product in type 1 diabetes. *Nat Med* (2017) 23(4):501–7. doi:10.1038/nm.4289
37. Phelps EA, Cianciaruso C, Michael IP, Pasquier M, Kanaani J, Nano R, et al. Aberrant accumulation of the diabetes autoantigen GAD65 in Golgi membranes in conditions of ER stress and autoimmunity. *Diabetes* (2016) 65(9):2686–99. doi:10.2337/db16-0180
38. Eizirik DL, Sammeth M, Bouckenooghe T, Bottu G, Sisino G, Igoillo-Esteve M, et al. The human pancreatic islet transcriptome: expression of candidate genes for type 1 diabetes and the impact of pro-inflammatory cytokines. *PLoS Genet* (2012) 8(3):e1002552. doi:10.1371/journal.pgen.1002552
39. Ortis F, Naamane N, Flamez D, Ladriere L, Moore F, Cunha DA, et al. Cytokines interleukin-1beta and tumor necrosis factor-alpha regulate different transcriptional and alternative splicing networks in primary beta-cells. *Diabetes* (2010) 59(2):358–74. doi:10.2337/db09-1159
40. Brooks-Worrell B, Gersuk VH, Greenbaum C, Palmer JP. Intermolecular antigen spreading occurs during the preclinical period of human type 1 diabetes. *J Immunol* (2001) 166(8):5265–70. doi:10.4049/jimmunol.166.8.5265
41. You S, Chatenoud L. Proinsulin: a unique autoantigen triggering autoimmune diabetes. *J Clin Invest* (2006) 116(12):3108–10. doi:10.1172/JCI30760
42. von Herrath M, Sanda S, Herold K. Type 1 diabetes as a relapsing-remitting disease? *Nat Rev Immunol* (2007) 7(12):988–94. doi:10.1038/nri2192

43. Willcox A, Richardson SJ, Bone AJ, Foulis AK, Morgan NG. Analysis of islet inflammation in human type 1 diabetes. *Clin Exp Immunol* (2009) 155(2):173–81. doi:10.1111/j.1365-2249.2008.03860.x
44. Pugliese A. Autoreactive T cells in type 1 diabetes. *J Clin Invest* (2017) 127(8):2881–91. doi:10.1172/JCI94549
45. Coppieters KT, Dotta F, Amirian N, Campbell PD, Kay TW, Atkinson MA, et al. Demonstration of islet-autoreactive CD8 T cells in insulitic lesions from recent onset and long-term type 1 diabetes patients. *J Exp Med* (2012) 209(1):51–60. doi:10.1084/jem.20111187
46. Atkinson MA, von Herrath M, Powers AC, Clare-Salzler M. Current concepts on the pathogenesis of type 1 diabetes – considerations for attempts to prevent and reverse the disease. *Diabetes Care* (2015) 38(6):979–88. doi:10.2337/dc15-0144
47. Arif S, Gibson VB, Nguyen V, Bingley PJ, Todd JA, Guy C, et al. Beta-cell specific T-lymphocyte response has a distinct inflammatory phenotype in children with type 1 diabetes compared with adults. *Diabet Med* (2017) 34(3):419–25. doi:10.1111/dme.13153
48. Heninger AK, Eugster A, Kuehn D, Buettner F, Kuhn M, Lindner A, et al. A divergent population of autoantigen-responsive CD4+ T cells in infants prior to beta cell autoimmunity. *Sci Transl Med* (2017) 9(378):eaaf8848. doi:10.1126/scitranslmed.aaf8848
49. Richardson SJ, Willcox A, Bone AJ, Morgan NG, Foulis AK. Immunopathology of the human pancreas in type-I diabetes. *Semin Immunopathol* (2011) 33(1):9–21. doi:10.1007/s00281-010-0205-0
50. Coppieters KT, Roep BO, von Herrath MG. Beta cells under attack: toward a better understanding of type 1 diabetes immunopathology. *Semin Immunopathol* (2011) 33(1):1–7. doi:10.1007/s00281-010-0236-6
51. Campbell-Thompson M, Fu A, Kaddis JS, Wasserfall C, Schatz DA, Pugliese A, et al. Insulitis and beta-cell mass in the natural history of type 1 diabetes. *Diabetes* (2016) 65(3):719–31. doi:10.2337/db15-0779
52. Campbell-Thompson M. Organ donor specimens: what can they tell us about type 1 diabetes? *Pediatr Diabetes* (2015) 16(5):320–30. doi:10.1111/pedi.12286
53. In't Veld P. Insulitis in human type 1 diabetes: the quest for an elusive lesion. *Islets* (2011) 3(4):131–8. doi:10.4161/isl.3.4.15728
54. Skog O, Korsgren S, Melhus A, Korsgren O. Revisiting the notion of type 1 diabetes being a T-cell-mediated autoimmune disease. *Curr Opin Endocrinol Diabetes Obes* (2013) 20(2):118–23. doi:10.1097/MED.0b013e32835edb89
55. Atkinson MA, Gianani R. The pancreas in human type 1 diabetes: providing new answers to age-old questions. *Curr Opin Endocrinol Diabetes Obes* (2009) 16(4):279–85. doi:10.1097/MED.0b013e32832e06ba
56. Kent SC, Mannering SI, Michels AW, Babon JAB. Deciphering the pathogenesis of human type 1 diabetes (T1D) by interrogating T cells from the "scene of the crime". *Curr Diab Rep* (2017) 17(10):95. doi:10.1007/s11892-017-0915-y
57. Gomez-Tourino I, Arif S, Eichmann M, Peakman M. T cells in type 1 diabetes: instructors, regulators and effectors: a comprehensive review. *J Autoimmun* (2016) 66:7–16. doi:10.1016/j.jaut.2015.08.012
58. Arif S, Tree TI, Astill TP, Tremble JM, Bishop AJ, Dayan CM, et al. Autoreactive T cell responses show proinflammatory polarization in diabetes but a regulatory phenotype in health. *J Clin Invest* (2004) 113(3):451–63. doi:10.1172/JCI19585
59. Walker LS, von Herrath M. CD4 T cell differentiation in type 1 diabetes. *Clin Exp Immunol* (2016) 183(1):16–29. doi:10.1111/cei.12672
60. Emamaullee JA, Davis J, Merani S, Toso C, Elliott JF, Thiesen A, et al. Inhibition of Th17 cells regulates autoimmune diabetes in NOD mice. *Diabetes* (2009) 58(6):1302–11. doi:10.2337/db08-1113
61. Marwaha AK, Crome SQ, Panagiotopoulos C, Berg KB, Qin H, Ouyang Q, et al. Cutting edge: increased IL-17-secreting T cells in children with new-onset type 1 diabetes. *J Immunol* (2010) 185(7):3814–8. doi:10.4049/jimmunol.1001860
62. Ferraro A, Socci C, Stabilini A, Valle A, Monti P, Piemonti L, et al. Expansion of Th17 cells and functional defects in T regulatory cells are key features of the pancreatic lymph nodes in patients with type 1 diabetes. *Diabetes* (2011) 60(11):2903–13. doi:10.2337/db11-0090
63. Schneider A, Rieck M, Sanda S, Pihoker C, Greenbaum C, Buckner JH. The effector T cells of diabetic subjects are resistant to regulation via CD4+ FOXP3+ regulatory T cells. *J Immunol* (2008) 181(10):7350–5. doi:10.4049/jimmunol.181.10.7350
64. D'Alise AM, Auyeung V, Feuerer M, Nishio J, Fontenot J, Benoist C, et al. The defect in T-cell regulation in NOD mice is an effect on the T-cell effectors. *Proc Natl Acad Sci U S A* (2008) 105(50):19857–62. doi:10.1073/pnas.0810713105
65. Hulme MA, Wasserfall CH, Atkinson MA, Brusko TM. Central role for interleukin-2 in type 1 diabetes. *Diabetes* (2012) 61(1):14–22. doi:10.2337/db11-1213
66. Garg G, Tyler JR, Yang JH, Cutler AJ, Downes K, Pekalski M, et al. Type 1 diabetes-associated IL2RA variation lowers IL-2 signaling and contributes to diminished CD4+CD25+ regulatory T cell function. *J Immunol* (2012) 188(9):4644–53. doi:10.4049/jimmunol.1100272
67. Brusko TM, Wasserfall CH, Clare-Salzler MJ, Schatz DA, Atkinson MA. Functional defects and the influence of age on the frequency of CD4+ CD25+ T-cells in type 1 diabetes. *Diabetes* (2005) 54(5):1407–14. doi:10.2337/diabetes.54.5.1407
68. Lindley S, Dayan CM, Bishop A, Roep BO, Peakman M, Tree TI. Defective suppressor function in CD4(+)CD25(+) T-cells from patients with type 1 diabetes. *Diabetes* (2005) 54(1):92–9. doi:10.2337/diabetes.54.1.92
69. Tang Q, Adams JY, Penaranda C, Melli K, Piaggio E, Sgouroudis E, et al. Central role of defective interleukin-2 production in the triggering of islet autoimmune destruction. *Immunity* (2008) 28(5):687–97. doi:10.1016/j.immuni.2008.03.016
70. Hull CM, Peakman M, Tree TIM. Regulatory T cell dysfunction in type 1 diabetes: what's broken and how can we fix it? *Diabetologia* (2017) 60(10):1839–50. doi:10.1007/s00125-017-4377-1
71. Miyara M, Sakaguchi S. Natural regulatory T cells: mechanisms of suppression. *Trends Mol Med* (2007) 13(3):108–16. doi:10.1016/j.molmed.2007.01.003
72. Goudy KS, Johnson MC, Garland A, Li C, Samulski RJ, Wang B, et al. Inducible adeno-associated virus-mediated IL-2 gene therapy prevents autoimmune diabetes. *J Immunol* (2011) 186(6):3779–86. doi:10.4049/jimmunol.1001422
73. Johnson MC, Garland AL, Nicolson SC, Li C, Samulski RJ, Wang B, et al. Beta-cell-specific IL-2 therapy increases islet Foxp3+Treg and suppresses type 1 diabetes in NOD mice. *Diabetes* (2013) 62(11):3775–84. doi:10.2337/db13-0669
74. Flores RR, Zhou L, Robbins PD. Expression of IL-2 in beta cells by AAV8 gene transfer in pre-diabetic NOD mice prevents diabetes through activation of FoxP3-positive regulatory T cells. *Gene Ther* (2014) 21(8):715–22. doi:10.1038/gt.2014.45
75. Long SA, Cerosaletti K, Bollyky PL, Tatum M, Shilling H, Zhang S, et al. Defects in IL-2R signaling contribute to diminished maintenance of FOXP3 expression in CD4(+)CD25(+) regulatory T-cells of type 1 diabetic subjects. *Diabetes* (2010) 59(2):407–15. doi:10.2337/db09-0694
76. Attridge K, Wang CJ, Wardzinski L, Kenefeck R, Chamberlain JL, Manzotti C, et al. IL-21 inhibits T cell IL-2 production and impairs Treg homeostasis. *Blood* (2012) 119(20):4656–64. doi:10.1182/blood-2011-10-388546
77. Arif S, Leete P, Nguyen V, Marks K, Nor NM, Estorninho M, et al. Blood and islet phenotypes indicate immunological heterogeneity in type 1 diabetes. *Diabetes* (2014) 63(11):3835–45. doi:10.2337/db14-0365
78. Sanda S, Roep BO, von Herrath M. Islet antigen specific IL-10+ immune responses but not CD4+CD25+FoxP3+ cells at diagnosis predict glycemic control in type 1 diabetes. *Clin Immunol* (2008) 127(2):138–43. doi:10.1016/j.clim.2007.12.003
79. Petrich de Marquesini LG, Fu J, Connor KJ, Bishop AJ, McLintock NE, Pope C, et al. IFN-gamma and IL-10 islet-antigen-specific T cell responses in autoantibody-negative first-degree relatives of patients with type 1 diabetes. *Diabetologia* (2010) 53(7):1451–60. doi:10.1007/s00125-010-1739-3
80. Jin Y, Chen X, Podolsky R, Hopkins D, Makala LH, Muir A, et al. APC dysfunction is correlated with defective suppression of T cell proliferation in human type 1 diabetes. *Clin Immunol* (2009) 130(3):272–9. doi:10.1016/j.clim.2008.10.005
81. Serreze DV, Gaskins HR, Leiter EH. Defects in the differentiation and function of antigen presenting cells in NOD/Lt mice. *J Immunol* (1993) 150(6):2534–43.
82. Katz JD, Ondr JK, Opoka RJ, Garcia Z, Janssen EM. Cutting edge: merocytic dendritic cells break T cell tolerance to beta cell antigens in nonobese diabetic mouse diabetes. *J Immunol* (2010) 185(4):1999–2003. doi:10.4049/jimmunol.1001398

83. Poligone B, Weaver DJ Jr, Sen P, Baldwin AS Jr, Tisch R. Elevated NF-kappaB activation in nonobese diabetic mouse dendritic cells results in enhanced APC function. *J Immunol* (2002) 168(1):188–96. doi:10.4049/jimmunol.168.1.188
84. Liu J, Beller DI. Distinct pathways for NF-kappa B regulation are associated with aberrant macrophage IL-12 production in lupus- and diabetes-prone mouse strains. *J Immunol* (2003) 170(9):4489–96. doi:10.4049/jimmunol.170.9.4489
85. Uno S, Imagawa A, Okita K, Sayama K, Moriwaki M, Iwahashi H, et al. Macrophages and dendritic cells infiltrating islets with or without beta cells produce tumour necrosis factor-alpha in patients with recent-onset type 1 diabetes. *Diabetologia* (2007) 50(3):596–601. doi:10.1007/s00125-006-0569-9
86. Serreze DV, Chapman HD, Varnum DS, Hanson MS, Reifsnyder PC, Richard SD, et al. B lymphocytes are essential for the initiation of T cell-mediated autoimmune diabetes: analysis of a new "speed congenic" stock of NOD.Ig mu null mice. *J Exp Med* (1996) 184(5):2049–53. doi:10.1084/jem.184.5.2049
87. Noorchashm H, Noorchashm N, Kern J, Rostami SY, Barker CF, Naji A. B-cells are required for the initiation of insulitis and sialitis in nonobese diabetic mice. *Diabetes* (1997) 46(6):941–6. doi:10.2337/diabetes.46.6.941
88. Marino E, Silveira PA, Stolp J, Grey ST. B cell-directed therapies in type 1 diabetes. *Trends Immunol* (2011) 32(6):287–94. doi:10.1016/j.it.2011.03.006
89. Cnop M, Welsh N, Jonas JC, Jorns A, Lenzen S, Eizirik DL. Mechanisms of pancreatic beta-cell death in type 1 and type 2 diabetes: many differences, few similarities. *Diabetes* (2005) 54(Suppl 2):S97–107. doi:10.2337/diabetes.54.suppl_2.S97
90. Simmons KM, Michels AW. Type 1 diabetes: a predictable disease. *World J Diabetes* (2015) 6(3):380–90. doi:10.4239/wjd.v6.i3.380
91. Regnell SE, Lernmark A. Early prediction of autoimmune (type 1) diabetes. *Diabetologia* (2017) 60(8):1370–81. doi:10.1007/s00125-017-4308-1
92. Ziegler AG, Rewers M, Simell O, Simell T, Lempainen J, Steck A, et al. Seroconversion to multiple islet autoantibodies and risk of progression to diabetes in children. *JAMA* (2013) 309(23):2473–9. doi:10.1001/jama.2013.6285
93. Chen C, Cohrs CM, Stertmann J, Bozsak R, Speier S. Human beta cell mass and function in diabetes: recent advances in knowledge and technologies to understand disease pathogenesis. *Mol Metab* (2017) 6(9):943–57. doi:10.1016/j.molmet.2017.06.019
94. Shields BM, McDonald TJ, Oram R, Hill A, Hudson M, Leete P, et al. C-peptide decline in type 1 diabetes has two phases: an initial exponential fall and a subsequent stable phase. *Diabetes Care* (2018) 41(7):1486–92. doi:10.2337/dc18-0465
95. Bougneres PF, Landais P, Boisson C, Carel JC, Frament N, Boitard C, et al. Limited duration of remission of insulin dependency in children with recent overt type I diabetes treated with low-dose cyclosporin. *Diabetes* (1990) 39(10):1264–72. doi:10.2337/diab.39.10.1264
96. Stiller CR, Dupre J, Gent M, Jenner MR, Keown PA, Laupacis A, et al. Effects of cyclosporine immunosuppression in insulin-dependent diabetes mellitus of recent onset. *Science* (1984) 223(4643):1362–7. doi:10.1126/science.6367043
97. Herold KC, Hagopian W, Auger JA, Poumian-Ruiz E, Taylor L, Donaldson D, et al. Anti-CD3 monoclonal antibody in new-onset type 1 diabetes mellitus. *N Engl J Med* (2002) 346(22):1692–8. doi:10.1056/NEJMoa012864
98. Shoda LK, Young DL, Ramanujan S, Whiting CC, Atkinson MA, Bluestone JA, et al. A comprehensive review of interventions in the NOD mouse and implications for translation. *Immunity* (2005) 23(2):115–26. doi:10.1016/j.immuni.2005.08.002
99. Perruche S, Zhang P, Liu Y, Saas P, Bluestone JA, Chen W. CD3-specific antibody-induced immune tolerance involves transforming growth factor-beta from phagocytes digesting apoptotic T cells. *Nat Med* (2008) 14(5):528–35. doi:10.1038/nm1749
100. Chatenoud L, Bluestone JA. CD3-specific antibodies: a portal to the treatment of autoimmunity. *Nat Rev Immunol* (2007) 7(8):622–32. doi:10.1038/nri2134
101. Belghith M, Bluestone JA, Barriot S, Megret J, Bach JF, Chatenoud L. TGF-beta-dependent mechanisms mediate restoration of self-tolerance induced by antibodies to CD3 in overt autoimmune diabetes. *Nat Med* (2003) 9(9):1202–8. doi:10.1038/nm924
102. Wallberg M, Recino A, Phillips J, Howie D, Vienne M, Paluch C, et al. Anti-CD3 treatment up-regulates programmed cell death protein-1 expression on activated effector T cells and severely impairs their inflammatory capacity. *Immunology* (2017) 151(2):248–60. doi:10.1111/imm.12729
103. Chatenoud L, Primo J, Bach JF. CD3 antibody-induced dominant self tolerance in overtly diabetic NOD mice. *J Immunol* (1997) 158(6):2947–54.
104. Keymeulen B, Vandemeulebroucke E, Ziegler AG, Mathieu C, Kaufman L, Hale G, et al. Insulin needs after CD3-antibody therapy in new-onset type 1 diabetes. *N Engl J Med* (2005) 352(25):2598–608. doi:10.1056/NEJMoa043980
105. Herold KC, Gitelman S, Greenbaum C, Puck J, Hagopian W, Gottlieb P, et al. Treatment of patients with new onset Type 1 diabetes with a single course of anti-CD3 mAb Teplizumab preserves insulin production for up to 5 years. *Clin Immunol* (2009) 132(2):166–73. doi:10.1016/j.clim.2009.04.007
106. Herold KC, Gitelman SE, Ehlers MR, Gottlieb PA, Greenbaum CJ, Hagopian W, et al. Teplizumab (anti-CD3 mAb) treatment preserves C-peptide responses in patients with new-onset type 1 diabetes in a randomized controlled trial: metabolic and immunologic features at baseline identify a subgroup of responders. *Diabetes* (2013) 62(11):3766–74. doi:10.2337/db13-0345
107. Herold KC, Gitelman SE, Masharani U, Hagopian W, Bisikirska B, Donaldson D, et al. A single course of anti-CD3 monoclonal antibody hOKT3gamma1(Ala-Ala) results in improvement in C-peptide responses and clinical parameters for at least 2 years after onset of type 1 diabetes. *Diabetes* (2005) 54(6):1763–9. doi:10.2337/diabetes.54.6.1763
108. Herold KC, Gitelman SE, Willi SM, Gottlieb PA, Waldron-Lynch F, Devine L, et al. Teplizumab treatment may improve C-peptide responses in participants with type 1 diabetes after the new-onset period: a randomised controlled trial. *Diabetologia* (2013) 56(2):391–400. doi:10.1007/s00125-012-2753-4
109. Long SA, Thorpe J, DeBerg HA, Gersuk V, Eddy J, Harris KM, et al. Partial exhaustion of CD8 T cells and clinical response to teplizumab in new-onset type 1 diabetes. *Sci Immunol* (2016) 1(5):eaai7793. doi:10.1126/sciimmunol.aai7793
110. Long SA, Thorpe J, Herold KC, Ehlers M, Sanda S, Lim N, et al. Remodeling T cell compartments during anti-CD3 immunotherapy of type 1 diabetes. *Cell Immunol* (2017) 319:3–9. doi:10.1016/j.cellimm.2017.07.007
111. Tooley JE, Vudattu N, Choi J, Cotsapas C, Devine L, Raddassi K, et al. Changes in T-cell subsets identify responders to FcR-nonbinding anti-CD3 mAb (teplizumab) in patients with type 1 diabetes. *Eur J Immunol* (2016) 46(1):230–41. doi:10.1002/eji.201545708
112. Vudattu NK, Herold KC. Treatment of new onset type 1 diabetes with teplizumab: successes and pitfalls in development. *Expert Opin Biol Ther* (2014) 14(3):377–85. doi:10.1517/14712598.2014.881797
113. Daifotis AG, Koenig S, Chatenoud L, Herold KC. Anti-CD3 clinical trials in type 1 diabetes mellitus. *Clin Immunol* (2013) 149(3):268–78. doi:10.1016/j.clim.2013.05.001
114. Ablamunits V, Henegariu O, Hansen JB, Opare-Addo L, Preston-Hurlburt P, Santamaria P, et al. Synergistic reversal of type 1 diabetes in NOD mice with anti-CD3 and interleukin-1 blockade: evidence of improved immune regulation. *Diabetes* (2012) 61(1):145–54. doi:10.2337/db11-1033
115. Sherry NA, Chen W, Kushner JA, Glandt M, Tang Q, Tsai S, et al. Exendin-4 improves reversal of diabetes in NOD mice treated with anti-CD3 monoclonal antibody by enhancing recovery of beta-cells. *Endocrinology* (2007) 148(11):5136–44. doi:10.1210/en.2007-0358
116. Hyslop CM, Tsai S, Shrivastava V, Santamaria P, Huang C. Prolactin as an adjunct for type 1 diabetes immunotherapy. *Endocrinology* (2016) 157(1):150–65. doi:10.1210/en.2015-1549
117. Parker MJ, Xue S, Alexander JJ, Wasserfall CH, Campbell-Thompson ML, Battaglia M, et al. Immune depletion with cellular mobilization imparts immunoregulation and reverses autoimmune diabetes in nonobese diabetic mice. *Diabetes* (2009) 58(10):2277–84. doi:10.2337/db09-0557
118. Haller MJ, Gitelman SE, Gottlieb PA, Michels AW, Perry DJ, Schultz AR, et al. Antithymocyte globulin plus G-CSF combination therapy leads to sustained immunomodulatory and metabolic effects in a subset of responders with established type 1 diabetes. *Diabetes* (2016) 65(12):3765–75. doi:10.2337/db16-0823
119. Hamad AR, Ahmed R, Donner T, Fousteri G. B cell-targeted immunotherapy for type 1 diabetes: what can make it work? *Discov Med* (2016) 21(115):213–9.
120. Musette P, Bouaziz JD. B cell modulation strategies in autoimmune diseases: new concepts. *Front Immunol* (2018) 9:622. doi:10.3389/fimmu.2018.00622
121. Hu CY, Rodriguez-Pinto D, Du W, Ahuja A, Henegariu O, Wong FS, et al. Treatment with CD20-specific antibody prevents and reverses autoimmune diabetes in mice. *J Clin Invest* (2007) 117(12):3857–67. doi:10.1172/JCI32405

122. Xiu Y, Wong CP, Bouaziz JD, Hamaguchi Y, Wang Y, Pop SM, et al. B lymphocyte depletion by CD20 monoclonal antibody prevents diabetes in nonobese diabetic mice despite isotype-specific differences in Fc gamma R effector functions. *J Immunol* (2008) 180(5):2863–75. doi:10.4049/jimmunol.180.5.2863
123. Fiorina P, Vergani A, Dada S, Jurewicz M, Wong M, Law K, et al. Targeting CD22 reprograms B-cells and reverses autoimmune diabetes. *Diabetes* (2008) 57(11):3013–24. doi:10.2337/db08-0420
124. Zekavat G, Rostami SY, Badkerhanian A, Parsons RF, Koeberlein B, Yu M, et al. In vivo BLyS/BAFF neutralization ameliorates islet-directed autoimmunity in nonobese diabetic mice. *J Immunol* (2008) 181(11):8133–44. doi:10.4049/jimmunol.181.11.8133
125. Marino E, Villanueva J, Walters S, Liuwantara D, Mackay F, Grey ST. CD4(+) CD25(+) T-cells control autoimmunity in the absence of B-cells. *Diabetes* (2009) 58(7):1568–77. doi:10.2337/db08-1504
126. Pescovitz MD, Greenbaum CJ, Krause-Steinrauf H, Becker DJ, Gitelman SE, Goland R, et al. Rituximab, B-lymphocyte depletion, and preservation of beta-cell function. *N Engl J Med* (2009) 361(22):2143–52. doi:10.1056/NEJMoa0904452
127. Cohen MD, Keystone E. Rituximab for rheumatoid arthritis. *Rheumatol Ther* (2015) 2(2):99–111. doi:10.1007/s40744-015-0016-9
128. Yi Z, Diz R, Martin AJ, Morillon YM, Kline DE, Li L, et al. Long-term remission of diabetes in NOD mice is induced by nondepleting anti-CD4 and anti-CD8 antibodies. *Diabetes* (2012) 61(11):2871–80. doi:10.2337/db12-0098
129. Phillips JM, Parish NM, Raine T, Bland C, Sawyer Y, De La Pena H, et al. Type 1 diabetes development requires both CD4+ and CD8+ T cells and can be reversed by non-depleting antibodies targeting both T cell populations. *Rev Diabet Stud* (2009) 6(2):97–103. doi:10.1900/RDS.2009.6.97
130. Hutchings P, O'Reilly L, Parish NM, Waldmann H, Cooke A. The use of a non-depleting anti-CD4 monoclonal antibody to re-establish tolerance to beta cells in NOD mice. *Eur J Immunol* (1992) 22(7):1913–8. doi:10.1002/eji.1830220735
131. Phillips JM, Harach SZ, Parish NM, Fehervari Z, Haskins K, Cooke A. Nondepleting anti-CD4 has an immediate action on diabetogenic effector cells, halting their destruction of pancreatic beta cells. *J Immunol* (2000) 165(4):1949–55. doi:10.4049/jimmunol.165.4.1949
132. Pullar CE, Morris PJ, Wood KJ. Altered proximal T-cell receptor signalling events in mouse CD4+ T cells in the presence of anti-CD4 monoclonal antibodies: evidence for reduced phosphorylation of Zap-70 and LAT. *Scand J Immunol* (2003) 57(4):333–41. doi:10.1046/j.1365-3083.2003.01241.x
133. Martin AJ, Clark M, Gojanovich G, Manzoor F, Miller K, Kline DE, et al. Anti-coreceptor therapy drives selective T cell egress by suppressing inflammation-dependent chemotactic cues. *JCI Insight* (2016) 1(17):e87636. doi:10.1172/jci.insight.87636
134. Orban T, Bundy B, Becker DJ, DiMeglio LA, Gitelman SE, Goland R, et al. Co-stimulation modulation with abatacept in patients with recent-onset type 1 diabetes: a randomised, double-blind, placebo-controlled trial. *Lancet* (2011) 378(9789):412–9. doi:10.1016/S0140-6736(11)60886-6
135. Orban T, Bundy B, Becker DJ, Dimeglio LA, Gitelman SE, Goland R, et al. Costimulation modulation with abatacept in patients with recent-onset type 1 diabetes: follow-up 1 year after cessation of treatment. *Diabetes Care* (2014) 37(4):1069–75. doi:10.2337/dc13-0604
136. Itoh N, Imagawa A, Hanafusa T, Waguri M, Yamamoto K, Iwahashi H, et al. Requirement of Fas for the development of autoimmune diabetes in nonobese diabetic mice. *J Exp Med* (1997) 186(4):613–8. doi:10.1084/jem.186.4.613
137. Chervonsky AV, Wang Y, Wong FS, Visintin I, Flavell RA, Janeway CA Jr, et al. The role of Fas in autoimmune diabetes. *Cell* (1997) 89(1):17–24. doi:10.1016/S0092-8674(00)80178-6
138. Xiao Z, Mohamood AS, Uddin S, Gutfreund R, Nakata C, Marshall A, et al. Inhibition of Fas ligand in NOD mice unmasks a protective role for IL-10 against insulitis development. *Am J Pathol* (2011) 179(2):725–32. doi:10.1016/j.ajpath.2011.04.016
139. Kalden JR, Schulze-Koops H. Immunogenicity and loss of response to TNF inhibitors: implications for rheumatoid arthritis treatment. *Nat Rev Rheumatol* (2017) 13(12):707–18. doi:10.1038/nrrheum.2017.187
140. Yang XD, Tisch R, Singer SM, Cao ZA, Liblau RS, Schreiber RD, et al. Effect of tumor necrosis factor alpha on insulin-dependent diabetes mellitus in NOD mice. I. The early development of autoimmunity and the diabetogenic process. *J Exp Med* (1994) 180(3):995–1004. doi:10.1084/jem.180.3.995
141. Chee J, Angstetra E, Mariana L, Graham KL, Carrington EM, Bluethmann H, et al. TNF receptor 1 deficiency increases regulatory T cell function in nonobese diabetic mice. *J Immunol* (2011) 187(4):1702–12. doi:10.4049/jimmunol.1100511
142. Mastrandrea L, Yu J, Behrens T, Buchlis J, Albini C, Fourtner S, et al. Etanercept treatment in children with new-onset type 1 diabetes: pilot randomized, placebo-controlled, double-blind study. *Diabetes Care* (2009) 32(7):1244–9. doi:10.2337/dc09-0054
143. Timper K, Hruz P, Beglinger C, Donath MY. Infliximab in the treatment of Crohn disease and type 1 diabetes. *Diabetes Care* (2013) 36(7):e90–1. doi:10.2337/dc13-0199
144. Tack CJ, Kleijwegt FS, Van Riel PL, Roep BO. Development of type 1 diabetes in a patient treated with anti-TNF-alpha therapy for active rheumatoid arthritis. *Diabetologia* (2009) 52(7):1442–4. doi:10.1007/s00125-009-1381-0
145. Tian Y, Cox MA, Kahan SM, Ingram JT, Bakshi RK, Zajac AJ. A context-dependent role for IL-21 in modulating the differentiation, distribution, and abundance of effector and memory CD8 T cell subsets. *J Immunol* (2016) 196(5):2153–66. doi:10.4049/jimmunol.1401236
146. Tian Y, Zajac AJ. IL-21 and T cell differentiation: consider the context. *Trends Immunol* (2016) 37(8):557–68. doi:10.1016/j.it.2016.06.001
147. Beringer A, Noack M, Miossec P. IL-17 in chronic inflammation: from discovery to targeting. *Trends Mol Med* (2016) 22(3):230–41. doi:10.1016/j.molmed.2016.01.001
148. Maurer MF, Garrigues U, Jaspers SR, Meengs B, Rixon MW, Stevens BL, et al. Generation and characterization of human anti-human IL-21 neutralizing monoclonal antibodies. *MAbs* (2012) 4(1):69–83. doi:10.4161/mabs.4.1.18713
149. Sutherland AP, Van Belle T, Wurster AL, Suto A, Michaud M, Zhang D, et al. Interleukin-21 is required for the development of type 1 diabetes in NOD mice. *Diabetes* (2009) 58(5):1144–55. doi:10.2337/db08-0882
150. Kuriya G, Uchida T, Akazawa S, Kobayashi M, Nakamura K, Satoh T, et al. Double deficiency in IL-17 and IFN-gamma signalling significantly suppresses the development of diabetes in the NOD mouse. *Diabetologia* (2013) 56(8):1773–80. doi:10.1007/s00125-013-2935-8
151. Spolski R, Kashyap M, Robinson C, Yu Z, Leonard WJ. IL-21 signaling is critical for the development of type I diabetes in the NOD mouse. *Proc Natl Acad Sci U S A* (2008) 105(37):14028–33. doi:10.1073/pnas.0804358105
152. Kenefeck R, Wang CJ, Kapadi T, Wardzinski L, Attridge K, Clough LE, et al. Follicular helper T cell signature in type 1 diabetes. *J Clin Invest* (2015) 125(1):292–303. doi:10.1172/JCI76238
153. McGuire HM, Walters S, Vogelzang A, Lee CM, Webster KE, Sprent J, et al. Interleukin-21 is critically required in autoimmune and allogeneic responses to islet tissue in murine models. *Diabetes* (2011) 60(3):867–75. doi:10.2337/db10-1157
154. Pham MN, von Herrath MG, Vela JL. Antigen-specific regulatory T cells and low dose of IL-2 in treatment of type 1 diabetes. *Front Immunol* (2015) 6:651. doi:10.3389/fimmu.2015.00651
155. Long SA, Buckner JH, Greenbaum CJ. IL-2 therapy in type 1 diabetes: "trials" and tribulations. *Clin Immunol* (2013) 149(3):324–31. doi:10.1016/j.clim.2013.02.005
156. Dwyer CJ, Ward NC, Pugliese A, Malek TR. Promoting immune regulation in type 1 diabetes using low-dose interleukin-2. *Curr Diab Rep* (2016) 16(6):46. doi:10.1007/s11892-016-0739-1
157. Bayer AL, Pugliese A, Malek TR. The IL-2/IL-2R system: from basic science to therapeutic applications to enhance immune regulation. *Immunol Res* (2013) 57(1–3):197–209. doi:10.1007/s12026-013-8452-5
158. Boyman O, Sprent J. The role of interleukin-2 during homeostasis and activation of the immune system. *Nat Rev Immunol* (2012) 12(3):180–90. doi:10.1038/nri3156
159. Setoguchi R, Hori S, Takahashi T, Sakaguchi S. Homeostatic maintenance of natural Foxp3(+) CD25(+) CD4(+) regulatory T cells by interleukin (IL)-2 and induction of autoimmune disease by IL-2 neutralization. *J Exp Med* (2005) 201(5):723–35. doi:10.1084/jem.20041982
160. Yu A, Zhu L, Altman NH, Malek TR. A low interleukin-2 receptor signaling threshold supports the development and homeostasis of T regulatory cells. *Immunity* (2009) 30(2):204–17. doi:10.1016/j.immuni.2008.11.014

161. Barron L, Dooms H, Hoyer KK, Kuswanto W, Hofmann J, O'Gorman WE, et al. Cutting edge: mechanisms of IL-2-dependent maintenance of functional regulatory T cells. *J Immunol* (2010) 185(11):6426–30. doi:10.4049/jimmunol.0903940
162. Koreth J, Matsuoka K, Kim HT, McDonough SM, Bindra B, Alyea EP III, et al. Interleukin-2 and regulatory T cells in graft-versus-host disease. *N Engl J Med* (2011) 365(22):2055–66. doi:10.1056/NEJMoa1108188
163. Saadoun D, Rosenzwajg M, Joly F, Six A, Carrat F, Thibault V, et al. Regulatory T-cell responses to low-dose interleukin-2 in HCV-induced vasculitis. *N Engl J Med* (2011) 365(22):2067–77. doi:10.1056/NEJMoa1105143
164. Grinberg-Bleyer Y, Baeyens A, You S, Elhage R, Fourcade G, Gregoire S, et al. IL-2 reverses established type 1 diabetes in NOD mice by a local effect on pancreatic regulatory T cells. *J Exp Med* (2010) 207(9):1871–8. doi:10.1084/jem.20100209
165. Rabinovitch A, Suarez-Pinzon WL, Shapiro AM, Rajotte RV, Power R. Combination therapy with sirolimus and interleukin-2 prevents spontaneous and recurrent autoimmune diabetes in NOD mice. *Diabetes* (2002) 51(3):638–45. doi:10.2337/diabetes.51.3.638
166. Long SA, Rieck M, Sanda S, Bollyky JB, Samuels PL, Goland R, et al. Rapamycin/IL-2 combination therapy in patients with type 1 diabetes augments Tregs yet transiently impairs beta-cell function. *Diabetes* (2012) 61(9):2340–8. doi:10.2337/db12-0049
167. Rosenzwajg M, Churlaud G, Mallone R, Six A, Derian N, Chaara W, et al. Low-dose interleukin-2 fosters a dose-dependent regulatory T cell tuned milieu in T1D patients. *J Autoimmun* (2015) 58:48–58. doi:10.1016/j.jaut.2015.01.001
168. Hartemann A, Bensimon G, Payan CA, Jacqueminet S, Bourron O, Nicolas N, et al. Low-dose interleukin 2 in patients with type 1 diabetes: a phase 1/2 randomised, double-blind, placebo-controlled trial. *Lancet Diabetes Endocrinol* (2013) 1(4):295–305. doi:10.1016/S2213-8587(13)70113-X
169. Sockolosky JT, Trotta E, Parisi G, Picton L, Su LL, Le AC, et al. Selective targeting of engineered T cells using orthogonal IL-2 cytokine-receptor complexes. *Science* (2018) 359(6379):1037–42. doi:10.1126/science.aar3246
170. Boyman O, Kovar M, Rubinstein MP, Surh CD, Sprent J. Selective stimulation of T cell subsets with antibody-cytokine immune complexes. *Science* (2006) 311(5769):1924–7. doi:10.1126/science.1122927
171. Webster KE, Walters S, Kohler RE, Mrkvan T, Boyman O, Surh CD, et al. In vivo expansion of T reg cells with IL-2-mAb complexes: induction of resistance to EAE and long-term acceptance of islet allografts without immunosuppression. *J Exp Med* (2009) 206(4):751–60. doi:10.1084/jem.20082824
172. Manirarora JN, Wei CH. Combination therapy using IL-2/IL-2 monoclonal antibody complexes, rapamycin, and islet autoantigen peptides increases regulatory T cell frequency and protects against spontaneous and induced type 1 diabetes in nonobese diabetic mice. *J Immunol* (2015) 195(11):5203–14. doi:10.4049/jimmunol.1402540
173. Spangler JB, Tomala J, Luca VC, Jude KM, Dong S, Ring AM, et al. Antibodies to interleukin-2 elicit selective T cell subset potentiation through distinct conformational mechanisms. *Immunity* (2015) 42(5):815–25. doi:10.1016/j.immuni.2015.04.015
174. Johnson MC, Wang B, Tisch R. Genetic vaccination for re-establishing T-cell tolerance in type 1 diabetes. *Hum Vaccin* (2011) 7(1):27–36. doi:10.4161/hv.7.1.12848
175. Grieger JC, Samulski RJ. Adeno-associated virus vectorology, manufacturing, and clinical applications. *Methods Enzymol* (2012) 507:229–54. doi:10.1016/B978-0-12-386509-0.00012-0
176. Manzoor F, Johnson MC, Li C, Samulski RJ, Wang B, Tisch R. beta-cell-specific IL-35 therapy suppresses ongoing autoimmune diabetes in NOD mice. *Eur J Immunol* (2017) 47(1):144–54. doi:10.1002/eji.201646493
177. Li C, Zhang L, Chen Y, Lin X, Li T. Protective role of adenovirus vector-mediated interleukin-10 gene therapy on endogenous islet beta-cells in recent-onset type 1 diabetes in NOD mice. *Exp Ther Med* (2016) 11(5):1625–32. doi:10.3892/etm.2016.3169
178. Mallol C, Casana E, Jimenez V, Casellas A, Haurigot V, Jambrina C, et al. AAV-mediated pancreatic overexpression of Igf1 counteracts progression to autoimmune diabetes in mice. *Mol Metab* (2017) 6(7):664–80. doi:10.1016/j.molmet.2017.05.007
179. Song S, Goudy K, Campbell-Thompson M, Wasserfall C, Scott-Jorgensen M, Wang J, et al. Recombinant adeno-associated virus-mediated alpha-1 antitrypsin gene therapy prevents type I diabetes in NOD mice. *Gene Ther* (2004) 11(2):181–6. doi:10.1038/sj.gt.3302156
180. Bluestone JA, Buckner JH, Fitch M, Gitelman SE, Gupta S, Hellerstein MK, et al. Type 1 diabetes immunotherapy using polyclonal regulatory T cells. *Sci Transl Med* (2015) 7(315):315ra189. doi:10.1126/scitranslmed.aad4134
181. Bluestone JA, Trotta E, Xu D. The therapeutic potential of regulatory T cells for the treatment of autoimmune disease. *Expert Opin Ther Targets* (2015) 19(8):1091–103. doi:10.1517/14728222.2015.1037282
182. Gitelman SE, Bluestone JA. Regulatory T cell therapy for type 1 diabetes: may the force be with you. *J Autoimmun* (2016) 71:78–87. doi:10.1016/j.jaut.2016.03.011
183. Tang Q, Henriksen KJ, Bi M, Finger EB, Szot G, Ye J, et al. In vitro-expanded antigen-specific regulatory T cells suppress autoimmune diabetes. *J Exp Med* (2004) 199(11):1455–65. doi:10.1084/jem.20040139
184. Putnam AL, Brusko TM, Lee MR, Liu W, Szot GL, Ghosh T, et al. Expansion of human regulatory T-cells from patients with type 1 diabetes. *Diabetes* (2009) 58(3):652–62. doi:10.2337/db08-1168
185. Miyara M, Chader D, Burlion A, Goldstein J, Sterlin D, Norol F, et al. Combination of IL-2, rapamycin, DNA methyltransferase and histone deacetylase inhibitors for the expansion of human regulatory T cells. *Oncotarget* (2017) 8(62):104733–44. doi:10.18632/oncotarget.10914
186. Lin L, Zhang J. Role of intestinal microbiota and metabolites on gut homeostasis and human diseases. *BMC Immunol* (2017) 18(1):2. doi:10.1186/s12865-016-0187-3
187. Alkanani AK, Hara N, Gottlieb PA, Ir D, Robertson CE, Wagner BD, et al. Alterations in intestinal microbiota correlate with susceptibility to type 1 diabetes. *Diabetes* (2015) 64(10):3510–20. doi:10.2337/db14-1847
188. Dunne JL, Triplett EW, Gevers D, Xavier R, Insel R, Danska J, et al. The intestinal microbiome in type 1 diabetes. *Clin Exp Immunol* (2014) 177(1):30–7. doi:10.1111/cei.12321
189. Akira S, Uematsu S, Takeuchi O. Pathogen recognition and innate immunity. *Cell* (2006) 124(4):783–801. doi:10.1016/j.cell.2006.02.015
190. Troutman TD, Bazan JF, Pasare C. Toll-like receptors, signaling adapters and regulation of the pro-inflammatory response by PI3K. *Cell Cycle* (2012) 11(19):3559–67. doi:10.4161/cc.21572
191. Markle JG, Frank DN, Mortin-Toth S, Robertson CE, Feazel LM, Rolle-Kampczyk U, et al. Sex differences in the gut microbiome drive hormone-dependent regulation of autoimmunity. *Science* (2013) 339(6123):1084–8. doi:10.1126/science.1233521
192. Murri M, Leiva I, Gomez-Zumaquero JM, Tinahones FJ, Cardona F, Soriguer F, et al. Gut microbiota in children with type 1 diabetes differs from that in healthy children: a case-control study. *BMC Med* (2013) 11:46. doi:10.1186/1741-7015-11-46
193. Tai N, Wong FS, Wen L. The role of gut microbiota in the development of type 1, type 2 diabetes mellitus and obesity. *Rev Endocr Metab Disord* (2015) 16(1):55–65. doi:10.1007/s11154-015-9309-0
194. de Goffau MC, Luopajarvi K, Knip M, Ilonen J, Ruohtula T, Harkonen T, et al. Fecal microbiota composition differs between children with beta-cell autoimmunity and those without. *Diabetes* (2013) 62(4):1238–44. doi:10.2337/db12-0526
195. Kostic AD, Gevers D, Siljander H, Vatanen T, Hyotylainen T, Hamalainen AM, et al. The dynamics of the human infant gut microbiome in development and in progression toward type 1 diabetes. *Cell Host Microbe* (2015) 17(2):260–73. doi:10.1016/j.chom.2015.01.001
196. Endesfelder D, Zu Castell W, Ardissone A, Davis-Richardson AG, Achenbach P, Hagen M, et al. Compromised gut microbiota networks in children with anti-islet cell autoimmunity. *Diabetes* (2014) 63(6):2006–14. doi:10.2337/db13-1676
197. Giongo A, Gano KA, Crabb DB, Mukherjee N, Novelo LL, Casella G, et al. Toward defining the autoimmune microbiome for type 1 diabetes. *ISME J* (2011) 5(1):82–91. doi:10.1038/ismej.2010.92
198. Marino E, Richards JL, McLeod KH, Stanley D, Yap YA, Knight J, et al. Gut microbial metabolites limit the frequency of autoimmune T cells and protect against type 1 diabetes. *Nat Immunol* (2017) 18(5):552–62. doi:10.1038/ni.3713

199. Clemente-Casares X, Tsai S, Huang C, Santamaria P. Antigen-specific therapeutic approaches in Type 1 diabetes. *Cold Spring Harb Perspect Med* (2012) 2(2):a007773. doi:10.1101/cshperspect.a007773
200. Miller SD, Turley DM, Podojil JR. Antigen-specific tolerance strategies for the prevention and treatment of autoimmune disease. *Nat Rev Immunol* (2007) 7(9):665–77. doi:10.1038/nri2153
201. Smith EL, Peakman M. Peptide immunotherapy for type 1 diabetes-clinical advances. *Front Immunol* (2018) 9:392. doi:10.3389/fimmu.2018.00392
202. Pozzilli P, Gisella Cavallo M. Oral insulin and the induction of tolerance in man: reality or fantasy? *Diabetes Metab Res Rev* (2000) 16(5):306–7. doi:10.1002/1520-7560(200009/10)16:5<306::AID-DMRR150>3.0.CO;2-J
203. Skyler JS. Type 1 diabetes TrialNet Study G. Update on worldwide efforts to prevent type 1 diabetes. *Ann N Y Acad Sci* (2008) 1150:190–6. doi:10.1196/annals.1447.055
204. Skyler JS, Krischer JP, Wolfsdorf J, Cowie C, Palmer JP, Greenbaum C, et al. Effects of oral insulin in relatives of patients with type 1 diabetes: the diabetes prevention trial – type 1. *Diabetes Care* (2005) 28(5):1068–76. doi:10.2337/diacare.28.5.1068
205. Pozzilli P, Pitocco D, Visalli N, Cavallo MG, Buzzetti R, Crino A, et al. No effect of oral insulin on residual beta-cell function in recent-onset type I diabetes (the IMDIAB VII). IMDIAB Group. *Diabetologia* (2000) 43(8):1000–4. doi:10.1007/s001250051482
206. Chaillous L, Lefevre H, Thivolet C, Boitard C, Lahlou N, Atlan-Gepner C, et al. Oral insulin administration and residual beta-cell function in recent-onset type 1 diabetes: a multicentre randomised controlled trial. Diabete Insuline Orale group. *Lancet* (2000) 356(9229):545–9. doi:10.1016/S0140-6736(00)02579-4
207. Wherrett DK, Bundy B, Becker DJ, DiMeglio LA, Gitelman SE, Goland R, et al. Antigen-based therapy with glutamic acid decarboxylase (GAD) vaccine in patients with recent-onset type 1 diabetes: a randomised double-blind trial. *Lancet* (2011) 378(9788):319–27. doi:10.1016/S0140-6736(11)60895-7
208. Ludvigsson J, Krisky D, Casas R, Battelino T, Castano L, Greening J, et al. GAD65 antigen therapy in recently diagnosed type 1 diabetes mellitus. *N Engl J Med* (2012) 366(5):433–42. doi:10.1056/NEJMoa1107096
209. Awate S, Babiuk LA, Mutwiri G. Mechanisms of action of adjuvants. *Front Immunol* (2013) 4:114. doi:10.3389/fimmu.2013.00114
210. Axelsson S, Hjorth M, Akerman L, Ludvigsson J, Casas R. Early induction of GAD(65)-reactive Th2 response in type 1 diabetic children treated with alum-formulated GAD(65). *Diabetes Metab Res Rev* (2010) 26(7):559–68. doi:10.1002/dmrr.1126
211. Alleva DG, Gaur A, Jin L, Wegmann D, Gottlieb PA, Pahuja A, et al. Immunological characterization and therapeutic activity of an altered-peptide ligand, NBI-6024, based on the immunodominant type 1 diabetes autoantigen insulin B-chain (9-23) peptide. *Diabetes* (2002) 51(7):2126–34. doi:10.2337/diabetes.51.7.2126
212. Walter M, Philotheou A, Bonnici F, Ziegler AG, Jimenez R, Group NBIS. No effect of the altered peptide ligand NBI-6024 on beta-cell residual function and insulin needs in new-onset type 1 diabetes. *Diabetes Care* (2009) 32(11):2036–40. doi:10.2337/dc09-0449
213. Thrower SL, James L, Hall W, Green KM, Arif S, Allen JS, et al. Proinsulin peptide immunotherapy in type 1 diabetes: report of a first-in-man Phase I safety study. *Clin Exp Immunol* (2009) 155(2):156–65. doi:10.1111/j.1365-2249.2008.03814.x
214. Alhadj Ali M, Liu YF, Arif S, Tatovic D, Shariff H, Gibson VB, et al. Metabolic and immune effects of immunotherapy with proinsulin peptide in human new-onset type 1 diabetes. *Sci Transl Med* (2017) 9(402):eaaf7779. doi:10.1126/scitranslmed.aaf7779
215. Donnelly JJ, Wahren B, Liu MA. DNA vaccines: progress and challenges. *J Immunol* (2005) 175(2):633–9. doi:10.4049/jimmunol.175.2.633
216. Abdulhaqq SA, Weiner DB. DNA vaccines: developing new strategies to enhance immune responses. *Immunol Res* (2008) 42(1–3):219–32. doi:10.1007/s12026-008-8076-3
217. Goudy KS, Wang B, Tisch R. Gene gun-mediated DNA vaccination enhances antigen-specific immunotherapy at a late preclinical stage of type 1 diabetes in nonobese diabetic mice. *Clin Immunol* (2008) 129(1):49–57. doi:10.1016/j.clim.2008.06.001
218. Tisch R, Wang B, Weaver DJ, Liu B, Bui T, Arthos J, et al. Antigen-specific mediated suppression of beta cell autoimmunity by plasmid DNA vaccination. *J Immunol* (2001) 166(3):2122–32. doi:10.4049/jimmunol.166.3.2122
219. Seifarth C, Pop S, Liu B, Wong CP, Tisch R. More stringent conditions of plasmid DNA vaccination are required to protect grafted versus endogenous islets in nonobese diabetic mice. *J Immunol* (2003) 171(1):469–76. doi:10.4049/jimmunol.171.1.469
220. Weaver DJ Jr, Liu B, Tisch R. Plasmid DNAs encoding insulin and glutamic acid decarboxylase 65 have distinct effects on the progression of autoimmune diabetes in nonobese diabetic mice. *J Immunol* (2001) 167(1):586–92. doi:10.4049/jimmunol.167.1.586
221. Roep BO, Solvason N, Gottlieb PA, Abreu JRF, Harrison LC, Eisenbarth GS, et al. Plasmid-encoded proinsulin preserves C-peptide while specifically reducing proinsulin-specific CD8(+) T cells in type 1 diabetes. *Sci Transl Med* (2013) 5(191):191ra82. doi:10.1126/scitranslmed.3006103
222. Keselowsky BG, Xia CQ, Clare-Salzler M. Multifunctional dendritic cell-targeting polymeric microparticles: engineering new vaccines for type 1 diabetes. *Hum Vaccin* (2011) 7(1):37–44. doi:10.4161/hv.7.1.12916
223. Lewis JS, Allen RP. An introduction to biomaterial-based strategies for curbing autoimmunity. *Exp Biol Med (Maywood)* (2016) 241(10):1107–15. doi:10.1177/1535370216650294
224. Bachelder EM, Pino EN, Ainslie KM. Acetalated dextran: a tunable and acid-labile biopolymer with facile synthesis and a range of applications. *Chem Rev* (2017) 117(3):1915–26. doi:10.1021/acs.chemrev.6b00532
225. Chen N, Collier MA, Gallovic MD, Collins GC, Sanchez CC, Fernandes EQ, et al. Degradation of acetalated dextran can be broadly tuned based on cyclic acetal coverage and molecular weight. *Int J Pharm* (2016) 512(1):147–57. doi:10.1016/j.ijpharm.2016.08.031
226. Wattendorf U, Coullerez G, Voros J, Textor M, Merkle HP. Mannose-based molecular patterns on stealth microspheres for receptor-specific targeting of human antigen-presenting cells. *Langmuir* (2008) 24(20):11790–802. doi:10.1021/la801085d
227. Kwon YJ, James E, Shastri N, Frechet JM. In vivo targeting of dendritic cells for activation of cellular immunity using vaccine carriers based on pH-responsive microparticles. *Proc Natl Acad Sci U S A* (2005) 102(51):18264–8. doi:10.1073/pnas.0509541102
228. Cruz LJ, Tacken PJ, Fokkink R, Joosten B, Stuart MC, Albericio F, et al. Targeted PLGA nano- but not microparticles specifically deliver antigen to human dendritic cells via DC-SIGN in vitro. *J Control Release* (2010) 144(2):118–26. doi:10.1016/j.jconrel.2010.02.013
229. Machen J, Harnaha J, Lakomy R, Styche A, Trucco M, Giannoukakis N. Antisense oligonucleotides down-regulating costimulation confer diabetes-preventive properties to nonobese diabetic mouse dendritic cells. *J Immunol* (2004) 173(7):4331–41. doi:10.4049/jimmunol.173.7.4331
230. Phillips B, Nylander K, Harnaha J, Machen J, Lakomy R, Styche A, et al. A microsphere-based vaccine prevents and reverses new-onset autoimmune diabetes. *Diabetes* (2008) 57(6):1544–55. doi:10.2337/db07-0507
231. Engman C, Wen Y, Meng WS, Bottino R, Trucco M, Giannoukakis N. Generation of antigen-specific Foxp3+ regulatory T-cells in vivo following administration of diabetes-reversing tolerogenic microspheres does not require provision of antigen in the formulation. *Clin Immunol* (2015) 160(1):103–23. doi:10.1016/j.clim.2015.03.004
232. Yeste A, Takenaka MC, Mascanfroni ID, Nadeau M, Kenison JE, Patel B, et al. Tolerogenic nanoparticles inhibit T cell-mediated autoimmunity through SOCS2. *Sci Signal* (2016) 9(433):ra61. doi:10.1126/scisignal.aad0612
233. Tsai S, Shameli A, Yamanouchi J, Clemente-Casares X, Wang J, Serra P, et al. Reversal of autoimmunity by boosting memory-like autoregulatory T cells. *Immunity* (2010) 32(4):568–80. doi:10.1016/j.immuni.2010.03.015
234. Clemente-Casares X, Blanco J, Ambalavanan P, Yamanouchi J, Singha S, Fandos C, et al. Expanding antigen-specific regulatory networks to treat autoimmunity. *Nature* (2016) 530(7591):434–40. doi:10.1038/nature16962
235. Trahtemberg U, Mevorach D. Apoptotic cells induced signaling for immune homeostasis in macrophages and dendritic cells. *Front Immunol* (2017) 8:1356. doi:10.3389/fimmu.2017.01356
236. Vanderlugt CL, Neville KL, Nikcevich KM, Eagar TN, Bluestone JA, Miller SD. Pathologic role and temporal appearance of newly emerging autoepitopes in relapsing experimental autoimmune encephalomyelitis. *J Immunol* (2000) 164(2):670–8. doi:10.4049/jimmunol.164.2.670
237. Lutterotti A, Yousef S, Sputtek A, Sturner KH, Stellmann JP, Breiden P, et al. Antigen-specific tolerance by autologous myelin peptide-coupled cells: a phase 1 trial in multiple sclerosis. *Sci Transl Med* (2013) 5(188):188ra75. doi:10.1126/scitranslmed.3006168

238. Peschl P, Reindl M, Schanda K, Sospedra M, Martin R, Lutterotti A. Antibody responses following induction of antigen-specific tolerance with antigen-coupled cells. *Mult Scler* (2015) 21(5):651–5. doi:10.1177/1352458514549405
239. Kaufman A, Herold KC. Anti-CD3 mAbs for treatment of type 1 diabetes. *Diabetes Metab Res Rev* (2009) 25(4):302–6. doi:10.1002/dmrr.933
240. Izquierdo C, Ortiz AZ, Presa M, Malo S, Montoya A, Garabatos N, et al. Treatment of T1D via optimized expansion of antigen-specific Tregs induced by IL-2/anti-IL-2 monoclonal antibody complexes and peptide/MHC tetramers. *Sci Rep* (2018) 8(1):8106. doi:10.1038/s41598-018-26161-6

Conflict of Interest Statement: The authors declare that the research was conducted in the absence of any commercial or financial relationships that could be construed as a potential conflict of interest.

Copyright © 2018 Kroger, Clark, Ke and Tisch. This is an open-access article distributed under the terms of the Creative Commons Attribution License (CC BY). The use, distribution or reproduction in other forums is permitted, provided the original author(s) and the copyright owner(s) are credited and that the original publication in this journal is cited, in accordance with accepted academic practice. No use, distribution or reproduction is permitted which does not comply with these terms.

frontiers in Immunology

ORIGINAL RESEARCH
published: 04 September 2018
doi: 10.3389/fimmu.2018.02022

A Type I Interferon and IL-10 Induced by *Orientia tsutsugamushi* Infection Suppresses Antigen-Specific T Cells and Their Memory Responses

Chan-Ki Min [1,2†], Hong-Il Kim [1,2†], Na-Young Ha [1,2], Yuri Kim [1,2], Eun-Kyung Kwon [1,2], Nguyen Thi Hai Yen [1,2], Je-In Youn [2,3], Yoon Kyung Jeon [4], Kyung-Soo Inn [5], Myung-Sik Choi [1] and Nam-Hyuk Cho [1,2,3,6]*

[1] Department of Microbiology and Immunology, Seoul National University College of Medicine, Seoul, South Korea, [2] Department of Biomedical Sciences, Seoul National University College of Medicine, Seoul, South Korea, [3] Wide River Institute of Immunology, Seoul National University College of Medicine, Gangwon-do, South Korea, [4] Department of Pathology, Seoul National University College of Medicine, Seoul, South Korea, [5] Department of Pharmaceutical Science, College of Pharmacy, Kyung Hee University, Seoul, South Korea, [6] Institute of Endemic Disease, Seoul National University Medical Research Center and Bundang Hospital, Seoul, South Korea

OPEN ACCESS

Edited by:
Gustavo Javier Martinez, Rosalind Franklin University of Medicine and Science, United States

Reviewed by:
Werner Solbach, Universität zu Lübeck, Germany
Yongliang Zhang, National University of Singapore, Singapore

***Correspondence:**
Nam-Hyuk Cho
chonh@snu.ac.kr

[†]These authors have contributed equally to this work

Specialty section:
This article was submitted to Microbial Immunology, a section of the journal Frontiers in Immunology

Received: *08 May 2018*
Accepted: *16 August 2018*
Published: *04 September 2018*

Citation:
Min C-K, Kim H-I, Ha N-Y, Kim Y, Kwon E-K, Yen NTH, Youn J-I, Jeon YK, Inn K-S, Choi M-S and Cho N-H (2018) A Type I Interferon and IL-10 Induced by Orientia tsutsugamushi Infection Suppresses Antigen-Specific T Cells and Their Memory Responses. Front. Immunol. 9:2022. doi: 10.3389/fimmu.2018.02022

Despite the various roles of type I interferon (type I IFN) responses during bacterial infection, its specific effects *in vivo* have been poorly characterized in scrub typhus caused by *Orientia tsutsugamushi* infection. Here, we show that type I IFNs are primarily induced via intracellular nucleic acids sensors, including RIG-I/MAVS and cGAS/STING pathways, during *O. tsutsugamushi* invasion. However, type I IFN signaling did not significantly affect pathogenesis, mortality, or bacterial burden during primary infection *in vivo*, when assessed in a mice model lacking a receptor for type I IFNs (IFNAR KO). Rather, it significantly impaired the induction of antigen-specific T cells and reduced memory T cell responses. IFNAR KO mice that recovered from primary infection showed stronger antigen-specific T cell responses, especially Th1, and more efficiently controlled bacteremia during secondary infection than wild type mice. Enhanced IL-10 expression by macrophages in the presence of type I IFN signaling might play a significant role in the suppression of antigen-specific T cell responses as neutralization or knock-out (KO) of IL-10 increased T cell responses *in vitro*. Therefore, induction of the type I IFN/IL-10 axis by *O. tsutsugamushi* infection might play a significant role in the suppression of T cell responses and contribute to the short longevity of cell-mediated immunity, often observed in scrub typhus patients.

Keywords: scrub typhus, *Orientia tsutsugamushi*, type I interferon, IL-10, T cells, memory response, cell-mediated immunity

INTRODUCTION

Type I interferons (type I IFNs), including IFN-α and IFN-β, have diverse effects on innate and adaptive immune responses during viral and bacterial infections (1–3). Even though the antiviral role of type I IFNs has well-established (1), they are now known to have a myriad of effects in infectious diseases and other immuno-pathological conditions, directly and/or indirectly through

the induction of inflammatory mediators (2, 4, 5). In particular, the effect of type I IFN signaling induced during bacterial infection is associated with various downstream beneficial or detrimental consequences for the host depending on the type of bacterial pathogen (3, 6). Therefore, it is critical to distinguish the specific pathogen type- and context-dependent effects of the type I IFN responses to understand the underlying mechanisms of immune modulation during bacterial infection, as well as to design preventive and therapeutic measures for each specific infectious disease.

Expression of type I IFNs by bacterial infection can be initiated by recognition of pathogen-associated molecular patterns (PAMPs), such as nucleic acids, cell wall components, and lipoproteins derived from invading pathogens. These bacterial PAMPs induce type I IFN responses through multiple signaling pathways of various pattern recognition receptor (PRR) systems, including Toll-like receptors (TLRs)-myeloid differentiation factor 88 (MyD88)/TIR domain-containing adaptor-inducing IFN-β (TRIF), retinoic acid-inducing gene-I (RIG-I)-mitochondrial antiviral-signaling protein (MAVS), and the cyclic GMP-AMP synthase (cGAS)-stimulator of IFN genes (STING) pathways (3, 7). All these pathways eventually turn on type I IFNs gene expression, as well as other pro-inflammatory cytokines, via activation of transcription factors, IFN-regulatory factors (IRFs) and nuclear factor-κB (NF-κB) (2). Secreted type I IFNs bind to, and signal through a heterodimeric receptor, composed of IFNAR1 and IFNAR2 (2). Downstream signaling of IFNAR1 and IFNAR2 activates transcription factors, STAT1, STAT2, and IRF9, to form the IFN-stimulated gene factor 3 (ISGF3) complex, which binds to IFN-stimulated response elements (ISREs) in gene promoters, leading to induction of a large number of IFN-stimulated genes (ISGs) (2). Depending on the type of stimulus, the strength and durability of type I IFN production may vary and positively or negatively influence innate immune cell activation and regulation of adaptive immune responses. The reasons and molecular details for the dual actions of type I IFNs in bacterial infections remain poorly understood (8).

Scrub typhus is an acute febrile illness caused by infection with *Orientia tsutsugamushi* (9). This bacterium is an obligate intracellular pathogen transmitted from infected chigger mites to humans (10). The disease is currently a growing threat in Asia and the western Pacific region due to its rising incidence and continuous local outbreaks. In addition, scrub typhus is also emerging in unexpected geographical regions such as South America and Africa (11, 12), where disease endemicity has not been previously reported. Even though early diagnosis followed by appropriate antibiotic therapy can efficiently control the febrile illness, several problems, including relatively high mortality in untreated patients or after delayed diagnosis (13), potential antibiotic resistance (14), recurrent infection in highly endemic areas (15), and growing urbanization primarily due to ecological changes of mite vectors (16), pose challenges in the endemic area. Moreover, an effective vaccine for human infection is not yet available despite continuous efforts since the 1940s (17, 18).

O. tsutsugamushi infects human when chiggers feed on tissue fluid and disseminates systemically, targeting multiple organs such as the lung, kidney, liver, brain, and spleen (19). The intracellular pathogen has tropism for dendritic cells, monocytes/macrophages, and endothelial cells (10), where it replicates in the cytosol and induces multiple inflammatory mediators. Additionally, systemic *O. tsutsugamushi* infection in humans causes neutrophilia and CD4 T lymphopenia in the acute phase, followed by proliferation of CD8 T cells with activated phenotype during convalescent phase (20). Such potent immuno-pathological changes in innate and adaptive immune system might be associated with clinical presentations of scrub typhus such as eschar, fever, rash, lymphadenopathy, systemic vasculitis, and multi-organ failure often observed in fatal cases. It is also notable that adaptive immunity generated by primary infection generally rapidly wanes and does not last longer than a few years after infection (21). Particularly, cellular immunity, including CD4 and CD8 T cells specific to *O. tsutsugamushi* antigens, quickly decline from 1 year after infection (21). The short longevity of antigen-specific adaptive immunity might be attributable to limited memory responses, as observed in early vaccine studies using whole bacterial antigens as well as in human patients. Nevertheless, the underlying mechanisms of the short immune memory are poorly understood and remain to be elucidated for developing protective and long-lasting immunity.

Several studies have reported that *O. tsutsugamushi* induces type I IFN responses in monocytes/macrophages and dendritic cells *in vitro* (22, 23), as well as in peripheral blood mononuclear cells from scrub typhus patients (24). In addition, expression of type I IFNs induced by *O. tsutsugamushi* infection in dendritic cells is significantly higher than those by other intracellular bacteria, including *Coxiella burnetii* and *Brucella abortus,* both of which reside in vacuolar compartments (23). Since the effect of type I IFNs on the intracellular replication of *O. tsutsugamushi* is generally marginal (25), further studies are required to determine the exact role of type I IFNs in *O. tsutsugamushi* infection. Here, we investigate the signaling pathways involved in induction of type I IFNs by *O. tsutsugamushi* using several genetic knock-out (KO) systems and search for the potential effects of type I IFN signaling on bacterial pathogenesis as well as on antigen-specific adaptive immunity using mutant mice lacking a receptor subunit for type I IFNs, IFNAR1.

MATERIALS AND METHODS

Ethics Statement

Animal experiments were approved by the Seoul National University Institutional Animal Care and Use Committee (SNU IACUC, Permit No. SNU-100414-1) and performed in strict accordance with the recommendations in the National Guide Line for the care and use of laboratory animals.

Mice

Type I IFN receptor α-chain knock-out (IFNAR KO) 129/SvEv mice (26) were kindly provided by Dr. Heung Kyu Lee (Korea Advanced Institute of Science and Technology) and backcrossed with C57BL/6J more than seven generations. Splenocytes and

bone marrow cells from MyD88-, TRIF- [MyD88 KO (27), TRIF KO (28)], and IL-10-deficient C57BL/6 mice were provided by Dr. Jong-Hwan Park in Chonnam National University. MAVS knock-out [MAVS KO (29)] mice on C57BL/6 background were generously provided by Dr. Shizuo Akira (Osaka University). IFNAR KO and wild type C57BL/6 mice (Orient Bio, Seongnam, South Korea) were housed and maintained in the specific pathogen-free facility at Seoul National University College of Medicine.

Cell Culture

L929 mouse fibroblast cells were obtained from American Type Culture Collection (Rockville, MD, USA) and cultured in complete Dulbecco's modified Eagle's medium (DMEM, Gibco, Grand Island, NY, USA) containing 10% (vol/vol) heat-inactivated fetal bovine serum (FBS, Gibco), 100 μg/ml of streptomycin, 100 U/ml of penicillin in humidified 5% CO_2 atmosphere at 37°C. Mouse embryonic fibroblasts (MEF) were isolated from wild type and various KO mice. Embryos were isolated at E13.5 and were chopped and treated with 0.5% Trypsine-EDTA for 5 min at 37°C. Isolated MEF cells were cultured in humidified 5% CO_2 atmosphere at 37°C. MEF cells derived from RIG-I or STING-deficient mice were kindly provided by Dr. Jae U. Jung (University of Southern California). Bone marrow-derived macrophages (BMDMs) were generated from the bone marrow of 6- to 12-week-old wild type or various KO C57BL/6 mice as previously described (30). Briefly, bone marrow cells were flushed out of femurs and tibias with serum-free DMEM, filtered through a nylon cell strainer (70-μm Nylon mesh; BD Biosciences, San Jose, CA, USA), and washed twice with serum-free DMEM. The cells were then cultured for 4 days in complete DMEM containing 10% L929 cell culture media as a source of M-CSF. Bone marrow-derived dendritic cells were also generated from the bone marrow cells by culturing them with complete Iscove's Modified Dulbecco's Medium (IMDM, Gibco) supplemented with 10% FBS, recombinant mouse GM-CSF (1.5 ng/ml; PeproTech, Rocky Hill, NJ, USA) and mouse IL-4 (1.5 ng/ml; PeproTech), penicillin (100 units/ml), streptomycin (100 μg/ml), gentamicin (50 μg/ml), L-glutamine (2 mM), and β-mercaptoethanol (50 nM; Gibco Invitrogen) for 6 days (31). Differentiated BMDCs were harvested using the CD11c microbeads kit (MACS, Gladbach, Germany).

Preparation of *Orientia tsutsugamushi* and Infection Study

O. tsutsugamushi Boryong strain was purified using a modified Percoll gradient purification method (17). *O. tsutsugamushi* was propagated in L929 cells. At 3–4 days post-infection, infectivity was determined using an indirect immunofluorescence assay. When an infection rate of >90% was achieved, the cells were harvested by centrifugation at 500 × g for 4 min. The cell pellet was resuspended with 6.5 ml of Tris-sucrose (TS) buffer (33 mM Tris-Cl [pH 7.4], 0.25 M sucrose) and the cells were homogenized using 100 strokes of a Polytron homogenizer (Wheaton Inc., Millville, NJ, USA) followed by centrifugation at 200 × g for 5 min. The supernatant was then mixed with 40% Percoll (Pharmacia Fine Chemicals, Uppsala, Sweden) in TS buffer and centrifuged at 25,000 × g for 60 min. The bacterial band was collected and centrifuged at 77,000 × g for 30 min. The bacterial pellet was washed three times in TS buffer, resuspended in DMEM and stored in liquid nitrogen until use. The infectivity titer of the inoculum was determined as previously described (17). For infection assays, cell cultures in 24 well plate were infected with 2.5×10^6 infected-cell counting unit (ICU) (17) of *O. tsutsugamushi* (∼4 bacteria/cell). In every infection study, we confirmed that more than 90% of the cells were infected with *O. tsutsugamushi* after 2 h of incubation. Fifty percent of lethal dose (LD_{50}) were determined in wild type C57BL/6J.

Histopathologic Analysis of Infected Tissues

All the isolated tissues were fixed in 4% paraformaldhehyde (Sigma-Aldrich, St. Louis, MO, USA) and embedded in paraffin. Tissue sections (10 μm thickness) were stained with hematoxylin and eosin. Stained lung tissue sections were scanned and scored at the pathology core facility of Seoul National University College of Medicine, following standard procedures. We used a 0–4 scoring system: grade 0, normal; grade 1, widening of alveolar septa with scattered inflammatory cells in focal areas of pulmonary parenchyma and focal inflammatory cells around bronchovascular bundles (<10% of lung); grade 2, widening of alveolar septa with scattered inflammatory cells in multifocal areas of pulmonary parenchyma and around bronchovascular bundles (10–50% of lung); grade 3, widening of alveolar septa with diffuse inflammatory cell infiltrates present in the pulmonary parenchyma and bronchovascular bundles (more than 50% of lung); grade 4, grade 3 criteria plus area of atelectasis.

Determination of Bacterial Load

Bacterial loads of infected tissues were assessed by quantitative real-time PCR (qRT-PCR) as previously described (32). Briefly, DNA was extracted from the tissue samples using a DNeasy Kit (Qiagen, Gaithersburg, MD, USA), and the bacterial load was determined by using a primer set derived from the 47 kDa gene: p47 forward (5′-AACTGATTTTATTCAAA CTAATGCTGCT-3′), p47 reverse (5′-TATGCCTGA GTAAGATACATGAATGGAATT-3′), and detecting probe (5′-6FAM-TGGGTAGCTTTGGTGGACCGATGTTTAATCT-TAMRA-3′). Bacterial loads were normalized to total μg of DNA per ml for the same sample and expressed as the number of 47 kDa gene copies per μg of total DNA.

RNA Purification and Quantitative Reverse Transcriptase PCR (qRT-PCR)

Total RNA was extracted from cells using Trizol reagent (Sigma-Aldrich, St. Louis, MO, USA) according to the manufacturer's instruction. Approximately 1 microgram of total RNA was reverse transcribed by Eco-dry cDNA Synthesis kit containing poly-dT primer (Clonetech, Mountain View, CA, USA). The quantification of cDNA was performed with gene specific primers using Power SYBR green PCR Master Mix (Applied Biosystems, Grand Island, NY, USA) and processed using the ABI 7500 (Applied Biosystems). The primer sequences are as follows: β-actin (forward: GTGACGTTGACATCCGTAAAGA,

reverse: GCCGGACTCATCGTACTCC), IFN-β3 (forward: ATGGTGGTCCGAGCAGAGAT, reverse: CCACCACTC ATTCTGAGGCA), and TNF-α3 (forward: TCCCCAAAGG GATGAGAAGTT, reverse: GTTTGCTACGACGTGGGCTAC). The relative level of gene expression was calculated by the 2^{-dCt} or the ddCt method (33), where β-actin transcripts was used for normalization. The qRT-PCR data represent the average of three independent experiments.

Cytokine Assay

The concentrations of cytokines in sera from infected mice or cell cultures were measured using mouse cytokine/chemokine magnetic bead panel 96-well plate assay according to the manufacturer's instructions (Merck Millipore, Darmstadt, Germany). The cytokines analyzed in this study are tumor necrosis factor (TNF-α), interferon-γ (IFN-γ), interleukin-2 (IL-2), IL-4, IL-6, IL-10, IL-1β, and IL-12(p70). Concentration of secreted IFN-β in cell culture supernatants were determined by ELISA (R&D systems, Minneapolis, MN, USA) according to the manufacturer's instruction.

Enzyme-Linked Immunosorbent Assay (ELISA)

The level of antibodies specific to TSA56 in the sera of infected mice was analyzed ELISA as previously described (34). Immunoassay plates (96-well plates; Nunc, Rochester, NY, USA) were coated with 100 μl of purified antigen at a concentration of 5 μg/ml at 4°C overnight. The plates were then blocked for 2 h at room temperature with PBS containing 1% BSA. Hundred microliters of serum samples serially diluted in two-fold were incubated for 2 h at room temperature. After washing with PBS containing 0.05% Tween20 (PBST), horseradish peroxidase (HRP)-conjugated goat anti-mouse IgG (Santa Cruz Biotechnology, Santa Cruz, CA, USA) was added and incubated for 2 h at room temperature. Wells were washed with PBST and incubated with 3,3′,5,5′-tetramethylbenzidine (TMB) peroxidase substrate solution (KPL, Gaithersburg, MD, USA) for 10 min. The reactions were stopped by addition of 1 M phosphoric acid solution. Absorbance was measured at 450 nm using a microplate reader (Beckman Coulter Inc., Fullerton, CA, USA).

Type I IFN Bioassay

Cell-culture supernatants from stimulated cells or sera from infected mice were incubated with L929 cells containing a stable IFN-stimulated response element-luciferase reporter plasmid [ISRE-luc (35)] for 4 h. The reporter cells were lysed in Passive Lysis Buffer (Promega, Madison, WI, USA) for 30 min at room temperature, mixed with firefly luciferin substrate (Promega), and measured on a luminometer (Becman coulter, Fullerton, CA, USA).

Cytokine Neutralization Assay

Splenocytes (2×10^6 cells/24-well) isolated from IFNAR KO mice were infected with *O. tsutsugamushi* for 1 day and further incubated in the presence of tetracycline (0.3 μg/ml) for 3 days. Neutralizing monoclonal antibodies, such as anti-IL-1β (clone B122, eBioscience, San Diego, CA, USA), anti-IL-6 (clone MP5-20F3, eBioscience), and anti-IL-10 (clone JES5-2A5, Biolegend, San Diego, CA, USA), as well as isotype control antibody (murine IgG_1, Biolegend), were added to the culture media (10 μg/ml each/24-well) of the infection assays. Cells were then stimulated with 10 μg of TSA56 for an additional 18 h and 1 μg of Golgiplug (BD Bioscience) for the final 6 h in humidified CO_2 atmosphere at 37°C. Harvested splenocytes were stained with specific antibodies and analyzed by flow cytometry as described below.

Flow Cytometry

Spelnocytes were stained with antibodies against the indicated surface molecules after blocking on ice for 30 min with ultra-block solution containing 10% rat sera, 10% hamster sera, 10% mouse sera (Sigma, St. Louis, MO, USA), and 10 μg/ml of anti-CD16/32 (2.4G2; BD Pharmingen, Franklin Lakes, NJ, USA). Anti-CD44 (IM7, from Biolegend), CD3 (145-2CD11), CD4 (RM4-5), CD69 (H1.2F3), CD8 (53-6.7) (from eBioscience), CD62L (MEL-1, from BD Pharmingen) antibodies, and annexin V (BD Pharmingen) conjugated to differential fluorescent dyes were used for flow cytometric analysis. Cells were also stained with 7-AAD (BD Pharmingen) for dead cell exclusion in some experiments. For intracellular detection of IFN-γ and TNF-α, splenocytes (1×10^6 cells) were stimulated with 10 μg of purified TSA56 antigen and 1 μg Golgiplug (BD Bioscience) for the final 6 h in humidified CO_2 atmosphere at 37°C. Stimulated cells were then stained with the indicated surface markers. Surface-stained cells were fixed and permeabilized with Fixation and Permeabilization Solution (BD Bioscience), followed by incubation with anti-IFN-γ (XMG1.2; BD Pharmingen) and TNF-α (MF6-XT22, Affymetrix, Cleveland, OH) antibodies. Fluorescence intensities of the stained molecules were examined on a FACS Fortessa II flow cytometer (BD Biosciences). Data were analyzed using Flowjo software (Tree Star, Ashland, OR, USA). Gating strategies for the flow cytometric analysis are summarized in **Figure S1** (Supplementary data).

Statistical Analysis

The data was analyzed using Graph Pad Prism 5.01 software (GraphPad Software, La Jolla, CA, USA). Statistical analysis was performed using two-tailed Student's *t*-test with 95% confidence interval or one-way analysis of variance (ANOVA) followed by Newman-Keuls *t*-test for comparisons of values among different groups. Data are expressed as the mean ± standard deviation. Statistical analysis on survival rates were performed using the Mantel-Cox Log Rank test. A p-value of < 0.05 was considered statistically significant.

RESULTS

Induction of Type I IFN Responses by *O. tsutsugamushi* Infection

To confirm the induction of type I IFNs by *O. tsutsugamushi*, non-phagocytic MEFs and phagocytic BMDMs were infected *in vitro* with *O. tsutsugamushi* and the relative levels of IFN-β transcripts were assessed by quantitative real-time PCR. The

results demonstrated a rapid upregulation of mRNA expression of IFN-β, as well as TNF-α, in MEFs and BMDMs with peak responses at 4 h after infection (**Figures 1A,B**). Secretion of type I IFNs from the infected cells was further confirmed by type I IFN bioassay using L929 cells harboring ISRE-luc after stimulation with culture supernatants collected from infected cells at the indicated times (**Figures 1A,B**, middle). Secreted IFN-β from infected BMDMs was also detectable by ELISA at 18 h after infection (**Figure 1C**). In addition, we also observed a gradual increase of type I IFN activity in the sera of infected mice, as measured type I IFN bioassay (**Figure 1D**). These results clearly demonstrate that type I IFN responses are significantly upregulated during *O. tsutsugamushi* infection *in vitro* and *in vivo*.

Role of Intracellular Nuclear Acid Sensor Pathways in the Induction of Type I IFN Responses by *O. tsutsugamushi* Infection

Induction of type I IFNs by the intracellular bacterial pathogen may be mediated by various innate pattern-recognition receptors (PRRs) during the infection process. In order to assess the potential role of diverse PRRs for the induction of type I IFNs in *O. tsutsugamushi* infection, we infected MEFs derived from KO mice lacking MAVS, RIG-I, or STING, and their wild type littermates (**Figure 2A**). Expression of IFN-β transcripts was severely impaired in MEFs deficient in intracellular nucleic acid sensors and adaptor compared to wild type MEFs. In addition, secretion of type I IFNs after the bacterial infection was abrogated in all the three KO MEFs, as measured by type I IFN bioassays (**Figure 2A**, middle). It is also notable that expression of TNF-α mRNAs was also drastically suppressed in all the KO MEFs upon bacterial infection, suggesting a significant role of RIG-I/MAVS and STING signaling pathways in non-phagocytic host cells. Since the potential role of other PRRs, including TLRs, for the induction of inflammatory cytokines during the bacterial infection has been reported (36), we examined the expression of type I IFN and TNF-α in professional phagocytic BMDMs lacking MyD88 or TRIF, the essential adaptors for TLR signaling. As seen in **Figure 2B**, expression of type I IFN was generally intact in BMDMs derived from the two different KO mice and comparable to that of wild type phagocytes. However, expression of TNF-α mRNAs was impaired in MyD88-deficient cells, but not in BMDMs lacking TRIF, indicating a specific role of MyD88 for the induction of TNF-α in professional phagocytes. Taken together, the induction of type I IFN responses during *O. tsutsugamushi* infection might be primarily associated with the RIG-I/MAVS and STING signaling pathways, with minor contribution by TLR signaling mediated by MyD88 and/or TRIF adaptors.

Role of Type I IFN Signaling in Pathogenesis and Bacterial Burden During *O. tsutsugamushi* Infection *in vivo*

In order to assess the effect of type I IFN responses on the pathogenesis of *O. tsutsugamushi* infection, we first evaluated the survival rate of wild type and mutant mice deficient in a receptor subunit for IFN-α and IFN-β (IFNAR KO) after intraperitoneal infection with fatal dose ($5 \times LD_{50}$) of *O. tsutsugamushi* (**Figure 3A**). Both the wild type and IFNAR KO mice similarly succumbed to *O. tsutsugamushi* infection within 3 weeks after infection. The survival rate of the IFNAR KO mice was not significantly different from wild type mice even when infected with lower ($1 \times LD_{50}$) or higher ($100 \times LD_{50}$) dose of the intracellular pathogen (**Figure S2** in Supplementary data). Nevertheless, we consistently observed that IFNAR KO mice more rapidly lost weight than wild type mice, but without statistical significance (**Figure 3A**, right). Since the lung and spleen are the primary target organs in the mouse infection model for scrub typhus (32), we also measured the bacterial loads and observed histopathologic changes in the infected organs of lethally infected mice at various time points (**Figures 3B–D** and **Figure S3** in Supplementary data). The bacterial burden in the lungs of infected mice gradually increased in both mice groups (**Figure 3B**). Pathologic examination of the lungs revealed that pulmonary lesions and interstitial pneumonia progressed similarly in wild type and IFNAR KO mice (**Figures 3C,D**). Even though the bacterial burdens and pathological changes in the lungs of IFNAR KO mice seem to be slightly more severe than wild type mice, those differences were not statistically significant. The spleens were also gradually enlarged with disintegration of follicular structures (**Figure S3**). The histological changes and the bacterial loads observed in the spleens of infected mice were also not significantly different between wild type and IFNAR KO mice (**Figure S3**). These results suggest that type I IFN signaling induced by *O. tsutsugamushi* infection does not significantly affect bacterial proliferation *in vivo* and the pathologic process of acute lethal infections.

Enhanced T Cell Responses and Memory Against *O. tsutsugamushi* Antigen in the Absence of Type I IFN Signaling

To evaluate whether type I IFN signaling affects immune responses against the bacterial pathogen, we infected wild type and IFNAR KO mice with a lethal dose ($5 \times LD_{50}$) of *O. tsutsugamushi* and examined various inflammatory cytokines in the plasma (**Figure 4A**). The inflammatory cytokines including IFN-γ, IL-6, 1L-10, and TNF-α gradually increased in both mice groups as the disease progressed. Interestingly, the plasma levels of IFN-γ in IFNAR KO mice were significantly higher than those of wild type mice at 12 days after infection, while responses of other inflammatory cytokines were similar between wild type and IFNAR KO mice (**Figure 4A**). This result prompted us to assess antigen-specific T cell responses in the infected mice since IFN-γ is a hallmark cytokine for Th1 response. We first measured the changes in the fraction of Th1 cells in the infected mice at 12 days after infection. Although the overall fractions of $CD4^+$ T cells of both mice groups were similar and significantly reduced by ∼35% among spleen lymphocytes at 12 days after infection, T-bet^+/$CD44^+$ activated Th1 cells in the spleens of IFNAR KO mice were significantly higher than those of wild type mice (**Figure 4B**). Furthermore, the proportion of IFN-γ-secreting Th1 cells was also upregulated among activated ($CD44^+$) T cell populations upon stimulation with

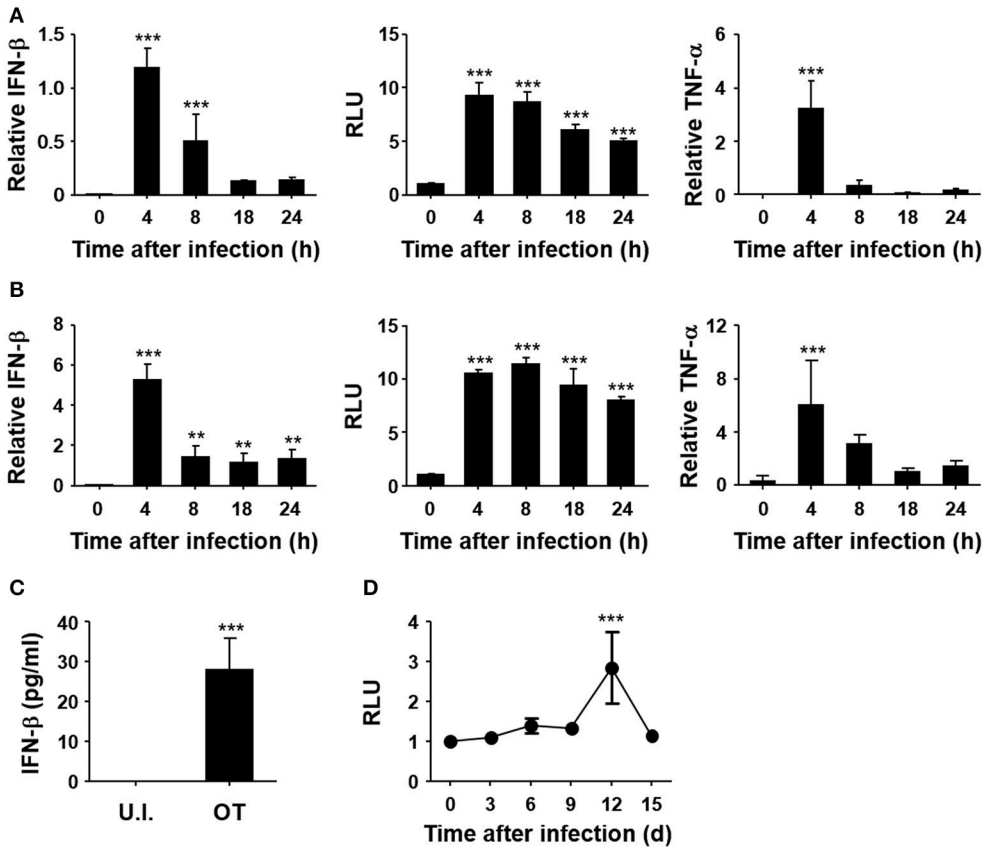

FIGURE 1 | Induction of type I IFN by *O. tsutsugamushi* infection. Mouse embryonic fibroblasts (MEFs, **A**) and bone marrow-derived macrophages (BMDMs, **B**) were infected with *O. tsutsugamushi* and harvested at the indicated time points. Total RNA was isolated from the infected cells and the relative levels of IFN-β (left) and TNF-α (right) transcripts, normalized with β-actin mRNA, were determined by qRT-PCR. Type I IFN bioactivity (middle) was also analyzed in L929 cells containing a stable ISRE-luciferase reporter plasmid after stimulation with culture supernatants collected at the indicated times. **(C)** Secreted IFN-β from infected BMDMs was analyzed by ELISA after 18 h of infection. U.I., uninfected; OT, *O. tsutsugamushi*-infected. **(D)** Mice were infected with 5 × LD_{50} of *O. tsutsugamushi* and type I IFN bioactivity in plasma collected at the indicated times was determined in L929 cells containing a stable ISRE-luciferase reporter plasmid. Data represent mean ± SD of three independent experiments. Statistical significance was determined by one-way analysis of variance (ANOVA) followed by Newman-Keuls *t*-test for comparisons with uninfected control. ***$p < 0.001$, **$p < 0.01$. RLU, relative luciferase unit.

TSA56, a major outer membrane antigen of *O. tsutsugamushi* (**Figure 4C**). These results clearly indicate that generation of antigen-specific Th1 lymphocytes were significantly enhanced in the absence of type I IFN signaling during acute bacterial infection.

In order to investigate whether enhanced T cell responses in the absence of type I IFN signaling during the acute phase of infection is linked to stronger memory T responses, we challenged the mice with lethal doses (5 × LD_{50}) of *O. tsutsugamushi* and treated them with tetracycline at 2 weeks after the initial infection. We confirmed the clearance of the bacterial pathogens by quantitation of bacterial genes in the lungs and spleens of infected mice and by observing mice morbidity during the third week after the pathogen challenge. At 6 weeks after the initial challenge with *O. tsutsugamushi*, splenocytes were collected from the cured mice and assessed for antigen-specific memory T cells by flow cytometry (**Figure 5A**). We observed there was no significant difference in the relative frequencies and absolute counts of T cells between wild type and IFNAR KO mice (**Table S1**). However, the proportion of IFN-γ-secreting CD4 T cells (average: 9.2%, $n = 5$) among memory T cells ($CD62L^{-}/CD44^{+}/CD4^{+}$) in IFNAR KO mice was three times higher than that of wild type mice (average: 2.8%, $n = 5$) when cells were stimulated with TSA56 (**Figure 5A**). Antibody (IgG) responses specific to TSA56 antigen were similar between wild type and IFNAR KO mice (**Figure 5B**). These results indicate that type I IFN responses induced by *O. tsutsugamushi* infection specifically suppress antigen-specific Th1 responses, but do not significantly affect humoral immunity against the bacterium. To assess the potential protective role of enhanced cellular memory against *O. tsutsugamushi*, we challenged the cured mice with lethal doses (5 × LD_{50}) of *O. tsutsugamushi* at 6 weeks after initial infection and observed the morbidity of infected mice. Both wild type and IFNAR KO mice showed no significant difference in morbidity and weight changes and all the mice were protected from the second challenge. However,

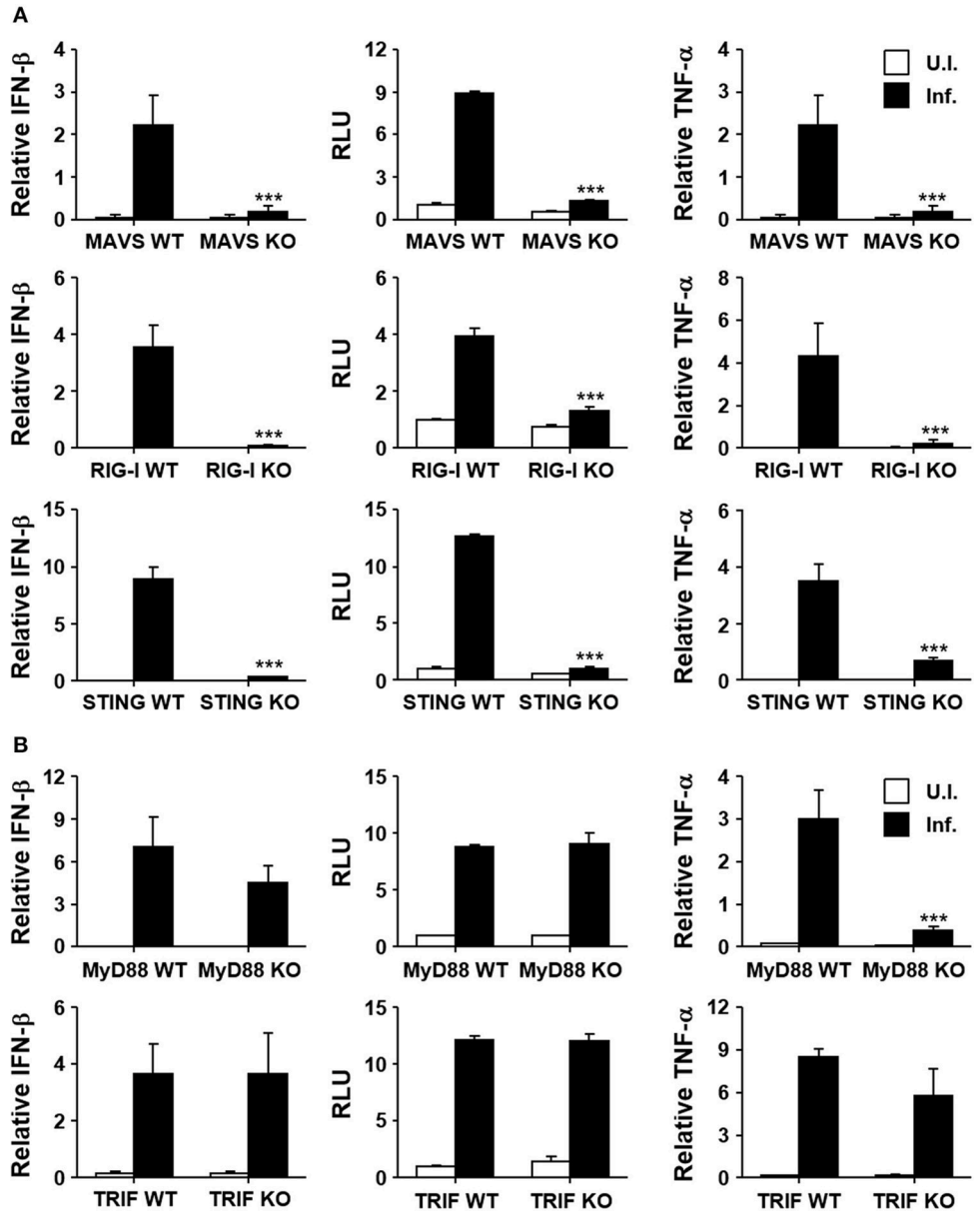

FIGURE 2 | Induction of type I IFN by *O. tsutsugamushi* infection through RIG-I/MAVS and STING. **(A)** MEFs derived from wild type (WT), MAVS-deficient (MAVS KO), RIG-I-deficient (RIG-I KO), or STING-deficient (STING KO) mice were infected with *O. tsutsugamushi* and the relative expression of IFN-β and TNF-α mRNA, as well as type I IFN bioactivity, were analyzed at 4 h after infection as describe in **Figure 1**. **(B)** BMDMs derived from wild type (WT), MyD88-deficient (MyD88 KO), or TRIF-deficient (TRIF KO) mice were infected with *O. tsutsugamushi* and the relative expression of IFN-β and TNF-α mRNA, as well as type I IFN bioactivity, were determined at 4 h after infection as described in **Figure 1**. Data represent mean ± SD of three independent experiments. Statistical significance was determined by two-tailed Student's *t*-test with 95% confidence interval for comparisons of values between wild type and KO cells after infection with *O. tsutsugamushi*. ***$p < 0.001$. RLU, relative luciferase unit. White box, uninfected (U.I.); black box, infected (Inf.).

O. tsutsugamushi was transiently detected in the lungs of several wild type mice at days 4 and 7 after infection, whereas the bacterial gene was barely detected in IFNAR KO mice after the second challenge (**Figure 5C**). These results suggest that enhanced T cell memory in IFNAR KO mice more efficiently protect them from systemic bacteremia after the second challenge than wild type mice.

Enhanced Expression of IL-10 by Type I IFN Response Is Associated With Suppression of T Cell Responses During the Acute Phase of Infection

To reveal the underlying mechanisms involved in the suppression of T cell responses by type I IFN responses during the acute phase

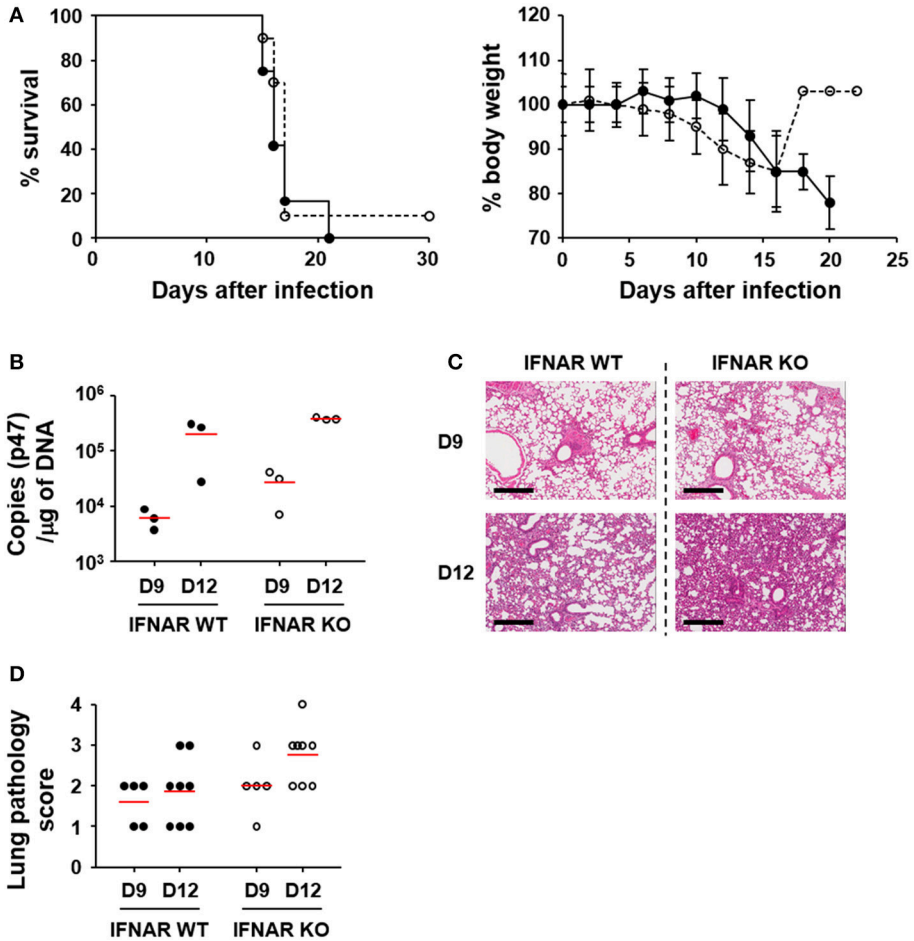

FIGURE 3 | Effect of type I IFN signaling on mortality, pathogenesis, and bacterial loads in *in vivo* infection of *O. tsutsugamushi*. **(A)** Wild type (black circle) and IFNAR-deficient (white circle) mice ($n = 10$) were intraperitoneally infected with 5 × LD_{50} of *O. tsutsugamushi* and survival rate and weight changes (relative to initial body weight on day 0) were monitored for a month. **(B)** Bacterial loads in the lungs of infected mice (wild type or IFNAR KO, $n = 3$/group) were assessed by qRT-PCR using primer sets detecting the p47 gene of *O. tsutsugamushi*. The infected tissues were collected at the indicated days after infection. **(C)** Lung tissue sections collected from mice at the indicated days after infection were stained with hematoxylin and eosin and representative scanned images are presented (see also **Figure S2**). Bar, 300 μm. **(D)** Pathological scores of infected lungs (D9: $n = 5$, D12: $n = 8$) are presented. Red lines, mean.

of bacterial infection, we performed *in vitro* infection assays using antigen-presenting phagocytes, BMDMs and BMDCs, from wild type and IFNAR KO mice and measured the levels of inflammatory cytokines produced upon *O. tsutsugamushi* infection (**Figure 6A**). Among the cytokines expressed by BMDMs infected with *O. tsutsugamushi*, the levels of IL-6 and IL-10 were significantly reduced in cells lacking IFNAR at 36 h after infection when compared to those of wild type macrophages. The production levels of IL-1β and TNF-α were similar in both primary phagocytic cells. In contrast, we observed significantly higher expression levels of IL-1β by IFNAR KO BMDCs than wild type dendritic cells when infected with the bacterial pathogen, whereas secretion of IL-6, IL-10, and TNF-α were similar in both dendritic cell groups. Expression of IL-12 (p70) was barely detectable in phagocytic cells infected with *O. tsutsugamushi* (data not shown). To further delineate the potential roles of the cytokines differentially expressed during the priming of naïve T cells, splenocytes prepared from IFNAR KO mice were infected with *O. tsutsugamushi* for 1 day, treated with tetracycline from the second day, and further incubated for 2 more days. Then, we assessed the percentile of IFN-γ or TNF-α producing CD4 or CD8 T cells by flow cytometry at 4 days after initial infection. In order to assess the potential effect of the inflammatory cytokines during *in vitro* T cell priming, we added specific monoclonal antibodies that neutralize the cytokines to the infection culture (**Figure S4** in Supplementary data). Addition of isotype control antibody, anti-IL-1β, IL-6, or IL-10 antibodies did not significantly affect the generation of T cells expressing IFN-γ or TNF-α during *in vitro* infection and T cell priming. However, anti-IL-10 antibody slightly, but not significantly, enhanced the IFN-γ producing CD4 and CD8 T cell fraction when compared to other groups, suggesting that neutralization of IL-10 produced by *O. tsutsugamushi* infection may further increase the generation of antigen-specific T cells

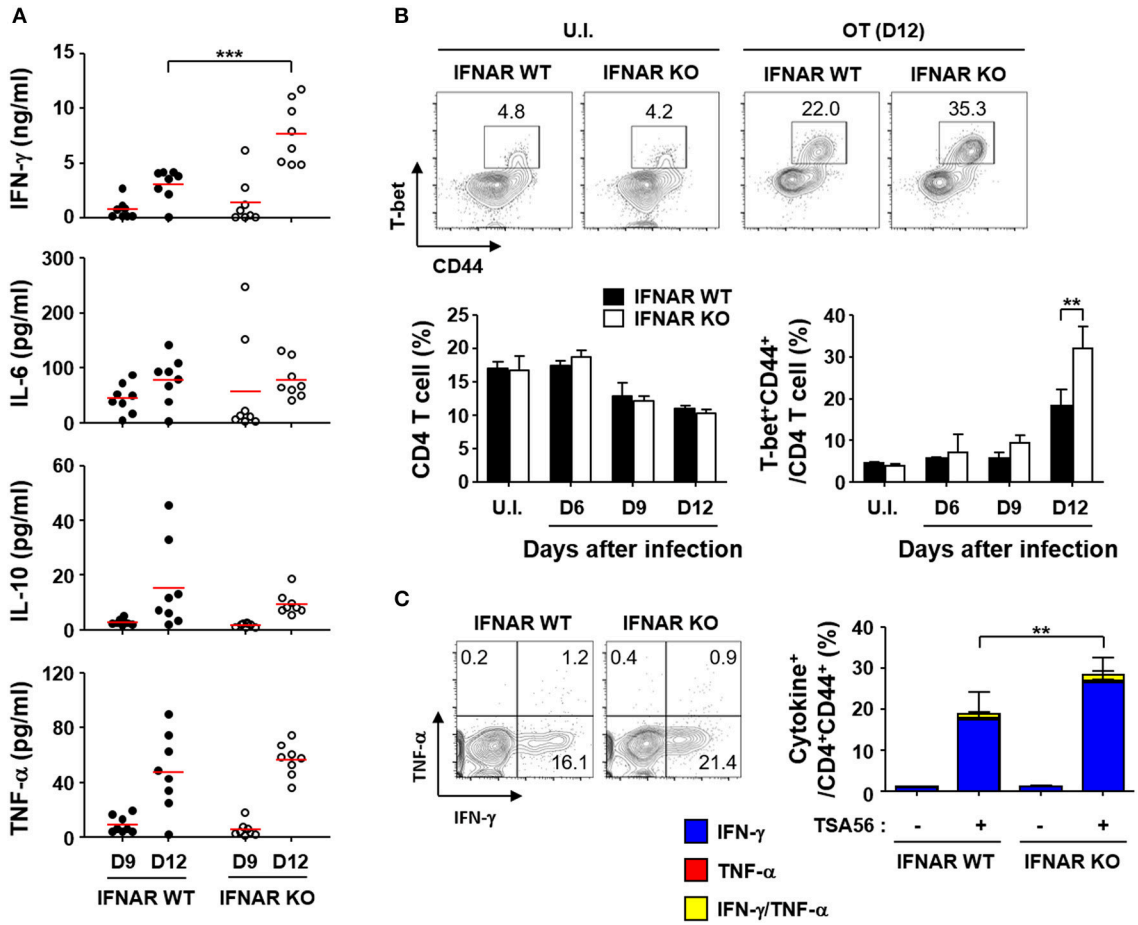

FIGURE 4 | Enhanced IFN-γ, Th1, and CD8 T cell responses by *O. tsutsugamushi* infection in the absence of type I IFN signaling. **(A)** Levels of cytokines in plasma collected at the indicated days after infection in wild type or IFNAR KO mice ($n = 8$/group) were determined. IL-2, IL-4, and IL-12p70 were barely detectable throughout the infection period (data not shown). Red line, mean; $^{***}p < 0.001$. **(B)** Proportion of T-bet^{+}CD44^{+} activated Th1 cells among CD4 T cells were analyzed in spleens of wild type and IFNAR KO mice infected by *O. tsutsugamushi*. Representative images of flow cytometric results are presented (upper) and proportion of CD4 T cells (lower left) and activated Th1 cells (lower right) are summarized ($n = 3$/group). Data represent mean + SD of three independent experiments. $^{**}p < 0.01$. U.I., uninfected; OT (D12), infected with *O. tsutsugamushi* for 12 days. **(C)** Splenocytes were collected from wild type and IFNAR KO mice at 12 days after infection with *O. tsutsugamushi* and production of IFN-γ and/or TNF-α in activated (CD44^{+}) CD4 T cells were analyzed by flow cytometry. Representative flow cytometric results are presented (left) and the percentile of cytokine positive cells among the activated T cell subsets are summarized (right graph) in the absence and presence of TSA56 antigen. Data represent mean + SD from wild type ($n = 5$) or IFNAR KO ($n = 8$) mice. $^{**}p < 0.01$. Blue box, IFN-γ-positive; red box, TNF-α-positve; yellow box, IFN-γ and TNF-α-positive.

during the priming stage in the absence of type I IFN signaling. To further confirm the role of secreted IL-10 in T cell priming, we isolated splenocytes from IL-10 KO mice, infected them with *O. tsutsugamushi*, and analyzed the number of IFN-γ or TNF-α producing T cells as described above. Both CD4 and CD8 T cell populations secreting TNF-α were significantly increased when wild type splenocytes were infected with *O. tsutsugamushi* ($p < 0.01$, **Figure 6B**). The proportion of CD4 T cells secreting TNF-α or IFN-γ and CD8 T cells producing IFN-γ were further elevated in infected IL-10 KO splenocytes ($p < 0.001$), indicating that expression of IL-10 during naive T cell priming upon infection suppresses the generation of T cell responses.

Taken together, macrophages infected with *O. tsutsugamushi* are the primary source of IL-10, which suppresses the generation of antigen-specific T cells, especially Th1 and CTLs, during the acute phase of infection. Type I IFN responses generated by *O. tsutsugamushi* infection enhances IL-10 secretion from macrophages, thereby impairing the initial priming of T cell responses as well as their long-term memory.

DISCUSSION

It was previously reported that induction of type I IFNs in monocyte/macrophages by *O. tsutsugamushi* is completely abrogated by heat-inactivation of the pathogen (22, 24). Considering that only live *O. tsutsugamushi* escapes into the cytosol from vesicular compartments or autophagosomes

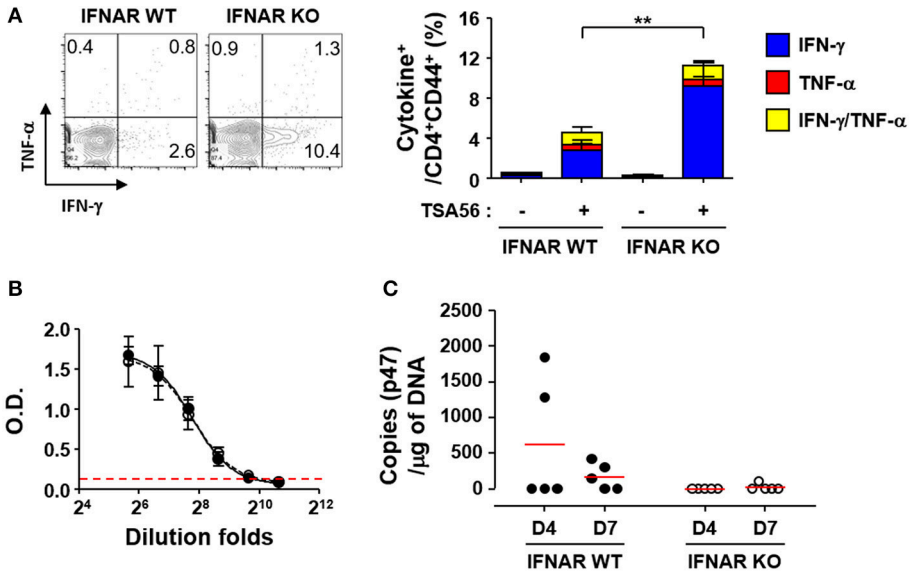

FIGURE 5 | Enhanced T cell memory responses by *O. tsutsugamushi* infection in the absence of type I IFN signaling. **(A)** Splenocytes were collected from cured wild type and IFNAR KO mice at 6 weeks after initial infection with *O. tsutsugamushi* and production of IFN-γ and/or TNF-α in activated ($CD44^+$) CD4 T cells were analyzed by flow cytometry. Mice were cured with tetracycline during the second week of lethal infection. Representative flow cytometric results are presented (left) and the percentile of cytokine positive cells among the activated T cell subsets are summarized (right graph) in the absence and presence of TSA56 antigen. Data represent mean + SD from wild type or IFNAR KO ($n = 5$) mice. $^{**}p < 0.01$. Blue box, IFN-γ-positive; red box, TNF-α-positve; yellow box, IFN-γ and TNF-α-positive. **(B)** Anti-TSA56 antibody (IgG) responses were analyzed in plasma from wild type (closed circles) and IFNAR KO (open circles) mice at 6 weeks after initial infection with *O. tsutsugamushi*. Optical densities (O.D.) of serially diluted samples ($n = 3$/group) were determined by ELISA. Red line: baseline O.D. + 3 × SD of plasma ($n = 3$, 1:100 diluted) from uninfected mice. **(C)** Bacterial loads in the lungs of infected mice (wild type or IFNAR KO, $n = 5$/group) were assessed by qRT-PCR using primer sets detecting the p47 gene of *O. tsutsugamushi*. Mice were again infected with *O. tsutsugamushi* at 6 weeks after the initial infection and the infected lungs were collected at the indicated days after the second infection and analyzed. Red line, mean.

of non-phagocytic and phagocytic host cells within a few hours after infection (31, 37, 38), active evasion from the vesicular compartments of host cells and subsequent exposure to intracellular PRRs is likely a critical opportunity for inducing type I IFNs. Our current results indicate that the RIG-I/MAVS and STING pathways are required for the induction of type I IFNs, but signaling adaptors for TLR pathways, MyD88 and TRIF, are dispensable in phagocytic cells (**Figure 2**). Since the cytosolic innate sensor systems detect nucleic acids from invading pathogen, active evasion from host trafficking vesicles and sequential release of nucleic acids from the bacteria may be the stimuli of cytosolic intracellular sensors. The ligand is possibly bacterial RNA, DNA, and/or cyclic dinucleotides (3). We also confirmed the role of cyclic GMP-AMP (cGAMP) synthase (cGAS), which detects cytosolic DNA and synthesizes cGAMP to stimulate STING, in expression of type I IFNs by knocking down cGAS in MEFs (**Figure S5** in Supplementary data). The involvement of the RIG-I/MAVS and cGAS/STING pathways in the induction of type I IFNs has been well-characterized in another intracellular pathogen, *Listeria monocytogenes*, that replicates in the cytosol of host cell (39, 40). Live *L. monocytogenes* actively escapes from phagosomes by expressing a cytolysin, listeolysin O (LLO), which disrupts the vacuolar membrane (41), and LLO-deficient *L. monocytogenes* fails to induce type I IFNs (39). Bacterial RNA and/or DNA can be released into cytosol either by an active secretion system or by bacteriolysis, which is recognized by RIG-I or IFI16/cGAS sensors, respectively (39, 40). IFI16 and cGAS co-localize with the bacterial DNA in the cytoplasm and are selectively recruited to DNA-activated STING signalosomes (40). Additionally, the downstream signaling components in RIG-I/MAVS and cGAS/STING pathways are physically and functionally interconnected, although distinct classes of receptors are responsible for RNA and DNA sensing (7). For example, the absence of STING expression is renders RIG-I unable to induce type I IFNs in response to cytoplasmic dsRNA (42) and Japanese encephalitis virus infection (43). Involvement of STING in transmitting RIG-I signaling might be mediated by the formation of the RIG-I/MAVS/STING complex upon intracellular pathogen infection (7). Conversely, knockdown of MAVS in host cells markedly reduces phosphorylation of TBK-1 and type I IFNs induced by cytoplasmic DNA (44). These may explain why the absence of one of the signaling components in either pathway abrogates the expression of type I IFNs by *O. tsutsugamushi* infection (**Figure 2**).

Second question is how nucleic acids of *O. tsutsugamushi* are released from the pathogen. It is interesting to note that mRNA expression of IFN-β peaked at 4 h after infection and decreased thereafter in both MEFs and BMDMs (**Figure 1**), suggesting a transient activation of type I IFNs during the early stage of intracellular invasion. Transient induction of IFN-β transcripts, peaking at 6 h after infection, in J774A.1 macrophages infected

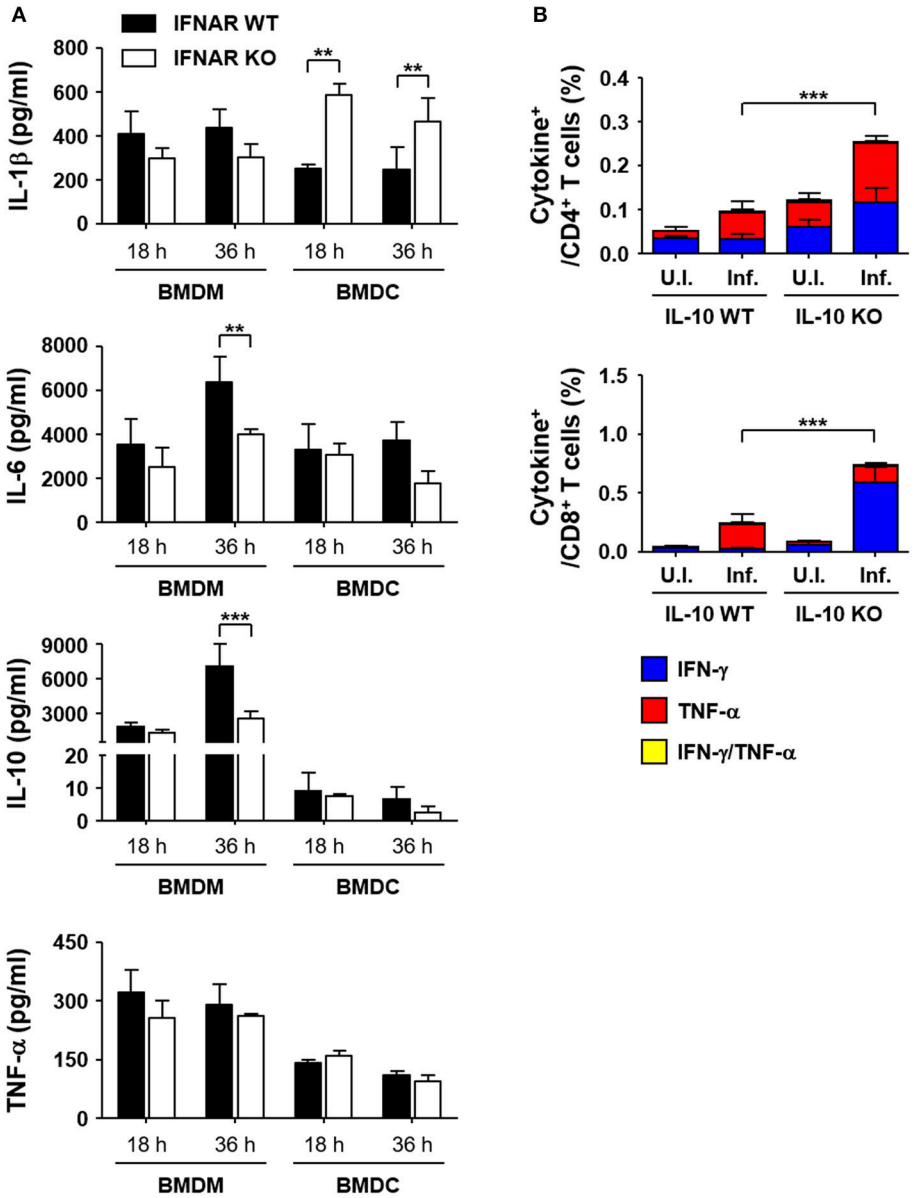

FIGURE 6 | Enhanced expression of IL-10 in macrophages infected with *O. tsutsugamushi* in the absence of type I IFN signaling and its role in T cell responses. **(A)** Levels of cytokines in culture supernatants of BMDMs or BMDCs infected with *O. tsutsugamushi* at the indicated times were analyzed. Phagocytic cells were differentiated from bone marrow cells from wild type (black box) and IFNAR KO (white box) mice and infected with the bacteria (~4 bacteria/cell). Data represent mean + SD from three independent experiments. $^{**}p < 0.01$; $^{***}p < 0.001$. (**B**) Splenocytes were collected from wild type and IL-10 KO mice infected with *O. tsutsugamushi*, and analyzed for production of IFN-γ and/or TNF-α in CD4 (upper) or CD8 T (lower) cells by flow cytometry. Splenocytes (2×10^6 cells/24-well) isolated from IL-10 KO mice were infected with *O. tsutsugamushi* for 1 day and further incubated in the presence of tetracycline (0.3 μg/ml) for 3 more days. Then, they were stained with specific antibodies and assessed by flow cytometry. Data represent mean + SD from three independent experiments. $^{***}p < 0.001$ for IFN-γ-positive T cells. Blue box, IFN-γ-positive; red box, TNF-α-positive; yellow box, IFN-γ and TNF-α-positive. U.I., uninfected; Inf., infected.

with *O. tsutsugamushi* was also observed in a previous study (22). Considering that escape of the intracellular pathogen from endocytic vesicles into the cytosol generally occurs within 2 h after infection (37), type I IFN transcripts might be transiently induced by *O. tsutsugamushi* during cytoplasmic invasion, but marginally generated during replication in the cytoplasm. Stimulation of nucleic acids-sensing pathways might be reduced during the subsequent cytoplasmic replication stage either by intermittent release of nucleic acids from the cytoplasmic bacteria or by active suppression of the signaling pathways. The true mechanisms induced by *O. tsutsugamushi* remain to be elucidated.

We also examined the potential role of type I IFN responses in *in vivo* pathogenesis of *O. tsutsugamushi* by infecting IFNAR KO

mice (**Figure 3** and **Figures S2**, **S3**). It is clear that the absence of type I IFN responses did not significantly affect the mortality of C57BL/6 mice (**Figure 3A** and **Figure S2**). The bacterial burdens in the lungs and spleens of infected mice were slightly higher in IFNAR KO mice, when compared to those of wild type, but not statistically significant (**Figure 3B** and **Figure S3**). In addition, the pathological changes of the lungs and spleens of IFNAR KO mice infected with *O. tsutsugamushi*, as well as weight changes, were not significantly different from those of wild type mice. Previously, it was reported that type I IFN induced by *Rickettsia prowazekii* or *Rickettsia conorii* suppresses the bacterial growth *in vitro* infection models (45, 46). However, type I IFN-mediated inhibition of *O. tsutsugamushi* replication *in vitro* varies but never becomes very pronounced (25). It was also shown that Addition of exogenous IFN-α/β (300–450 IU/ml), did not significantly affect the replication of *O. tsutsugamushi* Karp strain in MEFs derived from BALB/c and C3H mice, and Gilliam strain in C3H cells. A 50% decrease of plaque inhibition of Gilliam in BALB/c cells was achieved only with IFN-α/β concentrations over 300 IU/ml and the sensitivity of the Gilliam strain to IFN-α/β was at least 300-fold less than that of Encephalomyocarditis virus (25). Given that the concentration of IFN-β induced by BMDMs infected with *O. tsutsugamushi* Boryong strain, belonging to the Karp genogroup (47), is ∼30 pg/ml (**Figure 1C**, its concentration in plasma of infected mice was always below detection limit throughout the infection period) and 1 IU/ml of type I IFNs generally equals a few pg/ml range (48), physiological levels of type I IFNs induced by *O. tsutsugamushi* infection may not be sufficient to inhibit its replication *in vitro* and *in vivo*. Indeed, when we assessed replication of *O. tsutsugamushi* in BMBMs, there was no significant difference between wild type and IFNAR KO cells (data not shown). Therefore, endogenous type I IFN responses may have only marginal or no direct effects on the bacterial replication, but cytokine responses may critically indirectly influence inflammatory and/or antigen-specific immune responses.

When we assessed the levels of inflammatory cytokines in the sera of infected mice, the concentrations of IFN-γ, IL-6, IL-10, and TNF-α gradually increased in wild type mice, whereas IL-2, IL-4, and IL-12p70 were barely detectable throughout the infection period (**Figure 4A** and data not shown). Although the cytokine responses in IFNAR KO mice were similar to wild type, the level of IFN-γ was further elevated upon infection with *O. tsutsugamushi*, suggesting enhanced Th1 responses in the absence of type I IFN signaling. This phenotype was confirmed by a significant increase of T-bet^{+}CD44^{+} Th1 cell proportion, as well as IFN-γ-secreting activated CD4 T cells, among CD4 T cell population in IFNAR KO mice; however, the levels of CD4 T cell subsets were similarly decreased in both wild type and the mutant mice, potentially via cellular apoptosis, as we observed in scrub typhus patients previously (**Figures 4B,C** and **Table S2**) (20). The initial increase of antigen-specific Th1 responses were correlated with significant enhancement of memory T cells, and functionally associated with improved sterile immunity upon secondary bacterial challenge in IFNAR KO mice (**Figure 5**). Interestingly, TSA56-specific memory antibody (IgG) levels was not affected by the absence of type I IFN signaling, suggesting a specific role in downregulation of cell-mediated immunity, and no effect in humoral immune responses. Elevation of Th1 responses or systemic IFN-γ expression in the absence of type I IFN signaling have also been reported in mice models infected with *Ehrlichia* (49, 50), *Anaplasma* (51), *Chlamydia* (52), *Brucella* (53), and various other intracellular pathogens (3), but the negative effect of type I IFN responses on IFN-γ expression is either beneficial or detrimental to the host, depending on the pathogen. IFNAR KO mice were more resistant to fatal ehrlichiosis than wild type mice (49, 50), whereas *Ananaplasma phagocytophilum* infection was more highly pathogenic in STAT1 KO mice compared to wild type (51). In the case of primary lethal infection with *O. tsutsugamushi*, the magnitude of Th1 responses enhanced by the absence of type I IFN signaling may not be sufficient to provide protective cellular immunity. It was previously reported that CD8 T cell responses are required to protect against lethal infections with *O. tsutsugamushi*, but they also elicit specific pathologic tissue lesions in the liver and lung (54). Nevertheless, suppression of Th1 responses by type I IFNs during primary infection is clearly associated with reduced memory responses of antigen-specific T cells and may restrict sterile immunity against recurrent bacterial infection (**Figure 5**).

Finally, we tried to elucidate the underlying basis of how type I IFN responses induced by *O. tsutsugamushi* inhibit T cell responses. Among the various potential mechanisms exerted by type I IFNs, elevated IL-10 expression mediated by type I IFN signaling in infected macrophages might be one of the key factors in suppressing T cell responses (**Figure 6**) (2). The suppressive role of type I IFN/IL-10 during the generation of adaptive T cell immunity has been well-established in various infections (2, 55, 56). For example, IFNAR KO mice are less susceptible to *L. monocytogenes* infection since the intracellular pathogen induces massive apoptotic cell death of lymphocytes by type I IFN sensitization, subsequently leading to IL-10-mediated immunosuppression (55), which can reduce effector Th1 and/or CTL responses and the generation of memory CD4 and CD8 T cells (56, 57). Consistently, IL-10 KO mice are more resistant to *L. monocytogenes* infection, with enhanced control of bacterial replication in spleens and livers (55). In this study, we found that macrophages infected with *O. tsutsugamushi* massively produce IL-10 and wild type BMDMs (∼7.0 ng/ml) secrete 2.7 times more IL-10 compared to that of mutant BMDMs lacking IFNAR (∼2.6 ng/ml) at 36 h after infection, whereas the levels of IL-10 from BMDCs were generally <10 pg/ml in wild type and IFNAR KO cells (**Figure 6A**). Although the mechanisms by which type I IFNs promote IL-10 expression in macrophages are not fully understood, a recent study revealed central role of autocrine type I IFNs in increased production of IL-10 and increased IL-10 mRNA stability in macrophages, which is accompanied by increased STAT1 and IRF3 activation (58). The enhanced and prolonged expression of IL-10 is dependent on type I IFN-induced late ERK1/2 phosphorylation (58). Consistent with this, a previous study reported biphasic activation (an initial peak within 10–30 min and persistent activation from 2 to 8 h after infection) of ERK1/2 in murine macrophages supports positive feedback expression of IL-10 by induced type I IFNs (22). We also observed reduced IL-6

expression in IFNAR KO BMDMs at 36 h after infection and enhanced IL-1β secretion in BMDCs lacking IFNAR (**Figure 6A**). Even though the specific roles and regulatory mechanisms of reduced IL-6 expression in macrophages and enhanced IL-1β expression in dendritic cells during *O. tsutsugamushi* infection in the absence of type I IFN signaling needs to be further defined (2), our pilot study using specific neutralizing antibodies against the cytokines revealed that neutralization IL-10 enhances IFN-γ expression in T cells, whereas antibodies against IL-1β or IL-6 failed to do so (**Figure S4**). In addition, splenocytes derived from IL-10 KO mice produced significantly higher levels of IFN-γ when compared to those from wild type mice when infected with *O. tsutsugamushi* (**Figure 6B**). These clearly confirm the suppressive role of IL-10 in naïve T cell priming during bacterial infection. Enhanced expression of IL-10 by *O. tsutsugamushi* infection is consistent in *in vitro* and *in vivo* experiments, as well as studies in scrub typhus patients (10). Moreover, the potential role of IL-10 in the modulation of inflammatory responses and in wide spread tissue damage has also been documented during *O. tsutsugamushi* infection (59, 60).

Taken together, type I IFN responses induced by *O. tsutsugamushi* infection via intracellular nucleic acid sensor pathways in infected host cells contribute to enhanced production of IL-10, which in turn down-modulates antigen-specific T cells and their memory responses. We propose that the type I IFNs/IL-10 axis might play a critical role in suppressing the cellular immunity during acute phase infection, as well as the short longevity of T cell responses, often observed in scrub typhus patients.

AUTHOR CONTRIBUTIONS

C-KM and N-HC designed the experiments; C-KM, H-IK, N-YH, YK, E-KK, NY, YJ, and K-SI performed the experiments; C-KM, J-IY, YJ, K-SI, M-SC, and N-HC analyzed the results; C-KM, YJ, and N-HC wrote the manuscript; All authors read and approved the final manuscript.

FUNDING

This study was supported by the Basic Science Research Program through the National Research Foundation of Korea (NRF) funded by the Ministry of Science, ICT & Future Planning (2013R1A2A2A01007299). C-KM, H-IK, N-YH, YK, and NY received a scholarship from the BK21-plus education program provided by the National Research Foundation of Korea. The funders had no role in study design, data collection, and analysis, decision to publish, or preparation of the manuscript.

SUPPLEMENTARY MATERIAL

The Supplementary Material for this article can be found online at: https://www.frontiersin.org/articles/10.3389/fimmu.2018.02022/full#supplementary-material

REFERENCES

1. Crouse J, Kalinke U, Oxenius A. Regulation of antiviral T cell responses by type I interferons. *Nat Rev Immunol.* (2015) 15:231–42. doi: 10.1038/nri3806
2. McNab F, Mayer-Barber K, Sher A, Wack A, O'Garra A. Type I interferons in infectious disease. *Nat Rev Immunol.* (2015) 15:87–103. doi: 10.1038/nri3787
3. Snyder DT, Hedges JF, Jutila MA. Getting "inside" type I IFNs: type I IFNs in intracellular bacterial infections. *J Immunol Res.* (2017) 2017:9361802. doi: 10.1155/2017/9361802
4. Niewold TB. Type I interferon in human autoimmunity. *Front Immunol.* (2014) 5:306. doi: 10.3389/fimmu.2014.00306
5. Lee M, Rhee I. Cytokine signaling in tumor progression. *Immune Netw.* (2017) 17:214–27. doi: 10.4110/in.2017.17.4.214
6. Murira A, Lamarre A. Type-I interferon responses: from friend to foe in the battle against chronic viral infection. *Front Immunol.* (2016) 7:609. doi: 10.3389/fimmu.2016.00609
7. Zevini A, Olagnier D, Hiscottt J. Crosstalk between cytoplasmic RIG-I and STING sensing pathways. *Trends Immunol.* (2017) 38:194–205. doi: 10.1016/j.it.2016.12.004
8. Kovarik P, Castiglia V, Ivin M, Ebner F. Type I interferons in bacterial infections: a balancing act. *Front Immunol.* (2016) 7:652. doi: 10.3389/fimmu.2016.00652
9. Cho NH, Kim HR, Lee JH, Kim SY, Kim J, Cha S, et al. The *Orientia tsutsugamushi* genome reveals massive proliferation of conjugative type IV secretion system and host-cell interaction genes. *Proc Natl Acad Sci USA* (2007) 104:7981–6. doi: 10.1073/pnas.0611553104
10. Diaz FE, Abarca K, Kalergis AM. An update on host-pathogen interplay and modulation of immune responses during *Orientia tsutsugamushi* infection. *Clin Microbiol Rev.* (2018) 31:e00076-17. doi: 10.1128/CMR.00076-17
11. Maina AN, Farris CM, Odhiambo A, Jiang J, Laktabai J, Armstrong J, et al. Q fever, scrub typhus, and rickettsial diseases in children, Kenya, 2011-2012. *Emerg Infect Dis.* (2016) 22:883–6. doi: 10.3201/eid2205.150953
12. Weitzel T, Dittrich S, Lopez J, Phuklia W, Martinez-Valdebenito C, Velasquez K, et al. endemic scrub typhus in South America. *N Engl J Med.* (2016) 375:954–61. doi: 10.1056/NEJMoa1603657
13. Taylor AJ, Paris DH, Newton PN. A systematic review of mortality from untreated scrub typhus (*Orientia tsutsugamushi*). *PLoS Negl Trop Dis.* (2015) 9:e0003971. doi: 10.1371/journal.pntd.0003971
14. Mathai E, Rolain JM, Verghese GM, Abraham OC, Mathai D, Mathai M, et al. Outbreak of scrub typhus in southern India during the cooler months. *Ann N Y Acad Sci.* (2003) 990:359–64.
15. Koralur MC, Singh R, Varma M, Stenos J, Bairy I. Scrub typhus reinfection. *Trop Doct.* (2017) 48:69–72. doi: 10.1177/0049475517740310
16. Park SW, Ha NY, Ryu B, Bang JH, Song H, Kim Y, et al. Urbanization of scrub typhus disease in South Korea. *PLoS Negl Trop Dis.* (2015) 9:e0003814. doi: 10.1371/journal.pntd.0003814
17. Ha NY, Sharma P, Kim G, Kim Y, Min CK, Choi MS, et al. Immunization with an autotransporter protein of *Orientia tsutsugamushi* provides protective immunity against scrub typhus. *PLoS Negl Trop Dis.* (2015) 9:e0003585. doi: 10.1371/journal.pntd.0003585
18. Ha NY, Shin HM, Sharma P, Cho HA, Min CK, Kim HI, et al. Generation of protective immunity against *Orientia tsutsugamushi* infection by immunization with a zinc oxide nanoparticle combined with ScaA antigen. *J Nanobiotechnol.* (2016) 14:76. doi: 10.1186/s12951-016-0229-2
19. Moron CG, Popov VL, Feng HM, Wear D, Walker DH. Identification of the target cells of *Orientia tsutsugamushi* in human cases of scrub typhus. *Mod Pathol.* (2001) 14:752–9. doi: 10.1038/modpathol.3880385
20. Cho BA, Ko Y, Kim YS, Kim S, Choi MS, Kim IS, et al. Phenotypic characterization of peripheral T cells and their dynamics

in scrub typhus patients. *PLoS Negl Trop Dis.* (2012) 6:e1789. doi: 10.1371/journal.pntd.0001789
21. Ha NY, Kim Y, Min CK, Kim HI, Yen NTH, Choi MS, et al. Longevity of antibody and T-cell responses against outer membrane antigens of *Orientia tsutsugamushi* in scrub typhus patients. *Emerg Microbes Infect.* (2017) 6:e116. doi: 10.1038/emi.2017.106
22. Koo JE, Yun JH, Lee KH, Hyun JW, Kang HK, Jang WJ, et al. Activation of mitogen-activated protein kinases is involved in the induction of interferon beta gene in macrophages infected with *Orientia tsutsugamushi*. *Microbiol Immunol.* (2009) 53:123–9. doi: 10.1111/j.1348-0421.2008.00098.x
23. Gorvel L, Textoris J, Banchereau R, Ben Amara A, Tantibhedhyangkul W, von Bargen K, et al. Intracellular bacteria interfere with dendritic cell functions: role of the type I interferon pathway. *PLoS ONE* (2014) 9:e99420. doi: 10.1371/journal.pone.0099420
24. Tantibhedhyangkul W, Prachason T, Waywa D, El Filali A, Ghigo E, Thongnoppakhun W, et al. *Orientia tsutsugamushi* stimulates an original gene expression program in monocytes: relationship with gene expression in patients with scrub typhus. *PLoS Negl Trop Dis.* (2011) 5:e1028. doi: 10.1371/journal.pntd.0001028
25. Hanson B. Comparative susceptibility to mouse interferons of *Rickettsia tsutsugamushi* strains with different virulence in mice and of *Rickettsia rickettsii*. *Infect Immun.* (1991) 59:4134–41.
26. Muller U, Steinhoff U, Reis LF, Hemmi S, Pavlovic J, Zinkernagel RM, et al. Functional role of type I and type II interferons in antiviral defense. *Science* (1994) 264:1918–21. doi: 10.1126/science.8009221
27. Adachi O, Kawai T, Takeda K, Matsumoto M, Tsutsui H, Sakagami M, et al. Targeted disruption of the MyD88 gene results in loss of IL-1- and IL-18-mediated function. *Immunity* (1998) 9:143–50.
28. Yamamoto M, Sato S, Hemmi H, Hoshino K, Kaisho T, Sanjo H, et al. Role of adaptor TRIF in the MyD88-independent toll-like receptor signaling pathway. *Science* (2003) 301:640–3. doi: 10.1126/science.1087262
29. Sun Q, Sun L, Liu HH, Chen X, Seth RB, Forman J, et al. The specific and essential role of MAVS in antiviral innate immune responses. *Immunity* (2006) 24:633–42. doi: 10.1016/j.immuni.2006.04.004
30. Weischenfeldt J, Porse B. Bone Marrow-Derived Macrophages (BMM): isolation and applications. *CSH Protoc.* (2008) 2008:pdb.prot5080. doi: 10.1101/pdb.prot5080
31. Choi JH, Cheong TC, Ha NY, Ko Y, Cho CH, Jeon JH, et al. *Orientia tsutsugamushi* subverts dendritic cell functions by escaping from autophagy and impairing their migration. *PLoS Negl Trop Dis.* (2013) 7:e1981. doi: 10.1371/journal.pntd.0001981
32. Shelite TR, Saito TB, Mendell NL, Gong B, Xu G, Soong L, et al. A hematogenously disseminated *Orientia tsutsugamsushi*-infected murine model of scrub typhus. *PLoS Negl Trop Dis.* (2014) 8:e2966. doi: 10.1371/journal.pntd.0002966
33. Livak KJ, Schmittgen TD. Analysis of relative gene expression data using real-time quantitative PCR and the 2(T)(-Delta Delta C) method. *Methods* (2001) 25:402–8. doi: 10.1006/meth.2001.1262
34. Ha NY, Choi MS, Cho NH. Molecular characterization of sca genes found in *Orientia tsutsugamushi* genome. *J Bacteriol Virol.* (2013) 43:155–8. doi: 10.4167/jbv.2013.43.2.155
35. Uze G, Dimarco S, Mouchelvielh E, Monneron D, Bandu MT, Horisberger MA, et al. Domains of interaction between alpha-interferon and its receptor components. *J Mol Biol.* (1994) 243:245–57. doi: 10.1006/jmbi.1994.1651
36. Gharaibeh M, Hagedorn M, Lilla S, Hauptmann M, Heine H, Fleischer B, et al. Toll-like receptor 2 recognizes *Orientia tsutsugamushi* and increases susceptibility to murine experimental scrub typhus. *Infect Immun.* (2016) 84:3379–87. doi: 10.1128/IAI.00185-16
37. Chu H, Lee JH, Han SH, Kim SY, Cho NH, Kim IS, et al. Exploitation of the endocytic pathway by *Orientia tsutsugamushi* in nonprofessional phagocytes. *Infect Immun.* (2006) 74:4246–53. doi: 10.1128/IAI.01620-05
38. Ko Y, Choi JH, Ha NY, Kim IS, Cho NH, Choi MS. Active escape of *Orientia tsutsugamushi* from cellular autophagy. *Infect Immun.* (2013) 81:552–9. doi: 10.1128/IAI.00861-12
39. Abdullah Z, Schlee M, Roth S, Mraheil MA, Barchet W, Bottcher J, et al. RIG-I detects infection with live Listeria by sensing secreted bacterial nucleic acids. *EMBO J.* (2012) 31:4153–64. doi: 10.1038/emboj.2012.274
40. Hansen K, Prabakaran T, Laustsen A, Jorgensen SE, Rahbaek SH, Jensen SB, et al. *Listeria monocytogenes* induces IFN beta expression through an IFI16-, cGAS- and STING-dependent pathway. *EMBO J.* (2014) 33:1654–66. doi: 10.15252/embj.201488029
41. Cossart P, Vicente MF, Mengaud J, Baquero F, Perezdiaz JC, Berche P. Listeriolysin-O is essential for virulence of *Listeria monocytogenes* - direct evidence obtained by gene complementation. *Infect. Immun.* (1989) 57:3629–36.
42. Chen LL, Yang L, Carmichael GG. Molecular basis for an attenuated cytoplasmic dsRNA response in human embryonic stem cells. *Cell Cycle* (2010) 9:3552–64. doi: 10.4161/cc.9.17.12792
43. Nazmi A, Mukhopadhyay R, Dutta K, Basu A. STING mediates neuronal innate immune response following Japanese encephalitis virus infection. *Sci Rep.* (2012) 2:347. doi: 10.1038/srep00347
44. Suzuki T, Oshiumi H, Miyashita M, Aly HH, Matsumoto M, Seya T. Cell type-specific subcellular localization of phospho-TBK1 in response to cytoplasmic viral DNA. *PLoS ONE* (2013) 8:e83639. doi: 10.1371/journal.pone.0083639
45. Turco J, Winkler HH. Interferon-alpha-beta and *Rickettsia prowazekii* - induction and sensitivity. *Ann NY Acad Sci.* (1990) 590:168–86. doi: 10.1111/j.1749-6632.1990.tb42219.x
46. Colonne PM, Eremeeva ME, Sahni SK. Beta interferon-mediated activation of signal transducer and activator of transcription protein 1 interferes with *Rickettsia conorii* replication in human endothelial cells. *Infect Immun.* (2011) 79:3733–43. doi: 10.1128/IAI.05008-11
47. Kim G, Ha NY, Min CK, Kim HI, Yen NTH, Lee KH, et al. Diversification of *Orientia tsutsugamushi* genotypes by intragenic recombination and their potential expansion in endemic areas. *Plos Negl Trop Dis.* (2017) 11:e0005408. doi: 10.1371/journal.pntd.0005408
48. Benson N, de Jongh J, Duckworth JD, Jones HM, Pertinez HE, Rawal JK, et al. Pharmacokinetic-pharmacodynamic modeling of alpha interferon response induced by a Toll-like 7 receptor agonist in mice. *Antimicrob Agents Chemother.* (2010) 54:1179–85. doi: 10.1128/AAC.00551-09
49. Zhang Y, Thai V, McCabe A, Jones M, MacNamara KC. Type I interferons promote severe disease in a mouse model of lethal ehrlichiosis. *Infect Immun.* (2014) 82:1698–709. doi: 10.1128/IAI.01564-13
50. Yang Q, Stevenson HL, Scott MJ, Ismail N. Type I interferon contributes to noncanonical inflammasome activation, mediates immunopathology, and impairs protective immunity during fatal infection with lipopolysaccharide-negative ehrlichiae. *Am J Pathol.* (2015) 185:446–61. doi: 10.1016/j.ajpath.2014.10.005
51. Choi KS, Scorpio DG, Dumler JS. Stat1 negatively regulates immune-mediated injury with *Anaplasma phagocytophilum* infection. *J Immunol.* (2014) 193:5088–98. doi: 10.4049/jimmunol.1401381
52. Nagarajan UM, Prantner D, Sikes JD, Andrews CWJr, Goodwin AM, Nagarajan S, et al. Type I interferon signaling exacerbates *Chlamydia muridarum* genital infection in a murine model. *Infect Immun.* (2008) 76:4642–8. doi: 10.1128/IAI.00629-08
53. de Almeida LA, Carvalho NB, Oliveira FS, Lacerda TL, Vasconcelos AC, Nogueira L, et al. MyD88 and STING signaling pathways are required for IRF3-mediated IFN-beta induction in response to *Brucella abortus* infection. *PLoS ONE* (2011) 6:e23135. doi: 10.1371/journal.pone.0023135
54. Hauptmann M, Kolbaum J, Lilla S, Wozniak D, Gharaibeh M, Fleischer B, et al. Protective and Pathogenic Roles of CD8+ T Lymphocytes in Murine *Orientia tsutsugamushi* Infection. *PLoS Negl Trop Dis.* (2016) 10:e0004991. doi: 10.1371/journal.pntd.0004991
55. Carrero JA, Calderon B, Unanue ER. Lymphocytes are detrimental during the early innate immune response against *Listeria monocytogenes*. *J Exp Med.* (2006) 203:933–40. doi: 10.1084/jem.20060045
56. Tian Y, Mollo SB, Harrington LE, Zajac AJ. IL-10 regulates memory T cell development and the balance between Th1 and follicular Th cell responses during an acute viral infection. *J Immunol.* (2016) 197:1308–21. doi: 10.4049/jimmunol.1502481
57. Biswas PS, Pedicord V, Ploss A, Menet E, Leiner I, Pamer EG. Pathogen-specific CD8 T cell responses are directly inhibited by IL-10. *J Immunol.* (2007) 179:4520–8. doi: 10.4049/jimmunol.179.7.4520
58. Howes A, Taubert C, Blankley S, Spink N, Wu X, Graham CM, et al. Differential production of type I IFN determines the reciprocal levels of IL-10 and proinflammatory cytokines produced by

C57BL/6 and BALB/c macrophages. *J Immunol.* (2016) 197:2838–53. doi: 10.4049/jimmunol.1501923

59. Soong L, Mendell NL, Olano JP, Rockx-Brouwer D, Xu G, Goez-Rivillas Y, et al. An intradermal inoculation mouse model for immunological investigations of acute scrub typhus and persistent infection. *PLoS Negl Trop Dis.* (2016) 10:e0004884. doi: 10.1371/journal.pntd.0004884
60. Tsai MH, Chang CH, Tsai RK, Hong YR, Chuang TH, Fan KT, et al. Cross-regulation of proinflammatory cytokines by interleukin-10 and miR-155 in *Orientia tsutsugamushi*-infected human macrophages prevents cytokine storm. *J Invest Dermatol.* (2016) 136:1398–407. doi: 10.1016/j.jid.2015.11.034

Conflict of Interest Statement: The authors declare that the research was conducted in the absence of any commercial or financial relationships that could be construed as a potential conflict of interest.

Copyright © 2018 Min, Kim, Ha, Kim, Kwon, Yen, Youn, Jeon, Inn, Choi and Cho. This is an open-access article distributed under the terms of the Creative Commons Attribution License (CC BY). The use, distribution or reproduction in other forums is permitted, provided the original author(s) and the copyright owner(s) are credited and that the original publication in this journal is cited, in accordance with accepted academic practice. No use, distribution or reproduction is permitted which does not comply with these terms.

frontiers in Immunology

ORIGINAL RESEARCH
published: 09 October 2018
doi: 10.3389/fimmu.2018.02089

Deficient O-GlcNAc Glycosylation Impairs Regulatory T Cell Differentiation and Notch Signaling in Autoimmune Hepatitis

*Xiaohua Hao[1], Yufeng Li[1], Jianwen Wang[1], Jiali Ma[1], Shuli Zhao[2], Xiaohui Ye[1], Lingling He[1], Junru Yang[1], Meixin Gao[1], Fan Xiao[1] and Hongshan Wei[1]**

[1] Beijing Ditan Hospital, Capital Medical University, Beijing, China, [2] Central Laboratory of Nanjing First hospital, Nanjing Medical University, Nanjing, China

Post-translational modifications such as glycosylation play an important role in the functions of homeostatic proteins, and are critical driving factors of several diseases; however, the role of glycosylation in autoimmune hepatitis is poorly understood. Here, we established an O-GlcNAc glycosylation-deficient rat model by knocking out the *Eogt* gene by TALEN-mediated gene targeting. O-GlcNAc glycosylation deficiency overtly aggravated liver injury in concanavalin-A induced autoimmune hepatitis, and delayed self-recovery of the liver. Furthermore, flow cytometry analysis revealed increased $CD4^+$ T cell infiltration in the liver of rats with O-GlcNAc glycosylation deficiency, and normal differentiation of regulatory T cells (Tregs) in the liver to inhibit T cell infiltration could not be activated. Moreover, *in vitro* experiments showed that O-GlcNAc glycosylation deficiency impaired Treg differentiation to inhibit the Notch signaling pathway in $CD4^+$ T cells. These finding indicate that O-GlcNAc glycosylation plays a critical role in the activation of Notch signaling, which could promote Treg differentiation in the liver to inhibit T cell infiltration and control disease development in autoimmune hepatitis. Therefore, this study reveals a regulatory role for glycosylation in the pathogenesis of autoimmune hepatitis, and highlights glycosylation as a potential treatment target.

Keywords: O-GlcNAc glycosylation, autoimmune hepatitis, treg cells, EOGT, notch signaling pathway

OPEN ACCESS

Edited by:
Gustavo Javier Martinez, Rosalind Franklin University of Medicine and Science, United States

Reviewed by:
Yeonseok Chung, Seoul National University, South Korea
Marta A. Toscano, Instituto de Biología y Medicina Experimental (CONICET), Argentina

***Correspondence:**
Hongshan Wei
drwei@ccmu.edu.cn

Specialty section:
This article was submitted to Autoimmune and Autoinflammatory Disorders, a section of the journal Frontiers in Immunology

Received: *26 April 2018*
Accepted: *24 August 2018*
Published: *09 October 2018*

Citation:
Hao X, Li Y, Wang J, Ma J, Zhao S, Ye X, He L, Yang J, Gao M, Xiao F and Wei H (2018) Deficient O-GlcNAc Glycosylation Impairs Regulatory T Cell Differentiation and Notch Signaling in Autoimmune Hepatitis. Front. Immunol. 9:2089. doi: 10.3389/fimmu.2018.02089

INTRODUCTION

Autoimmune hepatitis (AIH) is a typical immune-mediated liver disease characterized by hepatocellular inflammation and immune-mediated destruction of the hepatic parenchyma, resulting in liver failure, cirrhosis and death (1). Although understanding of the specific triggers initiating the series of events in AIH development and progression is still at its rudimentary stage, multiple clinical and basic science studies have suggested that T lymphocytes likely act as primary drivers of autoimmune responses via the innate and adaptive immune systems (2, 3). Indeed, during the development of AIH, the main population of infiltrated immune cells is largely composed of $CD4^+$ and $CD8^+$ T lymphocytes, whose intrahepatic accumulation is associated with increased histological severity of hepatitis (4).

The liver is often considered a unique site of immune tolerance (5), and functions to systemically inhibit autoimmune responses against ectopic antigens (6). Although the specific mechanisms underlying immune tolerance in the liver remain unclear, regulatory T cells (Tregs) are known to mediate hepatic immune tolerance (6). Tregs are central to the regulation of self-tolerance and maintenance of tissue homeostasis by preventing the activation and expansion of auto-reactive T lymphocytes that contribute to autoimmune diseases, and limiting immune responses in allergic diseases, infections, transplantation, graft-vs.-host disease, and cancer (7–9). Experimental evidence suggests that AIH with immunoregulatory dysfunction is characterized by decreased amounts of Tregs and FOXP3 expression levels (10, 11). Meanwhile, reduction of Treg amounts has been described in peripheral blood with a parallel increase of Treg frequency along with effector cell numbers in the inflamed liver tissue (12). Therefore, regulating Treg activation and expansion appears to be essential for self-systematic inhibition of AIH.

The development and maintenance of immunosuppressive function in Tregs are crucially controlled by FOXP3 expression; therefore, such regulation mainly aim to modulate FOXP3 protein expression (13). The transcriptional activity of FOXP3 is modulated by accessory extracellular signal activation and intracellular transcription factors (14–16), whose functions are precisely modulated by post-translational modifications (PTMs) (17). Various studies have demonstrated that FOXP3 is regulated by PTMs, including acetylation, ubiquitination and phosphorylation (17). Surface glycosylation is another PTM, which is ubiquitous in mammalian cells; it also regulates T cell development, trafficking and function (18). Recently, Cabral et al. (19) reported that surface glycosylation of Tregs is important in determining the Treg phenotype and suppressive potency. However, the role of glycosylation in modulating Treg development and activation in AIH is poorly understood.

Concanavalin A (Con A) is a plant lectin that is widely used for inducing acute immune-mediated hepatitis with an activated inflammatory response (20, 21). Indeed, Con A-induced AIH is a typical and well-established model for investigating T cell-mediated liver injury, closely mimicking the pathogenic mechanisms and pathological changes observed in AIH patients (22). In this study, we established a Con A-induced AIH rat model in which the *Eogt* gene was knocked out by the transcription activator-like effector nuclease (TALEN) technology. *Eogt* encodes a key enzyme for O-GlcNAc glycosylation and catalyzes the transfer of N-acetyl glucosamine to serine or threonine residues of target extracellular proteins (23). This knockout resulted in O-GlcNAc glycosylation deficiency, and was used to examine the effects of glycosylation on Treg activation and development, as well as the associated liver injury in AIH and underlying mechanisms.

MATERIALS AND METHODS

TALEN Construction

A pair of TALENs targeting exon 5 of the rat *Eogt* gene (GenBank accession number: NM_001009502.1) were created by Cyagen Biosciences Inc. Each TALEN binds to 18 bp of DNA, and binding sites are separated by a 14-bp spacer region as illustrated in **Figure 1A**. The TALENs were assembled using TALE Toolkit (Addgene, catalog # 1000000019) according to published protocols (24). Final constructs were produced in the pRP[TALEN]-Hygro-CMV backbone plasmid (Cyagen Biosciences Inc.).

The TALEN plasmids were linearized with SmaI and used as templates for *in vitro* transcription with mMessage mMachine T7 Ultra Kit (Ambion) according to the manufacturer's instructions. Capped, polyA-tailed mRNAs were cleaned up with a MEGAclear kit (Ambion). The mRNAs were precipitated, washed and resuspended at 1 μg/μL in DEPC-treated H_2O. TALEN mRNAs were subsequently diluted in 0.1× TE buffer at a final concentration of 10 ng/μL, aliquoted, and stored at −80°C until use for embryo injection.

Microinjection of TALENs in Fertilized Eggs

All animal-based experimental procedures were approved by the Institutional Animal Care and Use Committee, Peking University Health Science Center (SCXK: 2011-0012). Rats were bred and maintained in accordance with the Peking University Health Science Center guidelines for use of Laboratory Animals. Sprague Dawley (SD) rats (Charles River Laboratories) were housed under specific pathogen-free conditions under a 12/12 h light/dark cycle (7:00–19:00). Female embryo donors were superovulated with 25 IU of pregnant mare serum gonadotropin (Sigma) between 11:00 and 12:00, followed by administration of 25 IU of human chorionic gonadotropin (Sigma) 24 h later, and subsequently individually caged with a male stud rat. The following morning, donors were sacrificed, and embryos were collected from oviducts and cultured in M16 medium (Millipore) at 37°C in 5% CO_2/95% air. Fertilized one-cell embryos were transferred to M2 medium (Millipore) for microinjection. TALEN mRNAs were injected into the cytoplasm using glass injection pipettes. Embryos that survived the injection procedure were surgically transferred to the oviduct of day-0.5 post coitum pseudopregnant recipient SD females that had successfully mated with vasectomized males.

Mutation Analysis

Offspring from injected embryos were screened for mutations in the *Eogt* locus by polymerase chain reaction (PCR) followed by DNA sequencing. Briefly, DNA was prepared from tail snips (∼0.5 cm) using E.Z.N.A.® Forensic DNA Extraction Kit (Omega BioTek, USA) according to the manufacturer's instructions. A portion of the *Eogt* locus that overlaps with the TALEN spacer region was amplified by PCR with the forward primer 5′-GTTTGCCACCAGTCCTGTCTGAAG-3′ and reverse primer 5′-CGCTACCTTATACGGACAGTGGGA-3′. PCR reactions included Taq 2X Master Mix (New England Biolabs Inc., Ipswich, MA, USA), and the amplification program consisted of 95°C for 5 min, followed by 30 cycles of 95°C for 30 s 58°C for 30 s and 72°C for 30 s, with a final extension at 72°C for 5 min. Ten microliters of PCR products were analyzed on ethidium bromide-stained 1.5% agarose gels in Tris–borate–EDTA buffer.

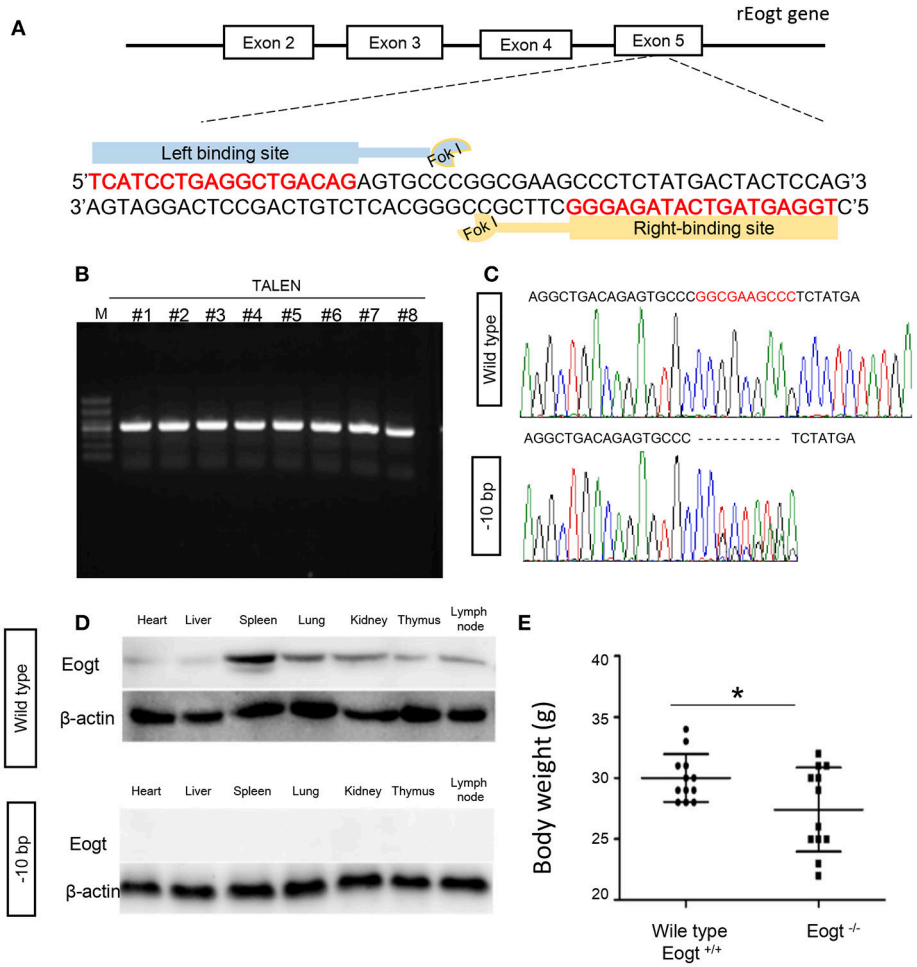

FIGURE 1 | Generation of Eogt1 knockout rats by TALEN-mediated gene targeting. **(A)** Schematic representation of the rEogt1 locus and rEogt1-TALEN design. Double-stranded DNA sequence of the rEogt1 locus that was targeted with TALENs. The TALEN binding sites are marked with red; **(B)** Agarose gel electrophoresis demonstrating products of the predicted size for the rEogt1 locus in 8 healthy offspring; **(C)** Representative genomic sequencing results of rEogt mutation around the target site. The black dotted line represents nucleotide deletions; **(D)** Western blot analysis of Eogt expression in the heart, liver, spleen, lung, kidney, thymus and lymph nodes of wild type and Eogt knockout rats; **(E)** Body weights in wild type and Eogt knockout rats on day 20 after birth. *$p < 0.05$, vs. WT control group.

In addition, *Eogt* PCR products from the founder rats were sequenced using the same primers described above. Positive founders were bred to the next generation, and the offspring were genotyped by PCR and DNA sequencing as described above.

Con A-Induced Autoimmune Liver Injury Model

Wild type ($Eogt^{+/+}$) and Eogt knockout ($Eogt^{-/-}$) SD rats (6–8 weeks old) were injected with Con A (Sigma-Aldrich) at 30 mg/kg body weight by the tail vein. The $Eogt^{+/+}$ and $Eogt^{-/-}$ groups each had 60 healthy adult male SD rats, which were randomly divided into 5 groups. Con A treatment was used to trigger AIH in a few hours, leading to hepatic dysfunction within 24 h. At 0, 12, 24, 48, and 72 h after injection, the experimental rats were sacrificed, and peripheral blood, and liver, spleen, and thymus samples were collected for further analysis.

Liver Function Marker Analysis

Serum alanine aminotransferase (ALT) and aspartate aminotransferase (AST) levels in $Eogt^{+/+}$ and $Eogt^{-/-}$ SD rats were detected on an Olympus AU 2700 analyzer (Olympus, Tokyo, Japan) according to the manufacturer's instructions.

Flow Cytometry Analysis of T Cell Subpopulations in Tissues

Over the last few decades, Tregs have been demonstrated to prevent $CD4^+$ T lymphocyte-mediated inflammatory diseases, including AIH (25). To assess whether Tregs are regulated by *Eogt* deletion, the population of $CD4^+FoxP3^+$ cells (Tregs) was detected in the liver of $Eogt^{+/+}$ and $Eogt^{-/-}$ rats after Con A injection by flow cytometry. For cell collection from the spleen, liver, and thymus, the organs were mechanically disrupted in a coffee grinder. Then, spleen and thymus cell suspensions were passed through a fine, 50-μm nylon mesh,

and cells were collected by centrifugation at 300 × *g* for 5 min. Liver cell suspension was centrifuged at 50 × *g* for 3 min twice to eliminate hepatocytes; non-parenchymal cells in the liver were collected following Percoll gradient separation. Cells were collected from peripheral blood by centrifugation at 2,000 × *g* for 15 min. Erythrocytes were removed by treating splenic cells with red blood cell lysis buffer (0.15 M NH_4Cl, 1.0 mM $KHCO_3$, 0.1 mM EDTA, pH 7.2) for 5 min and washing twice with cold phosphate-buffered saline (PBS). The resulting cells (1×10^6) were resuspended in PBS and incubated with the following anti-rat antibodies for 30 min at 4°C: anti-CD3-PerCP (eBioscience), anti-CD4-FITC (eBioscience), anti-CD25-APC (BD Bioscience), anti-Foxp3-PE (BD Bioscience), and isotype control antibodies (eBioscience, San Diego, CA). After incubation, the cells were washed twice with fluorescence-activating cell sorter (FACS) washing buffer, and 4×10^5 cells were collected by FACS Vantage SE (FACSCalibur, Becton Dickinson, San Jose, CA, USA) and analyzed with the CellQuest software (CellQuest Pro, Becton Dickinson).

$CD4^+$ T Cell Isolation and Con A Treatment

Con A-induced AIH is characterized by $CD4^+$ T lymphocyte infiltration in the liver, and $CD4^+$ T lymphocyte-mediated immune responses play an important role in the development and progression of AIH (26). Therefore, to assess whether loss of *Eogt* enhances $CD4^+$ T lymphocyte infiltration to further aggravate Con A-induced hepatic dysfunction, we monitored the dynamic changes of the $CD4^+$ T lymphocyte population in the liver. $CD4^+$ T cells were positively selected from rat splenocytes on a magnetic-activated cell-sorting system (MACS; Miltenyi Biotec, Germany). High-purity $CD4^+$ T cells were seeded in 96-well culture plates (5×10^5 cells/well) and cultured in RPMI 1640 (Gibco, Grand Island, NY, USA) with 10% fetal bovine serum, followed by the addition of 5 μg/mL Con A in 6 well plates. The experiment was repeated at least three times. The same concentration of PBS was added to control wells. All cells were collected after 0, 12, 24, 48, and 72 h for FACS analysis.

In vitro Treg Differentiation and Proliferation Assays

T cell subsets were obtained from single-cell suspensions of the spleen were prepared from 6-week-old r*Eogt*$^{+/+}$ or r*Eogt*$^{-/-}$ SD rats. Briefly, the harvested spleens were gently processed by gentle extrusion through a metal mesh into cold PBS, and spleen lymphocytes were isolated from the Percoll interphase. The harvested cells were aliquoted and stained with different antibody combinations for sorting naïve $CD4^+$ T cells (anti-CD4-PE, clone W3/25, BioLegend; anti-CD45RC-FITC, clone OX-22, Thermo Fisher Scientific) or Treg cells (anti-CD4-PE and anti-CD25-FITC), and subjected to flow cytometric sorting.

In Treg differentiation assays, the collected naïve $CD4^+$T cells ($CD4^+CD45RC^+$) were resuspended in complete RPMI 1640 medium supplemented with 2 ng/ml Rat TGFβ1 (Sino Biological), 100 U/ml Rat IL-2 (R&D systems), 1 μg/ml CD28 mAb (clone JJ319, BioLegend), seeded in 24-well plates pre-coated with anti-CD3ε antibody (clone 1F4, BioLegend), and incubated at 37°C with 5% CO2 for 4 days. Treg differentiation was assessed by Q-PCR analysis of Foxp3 mRNA levels and CD25/Foxp3 staining levels in flow cytometry analysis.

The proliferative capacity of Tregs after rEogt gene knockout was assessed with Cell Counting Kit-8 (CCK-8) according to the manufacturer's instructions. Briefly, the purified Tregs ($CD4^+CD25^+$) were seeded at a density of 5×10^3 cells in 96-well plates in quadruplicate, and incubated for 48 h in complete RPMI 1640 medium with equal amounts of Con A (0, 2, and 4 μg/ml) and recombinant 100 U/ml Rat IL-2 (25 ng/ml, R&D Systems) in a humid atmosphere with 5% CO2 at 37°C. Afterward, the supernatants were pulsed with the CCK-8 solution (1/10), and the cells were incubated for another 2 h at 37°C. Absorbance at 450 nm was determined on a microplate reader (BioTek, MQX200). All experiments were repeated three times.

Quantitative Real-Time PCR

Total RNA was isolated with TRIzol reagent (Invitrogen, Carlsbad, CA, USA) according to the manufacturer's instructions. A total of 1 μg RNA was used as a template for single-strand cDNA synthesis using oligo(dT) primers and TransScript®RT/RI Enzyme Mix (TransGen Biotech, Beijing, China). The resulting cDNA was amplified with TransStart® Top Green qPCR SuperMix (TransGen Biotech, Beijing, China) on an ABI Prism 7500 sequence detection system (Applied Biosystems, Foster City, CA, USA), programmed for 94°C for 30 s, followed by 40 cycles of 94°C for 5 s and 60°C for 30 s. Amplification results were analyzed with the ABI Prism 7500 software (Applied Biosystems), and expression levels of the genes of interest were normalized to the corresponding *Gapdh* results. The primer sequences are presented in **Table 1**.

TABLE 1 | Primer sequence used in Q-PCR.

Gene		Primer sequence
rRBPj	Forward	GGGTGTAGCCTCCTTTCT
	Reverse	TGTATTTGGACGATGGTTT
rNotch1	Forward	ATGACTGCCCAGGAAACAAC
	Reverse	ATGACTGCCCAGGAAACAAC
rJagged1	Forward	GCTTCGGCTCAGGGTCTA
	Reverse	AGTCACCTGGGAGTTTGC
rJagged2	Forward	CCAGGAAGTGGTCATATTCACGA
	Reverse	GCAGACAAGGCTTCCAACCAC
rHes1	Forward	GCTTCAGCGAGTGCATGAAC
	Reverse	CGGTGTTAACGCCCTCACA
rFoxp3	Forward	GGCCCTTCTCCAGGACAGA
	Reverse	GCTGATCATGGCTGGGTTGT
rCTLA-4	Forward	GGACTGAGGGCTGCTGACAC
	Reverse	GGCATGGTTCTGGATCGATG
rGITR	Forward	GCAGACTTTGGACCAACTGTTC
	Reverse	AGCGGCTGG GTATTGACCT
rGapdh	Forward	5′-AGGTCGGTGTGAACGGATTTG-3′
	Reverse	3′-GGGGTCGTTGATGGCAACA-5′

Western Blot

The samples were lysed in a buffer containing 50 mM Tris-HCl (pH 7.4), 150 mM NaCl, 1% NP40, 0.25% Na-deoxycholate, and 1 mM phenylmethylsulfonyl fluoride. After centrifugation, protein samples were subjected to 10% sodium dodecyl sulfate-polyacrylamide gel electrophoresis and transferred onto polyvinylidene fluoride (PVDF) membranes (Roche, Mannheim, Germany). The membranes were then blocked in TBST (1 mM Tris-HCl, pH 7.4, 150 mM NaCl, 0.05% Tween-20) containing 5% skim milk for 60 min, and incubated overnight at 4°C with diluted primary antibodies against GAPDH, β-actin, NALP2 and EOGT (Abcam, Database link: Q5NDL2), as well as cleaved caspase 3, cleaved caspase 7 and RBPJ (Cell Signaling Technology). After 3 washes with TBST for 5 min, the membranes were incubated with secondary antibodies in blocking buffer at room temperature for 1 h. Finally, chemiluminescence was used for detection, and images were acquired by autoradiography.

IMMUNOPRECIPITATION

For immunoprecipitation of total Notch1, lymphocyte lysates were incubated with Notch1 antibody (clone mN1A, Santa Cruz Biotechnology) at 2 mg/ml for 2 h at 4°C, and further incubated with protein G-coupled Sepharose beads (20 μL) for 1 h. After 5 washes with ice-cold washing buffer, total protein was eluted with SDS-PAGE sample loading buffer, and separated by 7% SDS-polyacrylamide gel electrophoresis followed by transfer onto polyvinylidene difluoride membranes (Millipore, Burlington, MA, USA). Finally, immunoblotting for the detection of O-GlcNAc and Notch1 was performed using anti-O-GlcNAc (clone CTD110.6, BioLegend) and anti-NOTCH1 antibodies, respectively.

Luminex Multiplex Assays

A Luminex assay (Luminex®) was used to determine the serum levels of 20 cytokines, including several interleukins (ILs), chemokines, and cytokines: GM-CSF, IFN-γ, IL-1β, IL-2, IL-4, IL-5, IL-6, IL-10, IL-13, TNF-a, G-CSF, Eotaxin, GRO-a, IP-10, MCP-1, MCP-3, MIP-1a, MIP-2, RANTES, and TGF-β.

Statistical Analysis

Data are mean ± SEM, and were assessed by Student's *t*-test with the GraphPad Prism 5.01 software (San Diego, CA, USA). $P < 0.05$ was considered statistically significant.

RESULTS

Eogt Knockout Rats Produced by TALEN-Mediated Gene Inactivation

To generate *Eogt* knockout rats, we designed a TALEN that targets the rat *Eogt* gene in exon 5 (**Figure 1A**). After transfer of TALEN mRNA-injected fertilized eggs to the uterus of a recipient, eight healthy offspring were produced. PCR products of around 500 bp were amplified from each animal corresponding to the portion of the *Eogt* locus overlapping with the TALEN spacer (**Figure 1B**). DNA sequence analysis further revealed that the PCR products of two females had a 10-bp deletion (−10 bp) in the spacer region (**Figure 1C**).

To generate offspring homozygous for this deletion, these female founder rats were mated with wild-type SD males, and six of the F1 offspring harbored the −10 bp allele. Heterozygous F1 offspring were then interbred to produce an F2 offspring, and DNA sequence analysis indicated that four of the F2 offspring were homozygous for the −10 bp allele. Western blot analysis further confirmed the successful establishment of *Eogt* knockout rats ($Eogt^{-/-}$) by the TALEN method, since the EOGT protein was detected in various tissues (heart, liver, spleen, lung, kidney, thymus and lymph nodes) of wild-type rats but not in any of the −10 bp animals (**Figure 1D**). Furthermore, body weights in $Eogt^{-/-}$ rats were significantly lower compared with those of $Eogt^{+/+}$ animals on day 20 after birth (**Figure 1E**).

Con A-Induced Liver Injury Is Aggravated in $Eogt^{-/-}$ Rats

After Con A injection, both $Eogt^{+/+}$ and $Eogt^{-/-}$ rats displayed hepatic dysfunction as evidenced by dynamic changes of ALT and AST levels (**Figure 2A**). At 12 h after Con A injection, serum ALT and AST levels were markedly increased in both groups; however, these levels were much higher in $Eogt^{-/-}$ rats. ALT and AST levels decreased from 12 to 24 h in $Eogt^{+/+}$ rats, but remained high in $Eogt^{-/-}$ animals. From 24 to 72 h, ALT and AST levels were gradually restored to normal levels in both groups (**Figure 2B**).

Western blot analysis further showed that the levels of apoptotic marker proteins, including cleaved caspases 3 and 7, were increased in the liver of Con A-treated $Eogt^{+/+}$ rats (**Figure 2C**), with more pronounced increases observed in $Eogt^{-/-}$ rats, indicating that *Eogt* knockout aggravated hepatic dysfunction (**Figure 2C**). Moreover, Con A-induced liver dysfunction and apoptosis were accompanied with overtly increased NALP2 levels, indicating the activation of inflammatory responses in the liver; the alteration was 3-fold higher in $Eogt^{-/-}$ rats compared with $Eogt^{+/+}$ animals (**Figures 2D,E**). Histological analysis confirmed that Con A-induced acute liver injury was more severe in $Eogt^{-/-}$ rats (**Figure 2F**).

Con A-Induced $Eogt^{-/-}$ Rats Show Abnormal Treg Activation

In Con A-treated $Eogt^{+/+}$ rats, the percentage of liver $CD4^+$ T lymphocyte was obviously increased in the first 12 h, and gradually decreased thereafter (**Figure 3A**). By contrast, Con A-treated $Eogt^{-/-}$ rats showed a continuous increase in liver $CD4^+$ T lymphocytes over the first 24 h, which then declined to the normal level (**Figure 3A**). The frequencies of $CD4^+$ T lymphocytes in peripheral blood were significantly decreased at 1 h after Con A injection in both $Eogt^{+/+}$ and $Eogt^{-/-}$ rats (**Figure 3B**), with no difference between the two groups. However, the recovery rate of peripheral blood $CD4^+$ T lymphocytes over the following 12–36 h was higher in $Eogt^{+/+}$ rats (**Figure 3B**). There were no significant differences in the

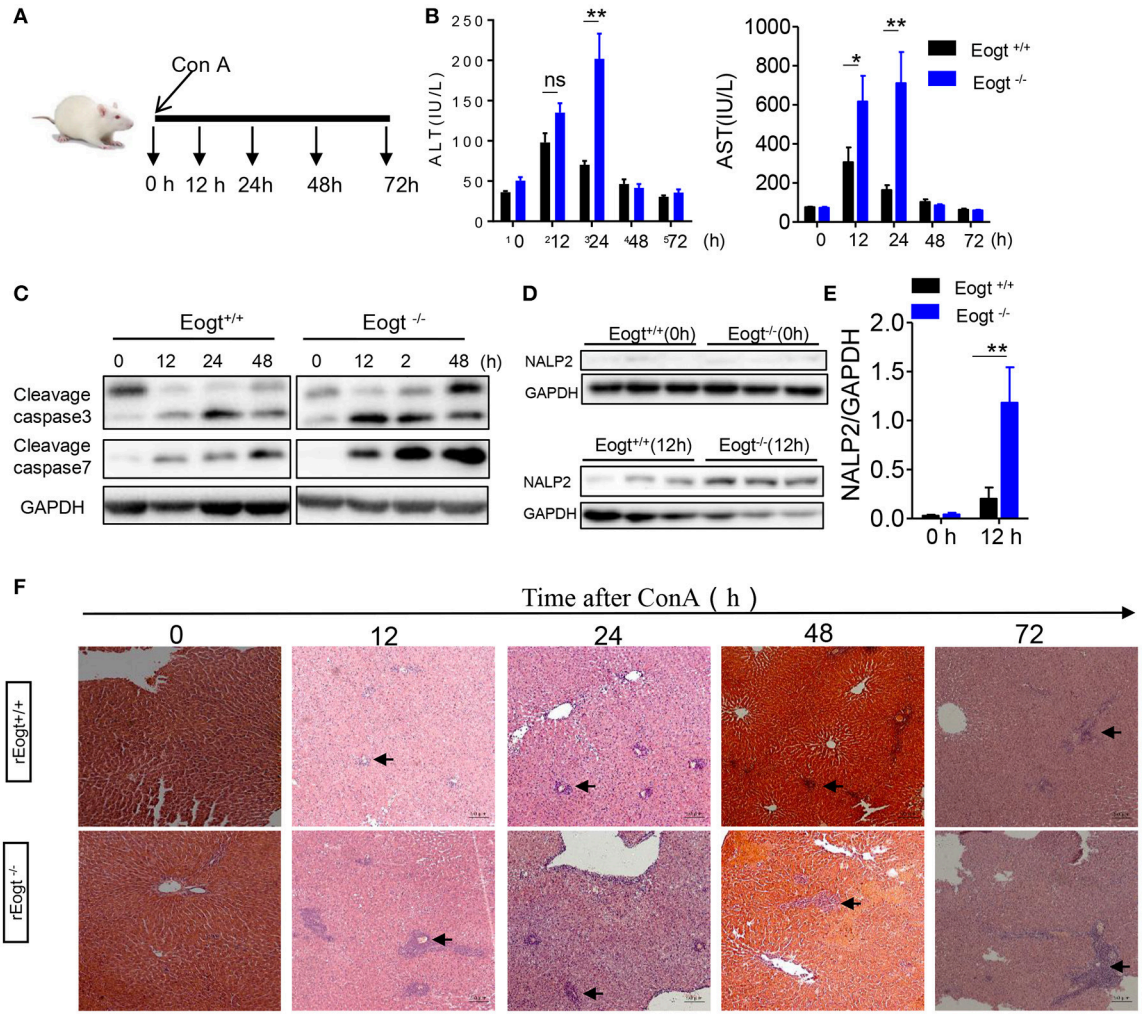

FIGURE 2 | Knockout Eogt aggravates concanavalin-A induced liver injury. **(A)** Schematic outline of concanavalin-A (Con A) administration in Eogt$^{+/+}$ and Eogt$^{-/-}$ rats. **(B)** ALT and AST levels in Eogt$^{+/+}$ and Eogt$^{-/-}$ rats after Con-A injection at 0, 12, 24, 48, and 72 h; **(C)** Western blot analysis of cleaved caspases 3 and 7 in the liver of Eogt+/+ and Eogt$^{-/-}$ rats after Con-A injection at 0, 12, 24, and 48 h; **(D)** Western blot analysis of NALP2 protein levels in the liver of Eogt$^{+/+}$ and Eogt$^{-/-}$ rats after Con-A injection at 0 and 12 h; **(E)** Quantification of NALP2 protein expression in **(D)**. **(F)** Representative H and E staining of liver sections after Con-A injection at 0, 12, 24, and 48 h. *$p < 0.05$; **$p < 0.01$, vs. WT control group.

dynamic changes of CD4$^+$ T lymphocytes in the spleen and lymph nodes between the two groups (**Figures 3C,D**).

In line with a previous report (26), we found that the population of liver CD4$^+$Foxp3$^+$ cells (Treg) was increased from 11.48 ± 0.93% to 26.42 ± 1.80% 12 h after Con A treatment in *Eogt*$^{+/+}$ rats, and returned to baseline levels at 24 and 48 h (**Figures 3E,F**). However, in *Eogt*$^{-/-}$ rats, the proportion of Tregs only increased slightly from 11.18 ± 1.15% to 13.67 ± 1.39% at 12 h after Con A treatment, which was significantly lower compared with that of *Eogt*$^{+/+}$ animals (**Figures 3E,F**).

EOGT Knockout Inhibits the Generation of iTregs From CD4$^+$CD45RC$^+$ T cells *in vitro*

To directly assess the role of EOGT on Treg proliferation and differentiation, we adopted flow cytometry to sort naive CD4$^+$ T cells (CD4$^+$CD45RC$^+$) (**Figures 4A,D**) and CD4$^+$CD25$^+$ Tregs (**Figures 4A,B**) from rat spleens. Although Con A could promote Treg proliferation in the presence of IL-2, no statistically significant differences were observed between the WT and KO groups with or without Con A (**Figure 4C**). Next, we adopted an *in vitro* culture system where naive CD4$^+$ T cells (CD4$^+$CD45RC$^+$) were differentiated into FoxP3$^+$ Tregs upon anti-CD3 mAb stimulation in the presence of TGF-β1, rIL-2 and anti-CD28 mAb. However, Foxp3 mRNA levels and the percentage of inducible regulatory T cells (CD25+Foxp3+) in KO induction groups were significantly lower compared with those of WT induction groups (**Figures 4E,F**).

Eogt Suppression Alters the Serum Levels of Chemokines

Since many cytokines and chemokines play important roles in the development of autoimmune hepatitis diseases, we next

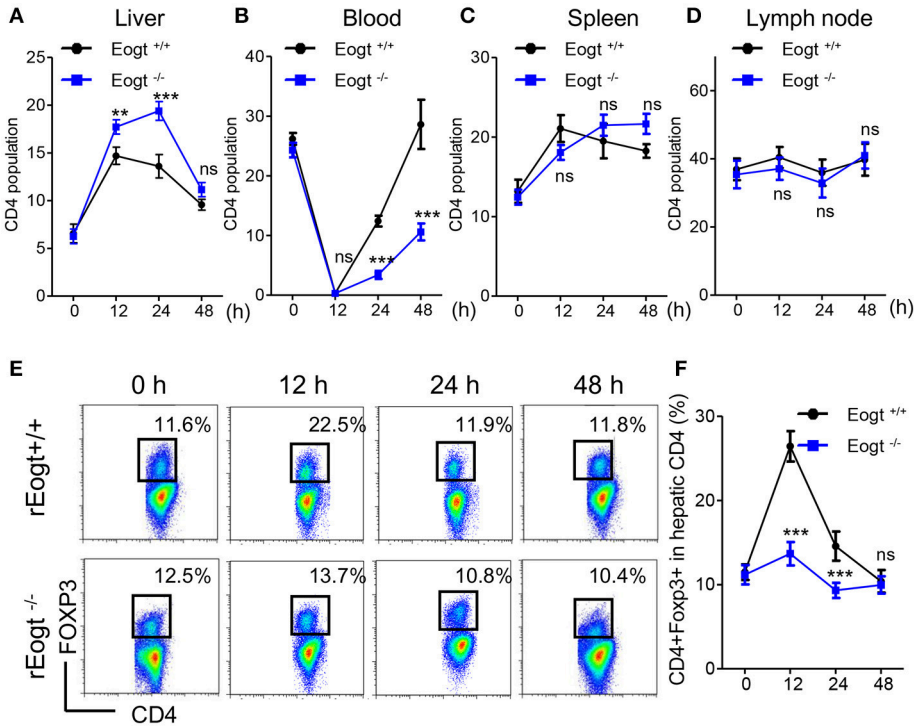

FIGURE 3 | Abnormal activation of Tregs in Eogt$^{-/-}$ rats after Concanavalin-A treatment. **(A–D)**. Flow cytometry analysis of CD4$^+$ T cells in the Liver **(A)**, Blood **(B)**, Spleen **(C)** and Lymph nodes **(D)** of Eogt$^{+/+}$ and Eogt$^{-/-}$ rats after Con-A injection at 0, 12, 24, and 48 h; **(E)** Flow cytometry assessment of CD4$^+$FOXP3$^+$ (Treg) cells in the Liver of Eogt$^{+/+}$ and Eogt$^{-/-}$ rats after Con-A injection at 0, 12, 24, and 48 h; **(F)** Quantification of Tregs in **(E)**. $^{**}p < 0.01$; $^{***}p < 0.001$, vs. WT control group.

determined the serum levels of select cytokines, including interleukins (ILs) and other inflammatory cytokines. Before Con A injection, serum RANTES and MIP-1α levels in *Eogt*$^{-/-}$ rats were significantly higher than those of *Eogt*$^{+/+}$ animals ($p < 0.05$, **Figures 5D,F**). With autoimmune hepatitis associated with Con A, the serum levels of some inflammatory cytokines (IL-2/4/10, IFNγ and TGF-β) were altered to varying degrees. However, as shown in **Figure 5**, serum IL-1β (12, 48, and 72 h), IL-2 (12, 48, and 72 h), IL-4 (12 h), RANTES (24, 48, and 72 h), IFNγ (12 h) and MIP-1α (12, 48, and 72 h) levels in Con A-treated *Eogt*$^{-/-}$ rats were significantly higher compared with those of Con A-treated *Eogt*$^{+/+}$ animals, while serum Eotaxin (12 h), IL-10 (48 and 72 h) and TGF-β (12 and 24 h) were significantly lower ($p < 0.05$ or 0.01). No variations of other cytokines in serum were observed (data not shown).

EOGT Inhibits Treg Activation via the Notch Signaling Pathway

To further assess the relationship between EOGT-mediated glycosylation and Treg activation, we performed MACS to separate CD4$^+$ T cells from *Eogt*$^{+/+}$ and *Eogt*$^{-/-}$ rat spleens. Flow cytometry analysis confirmed that a purity for the isolated CD4$^+$ T cells of 96.43 ± 2.67%. Next, we cultured the isolated CD4$^+$ T cells under Con A stimulation (5 μg/mL), and detected the Treg population by FACS. After 12 h, the proportion of Tregs were increased from 7.37 ± 0.47% to 17.73 ± 1.35% in the *Eogt*$^{+/+}$ CD4$^+$ T population (**Figures 6A,B**), whereas this increase was significantly lower in the *Eogt*$^{-/-}$ CD4+ T cells, from 6.73 ± 0.62% to 12.10 ± 1.50% (**Figures 6A,B**). Notch signaling has been reported to promote the differentiation and survival of Tregs (27–29). Meanwhile, glycosylation of the extracellular domain of Notch is important for activating Notch signaling (30). To determine whether loss of *Eogt* suppresses Notch signaling to prevent Treg differentiation, cultured CD4$^+$ T cells were collected after 6 h of Con A stimulation for gene expression analysis. Con A treatment did not alter the expression levels of *Notch1* and *Notch2* in *Eogt*$^{+/+}$ and *Eogt*$^{-/-}$ CD4$^+$ T cells (**Figure 6C**); meanwhile, Eogt knockout decreased Notch1 protein O-GlcNAcylation levels in lymphocytes in *Eogt*$^{-/-}$ rats (**Figure 6E**). However, the expression levels of *Rbpj* and *Hes1*, Notch signaling-activated genes, were markedly induced in *Eogt*$^{+/+}$ CD4$^+$ T cells but not in *Eogt*$^{-/-}$ counterparts (**Figure 6D**). Furthermore, Western blot demonstrated that *Eogt* knockout reduced the activation of RBPJ, the major transcriptional effector of Notch signaling (**Figure 6F**).

DISCUSSION

PTMs of proteins constitute one of the most effective methods to dynamically and rapidly regulate protein functions, and

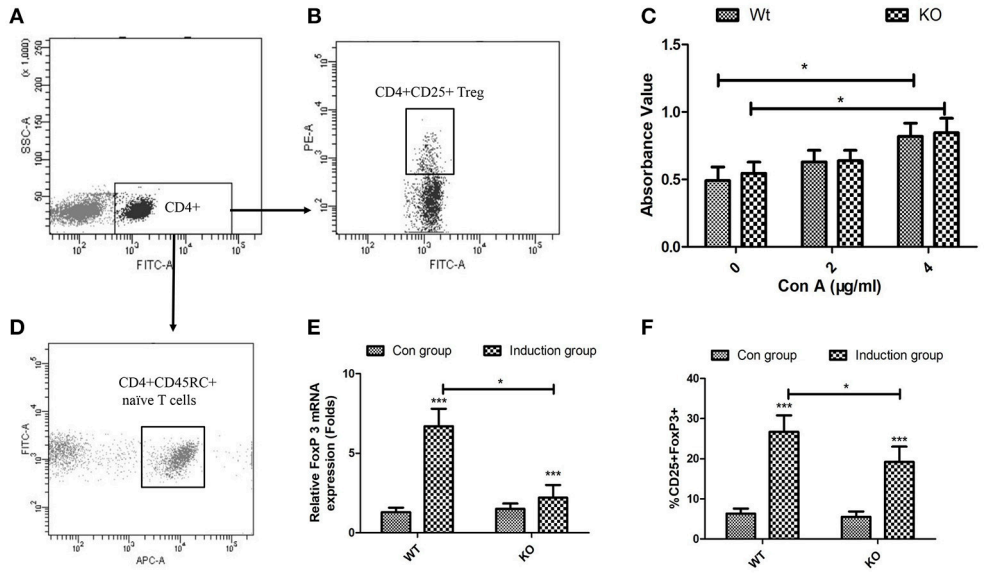

FIGURE 4 | Effects of EOGT knockout on Treg cell proliferation and differentiation. Flow cytometry for sorting naive $CD4^+$ T cells ($CD4^+CD45RC^+$) **(A,D)** and $CD4^+CD25^+$ Tregs **(A,B)** from rat spleens; **(C)** $CD4^+CD25^+$ Tregs from $Eogt^{+/+}$ and $Eogt^{-/-}$ rats treated with IL-2 without or with different Con A concentrations for 48 h; **(E)** Foxp3 mRNA levels and **(F)** percentages of regulatory T cells ($CD25^+Foxp3^+$) differentiated from naive $CD4^+$ T cells ($CD4^+CD45RC^+$). Data are mean ± SD from three independent experiments. $^*P < 0.05$; $^{***}p < 0.001$, vs. WT control group.

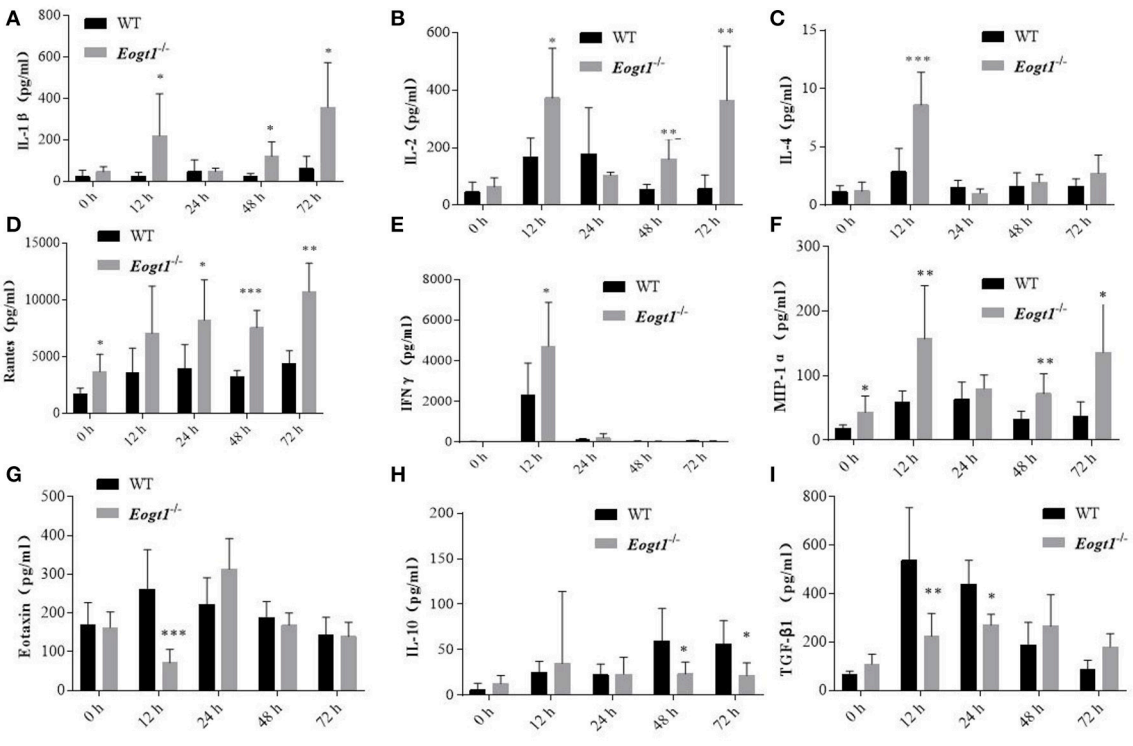

FIGURE 5 | Luminex multiplex analysis of cytokine levels in rat serum. Column charts respectively show serum levels of 9 cytokines in $Eogt^{+/+}$ and $Eogt^{-/-}$ rats after Con-A injection at 0, 12, 24, 48, and 72 h. Data are mean ± SD from three independent experiments. $^*P < 0.05$; $^{**}P < 0.01$, vs. WT control group. **(A)** IL-1β, **(B)** IL-2, **(C)** IL-4, **(D)** Rentes, **(E)** IFN-r, **(F)** MIP-1α, **(G)** Extaxin, **(H)** IL-10, **(I)** TGF-β1.

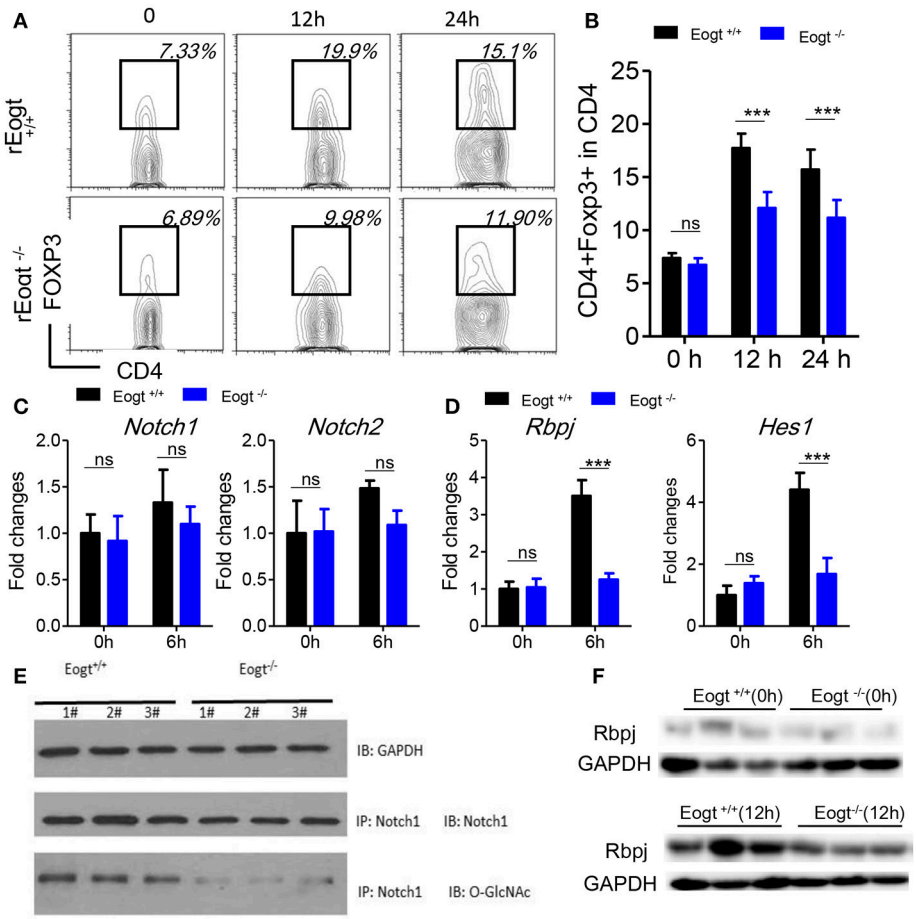

FIGURE 6 | Knockout of Eogt inhibits Treg differentiation via the NOTCH signaling pathway. **(A)** Flow cytometry analysis of $CD4^+FOXP3^+$ (Treg) cells in $Eogt^{+/+}$ ($n = 6$) and $Eogt^{-/-}$ ($n = 6$) $CD4^+$ T cells after *in vitro* treatment with Con A; **(B)** Quantification of Tregs in **(A)**; **(C)** Quantitative PCR analysis of *Nocth1* and *Nocth2* in $Eogt^{+/+}$ ($n = 6$) and $Eogt^{-/-}$ ($n = 6$) $CD4^+$ T cells after *in vitro* treatment with Con A; **(D)** Quantitative PCR analysis of *Rbpj* and Hes1 in $Eogt^{+/+}$ ($n = 6$) and $Eogt^{-/-}$ ($n = 6$) $CD4^+$ T cells after *in vitro* treatment with Con A; Western blot analysis of O-GlcNAc and Notch1 levels in lymphocytes **(E)** and Rbpj expression amounts in $Eogt^{+/+}$ ($n = 6$) and $Eogt^{-/-}$ ($n = 6$) $CD4^+$ T cells after *in vitro* treatment with Con A **(F)**. $^{***}p < 0.001$, vs. WT control group.

play important roles in several physiological and pathological processes; indeed, abnormalities of protein PTMs are both the causes and consequences of various diseases (31). In this study, the TALEN technology was applied to knock out the rat *Eogt* gene, which encodes the enzyme that catalyzes protein glycosylation, and demonstrated that this glycosylation deficiency could prevent Treg differentiation by suppressing Notch signaling, leading to $CD4^+$ T lymphocyte infiltration that resulted in the aggravation of hepatic dysfunction in Con A-induced AIH.

AIH is the most typical autoimmune disease, and characterized by a T-cell-rich infiltrate (32). In the course of disease development, effector T cells from peripheral blood are recruited to the inflamed liver, leading to the apoptosis of hepatocytes. Then, activated Tregs suppress the proliferation and cytokine secretion of infiltrating effector T cells (33). Previous studies demonstrated a reduction of Treg frequency in peripheral blood from AIH patients (10, 11), suggesting that Tregs are recruited to the inflamed liver along with effector T cells to control inflammation (12). In line with these previous reports, this study demonstrated a rapid reduction of $CD4^+$ T cells in peripheral blood and an accumulation of $CD4^+$ T cells in the liver following Con A treatment; however, the frequency of Tregs in the liver was largely different between $Eogt^{+/+}$ and $Eogt^{-/-}$ rats, with only a slight increase in the latter and a marked increase in the former. This *in vivo* finding might indicate that the recruited Tregs from peripheral blood only represent a small population of liver Tregs, and the main liver Treg population might instead originate from T cell differentiation in response to the hepatic microenvironment (34). We sorted Tregs ($CD4^+CD25^+FoxP3^+$) from liver samples after Con A-induced autoimmune liver injury at 12 h, and compared the mRNA levels of CTLA-4 and GITR in $CD4^+CD25^+Foxp3^+$ (Treg) cells. As shown in **Figure S1**, there were no significant differences in mRNA expression levels of CTLA-4 and GITR between the two subsets of WT and KO rats, suggesting that

abnormal Treg activation caused by Eogt knockout could be independent of Tregs' functional makers.

In vitro and *in vivo* studies have demonstrated that T cell receptor signaling, cytokines, and other signaling pathways play important roles in the development and differentiation of Tregs in disease (35–37). In a liver with AIH, the presence of transforming growth factor-beta released from hepatocytes or other activated non-parenchymal cells could promote Treg differentiation (38, 39). We further showed that Con A also regulated the differentiation of Tregs from $CD4^+$ T lymphocytes *in vitro*. Previous studies have shown that Con A-treated $CD4^+$ T cells have significantly increased levels of Notch1 (40), and activation of the Notch signaling pathway has been detected in induced Tregs (41). Although Con A did not upregulate *Notch1* in the $CD4^+$ T cell population in the present study, Notch signaling was activated upon Con A stimulation, which promoted the differentiation of Tregs mediated by glycosylation. Protein structure analysis revealed that the extracellular domain of Notch contains epidermal growth factor-like repeats, representing a consensus site for O-glycosylation catalyzed by EOGT (42). In addition, EOGT-mediated Notch signaling pathway activation has been confirmed in $Eogt^{-/-}$ mice (42).

The current study had several limitations. First, due to the lack of well-established *in vitro* rat Treg cell-differentiation conditions, we could only refer to the reported method of *in vitro* mouse Treg differentiation from naïve T cells. Secondly, as many immune cells as possible should be assessed in other immune organs (bone marrow, peripheral blood, spleen and lymph nodes etc.) to explore the role of Eogt knockout in the immune system. Thirdly, because liver samples in this study were not properly preserved, we could not detect the CD69 activation marker and the cleaved Notch intracellular domain (NICD) on $CD4^+$ T cells.

In summary, this study demonstrated that EOGT plays a critical role in AIH by regulating Treg differentiation via Notch signaling. In EOGT-deficient rats, Treg differentiation was clearly impaired due to inactivated Notch signaling, resulting in abnormal infiltration of the T cell population into the liver, which aggravates hepatic injury. Therefore, this study revealed a regulatory role for glycosylation in the pathogenesis of AIH, highlighting a potential therapeutic target.

ETHICS STATEMENT

This study was carried out in accordance with the recommendations of the international guidelines for the care and use of laboratory animals, Experimental Animal Care and Use Committee of Peking University Health Science Center. The protocol was approved by the Experimental Animal Care and Use Committee of Peking University Health Science Center.

AUTHOR CONTRIBUTIONS

HW, XH, and YL contributed to research design. XH, YL, JW, JM, SZ, XY, LH, JY, and MG, performed the research. FX and SZ provided innovative views and opinions. XH and YL analyzed the data. XH and SZ wrote the manuscript. HW revised the manuscript.

FUNDING

This work was supported by the National Natural Science Foundation of China (grant number: 30872243, 81071411 and 81271901).

SUPPLEMENTARY MATERIAL

The Supplementary Material for this article can be found online at: https://www.frontiersin.org/articles/10.3389/fimmu.2018.02089/full#supplementary-material

REFERENCES

1. Krawitt EL. Autoimmune hepatitis. *New England J Med.* (2006) 354:54–66. doi: 10.1056/NEJMra050408
2. Czaja AJ, Manns MP. Advances in the diagnosis, pathogenesis, and management of autoimmune hepatitis. *Gastroenterology* (2010) 139:58–72 e54. doi: 10.1053/j.gastro.2010.04.053
3. Hardtke-Wolenski M, Fischer K, Noyan F, Schlue J, Falk CS, Stahlhut M, et al. Genetic predisposition and environmental danger signals initiate chronic autoimmune hepatitis driven by $CD4^+$ T cells. *Hepatology* (2013) 58:718–28. doi: 10.1002/hep.26380
4. Taubert R, Hardtke-Wolenski M, Noyan F, Wilms A, Baumann AK, Schlue J, et al. Intrahepatic regulatory T cells in autoimmune hepatitis are associated with treatment response and depleted with current therapies. *J Hepatol.* (2014) 61:1106–14. doi: 10.1016/j.jhep.2014.05.034
5. Crispe IN. Hepatic T cells and liver tolerance. *Nat Rev Immunol.* (2003) 3:51–62. doi: 10.1038/nri981
6. Lüth S, Huber S, Schramm C, Buch T, Zander S, Stadelmann C, et al. Ectopic expression of neural autoantigen in mouse liver suppresses experimental autoimmune neuroinflammation by inducing antigen-specific Tregs. *J Clin Invest.* (2008) 118:3403–10. doi: 10.1172/JCI32132
7. Sakaguchi, S. Naturally arising Foxp3-expressing $CD25^+CD4^+$ regulatory T cells in immunological tolerance to self and non-self. *Nat Immunol.* (2005) 6:345–52. doi: 10.1038/ni1178
8. Belkaid Y, Rouse BT. Natural regulatory T cells in infectious disease. *Nat Immunol.* (2005) 6:353–60. doi: 10.1038/ni1181
9. Maloy KJ, Powrie F. Regulatory T cells in the control of immune pathology. *Nat Immunol.* (2001) 2:816–22. doi: 10.1038/ni0901-816
10. Longhi MS, Ma Y, Bogdanos DP, Cheeseman P, Mieli-Vergani G, Vergani D, et al. Impairment of CD4(+)CD25(+) regulatory T-cells in autoimmune liver disease. *J Hepatol.* (2004) 41:31–7. doi: 10.1016/j.jhep.2004.03.008
11. Longhi MS, Hussain MJ, Mitry RR, Arora SK, Mieli-Vergani G, Vergani D, et al. Functional study of $CD4^+CD25^+$ regulatory T cells in health and autoimmune hepatitis. *J Immunol.* (2006) 176:4484–91. doi: 10.4049/jimmunol.176.7.4484
12. Oo YH, Weston CJ, Lalor PF, Curbishley SM, Withers DR, Reynolds GM, et al. Distinct roles for CCR4 and CXCR3 in the recruitment and positioning of regulatory T cells in the inflamed human liver. *J Immunol.* (2010) 184:2886–98. doi: 10.4049/jimmunol.0901216
13. Rudensky AY. Regulatory T cells and Foxp3. *Immunol Rev.* (2011) 241:260–68. doi: 10.1111/j.1600-065X.2011.01018.x

14. Wu Y, Borde M, Heissmeyer V, Feuerer M, Lapan AD, Stroud JC, et al. FOXP3 controls regulatory T cell function through cooperation with NFAT. *Cell* (2006) 126:375–87. doi: 10.1016/j.cell.2006.05.042
15. Ono M, Yaguchi H, Ohkura N, Kitabayashi I, Nagamura Y, Nomura T, et al. Foxp3 controls regulatory T-cell function by interacting with AML1/Runx1. *Nature* (2007) 446:685–89. doi: 10.1038/nature05673
16. Asano N, Watanabe T, Kitani A, Fuss IJ, Strober W. Notch1 signaling and regulatory T cell function. *J Immunol.* (2008) 180:2796–804. doi: 10.4049/jimmunol.180.5.2796
17. van Loosdregt J, Coffer PJ. Post-translational modification networks regulating FOXP3 function. *Trends Immunol.* (2014) 35:368–78. doi: 10.1016/j.it.2014.06.005
18. Comelli EM, Sutton-Smith M, Yan Q, Amado M, Panico M, Gilmartin T, et al. Activation of murine $CD4^+$ and $CD8^+$ T lymphocytes leads to dramatic remodeling of N-linked glycans. *J Immunol.* (2006) 177:2431–40. doi: 10.4049/jimmunol.177.4.2431
19. Cabral J, Hanley SA, Gerlach JQ, O'Leary N, Cunningham S, Ritter T, et al. Distinctive surface glycosylation patterns associated with mouse and human CD4(+) Regulatory T cells and their suppressive function. *Front Immunol.* (2017) 8:987. doi: 10.3389/fimmu.2017.00987
20. Heymann F, Hamesch K, Weiskirchen R, Tacke F. The concanavalin A model of acute hepatitis in mice. *Lab Anim.* (2015) 49:12–20. doi: 10.1177/0023677215572841
21. Kusters S, Gantner F, Kunstle G, Tiegs G. Interferon gamma plays a critical role in T cell-dependent liver injury in mice initiated by concanavalin A. *Gastroenterology* (1996) 111:462–71.
22. Löhr HF, Schlaak JF, Lohse AW, Böcher WO, Arenz M, Gerken G, et al. Autoreactive $CD4^+$ LKM-specific and anticlonotypic T-cell responses in LKM-1 antibody-positive autoimmune hepatitis. *Hepatology* (1996) 24:1416–21. doi: 10.1002/hep.510240619
23. Varshney S, Stanley P. Biochem Soc trans. EOGT and O-GlcNAc on secreted and membrane proteins. *Biochem. Soc. Trans.* (2017) 45:401–8. doi: 10.1042/BST20160165
24. Sanjana NE, Cong L, Zhou Y, Cunniff MM, Feng G, Zhang F. A transcription activator-like effector toolbox for genome engineering. *Nat Protoc.* (2012) 7:171–92. doi: 10.1038/nprot.2011.431
25. Wing K, Sakaguchi S. Regulatory T cells exert checks and balances on self tolerance and autoimmunity. *Nat Immunol.* (2010) 11:7–13. doi: 10.1038/ni.1818
26. Yamashita J, Iwamura C, Sasaki T, Mitsumori K, Ohshima K, Hada K, et al. Apolipoprotein A-II suppressed concanavalin A-induced hepatitis via the inhibition of CD4 T cell function. *J Immunol.* (2011) 186:3410–20. doi: 10.4049/jimmunol.1002924
27. Charbonnier LM, Wang S, Georgiev P, Sefik E, Chatila TA. Control of peripheral tolerance by regulatory T cell-intrinsic Notch signaling. *Nat Immunol.* (2015) 16:1162–73. doi: 10.1038/ni.3288
28. Perumalsamy LR, Marcel N, Kulkarni S, Radtke F, Sarin A. Distinct spatial and molecular features of notch pathway assembly in regulatory T cells. *Sci Signal.* (2012) 5:ra53. doi: 10.1126/scisignal.2002859
29. Ou-Yang HF, Zhang HW, Wu CG, Zhang P, Zhang J, Li JC, et al. Notch signaling regulates the FOXP3 promoter through RBP-J- and Hes1-dependent mechanisms. *Mole Cell Biochem.* (2009) 320:109–14. doi: 10.1007/s11010-008-9912-4
30. Takeuchi H, Haltiwanger RS. Significance of glycosylation in Notch signaling. *Biochem Biophys Res Commun.* (2014) 453:235–42. doi: 10.1016/j.bbrc.2014.05.115
31. Li S, Iakoucheva LM, Mooney SD, Radivojac P. Loss of post-translational modification sites in disease. In: *Pacific Symposium Biocomputing.* (2010). p. 337–47. doi: 10.1142/9789814295291_0036
32. Oo YH, Hubscher SG, Adams DH. Autoimmune hepatitis: new paradigms in the pathogenesis, diagnosis, and management. *Hepatol Int.* (2010) 4:475–93. doi: 10.1007/s12072-010-9183-5
33. Oo YH, Adams DH. Regulatory T cells and autoimmune hepatitis: defective cells or a hostile environment? *J Hepatol.* (2012) 57:6–8. doi: 10.1016/j.jhep.2012.04.005
34. Oo YH, Adams DH. Regulatory T cells and autoimmune hepatitis: what happens in the liver stays in the liver. *J Hepatol.* (2014) 61:973–5. doi: 10.1016/j.jhep.2014.08.005
35. Kretschmer K, Apostolou I, Hawiger D, Khazaie K, Nussenzweig MC, von Boehmer H. Inducing and expanding regulatory T cell populations by foreign antigen. *Nat Immunol.* (2005) 6:1219–27. doi: 10.1038/ni1265
36. Chen W, Jin W, Hardegen N, Lei KJ, Li L, Marinos N, et al. Conversion of peripheral $CD4^+CD25^-$ naive T cells to $CD4^+CD25^+$ regulatory T cells by TGF-beta induction of transcription factor Foxp3. *J Exp Med.* (2003) 198:1875–86. doi: 10.1084/jem.20030152
37. Josefowicz SZ, Lu LF, Rudensky AY. Regulatory T cells: mechanisms of differentiation and function. *Ann Rev Immunol.* (2012) 30:531–64. doi: 10.1146/annurev.immunol.25.022106.141623
38. Knolle PA, Thimme R. Hepatic immune regulation and its involvement in viral hepatitis infection. *Gastroenterology* (2014) 146:1193–207. doi: 10.1053/j.gastro.2013.12.036
39. Carambia A, Freund B, Schwinge D, Heine M, Laschtowitz A, Huber S, et al. TGF-beta-dependent induction of CD4(+)CD25(+)Foxp3(+) Tregs by liver sinusoidal endothelial cells. *J Hepatol.* (2014) 61:594–99. doi: 10.1016/j.jhep.2014.04.027
40. Burghardt S, Erhardt A, Claass B, Huber S, Adler G, Jacobs T, et al. Hepatocytes contribute to immune regulation in the liver by activation of the notch signaling pathway in T cells. *J Immunol.* (2013) 191:5574–82. doi: 10.4049/jimmunol.1300826
41. Burghardt S, Claass B, Erhardt A, Karimi K, Tiegs G. Hepatocytes induce foxp3(+) regulatory T cells by notch signaling. *J Leukocyte Biol.* (2014) 96:571–77. doi: 10.1189/jlb.2AB0613-342RR
42. Sawaguchi S, Varshney S, Ogawa M, Sakaidani Y, Yagi, H, Takeshita, K, et al. O-GlcNAc on NOTCH1 EGF repeats regulates ligand-induced Notch signaling and vascular development in mammals. *eLife* (2017) 6:e24419. doi: 10.7554/eLife.24419

Conflict of Interest Statement: The authors declare that the research was conducted in the absence of any commercial or financial relationships that could be construed as a potential conflict of interest.

Copyright © 2018 Hao, Li, Wang, Ma, Zhao, Ye, He, Yang, Gao, Xiao and Wei. This is an open-access article distributed under the terms of the Creative Commons Attribution License (CC BY). The use, distribution or reproduction in other forums is permitted, provided the original author(s) and the copyright owner(s) are credited and that the original publication in this journal is cited, in accordance with accepted academic practice. No use, distribution or reproduction is permitted which does not comply with these terms.

frontiers in Immunology

ORIGINAL RESEARCH
published: 11 October 2018
doi: 10.3389/fimmu.2018.02347

IL-17RA-Signaling Modulates CD8+ T Cell Survival and Exhaustion During *Trypanosoma cruzi* Infection

Jimena Tosello Boari[1,2], *Cintia L. Araujo Furlan*[1,2], *Facundo Fiocca Vernengo*[1,2], *Constanza Rodriguez*[1,2], *María C. Ramello*[1,2], *María C. Amezcua Vesely*[1,2], *Melisa Gorosito Serrán*[1,2], *Nicolás G. Nuñez*[3,4], *Wilfrid Richer*[3,4], *Eliane Piaggio*[3,4], *Carolina L. Montes*[1,2], *Adriana Gruppi*[1,2] *and Eva V. Acosta Rodríguez*[1,2]*

[1] *Departamento de Bioquímica Clínica, Facultad de Ciencias Químicas, Universidad Nacional de Córdoba, Córdoba, Argentina,* [2] *Centro de Investigaciones en Bioquímica Clínica e Inmunología, CONICET, Córdoba, Argentina,* [3] *SiRIC TransImm "Translational Immunotherapy Team," Translational Research Department, Research Center, PSL Research University, INSERM U932, Institut Curie, Paris, France,* [4] *Centre d'Investigation Clinique Biothérapie CICBT 1428, Institut Curie, Paris, France*

OPEN ACCESS

Edited by:
Gustavo Javier Martinez, Rosalind Franklin University of Medicine and Science, United States

Reviewed by:
Seon Hee Chang, University of Texas MD Anderson Cancer Center, United States
Lawrence Kane, University of Pittsburgh, United States
Bertram Bengsch, Universitätsklinikum Freiburg, Germany

***Correspondence:**
Eva V. Acosta Rodríguez
eacosta@fcq.unc.edu.ar

Specialty section:
This article was submitted to T Cell Biology, a section of the journal Frontiers in Immunology

Received: *08 June 2018*
Accepted: *21 September 2018*
Published: *11 October 2018*

Citation:
Tosello Boari J, Araujo Furlan CL, Fiocca Vernengo F, Rodriguez C, Ramello MC, Amezcua Vesely MC, Gorosito Serrán M, Nuñez NG, Richer W, Piaggio E, Montes CL, Gruppi A and Acosta Rodríguez EV (2018) IL-17RA-Signaling Modulates CD8+ T Cell Survival and Exhaustion During Trypanosoma cruzi Infection. Front. Immunol. 9:2347. doi: 10.3389/fimmu.2018.02347

The IL-17 family contributes to host defense against many intracellular pathogens by mechanisms that are not fully understood. CD8+ T lymphocytes are key elements against intracellular microbes, and their survival and ability to mount cytotoxic responses are orchestrated by several cytokines. Here, we demonstrated that IL-17RA-signaling cytokines sustain pathogen-specific CD8+ T cell immunity. The absence of IL-17RA and IL-17A/F during *Trypanosoma cruzi* infection resulted in increased tissue parasitism and reduced frequency of parasite-specific CD8+ T cells. Impaired IL-17RA-signaling *in vivo* increased apoptosis of parasite-specific CD8+ T cells, while *in vitro* recombinant IL-17 down-regulated the pro-apoptotic protein BAD and promoted the survival of activated CD8+ T cells. Phenotypic, functional, and transcriptomic profiling showed that *T. cruzi*-specific CD8+ T cells derived from IL-17RA-deficient mice presented features of cell dysfunction. PD-L1 blockade partially restored the magnitude of CD8+ T cell responses and parasite control in these mice. Adoptive transfer experiments established that IL-17RA-signaling is intrinsically required for the proper maintenance of functional effector CD8+ T cells. Altogether, our results identify IL-17RA and IL-17A as critical factors for sustaining CD8+ T cell immunity to *T. cruzi.*

Keywords: IL-17, chagas disease, immunity, cellular, CD8+ T cells, exhausted T cells, effector function, apoptosis

INTRODUCTION

IL-17A and IL-17F were initially associated with the pathogenesis of autoinflammatory and autoimmune disorders (1). Nonetheless, the primary function of these cytokines is likely host protection against microbes. Indeed, mice deficient in IL-17A and/or IL-17F are highly susceptible to infection with a wide array of fungi and extracellular bacteria, as well as viruses and parasites (2, 3). We previously demonstrated that the IL-17 family of cytokines plays a critical role in host survival by regulating exuberant inflammation and immunopathology during infection with the protozoan *Trypanosoma cruzi* (4, 5). Additional data from our laboratory suggests that IL-17 plays additional protective roles against *T. cruzi* by modulating adaptive immunity.

The IL-17 family is comprised of 6 members, IL-17A to IL-17F, which have different cellular sources and expression patterns but often show overlapping activities. The cytokines signal through a receptor complex composed of at least two identical or different subunits of the IL-17R family (IL-17RA to IL-17RE). IL-17RA is the common signaling subunit used by at least four ligands: IL-17A, IL-17C, IL-17E, and IL-17F. IL-17 members regulate inflammation by recruiting and activating neutrophils, NK cells, and other cells of the innate immune system and by inducing several pro-inflammatory mediators (i.e., cytokines, chemokines, microbial peptides, and metalloproteinases). In addition, these cytokines play important roles during adaptive immune responses, including the modulation of germinal center reactions, as well as the regulation of Th1 and CD8+ cellular responses (6–9).

Infection with *T. cruzi* is known to cause Chagas disease, the third most frequent parasitic disease worldwide that is endemic in Latin America and is increasing globally due to migratory flows. Disease progression, from asymptomatic to severe cardiac and digestive forms, is linked to parasite heterogeneity and variable host immune responses. CD8+ T cell mediated immunity is essential for parasite control throughout the various stages of infection, although it is not sufficient for complete parasite elimination (10, 11). CD8+ T cell deficient mice are extremely susceptible to infection (12, 13), and strategies that improve specific CD8+ T cell responses result in increased host protection (11, 14, 15). This finding, coupled with the fact that parasite persistence correlates with disease severity in human and experimental models of *T. cruzi* infection (16, 17), have prompted efforts to better understand the mechanisms that promote anti-parasitic CD8+ T cell immunity.

The general features of protective CD8+ T cell responses (as defined with model viral and bacterial infections) consist of the generation and expansion of short-lived, highly functional effector populations with antimicrobial activities. After the pathogen has been cleared, most of the effector cells die and the few remaining cells differentiate into memory T cells, contributing to long-lived immunological protection (18). Persistently activated CD8+ T cells can become dysfunctional during certain chronic infections, which results in a hierarchical loss of effector functions and proliferation potential, as well as sustained expression of multiple inhibitory receptors. Severe exhaustion leads to pathogen-specific cells that are prone to deletion and have reduced ability to produce cytokines and degranulate. These exhausted CD8+ T cells fail to provide optimal protection and contribute to poor pathogen control (19). In addition to antigen-specific and co-stimulatory signals, which are the driving forces behind CD8+ T cell responses, various cytokines (i.e., IL-21, IL-2, IL-12) are required to provide the "third-signal" essential for protective CD8+ T cell immunity (20, 21).

Herein, we demonstrate that IL-17RA signaling is required for the maintenance of robust, specific CD8+ T cell responses that contribute to host resistance to *T. cruzi*. We show that absence of IL-17RA signaling during *T. cruzi* infection alters the transcriptional program of effector CD8+ T cells, and consequently affects their survival, effector function, and exhaustion. Our findings are relevant for gaining a better understanding of the role of the IL-17 family in the orchestration of protective immunity against infections.

MATERIALS AND METHODS

Mice

Mice used for experiments were sex- and age-matched (6 to 10 weeks-old). C57BL/6 mice were obtained from School of Veterinary, La Plata National University (La Plata, Argentina). IL-17RA KO mice were provided by Amgen Inc. (Master Agreement N° 200716544-002). IL-17A/IL-17F double KO mice (22) were kindly provided by Dr Immo Prinz. CD45.1 C57BL/6 mice (B6.SJL-*Ptprca Pepcb*/Boy) and CD8α KO mice (B6.129S2-Cd8atm1Mak/J) were obtained from The Jackson Laboratories (USA). CD45.1 × CD45.2 F1 WT mice bred in our animal facility. All animals were housed in the Facultad de Ciencias Químicas, Universidad Nacional de Córdoba.

Parasites and Experimental Infection

Bloodstream trypomastigotes of the Tulahuén strain of *T. cruzi* were obtained from BALB/c mice infected 10 days earlier. For experimental infection mice were inoculated intraperitoneally with 0.2 ml PBS containing 5×10^3 trypomastigotes (usual dose) or doses of 500 and 5×10^4 trypomastigotes when indicated. For infection of transferred CD8α knockout mice, parasite dose was 1,000 trypomastigotes.

Quantification of Parasite DNA in Tissues

Genomic DNA was purified from 50 μg of tissue (spleen, liver, and heart) using TRIzol Reagent (Life Technologies) following manufacturer's instructions. Satellite DNA from *T. cruzi* (GenBank AY520036) was quantified by real time PCR using specific Custom Taqman Gene Expression Assay (Applied Biosystem) using the primer and probe sequences described by Piron et al. (23). A sample was considered positive for the *T. cruzi* target when CT < 45. Abundance of satellite DNA from *T. cruzi* was normalized to GAPDH abundance (Taqman Rodent GAPDH Control Reagent, Applied Biosystem) and expressed as arbitrary units.

Cells and Culture

CD8+ T cells were isolated from the spleen by magnetic negative selection or cell sorting from pools of at least 3-5 mice. For magnetic cell purification the EasySep™ Mouse CD8+ T Cell Isolation Kit (Stemcell Technologies) were used according to the manufacturer's protocol. For cell sorting, spleen cell suspensions were surface stained and CD3+CD8+ T cells were sorted with a FACSAria II (BD Biosciences). During *in vitro* studies, CD8+ T cells (2×10^5) purified by magnetic selection were stimulated in 96-well plates coated with anti-CD3/anti-CD28 Abs (eBioscience, 2 and 1 μg/ml respectively) and incubated during 24 h in the presence of 100 ng/ml of recombinant IL-17A, IL-17F, IL-17C, and IL-17E (ImmunoTools, GmbH) and/or 50 ng/mL of IL-21 and TNF (ImmunoTools, GmbH). For camptothecin challenge, the drug was added in a concentration of 5 μM from the beginning of the culture.

Antibodies and Flow Cytometry

Cell suspensions were washed in PBS and incubated with LIVE/DEAD Fixable Cell Dead Stain (eBioscience) during 15 min at RT. Next, cells were washed and incubated with fluorochrome labeled-Abs for 20 min at 4°C (see below for details). To detect *T. cruzi* specific CD8+ T cells, H-2K(b) *T. cruzi* trans-sialidase amino acids 567-574 ANYKFTLV (TSKB20) APC-Labeled Tetramer (NIH Tetramer Core Facility) were incubated 20 min at 4°C before further surface staining with additional Abs. After further surface staining, cells were washed and acquired in a FACSCanto II (BD Biosciences). Blood was directly incubated with the indicated antibodies and erythrocytes were lysed with a 0.87% NH_4Cl buffer previously to acquisition. For Ki-67 intranuclear staining, cells were first stained on surface, washed and then fixed, permeabilized and stained with Foxp3/Transcription Factor Staining Buffers (eBioscience) following eBioscience One-step protocol: intracellular (nuclear) proteins.

Flow cytometry and/or cell sorting was performed with a combination of the following Abs (BD Biosciences, Biolegend, eBioscience, Life Technologies, Santa Cruz Biotechnology or Cell Signaling): FITC/AF488-labeled anti-mouse: CD8 (53-6.7), anti-CD25 (7D4), CD69 (H1.2F3), CD44 (IM7), Bcl-2 (10C4), IgG (polyclonal goat), and anti-rat IgG (polyclonal goat); PE-labeled anti-mouse: Fas (Jo2), CTLA-4 (UC10-4B9), PD-1 (RMP1-30), Ki-67 (SolA15), IL-17RA (PAJ17R), CD120b (TR75-89), Bim (rabbit. C34C5), rabbit IgG control isotype (DA1E); PECy7-labeled anti-mouse: CD8 (53-6.7), PD-1 (RMP1-30), FAS (Jo2) and anti-CD25 (P61.5); PerCPCy5.5-labeled anti-mouse: CD3 (145-2C11), CD45.2 (104); PerCP-eFluor 710 labeled anti-mouse: TIGIT (GIGD7); APC-Cy7/AF780-labeled anti-mouse: CD45.1 (A20) and CD62L (MEL-14); Biotin-labeled anti-mouse: BTLA (8F4) and PE-labeled Streptavidin; unlabeled anti-mouse: Bcl-xL (rabbit, 54H7), Bcl-2-associated death promoter (BAD) (rabbit, C-20), Bax (rabbit, P-19).

Quantification of IL-21

The concentration of IL-21 in the plasma of in plasma of infected WT and IL-17RA KO mice was assessed by ELISA using paired specific Abs (eBiosciences) according to standard protocols.

Evaluation of Proliferation and Apoptosis

T. cruzi-infected WT and IL-17RA KO mice were given BrdU (1 mg/ml, Sigma-Aldrich)/1% sucrose in the drinking water (carefully protected from light) ad libitum. After 5 days, mice were sacrificed and spleen mononuclear cells were collected and stained with surface antibodies. Incorporated BrdU was detected with a BrdU Flow kit according to the manufacturer's specifications (BD Biosciences).

Apoptosis was determined by Annexin V and 7AAD staining according to the manufacturer's specifications (BD Biosciences). Mitochondrial depolarization (ψ) was measured by FACS using 50 nM TMRE (Invitrogen) as described (24). When indicated, 7AAD or LIVE/DEAD Fixable Aqua dead cell stain was used in combination to identify live, early apoptotic and late apoptotic/necrotic cells.

Determination of CD8+ T Cell Effector Function *in vitro*

Spleen cell suspensions were cultured during 5 h with medium, 5 μg/ml TSKB20 (ANYKFTLV) peptide (Genscript Inc.), 50 nM PMA plus 0.5 μg/ml ionomycin (Sigma-Aldrich) in the presence of Monensin and Brefeldin A (eBioscience). When indicated a PE-labeled anti-CD107a mAb (eBioscience, eBio1D4B) was included during the culture period. After culture, the cells were surface stained, fixed and permeabilized with BD Cytofix/Cytoperm and Perm/Wash (BD Biosciences) according manufacturer's instruction. Cells were incubated with FITC-labeled antibodies to IFNγ (eBioscience, XMG1.2) or Perforin-1 (eBoscience, eBioOMAK-D), PerCP/PerCP-eFluor 710 labeled antibody to TNF (Biolegend, MP6-XT22) or Granzyme A (eBiosciences, GzA-3G8.5) and/or APC/AF647-labeled antibody to TNF (Biolegend, MP6-XT22) or Granzyme B (Biolegend, GB11). Stained cells were acquired on FACSCanto II (BD Biosciences).

Adoptive Cell Transfer

Competitive adoptive transfer experiments were performed by i.v. injection of recipient CD45.1+/CD45.2+ WT mice (F1 hybrid obtained by crossing CD45.1+ and CD45.2+ WT mice) or CD8α knockout mice with a mixture 1:1 of CD8+ T cells purified from spleen of CD45.1+ WT mice and CD45.2+ IL-17RA KO mice. Total 5×10^6 cells and 15×10^6 cells were injected in WT and CD8α knockout recipients, respectively. Recipient mice were immediately infected and frequency of the injected CD45.1+ WT and CD45.2+ IL-17RA KO cells within the total T cell population were determined in blood, spleen and liver at different days pi.

To address the relevance of CD8+ T cell-intrinsic IL-17RA signaling for *T. cruzi* infection progression, CD8α knockout hosts were injected i.v. with the same number (7×10^6) of CD8+ T cells purified from spleen of WT or IL-17RA KO mice and immediately infected. Transfer of equal number of CD8+ T cells in both mouse groups was evaluated 1 day after injection by analyzing the frequency of CD8+ T cells in blood. The progression of the infection was followed by the quantification of parasitemia and survival. Infected non-transferred CD8α knockout mice were used as control.

Treatment With Neutralizing Anti- IL-17A and PD-L1 Abs

To block the PD-1/PD-L1 pathway, infected WT and IL-17RA KO mice were injected i.p. with 200 μg rat anti-mouse PD-L1 antibody (10F.9G2, BioXcell) or total rat IgG isotype control (Jackson Research) every 3 days from 15 dpi until sacrifice at day 21 dpi. Infection matched WT mice were assayed in parallel as controls.

For the *in vivo* neutralization of IL-17A, infected WT mice were injected i.p. with 200 μg rat anti-mouse IL-17 antibody (17F3, BioXcell) or rat total IgG1 isotype control (MOPC-21, BioXcell) every 3 days from day 13 dpi until sacrifice at 21 dpi. Infection-matched IL-17RA KO mice were assayed in parallel as controls.

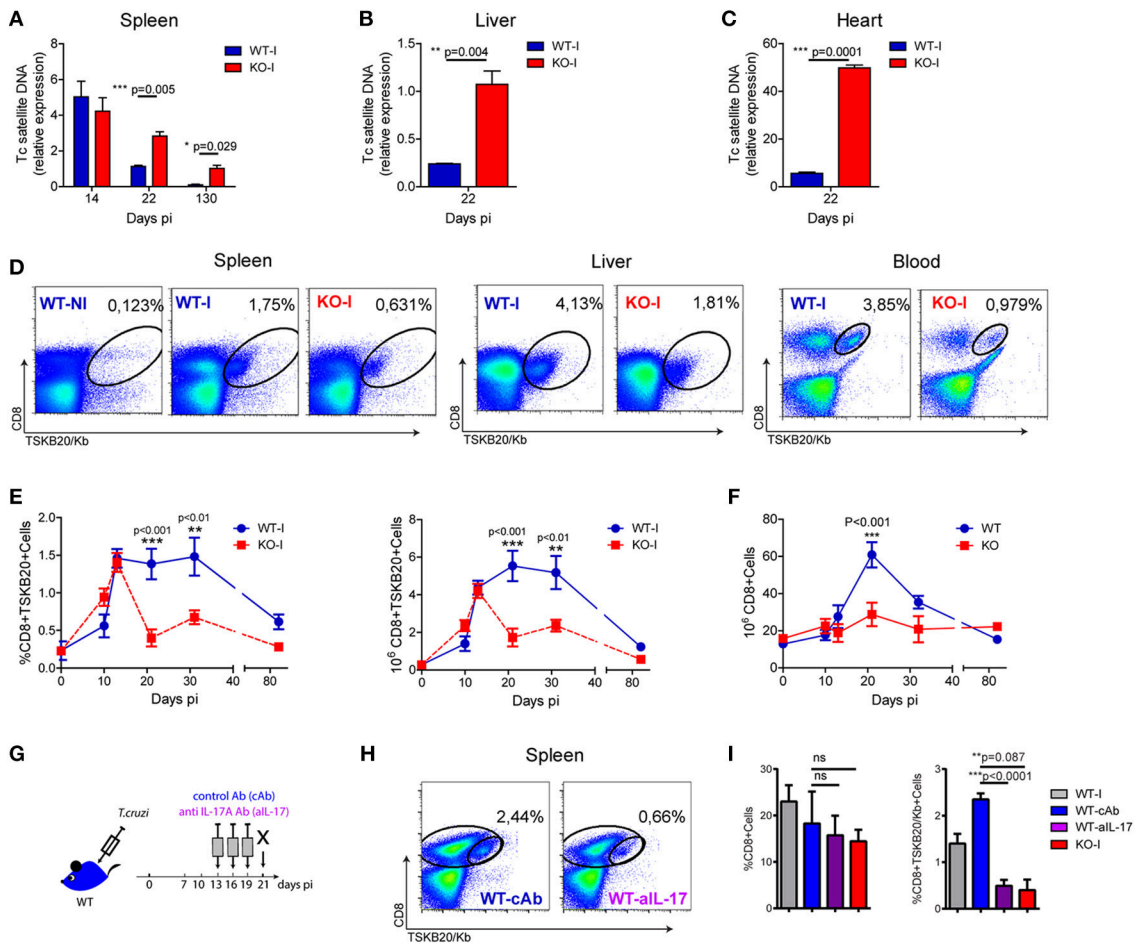

FIGURE 1 | Absence of IL-17RA signaling results in increased tissue parasitism and a reduced magnitude of parasite-specific CD8+ T cell responses. **(A-C)** Relative amount of *T. cruzi* satellite DNA in spleen **(A)**, liver **(B)** and heart **(C)** of infected WT and IL-17RA KO (KO) mice determined at the indicated dpi. Murine GAPDH was used for normalization. Data are presented as mean ± SD, $N = 5$ mice. *P* values calculated with two-tailed *T* test. **(D)** Representative plots of CD8 and TSKB20/Kb staining in spleen, liver and blood of WT and KO mice at 22 dpi (WT-I and KO-I, respectively). A representative plot of the staining of splenocytes from non-infected WT mice (WT-N) is shown for comparison. **(E)** Percentage and cell numbers of TSKB20/Kb+ CD8+ T cells and **(F)** cell numbers of total CD8+ T cells determined in spleen of WT and IL-17RA KO mice at different dpi. Data shown as mean ± SD, $N = 5–8$ mice. *P* values calculated using two-way ANOVA followed by Bonferroni's post-test. **(G)** Experimental layout of IL-17 neutralization in infected WT mice injected with control isotype or anti-IL-17 Abs (WT-cAb and WT-aIL-17, respectively). **(H)** Representative plots of CD8 and TSKB20/Kb staining in spleen and liver infected control and treated WT mice. **(I)** Percentage of total and TSKB20/Kb+ CD8+ T cells infected control and treated WT mice. Results from infection-matched WT (WT-I) and KO mice (KO-I) are shown for comparison. Data are representative of five **(A–F)**, and two **(G–I)** independent experiments.

Real-Time Quantitative PCR and DNA Microarray

RNA from total spleen tissue was purified using TRIzol Reagent (Life Technologies) following manufacturer's instructions. Oligo-dT and a MMLV reverse transcriptase kit (Invitrogen) were used for cDNA synthesis. IL-17RA, IL-17RC, and IL-17RD transcripts were quantified by real-time quantitative PCR on an ABI PRISM 7700 Sequence Detector (Perkin-Elmer Applied Biosystems) with Applied Biosystems predesigned TaqMan Gene Expression Assays and reagents according to the manufacturer's instructions. The following probes were used: Mm00434214_m1 for IL-17RA, Mm00506606_m1 for IL-17RC and Mm00460340_m1 for IL-17RD. For each sample, the mRNA abundance was normalized to the amount of 18S rRNA (Mm03928990_g1) and is expressed as arbitrary units (AU).

For gene-expression analysis, CD8+ T cells were purified by FACS from the spleen of non-infected and 22-day infected WT and IL-17RA KO mice and lysed with TRIzol reagent. Total RNA was extracted with the RNAeasy Mini Kit (Qiagen). RNA quality was verified in an Agilent Bioanalyzer and measured with a Nanodrop 1000 (Thermo Scientific). cDNA was hybridized on Affymetrix Mouse Gene 2.1 ST arrays as described elsewhere.

Analysis of Microarray Data

The microarray data from this publication have been deposited to the GEO database (https://www.ncbi.nlm.nih.gov/geo/) and assigned the identifier: GSE104886. Gene expression data was

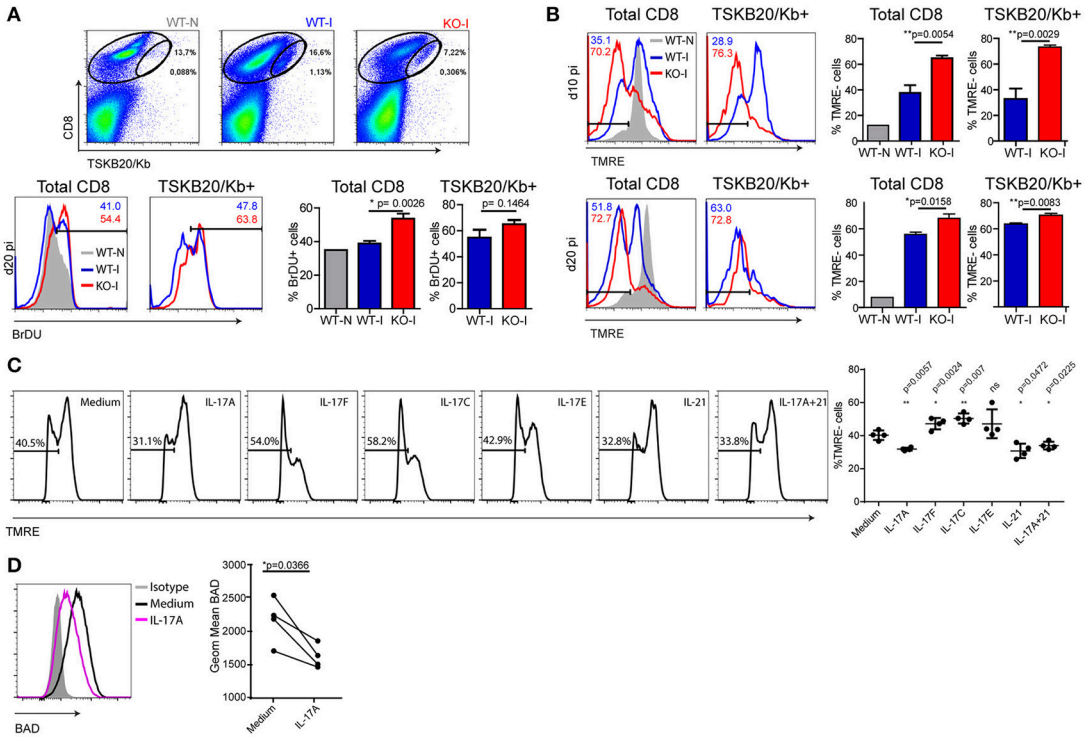

FIGURE 2 | IL-17RA signaling during *T. cruzi* infection promotes survival of CD8+ T cells. **(A)** Representative dot plots of CD8 and TSKB20/Kb staining and representative histograms of BrDU in cell suspensions from the spleen of WT and KO mice at 0 dpi (WT-N) and 20 dpi (WT-I and KO-I) and within the indicated total and TSKB20/Kb+ CD8+ T cell gates. Numbers in the histograms indicate the frequency of BrDU+ cells from the corresponding colored group. Histograms are representative of one out of five mice. Bars in the statistical analysis represent data as mean ± SD, $N = 5$ mice. *P* values were calculated with two-tailed *T* test. **(B)** Representative histograms of TMRE staining in total (left) and TSKB20/Kb+ (right) CD8+ T cells from the spleen of WT and IL17RA KO mice at 10 dpi (top) and 20 dpi (bottom). Numbers indicate the frequency of TMRE- (apoptotic) cells in total and TSKB20/Kb+ CD8+ T cells from the corresponding colored group. Gray tinted histogram show staining in CD8+ T cells from non-infected WT mice (WT-N). Histograms are representative of one out of five mice. Bars in the statistical analysis represent data as mean ± SD, $N = 5$ mice. *P* values were calculated with two-tailed *T* test. **(C, D)** Representative histograms of TMRE **(C)** and BAD **(D)** stainings in cultures of purified CD8+ T cells activated with coated anti-CD3 and anti-CD28 in the presence of the indicated cytokines. Statistical analysis in **(C)** shows the frequency of TMRE- (apoptotic) cells in each biological replicate ($N = 4$ mice) and the mean ± *SD*. *P* values calculated with paired two-tailed *T* test (ns, not significant). Statistical analysis in **(D)** represent protein expression as the geometric mean of fluorescence intensity in each replicate ($N = 4$ mice). Lines link paired samples. *P* values calculated with paired two-tailed *T* test. Data in **(A-D)** are representative of three and two independent experiments, respectively.

normalized using RMA algorithm on custom Brainarray CDF (v.22.0.0 ENTREZG). Plots of differential expressed genes in spleen CD8 T cells at day 0 post infection and day 22 post infection in WT and IL-17RA KO samples were defined using fold change [|log2FC| >log2(1.2)]. Bioinformatic analyses were performed with R software environment. Heatmaps were produced using Heatmapper (http://www.heatmapper.ca) and show gene expression of CD8+ T cells from WT and IL-17RA KO normalized by the average of the gene expression in non-infected counterparts, except specified. Gene Set Enrichment Analyses (GSEA) between the different spleen CD8 T cell samples were done using specific gene sets from the Molecular Signatures DB (MSigDB). Genes induced by the infection in WT and IL-17RA KO mice but showing significantly higher expression in IL-17RA KO mice were uploaded to Ingenuity Pahtway Analysis (Ingenuity® Systems, www.ingenuity.com) for the analysis of "Disease and bio-function," "Canonical pathway," and "Up-stream regulators." It was considered significantly activated (or inhibited) with an overlap $p \leq 0.05$ and an IPA activation Z-score as defined under each specific analysis category on the IPA website.

Statistics

Statistical significance of comparisons of mean values was assessed as indicated by a two-tailed Student's *t* test, two way ANOVA followed by Bonferroni's posttest and Gehan-Breslow-Wilcoxon Test using GraphPad software. $P < 0.05$ was considered statistically significant.

RESULTS

IL-17RA and IL-17A/IL-17F Deficiencies Compromise Parasite Control and Reduce the Magnitude of the Specific CD8+ T Cell Response During *T. cruzi* Infection

We previously showed that IL-17RA-signaling and IL-17-secreting B cells are required for host survival during *T. cruzi*

infection by, at least in part, regulating innate immunity and inflammation (4, 5). In addition, histological data from these initial studies suggested that infected IL-17RA knockout (KO) mice exhibited increased parasite levels in tissues, but similar levels of parasitemia, compared with those of their infected wildtype (WT) counterparts (4). To confirm this and to study possible additional protective mechanisms mediated by IL-17, we evaluated tissue parasitism in infected WT and IL-17RA KO mice. As determined by the amounts of parasite DNA quantified in the spleen, we observed that *T. cruzi* infected IL-17RA KO mice controlled tissue parasitism similar to WT mice during the first 2 weeks of infection (**Figure 1A**). However, IL-17RA KO mice failed to reduce the parasite burden at later stages of infection, as attested by the increased parasite load in the spleen at 22 and 130 days post-infection (dpi) (**Figure 1A**). Furthermore, increased parasite levels were also detected in other organs, such as liver and heart (**Figures 1B,C**).

Given that the aforementioned result suggested a deteriorated adaptive immune response, we focused on studying the role of IL-17RA in the development of parasite-specific CD8+ T cells. To this end, we examined the generation of CD8+ T cells specific for the immunodominant epitope TSKB20 (*T. cruzi* trans-sialidase amino acids 569-576 –ANYKFTLV–) (25) in infected IL-17RA KO and WT mice. We determined that the frequency of TSKB20-specific CD8+ T cells was reduced in the spleen, liver, and blood of infected IL-17RA KO mice at 20 dpi (**Figure 1D**). Kinetics studies showed that the frequency and absolute numbers of TSKB20-specific CD8+ T cells in the spleen of infected IL-17RA KO mice was similar to that of infected WT control mice up to 14 dpi, but these values dropped dramatically soon after (**Figure 1E**). Remarkably, total CD8+ T cell numbers at 20 dpi were also reduced in the spleen of infected IL-17RA KO mice (**Figure 1F**). In agreement with the notion that IL-17A and IL-17F are the major IL-17RA-signaling cytokines that modulate immune responses, IL-17A/IL-17F double knockout (DKO) mice also showed increased tissue parasitism in spleen and liver (**Supplementary Figure 1A**) and reduced frequency of parasite-specific CD8+ T cells in comparison to WT control mice (**Supplementary Figure 1B**).

Considering the kinetics of the TSKB20-specific CD8+ T cell immunity observed in infected IL-17RA KO mice (**Figure 1E**), along with our results showing that IL-17 production peaked around 14 dpi (4, 5), we speculated that IL-17RA signaling plays a role during the expansion and maintenance of parasite-specific CD8+ T cells after priming. To test this, we performed neutralization experiments in which infected WT mice were injected with anti-IL-17A antibodies (Abs) from 13 to 19 dpi (**Figure 1G**). A blockade of IL-17 signaling, specifically during the expansion/maintenance phase, resulted in a significant decrease in the frequency of TSKB20-specific T cells (**Figure 1H**). Indeed, mice treated with anti-IL-17 once the CD8+ T cell response was already established (from 13 to 19 dpi), showed a frequency of parasite-specific T cells comparable to that observed in infected IL-17RA KO mice that were devoid of IL-17 signaling throughout the entire infection period (**Figure 1I**).

Absence of IL-17RA Signaling During *T. cruzi* Infection Reduces the Survival of Total and Specific CD8+ T Cells

Considering the conventional kinetics of T cell responses (18), it was conceivable that the abortive CD8+ T cell response observed in infected IL-17RA KO mice could be a consequence of reduced cell expansion and/or increased contraction. To address the role of IL-17RA in CD8+ T cell proliferation, we assessed the *in vivo* incorporation of BrdU between 15 and 20 dpi, as these time points directly preceded the dramatic decrease in the numbers of specific CD8+ T cells in infected IL-17RA KO mice. The results depicted in **Figure 2A** demonstrate that the absence of IL-17RA does not compromise proliferation of CD8+ T cells during *T. cruzi* infection. Complementary studies of e*x vivo* detection of the Ki-67 antigen led to similar conclusions (**Supplementary Figure 2A**). We then tested a possible role of IL-17RA signaling in supporting CD8+ T cell survival. In comparison to their infected WT counterparts, total and TSKB20-specific CD8+ T cells from infected IL-17RA KO mice showed significantly higher frequencies of apoptotic cells as early as 10 dpi and also at later time points (20 dpi) (**Figure 2B**). Similar results were obtained by analyzing Annexin V+/7AAD- cells (**Supplementary Figure 2B**). In the same direction, total and parasite-specific CD8+ T cells from infected WT mice treated with anti-IL-17A Abs (**Figure 1H**) showed higher percentage of apoptotic cells than their counterparts from WT mice, and exhibited levels of apoptosis similar to that of infected IL-17RA KO mice (**Supplementary Figure 2C**).

Given the results described above, we evaluated whether cytokines that signal through IL-17RA were able to directly increase survival of activated CD8+ T cells. CD8+ T cells purified from the spleen of non-infected WT mice were activated for 24 h with plastic-coated anti-CD3 and anti-CD28 Abs in the presence of recombinant cytokines. The addition of IL-17A, but not IL-17F, IL-17C, or IL-17E, lead to a modest but significant reduction in the percentage of apoptotic activated CD8+ T cells (**Figure 2C**). Of note, the direct anti-apoptotic effect of IL-17 in CD8+ T cells was comparable to that of IL-21, a well-recognized survival factor for this population (26). We also determined that CD8+ T cells purified from the spleen of IL-17RA KO mice and activated *in vitro* were more susceptible to cell death (apoptosis and necrosis) induced by camptothecin (CPT) challenge than CD8+ T cells from WT mice (**Supplementary Figure 2D**). As expected based on the lack of IL-17RA expression, IL-17 was not able to reduce activation- or CPT-induced cell death in CD8+ T cells from IL-17RA KO mice. However, IL-17 also failed to reduce the cell death triggered by CPT in CD8+ T cells from WT mice. The differential effect of IL-17 in protecting CD8+ T cells from TCR- but not CPT-induced cell death may result from differences in the apoptotic signaling pathways triggered by these two treatments (27, 28). In an attempt to elucidate the mechanisms underlying the pro-survival effects of IL-17A against activation-induced apoptosis, we evaluated the expression of pro- and anti-apoptotic members of the Bcl-2 superfamily that are critically involved in the

regulation of T cell death (29). We determined that IL-17A significantly downregulated the expression of Bad (**Figure 2D**). Little to no changes were observed in other members such as Bcl-xL, Bcl-2, Bim, and Bax (**Supplementary Figure 2E**). Altogether, these results indicate that IL-17A may promote CD8+ T cell survival by down-regulating pro-apoptotic factors in the Bcl-2 family.

Absence of IL-17RA Perturbs the Transcriptional Program of CD8+ T Cells Activated During *T. cruzi* Infection

To gain further insights into the role of IL-17RA signaling during *T. cruzi* infection, we determined the gene expression profiles of purified CD8+ T cells using Affymetrix microarrays. Using gene expression data normalized to the corresponding non-infected samples, we compared the transcriptional changes induced by infection in CD8+ T cells from IL-17RA KO mice vs. WT mice in a fold change/fold change plot. We identified 4287 genes that showed significant expression differences (greater than 1.2 fold; $p < 0.05$) and grouped these genes into different sets according to the differential expression patterns (**Figure 3A**). Remarkably, 1,647 genes (pink, orange and red sets) were expressed at higher level in CD8+ T cells from IL-17RA KO infected mice in comparison to WT counterparts, whereas 2,640 genes (light green, green and dark sets) were expressed at lower levels. To further evaluate the biological characteristics of the transcriptional landscape of CD8+ T cells from infected IL-17RA KO vs. WT mice, we performed gene-enrichment set analysis (GSEA) for the genes that were differentially expressed. After conducting a broad analysis using gene ontology, as well as immunological and curated databases, we decided to focus on specific gene sets (Molecular Signatures DB-MSigDB) related to CD8+ T cell function and differentiation, such as GSEA26495 and GSEA41867. This supervised analysis showed that IL-17RA KO CD8+ T cells were significantly enriched in six gene sets in which the most enriched CD8+ T cell gene sets in the significance order (size of FWER *P* values) were $PD1^{hi}$ vs. $PD1^{low}$ ($p < 0.001$) and Naïve vs. $PD1^{low}$ ($p < 0.001$) (**Figure 3B**). These results denoted that CD8+ T cells derived from IL-17RA KO mice infected with *T. cruzi* showed a phenotype with characteristics of dysfunctional and, surprisingly, naïve cells.

We then analyzed the expression patterns of genes within the categories relevant for CD8+ T cell biology and IL-17RA signaling. Direct comparison of the gene expression profiles of CD8+ T cells from infected WT and IL-17RA KO mice after normalization of the date to gene expression in cell from non-infected mice revealed that absence of IL-17 expression resulted in important differencesin the transcriptional profile of CD8+ T cells (**Figure 3C**). Indeed, genes encoding activation and effector cell markers, such as the KLRG family molecules CD11c and CD69, showed a completely opposite pattern of expression in CD8+ T cells from infected IL-17RA KO vs. WT mice. Furthermore, CD8+ T cells from infected IL-17RA KO mice showed clearly increased expression of genes encoding inhibitory and death receptors, including *Ctla4, Havcr2* (Tim3), *Pdcd1* (PD1), *Tigit,* and *Fas*. We also analyzed how the absence of IL-17RA signaling affected the expression of genes encoding transcription factors (TFs) that regulate CD8+ T cell fate. Of note, there was a group of TF-encoding genes whose expression was significantly higher in CD8+ T cells from infected IL-17RA KO mice than in those of their WT counterparts. This group included genes such as *Foxo1*, *Irf4,* and *Foxo3* that are critical for the generation of effector CD8+ T cells (30, 31). Also, we determined that CD8+ T cells from infected WT and IL-17RA mice showed differences in the expression of many genes encoding effector molecules, cytokine receptors, homing and migration molecules, and apoptosis mediators, thus further supporting the fact that absence of IL-17RA influences CD8+ T cell fate. Finally, analysis of the gene expression of molecules associated to IL-17RA signaling (6) evidenced significant differences between CD8+ T cells from infected WT and IL-17RA KO mice. Thus, CD8+ T cells from WT mice showed increased amounts of transcripts encoding MMP-13, CCL-20, and IL-6 among others while CD8+ T cells from IL-17RA KO mice showed higher amounts of transcripts encoding TNF, IKBKb, CXCL-2, S100a8, MMP-8, and others (**Figure 3D**).

To broadly analyze the significance of the transcriptional differences between CD8+ T cells from infected IL-17RA KO mice and their WT counterparts, we performed an Ingenuity Pathway Analysis (IPA) on genes marked in red in **Figure 3A**. The genes were up-regulated in infected CD8+ T cells from both groups of mice, but were expressed at significantly higher levels in CD8+ T cells from IL-17RA KO mice. The top 20 "Diseases and Bio-functions," "Canonical pathways," and "Upstream regulators" that were most significantly altered in CD8+ T cells from IL-17RA KO mice infected with *T. cruzi* are shown in **Figures 3E–G**. Interestingly, "Cell death," "Apoptosis of Lymphocytes" bio-functions (**Figure 3E**) and the "p53 Signaling" (**Figure 3F**) canonical pathway emerged as significantly up-regulated. These results support the notion that the lack of IL-17RA signaling during *T. cruzi* infection significantly affected the survival and senescence status of CD8+ T cells, as well as various biological features. Finally, to elucidate which molecule/s were involved in the observed differences in gene expression, we performed an "upstream regulator analysis" (**Figure 3G**). Many modulators of the inflammatory responses, including the cytokines IL-2 and IL-6 and the NF-κB regulators CHUK and IKBKG, were significantly up-regulated in CD8+ T cells from infected IL-17RA KO mice. Conversely, the genes for MKL-2 and MKL-1, which interact with transcriptional regulator serum response factor, were down-regulated. Notably, IRF4, and to a lesser extent other TFs such as BATF, STAT1, and AHR, emerged as potential upstream regulators of the transcriptional program induced by *T. cruzi* infection in CD8+ T cells from IL-17RA KO mice.

Absence of IL-17RA Signaling During *T. cruzi* Infection Results in CD8+ T Cell Exhaustion

Given the results obtained from the microarray analysis, we performed a phenotypic characterization of the CD8+ T cells from the different experimental mouse groups. Analysis

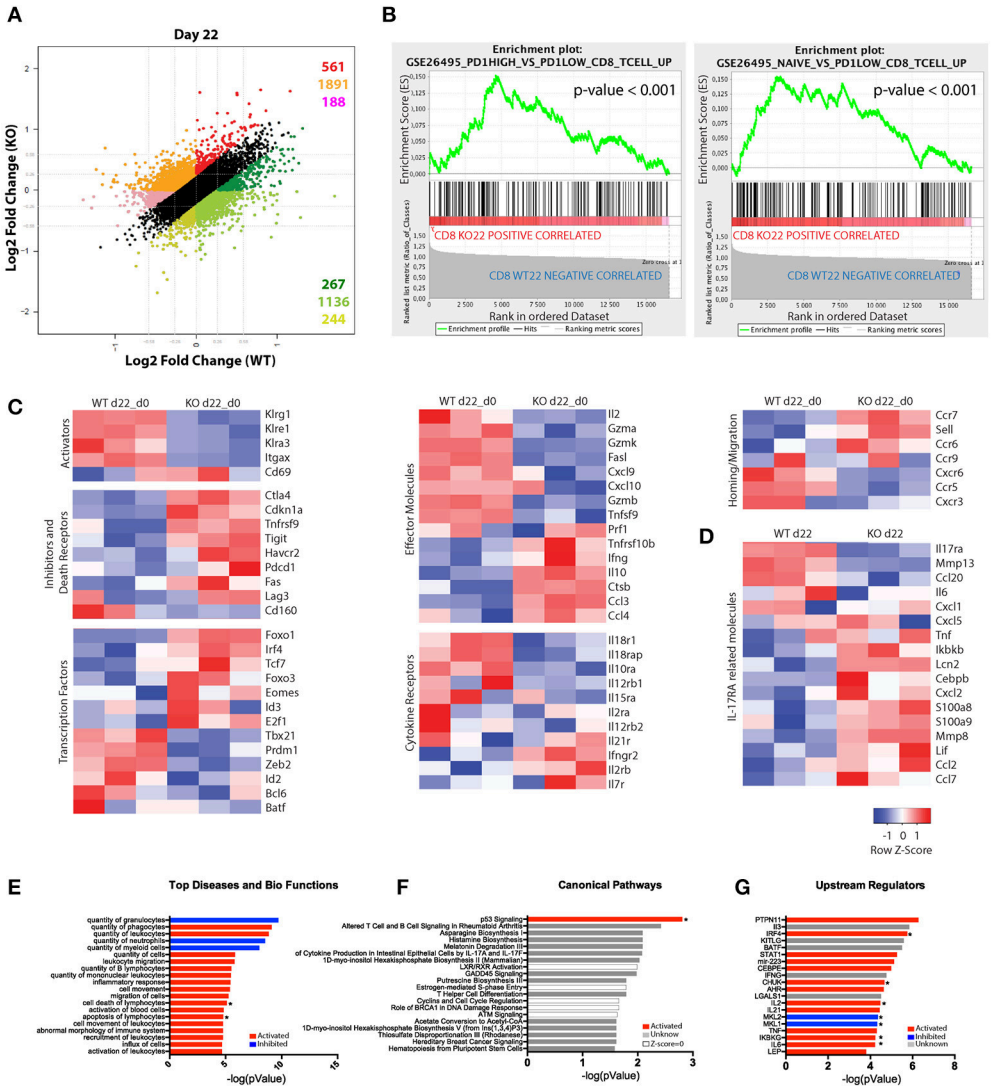

FIGURE 3 | Substantial differences in the gene-expression profile of CD8+ T cells from *T. cruzi*-infected IL-17RA KO and WT mice. **(A–F)** Microarray analysis of purified CD8+ T cells from infected WT (WT-I) and IL-17RA KO (KO-I) mice (22 dpi) and non-infected controls (WT-N and KO-N). $N = 3$ mice per group. **(A)** Dot plot displaying the number of genes that show a significant ≥1.2-fold difference in fold change expression of WT-I and KO-I relative to non-infected counterparts. Colors indicate sets of genes with different expression patterns. **(B)** Top two enrichment plots in KO-I ($p < 0.001$) determined by supervised analysis of all infection induced genes in WT-I and KO-I using GSEA26495 and GSEA41867 (MSigDB C5BP) signature gene sets. **(C)** Heat maps of expression of selected genes according to categories relevant to CD8+ T cell biology. The gene expression values of each sample were normalized by division to the average values of the corresponding samples from non-infected counterparts. **(D)** Heat map of expression of genes encoding molecules associated to IL-17RA signaling. Gene expression values represent non-normalized data from 3 mice. **(E–G)** IPA of genes induced by the infection but showing significantly higher expression in IL-17RA KO mice (red genes in **A**). Top 20 "Diseases and Bio-functions" **(E)**, "Canonical pathways" **(F)**, and "Up-stream regulators" **(G)** that were most significantly altered ($P < 0.05$ with Fischer's exact test) in KO mice are shown. The activation Z-score was calculated to predict activation (red), inhibition (blue), categories where no predictions can be made and unknown results (with Z-score close to 0). Categories significantly activated or inhibited according to Z-score are marked with a star.

of CD62L vs. CD44 expression showed that upon *T. cruzi* infection, more than 80% of the total CD8+ T cells from the spleen of infected WT and IL-17RA KO mice acquired an activated/effector phenotype characterized by $CD62L^{low}CD44^{hi}$ expression (**Figure 4A**). Within the TSKB20-specific population, the effector cells constituted more than 95% of the total number of cells. These results highlighted that CD8+ T cell activation triggered by *T. cruzi* infection is not compromised in the absence of IL-17RA. Indeed, total and parasite-specific CD8+ T cells from the infected IL-17RA KO mice had significantly elevated expression of prototypical activation markers such as CD69 and CD25 in comparison to that of CD8+ T cells from WT mice (**Figure 4B**), which corroborated the results from our microarray analysis.

We next determined the expression of inhibitory and death receptors in CD8+ T cells from WT and IL-17RA KO mice

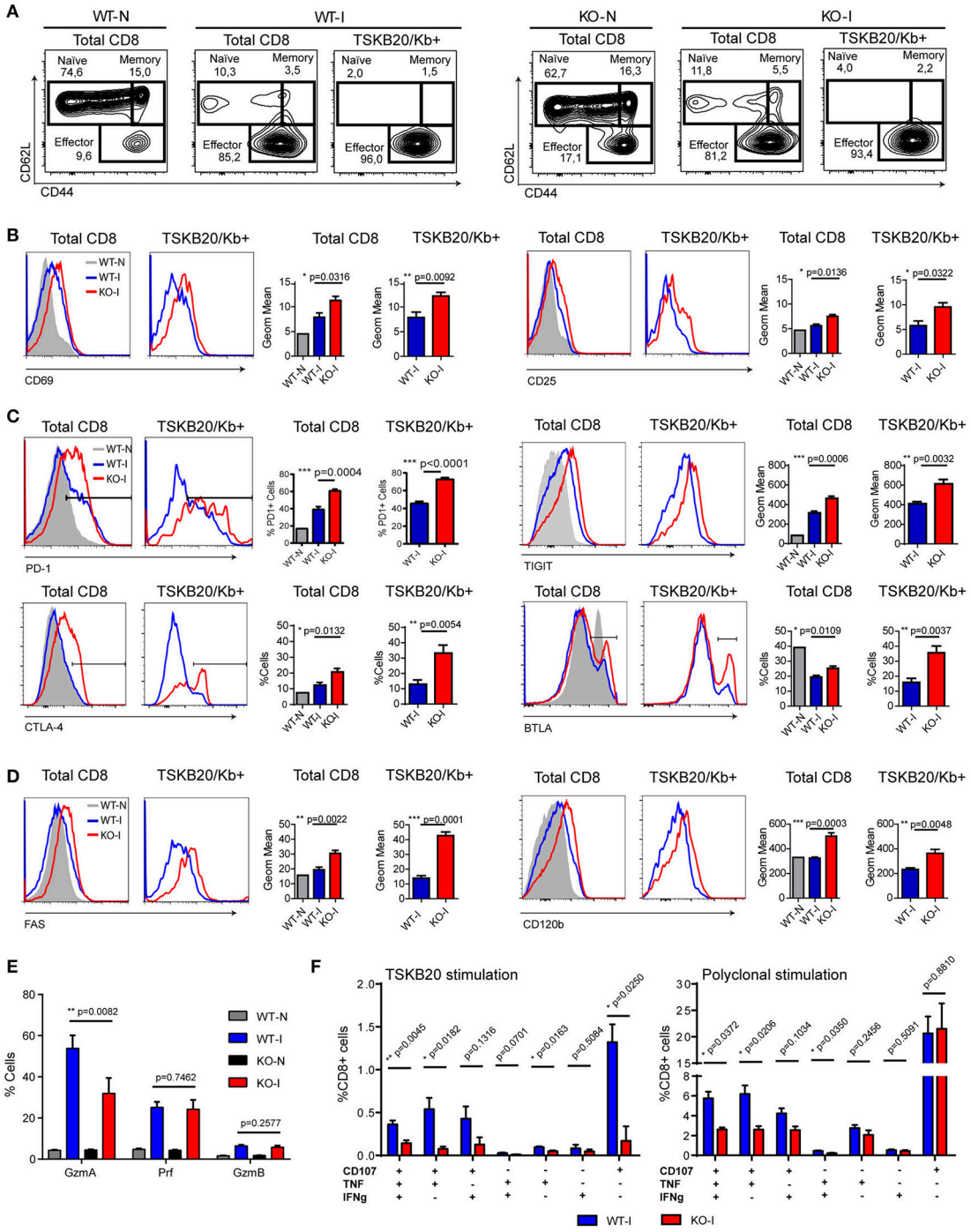

FIGURE 4 | CD8+ T cells from *T. cruzi* infected IL-17RA KO mice show phenotypic and functional features compatible with exhausted cells. Representative flow cytometry data that show the phenotype of total and TSKB20/Kb+ CD8+ T cells from the spleen of infected WT (WT-I) and IL-17RA (KO-I) mice (22 dpi). Stainings of non-infected WT (WT-N) and KO (KO-N) mice are showed in plots or gray tinted histograms for comparison. **(A)** Plots of CD62L vs. CD44 expression. Gates indicate the frequency of naïve, memory and effector subsets. **(B–D)** Representative histograms and statistical analysis of the geometric mean of expression or percentage of cells that express activation markers **(B)**, inhibitory receptors **(C)**, and death receptors **(D)** in total and TSKB20/Kb+ CD8+ T cells from the spleen of infected WT (WT-I) and IL-17RA (KO-I) mice (22 dpi). Data in statistical analysis **(B–D)** are presented as mean ± *SD*, $N = 4–6$ mice. **(E)** Percentage of CD8+ T cells from the spleen of non-infected (N) and 22-day infected (I) WT and KO mice expressing Granzyme A (GzmA), Perforin (Prf) or Granzime B (GzmB) after 5 h of PMA/Ionomycin stimulation. Data shown as mean ± *SD*, $N = 2–5$ mice. **(F)** Percentage of CD8+ T cells from the spleen of 22-day infected WT and KO mice that exhibit different combinations of effector functions including CD107a mobilization and/or IFNγ and/or TNF production upon 5 h of the indicated stimulation. Data shown as mean ± *SD*, $N = 5$ mice. Data were background subtracted. All *P* values were calculated using two-tailed *T* test. Data are representative of two-three independent experiments.

infected with *T. cruzi*. The total and TSKB20-specific CD8+ T cells from infected WT mice had an increased frequency of PD-1+ and CTLA-4+ cells, slightly higher TIGIT expression, and reduced frequency of BTLA+ cells compared to that of non-infected mice (**Figure 4C**). Notably, total and TSKB20-specific CD8+ T cells from infected IL-17RA KO mice showed significantly increased frequency of PD-1+, CTLA-4+ and BTLA+ cells as well as higher expression of TIGIT. Furthermore, these cells presented an apoptotic phenotype characterized by the expression of high levels of CD95/Fas and CD120b/TNF-R2 (**Figure 4D**). Total and TSKB20-specific CD8+ T cells from infected IL-17A/IL-17F DKO mice showed a profile of expression of inhibitory (PD-1) and death receptors (Fas/CD95) that was comparable to that of total and TSKB20-specific CD8+ T cells from infected IL-17RA KO mice (**Supplementary Figures 1C,D**).

Further phenotypic characterization included effector molecules involved in cytotoxicity such as Granzyme A (GzmA), Granzyme B (GzmB), and Perforin-1 (Prf). As GzmB and Prf were barely detectable *ex vivo* (data not shown), the expression of the three cytotoxic molecules was determined in splenocytes from non-infected and infected WT and IL-17RA KO mice after 5 h of stimulation with PMA/ionomycin (**Supplementary Figure 4A**). In agreement with the microarray data, we determined that CD8+ T cells from infected IL-17RA KO mice had significantly reduced expression of GzmA in comparison to their counterparts from infected WT mice, whereas the expression levels of GzmB and Prf were similar between both groups (**Figure 4E**).

To address whether the phenotypic features of CD8+ T cells elicited in absence of IL-17RA correlated with altered functionality, we compared the effector function of CD8+ T cells from infected WT and IL-17RA KO mice. To this end, we analyzed the mobilization of CD107a and secretion of effector cytokines upon specific and polyclonal activation *in vitro*. Stimulation of splenocytes from infected IL-17RA KO mice with the TSKB20 peptide resulted in a significant reduction of the frequency of CD8+ T cells with polyfunctional characteristics (i.e., surface CD107a expression and IFNγ and/or TNF production) in comparison to WT control mice (**Figure 4F**, left panel and **Supplementary Figure 3**). Although a poor response was anticipated due to the low frequency of TSKB20-specific CD8+ T cells in infected IL-17RA KO mice, the antigen-specific effector response of CD8+ T cells was not significantly different from background, suggesting the presence of both quantitative and qualitative defects. Polyclonal stimulation with PMA/ionomycin increased the percentage of CD8+ T cells from infected IL-17RA KO mice that had a polyfunctional response, although the magnitude of this effector response was significantly lower than that of WT mice (**Figure 4F**, right panel and **Supplementary Figure 3**).

To determine if the higher parasite burden in infected IL-17RA KO mice may underlie the upregulation of inhibitory receptors in CD8+ T cells from these mice, we evaluated the phenotype of CD8+ T cells from WT mice infected with increasing parasite doses. Interestingly, increasing the load of *T. cruzi* did not diminish the frequency of parasite-specific CD8+ T cells, nor did it promote the upregulation of the inhibitory and death receptors evaluated (**Supplementary Figures 4B–D**).

Checkpoint Blockade Partially Restores Parasite-Specific CD8+ T Cell Immunity and Enhances Parasite Control in Infected IL-17RA KO Mice

CD8+ T cell exhaustion has been associated with poor microbial control during infection with various pathogens, as well as with tumor progression in cancer. In these settings, a checkpoint blockade has been shown to efficiently restore the magnitude and functionality of effector T cells and minimize damage from the insult (32). Furthermore, a PD-L1 blockade has been effective in preventing T cell apoptosis in murine and human sepsis models (33, 34). Our results highlight that the absence of IL-17RA signaling during *T. cruzi* infection leads to poor CD8+ T cell effector function and parasite persistence. This prompted us to evaluate whether a checkpoint blockade could restore a resistance phenotype to infected IL-17RA KO mice. As PD-1 is highly expressed on parasite-specific CD8+ T cells from infected IL-17RA KO mice, we targeted this checkpoint receptor by injecting blocking anti-PD-L1 Abs at 15 and 18 dpi, before the contraction of a parasite-specific CD8+ T cell response (**Figure 5A**). We determined that PD-L1 blockade in infected IL-17RA KO significantly augmented the magnitude of the TSKB20-specific CD8+ T cell response by 21 dpi, particularly in the spleen and liver (**Figure 5B**). A similar response to treatment was observed in infected WT mice. Notably, the enhanced *T. cruzi*-specific CD8+ T cell immunity was correlated with a marked reduction in the levels of tissue parasitism (**Figure 5C**). In addition, inhibition of PD-L1 also lead to a milder infection, as highlighted by the significantly reduced levels of several damage biomarkers, such as the transaminase aspartate aminotransferase (AST), creatine kinase total (CK), and myocardial band (CK-MB) (**Figure 5D**). The rescue effects of the PD-L1 checkpoint blockade during *T. cruzi* infection, namely parasite persistence and tissue damage, were more impressive in IL-17RA KO mice than in WT mice, as they showed extremely high susceptibility to *T. cruzi* infection in the absence of treatment.

Intrinsic IL-17RA Signaling Modulates the Maintenance and Phenotype of CD8+ T Cells Activated During *T. cruzi* Infection

To understand if IL-17RA plays a direct role in the modulation of CD8+ T cell responses to *T. cruzi*, we first quantified the serum concentration of IL-21, a cytokine known to modulate CD8+ T cell immunity (35). Of note, we determined that in comparison to infected WT mice, infected IL-17RA KO mice displayed higher expression of IL-21 (**Figure 6A**). This result highlights that increased expression of IL-21 is not sufficient to compensate for the lack of IL-17RA signaling via restoring CD8+ T cell responses during *T. cruzi* infection.

We next evaluated the possibility of a direct effect of IL-17RA signaling in the modulation of CD8+ T cell responses, given that IL-17RA is upregulated in response to cytokines that boost CD8+ T cell responses such as IL-21 (26, 36). The IL-17RA

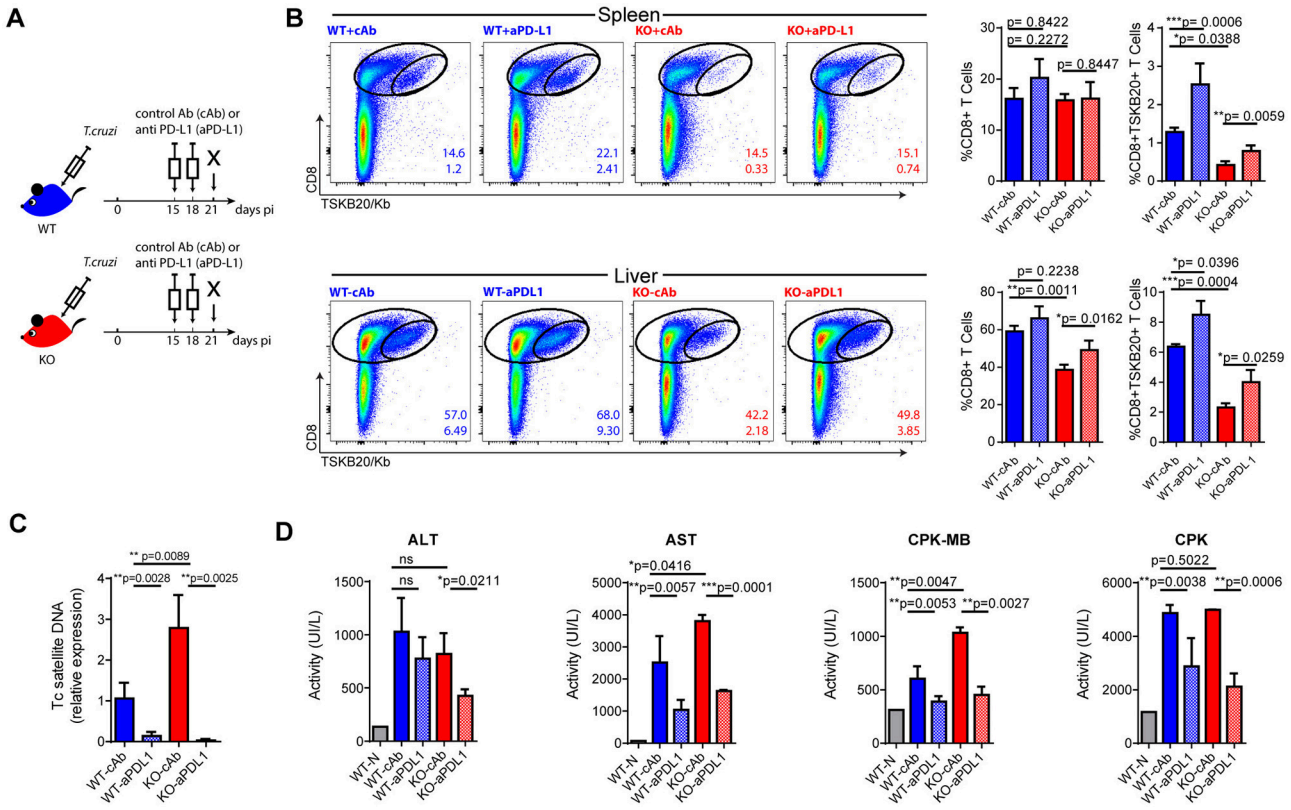

FIGURE 5 | Checkpoint blockade reinvigorates parasite-specific CD8+ T cell immunity and enhances parasite control in infected IL-17RA KO mice. **(A)** Layout of the checkpoint blockade experiment. **(B)** Representative plots and statistical analysis of CD8 and TSKB20/Kb staining in spleen and liver of the indicated experimental groups. Numbers within plots indicate the frequency of total CD8+ cells (up) and TSKB20-specific CD8+ T cells (down) at 21 dpi. Bar graphs represent data as mean ± *SD*, $N = 7$ mice. **(C)** Relative amount of *T. cruzi* satellite DNA in the spleens of the indicated experimental groups at 21 dpi. Murine GAPDH was used for normalization. Data are presented as mean ± *SD* relative to WT-cAb group, $N = 7$ mice. **(D)** Enzymatic activity (UI/L) of alanine transaminase (ALT), aspartate transaminase (AST), creatinine kinase-MB and creatinine phosphokinase (CPK) on plasma of the indicated experimental groups at 21 dpi. $N = 7$ mice. All *P* values were calculated with two-tailed *T* test. Data are representative of two independent experiments.

subunit interacts with IL-17RC to form the functional receptor for both IL-17A and IL-17F [reviewed in Gaffen (6)]. Recently, also IL-17RD was shown to bind to IL-17RA to differentially regulate IL-17A-inducing signaling pathways (37, 38). Therefore, we evaluated the mRNA levels of IL-17RA, IL-17RC, and IL-17RD by quantitative PCR. In agreement with published data, mRNA encoding IL-17RA were detected in splenic CD8+ T cells (**Figure 6B**). Transcripts encoding *Il17rc* and *Il17rd* were also detected in these cells, but at remarkably lower levels in comparison to *Il17ra*. Studies by flow cytometry confirmed the expression of IL-17RA on CD8+ T cells. Notably, IL-17RA expression varied depending on the CD8+ T cell subset, and was higher in memory cells defined as $CD44^{hi}CD62L^{hi}$ than in the effector ($CD44^{hi}CD62L^{lo}$) and naïve ($CD44^{lo}CD62L^{hi}$) subsets (**Figure 6C**). *T. cruzi* infection upregulated IL-17RA expression in CD8+ T cells, to levels and kinetics specific for each subset (**Figures 6C,D**). We observed that IL-17RA expression is substantially upregulated in bulk memory CD8+ T cells during *T. cruzi* infection, but is only transiently increased in bulk effector CD8+ T cells at early time points (**Figure 6D**). As expected given their effector nature, TSKB20-specific CD8+ T cells expressed IL-17RA at a level that was comparable to bulk effector cells.

To directly address the impact of intrinsic IL-17RA signaling in the development of CD8+ T cell responses during *T. cruzi* infection, we performed a series of adoptive transfer experiments. First, we transferred an equal number of congenically marked IL-17RA-deficient (CD45.2+) and WT (CD45.1+) CD8+ T cells into WT (CD45.1+/CD45.2+) recipient mice. Recipient mice were infected, and the presence of injected cells in the total and TSKB20-specific CD8+ T cell pools was examined at 20 dpi. As expected, no CD45.2+ KO or CD45.1+ WT CD8+ T cells were detected in infected F1 (CD45.1+/CD45.2+) WT hosts that were not injected (control mice). When analyzing the competitive adoptive transfer experiment, we observed that within the population of injected cells, IL-17RA KO CD8+ T cells were outcompeted by their WT counterparts in both total and parasite-specific CD8+ T cell subsets in all the organs examined, including blood and spleen (**Figure 6E**).

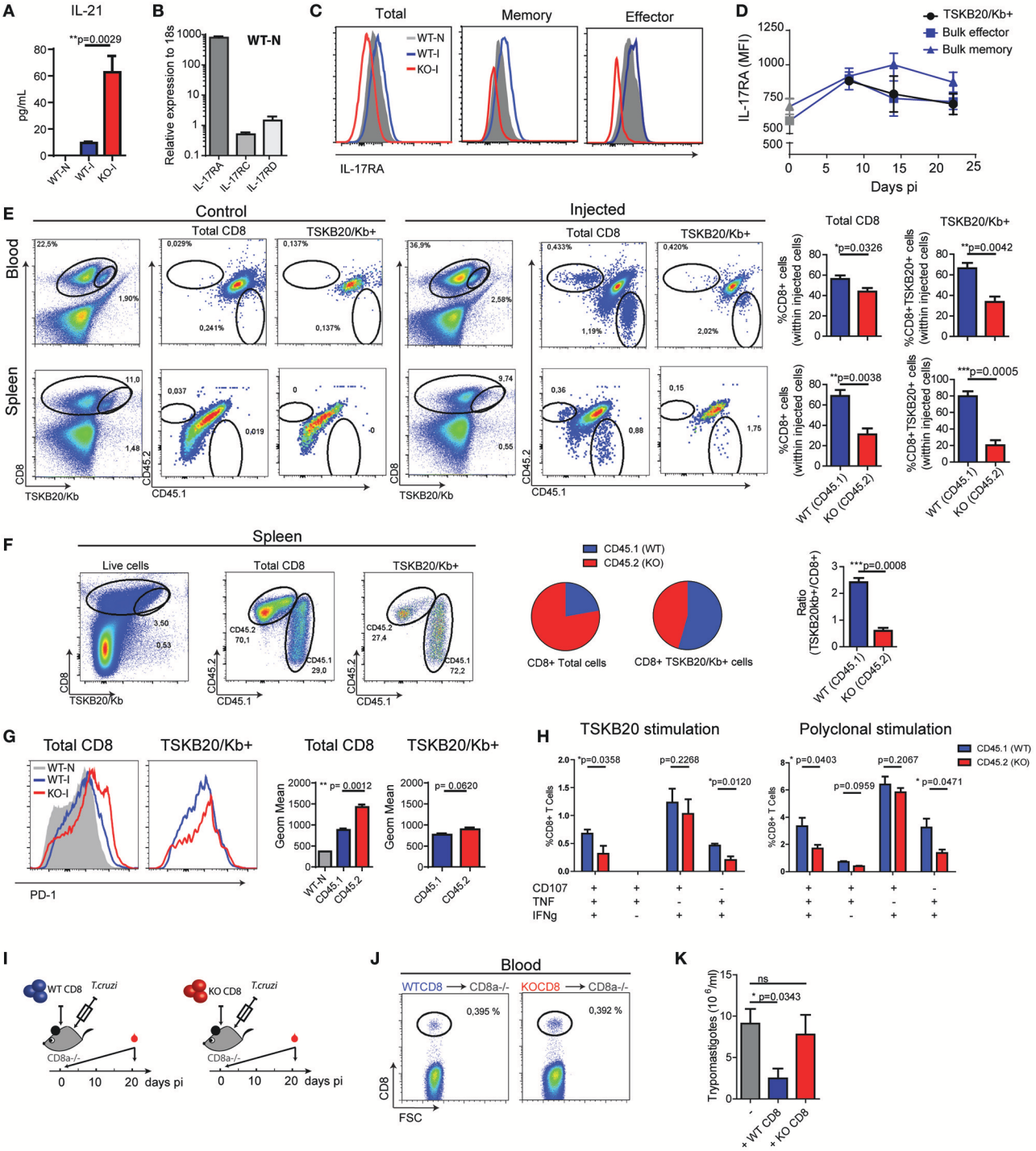

FIGURE 6 | Intrinsic IL-17RA-signaling modulates the maintenance, phenotype and function of CD8+ T cells during *T. cruzi* infection. **(A)** Concentration of IL-21 in plasma of infected (20 dpi) WT and IL-17RA KO mice. Data are presented as mean ± *SD*, $N = 4$ mice. **(B)** Amounts of *Il17ra, Il17rc,* and *Il17rd* transcript determined in CD8+ T cells purified from the spleen of non-infected WT mice, normalized to 18S RNA. Data are presented as mean ± *SD*, $N = 4$ mice **(C)** Representative histograms of the expression of IL-17RA (protein) on total, memory and effector CD8+ T cell subsets defined according to CD44 and CD62L staining in spleen cell suspensions from non-infected (N) and infected (I) WT mice (14 dpi). Staining of IL-17RA on spleen CD8+ T cells from IL-17RA KO mice is showed as negative control. **(D)** Kinetic evaluation of the upregulation of IL-17RA (MFI: mean of fluorescence intensity) induced by *T. cruzi* expression on bulk effector and memory CD8+ T cells and TSKB20-specific CD8+ T cells. Data in statistical analysis are presented as mean ± *SD*, $N = 4$. **(E)** Representative plots and statistical analysis of CD8 and TSKB20/Kb staining and of CD45.1 and CD45.2 staining within Total and TSKB20/Kb+ CD8+ T cells in the blood and spleen of infected CD45.1/CD45.2 WT

(Continued)

FIGURE 6 | recipient mice (20 dpi) non-injected (control) or injected with equal numbers of CD45.1+ WT and CD45.2+ KO CD8+ T cells. Numbers in the plots indicate the frequency of the correspondent cell subset. Bar graphs display the frequency of CD45.1+ WT cells and CD45.2+ KO cells within the indicated populations upon gating only in the injected cells. **(F)** Representative plots and statistical analysis of CD8 and TSKB20/Kb staining and of CD45.1 and CD45.2 staining within Total and TSKB20/Kb+ CD8+ T cells in the spleen of infected CD8α-/- recipients (17 dpi) injected with equal numbers of CD45.1+ WT and CD45.2+ KO CD8+ T cells. Pie charts display the frequency of CD45.1+ WT and CD45.2+ KO cells within the indicated gates. Bar graph shows the ratio between the frequencies of TSKB20/Kb+ CD8+ T cells and the total CD8+ T cells within CD45.1 WT and CD45.2 IL-17RA KO populations. **(G)** Representative histograms and statistical analysis of the geometric mean of PD-1 expression in total and TSKB20/Kb+ CD8+ T cells within CD45.1+ WT and CD45.2+ IL-17RA KO CD8+ T cells from the spleen of CD8α-/- recipient mice. Data in statistical analysis are presented as mean ± *SD*, $N = 4-6$ mice. **(H)** Percentage of polyfunctional effector cells denoted by expression CD107a, IFNγ and/or TNF upon 5 h of the indicated stimulation on CD45.1+ WT and CD45.2+ IL-17RA KO CD8+ T cells from the spleen of CD8α-/- recipient mice. Data shown as mean ± *SD*, $N = 4$ mice. Data were background subtracted. All *P* values in **(E–G)** were calculated using two-tailed *T* test. Data are representative of two independent experiments. **(I)** Experimental layout of the adoptive transfer of equal number of CD8+ T cells purified from WT mice or IL-17RA KO mice into CD8α knockout mice immediately followed by *T. cruzi* infection. $N = 3$ mice/group. **(J)** Representative dot plots of the frequency of CD8+ T cells determined 1 day after injection in blood of the different experimental groups. **(K)** Parasitemia (15 dpi) in the different experimental groups. Infected non-transferred CD8α knockout mice were used as control. *P* value calculated using Gehan-Breslow-Wilcoxon Test. Data in **(A–J)** are representative of two independent experiments.

To overcome the possible limitations derived from the presence of endogenous WT CD8+ T cells in lymphoreplete hosts, we repeated the competitive adoptive transfer experiment in CD8α-/- mice. At 17 dpi, the frequency of IL-17RA KO cells was double that of WT cells within the total population of CD8+ T cells (**Figure 6F**), likely as result of increased homeostatic proliferation of polyclonal IL-17RA KO CD8+ T cells (**Figure 2A**). In contrast, WT cells significantly outnumbered IL-17RA KO cells within the TSKB20-specific CD8+ T cell pool, indicating that intrinsic expression of IL-17RA provides a maintenance advantage for parasite-specific CD8+ T cells. Indeed, the ratio between the percentage of WT CD8+ T cells within TSKB20-specific gate and the polyclonal total CD8+ T cells was significantly higher than that of IL-17RA KO CD8+ T cells (**Figure 6F**). Phenotypic evaluation revealed that IL-17RA KO CD8+ T cells exhibited higher expression of the inhibitory receptor PD-1 (**Figure 6G**). Upon antigen specific stimulation with TSKB20, WT CD8+ T cells exhibited a significantly higher polyfunctional effector response in comparison to IL-17RA KO CD8+ T cell from the same host (**Figure 6H**, left panel and **Supplementary Figure 5**). An identical result was observed after polyclonal stimulation (**Figure 6H**, right panel and **Supplementary Figure 5**).

Finally, we aimed to address the relevance of CD8+ T cell-intrinsic IL-17RA signaling for host protection during *T. cruzi* infection. To this end, we evaluated the ability to control parasite replication in CD8α-/- mice transferred with IL-17RA KO CD8+ T cells in comparison to CD8α-/- mice transferred with WT CD8+ T cells (**Figure 6I**). As a control, we determined that the frequency of circulating CD8+ T cells at day one post-injection was the same between both groups of mice (**Figure 6J**). CD8α-/- mice were extremely susceptible to *T. cruzi* infection and displayed uncontrolled parasitemia at day 21, even with an infection dose of 100 trypomastigotes, which was 50 times less than the dose used in previous experiments. Furthermore, all these mice succumbed by day 25 post-infection (data not shown). Remarkably, the transfer of IL-17RA-sufficient WT CD8+ T cells, but not of IL-17RA-deficient KO CD8+ T cells, was able to enhance parasite control and significantly reduce parasitemia (**Figure 6K**).

DISCUSSION

During the last few decades, many reports have delineated the immunological mechanisms underlying IL-17-mediated roles in host protection against infection as well as in inflammatory diseases (39, 40). In this study, we uncover a novel mechanism by which IL-17RA signaling regulates CD8+ T cell responses and promotes protection against a protozoan infection. Our findings provide new elements to elucidate the cytokines and pathways leading to robust CD8+ T cell responses against infections with intracellular microbes and consequently, may have important implications for vaccine and therapy design.

The integral role of the IL-17 family in host defense against extracellular bacterial and fungal pathogens has been well established, and recent studies have implicated the family of genes in potentiating immunity against intracellular bacteria, viruses, and parasites (3). So far, the IL-17-dependent protective mechanisms were believed to be dependent on the activation of both non-immune and innate immune cells to sustain inflammation (8). Notably, the IL-17 family of proteins only indirectly promotes adaptive cellular immune responses (41, 42). In this regard, there is evidence to suggest the role of IL-17 cytokines in sustaining specific CD8+ T cell responses that promote host resistance to *Listeria* infection and melanoma (43, 44). In these settings, the IL-17-mediated induction of protective CD8+ T cells depended on enhanced recruitment of cross-presenting dendritic cells, although direct effects on CD8+ T cells were not ruled out. Very recently, IL-17 was shown to directly potentiate CD8+ T cell cytotoxicity against West Nile Virus infection (9). In line with this, we demonstrate that mice deficient in IL-17RA showed an abortive CD8+ T cell response during *T. cruzi* infection characterized by an early reduction in the number of parasite-specific CD8+ T cells. Concomitantly, infected IL-17RA KO mice showed poor control of the parasite in target tissues such as spleen, liver, and heart. By using different experimental approaches, including detailed phenotypic, functional and transcriptional profiling of CD8+ T cells from IL-17RA KO mice infected with *T. cruzi*, we demonstrated that CD8+ T cell-intrinsic IL-17RA signaling is required to sustain CD8+ T cell maintenance and pathogen-specific CD8+ T cell immunity, particularly during the expansion phase.

Whether one or more of the four cytokines that signal through IL-17RA is involved in these events is currently unknown. However, our results led us to postulate that IL-17A is the main cytokine involved in the IL-17RA-mediated effect of CD8+ T cells. This postulate is based on the marked similarities in the phenotype of the infected IL-17A/F DKO and IL-17RA KO mice and the significant consequences of the IL-17A neutralization in mice and IL-17A supplementation in CD8+ T cell cultures. Still, a possible role of other members of this family are not ruled out given that at least two other the IL-17RA signaling cytokines besides IL-17A (i.e., IL-17F and IL-17E/IL-25) are increased during *T. cruzi* infection (4). Regarding receptor expression, we determined that CD8+ T cells express the transcripts encoding not only IL-17RA but also IL-17RC and IL-17RD. Of note, we determined that *Il17ra* transcripts are present in significantly higher amounts than *Il17rc* and *Il17rd*. These findings are noteworthy as high levels of IL-17RA seem to be required for effective responses to IL-17 (45), and also because they also pose the question of whether IL-17RC or IL-17RD are effectively expressed on CD8+ T cells and required for IL-17 signal transduction. Although, the receptor complex formed by IL-17RA and IL-17RC is considered essential for IL-17 signal transduction (46), some studies reported that hematopoietic cell types (including T cells) show IL-17-dependent responses even in the absence of IL-17RC (47–49). It should be further established whether IL-17RD may interact with IL-17RA and replace IL-17RC to mediate the IL-17 signaling in these populations as previously reported (37). In the same direction, to dissect the precise signaling requirement for IL-17 signal transduction in CD8+ T cells may provide important information in terms of the IL-17 biology.

Besides a direct role of IL-17 cytokines, it is possible that a crosstalk of IL-17 with other cytokines that regulate CD8+ T cell fate such as IL-21 might be indirectly involved in the observed qualitative defects. In this regard, Hoft and colleagues described that TCR-transgenic CD4+ T cells specific for an immunodominant peptide of *T. cruzi* that were polarized *in vitro* into Th17 cells could potentiate CD8+ T cell immunity through a mechanism that is IL-21-dependent, but IL-17-independent (50). It remains to be established whether the *in vitro* generated Th17 cells are equivalent to those differentiated *in vivo* within the host during *T. cruzi* infection. Indeed, we determined that infected IL-17RA KO mice displayed higher concentrations of serum IL-21 than infected WT control mice, suggesting that the altered CD8+ T cell response observed in absence of IL-17RA signaling is unlikely to be a result of deficient IL-21 production.

CD8+ T cells from infected IL-17RA KO mice showed increased apoptosis and a transcriptional landscape associated with canonical cell death and senescence pathways. In addition, these cells exhibited high expression of multiple inhibitory and death receptors that correlated with reduced *ex vivo* effector responses and a gene signature that positively correlated with those defined for dysfunctional PD-1^{high} CD8+ T cells (51, 52). Altogether, these features partially resembled those of dysfunctional CD8+ T cells described in many chronic infections and cancer that are characterized by the progressive loss of T cell function, sustained expression of inhibitory receptors, and high susceptibility to deletion (53). Interestingly, we found that the functional CD8+ T cell response observed in *T. cruzi*-infected WT mice [this manuscript and (54)] was significantly impaired in the absence of IL-17RA signaling. In this regard, although it is conceivable that the increased tissue parasitism in IL-17RA KO mice favored CD8+ T cell exhaustion, infection of WT mice with increasing parasite loads does not induce expression of inhibitory receptors or deletion of parasite-specific CD8+ T cells, nor does it result in impaired CD8+ T cell cytotoxic effector function (55). As cytokines are essential for the regulation of exhaustion (20), we performed adoptive transfer experiments that supported the notion that IL-17 signaling influenced CD8+ T cell survival and function partially through cell intrinsic mechanisms. Interestingly, we determined that IL-17RA is expressed at different levels according to each particular CD8+ T cell subset. Specifically, IL-17RA expression was increased and sustained in memory cells, but was transiently up-regulated in activated effector cells at early stages of infection. These results, together with those showing that IL17RA downregulation is included in the gene signature of exhausted T cells (56, 57), suggest that the IL-17/IL-17RA pathway modulates CD8+ T cell fate, thus preventing cell exhaustion in activated cells and sustaining long-lasting cytotoxic responses. In this regard, adoptive transfer of WT, but not of IL-17RA KO CD8+ T cells, promoted parasite control in immuno-deficient CD8α-/- mice. In line with this, we demonstrated that anti-PD-L1 Abs during the CD8+ T cell expansion phase reinvigorated the parasite-specific CD8+ T cell responses in infected IL-17RA KO mice, thus restoring robust parasite control and reducing pathology to levels comparable to infected WT controls. Remarkably, we observed that a short regimen of PD-L1 neutralization increased the frequency of parasite-specific CD8+ T cells by two-fold in both treated groups, although the magnitude of the response in infected IL-17RA KO mice remained lower than in WT control mice. Given the high levels of inhibitory receptors in CD8+ T cells elicited by *T. cruzi* infection in absence of IL-17RA, it is likely that the combination of different checkpoint Abs may have a stronger effect in these settings, as reported in cancer models (58).

The role of checkpoint inhibitors during *T. cruzi* infection, particularly the PD-1/PD-L1 axis, has been understudied thus far. One report demonstrated that genetic disruption of this inhibitory pathway increased the effector immune response to favor parasite control, but also promoted cardiac pathology and compromised host resistance to the infection (59). In this context, our data provide evidence that a PD-L1 checkpoint blockade at the CD8+ T cell expansion phase not only restored resistance to *T. cruzi* absence of IL-17RA signaling, but also boosted protective CD8+ T cell immunity during the natural infection. These findings are relevant to a growing area of research aimed at investigating the therapeutic potential of immune checkpoint pathways during chronic infections (60). In recent years, several reports have shown that immune cell exhaustion or dysfunction is a common finding in human Chagas disease, particularly in patients with severe symptoms (61–64). There is certain consensus that even very low parasite loads in tissues may drive, in the long term of the human

infection (two decades), the expression of inhibitory receptors and cell dysfunction in T cells. Consequently, this likely drives an immune modulatory mechanism and reduced tissue damage in the later stages of infection. Interestingly, many reports have described that patients with moderate to severe chronic chagasic cardiomyopathy have reduced production of IL-17, supporting a protective role of the cytokine against cardiac damage (65, 66). Altogether, previous findings and those reported here support the hypothesis that elevated IL-17 production in the context of persistent parasite levels may prevent T cell dysfunction and the associated immune imbalance that cause chronic myocarditis. Given the relevance for the understanding of the immunopathology during human Chagas disease, this hypothesis merits further investigation in future studies.

The comparison of the transcriptome of CD8+ T cells from infected IL-17RA KO and WT mice supported the notion that IL-17RA signaling influences the transcriptional program of effector CD8+ T cells. These conclusions were based on the transcriptome of bulk CD8+ T cells and, consequently, may present some caveats as result of the heterogeneity of the sample and the "dilution" of the parasite-specific response. However, we determined that during *T. cruzi* infection most CD8+ T cells acquire an activated phenotype. Furthermore, total and TSKB20-specific CD8+ T cells from infected WT and IL-17RA KO mice exhibit similar expression of activation and differentiation markers and inhibitory and death receptors. Moreover, despite the fact that TSKB20-specific CD8+ T cells were the immunodominant population within effector cells, CD8+ T cells specific for other parasite peptides (i.e., TSKB18) were also detectable in infected WT and IL-17RA KO mice (data not shown). Accordingly, we consider that transcriptomic profiling of bulk CD8+ T cells activated during *T. cruzi* infection, though with some limitations, provides meaningful evidences about the role of IL-17RA signaling in dictating the transcriptional program of effector CD8+ T cells. Interestingly, the IPA analysis of the transcriptome of CD8+ T cells arising IL-17RA KO mice infected with *T. cruzi* highlighted IRF4 and, to a minor extent, BATF as potential upstream regulators of the IL-17RA phenotype. Notably, both TFs have been reported to be required for survival and differentiation of early effector CD8+ T cells (67–72). IRF4 promotes CD8+ T cell expansion and differentiation (69), but it also induces the expression of molecules associated with an exhausted status such as Blimp-1, CTLA-4, and IL-10 (73–75). Furthermore, BATF expression may be triggered by PD-1 ligation and associated with CD8+ T cell exhaustion during chronic viral infection in humans and mice (76). Very recently, IRF4 and BATF have been shown to form a TCR-responsive transcriptional circuit that establishes and sustains T cell exhaustion during chronic viral infection (77). Therefore, it is conceivable that sustained elevated levels of both TFs could result in the induction of cell death and exhaustion program observed in CD8+ T cells from infected IL-17RA KO mice. The link between IL-17RA signaling, expression of BATF and IRF-4, and CD8+ T cell exhaustion deserves further investigation using genetic dissection approaches.

In conclusion, our results provide evidence for a novel IL-17RA-mediated mechanism that potentiates immunity to intracellular pathogens such as *T. cruzi* by improving adaptive CD8+ T cell responses. These findings, taken together with the report showing that IL-17 controls functional competence of NK cells during a fungal infection (78), suggest that the IL-17 family is likely important for both the innate and adaptive arms of the cytotoxic response against pathogens. Although it remains to be determined whether this mechanism can be applied to host resistance mediated by IL-17 cytokines in the context of other infections, these findings have two fundamental repercussions in the field of IL-17-mediated immune responses. The first is that the prolonged targeting of the IL-17 pathways as part of an anti-inflammatory treatment during autoimmune diseases or cancer may potentially have harmful effects due to defective cytotoxic responses. The second is the notion that promoting the production of IL-17 cytokines during infection or vaccination may help to elicit stronger cytotoxic responses to fight against microbes, and eventually, tumors.

ETHICS STATEMENT

This study was carried out in accordance with the recommendations of Guide to the care and use of experimental animals (Canadian Council on Animal Care, 1993) and Institutional Animal Care and Use Committee Guidebook (ARENA/OLAW IACUC Guidebook, National Institutes of Health, 2002). The protocol was approved by the Institutional Animal Care and Use Committee (IACUC) Facultad de Ciencias Químicas, Universidad Nacional de Córdoba (Approval Number 981/15) (OLAW Assurance number A5802-01).

AUTHOR CONTRIBUTIONS

JT designed and performed most of the experiments, analyzed data, and wrote, commented on the manuscript. CA, FF, and CR performed experiments, analyzed data and commented on the manuscript. MR, MA, and MG performed experiments and commented on the manuscript. NN performed microarray experiment. WR analyzed microarray data. EP participated in microarray design and analysis and provided funding. CM and AG participated in data analysis, commented on the manuscript and provided funding. EA supervised the research, designed experiments, wrote the manuscript, and provided funding.

FUNDING

Research reported in this publication was supported by: Agencia Nacional de Promoción Científica y Técnica (PICT 2013-0070 and PICT 2015-0127), Secretaría de Ciencia y Técnica-Universidad Nacional de Córdoba, Fundación Florencio Fiorini and the National Institute of Allergy and Infectious Diseases of the National Institutes of Health under Award Number R01AI110340. The content is solely the responsibility of the authors and does not necessarily represent the official views of the funding agencies.

ACKNOWLEDGMENTS

We thank MP. Abadie, MP. Crespo, F. Navarro, D. Lutti, V. Blanco, A. Romero, L. Gatica and G. Furlán for their excellent technical assistance. We thank Dr. Immo Prinz for providing IL-17A/IL-17F double knockout mice. We acknowledge the NIH Tetramer Core Facility for provision of the APC-labeled TSKB20/Kb and TSKB18/Kb tetramers. We thank A. Rapinat and D. Gentien from Genomic Platform, from the translational research department from Institut Curie, Paris, for the transcriptome experiments.

This manuscript has been released as a pre-print at BioRxiv (79).

SUPPLEMENTARY MATERIAL

The Supplementary Material for this article can be found online at: https://www.frontiersin.org/articles/10.3389/fimmu.2018.02347/full#supplementary-material

Supplementary Figure 1 | Complementary evaluation of parasite-specific CD8+ T cell responses and tissue parasitism in *T. cruzi*-infected IL-17A/IL-17F DKO mice. **(A)** Relative amount of *T. cruzi* satellite DNA in spleen and liver of infected WT and IL-17A/IL-17F DKO mice determined at 22 dpi. Murine GAPDH was used for normalization. **(B)** Representative plots and statistical analysis of CD8 and TSKB20/Kb staining in spleen of WT and IL-17A/IL-17F DKO mice at 22 dpi. Numbers on plots represent the frequency of TSKB20/Kb+ CD8+ T cells. **(C–D)** Representative histograms and statistical analysis of the geometric mean expression of the inhibitory receptor PD-1 **(C)** and the death receptor CD95/Fas **(D)** in total and TSKB20/Kb+ spleen CD8+ T cells from WT and IL-17A/IL-17F DKO mice at 22 dpi. Gray tinted histogram show staining in CD8+ T cells from non-infected WT mice. Data in statistical analysis **(A–D)** are presented as mean ± *SD*, $N = 4–6$ mice. *P* values calculated with two-tailed *T* test. **(A–D)** Data are representative of at least three independent experiments.

Supplementary Figure 2 | Complementary studies of proliferation and apoptosis in total and parasite-specific CD8+ T cells in WT and IL-17RA KO infected mice. **(A,B)** Representative histograms and statistical analysis of Ki-67 **(A)** and Annexin V **(B)** staining within the 7ADD- gate in total (left) and TSKB20/Kb+ (right) CD8+ T cells from the spleen of WT and IL17RA KO mice at 10 dpi **(B)** and/or 20 dpi **(A,B)**. Gray tinted histogram show staining in CD8+ T cells from non-infected (N) WT mice. Histograms are representative of one out of five mice. Numbers indicate the frequency of Ki-67+ **(A)** and Annexin V+ **(B)** cells from the corresponding colored group. Bar graphs represent data as mean ± *SD*, $N = 4$ mice. *P* values calculated with two-tailed *T* test. **(C)** Representative histograms of TMRE staining in total (left) and TSKB20/Kb+ (right) CD8+ T cells from the spleen of infected WT mice treated with isotype control or anti-IL-17 as described in **Figure 1G**. Gray tinted histogram show staining in CD8+ T cells from non-infected WT mice. Numbers indicate the frequency of TMRElow (apoptotic) cells from the corresponding colored group. Histograms are representative of one out of seven mice. Bar graphs in the statistical analysis represent data as mean ± *SD*, $N = 7$ mice. *P* values calculated with two-tailed *T* test. **(D)** Representative plots ($N = 3$) of TMRE and LIVE/DEAD fixable aqua staining showing the frequency of cells in early apoptosis (TMRE LIVE/DEAD) and in late apoptosis/necrosis (TMRE LIVE/DEAD$^+$) within cell cultures of CD8+ T cells purified from non-infected WT and IL-17RA KO mice and activated during 24 h with coated anti-CD3 and anti-CD28 in the presence of the indicated combinations of medium, IL-17A (100 ng/mL) and camptothecin (CPT, 5 μM). **(E)** Representative histograms of the expression of Bcl-2, Bim and Bax in cultures of purified CD8+ T cells activated during 24 h with coated anti-CD3 and anti-CD28 in the presence of medium or IL-17A (100 ng/mL) as indicated. **(A–E)** Data are representative of two independent experiments.

Supplementary Figure 3 | Representative flow cytometry data plots of the evaluation of CD8+ T cell effector function. **(A)** Representative plots of the expression of Granzyme A (GzmA), Perforin (Prf) and Granzyme B (GrmB) determined after 5 h of PMA/ionomicin stimulation in spleen cells from non-infected (gray dots) and 22-day infected (blue dots) WT mice and in non-infected (black dots) and 22-day infected (red dots) IL-17RA KO mice. Plots are gated within CD8+ T cells. Numbers indicate the frequency of cells expressing the corresponding effector molecule within the infected groups. Data representative of two independent experiments with $N = 3$/group. **(B)** Representative plots and analysis strategy of the frequency of spleen CD8+ T cells from infected WT and IL-17RA KO mice (22dpi) showing a combination of three and two effector function including expression of CD107a, IFNγ and/or TNF upon 5 h of culture with the indicated stimulation. Plots are representative of one out of five mice. Data are representative of two independent experiments.

Supplementary Figure 4 | Increasing parasite doses did not diminish the frequency of parasite-specific CD8+ T cells cells or upregulated inhibitory receptors on CD8+ T cells. **(A)** Parasitemia at 22 dpi determined in the blood of WT mice infected with increasing doses of parasites (500, 5,000 and 50,000 tripomastigotes). **(B)** Representative plots and statistical analysis of CD8 and TSKB20/Kb staining in spleen of WT infected as described in **(A)**. **(C,D)** Statistical analysis of the geometric mean of expression of inhibitory **(C)** and death **(D)** receptors in total and TSKB20/Kb+ CD8+ T cells from WT mice infected as described in A. Data in statistical analysis are presented as mean ± *SD*, $N = 4–6$ mice. *P* values calculated with two-tailed *T* test. **(A–D)** Data are representative of at least 2 independent experiments.

Supplementary Figure 5 | Representative flow cytometry data plots of the evaluation of CD8+ T cell effector function in mice adoptively transferred. Representative plots and analysis strategy of the frequency of CD45.1+ WT and CD45.2+ IL-17RA KO CD8+ T cells from the spleen of CD8α-/- mice adoptively transferred and infected as indicated for **Figure 6E**. The plots show a combination of three and two effector function including expression of CD107a, IFNγ, and/or TNF upon 5 h of culture with the indicated stimulation. Plots are representative of one out of four mice. Data are representative of two independent experiments.

REFERENCES

1. Gaffen SL, Jain R, Garg AV, Cua DJ. The IL-23-IL-17 immune axis: from mechanisms to therapeutic testing. *Nat Rev Immunol.* (2014) 14:585–600. doi: 10.1038/nri3707
2. Jin W, Dong C. IL-17 cytokines in immunity and inflammation. *Emerg Microbes Infect*. (2013) 2:e60. doi: 10.1038/emi.2013.58
3. Cypowyj S, Picard C, Marodi L, Casanova JL, Puel A. Immunity to infection in IL-17-deficient mice and humans. *Eur J Immunol*. (2012) 42:2246–54. doi: 10.1002/eji.201242605
4. Tosello Boari J, Amezcua Vesely MC, Bermejo DA, Ramello MC, Montes CL, Cejas H, et al. IL-17RA Signaling reduces inflammation and mortality during *Trypanosoma cruzi* infection by recruiting suppressive IL-10-producing neutrophils. *PLoS Pathog.* (2012) 8:e1002658. doi: 10.1371/journal.ppat.1002658PPATHOGENS-D-11-02639
5. Bermejo DA, Jackson SW, Gorosito-Serran M, Acosta-Rodriguez EV, Amezcua-Vesely MC, Sather BD, et al. *Trypanosoma cruzi* trans-sialidase initiates a program independent of the transcription factors RORgammat and Ahr that leads to IL-17 production by activated B cells. *Nat Immunol.* (2013) 14:514–22. doi: 10.1038/ni.2569
6. Gaffen S. Structure and signalling in the IL-17 receptor family. *Nat Rev Immunol.* (2009) 9:556–67. doi: 10.1038/nri2586
7. Ouyang W, Kolls J, Zheng Y. The biological functions of T helper 17 cell effector cytokines in inflammation. *Immunity* (2008) 28:454–67. doi: 10.1016/j.immuni.2008.03.004
8. Iwakura Y, Ishigame H, Saijo S, Nakae S. Functional specialization of interleukin-17 family members. *Immunity* (2011) 34:149–62. doi: 10.1016/j.immuni.2011.02.012
9. Acharya D, Wang P, Paul AM, Dai J, Gate D, Lowery JE, et al. Interleukin-17A promotes CD8$^+$ T cell cytotoxicity to facilitate west

nile virus clearance. *J Virol.* (2017) 91:e01529-16. doi: 10.1128/JVI.01529-16
10. Junqueira C, Caetano B, Bartholomeu DC, Melo MB, Ropert C, Rodrigues MM, et al. The endless race between *Trypanosoma cruzi* and host immunity: lessons for and beyond Chagas disease. *Expert Rev Mol Med.* (2010) 12:e29. doi: 10.1017/S1462399410001560
11. Padilla A, Bustamante J, Tarleton R. $CD8^+$ T cells in *Trypanosoma cruzi* infection. *Curr Opin Immunol.* (2009) 21:385–90. doi: 10.1016/j.coi.2009.07.006
12. Tarleton RL. Depletion of $CD8^+$ T cells increases susceptibility and reverses vaccine-induced immunity in mice infected with *Trypanosoma cruzi*. *J Immunol.* (1990) 144:717–24.
13. Tzelepis F, de Alencar B, Penido M, Gazzinelli R, Persechini P, Rodrigues M. Distinct kinetics of effector $CD8^+$ cytotoxic T cells after infection with *Trypanosoma cruzi* in naive or vaccinated mice. *Infect Immun.* (2006) 74:2477–81. doi: 10.1128/IAI.74.4.2477-2481.2006
14. Jordan K, Hunter C. Regulation of $CD8^+$ T cell responses to infection with parasitic protozoa. *Exp Parasitol.* (2010) 126:318–25. doi: 10.1016/j.exppara.2010.05.008
15. Vasconcelos JR, Dominguez MR, Araujo AF, Ersching J, Tararam CA, Bruna-Romero O, et al. Relevance of long-lived CD8(+) T effector memory cells for protective immunity elicited by heterologous prime-boost vaccination. *Front Immunol.* (2012) 3:358. doi: 10.3389/fimmu.2012.00358
16. Zhang L, Tarleton RL. Parasite persistence correlates with disease severity and localization in chronic Chagas' disease. *J Infect Dis.* (1999) 180:480–6. doi: 10.1086/314889
17. Gutierrez FR, Guedes PM, Gazzinelli RT, Silva JS. The role of parasite persistence in pathogenesis of Chagas heart disease. *Parasite Immunol.* (2009) 31:673–85. doi: 10.1111/j.1365-3024.2009.01108.x
18. Zhang N, Bevan M. CD8(+) T cells: foot soldiers of the immune system. *Immunity* (2011) 35:161–8. doi: 10.1016/j.immuni.2011.07.010
19. Wherry EJ. T cell exhaustion. *Nat Immunol.* (2011) 12:492–9. doi: 10.1038/ni.2035
20. Cox M, Harrington L, Zajac A. Cytokines and the inception of CD8 T cell responses. *Trends Immunol.* (2011) 32:180–6. doi: 10.1016/j.it.2011.01.004
21. Kaech S, Cui W. Transcriptional control of effector and memory $CD8^+$ T cell differentiation. *Nat Rev Immunol.* (2012) 12:749–61. doi: 10.1038/nri3307
22. Haas JD, Ravens S, Duber S, Sandrock I, Oberdorfer L, Kashani E, et al. Development of interleukin-17-producing gammadelta T cells is restricted to a functional embryonic wave. *Immunity* (2012) 37:48–59. doi: 10.1016/j.immuni.2012.06.003
23. Piron M, Fisa R, Casamitjana N, Lopez-Chejade P, Puig L, Verges M, et al. Development of a real-time PCR assay for *Trypanosoma cruzi* detection in blood samples. *Acta Trop.* (2007) 103:195–200. doi: 10.1016/j.actatropica.2007.05.019
24. Amezcua Vesely MC, Schwartz M, Bermejo DA, Montes CL, Cautivo KM, Kalergis AM, et al. FcgammaRIIb and BAFF differentially regulate peritoneal B1 cell survival. *J Immunol.* (2012) 188:4792–800. doi: 10.4049/jimmunol.1102070
25. Martin D, Weatherly D, Laucella S, Cabinian M, Crim M, Sullivan S, et al. $CD8^+$ T-Cell responses to *Trypanosoma cruzi* are highly focused on strain-variant trans-sialidase epitopes. *PLoS Pathog.* (2006) 2:e77. doi: 10.1371/journal.ppat.0020077
26. Zeng R, Spolski R, Finkelstein S, Oh S, Kovanen P, Hinrichs C, et al. Synergy of IL-21 and IL-15 in regulating $CD8^+$ T cell expansion and function. *J Exp Med.* (2005) 201:139–48. doi: 10.1084/jem.20041057
27. Gaubin M, Autiero M, Basmaciogullari S, Metivier D, Mis hal Z, Culerrier R, et al. Potent inhibition of CD4/TCR-mediated T cell apoptosis by a CD4-binding glycoprotein secreted from breast tumor and seminal vesicle cells. *J Immunol.* (1999) 162:2631–8.
28. Stahnke K, Fulda S, Friesen C, Strauss G, Debatin KM. Activation of apoptosis pathways in peripheral blood lymphocytes by *in vivo* chemotherapy. *Blood* (2001) 98:3066–73. doi: 10.1182/blood.V98.10.3066
29. Renault TT, Chipuk JE. Getting away with murder: how does the BCL-2 family of proteins kill with immunity? *Ann N Y Acad Sci.* (2013) 1285:59–79. doi: 10.1111/nyas.12045
30. Hedrick SM, Hess Michelini R, Doedens AL, Goldrath AW, Stone EL. FOXO transcription factors throughout T cell biology. *Nat Rev Immunol.* (2012) 12:649–61. doi: 10.1038/nri3278
31. Huber M, Lohoff M. IRF4 at the crossroads of effector T-cell fate decision. *Eur J Immunol.* (2014) 44:1886–95. doi: 10.1002/eji.201344279
32. Pauken KE, Wherry EJ. Overcoming T cell exhaustion in infection and cancer. *Trends Immunol.* (2015) 36:265–76. doi: 10.1016/j.it.2015.02.008
33. Chang K, Svabek C, Vazquez-Guillamet C, Sato B, Rasche D, Wilson S, et al. Targeting the programmed cell death 1: programmed cell death ligand 1 pathway reverses T cell exhaustion in patients with sepsis. *Crit Care* (2014) 18:R3. doi: 10.1186/cc13176
34. Zhang Y, Zhou Y, Lou J, Li J, Bo L, Zhu K, et al. PD-L1 blockade improves survival in experimental sepsis by inhibiting lymphocyte apoptosis and reversing monocyte dysfunction. *Crit Care* (2010) 14:R220. doi: 10.1186/cc9354
35. Tian Y, Zajac AJ. IL-21 and T Cell differentiation: consider the context. *Trends Immunol.* (2016) 37:557–68. doi: 10.1016/j.it.2016.06.001
36. Lindemann M, Hu Z, Benczik M, Liu K, Gaffen S. Differential regulation of the IL-17 receptor by gammac cytokines: inhibitory signaling by the phosphatidylinositol 3-kinase pathway. *J Biol Chem.* (2008) 283:14100–8. doi: 10.1074/jbc.M801357200
37. Rong Z, Wang A, Li Z, Ren Y, Cheng L, Li Y, et al. IL-17RD (Sef or IL-17RLM) interacts with IL-17 receptor and mediates IL-17 signaling. *Cell Res.* (2009) 19:208–15. doi: 10.1038/cr.2008.320
38. Mellett M, Atzei P, Horgan A, Hams E, Floss T, Wurst W, et al. Orphan receptor IL-17RD tunes IL-17A signalling and is required for neutrophilia. *Nat Commun.* (2012) 3:1119. doi: 10.1038/ncomms2127
39. Conti HR, Gaffen SL. IL-17-mediated immunity to the opportunistic fungal pathogen *Candida albicans*. *J Immunol.* (2015) 195:780–8. doi: 10.4049/jimmunol.1500909
40. Song X, He X, Li X, Qian Y. The roles and functional mechanisms of interleukin-17 family cytokines in mucosal immunity. *Cell Mol Immunol.* (2016) 13:418–31. doi: 10.1038/cmi.2015.105
41. Khader SA, Gopal R. IL-17 in protective immunity to intracellular pathogens. *Virulence* (2010) 1:423–7. doi: 10.4161/viru.1.5.12862
42. Xu S, Cao X. Interleukin-17 and its expanding biological functions. *Cell Mol Immunol.* (2010) 7:164–74. doi: 10.1038/cmi.2010.21
43. Xu S, Han Y, Xu X, Bao Y, Zhang M, Cao X. IL-17A-producing gammadeltaT cells promote CTL responses against Listeria monocytogenes infection by enhancing dendritic cell cross-presentation. *J Immunol.* (2010) 185:5879–87. doi: 10.4049/jimmunol.1001763
44. Martin-Orozco N, Muranski P, Chung Y, Yang X, Yamazaki T, Lu S, et al. T helper 17 cells promote cytotoxic T cell activation in tumor immunity. *Immunity* (2009) 31:787–98. doi: 10.1016/j.immuni.2009.09.014
45. Shen F, Hu Z, Goswami J, Gaffen S. Identification of common transcriptional regulatory elements in interleukin-17 target genes. *J Biol Chem.* (2006) 281:24138–48. doi: 10.1074/jbc.M604597200
46. Gaffen SL. Recent advances in the IL-17 cytokine family. *Curr Opin Immunol.* (2011) 23:613–9. doi: 10.1016/j.coi.2011.07.006
47. Hsu H-C, Yang P, Wang J, Wu Q, Myers R, Chen J, et al. Interleukin 17-producing T helper cells and interleukin 17 orchestrate autoreactive germinal center development in autoimmune BXD2 mice. *Nat Immunol.* (2008) 9:166-75. doi: 10.1038/ni1552
48. Ishigame H, Kakuta S, Nagai T, Kadoki M, Nambu A, Komiyama Y, et al. Differential roles of interleukin-17A and−17F in host defense against mucoepithelial bacterial infection and allergic responses. *Immunity* (2009) 30:108–19. doi: 10.1016/j.immuni.2008.11.009
49. O'Connor W, Kamanaka M, Booth C, Town T, Nakae S, Iwakura Y, et al. A protective function for interleukin 17A in T cell-mediated intestinal inflammation. *Nat Immunol.* (2009) 10:603–9. doi: 10.1038/ni.1736
50. Cai CW, Blase JR, Zhang X, Eickhoff CS, Hoft DF. Th17 cells are more protective than Th1 cells against the intracellular parasite *Trypanosoma cruzi*. *PLoS Pathog.* (2016) 12:e1005902. doi: 10.1371/journal.ppat.1005902
51. Duraiswamy J, Ibegbu CC, Masopust D, Miller JD, Araki K, Doho GH, et al. Phenotype, function, and gene expression profiles of programmed death-1(hi) CD8 T cells in healthy human adults. *J Immunol.* (2011) 186:4200–12. doi: 10.4049/jimmunol.1001783

52. Doering TA, Crawford A, Angelosanto JM, Paley MA, Ziegler CG, Wherry EJ. Network analysis reveals centrally connected genes and pathways involved in $CD8^+$ T cell exhaustion versus memory. *Immunity* (2012) 37:1130–44. doi: 10.1016/j.immuni.2012.08.021
53. Attanasio J, Wherry EJ. Costimulatory and coinhibitory receptor pathways in infectious disease. *Immunity* (2016) 44:1052–68. doi: 10.1016/j.immuni.2016.04.022
54. Bustamante J, Bixby L, Tarleton R. Drug-induced cure drives conversion to a stable and protective $CD8^+$ T central memory response in chronic Chagas disease. *Nat Med*. (2008) 14:542–50. doi: 10.1038/nm1744
55. Tzelepis F, Persechini P, Rodrigues M. Modulation of $CD4^+$ T cell-dependent specific cytotoxic $CD8^+$ T cells differentiation and proliferation by the timing of increase in the pathogen load. *PLoS ONE* (2007) 2:e393. doi: 10.1371/journal.pone.0000393
56. Wherry EJ, Ha SJ, Kaech SM, Haining WN, Sarkar S, Kalia V, et al. Molecular signature of $CD8^+$ T cell exhaustion during chronic viral infection. *Immunity* (2007) 27:670–84. doi: 10.1016/j.immuni.2007.09.006
57. Bengsch B, Ohtani T, Herati RS, Bovenschen N, Chang KM, Wherry EJ. Deep immune profiling by mass cytometry links human T and NK cell differentiation and cytotoxic molecule expression patterns. *J Immunol Methods* (2018) 453:3–10. doi: 10.1016/j.jim.2017.03.009
58. Hellmann MD, Friedman CF, Wolchok JD. Combinatorial cancer immunotherapies. *Adv Immunol*. (2016) 130:251–77. doi: 10.1016/bs.ai.2015.12.005
59. Gutierrez FR, Mariano FS, Oliveira CJ, Pavanelli WR, Guedes PM, Silva GK, et al. Regulation of *Trypanosoma cruzi*-induced myocarditis by programmed death cell receptor 1. *Infect Immun*. (2011) 79:1873–81. doi: 10.1128/IAI.01047-10
60. Dyck L, Mills KHG. Immune checkpoints and their inhibition in cancer and infectious diseases. *Eur J Immunol*. (2017) 47:765–79. doi: 10.1002/eji.201646875
61. Lasso P, Mateus J, Pavia P, Rosas F, Roa N, Thomas MC, et al. Inhibitory receptor expression on $CD8^+$ T cells is linked to functional responses against *Trypanosoma cruzi* antigens in chronic chagasic patients. *J Immunol*. (2015) 195:3748–58. doi: 10.4049/jimmunol.1500459
62. Albareda MC, Laucella SA, Alvarez MG, Armenti AH, Bertochi G, Tarleton RL, et al. *Trypanosoma cruzi* modulates the profile of memory $CD8^+$ T cells in chronic Chagas' disease patients. *Int Immunol*. (2006) 18:465–71. doi: 10.1093/intimm/dxh387
63. Albareda MC, Olivera GC, Laucella SA, Alvarez MG, Fernandez ER, Lococo B, et al. Chronic human infection with *Trypanosoma cruzi* drives $CD4^+$ T cells to immune senescence. *J Immunol*. (2009) 183:4103–8. doi: 10.4049/jimmunol.0900852
64. Tarleton RL. $CD8^+$ T cells in *Trypanosoma cruzi* infection. *Semin Immunopathol*. (2015) 37:233–8. doi: 10.1007/s00281-015-0481-9
65. Guedes PM, Gutierrez FR, Silva GK, Dellalibera-Joviliano R, Rodrigues GJ, Bendhack LM, et al. Deficient regulatory T cell activity and low frequency of IL-17-producing T cells correlate with the extent of cardiomyopathy in human Chagas' disease. *PLoS Negl Trop Dis*. (2012) 6:e1630. doi: 10.1371/journal.pntd.0001630PNTD-D-11-01006
66. Magalhaes LM, Villani FN, Nunes Mdo C, Gollob KJ, Rocha MO, Dutra WO. High interleukin 17 expression is correlated with better cardiac function in human Chagas disease. *J Infect Dis*. (2013) 207:661–5. doi: 10.1093/infdis/jis724
67. Kuroda S, Yamazaki M, Abe M, Sakimura K, Takayanagi H, Iwai Y. Basic leucine zipper transcription factor, ATF-like (BATF) regulates epigenetically and energetically effector CD8 T-cell differentiation via Sirt1 expression. *Proc Natl Acad Sci USA*. (2011) 108:14885–9. doi: 10.1073/pnas.1105133108
68. Man K, Miasari M, Shi W, Xin A, Henstridge DC, Preston S, et al. The transcription factor IRF4 is essential for TCR affinity-mediated metabolic programming and clonal expansion of T cells. *Nat Immunol*. (2013) 14:1155–65. doi: 10.1038/ni.2710
69. Yao S, Buzo BF, Pham D, Jiang L, Taparowsky EJ, Kaplan MH, et al. Interferon regulatory factor 4 sustains $CD8^+$ T cell expansion and effector differentiation. *Immunity* (2013) 39:833–45. doi: 10.1016/j.immuni.2013.10.007
70. Raczkowski F, Ritter J, Heesch K, Schumacher V, Guralnik A, Hocker L, et al. The transcription factor interferon regulatory factor 4 is required for the generation of protective effector $CD8^+$ T cells. *Proc Natl Acad Sci USA*. (2013) 110:15019–24. doi: 10.1073/pnas.1309378110
71. Kurachi M, Barnitz RA, Yosef N, Odorizzi PM, DiIorio MA, Lemieux ME, et al. The transcription factor BATF operates as an essential differentiation checkpoint in early effector $CD8^+$ T cells. *Nat Immunol*. (2014) 15:373–83. doi: 10.1038/ni.2834
72. Grusdat M, McIlwain DR, Xu HC, Pozdeev VI, Knievel J, Crome SQ, et al. IRF4 and BATF are critical for CD8 T-cell function following infection with LCMV. *Cell Death Differ*. (2014) 21:1050–60. doi: 10.1038/cdd.2014.19
73. Kwon H, Thierry-Mieg D, Thierry-Mieg J, Kim HP, Oh J, Tunyaplin C, et al. Analysis of interleukin-21-induced Prdm1 gene regulation reveals functional cooperation of STAT3 and IRF4 transcription factors. *Immunity* (2009) 31:941–52. doi: 10.1016/j.immuni.2009.10.008
74. Cretney E, Xin A, Shi W, Minnich M, Masson F, Miasari M, et al. The transcription factors Blimp-1 and IRF4 jointly control the differentiation and function of effector regulatory T cells. *Nat Immunol*. (2011) 12:304–11. doi: 10.1038/ni.2006
75. Li P, Spolski R, Liao W, Wang L, Murphy TL, Murphy KM, et al. BATF-JUN is critical for IRF4-mediated transcription in T cells. *Nature* (2012) 490:543–6. doi: 10.1038/nature11530
76. Quigley M, Pereyra F, Nilsson B, Porichis F, Fonseca C, Eichbaum Q, et al. Transcriptional analysis of HIV-specific $CD8^+$ T cells shows that PD-1 inhibits T cell function by upregulating BATF. *Nat Med*. (2010) 16:1147–51. doi: 10.1038/nm.2232
77. Man K, Gabriel SS, Liao Y, Gloury R, Preston S, Henstridge DC, et al. Transcription factor IRF4 promotes $CD8^+$ T cell exhaustion and limits the development of memory-like T cells during chronic infection. *Immunity* (2017) 47:1129–41 e5. doi: 10.1016/j.immuni.2017.11.021
78. Bar E, Whitney PG, Moor K, Reis e Sousa C, LeibundGut-Landmann S. IL-17 regulates systemic fungal immunity by controlling the functional competence of NK cells. *Immunity* (2014) 40:117–27. doi: 10.1016/j.immuni.2013.12.002
79. Tosello Boari J, Araujo Furlan CL, Fiocca Vernengo F, Rodrigueza C, Ramello MC, Amezcua Vesely MC, et al. IL-17RA-signaling modulates $CD8^+$ T cell survival and exhaustion during *Trypanosoma cruzi* infection. *bioRxiv* [Preprint] (2018). doi: 10.1101/314336

Conflict of Interest Statement: The authors declare that the research was conducted in the absence of any commercial or financial relationships that could be construed as a potential conflict of interest.

Copyright © 2018 Tosello Boari, Araujo Furlan, Fiocca Vernengo, Rodriguez, Ramello, Amezcua Vesely, Gorosito Serrán, Nuñez, Richer, Piaggio, Montes, Gruppi and Acosta Rodríguez. This is an open-access article distributed under the terms of the Creative Commons Attribution License (CC BY). The use, distribution or reproduction in other forums is permitted, provided the original author(s) and the copyright owner(s) are credited and that the original publication in this journal is cited, in accordance with accepted academic practice. No use, distribution or reproduction is permitted which does not comply with these terms.

frontiers in Immunology

ORIGINAL RESEARCH
published: 15 October 2018
doi: 10.3389/fimmu.2018.02269

Alpha2beta1 Integrin (VLA-2) Protects Activated Human Effector T Cells From Methotrexate-Induced Apoptosis

Amna Abderrazak[1†], Mohammed-Amine El Azreq[1†], Dalila Naci[1‡], Paul R. Fortin[1,2] and Fawzi Aoudjit[1,3]*

[1] Axe de Recherche sur les Maladies Infectieuses et Immunitaires, Centre de Recherche du CHU De Québec-Université Laval, Québec, QC, Canada, [2] Division de Rhumatologie, Département de Médecine, Faculté de Médecine, Université Laval, Québec, QC, Canada, [3] Département de Microbiologie-Infectiologie et D'immunologie, Faculté de Médecine, Université Laval, Québec, QC, Canada

β1 integrins are critical for T cell migration, survival and costimulation. The integrin α2β1, which is a receptor for collagen, also named VLA-2, is a major costimulatory pathway of effector T cells and has been implicated in arthritis pathogenesis. Herein, we have examined its ability to promote methotrexate (MTX) resistance by enhancing effector T cells survival. Our results show that attachment of anti-CD3-activated human polarized Th17 cells to collagen but not to fibronectin or laminin led to a significant reduction of MTX-induced apoptosis. The anti-CD3+collagen-rescued cells still produce significant amounts of IL-17 and IFNγ upon their reactivation indicating that their inflammatory nature is preserved. Mechanistically, we found that the prosurvival role of anti-CD3+collagen involves activation of the MTX transporter ABCC1 (ATP Binding Cassette subfamily C Member 1). Finally, the protective effect of collagen/α2β1 integrin on MTX-induced apoptosis also occurs in memory $CD4^+$ T cells isolated from rheumatoid arthritis (RA) patients suggesting its clinical relevance. Together these results show that α2β1 integrin promotes MTX resistance of effector T cells, and suggest that it could contribute to the development of MTX resistance that is seen in RA.

Keywords: α2β1 integrin, collagen, cell adhesion, methotrexate, rheumatoid arthritis, apoptosis, T cells

OPEN ACCESS

Edited by:
María Fernanda Pascutti, Sanquin Diagnostic Services, Netherlands

Reviewed by:
Marta A. Toscano, Instituto de Biología y Medicina Experimental (IBYME), CONICET, Argentina
Zhe-Xiong Lian, South China University of Technology, China
Femke Van Wijk, University Medical Center Utrecht, Netherlands

***Correspondence:**
Fawzi Aoudjit
fawzi.aoudjit@crchudequebec.ulaval.ca

[†] These authors have contributed equally to this work

‡Present Address:
Dalila Naci, Peter Gilgan Center for Research and Learning, The Hospital for Sick Children, Toronto University, Toronto, ON, Canada

Specialty section:
This article was submitted to Autoimmune and Autoinflammatory Disorders, a section of the journal Frontiers in Immunology

Received: *19 June 2018*
Accepted: *12 September 2018*
Published: *15 October 2018*

Citation:
Abderrazak A, El Azreq MA, Naci D, Fortin PR and Aoudjit F (2018) Alpha2beta1 Integrin (VLA-2) Protects Activated Human Effector T Cells From Methotrexate-Induced Apoptosis. Front. Immunol. 9:2269. doi: 10.3389/fimmu.2018.02269

INTRODUCTION

Integrins are a large family of α/β transmembrane receptors playing a key role in cell-cell interactions and cell adhesion to the extracellular matrix (ECM). The very late activating antigens (VLA)-1 to -6 belonging to the β1 integrin subfamily are the most expressed ECM receptors by effector T cells. After activation, integrins induce T cell adhesion and migration through basement membranes and interstitial tissue in order to reach the inflammatory sites (1). In addition, β1 integrins also provide costimulatory signals to promote T cell survival and cytokine production (1).

The collagen-binding integrin α2β1 (VLA-2) has recently gained significant attention as one of the major integrin involved in T cell-mediated immunity. It is expressed on effector/memory T cells found in inflammatory tissues but not on naïve T cells (2–4). α2β1 integrin is found on Th1 cells (5) and it is the major integrin that binds collagen, which is expressed by human Th17 cells (6).

α2β1 integrin has been involved in Th17 and Th1 cell adhesion to collagen and in costimulation of IL-17 and IFNγ production (5–7). Furthermore, it promotes the survival of human effector T cells by inhibiting Fas-induced apoptosis (8). *In vivo* studies showed the implication of α2β1 integrin in the development of inflammatory diseases including experimental colitis (9), experimental autoimmune encephalomyelitis (10) and arthritis. In this case, we have shown that α2β1 integrin is expressed on RA synovial Th17 cells and its blockade reduces severity of collagen-induced arthritis and IL-7-induced bone loss in mice by reducing Th17 cell numbers and activity in the synovial tissue (11, 12).

RA is a disabling disease in which Th17 and Th1 cells play a central role in the resulting synovitis and cartilage and bone erosion. Despite the introduction of several biologics, MTX is still the first line in RA therapy and the most frequently used disease-modifying anti-rheumatic drug. However, 30–40% of patients fail to respond or end-up developing resistance, thus becoming unresponsive (13, 14). The mechanisms accounting for MTX resistance in RA are still unclear although increased metabolism, altered target enzymes, and defective cellular uptake or increased MTX efflux through the expression and activity of ATP-binding cassette (ABC) drug transporters have been proposed (13, 14). These drug transporters, which are involved in cancer chemoresistance (15), have the ability to function, in an ATP-dependent manner, as a pump in order to extrude various endogenous (steroids, metabolites, ions) or exogenous substrates (drugs) out of the cells.

MTX can act by blocking cell proliferation and cytokine production (16). However, one major effect of MTX is the induction of apoptosis in proliferating activated/effector T cells (16, 17). Decreased T cell numbers in the synovium of RA patients treated with MTX has also been reported (18, 19). Thus, it is likely that factors that promote resistance of effector T cells to apoptosis may have a significant role in MTX resistance. Since α2β1 integrin plays an important role in the survival and costimulation of effector T cell and in arthritis pathogenesis, we tested its contribution to MTX resistance using a tailored *in vitro* T cell model and T cells from RA patients. Our results show that α2β1 protects activated human polarized Th17 cells and RA effector/memory T cells from MTX-induced apoptosis through the ABC drug transporter ABCC1. Taken together our findings indicate that α2β1 integrin promotes Th17 cell resistance to MTX, and thus it could contribute to MTX resistance that is observed in RA.

MATERIALS AND METHODS

Reagents and Antibodies

Cell culture medium, X-vivo 15, was purchased from Lonza technologies (Walkersville, MD). Human cytokines (IL-6, TGF-β, IL-2, IL-1β, and IL-23) were purchased from R&D Systems (Minneapolis, MN). Type II collagen (referred hereafter as collagen) was from EPC Elastin Products Company (Owensville, MO), fibronectin, was from Sigma-Millipore (St. Louis, MO) and laminin-8 was from Biolamina (Stockholm, Sweden). The ABCC1 inhibitor MK571 and calcein-AM were from Calbiochem (San Diego, CA). The ABCG2 inhibitor, fumitremorgin c and ABCC1 inhibitor, reversan were from Sigma-Millipore (St-Louis, MO). MTX, the blocking anti-human α2 integrin (P1E6), the blocking anti-α2β1 integrin (BHA2.1) and their appropriate isotypic control antibodies were from EMD Millipore (Billerica, MA). The blocking anti-human β1 integrin (4B4) and its control isotypic antibody were purchased from Beckman Coulter (Brea, CA). CD3/CD28 Dynabeads were from Invitrogen Dynal AS (Oslo, Norway). The anti-CD3 mAb (OKT3), PE-conjugated anti-human IFNγ (B27), PE-conjugated anti-human α2 integrin (12F1), FITC-conjugated anti-human ABCC1 (QCRL-3), Alexa 647-conjugated anti-human IL-17 (N49-653), PE-conjugated anti-ABCG2 (ATP-binding cassette sub-family G member 2) (5D3), their appropriate control isotypic antibodies and the FITC-annexin V apoptotic kit were from BD Biosciences (San Diego, USA). Anti-β-actin (C2) and anti-caspase-3 (E-8) antibodies were from Santa Cruz Biotechnology (Santa Cruz, CA).

Ethical Statement

Our study was approved by the CHU de Québec-Université Laval ethical committee for clinical research. Healthy adult blood donors were recruited through the clinical research facility at the CHU de Québec-Université Laval Research Center. RA patients were recruited through the CHU de Québec-Université Laval Systemic Autoimmune Rheumatic Diseases Biobank and Repository Database. The CHU de Québec-Université Laval ethics committee has approved the biobank and its management (CÉR #B13-06-1243). Our experiments were conducted in accordance with the local ethical guidelines and regulations. RA patients and healthy donors provided and signed written consent forms before blood collection.

Naïve CD4$^+$ T Cells Isolation and Th17 Differentiation

PBMCs were collected from blood of healthy subject volunteers using ficoll gradients. Next we purified primary human naïve CD4$^+$T cells by negative selection using the EasySep human Naïve CD4$^+$ Cell Enrichment Kit from StemCell Technologies (Vancouver, BC) as described in manufacturer's instructions. We then generated Th17 cells after activation of naïve CD4$^+$ T cells during 6 days with CD3/CD28 beads (one bead/cell) in serum-free X-vivo medium in the presence of Th17 polarizing cytokines (TGFβ, IL-1β, IL-6, and IL-23) as we previously described (12).

RA Patients and CD45RO$^+$ Memory T Cells Isolation

PBMCs were isolated from peripheral blood of RA patients (n = 5) with established disease according to the American College of Rheumatology criteria (20). The patients were between 37 and 71 y old with disease duration of one year and received prednisone and MTX. We purified memory CD4$^+$ T cells by negative

Abbreviations: ABCC1, ATP Binding Cassette subfamily C Member 1; ABCG2, ATP-binding Cassette subfamily G member 2; Col, collagen; ECM, extracellular matrix; Fbn, fibronectin; Lam, laminin; MFI, mean fluorescence intensity; MTX, methotrexate; NS, non-specific band; PBMCs, Peripheral blood mononuclear cells; PLL, poly-L-lysine; PMA, Phorbol-12-Myristate 13-Acetate; RA, rheumatoid arthritis; sCol, soluble Col; TCR, T cell receptor.

selection using an appropriate kit from StemCell Technologies (Vancouver, BC). $CD4^+CD45RO^+$ T cells (1×10^6) in 1 ml of X-vivo medium were expanded with CD3/CD28 beads (one bead/cell) and IL-2 (50 Units/ml) for 6 days.

T Cell Activation and Apoptosis

Wells were first coated with 2 μg/ml of anti-CD3 mAb for 24 h at 4°C, after which, they were washed with PBS. The wells with or without anti-CD3 were then coated with 2 μg/ml collagen for 3 h at 37°C. After three washes with PBS, we seeded the cells for 3 h, and treated them with 10 μM of MTX for 24 h at 37°C. Cell apoptosis was determined using annexin V-FITC staining and measured by flow cytometry (BD FACSCALIBUR II cytometer).

Cell Adhesion Assays

Cell adhesion assays were conducted as described (7). A 96-well microtiter plate (TC plate, flat bottom, Falcon) was coated with 20 μg/ml of matrix proteins diluted in PBS overnight at 4°C. After three washes with PBS, wells were blocked with 1% BSA for 1 h at 37°C. Then, 10^5 cells in 100 μl of X-vivo medium activated or not with anti-CD3-coated beads were seeded into the wells. After 1 h, the cells were washed with PBS and fixed in a PBS solution containing 1% formaldehyde for 1 h at room temperature. The cells were washed and stained with a methanol solution containing 0.5% crystal violet. After four washes, we lysed the cells using a 1% SDS solution and determined the absorbance at 600 nm using an ELISA plate reader.

Expression of α2 Integrin, ABCC1, and ABCG2 Transporters

The cells were stained with (PE-conjugated) isotypic control, anti-α2 integrin, and anti-ABCG2 antibodies for 30 min on ice. For ABCC1 expression, we first permeabilized and fixed the cells with a cytoFix/CytoPerm kit (BD Biosciences) for 20 min, after which, we incubated them with FITC-conjugated isotypic control or anti-ABCC1 antibodies. The cells were washed and then analyzed for α2 integrin, ABCC1, and ABCG2 expression levels by flow cytometry (BD FACSCalibur II cytometer).

Quantitative RT-PCR

Total RNA isolation and cDNA preparation were carried out as we previously described (6). PCR reactions were performed with 1 μl of cDNA in a 20 μl of total volume containing SYBR Green I (Invitrogen, CA) for 35 cycles in Rotor-Gene 3000 operated with Rotor-Gene Software 9 version 6.0.19 (Corbett Research, Mortlake, New South Wales, Australia). For specificity, we performed the Melts procedure as we previously described (6). The housekeeping gene *β-actin* was used for normalization of *ABCC1* and *ABCG2* gene expression. As a calibrator, control PCR reactions using RNA from MCF-7 cells, which express both ABCC1 and ABCG2 (21) were used. Relative gene expression was calculated using the ΔΔCt comparative method and the formula: ΔΔCt= (Ct target gene-Ct β-actin) sample–(Ct target gene–Ct β-actin) calibrator. Primers for human *ABCC1*, *ABCG2,* and *β-actin* genes were as previously described (6, 22).

Caspase-3 Activation and Western Blot Analysis

Caspase-3 activation was evaluated by Western blot using anti-caspase-3 antibody, which recognizes the native and active caspase-3 fragments, as we previously described (23). Blots were stripped and then reprobed for loading control with anti-β-actin antibody.

IL-17 and IFNγ Quantification

After MTX treatment in the presence of anti-CD3+collagen, viable polarized Th17 cells (rescued cells) were isolated through a ficoll gradient (viability of more than 95%). Then, equal cell numbers of rescued cells and control cells (non-treated) were restimulated with anti-CD3+collagen for 24 h. The supernatants were collected for ELISA analysis in order to quantify IL-17 and IFNγ production using ELISA kits from R&D Systems (Minneapolis, USA).

For intracellular cytokine staining, arthritic effector/memory $CD4^+$ T cells were activated with 50 ng/ml of Phorbol-12-Myristate 13-Acetate (PMA) and 750 ng/ml of ionomycin in the presence of BD Golgi Plug (2 μg/ml) for 4 h. After permeabilisation and fixation with cytoFix/CytoPerm kit (BD Biosciences), the cells were stained with intracellular anti-IL-17 and anti-IFNγ antibodies and positive cells were evaluated by FACS analysis (BD FACSCalibur II).

Calcein-AM Intracellular Content

Human polarized Th17 cells in X-vivo medium were activated for 3 h with anti-CD3+collagen. The cells were then cultured for 1 h in medium containing 1 nM of calcein-AM, after which the cells were washed. The intracellular levels of calcein-AM were determined by flow cytometry (BD FACSCalibur II) using the FL-1 channel. Results are expressed as percentage of positive cells times (x) mean fluorescence intensity (MFI) giving a metric referred as integrated MFI, which reflects the total expression in positive cells (24). This method of quantification has been used in various studies including ours (25–28) and has therefore been applied throughout this study.

Statistical Analysis

The Student's *t*-test was used and $p<0.05$ was considered significant.

RESULTS

Collagen Protects Human Polarized Th17 Cells From MTX-Induced Apoptosis

In order to determine whether α2β1 integrin provides a survival advantage to Th17 cells, we first studied the effect of collagen on MTX-induced apoptosis in human polarized Th17 cells. As previously shown, 15–20 % of the cells produce IL-17 (12) (**Figure S1** in Supplementary material). MTX has been shown to induce apoptosis at 0.1–10 μM, which mimic the low doses administered to RA patients (17, 29, 30) and we have found that MTX at 10 μM is the optimal dose in our cell model. As shown in **Figure 1A**, adhesion to collagen slightly reduces MTX-induced apoptosis of polarized Th17 cells as evidenced by the

decrease in annexin-positive cells compared with cells treated only with MTX. Anti-CD3 alone did not show any effect on cell survival. However, culture of the cells on anti-CD3+collagen led to a 40% reduction in apoptosis. As a control, the non-integrin ligand poly-L-lysine had no effect on MTX-induced apoptosis. Of note, we also found that anti-CD3+collagen reduces MTX-induced apoptosis by 35–40% when MTX was used at 0.1 and 1 μM (data not shown).

To determine if the collagen effect is due to increased cell contacts with coated anti-CD3 mAb as a result of cell adhesion, we tested if collagen still has the ability to protect polarized Th17 cells from MTX-induced apoptosis when added in soluble form. We found that the soluble form of collagen has the same ability as immobilized collagen to protect the cells from MTX-induced apoptosis (**Figure 1B**) suggesting that the pro-survival effect of collagen is a result of its signaling function. Together, these results indicate that although collagen by itself has a small effect, it is the combination of anti-CD3+collagen that has produced the most important effect on cell survival.

Because MTX-induced apoptosis is associated with caspase-3 activation, we determined if anti-CD3+collagen costimulation inhibited caspase-3 activation in MTX-treated cells. Treatment of polarized Th17 cells with MTX is associated with caspase-3 activation as determined by the proteolysis of procaspase-3 leading to the generation of caspase-3 active fragments (**Figure 1C**). Activation of the cells with anti-CD3 mAb had no effect whereas their activation with collagen alone had only a minor effect. However, activation with anti-CD3+collagen effectively inhibited MTX-induced caspase-3 activation further indicating that anti-CD3+collagen signaling protects polarized Th17 cells from MTX-induced apoptosis.

To determine if the anti-CD3+collagen-rescued cells from MTX treatment were still able to produce IL-17, rescued cells (viable cells) were isolated through a ficoll gradient and restimulated with anti-CD3+collagen. The results show that these cells still produce significant amounts of IL-17 when compared to control cells that have not been treated with MTX (**Figure 1D**). In addition, since human polarized Th17 cells also contain Th1 cells (31, 32), we examined the production of IFNγ and found that upon restimulation with anti-CD3+collagen, MTX-rescued cells produce comparable levels of IFNγ than control cells (**Figure 1D**). These results indicate that under MTX conditions, costimulation with anti-CD3+collagen preserves the inflammatory nature of human polarized Th17 cells. As a control, costimulation of the rescued cells with anti-CD3+anti-CD28 antibodies also led to the production of comparable levels of IL-17 and IFNγ than control cells (data not shown) further supporting that the rescued cells kept their inflammatory function.

The Pro-survival Role of Collagen Is Mediated via α2β1 Integrin

Effector T cells are characterized by the expression of several members of β1 integrins that play an important role in their interactions with ECM proteins (1–4). Besides collagen, fibronectin and laminin are also two major matrix proteins. We thus examined if fibronectin and laminin, which bind to α4β1/α5β1 and α3β1/α6β1 integrins respectively could have a similar protective effect as collagen. To this end, we first assessed the ability of human polarized Th17 cells to attach to the various matrices. The results show that human polarized Th17 cells are capable of adhering to all matrices. Cell adhesion to fibronectin is slightly higher than to the other two matrices upon anti-CD3 activation, which increases cell adhesion to all matrices (**Figure 2A**). However, fibronectin and laminin had no effect on MTX-induced apoptosis in anti-CD3-treated cells (**Figure 2B**). Similar findings were obtained when fibronectin and laminin were added in their soluble forms (data not shown). Because human polarized Th17 cells express and use α2β1 integrin to attach to collagen, we verified if it transduces the protective effect of collagen. We found that incubation of the cells with blocking anti-β1 and anti-α2 integrin antibodies abrogated the collagen protective effect on MTX-induced apoptosis whereas the control antibody had no effect (**Figure 2C**). These results suggest the selective implication of α2β1 integrin in the resistance of effector T cells to MTX.

Collagen Promotes MTX Resistance via the ABCC1 Drug Transporter

We then sought to determine the mechanisms by which T cell adhesion to collagen promotes MTX resistance in activated human polarized Th17 cells. The drug transporters of the ABC subfamily have been highly associated with chemoresistance. Accordingly, we examined whether they could be involved in our cell model. ABCC1 and ABCG2 also known as MRP-1 and BCRP1 respectively are two major MTX transporters and reported to be expressed in T cells (33, 34). Thus, we first assessed whether these two transporters were expressed in human polarized Th17 cells. The results show that polarized human Th17 cells express slightly higher levels of ABCC1 than ABCG2 especially upon anti-CD3+collagen costimulation (**Figure 3A**). Quantification analysis indicates a 1.5 × fold increase in ABCC1 levels upon anti-CD3+collagen costimulation, which had no significant effect on ABCG2 protein levels (**Figure 3B**). The ABCC1 levels are 1.57 × fold higher than ABCG2 levels in anti-CD3+collagen-costimulated cells.

Because of the low levels detected by FACS, we sought to analyse the expression levels of ABCC1 and ABCG2 by quantitative RT-PCR (qRT-PCR), which is the preferred method for studying expression of ABC transporters in immune cells. Indeed, although functional but detection of protein levels of ABC transporters in human T cells is weak (35–37). We found that ABCC1 mRNA levels are three times higher than those of ABCG2 and costimulation with anti-CD3+collagen increases ABCC1 mRNA levels by 1.6 × fold but had no effect on ABCG2 mRNA levels (**Figure 3C**). Together, these results indicate that human polarized Th17 cells express higher levels of ABCC1 than ABCG2, which is in agreement with recent findings in human Th1 and Th17 cells (37). The discrepancies between the FACS and qRT-PCR quantification data with regard to the relative levels of ABCC1 *vs*. ABCG2 could be due to the low levels detected by FACS, which could be due to the efficacy of antibodies, and to the differences in the staining methods for ABCC1 and ABCG2.

We then determined the functionality of ABCC1 by evaluating the content of intracellular calcein-AM by FACS analysis. Calcein-AM is a specific substrate for ABCC1 and has been

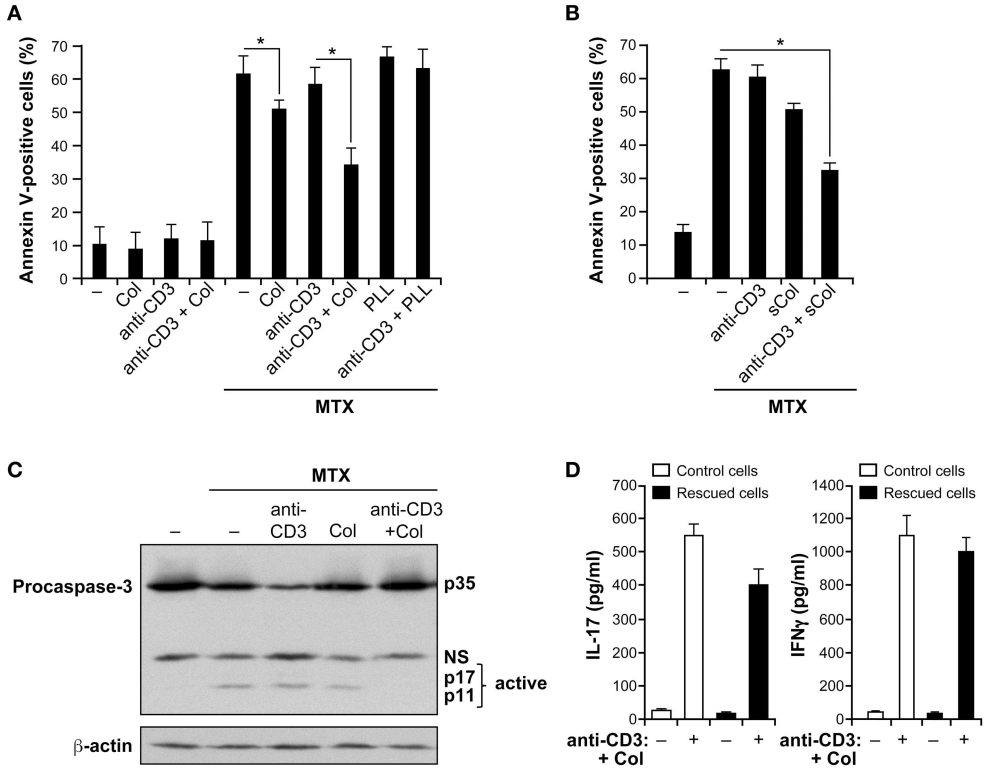

FIGURE 1 | Collagen promotes MTX resistance of activated human polarized Th17 cells. **(A)** Collagen protects human polarized Th17 cells from MTX-induced apoptosis. Cells were incubated or not (–) for 3 h with coated anti-CD3 mAb, collagen (Col) or as a control with poly-L-lysine (PLL) or in combination as described. Then, they were treated for 24 h with 10 μM of methotrexate (MTX) and apoptosis was evaluated using FITC-conjugated annexin V staining and FACS analysis. **(B)** Protective effect of soluble collagen. Cells were activated or not (–) for 3 h with 50 μg/ml of soluble Col (sCol), anti-CD3 mAb and with a combination of anti-CD3+sCol. They were then treated for 24 h with MTX and apoptosis was evaluated by annexin V staining and FACS analysis. **(C)** Collagen inhibits MTX-induced caspase-3 activation. Cells were activated for 3 h as indicated and then treated for 12 h with MTX. Cell lysates were prepared and analyzed for caspase-3 activation by Western blot (NS, non-specific band). Blots were stripped and reprobed with anti-β-actin Ab as a loading control. The results are representative of three independent experiments. **(D)** Anti-CD3+collagen stimulation preserves the inflammatory nature of polarized Th17 cells. Cells were activated with anti-CD3+Col and then treated with MTX. After 24 h, viable cells were isolated and stimulated or not (–) along with control cells with anti-CD3+Col. Supernatants were harvested 24 h later and the production of IL-17 and IFNγ was quantified by ELISA. The results in panels **(A,B,D)** are presented as mean ± SD calculated from three to five different experiments conducted in triplicates with human T cells isolated from different healthy blood donors. *$p < 0.05$.

used as a surrogate for MTX efflux and ABCC1 activity in multiple studies (38, 39). As shown, activation of the cells with anti-CD3+collagen reduces calcein-AM intracellular content by reducing the % of positive cells as well as the MFI, and this regulatory effect is partially reversed by the specific ABCC1 inhibitor, MK571 (**Figure 4A**). Quantification analysis taking into account the number of positive cells and MFI indicates a 40% reduction in total intracellular calcein-AM levels upon activation with anti-CD3+collagen and the MK571 inhibitor blocked the effect of anti-CD3+collagen by about 75% (**Figure 4B**). As a control, we also found that the effect of collagen on calcein-AM efflux is abolished with a blocking anti-α2β1 mAb (**Figure 4C**). These results indicate that collagen via α2β1 integrin enhances the expression and the function of ABCC1 in anti-CD3-activated polarized Th17 cells.

Using the specific ABCC1 inhibitor, MK571, we then studied the role of ABCC1 in MTX resistance of human polarized Th17 cells. Treatment with the MK571 inhibitor did not show any effect on MTX-induced apoptosis but inhibited the anti-CD3+collagen protective effect (**Figure 4D**). To confirm the effect of the MK571 inhibitor, we evaluated the effect of a second ABCC1 inhibitor named reversan (40). Similar to MK571, reversan abolished the protective effect of anti-CD3+collagen (**Figure 4E**). Interestingly, the specific ABCG2 inhibitor fumitremorgin C (41) had no effect. Taken together, these results show that collagen promotes MTX resistance of anti-CD3-activated human polarized Th17 cells by upregulating the function of ABCC1.

Collagen Promotes MTX Resistance of Arthritic T Cells

Next we analyzed whether the pro-survival role of collagen/α2β1 interaction occurs in RA with effector $CD4^+$T cells that have not been polarized *in vitro*. To this end, we examined whether it promotes MTX resistance of $CD4^+$ memory T cells isolated from RA patients. In agreement, we found that RA peripheral blood $CD4^+CD45RO^+$ T cells contain Th1, Th17, and Th17/Th1 subsets (**Figure 5A**); the main pathogenic Th

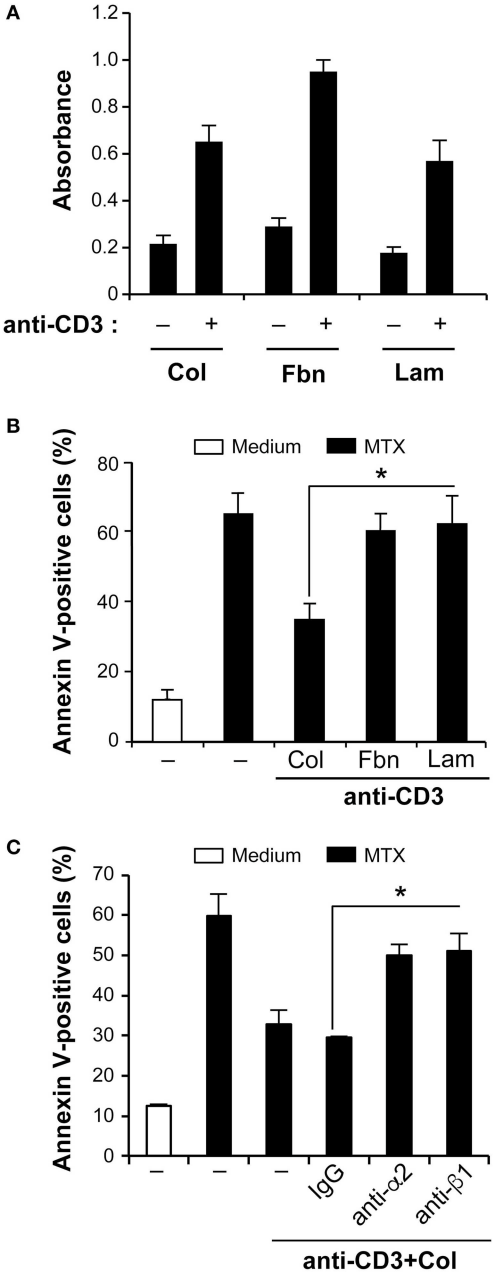

FIGURE 2 | Collagen-α2β1 integrin interaction protects human polarized Th17 cells from MTX-induced apoptosis. **(A)** Human polarized Th17 cells adhesion to matrix proteins. Control and anti-CD3-activated cells were cultured for 1 h in wells coated with Col, fibronectin (Fbn) or laminin (Lam). Cell Adhesion was quantified as described in the Materials and Methods section. **(B)** Differential effect of Col on MTX-induced apoptosis. Human polarized Th17 cells were cultured for 3 h with Col, Fbn or Lam in the presence of anti-CD3 mAb after which they were treated for 24 h with MTX. The cells were stained with annexin V and apoptosis was determined by FACS analysis. **(C)** Cells were first incubated for 1 h with 10 μg/ml of anti-alpha2 integrin (clone P1E6) and anti-beta1 integrin (clone 4B4) blocking mAbs or with isotypic control IgG. They were then activated with anti-CD3+Col and treated with MTX for 24 h. The cells were stained with annexin V and apoptosis was determined by FACS analysis. Results are presented as mean ± SD calculated from three independent experiments conducted in triplicates with T cells obtained from three different healthy donors. $^*p < 0.05$.

cells involved in RA pathogenesis (42). Because these cells are in a quiescent state, we reactivated them with anti-CD3 and anti-CD28 mAbs and expanded them with IL-2 for 1 week to sensitize them to MTX-induced apoptosis. Their activation also increased the levels of α2 integrin (**Figure 5B**) consistent with the upregulation of α2 integrin upon T cell activation and effector differentiation (1–4, 43). Furthermore, we found that these cells also express the drug transporter ABCC1 and their activation with anti-CD3+collagen also increases ABCC1 levels (**Figure 5C**).

We then examined the response of arthritic effector T cells to MTX. Activation of expanded-RA peripheral blood $CD4^+CD45RO^+$ T cells with anti-CD3+collagen reduced MTX-induced apoptosis by 38%. This effect was mediated by α2β1 integrin since it was reversed by incubating the cells with the blocking anti-α2β1 mAb (**Figure 5D**). In addition, the ABCC1 inhibitor MK571 also abrogated the pro-survival effect of collagen in anti-CD3-activated arthritic T cells (**Figure 5D**). Together these results show that arthritic effector T cells are also protected from MTX-induced apoptosis upon their attachment to collagen via α2β1/ABCC1 pathway.

DISCUSSION

The mechanisms underlying MTX failure in RA are still unclear and their elucidation could lead to more efficient therapies. Th17 and Th1 cells are critical effector cells in joint tissue damage and their resistance to MTX could contribute to MTX therapy failure in RA. Since MTX is associated with apoptosis of effector T cells, we have considered whether β1 integrins, which play an important role in cell survival, would provide a survival advantage to effector T cells under MTX therapeutic setting.

We found that collagen, which is abundant in the synovium, *via* its receptor, the integrin α2β1, protects human polarized Th17 cells from MTX-induced apoptosis. The strongest effect of collagen is seen only in anti-CD3-activated cells. This is likely due to the increased attachment of the cells to collagen upon stimulation via the T cell receptor (TCR), which occurs through α2β1 (**Figure 2A**) (6). Although TCR/CD3 activation alone did not protect human polarized Th17 from MTX-induced apoptosis, it is not excluded that additional pathways activated by the TCR/CD3 engagement could cooperate with α2β1 integrin in mediating T cell survival. Anti-CD3-activated human polarized Th17 cells also attach to fibronectin and laminin but these matrices did not influence MTX-induced apoptosis suggesting a differential implication of β1 integrins in the modulation of MTX-induced apoptosis, which could be due to their differential signaling capacities since both α and β integrin chains are known to induce cell signaling. The role of α2β1 integrin in T cell survival is reminiscent to previous work that showed that this collagen-binding integrin inhibits Fas-induced apoptosis in human effector T cells whereas fibronectin- and laminin-binding integrins did not (8). Taken together, these studies indicate that in addition to Fas-induced apoptosis, α2β1 integrin has also the ability to protect effector T cells during therapeutic setting.

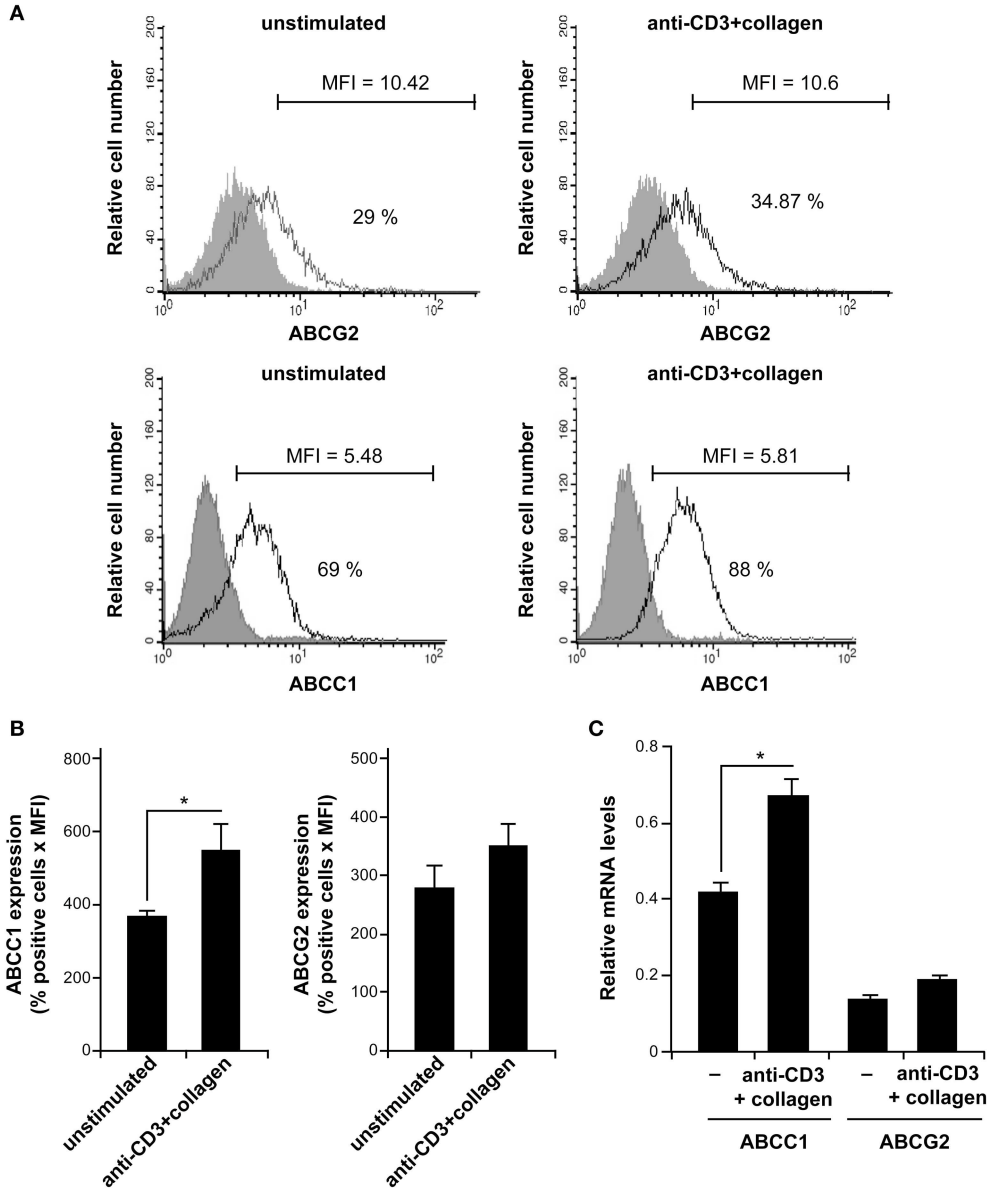

FIGURE 3 | Human polarized Th17 cells express ABCC1. **(A)** ABCC1 and ABCG2 expression. After 12 h of culture with or without stimulation with anti-CD3+Col, the cells were stained with specific anti-ABCC1 and anti-ABCG2 antibodies and analyzed by FACS analysis. The gray areas represent control stainings with appropriate conjugated-isotypic antibodies. Results are representative of five independent experiments conducted with T cells obtained from five different donors. The % of positive cells and MFI are indicated in each histogram. **(B)** Quantification of ABCC1 and ABCG2 expression levels. Results are expressed as % positive cells x MFI and the values represent mean ± SD calculated from five independent experiments conducted with T cells obtained from five different donors. **(C)** The ABCC1 and ABCG2 mRNA levels expressed in human polarized Th17 cells at the basal level and after anti-CD3+collagen stimulation were determined by qRT-PCR. The results represent mean values ± SD calculated from three independent experiments conducted in triplicates with T cells obtained from three different donors. $^*p < 0.05$.

MTX has been shown to act by blocking cell proliferation and cytokine production (16). Our results indicate that anti-CD3+collagen-rescued cells have kept their ability to produce IL-17 and IFNγ upon restimulation. This suggests that in addition of promoting survival, the anti-CD3+collagen signaling pathway also kept the inflammatory nature of human polarized Th17 cells, thus supporting the role of α2β1 integrin in MTX resistance.

We have also shown that the pro-survival role of α2β1 integrin under MTX setting occurs in the context of RA. Despite the fact that we did not have access to synovial fluids and were limited in RA samples and T cell numbers, we showed that memory $CD4^+$ T cells isolated from peripheral blood of RA patients are also rescued from MTX-induced apoptosis suggesting that this mechanism could be clinically relevant. Although, we could not examine the role of α2β1 integrin specifically in RA Th17 *vs.*

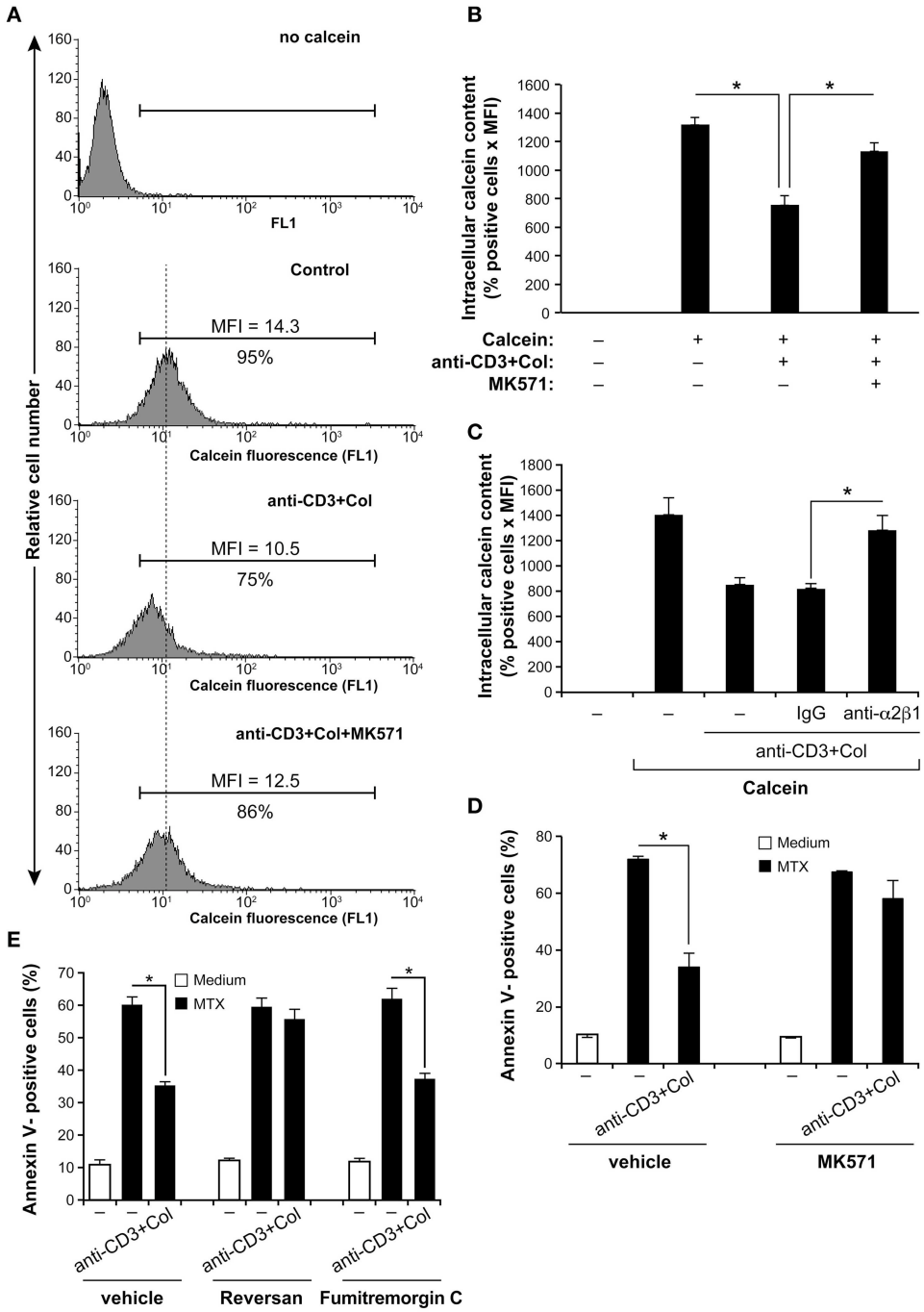

FIGURE 4 | Collagen promotes MTX resistance of activated human polarized Th17 cells *via* the drug transporter ABCC1. **(A)** Anti-CD3+Col costimulation reduces ABCC1 activity. After 3 h activation with anti-CD3+Col, the cells were incubated for 1 h with 1 nM of calcein-AM. As indicated, cells were pre-treated with 10 μM of MK571 (ABCC1 inhibitor) before being stimulated with anti-CD3+Col. Intracellular calcein-AM content was then determined by FACS using the FL-1 channel. Representative FACS profiles of intracellular calcein-AM content are shown. The % of positive cells and MFI are indicated. **(B)** Quantification of intracellular calcein-AM content. **(C)** The blocking anti-α2β1 integrin (BHA2.1) abolishes the effect of anti-CD3+Col on calcein-AM efflux. Cells were first incubated or not for 1 h with 10 μg/ml of BHA2.1 mAb or with isotypic control IgG, activated or not with anti-CD3+Col and then loaded with calcein-AM. Intracellular calcein-AM content was then determined by FACS analysis and quantified as above. **(D)** The MK571 inhibitor abolished the protective effect of anti-CD3+Col on MTX-induced apoptosis. Cells were treated as indicated and after 24 h of MTX treatment, the cells were stained with annexin V and analyzed by FACS. **(E)** The ABCC1 inhibitor reversan (10 μM) but not the ABCG2 inhibitor fumitremorgin C (10 μM) abrogates the protective effect of anti-CD3+collagen on MTX-induced apoptosis. Results (**(B–E)** panels) are presented as mean ± SD calculated from three independent experiments performed in triplicates with T cells obtained from three different donors. *$p < 0.05$.

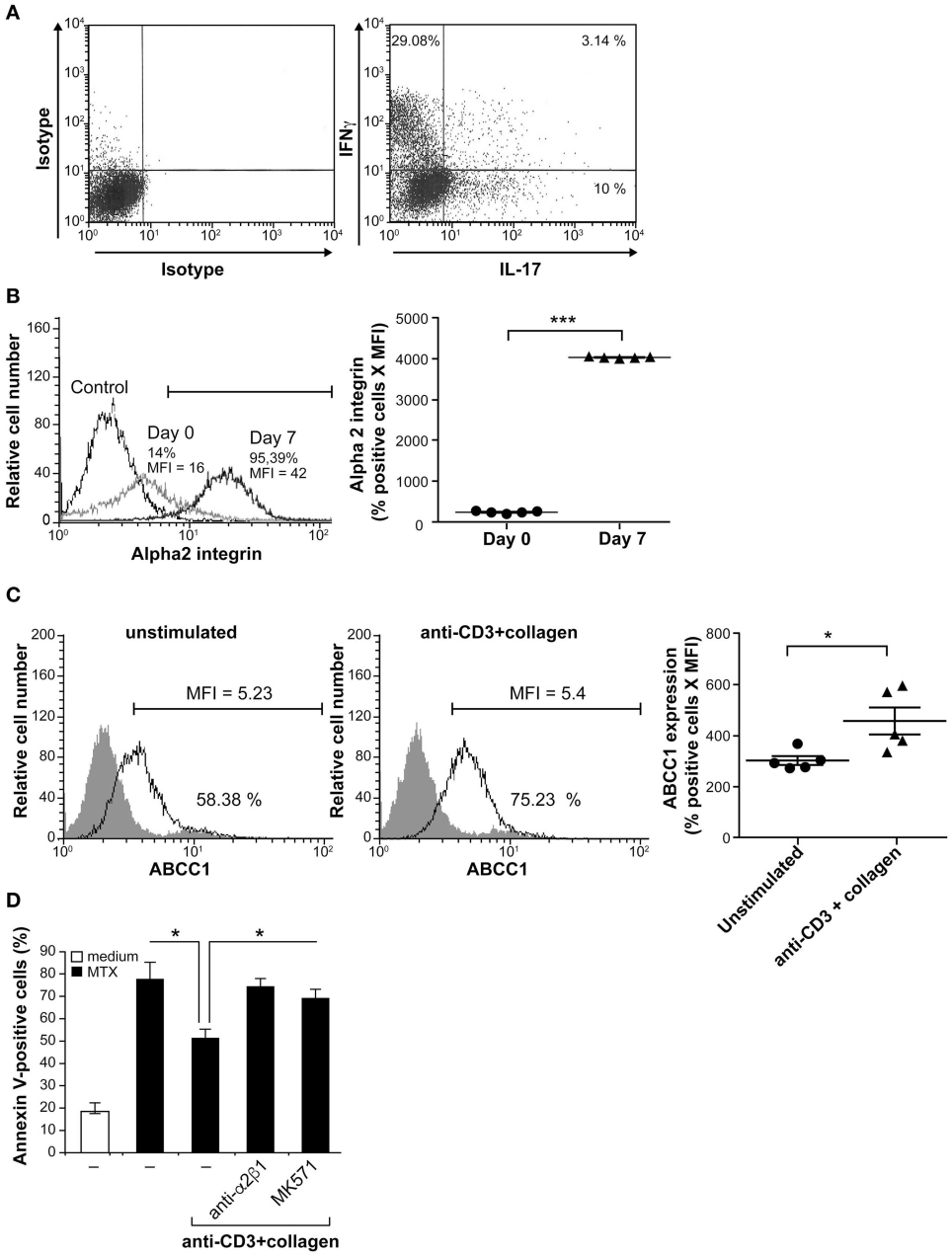

FIGURE 5 | Collagen protects arthritic effector/memory $CD4^+$ T cells from MTX-induced apoptosis. **(A)** FACS analysis of Th1 and Th17 in arthritic T cells. $CD4^+CD45RO^+$ T cells collected from peripheral blood of RA patients contain IL-17- and IFNγ-producing cells. After activation with PMA and ionomycin for 4 h in the presence of BD Golgi plug, the cells were stained with intracellular anti-IL-17 and anti-IFNγ antibodies and analyzed by FACS. The results are representative of five different RA patients. **(B)** α2 integrin expression was evaluated by FACS analysis on day 0 and day 7 (one week after *in vitro* expansion). **(C)** ABCC1 expression was evaluated by FACS analysis on day 7. The gray areas represent staining with appropriate conjugated-isotypic control antibodies. The scatter-bar plots (right panels in **(B)** and **(C)**) represent quantification of α2 integrin and ABCC1 expression levels respectively. Results are presented as mean ± SEM calculated from five independent experiments conducted with five different RA patients. $^{***}p < 0.001$; $^{*}p < 0.05$. **(D)** The blocking anti-α2β1 integrin mAb and the ABCC1 inhibitor MK571 inhibit the protective effect of anti-CD3+Col costimulation. *In vitro* expanded $CD4^+CD45RO^+$ T cells were stimulated during 3 h with anti-$CD3^+$Col, followed by a 24 h treatment with MTX. As indicated, the cells were we first pre-treated for 1 h prior their activation, with the blocking anti-α2β1 mAb (BHA2.1) and with the MK571 inhibitor. Apoptosis was measured following annexin V staining and FACS analysis. Results are presented as mean ± SD calculated from three different experiments conducted in triplicates with $CD4^+CD45RO^+$ T cells isolated from three RA patients. $^{*}p < 0.05$.

Th1 cells, it is likely that a similar mechanism occurs in both populations since α2β1 integrin is a costimulatory molecule for both Th1 and Th17 (5–7), and as shown in **Figure 1D**, both Th1 and Th17 can be protected by anti-CD3+collagen costimulation since MTX-rescued cells are able to produce IL-17 and IFNγ to the same extent as control cells upon restimulation. α2β1

integrin promotes arthritis pathogenesis by acting on synovial Th17 cells (11, 12) and on synovial fibroblasts (44). Whether it promotes MTX resistance of other cell types involved in arthritis pathogenesis remains to be determined.

Cell adhesion-mediated drug resistance is a well-studied process in oncology. Indeed, several studies both in solid tumors and in hematological malignancies have shown that attachment to ECM *via* integrins promotes the resistance of cancer cells to multiple drugs used in chemotherapy (45, 46). In this context, α2β1 integrin, which is an important integrin in cancer, has also been associated with drug resistance (47). This is particularly the case in human acute T lymphoblastic leukemia (T-ALL). Attachment of human T-ALL cell lines and blasts to collagen protected them from the cytotoxic action of doxorubicin (25, 48). The study reported herein indicates that the role of α2β1 integrin in chemoresistance is conserved in normal T cells and autoimmune diseases and suggests that as in cancer, cell adhesion-mediated drug resistance could contribute to therapy failures that are observed in the treatment of autoimmune diseases.

Mechanistically, our results support the implication of the drug transporter ABCC1 in MTX resistance. ABCG2 and ABCC1 are two major MTX transporters that have been associated with T cells (33, 34). We found that human effector T cells express higher levels of ABCC1 than ABCG2 and activation with anti-CD3+collagen enhanced the efflux activity of ABCC1. Furthermore, the specific ABCC1 inhibitors, MK571 and reversan, inhibited the protective effect of anti-CD3+collagen both in human polarized Th17 cells as well as in RA effector/memory T cells, whereas the ABCG2 inhibitor (fumitremorgin C) had no effect. A recent study found that CD147 promotes MTX resistance of immune cells through ABCG2 in psoriasis (49). However, this was analyzed in PBMCs and not specifically in T cells. ABCG2 has also been associated with MTX resistance of macrophages in RA synovial tissue but it was not detected in synovial T cells, which were rather shown to express ABCC1 (50). Recently, it was found that a subset of human inflammatory Th17 cells (Th17.1) express the drug transporter ABCB1 (also named PgP) and were refractory to glucocorticoids, although this occurred independently from ABCB1 (37). The authors of this study also found that ABCC1 is expressed at higher levels than ABCB1 and ABCG2 in the different human effector T cells including Th1, Th2, Th17, and the inflammatory Th17.1 subset. Together these studies suggest that ABCC1 could be the most important MTX transporter in T cells, whereas ABCG2 could be associated with monocytes/macrophages.

ABCC1, ABCG2 as well as ABCB1 are all expressed in RA (33, 51–53) but a clear implication of a particular transporter in predicting MTX response is unclear. However, the majority of these studies focused on RA PBMCs, which could be phenotypically and functionally different from the synovial immune cells that are directly associated with tissue damage. Indeed, microenvironmental cues are likely to influence the expression and function of MTX transporters expressed by the various immune cells infiltrating the synovium. In this context, our study reveals that integrins and attachment to collagen, which is abundant in the synovium, could be important factors in regulating activity of MTX transporters. The mechanisms of MTX resistance in RA are complex and could involve additional factors. Along these lines, a recent study showed that MTX resistance in RA could be correlated with weak levels of CD39 expressed by regulatory T cells (54).

Our results showed that activation with anti-CD3+collagen increased only slightly the ABCC1 levels suggesting that the effect of anti-CD3+collagen occurs mainly at the level of ABCC1 activity. This is in agreement with studies reporting that chemotaxis and migration of Langerhans cells and T cells to the lymph nodes is associated with the activation of ABCC1, which mediates efflux of sphingolipid and cysteinyl leukotriene (55, 56). Similarly, antigen-induced export of sphingosine-1 phosphate from mast cells is dependent on ABCC1 activation (57). It has previously been shown that ABCC1 localization in membrane lipid rafts and actin polymerization are both necessary for its activity (58). In addition, collagen/α2β1 integrin signaling enhances ABCC1 activity and doxorubicin resistance in acute T lymphoblastic leukemia *via* actin polymerization (25). Although the role of lipid rafts in ABCC1 activation is not firmly established (59), α2β1 integrin has previously been shown to localize into lipid rafts (60, 61). Thus, it is possible that anti-CD3-induced attachment of human effector T cells to collagen leads to cytoskeletal reorganization and thereby to increased ABCC1 localization, stability and function. Nonetheless, additional mechanisms such as receptor recycling and increased ATP production could also be involved.

Although reduction of purine-pyrimidine levels has been associated with MTX-induced apoptosis in T cells (16, 17, 29) folate co-therapy did not interfere with MTX clinical benefit (62) suggesting that apoptosis may not be critical for MTX action. However, this cannot be excluded since recent studies found that MTX-induced apoptosis in T cells is dependent on a reduction in tetrahydrobiopterin but not purine-pyrimidine levels (63, 64). Clearly additional studies are required to understand how MTX works in RA but regardless of its mode of action, the MTX resistance mechanism unraveled in our study is likely to affect its therapeutic benefit.

In summary, we have reported to our knowledge, a novel function for α2β1 integrin in human effector T cells consisting of mediating MTX resistance. This observation also occurs in effector RA T cells, but because of limited access to RA samples, we could not answer some key questions such as weather α2β1 expression and function correlates with MTX non-responders in RA. Our results do suggest that this could be case. Because α2β1 integrin is expressed on synovial Th17 cells of RA patients (11), it will be interesting to examine whether at the clinical level, it could represent a novel biomarker predicting MTX response in RA.

AUTHOR CONTRIBUTIONS

AA and MAE contributed to the design and execution of the experiments, data analysis and results interpretation and writing the manuscript. DN performed experiments and analyzed the

data. PF designed experiments, analyzed and interpreted the data. FA conceived and designed the study, supervised the work, analyzed the data and wrote the manuscript. All authors read and approved the final manuscript.

FUNDING

This study was supported by a grant (RGPIN-2017-06116) from the Natural Sciences and Engineering Research Council of Canada and by a grant (MOP-136819) from the Canadian Institutes of Health Research of Canada to FA.

SUPPLEMENTARY MATERIAL

The Supplementary Material for this article can be found online at: https://www.frontiersin.org/articles/10.3389/fimmu.2018.02269/full#supplementary-material

REFERENCES

1. Pribila JT, Quale AC, Mueller KL, Shimizu Y. Integrins and T cell-mediated immunity. *Annu Rev Immunol.* (2004) 22:157–80. doi: 10.1146/annurev.immunol.22.012703.104649
2. Krivacic KA, Levine AD. Extracellular matrix conditions T cells for adhesion to tissue interstitium. *J Immunol.* (2003) 170:5034–44. doi: 10.4049/jimmunol.170.10.5034
3. Kassiotis G, Gray D, Kiafard Z, Zwirner J, Stockinger B. Functional specialization of memory Th cells revealed by expression of integrin CD49b. *J Immunol.* (2006) 177:968–75. doi: 10.4049/jimmunol.177.2.968
4. Rao WH, Hales JM, Camp RD. Potent costimulation of effector T lymphocytes by human collagen type I. *J Immunol.* (2000) 165:4935–40. doi: 10.4049/jimmunol.165.9.4935
5. Sasaki K, Tsuji T, Jinushi T, Matsuzaki J, Sato T, Chamoto K, et al. Differential regulation of VLA-2 expression on Th1 and Th2 cells: a novel marker for the classification of Th subsets. *Int Immunol.* (2003) 15:701–10. doi: 10.1093/intimm/dxg066
6. Boisvert M, Chetoui N, Gendron S, Aoudjit F. Alpha2beta1 integrin is the major collagen-binding integrin expressed on human Th17 cells. *Eur J Immunol.* (2010) 40:2710–9. doi: 10.1002/eji.201040307
7. Boisvert M, Gendron S, Chetoui N, Aoudjit F. Alpha2beta1 integrin signaling augments T cell receptor-dependent production of interferon-gamma in human T cells. *Mol Immunol.* (2007) 44:3732–40. doi: 10.1016/j.molimm.2007.04.003
8. Gendron S, Couture J, Aoudjit F. Integrin alpha2beta1 inhibits Fas-mediated apoptosis in T lymphocytes by protein phosphatase 2A-dependent activation of the MAPK/ERK pathway. *J Biol Chem.* (2003) 278:48633–43. doi: 10.1074/jbc.M305169200
9. Lundberg S, Lindholm J, Lindbom L, Hellstrom PM, Werr J. Integrin alpha2beta1 regulates neutrophil recruitment and inflammatory activity in experimental colitis in mice. *Inflamm Bowel Dis.* (2006) 12:172–7. doi: 10.1097/01.MIB.0000217765.96604.83
10. Tsunoda I, Terry EJ, Marble BJ, Lazarides E, Woods C, Fujinami RS. Modulation of experimental autoimmune encephalomyelitis by VLA-2 blockade. *Brain Pathol.* (2007) 17:45–55. doi: 10.1111/j.1750-3639.2006.00042.x
11. El Azreq MA, Boisvert M, Cesaro A, Page N, Loubaki L, Allaeys I, et al. Alpha2beta1 integrin regulates Th17 cell activity and its neutralization decreases the severity of collagen-induced arthritis. *J Immunol. (*2013) 191:5941–50. doi: 10.4049/jimmunol.1301940
12. El Azreq MA, Arseneault C, Boisvert M, Page N, Allaeys I, Poubelle PE, et al. Cooperation between IL-7 Receptor and Integrin alpha2beta1 (CD49b) Drives Th17-Mediated Bone Loss. *J Immunol.* (2015) 195:4198–209. doi: 10.4049/jimmunol.1500437
13. van der Heijden JW, Dijkmans BA, Scheper RJ, Jansen G. Drug insight: resistance to methotrexate and other disease-modifying antirheumatic drugs from bench to bedside. *Nat Clin Pract Rheumatol.* (2007). 3:26–34. doi: 10.1038/ncprheum0380
14. Yu MB, Firek A, Langridge WHR. Predicting methotrexate resistance in rheumatoid arthritis patients. *Inflammopharmacology* (2018) 26:699–708. doi: 10.1007/s10787-018-0459-z
15. Robey RW, Pluchino KM, Hall MD, Fojo AT, Bates SE, Gottesman MM. Revisiting the role of ABC transporters in multidrug-resistant cancer. *Nat Rev Cancer* (2018) 18:452–64. doi: 10.1038/s41568-018-0005-8
16. Brown PM, Pratt AG, Isaacs JD. Mechanism of action of methotrexate in rheumatoid arthritis, and the search for biomarkers. *Nat Rev Rheumatol.* (2016) 12:731–42. doi: 10.1038/nrrheum.2016.175
17. Quemeneur L, Gerland LM, Flacher M, Ffrench M, Revillard JP, Genestier L. Differential control of cell cycle, proliferation, and survival of primary T lymphocytes by purine and pyrimidine nucleotides. *J Immunol.* (2003) 170:4986–95. doi: 10.4049/jimmunol.170.10.4986
18. Guggino G, Giardina A, Ferrante A, Giardina G, Schinocca C, Sireci G, et al. The *in vitro* addition of methotrexate and/or methylprednisolone determines peripheral reduction in Th17 and expansion of conventional Treg and of IL-10 producing Th17 lymphocytes in patients with early rheumatoid arthritis. *Rheumatol Int.* (2015) 35:171–5. doi: 10.1007/s00296-014-3030-2
19. Sandhu A, Ahmad S, Kaur P, Bhatnagar A, Dhawan V, Dhir V. Methotrexate preferentially affects Tc1 and Tc17 subset of CD8 T lymphocytes. *Clin Rheumatol.* (2018). doi: 10.1007/s10067-018-4011-8. [Epub ahead of print].
20. Aletaha D, Neogi T, Silman AJ, Funovits J, Felson DT, Bingham CO, et al. 2010 Rheumatoid arthritis classification criteria: an American college of rheumatology/European league against rheumatism collaborative initiative. *Arthritis Rheum.* (2010) 62:2569–81. doi: 10.1002/art.27584
21. DA Silva VA, DA Silva KA, Delou JM, LM DAF, Lopes AG, Capella MA. Modulation of ABCC1 and ABCG2 proteins by ouabain in human breast cancer cells. *Anticancer Res.* (2014) 34:1441–8.
22. Manceau S, Giraud C, Decleves X, Batteux F, Chereau C, Chouzenoux S, et al. Expression and induction by dexamethasone of ABC transporters and nuclear receptors in a human T-lymphocyte cell line. *J Chemother.* (2012) 24:48–55. doi: 10.1179/1120009X12Z.00000000010
23. Naci D, Aoudjit F. Alpha2beta1 integrin promotes T cell survival and migration through the concomitant activation of ERK/Mcl-1 and p38 MAPK pathways. *Cell Signal.* (2014) 26:2008–15. doi: 10.1016/j.cellsig.2014.05.016
24. Shooshtari P, Fortuno ES III, Blimkie D, Yu M, Gupta A, Kollmann TR, et al. Correlation analysis of intracellular and secreted cytokines via the generalized integrated mean fluorescence intensity. *Cytometry A* (2010) 77:873–80. doi: 10.1002/cyto.a.20943
25. El Azreq MA, Naci D, Aoudjit F. Collagen/beta1 integrin signaling up-regulates the ABCC1/MRP-1 transporter in an ERK/MAPK-dependent manner. *Mol Biol Cell* (2012) 23:3473–84. doi: 10.1091/mbc.E12-02-0132
26. El Azreq MA, Garceau V, Bourgoin SG. Cytohesin-1 regulates fMLF-mediated activation and functions of the beta2 integrin Mac-1 in human neutrophils. *J Leukoc Biol.* (2011) 89:823–36. doi: 10.1189/jlb.0410222
27. Darrah PA, Patel DT, De Luca PM, Lindsay RW, Davey DF, Flynn BJ, et al. Multifunctional TH1 cells define a correlate of vaccine-mediated protection against Leishmania major. *Nat Med.* (2007) 13:843–50. doi: 10.1038/nm1592
28. Han L, Wierenga AT, Rozenveld-Geugien M, van de Lande K, Vellenga E, Schuringa JJ. Single-cell STAT5 signal transduction profiling in normal and leukemic stem and progenitor cell populations reveals highly distinct cytokine responses. *PLoS ONE* (2009) 4:e7989. doi: 10.1371/journal.pone.0007989
29. Genestier L, Paillot R, Fournel S, Ferraro C, Miossec P, Revillard JP. Immunosuppressive properties of methotrexate: apoptosis and clonal deletion of activated peripheral T cells. *J Clin Invest.* (1998) 102:322–8. doi: 10.1172/JCI2676

30. Nielsen CH, Albertsen L, Bendtzen K, Baslund B. Methotrexate induces poly(ADP-ribose) polymerase-dependent, caspase 3-independent apoptosis in subsets of proliferating CD4+ T cells. *Clin Exp Immunol.* (2007) 148:288–95. doi: 10.1111/j.1365-2249.2007.03335.x
31. Volpe E, Servant N, Zollinger R, Bogiatzi SI, Hupe P, Barillot E, et al. A critical function for transforming growth factor-beta, interleukin 23 and proinflammatory cytokines in driving and modulating human T(H)-17 responses. *Nat Immunol.* (2008) 9:650–7. doi: 10.1038/ni.1613
32. Manel N, Unutmaz D, Littman DR. The differentiation of human T(H)-17 cells requires transforming growth factor-beta and induction of the nuclear receptor RORgammat. *Nat Immunol.* (2008) 9:641–9. doi: 10.1038/ni.1610
33. Marki-Zay J, Tauberne Jakab K, Szeremy P, Krajcsi P. MDR-ABC transporters: biomarkers in rheumatoid arthritis. *Clin Exp Rheumatol.* (2013) 31:779–87.
34. Assaraf YG. The role of multidrug resistance efflux transporters in antifolate resistance and folate homeostasis. *Drug Resist Updat.* (2006) 9:227–46. doi: 10.1016/j.drup.2006.09.001
35. Echevarria-Lima J, Rumjanek VM, Kyle-Cezar F, Harab RC, Leite AC, dos Santos Ornellas D, et al. HTLV-I alters the multidrug resistance associated protein 1 (ABCC1/MRP1) expression and activity in human T cells. *J Neuroimmunol.* (2007) 185:175–81. doi: 10.1016/j.jneuroim.2007.01.008
36. Dimeloe S, Frick C, Fischer M, Gubser PM, Razik L, Bantug GR, et al. Human regulatory T cells lack the cyclophosphamide-extruding transporter ABCB1 and are more susceptible to cyclophosphamide-induced apoptosis. *Eur J Immunol.* (2014) 44:3614–20. doi: 10.1002/eji.201444879
37. Ramesh R, Kozhaya L, McKevitt K, Djuretic IM, Carlson TJ, Quintero MA, et al. Pro-inflammatory human Th17 cells selectively express P-glycoprotein and are refractory to glucocorticoids. *J Exp Med.* (2014) 211:89–104. doi: 10.1084/jem.20130301
38. Schmitt SM, Stefan K, Wiese M. Pyrrolopyrimidine derivatives and purine analogs as novel activators of Multidrug Resistance-associated Protein 1 (MRP1, ABCC1). *Biochim Biophys Acta* (2017) 1859:69–79. doi: 10.1016/j.bbamem.2016.10.017
39. Lebedeva IV, Pande P, Patton WF. Sensitive and specific fluorescent probes for functional analysis of the three major types of mammalian ABC transporters. *PLoS ONE* (2011) 6:e22429. doi: 10.1371/journal.pone.0022429
40. Burkhart CA, Watt F, Murray J, Pajic M, Prokvolit A, Xue C, et al. Small-molecule multidrug resistance-associated protein 1 inhibitor reversan increases the therapeutic index of chemotherapy in mouse models of neuroblastoma. *Cancer Res.* (2009) 69:6573–80. doi: 10.1158/0008-5472.CAN-09-1075
41. Galetti M, Petronini PG, Fumarola C, Cretella D, La Monica S, Bonelli M, et al. Effect of ABCG2/BCRP expression on efflux and uptake of gefitinib in NSCLC cell lines. *PLoS ONE* (2015) 10:e0141795. doi: 10.1371/journal.pone.0141795
42. Lubberts E. The IL-23-IL-17 axis in inflammatory arthritis. *Nat Rev Rheumatol.* (2015) 11:415–29. doi: 10.1038/nrrheum.2015.53
43. El Azreq MA, Aoudjit F. Collagen-binding integrins in the pathogenesis of rheumatoid arthritis. *Austin J Clin Immunol.* (2014). 1:1006.
44. Peters MA, Wendholt D, Strietholt S, Frank S, Pundt N, Korb-Pap A, et al. The loss of alpha2beta1 integrin suppresses joint inflammation and cartilage destruction in mouse models of rheumatoid arthritis. *Arthritis Rheum.* (2012) 64:1359–68. doi: 10.1002/art.33487
45. Aoudjit F, Vuori K. Integrin signaling in cancer cell survival and chemoresistance. *Chemother Res Pract.* (2012) 2012:283181. doi: 10.1155/2012/283181
46. Zutter MM. Integrin-mediated adhesion: tipping the balance between chemosensitivity and chemoresistance. *Adv Exp Med Biol.* (2007) 608:87–100. doi: 10.1007/978-0-387-74039-3_6
47. Naci D, Vuori K, Aoudjit F. Alpha2beta1 integrin in cancer development and chemoresistance. *Semin Cancer Biol.* (2015) 35:145–53. doi: 10.1016/j.semcancer.2015.08.004
48. Naci D, El Azreq MA, Chetoui N, Lauden L, Sigaux F, Charron D, et al. Alpha2beta1 integrin promotes chemoresistance against doxorubicin in cancer cells through extracellular signal-regulated kinase (ERK). *J Biol Chem.* (2012) 287:17065–76. doi: 10.1074/jbc.M112.349365
49. Zhao S, Chen C, Liu S, Zeng W, Su J, Wu L, et al. CD147 promotes MTX resistance by immune cells through up-regulating ABCG2 expression and function. *J Dermatol Sci.* (2013) 70:182–9. doi: 10.1016/j.jdermsci.2013.02.005
50. van der Heijden JW, Oerlemans R, Tak PP, Assaraf YG, Kraan MC, Scheffer GL, et al. Involvement of breast cancer resistance protein expression on rheumatoid arthritis synovial tissue macrophages in resistance to methotrexate and leflunomide. *Arthritis Rheum.* (2009) 60:669–77. doi: 10.1002/art.24354
51. Micsik T, Lorincz A, Gal J, Schwab R, Petak I. MDR-1 and MRP-1 activity in peripheral blood leukocytes of rheumatoid arthritis patients. *Diagn Pathol.* (2015) 10:216. doi: 10.1186/s13000-015-0447-1
52. Prasad S, Tripathi D, Rai MK, Aggarwal S, Mittal B, Agarwal V. Multidrug resistance protein-1 expression, function and polymorphisms in patients with rheumatoid arthritis not responding to methotrexate. *Int J Rheum Dis.* (2014) 17:878–86. doi: 10.1111/1756-185X.12362
53. Garcia-Carrasco M, Mendoza-Pinto C, Macias Diaz S, Vera-Recabarren M, Vazquez de Lara L, Mendez Martinez S, et al. P-glycoprotein in autoimmune rheumatic diseases. *Autoimmun Rev.* (2015) 14:594–600. doi: 10.1016/j.autrev.2015.02.006
54. Peres RS, Liew FY, Talbot J, Carregaro V, Oliveira RD, Almeida SL, et al. Low expression of CD39 on regulatory T cells as a biomarker for resistance to methotrexate therapy in rheumatoid arthritis. *Proc Natl Acad Sci USA.* (2015) 112:2509–14. doi: 10.1073/pnas.1424792112
55. Honig SM, Fu S, Mao X, Yopp A, Gunn MD, Randolph GJ, et al. FTY720 stimulates multidrug transporter- and cysteinyl leukotriene-dependent T cell chemotaxis to lymph nodes. *J Clin Invest.* (2003) 111:627–37. doi: 10.1172/JCI16200
56. Robbiani DF, Finch RA, Jager D, Muller WA, Sartorelli AC, Randolph GJ. The leukotriene C(4) transporter MRP1 regulates CCL19 (MIP-3beta, ELC)-dependent mobilization of dendritic cells to lymph nodes. *Cell* (2000) 103:757–68. doi: 10.1016/S0092-8674(00)00179-3
57. Mitra P, Oskeritzian CA, Payne SG, Beaven MA, Milstien S, Spiegel S. Role of ABCC1 in export of sphingosine-1-phosphate from mast cells. *Proc Natl Acad Sci USA.* (2006) 103:16394–9. doi: 10.1073/pnas.0603734103
58. Hummel I, Klappe K, Ercan C, Kok JW. Multidrug resistance-related protein 1 (MRP1) function and localization depend on cortical actin. *Mol Pharmacol.* (2011) 79:229–40. doi: 10.1124/mol.110.069013
59. Meszaros P, Klappe K, Hummel I, Hoekstra D, Kok JW. Function of MRP1/ABCC1 is not dependent on cholesterol or cholesterol-stabilized lipid rafts. *Biochem J.* (2011) 437:483–91. doi: 10.1042/BJ20110427
60. Holleran BJ, Barbar E, Payet MD, Dupuis G. Differential recruitment of alpha2beta1 and alpha4beta1 integrins to lipid rafts in Jurkat T lymphocytes exposed to collagen type IV and fibronectin. *J Leukoc Biol.* (2003) 73:243–52. doi: 10.1189/jlb.0902439
61. Karjalainen M, Kakkonen E, Upla P, Paloranta H, Kankaanpaa P, Liberali P, et al. A Raft-derived, Pak1-regulated entry participates in alpha2beta1 integrin-dependent sorting to caveosomes. *Mol Biol Cell.* (2008) 19:2857–69. doi: 10.1091/mbc.E07-10-1094
62. Whittle SL, Hughes RA. Folate supplementation and methotrexate treatment in rheumatoid arthritis: a review. *Rheumatology* (2004) 43:267–71. doi: 10.1093/rheumatology/keh088
63. Spurlock CF III, Aune ZT, Tossberg JT, Collins PL, Aune JP, Huston JW III, et al. Increased sensitivity to apoptosis induced by methotrexate is mediated by JNK. *Arthritis Rheum.* (2011) 63:2606–16. doi: 10.1002/art.30457
64. Spurlock CF III, Tossberg JT, Fuchs HA, Olsen NJ, Aune TM. Methotrexate increases expression of cell cycle checkpoint genes via JNK activation. *Arthritis Rheum.* (2012) 64:1780–9. doi: 10.1002/art.34342

Conflict of Interest Statement: The authors declare that the research was conducted in the absence of any commercial or financial relationships that could be construed as a potential conflict of interest.

Copyright © 2018 Abderrazak, El Azreq, Naci, Fortin and Aoudjit. This is an open-access article distributed under the terms of the Creative Commons Attribution License (CC BY). The use, distribution or reproduction in other forums is permitted, provided the original author(s) and the copyright owner(s) are credited and that the original publication in this journal is cited, in accordance with accepted academic practice. No use, distribution or reproduction is permitted which does not comply with these terms.

frontiers in Immunology

MINI REVIEW
published: 16 October 2018
doi: 10.3389/fimmu.2018.02389

γδ T Lymphocytes: An Effector Cell in Autoimmunity and Infection

Carolina Maiumi Shiromizu[1] *and Carolina Cristina Jancic*[1,2]*

[1] *Laboratorio de Inmunidad Innata, Instituto de Medicina Experimental (IMEX) — CONICET, Academia Nacional de Medicina, Buenos Aires, Argentina,* [2] *Departamento de Microbiología, Parasitología e Inmunología, Facultad de Medicina, Universidad de Buenos Aires, Buenos Aires, Argentina*

γδ T cells are non-conventional lymphocytes which show several properties of innate immune cells. They present a limited TCR repertoire and circulate as cells with a pre-activated phenotype thus being able to generate rapid immune responses. γδ T cells do not recognize classical peptide antigens, their TCRs are non-MHC restricted and they can respond to pathogen-associated molecular patterns and to cytokines in absence of TCR ligands. They also recognize self-molecules induced by stress, which indicate infection and cellular transformation. All these features let γδ T cells act as a first line of defense in sterile and non-sterile inflammation. γδ T cells represent 1–10% of circulating lymphocytes in the adult human peripheral blood, they are widely localized in non-lymphoid tissues and constitute the majority of immune cells in some epithelial surfaces, where they participate in the maintenance of the epithelial barriers. γδ T cells produce a wide range of cytokines that orchestrate the course of immune responses and also exert high cytotoxic activity against infected and transformed cells. In contrast to their beneficial role during infection, γδ T cells are also implicated in the development and progression of autoimmune diseases. Interestingly, several functions of γδ T cells are susceptible to modulation by interaction with other cells. In this review, we give an overview of the γδ T cell participation in infection and autoimmunity. We also revise the underlying mechanisms that modulate γδ T cell function that might provide tools to control pathological immune responses.

Keywords: γδ T lymphocytes, inflammation, autoimmunity, infection, innate cells

OPEN ACCESS

Edited by:
Gustavo Javier Martinez, Rosalind Franklin University of Medicine and Science, United States

Reviewed by:
Jun-ichi Kira, Kyushu University, Japan
Irah L. King, McGill University, Canada

***Correspondence:**
Carolina Cristina Jancic
cjancic@gmail.com

Specialty section:
This article was submitted to T Cell Biology, a section of the journal Frontiers in Immunology

Received: *29 May 2018*
Accepted: *26 September 2018*
Published: *16 October 2018*

Citation:
Shiromizu CM and Jancic CC (2018) γδ T Lymphocytes: An Effector Cell in Autoimmunity and Infection. Front. Immunol. 9:2389. doi: 10.3389/fimmu.2018.02389

INTRODUCTION

γδ T cells are non-conventional T lymphocytes present in blood and tissues with a restricted TCR repertoire. During the ontogeny in the thymus, γδ T cells develop before αβ T lymphocytes and are abundant during the first weeks of fetal development. However, after birth, they constitute a minor fraction of thymocytes. This is similar in humans and rodents (1). In healthy adult humans, they represent 1–10% of the total circulating lymphocytes with a phenotype mainly CD4/CD8 double negative (2). They are found in high proportion in epithelial tissues, being particularly abundant in the intestine (3). In homeostatic conditions, γδ T cells can display a pre-activated and memory phenotype and the high frequency of these cells enables rapid responses without the presence of cognate TCR agonists and/or cellular expansion (1). γδ T cells can recognize many microorganisms and infected or transformed host cells (4) and exert a direct cytotoxic activity, which involves secretory, and non-secretory pathways, i.e., the release of granzymes and perforins and the engagement of Fas and TNF-related apoptosis-inducing ligand receptors, respectively

(5–7). Moreover, γδ T cells can propitiate the healing of damaged tissues and maintain the epithelial integrity (8). They can also generate memory cells, hence acting like adaptive immune T cells (9). Interestingly, and similar to conventional T lymphocytes, γδ T cells can differentiate into different effector profiles, and produce different chemokines and a wide array of cytokines including IFN-γ, TNF-α, IL-17, IL-21, and IL-22 (10). Recently, it has been reported in a murine model that in adipose tissue γδ T cells are abundant and they participate in the regulation of body temperature, through the production of IL-17A and TNF-α, and through the maintenance of catecholamine sensitivity for lipolysis induction. Moreover, in adipose tissue, γδ T cells let the recruitment and homeostatic expansion of regulatory T cells (11).

Regarding the effector profiles in mice, γδ T cells complete their functional differentiation in the fetal thymus (12). It has been shown, that γδ T cells that bind antigens with low affinity will produce IL-17, while those that bind antigen with high affinity will secrete IFN-γ (13). Another difference between human and mouse γδ T cells is their classification. In humans, γδ T cells are classified according to their Vδ gene segment used. Until now only three true Vδ genes exist: Vδ1-3; and seven functional Vγ gene segments: Vγ2-5, Vγ8, Vγ9, and Vγ11. While in mice γδ T cell subsets are named according to the Vγ chain used (14). Of note, the data describing the γδ T cell subsets of a particular species cannot be translated directly to another species because each repertoire is unique. The γδ TCR repertoire is restricted and is associated with the tissue distribution (5). The limited γδ TCR repertoire is consistent with their capacity to recognize conserved pathogen-derived antigens and self-molecules expressed under cellular stress conditions (5). Their tissue distribution and their capacity to recognize and rapidly respond to self- and non-self-conserved antigens allow them to act as the first line of defense in peripheral tissues (4). In humans, Vδ1+ T cells are abundant in the epithelium (8, 15, 16), they recognize molecules of the non-classical MHC family, either with or without loaded antigens, such as CD1a, c and d; and the molecules induced by stress: MICA/B and ULBP (5). Beside, Vδ3+ T cells are enriched in the liver and the intestine (17, 18). They can express CD4 or CD8 though the majority are double negative (CD4-CD8-). Vδ3+ T cells also express CD56, CD161, CD28, HLA-DR, and NKG2D, and some of them recognize CD1d and can exert cytotoxicity on CD1d+ target cells similar to Vδ1+ T cells (19). In humans and non-human primates, γδ T cells bearing the Vδ2 chain are the main subset present in peripheral blood and this δ chain is generally associated to the Vγ9. During infection, Vδ2Vγ9 T cells can be recruited to peripheral tissues where they contribute to the eradication of local infection (20).

Like αβ T lymphocytes, the activation of γδ T cells through the TCR requires the participation of accessory molecules. CD27 and NKG2D have been identified as co-effectors of the TCR activation (21, 22), but there is no clear consensus about the accessory molecules involved. Strikingly, in the past few years, it has been described the participation of CD277 [Butyrophilin(BTN)3A1] as a phosphoantigen presenting molecule specific for Vγ9Vδ2 TCR. According, phosphoantigen recognition is not restricted to the presentation in MHC molecules and it is independent of professional antigen presenting cells, but requires cellular contact and non-polymorphic presenting molecules (23). The main above mentioned functions reported for γδ T cells are summarized in **Figure 1**.

γδ T CELLS IN INFECTION

γδ T cells are key effectors in the immune response against microorganisms. In many microbial infections, the number of γδ T cells increases locally and/or systemically after a few days post-infection, being able to reach a 50% of the total circulating T cells (24). A hallmark of γδ T cells is that they can recognize a broad spectrum of endogenous and exogenous antigens widespread in nature, i.e., bacteria, protozoa, and infected or transformed host cells (4). To recognize these ligands, γδ T cells employ the TCRs and receptors such as TLRs, NOTCH, NKG2D (1, 24). The rapid effector responses elicited in infectious processes are similar to those generated by innate immune cells, a property related to their ability to be activated without an antigenic priming (5). γδ T cells can directly kill infected cells by releasing the content of cytotoxic granules and bacteriostatic or lytic molecules such as granulysin and defensins (7, 25). Furthermore, they have an indirect action on the elimination of microbes by producing cytokines that promote inflammation and by inducing the antibacterial functions of immune and epithelial cells (26). As we previously mentioned, γδ T cells can differentiate into different effector profiles depending on the pathophysiological context. They can produce IFN-γ and TNF-α in response to intracellular pathogens, IL-4, IL-5, IL-13 during parasite immune responses, and IL-17 in defense against extracellular bacteria and fungi (27). Accordingly mice lacking this cell subset (TCRδ KO mice) are more susceptible to suffer infections by bacteria (*Nocardia* spp., *Klebsiella* spp., *Listeria* spp., *Escherichia coli*, *Salmonella* spp., *Mycobacterium* spp., and *Pseudomonas* spp.) and parasites (*Plasmodium spp.*), demonstrating a critical role of IL-17-producing γδ T cells in these processes (28). The basis of the effector function of this T cell subset is controlling neutrophil recruitment in inflamed tissues. Interestingly, at sites of inflammation, neutrophils not only exert their microbicidal activity but also regulate (inhibit or stimulate) γδ T cell functions, as it has been extensively demonstrated (29–31).

Microbial recognition by Vγ9Vδ2 T cells involves phosphoantigens which are non-peptidic low molecular weight antigens with phosphate moieties, which are not only produced by prokaryotic but also eukaryotic cells. However, microbes' phosphoantigens are extremely potent activators of Vγ9Vδ2 T cells in contrast to endogenous phosphoantigens i.e., isopentenyl pyrophosphate (IPP) which is 10,000-folds less effective to induce cellular activation (32, 33). Noteworthy, eukaryotic cells under increased metabolic activity, can augment the production of IPP, i.e., tumor cells, and consequently activate γδ T cells efficiently (18). The phosphoantigen (E)-4-hydroxy-3-methyl-but-2-enyl pyrophosphate (HMBPP), an intermediate of the non-mevalonate pathway, generated by many bacteria, among them *Mycobacterium tuberculosis* (Mtb), *Mycobacterium bovis*, *Listeria monocytogenes, E. coli, Salmonella typhimurium,* and certain parasites such as *Plasmodium falciparum* and *Toxoplasma*

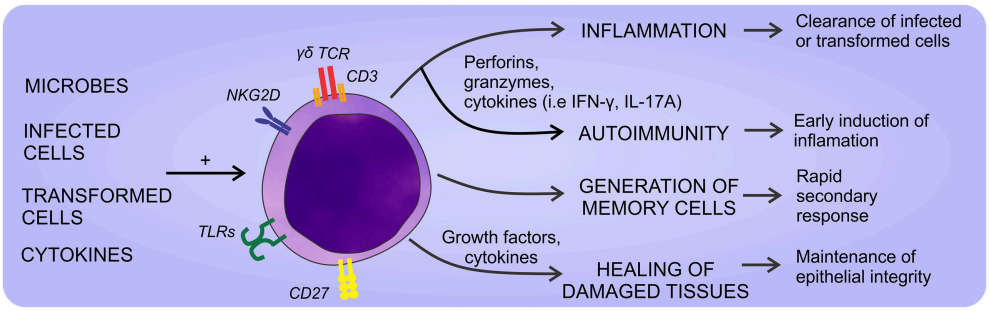

FIGURE 1 | General aspects of γδ T cell physiology. γδ T cells can sense a wide array of self- and non-self-stimuli that promote different responses. Thus, they can eliminate infected or transformed cells, heal damaged tissues, and eventually promote the development of autoimmune diseases if their response is exacerbated.

gondii is an extremely potent activator of Vγ9Vδ2 T cells (33, 34). Thanks to the presence of this metabolite, Vγ9Vδ2 T cells can be activated, proliferate and produce Th1-cytokines (IFN-γ and TNF-α) (29), thus mounting a rapid response against the microbes. Moreover, during Mtb or *L. monocytogenes* infections they produce IL-17 which prompts the recruitment of neutrophil and their immune response (35). In acute infections by Mtb and HMBPP-producing microbes, this cell subset expand and in re-infections they mount a secondary memory-like response (36). Furthermore, the production of IFN-γ by stimulated-Vγ9Vδ2 T cells may contribute to the immune response against Mtb as well as to control tuberculosis lesions since they are present in lung granuloma (37). Vγ9Vδ2 T cells also limit the development of intracellular Mtb by the action of perforins, granzymes, and granulysin (20). Additionally, they can promote airway CD8+ and Th1 CD4+ responses of conventional T cells specific for Mtb, through the production of IL-12 in response to phosphoantigen activation (20). In a non-human primate model of Mtb infection, *ex vivo* activation of Vγ9Vδ2 T cells by exogenous HMBPP up-regulates their IFN-γ production. This treatment promotes the inhibition of IL-22 production, which is associated with severe lesions (38). These results might be helpful to develop novel therapeutic strategies to control Mtb infection and persistence and to induce the activation of immune cells by IFN-γ in order to eliminate intracellular Mtb (**Figure 2A**).

In patients with viral infections, Vδ3+ T cells are enriched. In hepatitis C virus (HCV) infections, it has been observed the expansion of several Vδ3+ T cell clones in peripheral blood (39). In the liver, these cells can mount a response against virus-infected hepatocytes and non-infected host cells, suggesting that they may contribute to the hepatic damage (40). Additionally, there is a higher frequency of IFN-γ-producing Vδ1+ cells, which correlates with disease evolution (41). During the immune response against viral infections, the recognition of non-classical MHC molecules by Vδ2- T cells is determinant but also participate Vγ9Vδ2 T cells. It has been demonstrated that activated Vγ9Vδ2 T cells can inhibit sub-genomic HCV replication by the production of IFN-γ (41, 42). In the same way, patients suffering chronic hepatitis B virus (HBV) infection, have a reduction in the circulating Vδ2+ T cells, in the production of IFN-γ and in the cytotoxicity mediated by γδ T cells. These events correlate with the persistence of HBV infection (43). Noteworthy, in mouse models of infection by West Nile virus and herpes simplex virus type 2, it has been shown that γδ T cells play a critical role in the generation of conventional CD8+ and CD4+ memory T cells, respectively (44, 45). Importantly, γδ T cells also participate in anti-viral response early in life. It has been reported that they can mount a functional immune response to cytomegalovirus infection during development in uterus, pointing out the key role of γδ T cells in fetal life (46).

Furthermore, γδ T cells participate in antifungal immunity. It has been reported that Vδ1+ T cells can selectively respond to *Candida albicans*, by producing high levels of IL-17 (47).

Given the beneficial role of Vγ9Vδ2 T cells in the clearance of microbes, the *in vivo* effect of T cell activation by phosphoantigens administered exogenously was tested in primates (48). In an infection model induced by *Yersinia pestis*, phosphoantigen treatment provoked faster pathogen clearance and restoration of inflamed tissues (49). Moreover, during chronic viral infections, where Vγ9Vδ2 T cells are decreased and their functions are impaired (50, 51), it has been proposed the administration of phosphoantigens to help restore the γδ T cell functions. Furthermore, in a non-human primate model, it was reported that after administration of HMBPP, the plasma levels of IFN-γ increased, and this effect was even higher when administered with IFN-α (52), showing a new approach to boost Vγ9Vδ2 T cell response in viral infection (**Figure 2A**). In this work authors also explored, *in vitro*, the effect of this combined therapy in HCV-infected patients obtaining the same results (52).

γδ T CELLS IN AUTOIMMUNITY

It is well established that IL-17A plays a crucial role in the development and progression of autoimmune diseases (53, 54). Even though the main source of IL-17A is the Th17 CD4+ αβ T cell population, in the onset of autoimmune pathologies, innate immune cells, especially those belonging to the γδ T cell subset, also contribute to the production of IL-17A (55). Human IL-17A-producing γδ T cells are generated in the periphery and can be recruited to inflamed tissues where they accumulate (56, 57). This

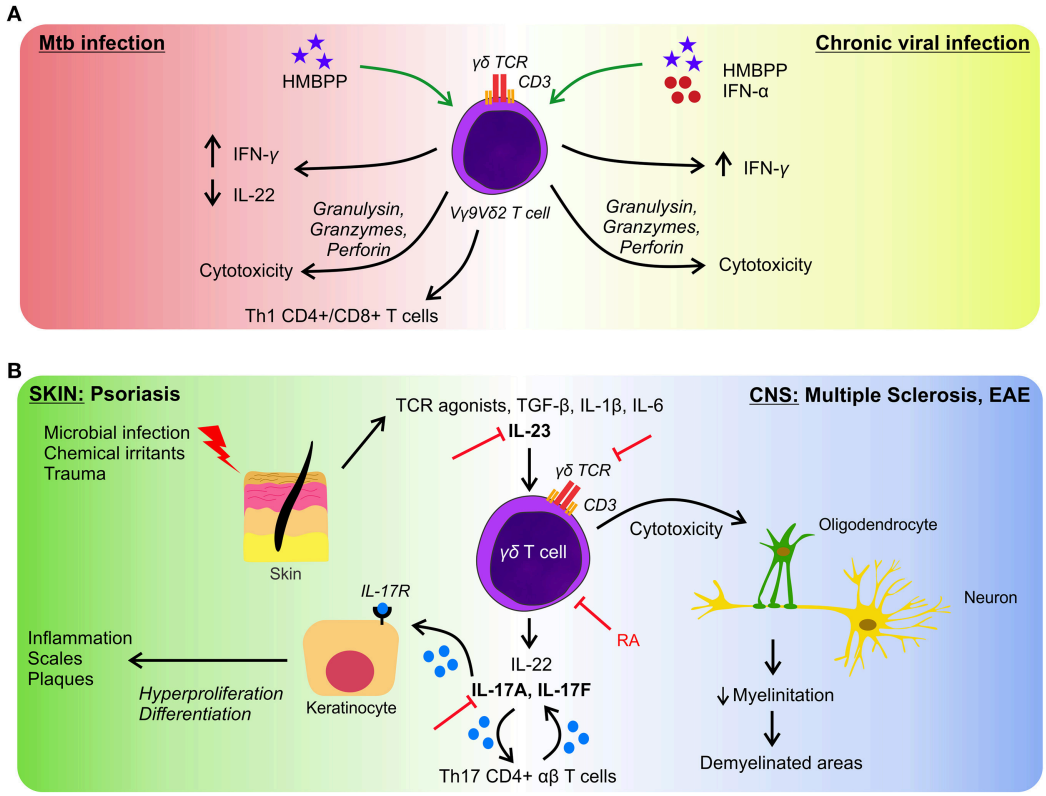

FIGURE 2 | γδ T cells in infection and autoimmunity. **(A)** In response to Mtb infection, γδ T cells produce inflammatory cytokines and exert cytotoxicity on infected cells (left side), similar effector functions are performed in response to several viruses (right side). But in chronic infections γδ T cells are less effective to control microbes. Green arrows represent the proposed approaches to boost the activation of γδ T lymphocytes. **(B)** γδ T cells participate in the initiation and development of autoimmune diseases. As examples we represent pathologies in skin (left side) and in CNS (right side) both having in common an axis governed by the activation of γδ T cells and by the production of IL-17 and IL-22. Figure shows different targets to block autoimmunity manifestations (red lines). RA, retinoic acid.

process takes place more rapidly compared to the activation of conventional T lymphocytes. In fact, γδ T cells can be activated in the absence of a cognate TCR ligand which allows them to be powerful early inducers of inflammation in autoimmune diseases. As demonstrated *in vitro*, several molecules are involved in the differentiation into the Th17 cytokine-profile, among them: TCR agonists, IL-1β, IL-6, IL-23, and TGF-β (57, 58). Interestingly, in patients with autoimmune liver disease such as autoimmune hepatitis, primary sclerosing cholangitis, or primary biliary cirrhosis, there is a significantly increase of γδ T cells (Vδ1+, Vδ2+, and Vδ3+) in peripheral blood and liver, supporting the participation of this subset in autoimmunity (18).

In the next paragraphs, we summarize the published data describing the role of γδ T cells in psoriasis and multiple sclerosis as two examples of autoimmune diseases where the role of γδ T cells has been extensively studied.

Autoimmunity in Skin

In steady-state conditions, in the skin and the intestine, γδ T cells are abundant and in conjunction with other immune cells, they act as sentinels and support the integrity of the epithelial barriers (59, 60). In human skin, local γδ T cells display an oligoclonal repertoire governed by the expression of Vδ1 chain (61). A well-characterized inflammatory condition in the skin is psoriasis. It is an autoimmune disease which can be triggered by microbial infections, chemical irritants or trauma. Once the pathological process starts, the innate and adaptive immune system activate and result in the hyperproliferation and the aberrant differentiation of keratinocytes, a key step in the pathophysiology of psoriasis. There is also an increase in the levels of IFN-γ and IL-23, which cause an immune-mediated dermatosis with skin lesions (62). In *in vivo* murine models of psoriasis induced by Imiquimod (TLR7/8 agonist) (63), γδ T cells were found to be necessary and sufficient to trigger skin lesions such as plaque formation, with a critical role of the axis IL-23/IL-17/IL-22. In fact, dermal γδ T cells easily proliferate and produce IL-17A, IL-17F, and IL-22 in response to IL-1β and IL-23 stimulation (63). Remarkably, γδ T cells have been proposed to initiate and precede the participation of conventional Th17 cells in psoriasis (64). In accordance, the genetic deletion of IL-17A, IL-17F, and IL-22 has shown to protect mice from Imiquimod-induced inflammation (65). Similarly, human dermal IL-17-producing γδ T cells appear to play a pathogenic role in psoriasis, as supported by evidence indicating an abundance of γδ T cells in skin biopsies from psoriasis patients, which upon stimulation with IL-23 *in vitro*, increase the IL-17 production to levels higher than αβ T cells (63). Moreover, a reduction in peripheral blood CLA+ CCR6+ Vγ9Vδ2+ T cells is observed in psoriasis patients

which correlates with the severity of the pathology (66). The γδ T cells present in psoriasis skin are the Vδ1+ subset and the recently reported Vδ2+ recruited from the blood. However, this finding remain controversial because Vγ9Vδ2+ T cells are normally rare in the dermis and exhibit a low capacity to produce IL-17 (67).

Interestingly, there is different preclinical and clinical data concerning the therapeutic strategies to treat psoriasis. Based on the components involved in the onset and progression of the disease, several molecular target has been studied. Remarkably, drugs that target IL-17 and IL-23 have shown notable efficacy (68), and some of them have been licensed to treat moderate and severe psoriasis (68, 69). Given the active role of γδ T cells in the development of autoimmunity, it is possible to speculate that the mentioned immunotherapies could act not only on conventional Th17 T cells but also on γδ T lymphocytes because they express IL-23R and produce substantial quantities of IL-17A and IL-22 (**Figure 2B**).

Autoimmunity in the Central Nervous System

Even if the role of γδ T cells in multiple sclerosis (MS) has not been completely elucidated, numerous studies have found that γδ T cells are associated with this pathology. It has been reported that γδ T cells are cytotoxic against oligodendrocytes, which participate in the myelinization of neurons, therefore, γδ T cells are implicated in the pathogenesis of MS and in its murine model, the experimental autoimmune encephalomyelitis (EAE) (70, 71). Noteworthy, it has been shown in patients suffering MS that γδ T cells accumulate in plaques and in chronically demyelinated areas of the central nervous system (CNS); and that IL-17A-producing γδ T cells increase in cerebrospinal fluids and in brain lesions (72, 73). As expected, in peripheral blood and CNS IL-17 is elevated (74). Recently it has been reported that circulating Vδ2+ T cells are decreased in MS, and it was found a negative correlation between the percentages of Vδ2+Vγ9+ T cells and the disease severity (75). These findings led to suggest that the decrease in Vδ2+ T cells impaired an effective control of auto-reactive αβ T lymphocytes (75). Additionally, in the CNS of mice with EAE, different subsets of γδ T cells were identified, among them the more abundant are: Vγ1, Vγ4, Vγ5, and Vγ6. These T cells infiltrate the brain and spinal cord in the early phases of EAE (10, 76–78). Interestingly, these subsets display different cytokine profiles, being the Vγ4+ cells, the most abundant, and the ones that produce high levels of IL-17 (76, 79). Thus, γδ T cells could be the initiators of the inflammation and the inductors of Th17 cells by producing IL-17 and IL-21 in the early phases of EAE, causing the amplification of Th17 responses (10). Of note, γδ T cells also play a beneficial role during EAE, as mediators in the resolution of the inflammation. The subset involved in the tissue repairing phase is suggested to be Vγ1, which could enhance the effector function of the regulatory T cells recruited (76), inhibit the differentiation to Th17 profile by the production of IFN-γ (80), and trigger apoptosis of pathogenic CD4+ T cells through the Fas-FasL pathway.

In vivo experimental data support that γδ T cells have a deleterious role in MS, i.e., in the relapsing-remitting EAE model, treating mice with TCRδ depleting antibodies immediately before the onset or during the chronic phase of the disease produces a reduction of the disease (81); and in knockout mice for IL-1RI the severity of the EAE is very decreased, demonstrating the participation of IL-1β in the induction of IL-17-producing T cells (82). Interestingly, another molecule that could modulate γδ T cells in EAE is retinoic acid. Raverdeau and co-workers demonstrated that retinoic acid treatment suppressed the production of IL-17A by murine γδ T cells *in vivo* and they also observed a reduction in the number of γδ T cells infiltrating the CNS (83). Altogether, these data show the role of new molecules that could be used to design immunotherapeutic strategies, providing new alternatives to treat autoimmunity (**Figure 2B**).

CONCLUDING REMARKS

In the last few years, immunotherapies based on γδ T cells have gained a great interest, supported by the anti-microbial and anti-tumor capabilities of these cells. Interestingly, these cells could be suppressed when their response is exacerbated such as in autoimmunity or some infectious conditions or could be stimulated when their response is not optimal i.e., in chronic infections. Moreover, γδ T cells can be manipulated *ex vivo* or *in vivo* to achieve an efficient immune response against infected or transformed cells. Nevertheless, further studies are necessary to address the most beneficial therapeutic approaches to modulate the self and non-self-immune response mediated by γδ T cells.

AUTHOR CONTRIBUTIONS

CS designed and performed figures and revised the manuscript. CJ wrote the manuscript.

FUNDING

CJ is funded by Consejo Nacional de Investigaciones Científicas y Técnicas and Agencia Nacional de Promoción Científica y Tecnológica—FonCyT (PICT2016/700).

ACKNOWLEDGMENTS

We thank Dr. Analia Trevani for critical reading of the manuscript.

REFERENCES

1. Bonneville M, O'Brien RL, Born WK. γδ T cell effector functions: a blend of innate programming and acquired plasticity. *Nat Rev Immunol.* (2010) 10:467–78. doi: 10.1038/nri2781
2. Dar AA, Patil RS, Chiplunkar SV. Insights into the relationship between Toll Like Receptors and γδ T cell responses. *Front Immunol.* (2014) 5:366. doi: 10.3389/fimmu.2014.00366
3. Hoytema van Konijnenburg DP, Reis BS, Pedicord VA, Farache J, Victora GD, Mucida D. Intestinal epithelial and intraepithelial T cell

crosstalk mediates a dynamic response to infection. *Cell* (2017) 171:1–12. doi: 10.1016/j.cell.2017.08.046
4. Hayday AC. γδ cells: A right time and a right place for a conserved third way of protection. *Annu Rev Immunol.* (2000) 18:975–1026. doi: 10.1146/annurev.immunol.18.1.975
5. Vantourout P, Hayday A. Six-of-the-best: unique contributions of γδ T cells to immunology. *Nat Rev Immunol.* (2013) 13:88–100. doi: 10.1038/nri3384
6. Qin G, Mao H, Zheng J, Sia SF, Liu Y, Chan PL, et al. Phosphoantigen-expanded human γδ T cells display potent cytotoxicity against monocytederived macrophages infected with human and avian influenza viruses. *J Infect Dis.* (2009) 200:858–65. doi: 10.1086/605413
7. Dieli F, Troye-Blomberg, M, Ivanyi J, Fournié JJ, Krensky AM, Bonneville M, et al. Granulysin-dependent killing of intracellular and extracellular *Mycobacterium tuberculosis* by Vγ9/Vδ2 T lymphocytes. *J Infect Dis.* (2001) 184:1082–5. doi: 10.1086/323600
8. Toulon A, Lionel B, Taylor KR, Tenenhaus M, Bhavsar D, Lanigan C, et al. A role for human skin-resident T cells in wound healing. *J Exp Med.* (2009) 206:743–50. doi: 10.1084/jem.20081787
9. McGinley AM, Edwards SC, Raverdeau M, Mills KH. Th17 cells, γδ T cells and their interplay in EAE and multiple sclerosis. *J Autoimmun.* (2018) 87:97–108. doi: 10.1016/j.jaut.2018.01.001
10. Sutton CE, Lalor SJ, Sweeney CM, Brereton CF, Lavelle EC, Mills KH. Interleukin-1 and IL-23 induce innate IL-17 production from γδ T cells, amplifying Th17 responses and autoimmunity. *Immunity* (2009) 31:331–41. doi: 10.1016/j.immuni.2009.08.001
11. Kohlgruber AC, Gal-Oz ST , La Marche NM, Shimazaki M, Duquette D, Nguyen HN, et al. γδ T cells producing interleukin-17A regulate adipose regulatory T cell homeostasis and thermogenesis. *Nat Immunol.* (2018) 19:464–74. doi: 10.1038/s41590-018-0094-2
12. Shibata K, Yamada H, Nakamura R, Sun X, Itsumi M, Yoshikai Y. Identification of CD25+ γδ T cells as fetal thymus-derived naturally occurring IL-17 producers. *J Immunol.* (2008) 181:5940–7. doi: 10.4049/jimmunol.181.9.5940
13. Jensen KDC, Su X, Shin S, Li L, Youssef S, Yamasaki S, et al. Thymic selection determines γδ T cell effector fate: antigen-naive cells make interleukin-17 and antigen-experienced cells make interferon gamma. *Immunity* (2008) 29:90–100. doi: 10.1016/j.immuni.2008.04.022
14. Adams EJ, Gu S, Luoma AM. Human γδ T cells: Evolution and ligand recognition. *Cell Immunol.* (2015) 296:31–40. doi: 10.1016/j.cellimm.2015.04.008
15. Chien YH, Meyer C, Bonneville M. γδ T cells: first line of defense and beyond. *Ann Rev Immunol.* (2014) 32:121–55. doi: 10.1146/annurev-immunol-032713-120216
16. Dunne MR, Eliott L, Hussey S, Mahmud N, Kelly J, Doherty DG, et al. Persistent changes in circulating and intestinal γδ T cell subsets, invariant natural killer T cells and mucosal-associated invariant T cells in children and adults with coeliac disease. *PLoS ONE* (2013) 4:e76008. doi: 10.1371/journal.pone.0076008
17. Kenna T, Golden-Mason L, Norris S, Hegarty JE, O'Farrelly C, Dohertye DG. Distinct subpopulations of γδ T cells are present in normal and tumor-bearing human liver. *Clin Immunol.* (2004) 113:56–63. doi: 10.1016/j.clim.2004.05.003
18. Doherty DG. Immunity, tolerance and autoimmunity in the liver: A comprehensive review. *J Autoimmun.* (2016) 66:60–75. doi: 10.1016/j.jaut.2015.08.020
19. Mangan BA, Dunne MR, O'Reilly VP, Dunne PJ, Exley MA, O'Shea D, et al. Cutting Edge: CD1d restriction and Th1/Th2/Th17 cytokine secretion by human Vδ3 T cells. *J Immunol.* (2013) 191:30–4. doi: 10.4049/jimmunol.1300121
20. Chen C, Yao S, Huang D, Wei H, Sicard H, Zeng G, et al. Phosphoantigen/IL2 expansion and differentiation of Vγ2Vδ2 T cells increase resistance to tuberculosis in nonhuman primates. *PLoS Pathog.* (2013) 9:e1003501. doi: 10.1371/journal.ppat.1003501
21. deBarros A, Chaves-Ferreira M, d'Orey F, Ribot JC, Silva-Santos B. CD70–CD27 interactions provide survival and proliferative signals that regulate T cell receptor-driven activation of human γδ peripheral blood lymphocytes. *Eur J Immunol.* (2011) 41:195–201. doi: 10.1002/eji.201040905
22. Ribot JC, deBarros A, Silva-Santos B. Searching for "signal 2": costimulation requirements of γδ T cells. *Cell Mol Life Sci.* (2011) 68:2345–55. doi: 10.1007/s00018-011-0698-2
23. Rhodes DA. Reith W, Trowsdale J. Regulation of immunity by butyrophilins. *Ann Rev Immunol.* (2016) 34:151–72. doi: 10.1146/annurev-immunol-041015-055435
24. Wesch D, Peters C, Oberg HH, Pietschmann K, Kabelitz D. Modulation of γδ T cell responses by TLR ligands. *Cell Mol Life Sci.* (2011) 68:2357–70. doi: 10.1007/s00018-011-0699-1
25. Dudal S, Turriere C, Bessoles S, Fontes P, Sanchez F, Liautard J, et al. Release of LL-37 by activated human Vγ9Vδ2 T cells: a microbicidal weapon against *Brucella suis*. *J Immunol.* (2006) 177:5533–9. doi: 10.4049/jimmunol.177.8.5533
26. Hamada S, Umemura M, Shiono T, Tanaka K, Yahagi A, Begum MD, et al. IL-17A produced by γδ T cells plays a critical role in innate immunity against *Listeria monocytogenes* infection in the liver. *J Immunol.* (2008) 181:3456–63. doi: 10.4049/jimmunol.181.5.3456
27. Harly C, Peigné C, Scotet E. Molecules and mechanisms implicated in the peculiar antigenic activation process of human Vγ9Vδ2 T cells. *Front Immunol.* (2015) 5:657. doi: 10.3389/fimmu.2014.00657
28. Sutton CE, Mielke LA, Milles KH. IL-17 producing γδ T cells and innate lymphoid cells. *Eur J Immunol.* (2012) 42:2221–31. doi: 10.1002/eji.201242569
29. Sabbione F, Gabelloni ML, Ernst G, Gori MS, Salamone GV, Oleastro M, et al. Neutrophils suppress γδ T-cell function. *Eur J Immunol.* (2014) 44:819–30. doi: 10.1002/eji.201343664
30. Towstyka NY, Shiromizu CM, Keitelman I, Sabbione F, Salamone GV, Geffner JR, et al. Modulation of γδ T-cell activation by neutrophil elastase. *Immunology* (2018) 153:225–37. doi: 10.1111/imm.12835
31. Kalyan S, Kabelitz D. Defining the nature of human γδ T cells: a biographical sketch of the highly empathetic. *Cell Mol Immunol.* (2013) 10:21–9. doi: 10.1038/cmi.2012.44
32. Hintz M, Reichenberg A, Altincicek B, Bahr U, Gschwind RM, Kollas AK, et al. Identification of (E)-4-hydroxy-3-methyl-but-2-enyl pyrophosphate as a major activator for human γδ T cells in *Escherichia coli*. *FEBS Lett* (2001) 509:317–22. doi: 10.1016/S0014-5793(01)03191-X
33. Eberl M, Hintz M, Reichenberg A, Kollas AK, Wiesner J, Jomaa H. Microbial isoprenoid biosynthesis and human γδ T cell activation. *FEBS Lett.* (2003) 544:4–10. doi: 10.1016/S0014-5793(03)00483-6
34. Belmant C, Espinosa E, Poupot R, Peyrat MA, Guiraud M, Poquet Y, et al. 3-Formyl-1-butyl pyrophosphate: a novel mycobacterial metabolite-activating human γδ T cells. *J Biol Chem.* (1999) 274:32079–84.
35. Poggi A, Catellan S, Musso A, Zocchi MR. γδ T lymphocytes producing IFN-γ and IL-17 in response to *Candida albicans* or mycobacterial antigens: possible implications for acute and chronic inflammation. *Curr Med Chem.* (2009) 16:4743–9. doi: 10.2174/092986709789878238
36. Shen Y, Zhou D, Qiu L, Lai X, Simon M, Shen L, et al. Adaptive immune response of Vγ2Vδ2+ T cells during mycobacterial infections. *Science* (2002) 295:2255–8. doi: 10.1126/science.1068819
37. Huang D, Shen Y, Qiu L, Chen CY, Shen L, Estep J, et al. Immune distribution and localization of phosphoantigen-specific Vγ2Vδ2 T cells in lymphoid and nonlymphoid tissues in *Mycobacterium tuberculosis* Infection. *Infect Immun.* (2007) 76:426–36. doi: 10.1128/IAI.01008-07
38. Qiu L, Huang D, Chen CY, Wang R, Shen L, Shen Y, et al. Severe tuberculosis induces unbalanced up-regulation of gene networks and overexpression of IL-22, MIP-1α, CCL27, IP-10, CCR4, CCR5, CXCR3, PD1, PDL2, IL-3, IFNbeta, TIM1, and TLR2 but low antigen-specific cellular responses. *J Infect Dis.* (2008) 198:1514–9. doi: 10.1086/592448
39. Ravens S, Hengst J, Schlapphoff V, Deterding K, Dhingra A, Schultze-Florey C, et al. Human γδ T cell receptor repertoires in peripheral blood remain stable despite clearance of persistent hepatitis C virus infection by direct-acting antiviral drug therapy. *Front Immunol.* (2018) 9:510. doi: 10.3389/fimmu.2018.00510
40. Tseng CTK, Miskovsky E, Houghton M, Klimpel GR. Characterization of liver T-cell receptor γδ T cells obtained from individuals chronically infected with hepatitis C virus (HCV): evidence for these T cells playing a role in the liver pathology associated with HCV infections. *Hepatology* (2001) 33:1312–20. doi: 10.1053/jhep.2001.24269

41. Agrati C, D'Offizi G, Narciso P, Abrignani S, Ippolito G, Colizzi V, et al. Vδ1 T lymphocytes expressing a Th1 phenotype are the major γδ T cell subset infiltrating the liver of HCV-infected persons. *Mol Med.* (2001) 7:11–9.
42. Agrati C, Alonzi T, De Santis R, Castilletti C, Abbate I, Capobianchi MR, et al. Activation of Vγ9Vδ2 T cells by non-peptidic antigens induces the inhibition of subgenomic HCV replication. *Int Immunol.* (2006) 18:11–8. doi: 10.1093/intimm/dxh337
43. Rajoriya N, Fergusson JR, Leithead JA, Klenerman P. γδ T-lymphocytes in hepatitis C and chronic liver disease. *Front Immunol.* (2014) 5:1–9. doi: 10.3389/fimmu.2014.00400
44. Nishimura H, Yajima T, Kagimoto Y, Ohata M, Watase T, Kishihara K, et al. Intraepithelial γδ T cells may bridge a gap between innate immunity and acquired immunity to herpes simplex virus type 2. *J Virol.* (2004) 78:4927–30. doi: 10.1128/JVI.78.9.4927-4930.2004
45. Wang T, Gao Y, Scully E, Davis CT, Anderson JF, Welte T, et al. γδ T cells facilitate adaptive immunity against West Nile virus infection in mice. *J Immunol.* (2006) 177:1825–32. doi: 10.4049/jimmunol.177.3.1825
46. Vermijlen D, Brouwer M, Donner C, Liesnard C, Tackoen M, Van Rysselberge M, et al. Human cytomegalovirus elicits fetal γδ T cell responses in utero. *J Exp Med.* (2010) 207:807–21. doi: 10.1084/jem.20090348
47. Fenoglio D, Poggi A, Catellani S, Battaglia F, Ferrera A, Setti M, et al. Vδ1 T lymphocytes producing IFN-γ and IL-17 are expanded in HIV-1–infected patients and respond to *Candida albicans*. *Blood* (2009) 113:6611–8. doi: 10.1182/blood-2009-01-198028
48. Sicard H, Ingoure S, Luciani B, Serraz C, Fournié JJ, Bonneville M, et al. *In vivo* immunomanipulation of Vγ9Vδ2 T cells with a synthetic phosphoantigen in a preclinical nonhuman primate model. *J Immunol.* (2005) 175:5471–80. doi: 10.4049/jimmunol.175.8.5471
49. Huang D, Chen CY, Ali Z, Shao L, Shen L, Lockman HA, et al. Antigen-specific Vγ2Vδ2 T effector cells confer homeostatic protection against pneumonic plaque lesions. *Proc Natl Acad Sci USA*. (2009) 106:7553–8. doi: 10.1073/pnas.0811250106
50. Par G, Rukavina D, Podack ER, Horanyi M, Szekeres-Bartho J, Hegedüs G, et al. Decrease in CD3-negative-CD8dim^{+} and Vδ2/Vγ9 TcR+ peripheral blood lymphocyte counts, low perforin expression and the impairment of natural killer cell activity is associated with chronic hepatitis C virus infection. *J Hepatol.* (2002) 37:514–22. doi: 10.1016/S0168-8278(02)00218-0
51. Riedel DJ, Sajadi M, Armstrong CL,Cummings JS, Cairo C, Redfield RR, et al. Natural viral suppressors of HIV-1 have a unique capacity to maintain γδ T cells. *AIDS* (2009) 23:1955–64. doi: 10.1097/QAD.0b013e32832ff1ff
52. Cimini E, Bonnafous C, Bordoni V, Lalle E, Sicard H, Sacchi A, et al. Interferon-α improves phosphoantigen-induced Vγ9Vδ2 T-cells interferon-γ production during chronic HCV infection. *PLoS ONE* (2012) 7:e37014. doi: 10.1371/journal.pone.0037014
53. Isailovic N, Daigo K, Mantovani A, Selmi C. Interleukin-17 and innate immunity in infections and chronic inflammation. *J Autoimmun.* (2015) 60:1–11. doi: 10.1016/j.jaut.2015.04.006
54. Burkett PR, Meyer zu Horste G, Kuchroo VK. Pouring fuel on the fire: Th17 cells, the environment, and autoimmunity. *J Clin Invest.* (2015) 125:2211–9. doi: 10.1172/JCI78085
55. Hirota K, Duarte JH, Veldhoen M, Hornsby E, Li Y, Cua DJ, et al. Fate mapping of IL-17-producing T cells in inflammatory responses. *Nat Immunol.* (2011) 12:255–63. doi: 10.1038/ni.1993
56. Papotto PH, Reinhardt A, Prinz I, Silva-Santos B. Innately versatile: γδ17 T cells in inflammatory and autoimmune diseases. *J Autoimmun.* (2018) 87:26–37. doi: 10.1016/j.jaut.2017.11.006
57. Caccamo N, Le Mendola C, Orland V, Meraviglia S, Todaro M, Stassi G, et al. Differentiation, phenotype and function of interleukin-17-producing human Vγ9Vδ2 T cells. *Blood* (2011) 118:129–38. doi: 10.1182/blood-2011-01-331298
58. Moens E, Brouwer M, Dimova T, Goldman M, Willems F, Vermijlen D. IL-23R and TCR signaling drives the generation of neonatal Vγ9Vδ2 T cells expressing high levels of cytotoxic mediators and producing IFN-γ and IL-17. *J Leuk Biol.* (2011) 89:743–52. doi: 10.1189/jlb.0910501
59. Jameson J, Ugarte K, Chen N, Yachi P, Fuchs E, Boismenu R, et al. A role for skin γδ T cells in wound repair. *Science* (2002) 296:747–49. doi: 10.1126/science.1069639
60. Hayday AC. γδ T cells and the lymphoid stress-surveillance response. *Immunity* (2009) 31:184–96. doi: 10.1016/j.immuni.2009.08.006
61. Holtmeier W, Pfänder M, Hennemann A, Caspary WF, Zollner TM, Kaufmann R. The TCR-δ repertoire in normal human skin is restricted and distinct from the TCR-δ repertoire in the peripheral blood. *J Invest Dermatol.* (2001) 116:275–90. doi: 10.1046/j.1523-1747.2001.01250.x
62. Chan JR, Blumenschein W, Murphy E, Diveu C, Wiekowski M, Abbondanzo S, et al. IL-23 stimulates epidermal hyperplasia via TNF and IL-20R2-dependent mechanisms with implications for psoriasis pathogenesis. *J Exp Med.* (2006) 203:2577–87. doi: 10.1084/jem.20060244
63. Cai Y, Shen X, Ding C, Qi C, Li K, Li X, et al. Pivotal role of dermal IL-17-producing γδ T cells in skin inflammation. *Immunity* (2011) 35:596–610. doi: 10.1016/j.immuni.2011.08.001
64. Diani M, Altomare G, Reali E. T cell responses in psoriasis and psoriatic arthritis. *Autoimmun Rev.* (2015) 14:286–92. doi: 10.1016/j.autrev.2014.11.012
65. Pantelyushin S, Haak S, Ingold B, Kulig P, Heppner FL, Navarini AA, et al. Rorγ+ innate lymphocytes and γδ T cells initiate psoriasiform plaque formation in mice. *J Clin Invest.* (2012) 122:2252–6. doi: 10.1172/JCI61862
66. Laggner U, Di Meglio P, Perera GK, Hundhausen C, Lacy KE, Ali N, et al. Identification of a novel proinflammatory human skin-homing Vγ9Vδ2 T cell subset with a potential role in psoriasis. *J Immunol.* (2011) 187:2783–93. doi: 10.4049/jimmunol.1100804
67. O'Brien RL, Born WK. Dermal γδ T cells – What have we learned? *Cell Immunol.* (2015) 296:62–9. doi: 10.1016/j.cellimm.2015.01.011
68. Teng MW, Bowman EP, McElwee JJ, Smyth MJ, Casanova JL, Cooper AM, et al. IL-12 and IL-23 cytokines: from discovery to targeted therapies for immune-mediated inflammatory diseases. *Nat Med.* (2015) 21:719–29. doi: 10.1038/nm.3895
69. Kirkham BW, Kavanaugh A, Reich K. Interleukin-17A: a unique pathway in immune-mediated diseases: psoriasis, psoriatic arthritis and rheumatoid arthritis. *Immunology* (2014) 141:133–42. doi: 10.1111/imm.12142
70. Freedman MS, Ruijs TC, Selin LK, Antel JP. Peripheral blood γδ T cells lyse fresh human braindderived oligodendrocytes. *Ann Neurol.* (1991) 30:794–800.
71. Zeine R, Pon R, Ladiwala U, Antel JP, Filion LG, Freedman MS. Mechanism of γδ T cell-induced human oligodendrocyte cytotoxicity: relevance to multiple sclerosis. *J Neuroimmunol.* (1998) 87:49–61.
72. Schirmer L, Rothhammer V, Hemmer B. Enriched CD161high CCR6+ γδ T cells in the cerebrospinal fluid of patients with multiple sclerosis. *JAMA Neurol.* (2013) 70:345–51. doi: 10.1001/2013.jamaneurol.409
73. Tzartos JS, Friese MA, Craner MJ, Palace J, Newcombe J, Esiri MM, et al. Interleukin-17 production in central nervous system-infiltrating T cells and glial cells is associated with active disease in multiple sclerosis. *Am J Pathol.* (2008) 172:146–55. doi: 10.2353/ajpath.2008.070690
74. Kurasawa K, Hirose K, Sano H, Endo H, Shinkai H, Nawata Y, et al. Increased interleukin-17 production in patients with systemic sclerosis. *Arthritis Rheum.* (2000) 43:2455–63. doi: 10.1002/1529-0131(200011)43:11<2455::AID-ANR12>3.0.CO;2-K
75. Maimaitijiang G, Shinoda K, Nakamura Y, Masaki K, Matsushita T, Isobe N, et al. Association of decreased percentage of Vδ2+Vγ9+ γδ T cells with disease severity in multiple sclerosis. *Front Immunol.* (2018) 9:748. doi: 10.3389/fimmu.2018.00748
76. Blink SE, Caldis MW, Goings GE, Harp CT, Malissen B, Prinz I, et al. γδ T cell subsets play opposing roles in regulating experimental autoimmune encephalomyelitis. *Cell Immunol.* (2014) 290:39–51. doi: 10.1016/j.cellimm.2014.04.013
77. Lalor SJ, Dungan LS, Sutton CE, Basdeo SA, Fletcher JM, Mills KH. Caspase-1-processed cytokines IL-1β and IL-18 promote IL-17 production by γδ and CD4 T cells that mediate autoimmunity. *J Immunol.* (2011) 186:5738–48. doi: 10.4049/jimmunol.1003597
78. Wohler JE, Smith SS, Zinn KR, Bullard DC, Barnum SR. γδ T cells in EAE: early trafficking events and cytokine requirements. *Eur J Immunol.* (2009) 39:1516–26. doi: 10.1002/eji.200839176
79. Papotto PH, Ribot JC, Silva-Santos B. IL-17+ γδ T cells as kick-starters of inflammation. *Nat Immunol.* (2017) 18:604–11. doi: 10.1038/ni.3726
80. Ottum PA, Arellano G, Reyes LI, Iruretagoyena M, Naves R. Opposing roles of interferon-γ on cells of the central nervous system in autoimmune neuroinflammation. *Front Immunol.* (2015) 6:539. doi: 10.3389/fimmu.2015.00539

81. Rajan AJ, Gao Y, Raine CS, Brosnan CF. A pathogenic role for γδ T cells in relapsing-remitting experimental allergic encephalomyelitis in the SJL mouse. *J Immunol.* (1996) 157:941–49.
82. Sutton C, Brereton C, Keogh B, Mills KH, Lavelle EC. A crucial role for interleukin (IL)-1 in the induction of IL-17 producing T cells that mediate autoimmune encephalomyelitis. *J Exp Med.* (2006) 203:1685–91. doi: 10.1084/jem.20060285
83. Raverdeau M, Breen CJ, Misiak A, Mills KH. Retinoic acid suppresses IL-17 production and pathogenic activity of γδ T cells in CNS autoimmunity. *Immuno Cell Biol.* (2016) 94:763–73. doi: 10.1038/icb.2016.39

Conflict of Interest Statement: The authors declare that the research was conducted in the absence of any commercial or financial relationships that could be construed as a potential conflict of interest.

Copyright © 2018 Shiromizu and Jancic. This is an open-access article distributed under the terms of the Creative Commons Attribution License (CC BY). The use, distribution or reproduction in other forums is permitted, provided the original author(s) and the copyright owner(s) are credited and that the original publication in this journal is cited, in accordance with accepted academic practice. No use, distribution or reproduction is permitted which does not comply with these terms.

frontiers in Immunology

ORIGINAL RESEARCH
published: 23 October 2018
doi: 10.3389/fimmu.2018.02443

Phenotype, Polyfunctionality, and Antiviral Activity of *in vitro* Stimulated CD8$^+$ T-Cells From HIV$^+$ Subjects Who Initiated cART at Different Time-Points After Acute Infection

Jimena Salido[1], *María Julia Ruiz*[1†], *César Trifone*[1], *María Inés Figueroa*[2], *María Paula Caruso*[1], *María Magdalena Gherardi*[1], *Omar Sued*[2], *Horacio Salomón*[1], *Natalia Laufer*[1,3], *Yanina Ghiglione*[1] *and Gabriela Turk*[1*]

[1] Consejo Nacional de Investigaciones Científicas y Técnicas (CONICET)-Universidad de Buenos Aires, Instituto de Investigaciones Biomédicas en Retrovirus y Sida (INBIRS), Buenos Aires, Argentina, [2] Fundación Huésped, Buenos Aires, Argentina, [3] Hospital General de Agudos "Dr. JA Fernández," Buenos Aires, Argentina

OPEN ACCESS

Edited by:
Gustavo Javier Martinez,
Rosalind Franklin University of Medicine and Science, United States

Reviewed by:
Sunil Joshi,
University of Miami, United States
Masaaki Miyazawa,
Kindai University, Japan

***Correspondence:**
Gabriela Turk
gturk@fmed.uba.ar

†Present Address:
María Julia Ruiz,
Centre de Recherche du Centre Hospitalier de l'Université de Montréal, Montréal, QC, Canada

Specialty section:
This article was submitted to Microbial Immunology, a section of the journal Frontiers in Immunology

Received: 24 July 2018
Accepted: 02 October 2018
Published: 23 October 2018

Citation:
Salido J, Ruiz MJ, Trifone C, Figueroa MI, Caruso MP, Gherardi MM, Sued O, Salomón H, Laufer N, Ghiglione Y and Turk G (2018) Phenotype, Polyfunctionality, and Antiviral Activity of in vitro Stimulated CD8$^+$ T-Cells From HIV$^+$ Subjects Who Initiated cART at Different Time-Points After Acute Infection. Front. Immunol. 9:2443. doi: 10.3389/fimmu.2018.02443

Since anti-HIV treatment cannot cure the infection, many strategies have been proposed to eradicate the viral reservoir, which still remains as a major challenge. The success of some of these strategies will rely on the ability of HIV-specific CD8$^+$ T-cells (CD8TC) to clear reactivated infected cells. Here, we aimed to investigate the phenotype and function of *in vitro* expanded CD8TC obtained from HIV$^+$ subjects on combination antiretroviral therapy (cART), either initiated earlier (median = 3 months postinfection, ET: Early treatment) or later (median = 20 months postinfection, DT: Delayed treatment) after infection. Peripheral blood mononuclear cells from 12 DT and 13 ET subjects were obtained and stimulated with Nef and Gag peptide pools plus IL-2 for 14 days. ELISPOT was performed pre- and post-expansion. CD8TC memory/effector phenotype, PD-1 expression, polyfunctionality (CD107a/b, IFN-γ, IL-2, CCL4 (MIP-1β), and/or TNF-α production) and antiviral activity were evaluated post-expansion. Magnitude of ELISPOT responses increased after expansion by 10^3 times, in both groups. Expanded cells were highly polyfunctional, regardless of time of cART initiation. The memory/effector phenotype distribution was sharply skewed toward an effector phenotype after expansion in both groups although ET subjects showed significantly higher proportions of stem-cell and central memory CD8TCs. PD-1 expression was clustered in HIV-specific effector memory CD8TCs, subset that also showed the highest proportion of cytokine–producing cells. Moreover, PD-1 expression directly correlated with CD8TC functionality. Expanded CD8TCs from DT and ET subjects were highly capable of mediating antiviral activity, measured by two different assays. Antiviral function directly correlated with the proportion of fully differentiated effector cells (viral inhibition assay) as well as with CD8TC polyfunctionality and PD-1 expression (VITAL assay). In sum, we show that, despite being dampened in subjects on cART, the HIV-specific CD8TC response could be selectively stimulated and expanded *in vitro*, presenting a high

proportion of cells able to carry-out multiple effector functions. Timing of cART initiation had an impact on the memory/effector differentiation phenotype, most likely reflecting how different periods of antigen persistence affected immune function. Overall, these results have important implications for the design and evaluation of strategies aimed at modulating CD8TCs to achieve the HIV functional cure.

Keywords: HIV functional cure, expanded CD8$^+$ T-cell response, polyfunctionality and phenotype, antiviral activity, time of cART initiation

INTRODUCTION

Infection with Human Immunodeficiency Virus (HIV) causes an irreversible and profound deterioration of the immune system as well as abrogated T cell homeostasis, ultimately leading to the development of acquired immunodeficiency syndrome (AIDS) in the vast majority of infected persons. Despite dramatic advances made over the past three decades, it still constitutes a major public health concern worldwide. Following virus transmission, acute/early phase of infection is characterized by a high-level peak of viremia, rapid loss of CD4$^+$ T-cells in both peripheral blood and mucosal lymphoid tissues, and clinical symptoms (1–3). Emergence of HIV-specific CD8$^+$ T-cell response is associated with the drop of plasma viremia to a stable level, known as the viral set-point (4).

Since the implementation of combination antiretroviral therapy (cART), AIDS-associated death rates have decreased drastically, and morbidity and mortality of HIV$^+$ subjects have been considerably reduced (with a concomitant improvement in their quality of life). Besides, transmission risks have diminished (with an impact on the global epidemic dynamics) (5). cART can quickly and persistently suppress viral replication but, if treatment is interrupted, plasma viral load (VL) rapidly increases (6, 7). The failure to eradicate HIV infection is due to the intrinsic stability of the viral genome in latently infected CD4$^+$ T-cells and also other long-lived cells (8). Consequently, cART is currently a lifelong treatment with some limitations: the need of daily doses, the development of viral resistance, toxicity, and the impossibility to clear the infection. Moreover, even effectively treated HIV-infected individuals have a greater risk of experiencing non-AIDS related morbidity and mortality events than age-matched HIV-uninfected adults (including accelerated immune aging, higher cardiovascular risk, coagulopathies and other metabolic disorders), indicating that even effective cART cannot fully restore health (9). In this line, the idea of developing a cure for HIV infection has gained intense interest over the last years; this is the development of a therapeutic intervention or approach that controls (functional cure or long-term remission in the absence of cART) or eliminates (sterilizing cure) HIV infection (3, 10). To pursue this objective, several strategies are being investigated as reviewed in Deeks et al. (3) and Pitman et al. (11). Many of these strategies, such as the "shock and kill" model, require the preexistence of cellular responses being able to actively clear reactivated and/or persistent virus. However, CD8$^+$ T-cell responses are severely waned in subjects on cART, limiting thus these approaches (12).

During the natural course of infection, HIV-specific CD8$^+$ T-cells play a central role in the control of viral replication, particularly during acute infection (2, 4, 12). In this setting, our group has provided evidence regarding different qualitative aspects of the response (specificity, functionality, and phenotype) that better associate with virus control in an acute infection cohort from Argentina (13, 14). Progressive infection is characterized by the presence of a narrow, oligofunctional and exhausted cellular response. As subjects initiate cART, the magnitude of the CD8$^+$ T-cell response declines rapidly (15–20) though some publications have demonstrated that the remaining cells still possess antiviral functions (21–23). Importantly, it has been recently illustrated in a non-human primate model that CD8$^+$ T-cells might have a role in controlling viral production even on cART (24). Moreover, some studies have indicated that CD8$^+$ T-cells still exert selective pressure in subjects on cART, suggesting that this response might be acting on viral residual replication as reviewed in McIlroy (25). Finally, different attributes of the CD8$^+$ T-cell response have been related to the reservoir size once the subjects are on treatment (26–30). However, cART interruption leads to rapid viral rebound, indicating that control mediated by CD8$^+$ T-cells is temporal and inefficient (31).

Thus, the success of the strategies aimed at eliminating the viral reservoir using HIV-specific memory CD8$^+$ T-cells that persist after cART initiation will require refined knowledge about the functional and phenotypic properties of these cells. Here, we aimed to investigate the phenotype and function of *in vitro* expanded CD8$^+$ T-cells from HIV$^+$ subjects on cART who initiated treatment either early or late after infection. Results indicated that HIV-specific cells can be selectively stimulated and expanded *in vitro*, presenting a high proportion of cells able to carry out multiple effector functions. On the contrary, cART initiation timing had an impact on the memory/effector differentiation phenotype. Despite this, expanded cells from both groups had potent antiviral activity. Thus, we propose that despite differences in the duration of antigen persistence, HIV-specific CD8$^+$ T-cells remain detectable and functional but should be boosted in order to support viral clearance.

MATERIALS AND METHODS

Study Subjects

Twenty-five HIV$^+$ subjects were enrolled during acute/early infection and followed up longitudinally as part of the *Grupo*

Argentino de Seroconversión study group. Enrollment criteria were described elsewhere (32, 33). Twelve subjects initiated cART after 4 months since the estimated date of infection (from now on Delayed Treatment (DT) group), and 13 initiated cART within 4 months post-infection (Early Treatment group, ET). For this study, samples were collected from study participants at ∼12 months post-cART initiation.

This study was reviewed and approved by two institutional review boards: *Comité de Bioética Humana, Fundación Huésped*, and *Comité de Ética Humana, Facultad de Medicina, Universidad de Buenos Aires,* Buenos Aires, Argentina. All participants provided written informed consents and agreed to participate in this study in line with the Declaration of Helsinki.

Samples

Forty ml of whole blood were collected from study participants, centrifuged to separate plasma, and stored at −80°C. Peripheral blood mononuclear cells (PBMCs) were isolated by Ficoll-Hypaque density gradient centrifugation (Amersham, Sweden) and cryopreserved for subsequent functional assays. Plasma viral load (VL) was determined by branched-DNA, Versant HIV-1 RNA 3.0 assay (Siemens Healthcare, UK). $CD4^+$ and $CD8^+$ T-cell counts were determined using TruCount absolute-count tubes (BD Bioscences, USA) on a BD FACSCalibur flow cytometer.

Peptide Pools

Potential T-cell epitope (PTE) peptide panels corresponding to Nef (unique pool, $n = 127$ peptides) and Gag [2 pools: p17 ($n = 97$) and p24 ($n = 128$)] HIV proteins and the cytomegalovirus (CMV), Epstein-Barr virus, and influenza virus (CEF) peptide pool were obtained from the NIH AIDS Reagent Program (34, 35). Lyophilized peptides were dissolved in dimethyl sulfoxide (DMSO) at 40 μg/μl and stored at −20°C.

HIV-Specific $CD8^+$ T-Cell Expansion

Cryopreserved PBMCs were thawed in PBS (Sigma-Aldrich), 2% fetal bovine serum [FBS; Gibco BRL], and 1 mM EDTA supplemented with 25 U/ml DNase I (Benzonase nuclease; Sigma-Aldrich) and then rested overnight (ON) in DNase-free complete RPMI medium (RPMIc; RPMI 1640 [Gibco BRL], 10% fetal bovine serum [FBS; Gibco BRL], 2 mM L-glutamine [Gibco BRL], 100 U/ml penicillin [Gibco BRL], 100 μg/ml streptomycin [Gibco BRL], 10mM HEPES [Gibco BRL]). Rested PBMCs were cultured in 12-well plates at a density of 2–3 × 10^6 cells/ml in cRPMI medium supplemented with 100 U/ml IL-2 (Biolegend Inc, USA) and in the presence of 1 μg/ml of the corresponding HIV peptide pool or CEF peptide pools, for 14 days. Medium was replaced every 72 h with freshly-prepared cRPMI supplemented with IL-2. Expanded cells were subsequently studied by ELISPOT, flow cytometry, and antiviral activity assays (**Figure 1**).

ELISPOT Assay

Interferon gamma (IFN-γ)-secreting cells were evaluated by ELISPOT before and after HIV-specific $CD8^+$ T-cell expansion (pre-expansion, i.e., immediately after PBMC ON rest, and post-expansion) following the protocols published previously (13, 36, 37).

Flow Cytometry

$CD8^+$ T-cell phenotype and functionality were evaluated in 14-day expanded cells by flow cytometry as reported by our group, with modifications (13, 14, 38). Briefly, cells were re-stimulated with the designated peptide pool (same used for expansion, at 2 μg/ml) or DMSO (to account for background) plus costimulatory antibodies (anti-CD28 and anti-CD49d; 1 μg/ml; BD Biosciences), monensin (Golgistop, 0.7 μl/ml; BD Biosciences) and brefeldin A (10 μg/ml; BD Biosciences) for 5 h at 37°C. Anti-CD107a/b-FITC antibodies (BD Biosciences) were also added to identify degranulating cells. For the functionality panel, cells were stained upon stimulation with Zombie NIR™ Fixable Viability Kit (Biolegend, USA), and the following conjugated antibodies: anti-CD14-V450, anti-CD19-V450, anti-CD3-BV786, anti-CD8-APC, and anti-CD4-BV650 (BD Biosciences). Then, cells were permeabilized (Permeabilization Wash Buffer, Biolegend), fixed (Fixation Buffer, Biolegend), and subsequently stained using anti-IL-2–PerCP-Cy5.5, anti-TNF-α-PECy7, anti-IFN-γ-BV711, and anti-CCL4-PE conjugated antibodies (BD Biosciences).

In parallel, $CD8^+$ T-cell memory phenotype was studied. Cells were shortly stimulated as described above and afterwards stained with Zombie NIR™ Fixable Viability Kit plus the following conjugated antibodies: anti-CCR7-Alexa700, anti-PD-1-PE, anti-CD3-BV786, anti-CD8-APC, anti-CD4-BV650, anti-CD14-V450, anti-CD19-V450, anti-CD45RO-PerCPCy5.5, and anti-CD95-PE-CF594 (BD Biosciences, USA). Then, cells were permeabilized, fixed and stained with anti-IL-2, anti-TNF-α, and anti-IFN-γ antibodies, all of them conjugated to FITC (BD Biosciences) to identify specific cells regardless of its function.

Flow cytometry data acquisition was performed on a 3-laser 14-color BD FACSAria FUSION flow cytometer using the BD FACSDiva v 8.0.1 software (BD Biosciences). Instrument settings and fluorescence compensation were performed using unstained samples and single stained BD CompBeads (BD Bioscience). Isotype controls, consisting of expanded, stimulated cells stained with conjugated antibodies to CD14, CD19, CD3, CD4, and CD8 surface molecules plus the isotype controls corresponding to the CCR7, CD45RO, CD95, PD-1, and/or the corresponding intracellular marker staining, were performed for each individual in order to set negative populations accurately.

Acquired data was analyzed using FlowJo v10 (Data Analysis Software, LLC). Gating strategy was performed as shown in **Figure S1**. First, single cells were selected in a forward scatter area (FSC-A) vs. FSC-Height plot. Then, dead cells were excluded on the bases of Zombie NIR™ fluorescence and monocytes as well as B lymphocytes were also excluded on the bases of V450 fluorescence (CD14 and CD19 staining). Subsequently, the lymphocyte population was selected in a FSC-A vs. side scatter (SSC) plot. Samples with at least 100,000 events in the lymphocyte gate were included in subsequent analyses. Finally, $CD3^+$ $CD8^+$ (or $CD4^+$) cells were gated in CD3-vs.-CD8 (or CD4) dot plots.

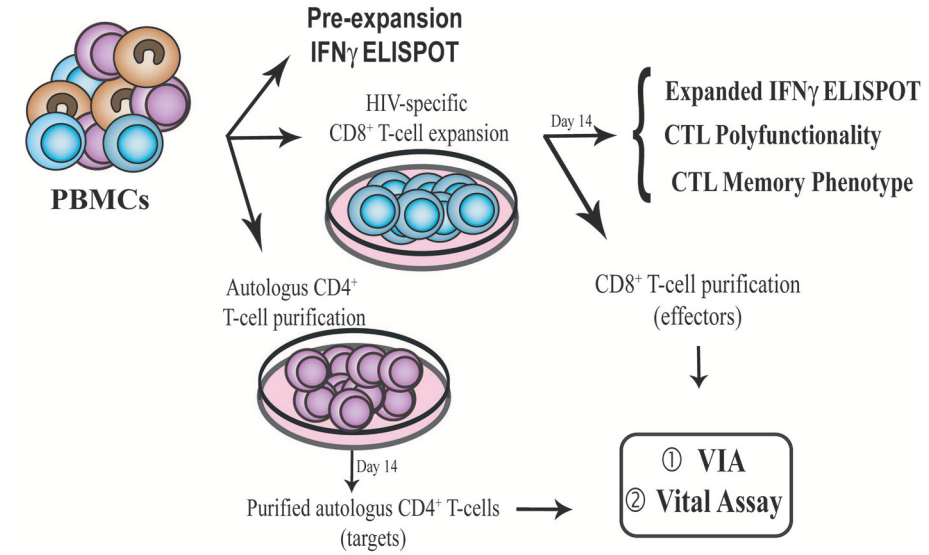

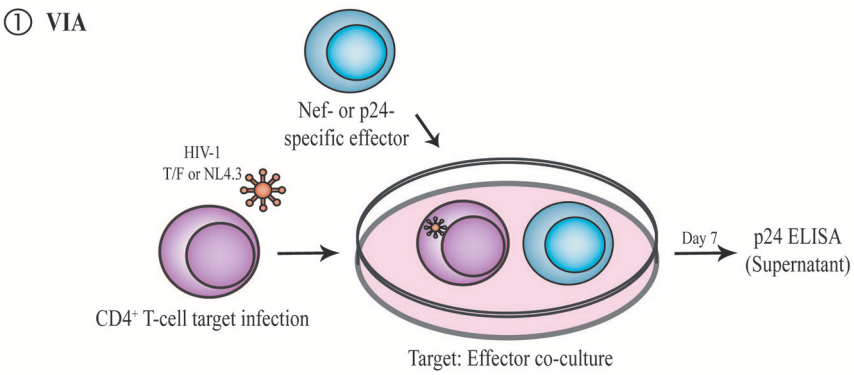

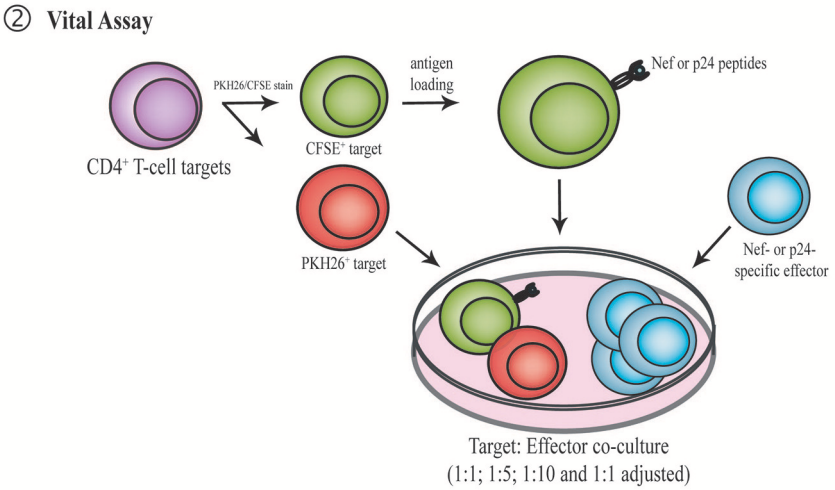

FIGURE 1 | Schematic representation of the experimental design. PBMC samples were obtained from enrolled subjects. First, IFN-γ ELISPOT was performed directly *ex vivo* (pre-expansion). PBMCs were then expanded for 14 days in the presence of Nef or p24 peptide pool, generating Nef-specific and p24-specific effector. At day 14, IFN-γ ELISPOT, $CD8^+$ T-cell polyfunctionality and $CD8^+$ T-cell phenotype (CCR7, CD45RO, CD95, and PD-1) were evaluated by flow cytometry. Expanded $CD8^+$ T-cells were also purified and used as effectors in the VIA (1) and VITAL (2) assays. In parallel, autologous $CD4^+$ T-cells were purified with CD3.8 bispecific antibodies to generate $CD4^+$ target cells. See M&M for further details. PBMC, Peripheral blood mononuclear cells; VIA, Viral inhibition assay; CTL, $CD8^+$ T-lymphocyte.

To study $CD8^+$ T-cell polyfunctionality, CD8 vs. CD107a/b, IFN-γ, IL-2, CCL4, or TNF-α plots were constructed. After the gates for each function were created, the Boolean gate platform was used to create the full array of obtainable combinations, equating to 32 possible combinations. Data presented correspond to background-subtracted results using the DMSO plus CD28/CD49d stimulation. This was performed on a cytokine-subset-by-cytokine-subset basis, i.e., subtracting the result from this condition for a given cytokine subset to the same subset of a peptide-stimulated condition. One standard deviation (SDs) above background was set as the threshold for determining positive responses. Values below this threshold were set at 0.

For phenotype analysis, HIV-specific $CD8^+$ T-cells were identified in a CD8 vs. FITC plot (CD107a/b, IFN-γ, IL-2, CCL4, and TNF-α). A positive cytokine response was defined as at least twice the background value, >0.05% after subtraction of background and at least 1,000 events. This criterion was established to minimize the possibility of error due to a low number of events when further subdividing these cells into the different memory subsets. To analyze the distribution of the different phenotype subsets, CD45RO vs. CCR7 density plots were constructed on both bulk and HIV-specific $CD8^+$ T-cells to identify central memory T-cells (T_{CM}, $CCR7^+/CD45RO^+$), effector memory T-cells (T_{EM}, $CCR7^-/CD45RO^+$), and terminal effector T-cells (T_{TE}, $CCR7^-/CD45RO^-$). CD95 expression was analyzed within the $CD45RO^-CCR7^+$ cells thus defining naïve T-cells (T_N, $CCR7^+/CD45RO^-/CD95^-$) and stem-cell memory T-cells (T_{SCM}, $CCR7^+/CD45RO^-/CD95^+$). Additionally, PD-1 expression was studied both on bulk (total and also within each memory subpopulations) and HIV-specific $CD8^+$ T-cells.

$CD8^+$ T-Cell Antiviral Activity

Antiviral activity of expanded $CD8^+$ T-cells was evaluated by two different assays (**Figure 1**): The Viral Inhibition Assay [VIA, (13, 39, 40)] and the VITAL assay [adapted from Hermans et al. (41)]. In the former, both cytolitic and non-cytolitic mechanisms of viral inhibition are accounted while in the latter direct cell-mediated toxicity is measured. For both assays, target (autologous $CD4^+$ T-cells) and effector (expanded $CD8^+$ T-cells) were prepared following the same procedure:

Generation and Isolation of Expanded Nef- and p24-Specific Effector $CD8^+$ T-Cells

PBMCs were thawed and stimulated with either peptide pools spanning Nef or p24 proteins as stated above (day 0). At day 13 post-expansion and after a 5-h short re-stimulation (as described previously), percentages of cytokine-producing cells and degranulating cells (i.e., total HIV-specific cells) were assessed by flow cytometry. At day 14, expanded $CD8^+$ T-cells were isolated by positive selection using Anti-Human CD8 Magnetic Particles (BD Biosciences).

Generation of Autologous $CD4^+$ T-Cell Targets

PBMCs were thawed and cultured in cRPMI medium supplemented with 50 U/ml IL-2 plus 0.5 μg/ml CD3/8 bi-specific antibody (obtained through the NIH AIDS Reagent Program, Division of AIDS, NIAID, NIH: Anti-Human CD3/8 Bi-specific Monoclonal from Drs. Johnson Wong and Galit Alter). PBMC treatment with CD3/8 bi-specific antibody results in the elimination of $CD8^+$ T-cells and purification of activated $CD4^+$ T-cells. To determine purity, expanded $CD4^+$ T-cell were stained with Zombie viability kit, anti-CD3-PECy7, anti-CD4-PerCP, and anti-CD8-BV510 at day 13. In all cases, 90% purity was achieved.

Viral Inhibition Assay (VIA) (Figure 1)

Target cells (purified and activated $CD4^+$ T-cells) were infected in parallel with 4 different viral strains: an X4-tropic laboratory strain (NL4-3) and three HIV-1 clade B transmitted/founder (T/F) primary viruses selected from the full panel of T/F Infectious Molecular Clones available at the NIH AIDS Reagent program (Division of AIDS, NIAID, NIH: Cat #11742 (X4-tropic T/F virus, from now on Virus 4, V4), cat #11746 (R5-tropic T/F virus obtained after an event of heterosexual transmission, from now on Virus 8, V8), and Cat #11749 (R5-tropic T/F virus obtained after an event of male-to-male transmission, from now on Virus 9, V9) from Dr. John Kappes (42–45). Pseudotyped viral stocks were produced by co-transfecting 293T cells with the corresponding HIV plasmid together with a plasmid encoding the Vesicular Stomatitis Virus (VSV) protein G, using the X-treme GENE 9 DNA transfection reagent (Roche, Switzerland). Culture supernatants were harvested 48 h post-transfection clarified by centrifugation at 600 g for 15 min at 4°C, fractioned and stored at −80°C until use. Viral titer was estimated by p24 antigen quantitation by ELISA (Sino Biological Inc., China).

Viruses were added to target cells at 15 ng p24/100,000 $CD4^+$ T-cells. In order to improve infection efficiency, plates were first centrifuged at 1,200 g for 1 h at 22°C (spinoculation), and then viral adsorption was let to proceed for an extra hour at 37°C in a humidified CO_2 incubator. After infection, cells were washed twice and co-cultured at 1:1 ratio with purified expanded Nef-specific or p24-specific $CD8^+$ T-cells (effectors) in U-bottom 96-well plates, in cRPMI medium containing 10 U/ml IL-2. Infectivity controls consisted of infected $CD4^+$ T-cell targets without $CD8^+$ T-cell effectors. Uninfected controls consisted of uninfected target cells without effectors. All conditions were assayed in triplicate. At day 4 post-infection, half of the culture supernatant was removed and replenished with fresh medium. At day 7, supernatants were collected and stored at −20°C until p24 antigen quantitation by ELISA. $CD8^+$ T-cell anti-HIV suppressive capacity was calculated as the $\log_{10}$ of the percentage of p24 antigen loss when $CD8^+$ T-cells were present in the culture compared to $CD4^+$ T-cell infected controls without effectors, for each virus.

In vitro Cell Killing Assay (VITAL Assay, Figure 1)

2×10^6 cells/ml target cells (purified and activated $CD4^+$ T-cells) were first stained with 1 μM of CFSE (Molecular Probes, USA) at 37°C for 8 min, followed by the addition of an equal volume of FBS to quench the reaction. After CFSE staining, cells were loaded with peptide antigens by incubation for 2 h in cRPMI supplemented with 2 μg/ml of either Nef or p24 peptide pool. In parallel, untreated $CD4^+$ T-cells (i.e., not loaded

with peptides) were labeled with 2 μM PKH26 red fluorescent cell linker (Sigma-Aldrich, USA). Peptide-loaded $CFSE^+$ and unloaded $PKH26^+$ cells were extensively washed, combined and plated in U-bottomed 96-well plates at 5×10^4 cells of each fluorescent population per well. Nef- or p24-specific effector cells were added to the corresponding wells at the indicated target-to-effector (T:E) ratios (1:1, 1:5, 1:10 and 1:1 adjusted [i.e., 1:1 ratio adjusted to proportion of specific $CD8^+$ T-cell effectors as determined by intracellular staining and flow cytometry]), in triplicate. Following overnight incubation at 37°C, cells were stained with Zombie Viability Kit and anti-CD3-PECy7, anti-CD4-PerCP, and anti-CD8-BV510 antibodies, and analyzed in a 2-laser, 8-color BD FACSCanto flow cytometer. Data acquisition was performed using the BD FACSDiva software and analyzed subsequently with FlowJo v10 software (Data Analysis Software, LLC). Initial gating was performed in a FSC-A *vs*. FSC-H plot to exclude doublets, and then lymphocytes were selected in a FSC-H vs. SSC-A plot. Subsequently, Zombie- negative cells (i.e., living cells) were gated. Then, $CD3^+CD4^+$ cells were selected and the analysis was performed on this population. CFSE vs. PKH26 plots were constructed, and cell survival of antigen-loaded targets cells (CFSE-positive) in the presence of effectors was determined compared to conditions without effector cells. Adjusted survival was calculated as the mean percentage of $CFSE^+$ events with added effector *vs*. the condition with no effectors. Finally, the percentage of specific lysis was calculated using the equation: %specific lysis: 100—%adjusted survival.

Data Analysis

The presumed date of infection was estimated as reported previously (32, 33). Date of cART initiation was informed by clinicians. Most data was expressed as median values with interquartile ranges (25 to 75%, IQ25-75) and analyzed by nonparametric methods using GraphPad Prism 7 software, unless otherwise stated. Inter- and intra-group comparisons were performed using Mann-Whitney and Wilcoxon tests, respectively. Correlation analyses were performed using the Spearman's rank test. In this case, *p*-values were adjusted for multiple comparisons using a false discovery rate (FDR) procedure, according to the Benjamini and Hochberg method, using the GraphPad Prism 7 software.

For the polyfunctionality analysis and cell phenotype data sets generated by flow cytometry, SPICE 6.0 software (https://niaid.github.io/spice/) was used following the experimental and technical considerations published by the software developers (46). In particular, Student's *t*-test and a partial permutation test were used to compare distribution profiles between groups.

All tests were considered significant when the *p*-value was <0.05. Adjusted *p*-values for correlation analyses were considered significant when <0.1.

RESULTS

Study Subjects

Twenty-five HIV^+ subjects were enrolled during acute/early HIV infection (within 6 months from presumed date of infection) and followed up for over at least 1 year after cART initiation. Subjects were segregated into two subgroups according to cART initiation timing. A 4-month post-presumed date of infection cut-off was selected based on the fact that $CD8^+$ T-cells are key players in viral set point establishment, which is usually reached around 4 months post-infection (2, 47). Thus, the responses evaluated would represent pre- and post-set-point scenarios. Delayed Treatment group (DT; 12 subjects) included subjects who initiated treatment after 4 months from presumed date of infection (median time to cART initiation = 20 months, [Interquartile range IQ25-75: 9.5–24.25 months]) while Early Treatment group (ET; 13 subjects) included subjects who started cART within 4 months post-presumed date of infection (median time to cART initiation = 3 months [IQ 25–75: 2–3.5 months]). All samples used for the study were obtained at ∼1 year after treatment initiation (DT: median time on cART = 13 months [IQ25-75: 5.75–18 months]; ET: median = 14 months [IQ25-75: 12–16.5 months]). Detailed descriptions of participants are shown in **Table 1**.

Median pre-treatment plasma VL was significantly higher in ET compared to DT (283,441 RNA copies [IQ25-75: 31,443–500,000] and 38,407 RNA copies/ml [IQ 25-75: 11,349–122,260], respectively; $p = 0.0207$). This reflects the fact that DT individuals already reached the VL set point by the moment of cART initiation while ET individuals had not reached that stage yet. All samples obtained after cART initiation and used for this study had undetectable plasma VL (lower limit of detection 50 RNA copies/ml).

Pre-treatment $CD4^+$ T-cell counts and CD4/CD8 ratios did not differ between groups (DT: median $CD4^+$ T-cell count = 370 cells/μl [IQ25-75: 290.3–450.8], Median CD4/CD8 ratio = 0.45 [IQ25-75: 0.33–0.66]. ET: median $CD4^+$ T-cell count = 435 cells/μl [IQ25-75: 334.5–640.5], Median CD4/CD8 ratio= 0.33 [IQ25-75: 0.18–0.68]). Both groups experienced significant improvements in both parameters by 1 year after cART initiation compared to the pre-cART determination (DT: median $CD4^+$ T-cell count=549 cells/μl [IQ25-75: 506.8–732], $p = 0.002$; median CD4/CD8 ratio = 0.755 [IQ25-75: 0.67–1.26], $p = 0.0005$; ET: median $CD4^+$ T-cell count = 829 cells/μl [IQ25-75: 625.5–1053], $p = 0.0005$; median CD4/CD8 ratio = 1.32 [IQ25-75: 0.89–1.74], $p = 0.0002$). Moreover, both $CD4^+$ T-cell count and CD4/CD8 ratio evaluated on-cART were significantly higher in ET vs. DT ($p = 0.025$ and $p = 0.014$, respectively), mirroring a poorer $CD4^+$ T-cell recovery in DT after a longer period prior cART initiation.

HIV-Specific T-Cells From DT and ET Subjects on cART Could Be Equally Expanded *in vitro*

Based on the notion that HIV-specific $CD8^+$ T-cell frequency decays significantly following cART initiation, and that the median half-life for the rate of decay is around 40 weeks (16), we first evaluated whether HIV-specific $CD8^+$ T-cells from DT and ET subjects after 1 year of cART could be expanded in an *in vitro* model. For this, PBMCs were stimulated with HIV peptide pools spanning Nef and Gag (sum of anti-p24 and p17 responses) proteins or the control CEF pool; plus IL-2 for 14 days and specific responses were evaluated pre- and post-expansion by

TABLE 1 | Clinical data corresponding to HIV$^+$ subjects enrolled per study group.

ID[a]	Time to cART (months)[b]	Time on cART (months)[c]	Pre-treatment Viral Load[d,e]	CD4 count		CD4/CD8	
				Before cART[d,f]	On cART[f,g]	Before cART[d,f]	On cART[f,g]
DT1	50	22	48526	383	524	0.72	1.35
DT2	22	18	132317	324	297	0.46	0.52
DT3	8	18	125716	391	711	0.48	0.65
DT4	11	5	27244	465	535	0.45	0.74
DT5	25	5	4612	408	739	0.48	1.00
DT6	19	15	66929	246	501	0.24	0.62
DT7	50	5	15297	330	468	0.42	0.77
DT8	5	12	>500000	279	528	0.26	0.72
DT9	21	14	28288	184	579	0.30	0.88
DT10	13	20	1702	357	563	0.44	0.72
DT11	22*	12	10033	819	819	0.88	1.36
DT12	9	8	111893	629	880	0.85	1.53
ET1	2	14	>500000	627	594	0.66	0.89
ET2	4	18	283441	187	522	0.20	0.88
ET3	1	11	36338	768	1099	1.18	1.83
ET4	3	14	17292	612	1342	0.33	1.32
ET5	3	15	20106	787	829	1.06	1.69
ET6	2	18	>500000	421	854	0.31	1.89
ET7	1	13	>500000	435	942	0.13	1.52
ET8	3	12	172468	435	657	0.59	1.16
ET9	3	17	26547	400	728	0.70	1.79
ET10	3*	11	231360	330	1080	0.18	1.24
ET11	2	12	>500000	654	1026	0.42	1.47
ET12	4	16	>500000	339	691	0.08	0.66
ET13	4	12	>500000	213	386	0.19	0.81

[a] *DT, Delayed Treatment Group; ET, Early Treatment Group.*
[b] *Relative to the presumed date of infection.*
[c] *Time from the moment of cART initiation to sample obtaining.*
[d] *Determinations evaluated at the closest sample obtained before cART initiation.*
[e] *Versant HIV-1 RNA 3.0 assay, Siemens. Lower and upper detection limits are 50 and 500,000 RNA copies/ml, respectively (1.7 and 5.7 log_{10}).*
[f] *Determined by flow cytometry.*
[g] *Determinations evaluated in samples used in this study.*
[*] *Estimated time to cART initiation, as informed by the clinician.*

ELISPOT (**Figure 2A**). Median pre-expansion responses found in DT were 30 SFU/10^6 PBMC (IQ25-75 25–65) for Nef, 107.5 (58.75–257.5) for Gag and 147.5 (51.25–366.3) for CEF peptides. No significant differences were found when comparing pre-expansion DT responses with those evaluated in ET, which were as follows: 25 (25–55) for Nef, 40 (25–346.3) for Gag, and 117.5 (25–495) for CEF peptides. After expansion, responses to all antigens tested were significantly increased in both study groups (by 10^3 times) and were predominantly mediated by CD8$^+$ T-cells, as observed later by flow cytometry (as explained below) which is consistent with higher representation of MHC-class I restricted peptides within the PTE peptide pools. Post-expansion magnitude in DT was 9,390 SFU/10^6 PBMC (IQ25–75 2,800–255,455) for Nef ($p = 0.0039$, compared to the pre-expansion condition), 7,700 (3,415–507,893) for Gag ($p = 0.002$) and 253,155 (617.5–500,000) for CEF ($p = 0.0176$). Similarly, post-expansion magnitude in ET was 2,110 (441.3–5,900) for Nef ($p = 0.0005$), 3,105 (1,365–4,578) for Gag ($p = 0.0005$) and 8,740 (940–500,000) for CEF ($p = 0.0005$). No differences were observed between DT and ET, for any of the antigen used. Then, the relative contribution of each antigen to the total post-expansion anti-HIV response was analyzed to provide an image of the response breadth for both groups (**Figure 2B**). DT individuals showed an even contribution of anti-Nef, p17 and p24 responses to the total HIV response. Although the distribution was not different from ET ($p = 0.1786$), it is worth highlighting that ET showed a lower contribution of anti-p17 responses and a higher contribution of anti-Nef responses, resulting globally in a narrower response mostly directed toward Nef and p24. Moreover, no differences were found when comparing the pre- and post-expansion distribution intragroups (not shown). Finally, the mean spot size was recorded

in both pre- and post-expansion conditions as a measure of the amount of IFN-γ produced by the individual specific T-cells (**Figure 2C**). Mean spot size significantly increased after expansion with all antigens tested. No significant differences were observed between DT and ET subjects. In sum, the magnitude of HIV-specific cellular responses could be equally expanded *in vitro* both in DT and ET subjects, and cells showed higher potential to secrete IFN-γ after stimulation. Of note, this parameter has been associated with higher T-cell avidity and a polyfunctional profile (13, 48, 49). Finally, DT subjects displayed a broader response to HIV peptide pools after expansion than ET subjects.

Polyfunctionality of Expanded CD8$^+$ T-Cells Is Not Conditioned by cART Initiation Timing

T-cell polyfunctionality has been largely considered an important metric reflecting the quality of the T-cell response (50). Thus, the capacity to degranulate (evaluated by the mobilization of CD107a/b to the plasma membrane) and to produce IFN-γ, IL-2, CCL4 (MIP-1β), and TNF-α was evaluated post-expansion by flow cytometry (gating strategy is shown in **Figure S1**). From this point forward, only CD8$^+$ T-cells expanded with Nef and p24 peptide pools were analyzed. p17-specific cells were excluded because, in this model, they proved limited expansion potential. It was observed that, as aforementioned, CD8$^+$ T-cells were preferentially expanded in our model, and CD4$^+$ T-cells represented only a small proportion of cells after expansion (data not shown). When analyzing CD8$^+$ T-cells expressing each of the functions either alone or in combination, and in consonance with the ELISPOT results, it was first noted that the proportion of responsive cells was much higher than that found when evaluating this parameter directly *ex vivo* (13, 14, 51). This finding is in line with the specific proliferation and survival of HIV-specific cells after the *in vitro* expansion. No significant differences were observed between DT and ET subjects either when polyfunctionality was analyzed as a whole or when functions were analyzed individually or combined (**Figure 3A**). Then, the same analysis was performed but splitting the responses toward the different HIV antigens and CEF (**Figure 3B**). In this case, total proportion of mono, bi, tri, tetra, and pentafunctional cells were analyzed independently of any particular function due to the low number of positive responses when fragmenting the analysis. By doing this, no differences were observed in the polyfunctional profile of expanded Nef-specific, p24-specific, even in CEF-specific CD8$^+$ T-cells obtained from ET. Only a non-significant reduction in the proportion of pentafunctional Nef-specific and p24-specific cells was observed when compared to CEF-specific cells from the same group. Conversely, expanded p24-specific CD8$^+$ T-cells from DT subjects showed an enrichment of monofunctional cells compared to Nef-specific ($p = 0.042$) and CEF-specific ($p = 0.16$) cells. Overall, expanded HIV-specific CD8$^+$ T-cells from DT and ET subjects showed a polyfunctional response comparable to CEF-specific responses, with high proportions of tetra and pentafunctional cells.

Time to cART Initiation Impacts on CD8$^+$ T-Cell Memory/Effector Phenotype Distribution Post-expansion

Cell phenotype was then evaluated by flow cytometry (**Figure S1**). Distribution of naïve (T_N), stem-cell memory (T_{SCM}), central memory (T_{CM}), effector memory (T_{EM}), and terminal effector (T_{TE}) T-cells was studied both on bulk and HIV-specific CD8$^+$ T-cells. In addition, expression of PD-1 was monitored. As expected, the general memory phenotype distribution was sharply skewed toward an effector phenotype after expansion. When analyzing the distribution of memory phenotype within the bulk CD8$^+$ T-cell compartment, the following hierarchy emerged in both groups: $T_{TE} > T_{EM} > T_{SCM} > T_{CM} > T_N$ (**Figure 4A**). However, the global distribution was significantly different between DT and ET ($p = 0.0051$) driven by intergroup differences in the proportion of various sub-populations: ET subjects showed significantly higher proportions of T_{SCM} (median % 11.93 vs. 4.21, $p = 0.003$) and T_{CM} (median % 1.9 vs. 1.00, $p = 0.016$) subsets, and significantly lower proportions of T_{TE} (median % 44.35 vs. 73.70, $p = 0.003$). Percentages of T_N cells were minimum in both groups (0.22 and 0.64% in DT and ET, respectively). Within the HIV-specific compartment, T_{EM} and T_{TE} were exclusively found among cells from DT while in ET subjects T_{SCM} and T_{CM} were also observed. The same pattern was observed for Nef-specific and p24-specific responses as well as for the CEF-specific response when analyzed separately (**Figure 4B**). In this case, the differences observed were not statistically significant, most likely due to the reduced numbers of positive responses when the analysis was segregated across antigens.

Then, we sought to analyze PD-1 expression in expanded cells. First, it was observed that the PD-1 expression was markedly lower in expanded cells compared to previous studies in a similar population but measuring PD-1 expression directly *ex vivo* (not shown) (14, 52–54). No significant differences were observed in PD-1 expression either at the bulk or HIV-specific CD8$^+$ T-cells compartments, between DT and ET groups (**Figure 5A**). On the other hand, HIV-specific cells showed significantly higher PD-1 expression compared to the bulk compartment, both in DT ($p = 0.0268$) and ET ($p < 0.0001$) which is in consonance with previous observations in other settings (14, 55, 56). Then, the distribution of different memory/effector phenotypes was investigated within the PD-1$^+$ events (only for the bulk compartment) (**Figure 5B**). The global distribution of subsets was significantly different between groups ($p = 0.0339$), with DT subjects showing an increased representation of CD8$^+$ T_{TE} cells within the PD-1$^+$ events, compared to ET subjects ($p = 0.026$) who, in turn, showed higher proportions of T_{SCM} and T_{CM} CD8$^+$ PD-1$^+$ cells ($p = 0.023$ and $p = 0.013$, respectively). Subsequently, we aimed to analyze the PD-1 expression distribution along the different memory/effector phenotypes. Due to the reduced number of events within the T_N, $T_{SCM,}$ and T_{CM} subsets, this analysis could only be performed on the bulk CD8$^+$ T_{EM} and T_{TE} subsets. In both DT and ET subjects, PD-1 expression was significantly higher in T_{EM} compared to T_{TE} subsets (**Figure S2A**). Likewise, T_{EM} CD8$^+$ cells showed a

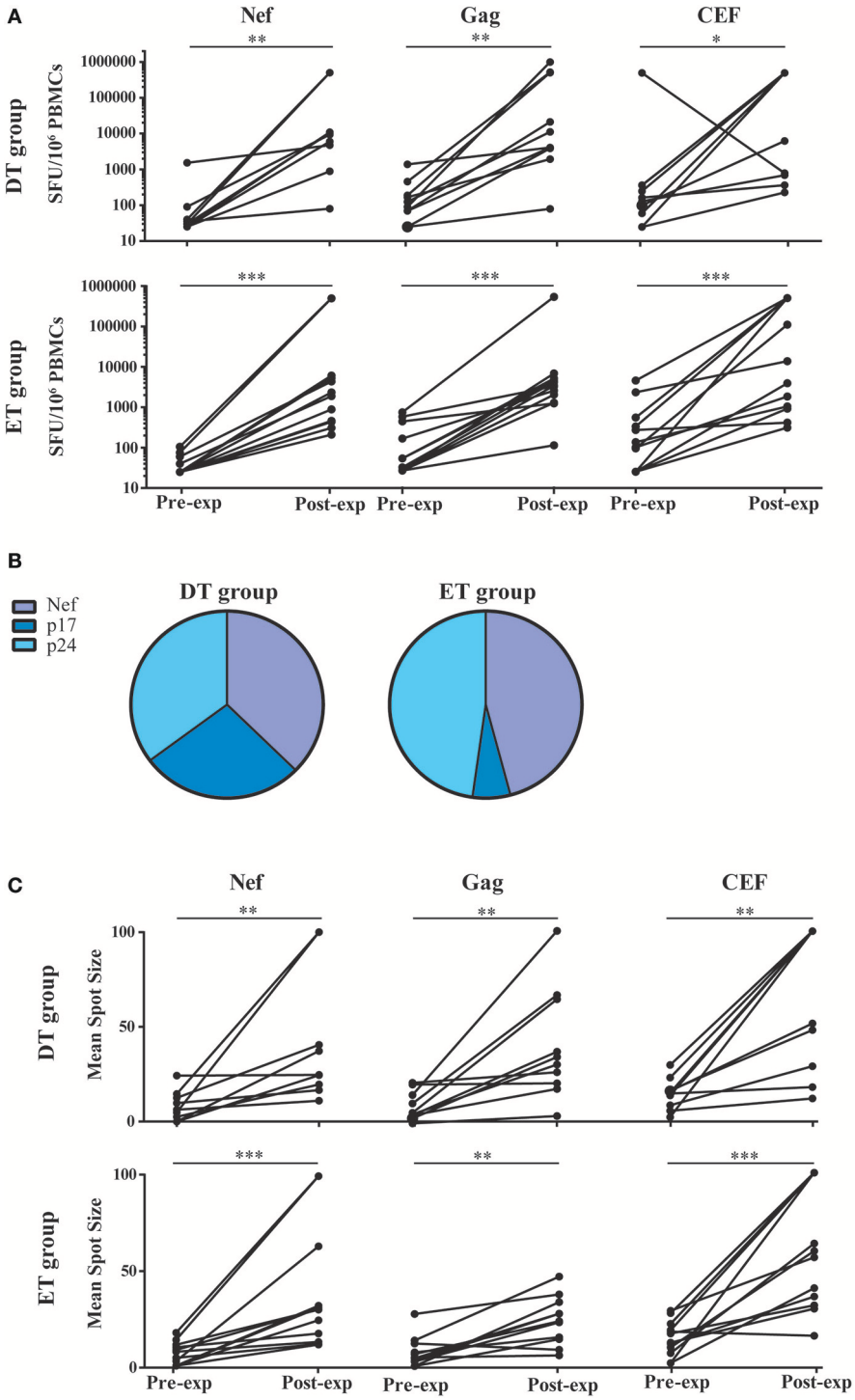

FIGURE 2 | ELISPOT screening of HIV-specific T-cell response before and after *in vitro* expansion, in samples from DT and ET individuals obtained after one year on cART. **(A)** Magnitude of total anti-Nef, anti-Gag (sum of anti-p17 and anti-p24 responses), and anti-CEF IFN-γ-producing cellular responses, expressed as spot forming units (SFU)/10^6 PBMCs, measured pre- and post-expansion *in vitro* on a subject-by-subject basis (each represented by a line). **(B)** Relative contribution of each antigen to the total HIV post-expansion response expressed as the percentage out of the total sum of the specific response (sum of the magnitude obtained for all Nef, p17 and p24 antigens), for DT (left pie) and ET (right pie) subjects. **(C)** Mean spot size obtained for HIV and CEF peptide pools at pre- and post-expansion conditions. HIV mean spot sizes represent the average mean spot sizes out of all Nef, Gag, and CEF pools for which a positive response was obtained in the ELISPOT assay on a subject-by-subject basis. Intragroup differences were analyzed using Wilcoxon test. Asterisks denote different *P* values: $^*p < 0.05$; $^{**}p < 0.01$; $^{***}p < 0.005$. DT, Delayed treatment ($N = 10$); ET, Early treatment ($N = 13$).

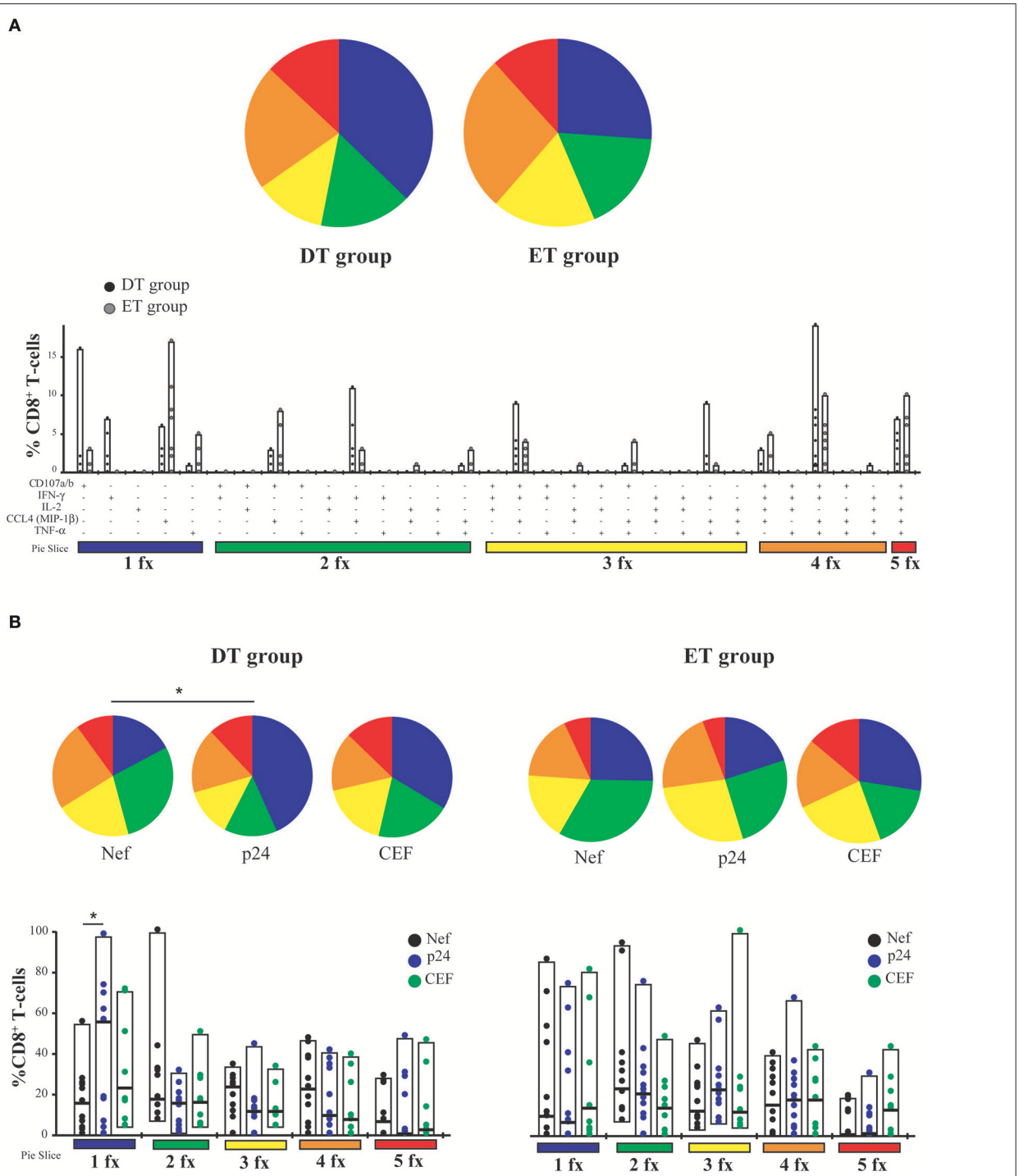

FIGURE 3 | $CD8^+$ T-cell polyfunctionality analysis after *in vitro* expansion with specific peptides. **(A)** Pies depict the distribution of mono-(blue), bi-(green), tri-(yellow), tetra-(orange), and penta-functional (red) cells within HIV specific $CD8^+$ T-cells, for DT and ET subjects. Bar charts represent the proportion of HIV-specific $CD8^+$ T-cells displaying each particular function or combination of functions (31 possible combinations of positive responses). The color code shown at the bottom mirrors the one shown in the pies. Black dots represent DT subjects and gray dots represent ET subjects. Boxes extend from min to max, horizontal bar within boxes represent median values **(B)** Polyfunctional profile for $CD8^+$ T-cells with different specificities (Nef, p24 or CEF) within DT group (left panel) and ET group (right panel). This analysis was performed considering cells that were able to mediate either one, two, three, four, or five functions, regardless of any particular function or function combination (block analysis). Analyses were performed with SPICE software. When analyzing global distribution (pies) permutation tests were applied, instead when analyzing bar graphs, Student *T*-test were used. *$p < 0.05$. DT, Delayed treatment ($N = 11$ for Nef- and p24-specific responses, $N = 8$ for CEF-specific responses); ET, Early treatment ($N = 12$ for Nef- and p24-specific responses, $N = 9$ for CEF-specific responses).

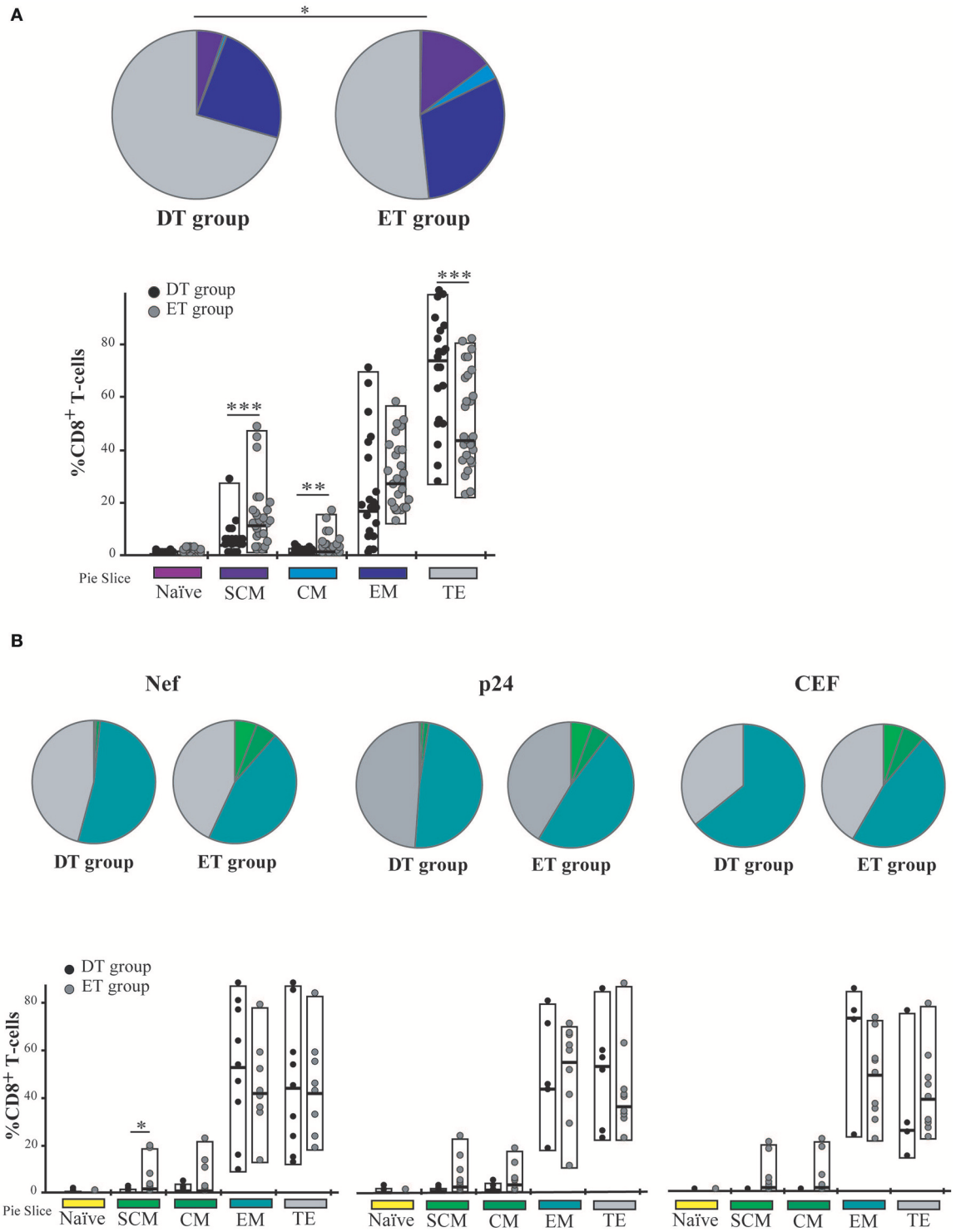

FIGURE 4 | Memory/effector phenotype analysis on expanded CD8$^+$ T-cells from DT and ET individuals. **(A)** Distribution of effector/memory subsets in bulk CD8$^+$ T-cells analyzed post-expansion. DT, Delayed treatment ($N = 11$ subjects, total 22 responses); ET, Early treatment ($N = 13$ subjects, total 26 responses). **(B)** Distribution of effector/memory subsets in Nef-, p24-, and CEF-specific CD8$^+$ T-cells, identified on the bases of cytokine production and/or degranulation capacity. DT, Delayed treatment ($N = 10$ Nef-specific responses, $N = 8$ p24-specific responses, $N = 5$ CEF-specific responses); ET, Early treatment ($N = 12$ Nef-specific responses, $N = 12$ p24-specific responses, $N = 10$ CEF-specific responses). In **(A,B)**, analyses were performed with SPICE software. In bar graphs, the color code shown at the bottom mirrors the one shown in the pies. Black dots represent DT subjects and gray dots represent ET subjects. Boxes extend from min to max, horizontal bar within boxes represent median values. When analyzing global distribution (pies) permutation tests were applied, instead when analyzing bar graphs, Student *T*-test were used. $^*p \leq 0.05$; $^{**}p \leq 0.01$; $^{***}p \leq 0.005$. SCM, Stem cell memory; CM, Central memory; EM, Effector memory; TE, Terminal effector.

significantly higher proportion of degranulating and/or cytokine-producing cells compared to T_{TE} in both groups (**Figure S2B**) pointing to a rheostat-like function of PD-1 rather than being merely a marker of cell exhaustion.

Overall, both at the bulk and HIV-specific compartments, ET subjects showed a preservation of early differentiated cells (T_{SCM} and T_{CM}), which was also represented as a higher proportion of T_{SCM} and T_{CM} cells within the PD-1^+ compartment. DT subjects showed a differentiated profile with increased representation of cells with effector phenotype (T_{EM} and T_{TE}). PD-1 expression was concentrated in HIV-specific $CD8^+$ T_{EM} cells.

Expanded $CD8^+$ T-Cells From DT and ET Subjects Were Highly Capable of Mediating Antiviral Activity

The capacity of *in vitro* expanded $CD8^+$ T-cells to exert viral inhibition by cytolitic and non-cytolitic mechanisms was evaluated by two different assays (see M&M and **Figure 1**). First, the VIA assay (which measures the magnitude of the overall $CD8^+$ T-cell antiviral potency comprising both cytolytic and non-cytolytic pathways) (39) was performed to evaluate the ability of expanded cells (either expanded with Nef or p24 peptides) to suppress the replication of one lab-adapted HIV strain (NL4-3) and three T/F primary strains (V4, V8, and V9). A significant capacity to mediate viral inhibition was observed both for Nef-specific and p24-specific cells from DT and ET subjects toward all viruses assayed (**Figure 6A**). Within Nef-specific $CD8^+$ T-cells, no significant differences were found between groups in their capacity to mediate VIA, although a trend was evident toward DT individuals displaying a higher capacity ($p = 0.0616$). In contrast, p24-specific $CD8^+$ T-cells from DT subjects showed a significantly stronger antiviral activity compared to p24-specific cells from ET subjects ($p = 0.005$). No significant differences were observed when analyzing Nef-specific and p24-specific cells within each study group. In parallel, the VITAL assay (which depicts direct cytotoxicity) was performed. **Figure 6B** shows dot-plots obtained from one representative assay, which depicts specific progressive loss of antigen-loaded $CFSE^+$ target cells as effectors are added at increasing ratios. Compiled data indicated that no significant difference could be observed between DT and ET individuals at any E:T ratio evaluated, regardless of $CD8^+$ T-cell specificity (**Figure 6C**). When performing an intragroup response analysis (i.e., comparing Nef-specific vs. p24-specific $CD8^+$ T-cells from DT or ET subjects), no differences were found (Wilcoxon's test $p > 0.05$). Only a tendency toward Nef-specific $CD8^+$ T-cells was evidenced showing an improved capacity to mediate a direct cytolytic activity compared to p24-specific $CD8^+$ T-cells in both groups.

Full Differentiation, Polyfunctionality, and PD-1 Expression of $CD8^+$ T-Cells Relate to Antiviral Function in This Expanded Model

Thus, we sought to investigate the relationship between $CD8^+$ T-cell phenotype and functionality (in terms of cytokine production and degranulation capacity) post *in vitro* expansion, and the magnitude of antiviral activity measured by VIA and VITAL assays. For this, results obtained with Nef- and p24-specific effectors were merged, due to no intragroup differences (i.e., within DT or ET subjects). First, a potential association with the results from the VIA assay was investigated. Activity against all viruses was examined. Correlation analysis revealed that the magnitude of VIA was inversely correlated with the proportion of bulk $CD8^+$ T_{SCM} cells ($r = -0.2634$, $p = 0.0054$), bulk $CD8^+$ T_{CM} cells ($r = -0.2058$, $p = 0.031$), and directly with the proportion of bulk $CD8^+$ T_{TE} cells ($r = 0.1878$, $p = 0.0495$). All correlations remained statistically significant after adjusting for multiple comparisons ($p = 0.0270$, $p = 0.0775$, and $p = 0.0825$, respectively). Furthermore, an inverse correlation with the proportion of HIV-specific $CD8^+$ T_{SCM} cells was found ($r = -0.2529$, $p = 0.0195$, adjusted $p = 0.0713$; **Figure 7A**). On the other hand, no significant correlations were found when analyzing the capacity of cells to mediate degranulation and/or secrete cytokines. Second, the magnitude of VITAL assay, at 1:5 T:E ratio, was inversely correlated with the proportion of HIV-specific $CD8^+$ T_{SCM} cells ($r = -0.4677$, $p = 0.0376$, adjusted $p = 0.0627$), inversely with HIV-specific $CD8^+$ T_{CM} cells ($r = -0.7228$, $p = 0.0003$, adjusted $p = 0.015$), and directly correlated with the proportion of HIV-specific $CD8^+$ T_{TE} cells ($r = 0.5035$, $p = 0.0280$, adjusted $p = 0.0627$) (**Figure 7B**). Additionally, correlations between VITAL magnitude and $CD8^+$ T-cell functionality were also found: direct correlations with the proportion of degranulating cells ($r = 0.5065$, $p = 0.0162$, adjusted $p = 0.0432$), IFN-γ-producing ($r = 0.563$, $p = 0.0064$, adjusted $p = 0.0259$), CCL4-producing ($r = 0.5957$, $p = 0.0034$, adjusted $p = 0.0259$), and TNF-α-producing $CD8^+$ T-cells ($r = 0.5494$, $p = 0.0081$, adjusted $p = 0.0259$), as well as with proportions of polyfunctional cells able to degranulate and secrete IFN-γ alone or plus one or two extra functions, regardless of any particular one ($r = 0.4652$, $p = 0.0291$, adjusted $p = 0.0582$; $r = 0.5671$, $p = 0.0059$, adjusted $p = 0.0259$, $r = 0.549$, $p = 0.0081$, adjusted $p = 0.0259$, respectively), and also tetrafunctional cells able to degranulate, express IFN-γ and TNF-α plus 1 extra functions ($r = 0.4767$, $p = 0.0249$, adjusted $p = 0.0569$) (**Figure 7C**). Finally, PD-1 expression within HIV-specific cells proved to directly correlate with direct cytotoxicity (VITAL assay 1:5 ratio; $r = 0.4861$, $p = 0.0160$, adjusted $p = 0.032$), the proportion of degranulating cells ($r = 0.699$, $p = 0.0012$, adjusted $p = 0.0063$), IFN-γ-producing $CD8^+$ T-cells ($r = 0.7647$, $p = 0.0002$, adjusted $p = 0.0014$), CCL4-producing $CD8^+$ T-cells ($r = 0.7661$, $p = 0.0002$, adjusted $p = 0.0014$) and TNF-α producing $CD8^+$ T-cells ($r = 0.8493$, $p < 0.0001$, adjusted $p = 0.0014$). Interestingly, PD-1 expression within HIV-specific cells also directly correlated with the proportion of degranulating polyfunctional cells that concomitantly secrete IFN-γ, TNF-α plus one extra function ($r = 0.6809$, $p = 0.0019$, adjusted $p = 0.008$) (**Figure 7D**). Overall, this data points toward the need to fully differentiate into an effector phenotype to gain maximum antiviral activity in both assays. VITAL assay better correlated with subsets of functions containing degranulating cells, thus reflecting the nature of the assay. Of note, correlations with the proportion of IFN-γ and TNF-α-producing $CD8^+$ T-cells might be driven by a high

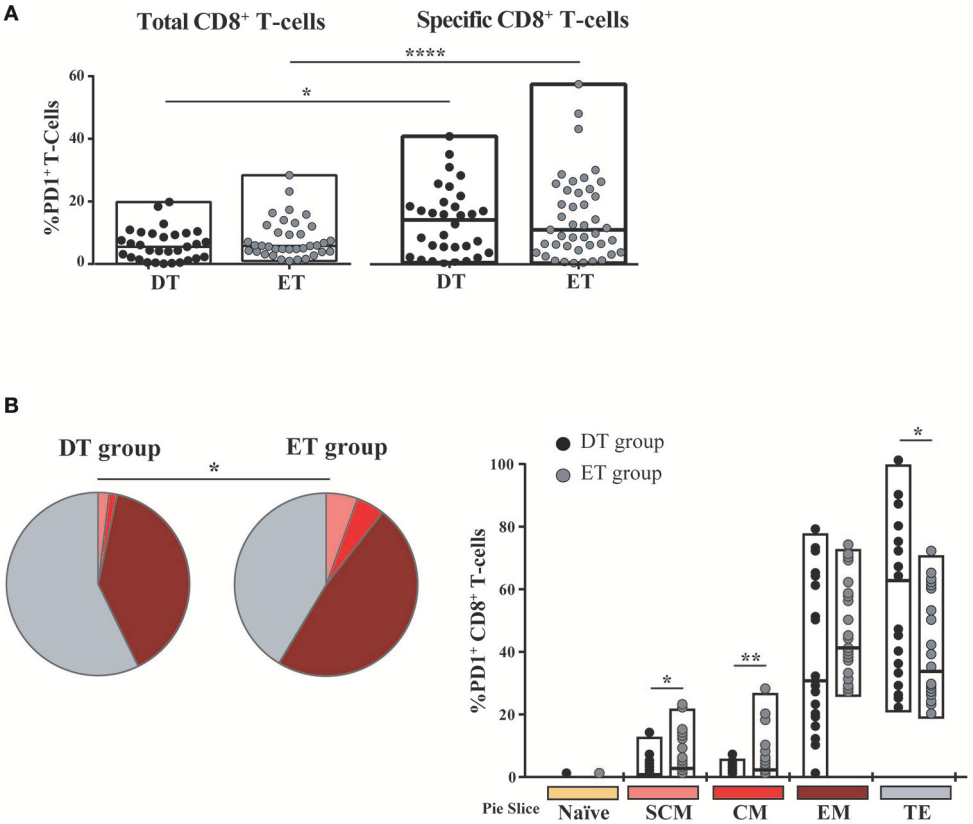

FIGURE 5 | PD-1 expression on expanded CD8$^+$ T-cells from DT and ET individuals. **(A)** Post-expansion percentages of bulk and HIV-specific PD-1$^+$ CD8$^+$ T-cells. Boxes extend from min to max. Horizontal bar within boxes represent the median. *$p \leq 0.05$; ****$p \leq 0.0001$ according to Wilcoxon's test. **(B)** Distribution of effector/memory phenotypes within bulk PD-1$^+$ CD8$^+$ T-cells analyzed post-expansion. Analysis was performed with SPICE software. In bar graphs, the color code shown at the bottom mirrors the one shown in the pies. Black dots represent DT subjects and gray dots represent ET subjects. Boxes extend from min to max, horizontal bar within boxes represent median values. When analyzing global distribution (pies) permutation tests were applied, instead when analyzing bar graphs, Student *T*-test were used. *$p \leq 0.05$; **$p \leq 0.01$. DT, Delayed treatment ($N = 11$ subjects, 21 responses). ET, Early treatment ($N = 13$ subjects, 26 responses). SCM, Stem cell memory; CM, Central memory; EM, Effector memory; TE, Terminal effector.

coexpression with CD107a/b$^+$ cells. Interestingly, PD-1 appeared as a marker of polyfunctional expanded cells able to mediate direct cytolysis.

DISCUSSION

Combination antiretroviral treatment has largely improved HIV$^+$ individual's quality of life and expectancy. Nevertheless, it cannot eliminate the viral reservoir by itself, precluding thus the cure of the infection. Many strategies have been proposed to eradicate the viral reservoir. The success of some of these strategies, such as the "shock and kill" approach, will rely mainly on the ability of HIV-specific CD8$^+$ T-cells to clear reactivated infected cells. Nevertheless, our knowledge regarding the quality of remaining CD8$^+$ T-cell responses on-cART is not accurate. Pivotal studies indicated that cART-treated individuals retain CD8$^+$ T-cells that, upon *ex vivo* expansion, are able to exert antiviral activity *in vitro*, even against reactivated cells (i.e., latently infected CD4$^+$ T-cells exposed to latency reversal agents) (57–59), although the depletion of infected cells is not complete (60). Yet, the functional and phenotypic characteristics needed to boost in the quest of a functional cure are not thoroughly understood. Here, we performed a comprehensive evaluation of the quality of *in vitro* expanded CD8$^+$ T-cells obtained from HIV$^+$ subjects who initiated cART at early (<4 month) or delayed (>4 month) time-points post-infection. Results indicated that (i) Nef- and p24-specific T-cell responses could be expanded *in vitro,* both in DT and ET subjects; (ii) expanded cells were highly polyfunctional; (iii) after expansion, the memory/effector differentiation profile was sharply skewed toward an effector phenotype, although ET subjects showed preserved proportions of T_N, $T_{SCM,}$ and T_{CM} subsets; (iv) expanded CD8$^+$ T-cells were highly capable of mediating antiviral activity and the magnitude of these activities were related to the proportion of fully-differentiated effector cells as well as with CD8$^+$ T-cell functionality; (v) PD-1 expression in expanded cells was mainly concentrated in HIV-specific T_{EM} CD8$^+$ cells and correlated to cell polyfunctionality and cytolytic activity.

Compiling evidence depicts the profound benefits that early initiation of cART has on both virologic and immunologic

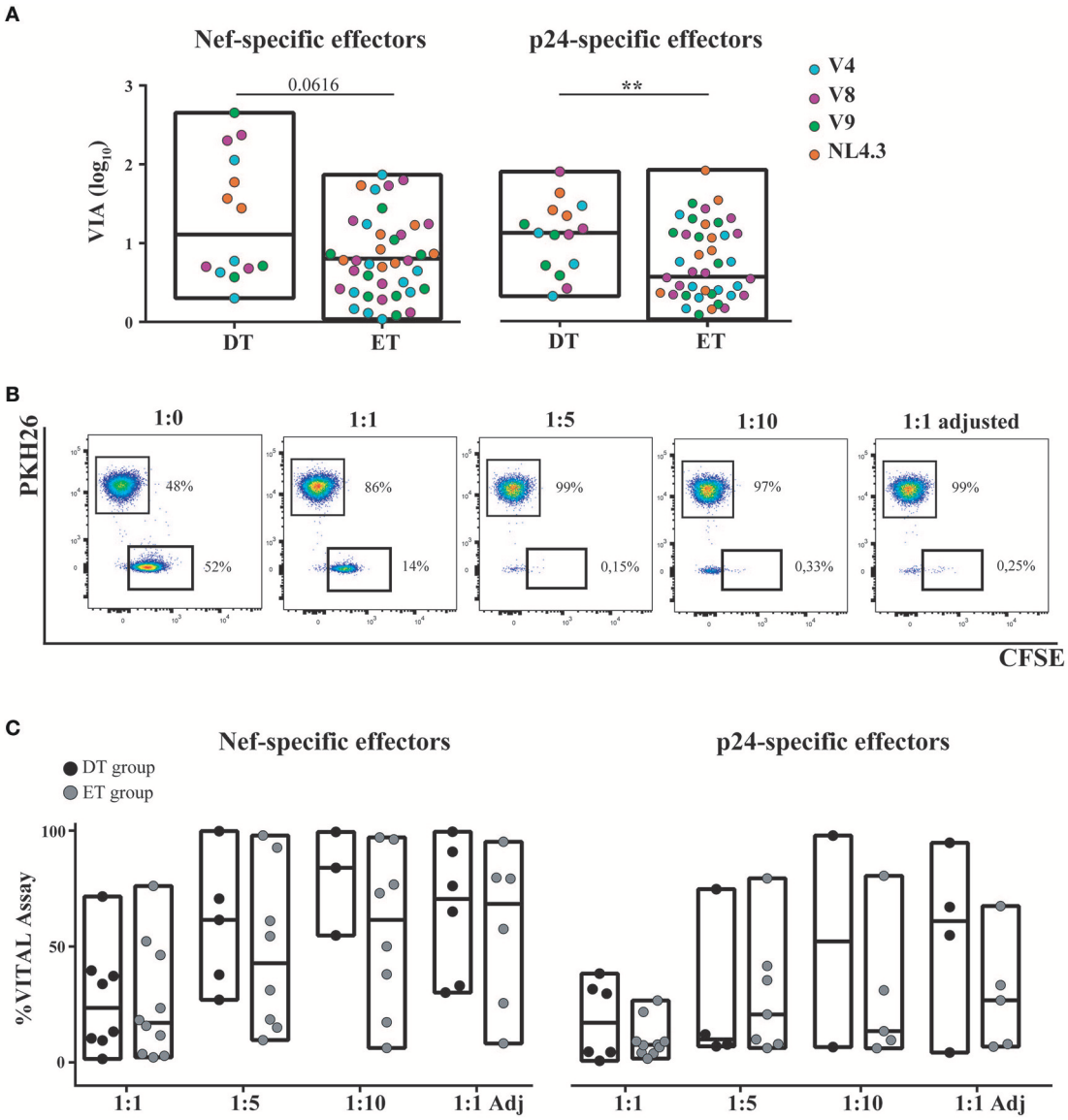

FIGURE 6 | Capacity of *in vitro* expanded CD8$^+$ T-cells to exert viral inhibition by cytolytic and non-cytolytic mechanisms. **(A)** *In vitro* viral inhibition assay (VIA) mediated by Nef-specific (left panel) and p24-specific (right panel) CD8$^+$ T-cells. VIA was expressed as the $\log_{10}$ of the proportion of p24 antigen lost when effector CD8$^+$ T-cells were present in the culture, compared to target cells (infected autologous CD4$^+$ T-cells) alone. Dots represent individual subjects. The different viral strains employed in the experiment are displayed in a different color. DT, Delayed treatment ($N = 4$ subjects, 14 Nef-specific responses and 15 p24-specific responses); ET, Early treatment ($N = 12$ subjects, 40 Nef-specific responses and 41 p24-specific responses). **(B)** Dot-plots obtained in one representative VITAL assay. At the 1:0 T:E ratio (far left panel), an even distribution of peptide-loaded (CFSE$^+$PKH26$^-$) targets and not-loaded targets (CFSE$^-$PKH26$^+$) targets is observed. From left to right, increasing ratios of effectors (1:1, 1:1 adjusted [i.e., 1:1 ratio adjusted to proportion of specific CD8$^+$ T-cell effectors as determined by intracellular staining and flow cytometry], 1:5 and 1:10) are shown and the concomitant loss of antigen-loaded targets is observed. **(C)** Percentage of specific lysis exerted by Nef-specific (left panel) and p24-specific (right panel) CD8$^+$ T-cells, as determined by the VITAL assay. Results for DT and ET subjects are shown at the different T:E ratios evaluated. DT, Delayed treatment ($N = 7$ subjects for Nef-specific responses and $N = 6$ subjects for p24-specific responses). ET, Early treatment ($N = 10$ subjects, both for Nef- and p24-specific responses). Black dots represent DT subjects and gray dots represent ET subjects. In **(A,C)**, boxes extend from min to max values. Horizontal lines within boxes represent the median values. In **(A)**, intergroup differences were analyzed using Mann-Whitney test; $^{**}p < 0.01$.

parameters in infected individuals (26, 27, 31, 47). Longer antigen persistence was shown to be deleterious on HIV-specific CD8$^+$ T-cells, resulting in an exhausted and hyperactivated immune response (27, 61). Furthermore, the latent reservoir is not only larger in size but also altered in its composition, possibly containing variants resistant to dominant CD8$^+$ T-cell responses, rendering immune eradication therapies less efficient in individuals initiating cART during chronic infection (58). So far, few works have studied the differences in breadth and magnitude of CD8$^+$ T-cell responses arising from starting cART

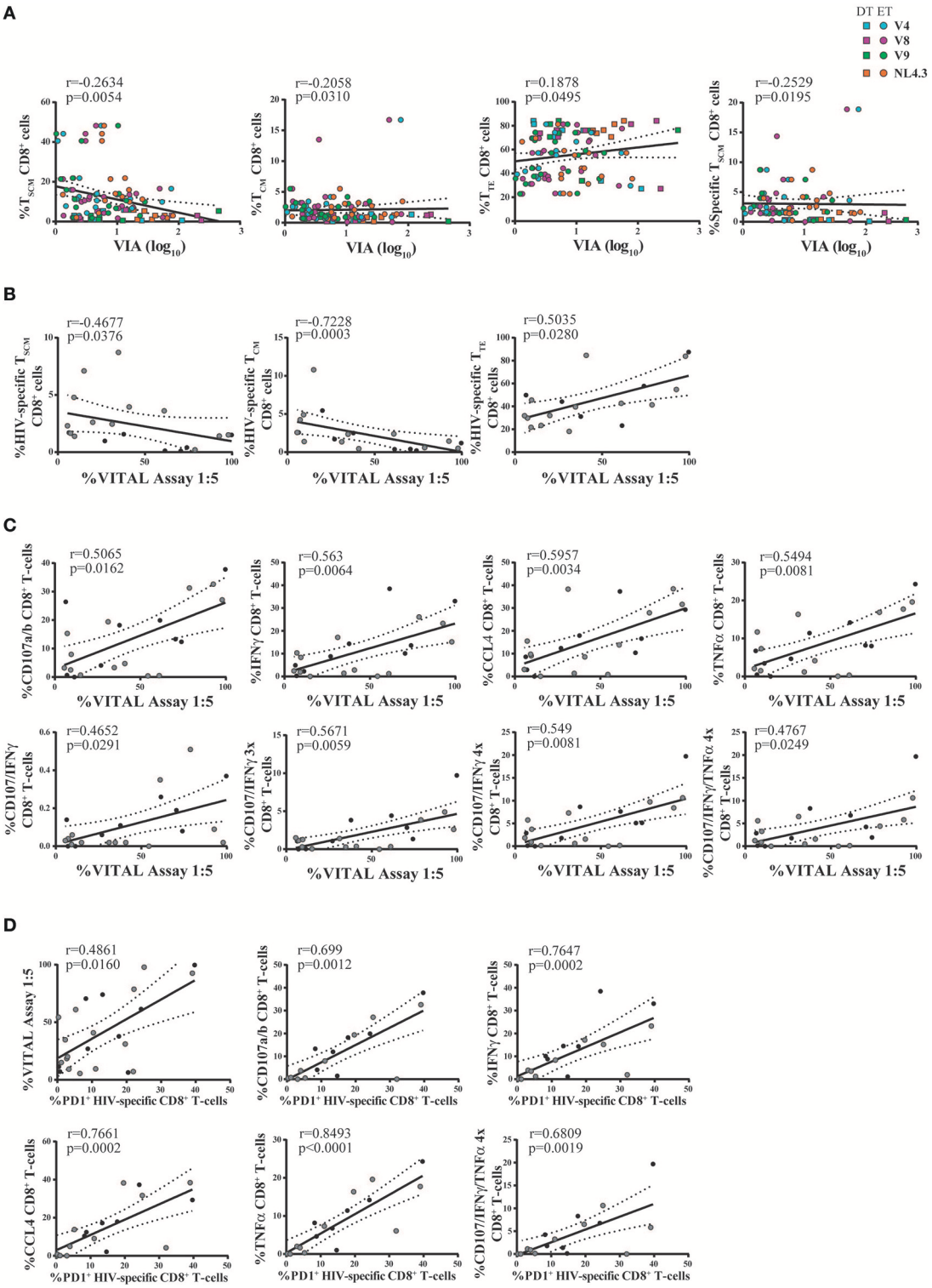

FIGURE 7 | Correlation analyses between antiviral activity versus cell phenotype and functionality of expanded CD8$^+$ T-cells. **(A)** Correlations between VIA magnitude (evaluated against all viruses and merging data from Nef-specific and p24-specific effectors) and bulk and HIV-specific CD8$^+$ T-cell memory phenotype. Square dots represent DT subjects and round dots represent ET subjects. The different viral strains employed in the VIA experiment are displayed in a different color, matching the color code showed in **Figure 6 A**. **(B,C)** Correlations between VITAL magnitude and the proportions of HIV-specific CD8$^+$ T-cell memory phenotype **(B)**, and the proportions of CD8$^+$ T-cell functionality **(C)**. **(D)** Correlations between the percentage of PD-1 expressing HIV-specific CD8$^+$ T-cells and cell functionality. **(B–D)** Black dots represent DT subjects and gray dots represent ET subjects. *r* and *p* values correspond to Spearman's correlations.

at different time-points after infection (54, 62, 63), but no evaluation has been focused on how those differences impact on the final antiviral activity, an important issue to be addressed when assessing functional cure strategies. In this context, we aimed to assess whether the moment of cART initiation (relative to the presumed date of infection) has an impact on post-expansion HIV-specific $CD8^+$ T-cell responses.

Because $CD8^+$ T-cell responses in subjects on cART are dramatically diminished (15–20), an *in vitro* cell expansion protocol was implemented. Several and diverse works have proven its utility in boosting HIV-specific responses to optimal activity (23, 40, 54, 57–59, 64–67). This work analyzed HIV-specific $CD8^+$ T-cell responses against Gag and Nef peptide pools based on a number of reasons: (1) during acute infection, Nef is the immunodominant target (68–70), though the response broadens afterwards to epitopes within other viral proteins including Gag (71–75), (2) higher frequencies of $CD8^+$ T-cells with polyfunctional responses to Gag and Nef were associated with lower viral set-points (76), (3) Gag-specific $CD8^+$ T-cell responses were associated with virus control in different settings (72–74, 77); particularly, early anti-Gag immunodominance was associated with improved antiviral activity and also with lower rate of disease progression (13); (4) expandable Gag responses were associated with strong antiviral activity and lower residual viral loads in Elite Controllers (40, 66); (5) Nef protein is detectable in PBMCs from subjects under cART (78) and (6) $CD4^+$ T-cells from individuals on prolonged therapy contain "defective" proviral sequences that are able to express Nef (79). Despite being the $CD8^+$ T-cell response very low and at times almost undetectable before stimulation, we were able to specifically and significantly expand it in both groups of individuals. However, DT subjects displayed a more homogeneous response, in terms of specificity, than ET subjects, for whom the post-expansion response was narrower. This could likely occur due to a longer period of antigen stimulation, which would have allowed $CD8^+$ T-cells from DT to develop into a broader-spectrum of specificities to different viral antigens. In consonance with the results obtained by Deng et al. a broader $CD8^+$ T-cell response would be favorable when the elimination of reactivated viruses is required (58). Nevertheless, it is worth noting that anti-Nef and anti-p24 responses were equally expandable in both groups.

Early reports comparing the capacity of $CD8^+$ T-cells to degranulate and secrete multiple soluble mediators upon stimulation, between individuals with progressive vs. long-term nonprogressive HIV infection, have suggested that $CD8^+$ T-cell polyfunctionality would be a functional correlate of virus control (76, 80). Later, it was shown that polyfunctionality does not necessarily correlate with disease progression (13). Instead, lack of T-cell polyfunctionality would be the consequence of constant antigen stimulation during viremic chronic infection, which ultimately may lead to cell exhaustion and functional impairment (81, 82). In any case, $CD8^+$ T-cell polyfunctionality relates to a beneficial response. Here, a significant proportion of peptide-expanded $CD8^+$ T-cells presented the ability to mediate different and simultaneous functions. In this line, several reports have evidenced the significant presence of polyfunctional cells upon expansion with specific peptides (40, 48). Particularly, Ndhlovu et al. (40) showed that, after expansion with a similar protocol to the one used here, Elite controllers had significantly higher frequencies of polyfunctional cells compared to a group of chronically infected subjects on cART. Contrary to the findings of Ndhlovu et al. we did not observe differences between study groups, i.e., polyfunctionality was equally evident in DT and ET subjects. One point to be considered is that DT and ET groups are less polar than Elite controllers and chronics on cART. Thus, more subtle differences might exist between DT and ET which could not be evidenced here. Regarding time to cART initiation, a similar study also indicated that it did not impact $CD8^+$ T-cell polyfunctionality profile, although evaluated directly *ex vivo* (54).

$CD8^+$ T-cells follow a progressive pathway of differentiation from naïve T-cells into different memory/effector subsets. Each subset is characterized by self-renewal, proliferative and functional attributes (83). Memory $CD8^+$ T-cell differentiation in progressive HIV infection is severely skewed, reflecting improper terminal differentiation of effector cells (14, 84, 85). Interestingly, the early deterioration of $CD8^+$ T-cell differentiation pathway was directly associated with disease progression (14, 86), while effective cART seems not to restore this phenomenon completely (65). Here, $CD8^+$ T-cell memory/effector differentiation was evaluated post-expansion in cells from DT and ET subjects. In this condition of strong antigen triggering and cytokine-driven proliferation signaling, a considerable extent of differentiation to effector phenotypes was expected. However, this was not equally represented by the two study groups included in this work: ET subjects had increased proportions of T_N, $T_{SCM,}$ and T_{CM} upon expansion. Initially, this could have been considered as an advantage since less differentiated cells with improved proliferative and self-renewal capacities were preserved. However, as will be later discussed, it inversely correlated with antiviral function. $CD8^+$ T_{SCM} cells have been described as a subset of antigen-experienced cells that retain a core of genes expressed by T_N cells, and also display superior ability to proliferate homeostatically and persist in the long term (83). Recently, it has been reported that HIV^+ subjects receiving cART have higher proportions of $CD8^+$ T_{SCM} cells and that this proportion even increases as time on cART extends (87). Since DT and ET subjects have a similar median time on cART at the moment of sampling, it would be interesting to evaluate if a higher representation of $CD8^+$ T_{SCM} cells after expansion could be reflecting an increase in the frequency of T_{SCM} cells before expansion. This in turn, would be a consequence of the earliest cART initiation. For regimens of adoptive cell transfer, widely explored in the field of cancer and Epstein-Barr virus–associated malignancies, it is known that $CD8^+$ T-cell differentiation widely affects the anti-tumoral response: although effector memory cells have fully functional differentiation, the diminished proliferative capacity severely compromises the success of the adoptive transfer because the effect is transient. Thus, strategies for limiting *ex vivo* differentiation but retaining functional differentiation are being evaluated (88). The same reasoning could apply in this context: ET subjects harbor the advantage of a preserved T_{SCM} subset but strategies to potentiate their antiviral activity should be explored.

Apart from memory/effector phenotype, the expression of PD-1 was investigated post-expansion. PD-1 is an inhibitory coreceptor that is involved in the fine-tuned regulation of the threshold of antigen responses of T and B cells. It is endowed with unique modulatory functions where its presence/absence matters but also its expression level is crucial (89, 90). During chronic viral infections, extremely high and persistent PD-1 expression has been found in T cells. This PD-1^{high} phenotype has been consistently associated with a state of cellular exhaustion in the context of different persistent viral infections, including HIV (14, 55, 56, 89, 91, 92). In this study, PD-1 expression in expanded $CD8^+$ T-cells was low compared to other reports measuring PD-1 expression directly *ex vivo*, as already mentioned. This could be the result of PD-1 down-modulation or death of PD-1^+ cells during expansion. The latter would be in consonance with the notion that exhausted PD-1^+ cells show decreased telomerase activity and telomere lengths rendering them more susceptible to cell death (93, 94). Expanded PD-1^+ cells were concentrated in the HIV-specific compartment, particularly within $CD8^+$ T_{EM} and T_{TE} cells. In addition, positive correlations were found between PD-1 expression on expanded HIV-specific cells and $CD8^+$ T-cell functionality. This is in line with data provided by Hokey et al., who found high PD-1 expression on cells with activated memory and effector phenotypes despite decreased telomere lengths, suggesting PD-1 could play a costimulatory role in $CD8^+$ T-cell populations (95). Moreover, a recent report showed that tumor-reactive $CD8^+$ T-cells that persist after adoptive cell-transfer therapy, and associate with tumor regression, are mostly polyfunctional and simultaneously express high levels of PD-1 (96). This data highlights the fact that the PD-1 role in the context of viral reactivation needs further research. Many studies have already proven the benefits of PD-1 signaling inhibition by anti-PD-1L (anti-PD-1 ligand] at the moment of $CD8^+$ T cell stimulation, (93, 97). Combination therapies that stimulate and simultaneously modulate the specific immune response (through PD-1 blocking for instance) are believed to be the optimal approaches for future therapeutic schemes (98, 99).

Then, we aimed to analyze whether $CD8^+$ T-cells quality and phenotype would have an impact on the global capacity to mediate viral inhibition. To attain this, two different approaches were used. VIA is a versatile technique that allowed us to investigate $CD8^+$ T-cell-mediated inhibition of viral replication of four different virus strains, three HIV-1 primary isolates and a laboratory strain. Even though it provides a global picture of the antiviral response, it cannot discriminate if cytotoxicity plays a relevant antiviral role in this expansion model. To assess this aspect, Herman's VITAL assay was implemented. This method particularly evaluates the direct cytotoxicity, requiring cell-to-cell contact between peptide-loaded target cells and effectors. Thus, this was carried out concomitantly with VIA to assess the contribution of cytolytic mechanisms to the global antiviral response. We considered relevant to perform such a discrimination because in a context of functional cure, strong cytolytic activity would be preferred over non-cytolytic mechanisms to eliminate reactivated cells (100). In this fashion, these experiments provide complementary data, granting a larger picture of the immune response. Here, both Nef- and p24-specific cells from DT and ET individuals were able to mediate VIA against the broad repertoire of viruses assayed, including clinically relevant viral strains. HIV-specific cells from DT group were prone to display greater inhibitory activity than ET but it was only statistically different from p24-specific cells. Bulk $CD8^+$ T-cell differentiation level correlated with VIA magnitude, stating that complete differentiation was needed to be achieved in order to mediate viral inhibition. We have already proven that terminal memory differentiation was needed to exert optimal antiviral activity in subjects off-cART and measured directly *ex vivo* (14). Here, this association was maintained even after expansion and in subjects on cART. This is consistent with reports that proved effector memory T-cells efficiency at controlling new infections because they are endowed with more immediate effector functions (27, 101). For VITAL assay, no differences were found between groups. Furthermore, VITAL magnitude correlated with a higher proportion of HIV-specific terminal effector cells. We also found that cells able to degranulate and secrete IFNγ or TNFα, either as unique functions or combined, exerted a greater cytolityc activity. In this line, it has been shown that CD107a/b surface expression was associated with the capacity of antigen-specific $CD8^+$ T-cells to eliminate infected cells as observed in VIA assays (13, 102). Additionally, CCL4 has been shown to interfere with HIV infection by blocking the binding to CCR5 coreceptor and has been associated with higher VIA magnitude (102). In our model, no differences were found in the total percentage of CCL4-expressing $CD8^+$ T-cells between groups, which is consistent with the lack of difference in VIA magnitude. To date, no reports associated VITAL assays with the level of degranulation post-expansion in HIV-specific cells, representing a novel finding. Of note, most correlations found for VITAL assay were driven by results obtained for Nef-specific responses. Moreover, a tendency toward Nef-specific cells able to mediate stronger direct cytotoxicity was evidenced. Given that $CD4^+$ T-cells from HIV^+ subjects on treatment upregulate HIV-1 mRNA within 1 h of stimulation and produce extracellular virus as early as six-h poststimulation, $CD8^+$ T-cells that recognize specifically early gene products, such as Nef, would be most beneficial in functional cure approaches. Additionally, they would effectively kill reactivated cells before viral spread and Nef-mediated MHC-downmodulation (67). Indeed, recent findings indicated that ongoing Nef-expression in treated subjects is associated with the maintenance of Nef-specific $CD8^+$ T-cells (28). Not only our results suggest that direct cytotoxicity was mediated more efficiently by Nef-specific $CD8^+$ T-cells, but also, for the reasons above stated, it would be an important target to boost in functional cure approaches and vaccine formulations.

Overall, this is a novel comprehensive study evaluating the quality of *in vitro* expanded $CD8^+$ T-cells from DT and ET HIV^+ subjects with relevant implication in the design and evaluation of functional cure strategies relying on $CD8^+$ T-cell-mediated killing among others. Limitations of this study include, but might not be restricted to: (i) the use of a strong and prolonged stimulation protocol for T-cell expansion might mask subtle inter-group differences, for instance as a consequence

of activation-induced cell death of certain cell subsets and survival of others common to both groups, thus we cannot exclude the possibility that with alternative expansion protocols (such as by using IL-7 or IL-15) differences may arise; (ii) identification of HIV-specific cells by combining molecules with the same fluorochrome leads to the underestimation of the specific response which might be mistakenly considered within the bulk compartment; (iii) production of perforins and granzymes, which were already described as key components of $CD8^+$ T-cell antiviral function, were not measured, and thus not accounted, for depicting $CD8^+$ T-cell quality; (iv) DT group is highly heterogenous which might potentially lead to data misinterpretation; (v) ET subjects might have initiated treatment even after seroconversion so they do not represent really early treated subjects such as those defined in other cohorts (27). This last point might instead be interpreted as an advantage in terms of potential translation of the results to the every-day practice. Detection of an acutely infected subject is extremely unusual, being mostly diagnosed at late Fiebig stages (IV to VI). Therefore, the scenario presented here would better approximate to a real context.

In sum, low frequency of HIV-specific $CD8^+$ T-cells from subjects on-ART for at least 1 year were readily expandable *in vitro* and retained antiviral functions. Minor qualitative differences were observed in expandable $CD8^+$ T-cell responses between DT and ET subjects, mostly related to the memory/effector differentiation profile. Thus, the initiation of cART before the viral set-point did not represent a major benefit in terms of post-expansion $CD8^+$ T-cell quality in our model. In other words, having started cART during chronic infection would not represent an obstacle to undergo immunomodulatory approaches. Studies aimed at determining how the quality of the pre-cART response relates to the post-expansion scenario and how all these parameters relate to the viral reservoir are being conducted. Although we showed here that *in vitro* expansion results in a fully antiviral functional response, it remains to be elucidated if this kind of responses (with the proper specificity and functionality), can be elicited *in vivo* (through therapeutic vaccination, for instance) or if an adoptive transfer strategy would be the best option to achieve a functional cure for HIV. Additionally, the inclusion of immunomodulators (immune checkpoint inhibitors and/or agonist of stimulatory pathways) should be considered to overcome the intrinsic immune damage caused by the infection in each particular subjects, leading to the development of tailor-made regimens. In any case, these results add important information to rationally design and/or evaluate future strategies to modulate not only anti-HIV T-cell responses but also immune responses toward other persistent pathogens.

AUTHOR CONTRIBUTIONS

GT conceived the study. JS, YG, and GT designed the experiments. JS, MR, CT, MC, and YG performed experiments. MF, OS, and NL contributed samples and gathered clinical data. JS, MG, HS, NL, YG, and GT analyzed and interpreted the data. JS and GT wrote the manuscript. All authors read and approved the final version.

FUNDING

This work was supported by grants from the Agencia Nacional de Promoción Científica y Tecnológica (ANPCyT) and GlaxoSmithKline (PICTO-GSK2013, Grant #0006), and from the Universidad de Buenos Aires (UBACyT2017, Grant # 20020160100008BA) to GT.

ACKNOWLEDGMENTS

Authors specially acknowledge study participants for agreeing to collaborate in this study and to provide blood samples. We thank Mr. Sergio Mazzini for language assistance during manuscript preparation.

SUPPLEMENTARY MATERIAL

The Supplementary Material for this article can be found online at: https://www.frontiersin.org/articles/10.3389/fimmu.2018.02443/full#supplementary-material

Figure S1 | Gating strategy used for the identification of the studied cellular populations, by flow cytometry. **(A)** To study $CD8^+$ T-cell polyfunctionality, initial gating was performed on a forward scatter area (FSC-A) vs. FSC-height (FSC-H) plot to remove doublets. Dead cells were then excluded on the bases of Zombie NIR fluorescence. Then, gating was performed on CD14/CD19 negative cells in order to exclude monocytes and B lymphocytes, and then small lymphocytes were selected in FSC vs. side scatter (SSC) plot. Subsequently, $CD3^+$ cells were gated in a CD3 vs. SSH dot plot, and then a CD8 vs. CD4 dot-plot was constructed to identify $CD8^+$ events. To study $CD8^+$ T-cell polyfunctionality, plots were derived from the $CD8^+$ gate to study each particular function: degranulation (evidenced as CD107a/b mobilization) and production of IFN-γ, IL-2, CCL4, and TNF-α. Cells capable of exerting multiple functions simultaneously (degranulating and/or secreting multiple cytokines; 2, 3, 4, or 5 functions) were identified using the Boolean gating strategy available at FlowJo v10 software. **(B)** For the phenotype panel, the initial gating strategy was identical to the polyfunctionality panel up-to-the point of CD8 vs. CD4 plot. There, $CD8^+$ events were gated to define bulk $CD8^+$ T-cells and a CD8 vs. FITC plot was derived to identify HIV-specific $CD8^+$ T-cells (defined as the ones degranulating and/or expressing cytokines, all stained in FITC). Subsequent analyses were performed on both populations as shown by overlaid dot-plots and overlaid histograms. To analyze the distribution of the different phenotype subsets, CD45RO vs. CCR7 density plots were constructed to identify central memory T-cells (T_{CM}, $CCR7^+/CD45RO^+$), effector memory T-cells (T_{EM}, $CCR7^-/CD45RO^+$) and terminal effector T-cells (T_{TE}, $CCR7^-/CD45RO^-$). CD95 expression was analyzed within the $CD45RO^-CCR7^+$ cells thus defining naïve T-cells (T_N, $CCR7^+/CD45RO^-/CD95^-$) and stem-cell memory T-cells (T_{SCM}, $CCR7^+/CD45RO^-/CD95^+$). Additionally, PD-1 expression was evaluated. In **(A,B)** illustration data represent cells derived from one representative subject, stimulated for 14 days with the HIV Nef peptide pool.

Figure S2 | (A) Proportion of $PD\text{-}1^+$ cells observed post-expansion on bulk $CD8^+$ TEM and TTE cells from DT and ET individuals. **(B)** Proportion of HIV-specific cells (either Nef-specific or p24-specific) cells, identified on the bases of cytokine production and/or degranulation capacity, observed post-expansion on $CD8^+$ TEM and TTE cells from DT and ET individuals. In **(A,B)**, boxes extend from min to max. Horizontal bar within boxes represent the median. $^{****}p \leq 0.0001$ according to Wilcoxon's test.

REFERENCES

1. Ambrosioni J, Nicolas D, Sued O, Aguero F, Manzardo C, Miro JM. Update on antiretroviral treatment during primary HIV infection. *Expert Rev Anti Infect Ther.* (2014) 12:793–807. doi: 10.1586/14787210.2014.913981
2. Maartens G, Celum C, Lewin SR. HIV infection: epidemiology, pathogenesis, treatment, and prevention. *Lancet* (2014) 384:258–71. doi: 10.1016/S0140-6736(14)60164-1
3. Deeks SG, Lewin SR, Ross AL, Ananworanich J, Benkirane M, Cannon P, et al. International AIDS society global scientific strategy: towards an HIV cure 2016. *Nat Med.* (2016) 22:839–50. doi: 10.1038/nm.4108
4. McDermott AB, Koup RA. CD8(+) T cells in preventing HIV infection and disease. *AIDS* (2012) 26:1281–92. doi: 10.1097/QAD.0b013e328353bcaf
5. Hull M, Lange J, Montaner JS. Treatment as prevention–where next? *Curr HIV/AIDS Rep.* (2014) 11:496–504. doi: 10.1007/s11904-014-0237-5
6. Davey RT Jr, Bhat N, Yoder C, Chun TW, Metcalf JA, Dewar R, et al. HIV-1 and T cell dynamics after interruption of highly active antiretroviral therapy (HAART) in patients with a history of sustained viral suppression. *Proc Natl Acad Sci USA.* (1999) 96:15109–14. doi: 10.1073/pnas.96.26.15109
7. Lewin SR, Rouzioux C. HIV cure and eradication: how will we get from the laboratory to effective clinical trials? *AIDS* (2011) 25:885–97. doi: 10.1097/QAD.0b013e3283467041
8. Katlama C, Deeks SG, Autran B, Martinez-Picado J, van Lunzen J, Rouzioux C, et al. Barriers to a cure for HIV: new ways to target and eradicate HIV-1 reservoirs. *Lancet* (2013) 381:2109–17. doi: 10.1016/S0140-6736(13)60104-X
9. Deeks SG, Tracy R, Douek DC. Systemic effects of inflammation on health during chronic HIV infection. *Immunity* (2013) 39:633–45. doi: 10.1016/j.immuni.2013.10.001
10. Dube K, Sylla L, Dee L, Taylor J, Evans D, Bruton CD, et al. Research on HIV cure: mapping the ethics landscape. *PLoS Med.* (2017) 14:e1002470. doi: 10.1371/journal.pmed.1002470
11. Pitman MC, Lau JSY, McMahon JH, Lewin SR. Barriers and strategies to achieve a cure for HIV. *Lancet HIV* (2018) 5:e317–28. doi: 10.1016/S2352-3018(18)30039-0
12. Jones RB, Walker BD. HIV-specific CD8(+) T cells and HIV eradication. *J Clin Invest.* (2016) 126:455–63. doi: 10.1172/JCI80566
13. Turk G, Ghiglione Y, Falivene J, Socias ME, Laufer N, Coloccini RS, et al. Early Gag immunodominance of the HIV-specific T-cell response during acute/early infection is associated with higher $CD8^+$ T-cell antiviral activity and correlates with preservation of the $CD4^+$ T-cell compartment. *J Virol.* (2013) 87:7445–62. doi: 10.1128/JVI.00865-13
14. Ghiglione Y, Falivene J, Ruiz MJ, Laufer N, Socias ME, Cahn P, et al. Early skewed distribution of total and HIV-specific $CD8^+$ T-cell memory phenotypes during primary HIV infection is related to reduced antiviral activity and faster disease progression. *PLoS ONE* (2014) 9:e104235. doi: 10.1371/journal.pone.0104235
15. Kalams SA, Goulder PJ, Shea AK, Jones NG, Trocha AK, Ogg GS, et al. Levels of human immunodeficiency virus type 1-specific cytotoxic T-lymphocyte effector and memory responses decline after suppression of viremia with highly active antiretroviral therapy. *J Virol.* (1999) 73:6721–8.
16. Casazza JP, Betts MR, Picker LJ, Koup RA. Decay kinetics of human immunodeficiency virus-specific $CD8^+$ T cells in peripheral blood after initiation of highly active antiretroviral therapy. *J Virol.* (2001) 75:6508–16. doi: 10.1128/JVI.75.14.6508-6516.2001
17. Conrad JA, Ramalingam RK, Duncan CB, Smith RM, Wei J, Barnett L, et al. Antiretroviral therapy reduces the magnitude and T cell receptor repertoire diversity of HIV-specific T cell responses without changing T cell clonotype dominance. *J Virol.* (2012) 86:4213–21. doi: 10.1128/JVI.06000-11
18. Ogg GS, Jin X, Bonhoeffer S, Moss P, Nowak MA, Monard S, et al. Decay kinetics of human immunodeficiency virus-specific effector cytotoxic T lymphocytes after combination antiretroviral therapy. *J Virol.* (1999) 73:797–800.
19. Migueles SA, Weeks KA, Nou E, Berkley AM, Rood JE, Osborne CM, et al. Defective human immunodeficiency virus-specific $CD8^+$ T-cell polyfunctionality, proliferation, and cytotoxicity are not restored by antiretroviral therapy. *J Virol.* (2009) 83:11876–89. doi: 10.1128/JVI.01153-09
20. Janbazian L, Price DA, Canderan G, Filali-Mouhim A, Asher TE, Ambrozak DR, et al. Clonotype and repertoire changes drive the functional improvement of HIV-specific CD8 T cell populations under conditions of limited antigenic stimulation. *J Immunol.* (2012) 188:1156–67. doi: 10.4049/jimmunol.1102610
21. Weekes MP, Wills MR, Sissons JG, Carmichael AJ. Large HIV-specific CD8 cytotoxic T-lymphocyte (CTL) clones reduce their overall size but maintain high frequencies of memory CTL following highly active antiretroviral therapy. *Immunology* (2006) 118:25–38. doi: 10.1111/j.1365-2567.2006.02334.x
22. Rehr M, Cahenzli J, Haas A, Price DA, Gostick E, Huber M, et al. Emergence of polyfunctional $CD8^+$ T cells after prolonged suppression of human immunodeficiency virus replication by antiretroviral therapy. *J Virol.* (2008) 82:3391–404. doi: 10.1128/JVI.02383-07
23. Lam S, Sung J, Cruz C, Castillo-Caro P, Ngo M, Garrido C, et al. Broadly-specific cytotoxic T cells targeting multiple HIV antigens are expanded from HIV^+ patients: implications for immunotherapy. *Mol Ther.* (2015) 23:387–95. doi: 10.1038/mt.2014.207
24. Cartwright EK, Spicer L, Smith SA, Lee D, Fast R, Paganini S, et al. CD8(+) Lymphocytes are required for maintaining viral suppression in SIV-infected macaques treated with short-term antiretroviral therapy. *Immunity* (2016) 45:656–68. doi: 10.1016/j.immuni.2016.08.018
25. McIlroy D. Do HIV-specific CTL continue to have an antiviral function during antiretroviral therapy? If not, why not, and what can be done about it? *Front Immunol.* (2013) 4:52. doi: 10.3389/fimmu.2013.00052
26. Buzon MJ, Martin-Gayo E, Pereyra F, Ouyang Z, Sun H, Li JZ, et al. Long-term antiretroviral treatment initiated at primary HIV-1 infection affects the size, composition, and decay kinetics of the reservoir of HIV-1-infected CD4 T cells. *J Virol.* (2014) 88:10056–65. doi: 10.1128/JVI.01046-14
27. Takata H, Buranapraditkun S, Kessing C, Fletcher JL, Muir R, Tardif V, et al. Delayed differentiation of potent effector CD8(+) T cells reducing viremia and reservoir seeding in acute HIV infection. *Sci Transl Med.* (2017) 9:eaag1809. doi: 10.1126/scitranslmed.aag1809
28. Thomas AS, Jones KL, Gandhi RT, McMahon DK, Cyktor JC, Chan D, et al. T-cell responses targeting HIV Nef uniquely correlate with infected cell frequencies after long-term antiretroviral therapy. *PLoS Pathog.* (2017) 13:e1006629. doi: 10.1371/journal.ppat.1006629
29. Yue FY, Cohen JC, Ho M, Rahman AK, Liu J, Mujib S, et al. HIV-specific granzyme B-secreting but not gamma interferon-secreting T cells are associated with reduced viral reservoirs in early HIV infection. *J Virol.* (2017) 91:e02233–16. doi: 10.1128/JVI.02233-16
30. Ghiglione Y, Trifone C, Salido J, Rhodes A, Ruiz MJ, Polo ML, et al. PD-1 expression in HIV-specific $CD8^+$ T-cells prior to antiretroviral therapy is associated with HIV persistence. *J Acquir Immune Defic Syndr.* (in press).
31. Saez-Cirion A, Bacchus C, Hocqueloux L, Avettand-Fenoel V, Girault I, Lecuroux C, et al. Post-treatment HIV-1 controllers with a long-term virological remission after the interruption of early initiated antiretroviral therapy ANRS VISCONTI Study. *PLoS Pathog.* (2013) 9:e1003211. doi: 10.1371/journal.ppat.1003211
32. Socias ME, Sued O, Laufer N, Lazaro ME, Mingrone H, Pryluka D, et al. Acute retroviral syndrome and high baseline viral load are predictors of rapid HIV progression among untreated Argentinean seroconverters. *J Int AIDS Soc.* (2011) 14:40. doi: 10.1186/1758-2652-14-40
33. Turk G, Ghiglione Y, Hormanstorfer M, Laufer N, Coloccini R, Salido J, et al. Biomarkers of progression after HIV acute/early infection: nothing compares to CD4(+) T-cell count? *Viruses* (2018) 10:E34. doi: 10.3390/v10010034
34. Currier JR, Kuta EG, Turk E, Earhart LB, Loomis-Price L, Janetzki S, et al. A panel of MHC class I restricted viral peptides for use as a quality control for vaccine trial ELISPOT assays. *J Immunol Methods* (2002) 260:157–72. doi: 10.1016/S0022-1759(01)00535-X
35. Malhotra U, Li F, Nolin J, Allison M, Zhao H, Mullins JI, et al. Enhanced detection of human immunodeficiency virus type 1 (HIV-1) Nef-specific T cells recognizing multiple variants in early HIV-1 infection. *J Virol.* (2007) 81:5225–37. doi: 10.1128/JVI.02564-06
36. Turk G, Gherardi MM, Laufer N, Saracco M, Luzzi R, Cox JH, et al. Magnitude, breadth, and functional profile of T-cell responses during human immunodeficiency virus primary infection with B and BF viral variants. *J Virol.* (2008) 82:2853–66. doi: 10.1128/JVI.02260-07

37. Ruiz MJ, Salido J, Abusamra L, Ghiglione Y, Cevallos C, Damilano G, et al. Evaluation of different parameters of humoral and cellular immune responses in HIV serodiscordant heterosexual couples: humoral response potentially implicated in modulating transmission rates. *EBioMedicine* (2017) 26:25–37. doi: 10.1016/j.ebiom.2017.11.001
38. Ghiglione Y, Ruiz MJ, Salido J, Trifone C, Sued O, Martin Y, et al. Modification of the HIV-specific CD8$^+$ T-cell response in an HIV elite controller after chikungunya virus infection. *AIDS* (2016) 30:1905–11. doi: 10.1097/QAD.0000000000001129
39. Saez-Cirion A, Shin SY, Versmisse P, Barre-Sinoussi F, Pancino G. *Ex vivo* T cell-based HIV suppression assay to evaluate HIV-specific CD8$^+$ T-cell responses. *Nat Protoc.* (2010) 5:1033–41. doi: 10.1038/nprot.2010.73
40. Ndhlovu ZM, Proudfoot J, Cesa K, Alvino DM, McMullen A, Vine S, et al. Elite controllers with low to absent effector CD8$^+$ T cell responses maintain highly functional, broadly directed central memory responses. *J Virol.* (2012) 86:6959–69. doi: 10.1128/JVI.00531-12
41. Hermans IF, Silk JD, Yang J, Palmowski MJ, Gileadi U, McCarthy C, et al. The VITAL assay: a versatile fluorometric technique for assessing CTL- and NKT-mediated cytotoxicity against multiple targets *in vitro* and *in vivo*. *J Immunol Methods* (2004) 285:25–40. doi: 10.1016/j.jim.2003.10.017
42. Keele BF, Giorgi EE, Salazar-Gonzalez JF, Decker JM, Pham KT, Salazar MG, et al. Identification and characterization of transmitted and early founder virus envelopes in primary HIV-1 infection. *Proc Natl Acad Sci USA.* (2008) 105:7552–7. doi: 10.1073/pnas.0802203105
43. Salazar-Gonzalez JF, Bailes E, Pham KT, Salazar MG, Guffey MB, Keele BF, et al. Deciphering human immunodeficiency virus type 1 transmission and early envelope diversification by single-genome amplification and sequencing. *J Virol.* (2008) 82:3952–70. doi: 10.1128/JVI.02660-07
44. Lee HY, Giorgi EE, Keele BF, Gaschen B, Athreya GS, Salazar-Gonzalez JF, et al. Modeling sequence evolution in acute HIV-1 infection. *J Theor Biol.* (2009) 261:341–60. doi: 10.1016/j.jtbi.2009.07.038
45. Salazar-Gonzalez JF, Salazar MG, Keele BF, Learn GH, Giorgi EE, Li H, et al. Genetic identity, biological phenotype, and evolutionary pathways of transmitted/founder viruses in acute and early HIV-1 infection. *J Exp Med.* (2009) 206:1273–89. doi: 10.1084/jem.20090378
46. Roederer M, Nozzi JL, Nason MC. SPICE: exploration and analysis of post-cytometric complex multivariate datasets. *Cytometry A* (2011) 79:167–74. doi: 10.1002/cyto.a.21015
47. Macatangay BJ, Rinaldo CR. Preserving HIV-specific T cell responses: does timing of antiretroviral therapy help? *Curr Opin HIV AIDS* (2015) 10:55–60. doi: 10.1097/COH.0000000000000124
48. Almeida JR, Price DA, Papagno L, Arkoub ZA, Sauce D, Bornstein E, et al. Superior control of HIV-1 replication by CD8$^+$ T cells is reflected by their avidity, polyfunctionality, and clonal turnover. *J Exp Med.* (2007) 204:2473–85. doi: 10.1084/jem.20070784
49. Rodriguez AM, Pascutti MF, Maeto C, Falivene J, Holgado MP, Turk G, et al. IL-12 and GM-CSF in DNA/MVA immunizations against HIV-1 CRF12_BF Nef induced T-cell responses with an enhanced magnitude, breadth and quality. *PLoS ONE* (2012) 7:e37801. doi: 10.1371/journal.pone.0037801
50. Seder RA, Darrah PA, Roederer M. T-cell quality in memory and protection: implications for vaccine design. *Nat Rev Immunol.* (2008) 8:247–58. doi: 10.1038/nri2274
51. Vigano S, Bellutti Enders F, Miconnet I, Cellerai C, Savoye AL, Rozot V, et al. Rapid perturbation in viremia levels drives increases in functional avidity of HIV-specific CD8 T cells. *PLoS Pathog.* (2013) 9:e1003423. doi: 10.1371/journal.ppat.1003423
52. Grabmeier-Pfistershammer K, Steinberger P, Rieger A, Leitner J, Kohrgruber N. Identification of PD-1 as a unique marker for failing immune reconstitution in HIV-1-infected patients on treatment. *J Acquir Immune Defic Syndr.* (2011) 56:118–24. doi: 10.1097/QAI.0b013e3181fbab9f
53. Serrano-Villar S, Sainz T, Lee SA, Hunt PW, Sinclair E, Shacklett BL, et al. HIV-infected individuals with low CD4/CD8 ratio despite effective antiretroviral therapy exhibit altered T cell subsets, heightened CD8$^+$ T cell activation, and increased risk of non-AIDS morbidity and mortality. *PLoS Pathog.* (2014) 10:e1004078. doi: 10.1371/journal.ppat.1004078
54. Jensen SS, Fomsgaard A, Larsen TK, Tingstedt JL, Gerstoft J, Kronborg G, et al. Initiation of Antiretroviral Therapy (ART) at different stages of HIV-1 disease is not associated with the proportion of exhausted CD8$^+$ T Cells. *PLoS ONE* (2015) 10:e0139573. doi: 10.1371/journal.pone.0139573
55. Day CL, Kaufmann DE, Kiepiela P, Brown JA, Moodley ES, Reddy S, et al. PD-1 expression on HIV-specific T cells is associated with T-cell exhaustion and disease progression. *Nature* (2006) 443:350–4. doi: 10.1038/nature05115
56. Trautmann L, Janbazian L, Chomont N, Said EA, Gimmig S, Bessette B, et al. Upregulation of PD-1 expression on HIV-specific CD8$^+$ T cells leads to reversible immune dysfunction. *Nat Med.* (2006) 12:1198–202. doi: 10.1038/nm1482
57. Shan L, Deng K, Shroff NS, Durand CM, Rabi SA, Yang HC, et al. Stimulation of HIV-1-specific cytolytic T lymphocytes facilitates elimination of latent viral reservoir after virus reactivation. *Immunity* (2012) 36:491–501. doi: 10.1016/j.immuni.2012.01.014
58. Deng K, Pertea M, Rongvaux A, Wang L, Durand CM, Ghiaur G, et al. Broad CTL response is required to clear latent HIV-1 due to dominance of escape mutations. *Nature* (2015) 517:381–5. doi: 10.1038/nature14053
59. Sung JA, Lam S, Garrido C, Archin N, Rooney CM, Bollard CM, et al. Expanded cytotoxic T-cell lymphocytes target the latent HIV reservoir. *J Infect Dis.* (2015) 212:258–63. doi: 10.1093/infdis/jiv022
60. Huang SH, Ren Y, Thomas AS, Chan D, Mueller S, Ward AR, et al. Latent HIV reservoirs exhibit inherent resistance to elimination by CD8$^+$ T cells. *J Clin Invest.* (2018) 128:876–89. doi: 10.1172/JCI97555
61. Mylvaganam GH, Silvestri G, Amara RR. HIV therapeutic vaccines: moving towards a functional cure. *Curr Opin Immunol.* (2015) 35:1–8. doi: 10.1016/j.coi.2015.05.001
62. Jain V, Hartogensis W, Bacchetti P, Hunt PW, Hatano H, Sinclair E, et al. Antiretroviral therapy initiated within 6 months of HIV infection is associated with lower T-cell activation and smaller HIV reservoir size. *J Infect Dis.* (2013) 208:1202–11. doi: 10.1093/infdis/jit311
63. Rutishauser RL, Hartogensis W, Deguit CD, Krone M, Hoh R, Hecht FM, et al. Early and delayed antiretroviral therapy results in comparable reductions in CD8(+) T cell exhaustion marker expression. *AIDS Res Hum Retrovirus* (2017) 33:658–67. doi: 10.1089/aid.2016.0324
64. Chapuis AG, Casper C, Kuntz S, Zhu J, Tjernlund A, Diem K, et al. HIV-specific CD8$^+$ T cells from HIV$^+$ individuals receiving HAART can be expanded *ex vivo* to augment systemic and mucosal immunity *in vivo*. *Blood* (2011) 117:5391–402. doi: 10.1182/blood-2010-11-320226
65. Emu B, Moretto WJ, Hoh R, Krone M, Martin JN, Nixon DF, et al. Composition and function of T cell subpopulations are slow to change despite effective antiretroviral treatment of HIV disease. *PLoS ONE* (2014) 9:e85613. doi: 10.1371/journal.pone.0085613
66. Ndhlovu ZM, Stampouloglou E, Cesa K, Mavrothalassitis O, Alvino DM, Li JZ, et al. The breadth of expandable memory CD8$^+$ T cells inversely correlates with residual viral loads in HIV elite controllers. *J Virol.* (2015) 89:10735–47. doi: 10.1128/JVI.01527-15
67. Walker-Sperling VE, Cohen VJ, Tarwater PM, Blankson JN. Reactivation kinetics of HIV-1 and susceptibility of reactivated latently infected CD4$^+$ T cells to HIV-1-specific CD8$^+$ T cells. *J Virol.* (2015) 89:9631–8. doi: 10.1128/JVI.01454-15
68. Lichterfeld M, Yu XG, Cohen D, Addo MM, Malenfant J, Perkins B, et al. HIV-1 Nef is preferentially recognized by CD8 T cells in primary HIV-1 infection despite a relatively high degree of genetic diversity. *AIDS* (2004) 18:1383–92. doi: 10.1097/01.aids.0000131329.51633.a3
69. Gray CM, Mlotshwa M, Riou C, Mathebula T, de Assis Rosa D, Mashishi T, et al. Human immunodeficiency virus-specific gamma interferon enzyme-linked immunospot assay responses targeting specific regions of the proteome during primary subtype C infection are poor predictors of the course of viremia and set point. *J Virol.* (2009) 83:470–8. doi: 10.1128/JVI.01678-08
70. Adland E, Carlson JM, Paioni P, Kloverpris H, Shapiro R, Ogwu A, et al. Nef-specific CD8$^+$ T cell responses contribute to HIV-1 immune control. *PLoS ONE* (2013) 8:e73117. doi: 10.1371/journal.pone.0073117
71. Masemola A, Mashishi T, Khoury G, Mohube P, Mokgotho P, Vardas E, et al. Hierarchical targeting of subtype C human immunodeficiency virus type 1 proteins by CD8$^+$ T cells: correlation with viral load. *J Virol.* (2004) 78:3233–43. doi: 10.1128/JVI.78.7.3233-3243.2004

72. Zuniga R, Lucchetti A, Galvan P, Sanchez S, Sanchez C, Hernandez A, et al. Relative dominance of Gag p24-specific cytotoxic T lymphocytes is associated with human immunodeficiency virus control. *J Virol.* (2006) 80:3122–5. doi: 10.1128/JVI.80.6.3122-3125.2006
73. Geldmacher C, Currier JR, Herrmann E, Haule A, Kuta E, McCutchan F, et al. CD8 T-cell recognition of multiple epitopes within specific Gag regions is associated with maintenance of a low steady-state viremia in human immunodeficiency virus type 1-seropositive patients. *J Virol.* (2007) 81:2440–8. doi: 10.1128/JVI.01847-06
74. Kiepiela P, Ngumbela K, Thobakgale C, Ramduth D, Honeyborne I, Moodley E, et al. $CD8^+$ T-cell responses to different HIV proteins have discordant associations with viral load. *Nat Med.* (2007) 13:46–53. doi: 10.1038/nm1520
75. Streeck H, Jolin JS, Qi Y, Yassine-Diab B, Johnson RC, Kwon DS, et al. Human immunodeficiency virus type 1-specific $CD8^+$ T-cell responses during primary infection are major determinants of the viral set point and loss of $CD4^+$ T cells. *J Virol.* (2009) 83:7641–8. doi: 10.1128/JVI.00182-09
76. Riou C, Burgers WA, Mlisana K, Koup RA, Roederer M, Abdool Karim SS, et al. Differential impact of magnitude, polyfunctional capacity, and specificity of HIV-specific $CD8^+$ T cell responses on HIV set point. *J Virol.* (2014) 88:1819–24. doi: 10.1128/JVI.02968-13
77. Ferrando-Martinez S, Casazza JP, Leal M, Machmach K, Munoz-Fernandez MA, Viciana P, et al. Differential Gag-specific polyfunctional T cell maturation patterns in HIV-1 elite controllers. *J Virol.* (2012) 86:3667–74. doi: 10.1128/JVI.07034-11
78. Mujib S, Saiyed A, Fadel S, Bozorgzad A, Aidarus N, Yue FY, et al. Pharmacologic HIV-1 Nef blockade promotes CD8 T cell-mediated elimination of latently HIV-1-infected cells *in vitro*. *JCI Insight* (2017) 2:e93684. doi: 10.1172/jci.insight.93684
79. Imamichi H, Dewar RL, Adelsberger JW, Rehm CA, O'Doherty U, Paxinos EE, et al. Defective HIV-1 proviruses produce novel protein-coding RNA species in HIV-infected patients on combination antiretroviral therapy. *Proc Natl Acad Sci USA*. (2016) 113:8783–88. doi: 10.1073/pnas.1609057113
80. Betts MR, Nason MC, West SM, De Rosa SC, Migueles SA, Abraham J, et al. HIV nonprogressors preferentially maintain highly functional HIV-specific $CD8^+$ T cells. *Blood* (2006) 107:4781–9. doi: 10.1182/blood-2005-12-4818
81. Streeck H, Brumme ZL, Anastario M, Cohen KW, Jolin JS, Meier A, et al. Antigen load and viral sequence diversification determine the functional profile of HIV-1-specific $CD8^+$ T cells. *PLoS Med.* (2008) 5:e100. doi: 10.1371/journal.pmed.0050100
82. Ferrari G, Korber B, Goonetilleke N, Liu MK, Turnbull EL, Salazar-Gonzalez JF, et al. Relationship between functional profile of HIV-1 specific CD8 T cells and epitope variability with the selection of escape mutants in acute HIV-1 infection. *PLoS Pathog.* (2011) 7:e1001273. doi: 10.1371/journal.ppat.1001273
83. Mahnke YD, Brodie TM, Sallusto F, Roederer M, Lugli E. The who's who of T-cell differentiation: human memory T-cell subsets. *Eur J Immunol.* (2013) 43:2797–809. doi: 10.1002/eji.201343751
84. Champagne P, Ogg GS, King AS, Knabenhans C, Ellefsen K, Nobile M, et al. Skewed maturation of memory HIV-specific CD8 T lymphocytes. *Nature* (2001) 410:106–11. doi: 10.1038/35065118
85. Addo MM, Draenert R, Rathod A, Verrill CL, Davis BT, Gandhi RT, et al. Fully differentiated HIV-1 specific $CD8^+$ T effector cells are more frequently detectable in controlled than in progressive HIV-1 infection. *PLoS ONE* (2007) 2:e321. doi: 10.1371/journal.pone.0000321
86. Burgers WA, Riou C, Mlotshwa M, Maenetje P, de Assis Rosa D, Brenchley J, et al. Association of HIV-specific and total $CD8^+$ T memory phenotypes in subtype C HIV-1 infection with viral set point. *J Immunol.* (2009) 182:4751–61. doi: 10.4049/jimmunol.0803801
87. Vigano S, Negron J, Ouyang Z, Rosenberg ES, Walker BD, Lichterfeld M, et al. Prolonged antiretroviral therapy preserves HIV-1-specific CD8 T cells with stem cell-like properties. *J Virol.* (2015) 89:7829–40. doi: 10.1128/JVI.00789-15
88. Restifo NP, Dudley ME, Rosenberg SA. Adoptive immunotherapy for cancer: harnessing the T cell response. *Nat Rev Immunol.* (2012) 12:269–81. doi: 10.1038/nri3191
89. Breton G, Chomont N, Takata H, Fromentin R, Ahlers J, Filali-Mouhim A, et al. Programmed death-1 is a marker for abnormal distribution of naive/memory T cell subsets in HIV-1 infection. *J Immunol.* (2013) 191:2194–204. doi: 10.4049/jimmunol.1200646
90. Okazaki T, Chikuma S, Iwai Y, Fagarasan S, Honjo T. A rheostat for immune responses: the unique properties of PD-1 and their advantages for clinical application. *Nat Immunol.* (2013) 14:1212–18. doi: 10.1038/ni.2762
91. Barber DL, Wherry EJ, Masopust D, Zhu B, Allison JP, Sharpe AH, et al. Restoring function in exhausted CD8 T cells during chronic viral infection. *Nature* (2006) 439:682–7. doi: 10.1038/nature04444
92. Yamamoto T, Price DA, Casazza JP, Ferrari G, Nason M, Chattopadhyay PK, et al. Surface expression patterns of negative regulatory molecules identify determinants of virus-specific $CD8^+$ T-cell exhaustion in HIV infection. *Blood* (2011) 117:4805–15. doi: 10.1182/blood-2010-11-317297
93. Zangeneh Z, Golmoghaddam H, Emad M, Erfani N, Doroudchi M. Elevated PD-1 expression and decreased telomerase activity in memory T cells of patients with symptomatic Herpes Zoster infection. *Cell Mol Biol.* (2014) 60:13–21. doi: 10.14715/cmb/2014.60.4.3
94. Bellon M, Nicot C. Telomere dynamics in immune senescence and exhaustion triggered by chronic viral infection. *Viruses* (2017) 9:289. doi: 10.3390/v9100289
95. Hokey DA, Johnson FB, Smith J, Weber JL, Yan J, Hirao L, et al. Activation drives PD-1 expression during vaccine-specific proliferation and following lentiviral infection in macaques. *Eur J Immunol.* (2008) 38:1435–45. doi: 10.1002/eji.200737857
96. Donia M, Kjeldsen JW, Andersen R, Westergaard MCW, Bianchi V, Legut M, et al. PD-1(+) Polyfunctional T cells dominate the periphery after tumor-infiltrating lymphocyte therapy for cancer. *Clin Cancer Res.* (2017) 23:5779–88. doi: 10.1158/1078-0432.CCR-16-1692
97. Lichterfeld M, Mou D, Cung TD, Williams KL, Waring MT, Huang J, et al. Telomerase activity of HIV-1-specific $CD8^+$ T cells: constitutive up-regulation in controllers and selective increase by blockade of PD ligand 1 in progressors. *Blood* (2008) 112:3679–87. doi: 10.1182/blood-2008-01-135442
98. Porichis F, Kaufmann DE. Role of PD-1 in HIV pathogenesis and as target for therapy. *Curr HIV/AIDS Rep.* (2012) 9:81–90. doi: 10.1007/s11904-011-0106-4
99. Pantaleo G, Levy Y. Therapeutic vaccines and immunological intervention in HIV infection: a paradigm change. *Curr Opin HIV AIDS* (2016) 11:576–84. doi: 10.1097/COH.0000000000000324
100. Brockman MA, Jones RB, Brumme ZL. Challenges and Opportunities for T-cell-mediated strategies to eliminate HIV reservoirs. *Front Immunol.* (2015) 6:506. doi: 10.3389/fimmu.2015.00506
101. Masopust D, Picker LJ. Hidden memories: frontline memory T cells and early pathogen interception. *J Immunol.* (2012) 188:5811–7. doi: 10.4049/jimmunol.1102695
102. Freel SA, Picking RA, Ferrari G, Ding H, Ochsenbauer C, Kappes JC, et al. Initial HIV-1 antigen-specific $CD8^+$ T cells in acute HIV-1 infection inhibit transmitted/founder virus replication. *J Virol.* (2012) 86:6835–46. doi: 10.1128/JVI.00437-12

Conflict of Interest Statement: The authors declare that the research was conducted in the absence of any commercial or financial relationships that could be construed as a potential conflict of interest.

Copyright © 2018 Salido, Ruiz, Trifone, Figueroa, Caruso, Gherardi, Sued, Salomón, Laufer, Ghiglione and Turk. This is an open-access article distributed under the terms of the Creative Commons Attribution License (CC BY). The use, distribution or reproduction in other forums is permitted, provided the original author(s) and the copyright owner(s) are credited and that the original publication in this journal is cited, in accordance with accepted academic practice. No use, distribution or reproduction is permitted which does not comply with these terms.

frontiers in Immunology

MINI REVIEW
published: 25 October 2018
doi: 10.3389/fimmu.2018.02372

Harnessing the Induction of CD8+ T-Cell Responses Through Metabolic Regulation by Pathogen-Recognition-Receptor Triggering in Antigen Presenting Cells

Francesco Nicoli[1]*, *Stéphane Paul*[2] and *Victor Appay*[3,4]*

[1] Department of Molecular Medicine, University of Padua, Padua, Italy, [2] GIMAP/EA3064, Université de Lyon, CIC 1408 Vaccinology, Saint-Etienne, France, [3] Sorbonne Université, INSERM, Centre d'Immunologie et des Maladies Infectieuses, Paris, France, [4] International Research Center of Medical Sciences, Kumamoto University, Kumamoto, Japan

OPEN ACCESS

Edited by:
María Fernanda Pascutti, Sanquin Diagnostic Services, Netherlands

Reviewed by:
Alberto Bosque, George Washington University, United States
Clovis Steve Palmer, Burnet Institute, Australia

***Correspondence:**
Francesco Nicoli
nclfnc1@unife.it
Victor Appay
victor.appay@upmc.fr

Specialty section:
This article was submitted to T Cell Biology, a section of the journal Frontiers in Immunology

Received: *11 July 2018*
Accepted: *24 September 2018*
Published: *25 October 2018*

Citation:
Nicoli F, Paul S and Appay V (2018) Harnessing the Induction of CD8+ T-Cell Responses Through Metabolic Regulation by Pathogen-Recognition-Receptor Triggering in Antigen Presenting Cells. Front. Immunol. 9:2372. doi: 10.3389/fimmu.2018.02372

Cytotoxic CD8+ T-cells are key players of the immune responses against viruses. During the priming of a CD8+ T-cell response, the activation of a naïve T-cell by a professional antigen presenting cell (APC) involves the induction of various intracellular and metabolic pathways. The modulation of these pathways at the level of APCs or T-cells offers great potential to enhance the induction of robust effector cells and the generation of long-lived memory cells. On the one hand, signaling through pathogen recognition receptors (PRRs) expressed by APCs can greatly influence T-cell priming, and the potential of several PRR ligands as adjuvants are being studied. On the other hand, the engagement of several metabolic processes, at play in APCs and T-cells upon stimulation, implies that modulating cellular metabolism can impact on priming efficacy. Here, we review recent efforts to understand the interplay between PRR mediated signaling and metabolic pathway modulation in this context, through three examples: interplay between TLR4 and fatty acid metabolism, between TLR9 and IDO, and between STING and autophagy. These initial works highlight the potential for harnessing the induction of antiviral CD8+ T-cell responses using synergistic modulation of metabolic and PRR pathways.

Keywords: immunometabolism, pathogen-recognition-receptor, TLR4, TLR9, STING, adjuvants, CD8+ T-cell priming

INTRODUCTION

CD8+ T-cells are major actors of the fight against viruses. Owing to their capacity, through T-cell receptor (TCR)—peptide Major Histocompatibility Complex (pMHC) interactions, to recognize a diversity of antigens presented on virus infected cells, CD8+ T-cells can directly kill target cells. However, rather than their quantity or frequency, their quality, or aptitude to engage multiple effector functions, represents an important basis of their efficacy in viral infection settings (1, 2). Induction of CD8+ T-cells with superior qualitative properties is therefore a primary goal of vaccines and immunotherapies in this context. The acquisition of functional attributes by CD8+ T-cells is crucially dependent on the priming step of the response, when antigen specific naïve precursors get activated and expand in response to the presentation of their cognate antigen

by dendritic cells (DCs) (3, 4). In recent years, we have gained increasing knowledge about the determinants of the quality of $CD8^+$ T-cells, and how to influence them upon priming. For instance, dendritic cells (DCs) govern the nature of primed $CD8^+$ T-cells via the provision of processed antigens in the form of pMHC class I molecules (signal I) and other important signals, including costimulatory interactions (signal II) and inflammatory cytokines (signal III) (5). Much effort has been focused on the modulation of DC function through pathogen-recognition-receptor (PRR) triggering (6, 7), as PRR ligands can modulate these different signals and thereby enhance the priming process to elicit more robust T-cell responses (7–9). Molecules, such as Toll-like receptor (TLR) ligands, can improve the immunogenicity of antigens by mimicking pathogen-associated "danger" signals in order to improve T-cell immunity (10, 11).

Moreover, new insights into cellular metabolism have underlined the tight connection existing between metabolic and functional properties of immune cells (12). For instance, recent studies have demonstrated that aerobic or catabolic metabolic processes and mitochondrial biogenesis control $CD8^+$ T-cell effector and memory cell formation (13, 14). In response to activation, $CD8^+$ T-cells undergo a metabolic transition or reprogramming. Quiescent naive T-cells have a low metabolic demand and rely primarily on oxidative phosphorylation (OXPHOS) (15, 16). Upon activation though, they switch to a AKT/mTOR-orchestrated reliance on multiple metabolic pathways including aerobic glycolysis, glutaminolysis and OXPHOS, which are important for the acquisition of effector functions and sustained proliferation (15–18). Eventually, memory $CD8^+$ T-cells regain a more catabolic metabolism and preferentially rely on fatty acid (FA) synthesis to fuel FA oxidation and enhance mitochondria respiratory capacity, and thus provide survival advantages (19). Cellular metabolic intermediates are therefore major regulators of $CD8^+$ T-cell activation and can dictate functional performance of effector cells upon priming (20). This opens new avenues to modulate cellular metabolic activity in order to promote the induction of high quality immune responses and enhance antiviral as well as antitumor $CD8^+$ T-cell immunity. In this review, we discuss initial considerations regarding the metabolic parallels between PRR- or TCR-mediated stimulation, and recent works highlighting how the quality of primed $CD8^+$ T-cells may be altered through metabolic regulation of T-cells or DCs using PRR agonists.

DIFFERENCES AND SIMILARITIES BETWEEN PRR- AND TCR-INDUCED METABOLIC REPROGRAMMING

The activation of both APCs via PRRs and T-cells via TCR is energetically reliant on the adoption of anabolic processes, and in particular on the consumption of glucose and production of lactate by a metabolic pathway called Warburg metabolism or aerobic glycolysis (15, 21–27). The rapid engagement of glycolysis has been shown in response to a broad array of PRR agonists, including ligands for TLR2, 4, 7, 9, and C-type lectin receptors, and is essential to support their stimulatory effects (22–25). Similarly, glycolysis is required for differentiation into effector cells and cytokine secretion in T lymphocytes upon TCR-mediate activation (26, 27).

The anabolic processes that regulate the activation of both DCs and T-cells are under the control of mTOR (15, 21), which is essential for differentiation of T-cells (28, 29) as well as for the maturation, differentiation, survival and T-cell stimulatory activity of DCs (21, 30–34). The glycolytic burst occurring in APC and T-cell upon activation is also supported by mTOR, via the transcription factors Hypoxia-inducible factor-1α (HIF-1α), that prompts the expression of key glycolytic enzymes (35–37). However, it has been reported that TCR-induced proliferation may occur also in the presence of mTOR inhibition (28, 29), which instead improves pro-inflammatory effects of TLR stimulation, resulting in enhanced IL-12 production and reduced IL-10 release by DCs (33, 38, 39), depending on the DC type (33). Therefore, the exact involvement of mTOR in integrating TCR and PRR signaling is not completely understood, and clues indicate a different role for this kinase in DC and T-cell activation.

Of note, TLR-induced metabolic reprogramming involves also the activation of *de novo* fatty acid synthesis (FAS) (23), required for the production of membranes to expand organelles (23). Interestingly, FAS is induced also after T-cell activation, and necessary for their expansion (12, 40). The induction of FAS upon PRR and TCR stimulation leads to the storage of fatty acids in lipid droplets (23, 41), whose function still remains controversial. Indeed, DCs with high content of lipids have been shown to better activate T-cells in the liver (42) but displayed diminished priming capacity within tumors (43). In addition, while storage of FA into triacylglycerol may be a mechanism exerted to avoid lipotoxicity (44), excess on neutral lipids has also been shown to induce apoptosis in T-cells (45).

INTERPLAY BETWEEN TLR4 AND FATTY ACID METABOLISM

The canonical Toll-like receptor 4 (TLR4) signaling cascade is initiated when lipid A (the membrane anchor of lipopolysaccharide [LPS]) is bound by the extracellular region of CD14, which complexes with MD2 and binds to membrane-bound TLR4 (46). Dimerization of these molecules with another lipid A-MD2-TLR4 complex creates a functional TLR4 signaling complex (47). Binding of a TLR4 agonist like lipid A initiates an innate immune response that can drive the development of antigen-specific acquired immunity (48). Mimicking the innate sensing of molecular patterns derived from microbes—pathogenic and non-pathogenic—to activate of immune cells, TLR4 agonist molecules show great promise for use as immunotherapeutic adjuvants to potentiate host responses in component vaccines [Reviewed in Reed et al. (48)].

With respect to metabolism, TLR4 stimulation has been linked with FA-induced inflammation in a number of pathologic conditions, including insulin resistance, retinal impairment, atherosclerosis and myocardial injury observed during diabetes

and obesity (49–54). Long chain, saturated FAs (SFAs) require TLR4 to exert pro-inflammatory effects (55), and have been suggested to bind it (53, 56). Lipid A itself is acylated with SFAs (57), whose number, length and saturation determine the TLR4 agonistic properties of LPS (49, 57). Conversely, poly-unsaturated FAs (PUFAs) inhibit TLR4 activation (49, 58). Notably, a similar pattern has been shown for another bacterial cell wall sensor, TLR2 (59). More recently, it has been proposed that SFAs may act as agonists of TLR4 without binding it (55, 60). SFAs may indeed be able to induce TLR4 dimerization in lipid rafts, in a ligand-independent manner (61), a step that is inhibited by PUFA. Irrespective of the mechanisms, evidence is concordant in suggesting that saturated and polyunsaturated FAs exert opposite effects on TLR4-mediated inflammatory response and APC activation. Indeed, SFAs may up-regulate the expression of costimulatory molecules and cytokines, resulting in increased T-cell activation capacity, while these effects are inhibited by PUFA (62). Several lines of evidence suggest that PUFA may reduce the induction of T-cell responses (63–65), acting on both APCs and T-cells. In addition to preventing TLR4 dimerization in lipid rafts and inhibiting downstream kinases (61, 66), PUFA can affect lipid rafts composition in T-cells, altering TCR signaling (67, 68) and resulting in hampered T-cell functionality (68–70). Overall, SFAs may favor co-stimulation delivered by APCs to T-cells and favor both TLR4 and TCR signaling (71), thus potentially boosting priming capacity (**Figure 1A**).

However, the role of specific FA species on T-cell functionality is not yet completely understood (44). Although it appears clear that FA are required during T-cell expansion (72), their excess may result in reduced T-cell proliferation and increases apoptosis (44, 73), and their use as energy source (fatty acid oxidation—FAO) was initially considered not to contribute to T-cell expansion following priming (74), although important for the transition of primed T-cells toward memory (74). Conversely, it has been recently discovered that FAO may sustain metabolic shift occurring upon TLR4 and TCR stimulation, in low glucose concentration conditions (75, 76) and during graft-vs.-host disease (77), suggesting a potential role for FAO in T-cell priming. SFA-mediated pro-inflammatory signaling requires their ligation with coenzyme A, a necessary step for SFA oxidation (55), indicating that FAO may be important to facilitate pro-inflammatory effects. This indicates therefore that the enhancement of FA catabolism may synergize with TLR4 activation to boost T-cell priming. Although further studies are necessary to better understand the underlying mechanisms, three hypotheses about the role of FAO in boosting T-cell priming may be proposed: (i) the induction of pro-inflammatory signals; (ii) the provision of additional energy sources to the activated APCs and T-cells, and (iii) the removal of high (and potentially toxic) concentration of SFAs or of FA with inhibitory activity (such as PUFA).

INTERPLAY BETWEEN TLR9 AND IDO

TLR9 is an endosomal receptor recognizing specific unmethylated CpG motifs present at high frequency in bacterial genome but absent in the mammalian one. TLR9 signals via the adaptor protein MyD88, leading to the production of pro-inflammatory cytokines (after activation of the NF-κB pathway) and type I interferon (after activation of the IRF7 pathway) (78–80). Interestingly, TLR9 has also been identified as a specific sensor of RNA:DNA hybrids, a key intermediate component essential to the replication during infection. The use of TLR9 agonists as vaccine adjuvant presents a great potential [Reviewed in Scheiermann and Klinman (81)], and DNA vaccines containing unmethylated CpG motifs show an enhanced immunogenicity (7, 82).

Nonetheless, increasing evidence indicates that TLR9 stimulation may also have immunosuppressive/tolerogenic effects. Despite the lack of consensus on this issue, the major mechanism explaining this phenomenon is the TLR9-mediated modulation of Indoleamine 2,3-dioxygenase (IDO), that catalyzes the first step of tryptophan catabolism (**Figure 1B**). *In vivo* systemic treatment with different TLR9-ligands could decrease the onset/severity of autoimmune diseases but increase susceptibility to infections in a IDO-dependent manner (83–87). Indeed, high CpG oligodeoxynucleotide doses may induce IDO in pDCs and splenocytes (86, 88), reducing the secretion of pro-inflammatory cytokines and favoring the expression of PD-L1, fostering the acquisition of suppressive activity by Tregs (89) and reducing antigen-specific T-cell expansion (86, 88, 90). Nonetheless, TLR9-mediated IDO induction of immunosuppressive properties depends on the type of TLR9 ligand used, as well as on the dose and route of administration (85–87, 90). The induction of IDO expression is a well-known immunosuppressive mechanism, which is also observed in several viral infections (91, 92). In addition to TLRs, IDO expression may also be induced upon stimulation of several receptors, including those for type I and II interferons, CD40L and TGFβ (93). Tryptophan degradation in the kynurenine pathway (KP), whose first step is mediated by IDO, may lower the concentrations of this amino acid, essential for cell survival and proliferation, and result in the synthesis of KP metabolites with immunosuppressive activity (93). Tryptophan depletion inhibits mTORC1 activity in T-cells as well as their proliferation (93, 94), while moDCs and pDCs expressing IDOs might prompt Treg expansion and suppressive activity (95, 96). As a result, T-cell priming efficacy and the generation of robust antiviral and memory responses was shown to be ameliorated by the use of IDO inhibitors *in vivo* (97–99). The use of IDO inhibitors may therefore reduce immunosuppressive effects of TLR9 ligands and boost its adjuvant activity, favoring the induction of strong antiviral and antitumor T-cell responses (**Figure 1B**).

INTERPLAY BETWEEN STING AND AUTOPHAGY

In the recent years, a strong enthusiasm for the study of the stimulator of interferon genes (STING) pathway has led to a better knowledge of the complexity of cytosolic DNA sensors (100). First identified as an adaptor protein mediating innate immune signaling induced by cytosolic DNA sensors, STING's

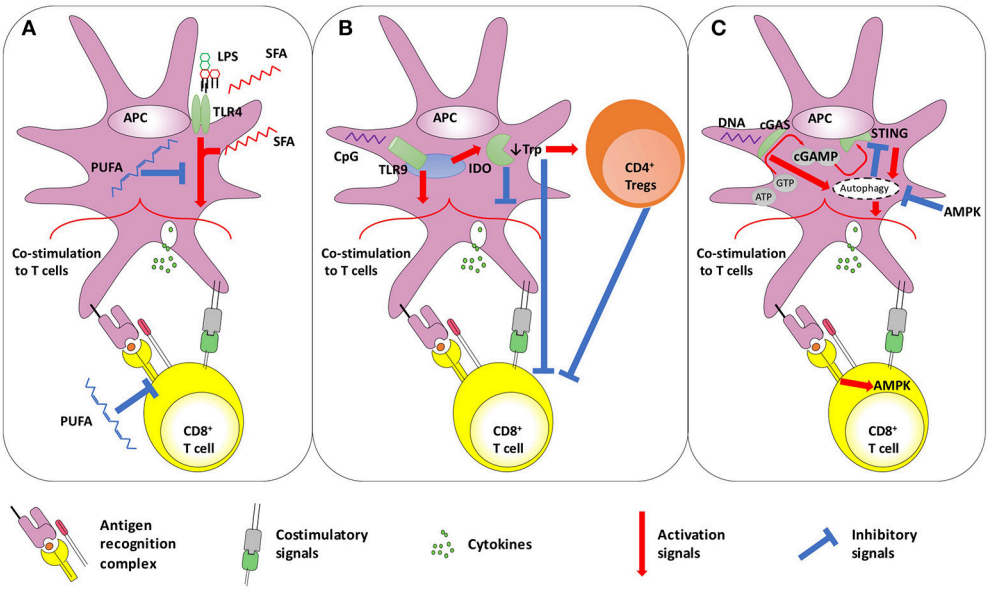

FIGURE 1 | Schematic representation of the interplay between **(A)** TLR4 and fatty acid metabolism, **(B)** TLR9 and IDO, and **(C)** STING and autophagy. **(A)** TLR4 activation on APCs improves $CD8^+$ T-cell priming. In addition to LPS, SFA are also thought to trigger TLR4. However, it has also been proposed that SFA act on TLR4-downstream pathways. In contrast, PUFA display anti-inflammatory effects, by dampening both TLR4- and TCR-induced signaling. **(B)** Dual role of TLR9 stimulation on T-cell activation. The TLR9 ligand CpG shows adjuvant effects, improving the co-stimulation delivered by APCs to T-cells. However, some reports highlighted that the same pathway may also trigger negative regulators of immunity, such as IDO that down-modulates APC-provided co-stimulation and favors Treg activity. Furthermore, IDO mediates tryptophan deprivation, with has negative consequences on T-cell functionality. **(C)** The autophagy-STING loop. The cytosolic DNA sensors cGAS converts ATP and GTP into the dinucleotide cGAMP, which triggers STING. Both cGAS and STING may promote authophagy, that can be involved in two distinct processes: inducing APC-delivered co-stimulation to T-cells, and STING degradation to avoid its permanent activation. The latter process seems under the control of AMPK, a kinase also acting in downstream TCR signaling in T-cells. AMPK, AMP-activated protein kinase; APC, antigen presenting cell; ATP, Adenosine Triphosphate; cGAMP, cyclic guanosine monophosphate–adenosine monophosphate; cGAS, cGAMP synthase; CpG, CpG oligodeoxynucleotides; GTP, Guanosine Triphosphate; IDO, Indoleamine 2;3-dioxygenase; Trp, tryptophan; LPS, lipopolysaccharide; PUFA, poly-unsaturated fatty acids; SFA, saturated fatty acids; STING, stimulator of interferon genes; TLR, toll like receptor.

function as cyclic di-nucleotide sensor has been described only recently (101), generating great enthusiasm for its potential use in cancer immunotherapy [Reviewed in Iurescia et al. (102)]. STING is a receptor for cyclic guanosine monophosphate–adenosine monophosphate (cGAMP), which can be synthesized by cGAS (cGAMP synthase), a member of the nucleotidyl transferase family. The latter plays a role in the recognition of HIV and other retroviruses leading to the synthesis of cGAMP (103). The produced cGAMP acts as an endogenous second messenger that binds to STING, leading to the activation of IRF3 and the induction of type I interferon synthesis (101). In addition to its major role for RNA virus sensing, it has been shown that cGAS expression also broadly inhibits several DNA viruses. However, the effect of cGAS is not limited to viruses. It acts as a DNA sensor responsible for the recognition of *Mycobacterium tuberculosis*, leading to the activation of the STING pathway. The recognition of this bacteria, as well as others, is made through cyclic-di-AMP, a bacterial cyclic di-nucleotide (CDN) leading to the production of IFN-β. CDN are also able to stimulate STING directly, and to activate an innate immune response leading to the induction of type I interferons. Interestingly, it has been demonstrated that RNA:DNA hybrids are also sensed by the immune system through the cGAS-STING pathway, inducing a strong type I interferon response. cGAMP has proven to be an effective adjuvant, able to boost the production of antigen-specific antibodies and T-cell responses after an intramuscular administration in mice. It has been recently evidenced that cGAMP is a promising mucosal adjuvant. STING agonists are also novel and highly promising immunomodulators for cancer immunotherapy (104). Its activation by CDN has proved to be efficient for anti-tumoral vaccination against metastatic breast cancer. Surprisingly, the STING pathway can also be triggered upon mitochondrial damage through the generation of mitochondrial ROS and the release of endogenous DNA into the cytosol.

Increasing evidence indicates that pathogen-derived CDN may trigger autophagy via STING (105–107), which forms cytoplasmic structures with LC3 and Atg9a, two proteins involved in the autophagy process (108). However, controversies exist about the significance of STING-induced autophagy. Indeed, STING and TBK1 migrates together via an autophagy-like process (109), and autophagy inhibition in cells infected with viruses known to activate STING dampens type I interferon production (107, 109). This suggests that autophagy seems essential to STING mediated pro-inflammatory effects (**Figure 1C**). Consistently, downstream STING type I IFN induction is dependent on Vps34 (110), a phosphatidylinositol 3-kinase (PI3K) required for autophagy initiation (111).

However, other two important autophagy-related proteins, Beclin-1 and the serine/threonine protein kinase ULK1, are dispensable for STING pro-inflammatory effects (110) but, rather, involved in STING degradation. ULK1 is activated, after the formation of STING-dependent autophagosomes, by the same cyclic dinucleotides that activate STING, but mediates its phosphorylation and blocking (110), while Beclin-1 interacts with cGAS to promote autophagy in a STING-independent manner, dampening interferon responses (112). Thus, autophagy would prompt STING degradation to avoid its chronic activity (110, 113). The dual role of autophagy in STING stimulation, delivering STING pro-inflammatory signaling at first and then mediating its degradation, suggests a temporal biphasic function of this metabolic process. Interestingly, a similar pattern has been described in T-cell activation: autophagy has been shown to first support NF-κB signaling in T-cells to then downregulate it (114, 115). Autophagy is activated and needed at the beginning of TCR stimulation to sense, and thus activate, mTOR (116, 117); then mTOR itself shuts down autophagy, which seems no longer required for effector cell generation, although essential for memory cell formation (117–119).

Further studies are needed to investigate which autophagy-related proteins should be targeted to improve STING adjuvant effects, enhancing downstream signaling and postponing its degradation to ensure prolonged STING activity at least during the initial phases of T-cell priming. Notably, cGAS-Beclin-1 mediated STING regulation is prompted by ligands, but not products of cGAS (such as 2′3′cGAMP), suggesting that the use of direct STING agonists may overcome this control mechanism leaving unaffected STING-induced autophagy. In addition, as the ULK1-dependent negative feedback is regulated by AMPK (110), whose inhibition leads to ULK1 activation, STING degradation and type I IFN response reduction (110, 120), AMPK activators might be used to prolong STING activity. It should be noted that AMPK has often been considered as anti-inflammatory, also for its capacity to suppress mTOR activity (121), which is required for T-cell activation. Nevertheless, AMPK activation occurs during and is essential for primary T-cell responses (74, 121, 122), may boost the generation of memory cells (74, 121), restore the functionality of exhausted effector cells (123) and generate robust effector cells starting from naïve cells (121, 123). Therefore, the potential use of AMPK activators in combination with STING ligands for priming of T-cell responses should be further explored with the aim to prolong STING pro-inflammatory activity, counteract exhaustion and prompt the generation of the memory pool.

CONCLUDING REMARKS

The discovery of PRRs and their ligands certainly represents one of the most fundamental advances of modern immunology with many, some yet to discover, applications in the context of vaccine development. In the recent years, our growing perception of the importance of immunometabolism is also opening new directions for immune interventions. Although it is still early days, the examples discussed in the present review provide clear evidence that combining our knowledge on metabolic immune regulation and PRR pathway activation offer great potential to influence the induction of potent immune responses. It will be important to assess the prospective use of such therapeutic approaches in animal or pre-clinical studies in order to better characterize benefits and drawbacks of these strategies in *in vivo* settings. Eventually, the combination of metabolic regulators and PRR based adjuvants may prove particularly effective in context of difficult to vaccinate populations, such as the elderly, whom immune cells present both metabolic and functional alterations, and overall suboptimal immune responsiveness.

AUTHOR CONTRIBUTIONS

FN, SP, and VA reviewed the literature and wrote the manuscript.

FUNDING

FN was funded by the Agence Nationale de la Recherche (ANR Project 14-CE14-0030-01).

REFERENCES

1. Nicoli F, Gallerani E, Skarlis C, Sicurella M, Cafaro A, Ensoli B, et al. Systemic immunodominant CD8 responses with an effector-like phenotype are induced by intravaginal immunization with attenuated HSV vectors expressing HIV Tat and mediate protection against HSV infection. *Vaccine* (2016) 34:2216–24. doi: 10.1016/j.vaccine.2016.03.022
2. Almeida JR, Price DA, Papagno L, Arkoub ZA, Sauce D, Bornstein E, et al. Superior control of HIV-1 replication by CD8+ T cells is reflected by their avidity, polyfunctionality, and clonal turnover. *J Exp Med.* (2007) 204:2473–85. doi: 10.1084/jem.20070784
3. Mercado R, Vijh S, Allen SE, Kerksiek K, Pilip IM, Pamer EG. Early programming of T cell populations responding to bacterial infection. *J Immunol.* (2000) 165:6833–9. doi: 10.4049/jimmunol.165.12.6833
4. Badovinac VP, Porter BB, Harty JT. CD8+ T cell contraction is controlled by early inflammation. *Nat Immunol.* (2004) 5:809–17. doi: 10.1038/ni1098
5. Mescher MF, Curtsinger JM, Agarwal P, Casey KA, Gerner M, Hammerbeck CD, et al. Signals required for programming effector and memory development by CD8+ T cells. *Immunol Rev.* (2006) 211:81–92. doi: 10.1111/j.0105-2896.2006.00382.x
6. Banchereau J, Palucka AK. Dendritic cells as therapeutic vaccines against cancer. *Nat Rev Immunol.* (2005) 5:296–306. doi: 10.1038/nri1592
7. Gutjahr A, Tiraby G, Perouzel E, Verrier B, Paul S. Triggering intracellular receptors for vaccine adjuvantation. *Trends Immunol.* (2016) 37:573–87. doi: 10.1016/j.it.2016.07.001
8. Nicoli F, Finessi V, Sicurella M, Rizzotto L, Gallerani E, Destro F, et al. The HIV-1 Tat protein induces the activation of CD8(+) T cells and affects *in vivo* the magnitude and kinetics of antiviral responses. *PLoS ONE* (2013) 8:e77746. doi: 10.1371/journal.pone.0077746
9. Pavot V, Rochereau N, Resseguier J, Gutjahr A, Genin C, Tiraby G, et al. Cutting edge: new chimeric NOD2/TLR2 adjuvant drastically increases vaccine immunogenicity. *J Immunol.* (2014) 193:5781–5. doi: 10.4049/jimmunol.1402184
10. Kawai T, Akira S. The role of pattern-recognition receptors in innate immunity: update on Toll-like receptors. *Nat Immunol.* (2010) 11:373–84. doi: 10.1038/ni.1863
11. Coffman RL, Sher A, Seder RA. Vaccine adjuvants: putting innate immunity to work. *Immunity* (2010) 33:492–503. doi: 10.1016/j.immuni.2010.10.002
12. Zhang L, Romero P. Metabolic control of CD8(+) T cell fate decisions and antitumor immunity. *Trends Mol Med.* (2018) 24:30–48. doi: 10.1016/j.molmed.2017.11.005

13. Ron-Harel N, Santos D, Ghergurovich JM, Sage PT, Reddy A, Lovitch SB, et al. Mitochondrial biogenesis and proteome remodeling promote one-carbon metabolism for T cell activation. *Cell Metab.* (2016) 24:104–17. doi: 10.1016/j.cmet.2016.06.007
14. van der Windt GJ, O'Sullivan D, Everts B, Huang SC, Buck MD, Curtis JD, et al. CD8 memory T cells have a bioenergetic advantage that underlies their rapid recall ability. *Proc Natl Acad Sci USA.* (2013) 110:14336–41. doi: 10.1073/pnas.1221740110
15. Almeida L, Lochner M, Berod L, Sparwasser T. Metabolic pathways in T cell activation and lineage differentiation. *Semin Immunol.* (2016) 28:514–24. doi: 10.1016/j.smim.2016.10.009
16. van der Windt GJ, Pearce EL. Metabolic switching and fuel choice during T-cell differentiation and memory development. *Immunol Rev.* (2012) 249:27–42. doi: 10.1111/j.1600-065X.2012.01150.x
17. Cham CM, Driessens G, O'Keefe JP, Gajewski TF. Glucose deprivation inhibits multiple key gene expression events and effector functions in CD8+ T cells. *Eur J Immunol.* (2008) 38:2438–50. doi: 10.1002/eji.200838289
18. Wang R, Dillon CP, Shi LZ, Milasta S, Carter R, Finkelstein D, et al. The transcription factor Myc controls metabolic reprogramming upon T lymphocyte activation. *Immunity* (2011) 35:871–82. doi: 10.1016/j.immuni.2011.09.021
19. O'Sullivan D, van der Windt GJ, Huang SC, Curtis JD, Chang CH, Buck MD, et al. Memory CD8(+) T cells use cell-intrinsic lipolysis to support the metabolic programming necessary for development. *Immunity* (2014) 41:75–88. doi: 10.1016/j.immuni.2014.06.005
20. Shehata HM, Murphy AJ, Lee MKS, Gardiner CM, Crowe SM, Sanjabi S, et al. Sugar or fat?-metabolic requirements for immunity to viral infections. *Front Immunol.* (2017) 8:1311. doi: 10.3389/fimmu.2017.01311
21. Pearce EJ, Everts B. Dendritic cell metabolism. *Nat Rev Immunol.* (2015) 15:18–29. doi: 10.1038/nri3771
22. Krawczyk CM, Holowka T, Sun J, Blagih J, Amiel E, DeBerardinis RJ, et al. Toll-like receptor–induced changes in glycolytic metabolism regulate dendritic cell activation. *Blood* (2010) 115:4742–9. doi: 10.1182/blood-2009-10-249540
23. Everts B, Amiel E, Huang SC, Smith AM, Chang CH, Lam WY, et al. TLR-driven early glycolytic reprogramming via the kinases TBK1-IKKvarepsilon supports the anabolic demands of dendritic cell activation. *Nat Immunol.* (2014) 15:323–32. doi: 10.1038/ni.2833
24. Dominguez-Andres J, Arts RJW, Ter Horst R, Gresnigt MS, Smeekens SP, Ratter JM, et al. Rewiring monocyte glucose metabolism via C-type lectin signaling protects against disseminated candidiasis. *PLoS Pathog.* (2017) 13:e1006632. doi: 10.1371/journal.ppat.1006632
25. Saas P, Varin A, Perruche S, Ceroi A. Recent insights into the implications of metabolism in plasmacytoid dendritic cell innate functions: potential ways to control these functions. *F1000Res.* (2017) 6:456. doi: 10.12688/f1000research.11332.1
26. Michalek RD, Gerriets VA, Jacobs SR, Macintyre AN, MacIver NJ, Mason EF, et al. Cutting edge: distinct glycolytic and lipid oxidative metabolic programs are essential for effector and regulatory CD4+ T cell subsets. *J Immunol.* (2011) 186:3299–303. doi: 10.4049/jimmunol.1003613
27. Menk AV, Scharping NE, Moreci RS, Zeng X, Guy C, Salvatore S, et al. Early TCR signaling induces rapid aerobic glycolysis enabling distinct acute T cell effector functions. *Cell Rep.* (2018) 22:1509–21. doi: 10.1016/j.celrep.2018.01.040
28. Delgoffe GM, Kole TP, Zheng Y, Zarek PE, Matthews KL, Xiao B, et al. The mTOR kinase differentially regulates effector and regulatory T cell lineage commitment. *Immunity* (2009) 30:832–44. doi: 10.1016/j.immuni.2009.04.014
29. Araki K, Turner AP, Shaffer VO, Gangappa S, Keller SA, Bachmann MF, et al. mTOR regulates memory CD8 T-cell differentiation. *Nature* (2009) 460:108–12. doi: 10.1038/nature08155
30. Woltman AM, van der Kooij SW, Coffer PJ, Offringa R, Daha MR, van Kooten C. Rapamycin specifically interferes with GM-CSF signaling in human dendritic cells, leading to apoptosis via increased p27KIP1 expression. *Blood* (2003) 101:1439–45. doi: 10.1182/blood-2002-06-1688
31. Hackstein H, Taner T, Zahorchak AF, Morelli AE, Logar AJ, Gessner A, et al. Rapamycin inhibits IL-4–induced dendritic cell maturation *in vitro* and dendritic cell mobilization and function *in vivo*. *Blood* (2003) 101:4457–63. doi: 10.1182/blood-2002-11-3370
32. Monti P, Mercalli A, Leone BE, Valerio DC, Allavena P, Piemonti L. Rapamycin impairs antigen uptake of human dendritic cells. *Transplantation* (2003) 75:137–45. doi: 10.1097/00007890-200301150-00025
33. Haidinger M, Poglitsch M, Geyeregger R, Kasturi S, Zeyda M, Zlabinger GJ, et al. A versatile role of mammalian target of rapamycin in human dendritic cell function and differentiation. *J Immunol.* (2010) 185:3919–31. doi: 10.4049/jimmunol.1000296
34. Yang CS, Song CH, Lee JS, Jung SB, Oh JH, Park J, et al. Intracellular network of phosphatidylinositol 3-kinase, mammalian target of the rapamycin/70 kDa ribosomal S6 kinase 1, and mitogen-activated protein kinases pathways for regulating mycobacteria-induced IL-23 expression in human macrophages. *Cell Microbiol.* (2006) 8:1158–71. doi: 10.1111/j.1462-5822.2006.00699.x
35. Land SC, Tee AR. Hypoxia-inducible factor 1alpha is regulated by the mammalian target of rapamycin (mTOR) via an mTOR signaling motif. *J Biol Chem.* (2007) 282:20534–43. doi: 10.1074/jbc.M611782200
36. Finlay DK, Rosenzweig E, Sinclair LV, Feijoo-Carnero C, Hukelmann JL, Rolf J, et al. PDK1 regulation of mTOR and hypoxia-inducible factor 1 integrate metabolism and migration of CD8+ T cells. *J Exp Med.* (2012) 209:2441–53. doi: 10.1084/jem.20112607
37. Cheng SC, Quintin J, Cramer RA, Shepardson KM, Saeed S, Kumar V, et al. mTOR- and HIF-1alpha-mediated aerobic glycolysis as metabolic basis for trained immunity. *Science* (2014) 345:1250684. doi: 10.1126/science.1250684
38. Ohtani M, Nagai S, Kondo S, Mizuno S, Nakamura K, Tanabe M, et al. Mammalian target of rapamycin and glycogen synthase kinase 3 differentially regulate lipopolysaccharide-induced interleukin-12 production in dendritic cells. *Blood* (2008) 112:635–43. doi: 10.1182/blood-2008-02-137430
39. Weichhart T, Werzowa J, Horl WH, Saemann MD. Biological action of rapamycin in renal transplantation. *Am J Kidney Dis.* (2008) 51:531; author reply 531–2. doi: 10.1053/j.ajkd.2007.09.027
40. Kidani Y, Elsaesser H, Hock MB, Vergnes L, Williams KJ, Argus JP, et al. Sterol regulatory element-binding proteins are essential for the metabolic programming of effector T cells and adaptive immunity. *Nat Immunol.* (2013) 14:489–99. doi: 10.1038/ni.2570
41. Angela M, Endo Y, Asou HK, Yamamoto T, Tumes DJ, Tokuyama H, et al. Fatty acid metabolic reprogramming via mTOR-mediated inductions of PPARgamma directs early activation of T cells. *Nat Commun.* (2016) 7:13683. doi: 10.1038/ncomms13683
42. Ibrahim J, Nguyen AH, Rehman A, Ochi A, Jamal M, Graffeo CS, et al. Dendritic cell populations with different concentrations of lipid regulate tolerance and immunity in mouse and human liver. *Gastroenterology* (2012) 143:1061–72. doi: 10.1053/j.gastro.2012.06.003
43. Herber DL, Cao W, Nefedova Y, Novitskiy SV, Nagaraj S, Tyurin VA, et al. Lipid accumulation and dendritic cell dysfunction in cancer. *Nat Med.* (2010) 16:880–6. doi: 10.1038/nm.2172
44. de Jong AJ, Kloppenburg M, Toes RE, Ioan-Facsinay A. Fatty acids, lipid mediators, and T-cell function. *Front Immunol.* (2014) 5:483. doi: 10.3389/fimmu.2014.00483
45. Al-Saffar NM, Titley JC, Robertson D, Clarke PA, Jackson LE, Leach MO, et al. Apoptosis is associated with triacylglycerol accumulation in Jurkat T-cells. *Br J Cancer* (2002) 86:963–70. doi: 10.1038/sj.bjc.6600188
46. Gregg KA, Harberts E, Gardner FM, Pelletier MR, Cayatte C, Yu L, et al. Rationally designed TLR4 ligands for vaccine adjuvant discovery. *MBio* (2017) 8:e00492-17. doi: 10.1128/mBio.00492-17
47. Park SN, Noh KT, Jeong YI, Jung ID, Kang HK, Cha GS, et al. Rhamnogalacturonan II is a Toll-like receptor 4 agonist that inhibits tumor growth by activating dendritic cell-mediated CD8+ T cells. *Exp Mol Med.* (2013) 45:e8. doi: 10.1038/emm.2013.14
48. Reed SG, Hsu FC, Carter D, Orr MT. The science of vaccine adjuvants: advances in TLR4 ligand adjuvants. *Curr Opin Immunol.* (2016) 41:85–90. doi: 10.1016/j.coi.2016.06.007
49. Rogero MM, Calder PC. Obesity, inflammation, toll-like receptor 4 and fatty acids. *Nutrients* (2018) 10:E432. doi: 10.3390/nu10040432
50. Shi H, Kokoeva MV, Inouye K, Tzameli I, Yin H, Flier JS. TLR4 links innate immunity and fatty acid-induced insulin resistance. *J Clin Invest.* (2006) 116:3015–25. doi: 10.1172/JCI28898

51. Ding Y, Subramanian S, Montes VN, Goodspeed L, Wang S, Han C, et al. Toll-like receptor 4 deficiency decreases atherosclerosis but does not protect against inflammation in obese low-density lipoprotein receptor-deficient mice. *Arterioscler Thromb Vasc Biol.* (2012) 32:1596–604. doi: 10.1161/ATVBAHA.112.249847
52. Kim F, Pham M, Luttrell I, Bannerman DD, Tupper J, Thaler J, et al. Toll-like receptor-4 mediates vascular inflammation and insulin resistance in diet-induced obesity. *Circ Res.* (2007) 100:1589–96. doi: 10.1161/CIRCRESAHA.106.142851
53. Wang Y, Qian Y, Fang Q, Zhong P, Li W, Wang L, et al. Saturated palmitic acid induces myocardial inflammatory injuries through direct binding to TLR4 accessory protein MD2. *Nat Commun.* (2017) 8:13997. doi: 10.1038/ncomms13997
54. Lee JJ, Wang PW, Yang IH, Huang HM, Chang CS, Wu CL, et al. High-fat diet induces toll-like receptor 4-dependent macrophage/microglial cell activation and retinal impairment. *Invest Ophthalmol Vis Sci.* (2015) 56:3041–50. doi: 10.1167/iovs.15-16504
55. Lancaster GI, Langley KG, Berglund NA, Kammoun HL, Reibe S, Estevez E, et al. Evidence that TLR4 is not a receptor for saturated fatty acids but mediates lipid-induced inflammation by reprogramming macrophage metabolism. *Cell Metab.* (2018) 27:1096–110.e5. doi: 10.1016/j.cmet.2018.03.014
56. Rocha DM, Caldas AP, Oliveira LL, Bressan J, Hermsdorff HH. Saturated fatty acids trigger TLR4-mediated inflammatory response. *Atherosclerosis* (2016) 244:211–5. doi: 10.1016/j.atherosclerosis.2015.11.015
57. Steimle A, Autenrieth IB, Frick JS. Structure and function: lipid A modifications in commensals and pathogens. *Int J Med Microbiol.* (2016) 306:290–301. doi: 10.1016/j.ijmm.2016.03.001
58. Lee JY, Ye J, Gao Z, Youn HS, Lee WH, Zhao L, et al. Reciprocal modulation of Toll-like receptor-4 signaling pathways involving MyD88 and phosphatidylinositol 3-kinase/AKT by saturated and polyunsaturated fatty acids. *J Biol Chem.* (2003) 278:37041–51. doi: 10.1074/jbc.M305213200
59. Lee JY, Zhao L, Youn HS, Weatherill AR, Tapping R, Feng L, et al. Saturated fatty acid activates but polyunsaturated fatty acid inhibits Toll-like receptor 2 dimerized with Toll-like receptor 6 or 1. *J Biol Chem.* (2004) 279:16971–9. doi: 10.1074/jbc.M312990200
60. Hwang DH, Kim JA, Lee JY. Mechanisms for the activation of Toll-like receptor 2/4 by saturated fatty acids and inhibition by docosahexaenoic acid. *Eur J Pharmacol.* (2016) 785:24–35. doi: 10.1016/j.ejphar.2016.04.024
61. Wong SW, Kwon MJ, Choi AM, Kim HP, Nakahira K, Hwang DH. Fatty acids modulate Toll-like receptor 4 activation through regulation of receptor dimerization and recruitment into lipid rafts in a reactive oxygen species-dependent manner. *J Biol Chem.* (2009) 284:27384–92. doi: 10.1074/jbc.M109.044065
62. Weatherill AR, Lee JY, Zhao L, Lemay DG, Youn HS, Hwang DH. Saturated and polyunsaturated fatty acids reciprocally modulate dendritic cell functions mediated through TLR4. *J Immunol.* (2005) 174:5390–7. doi: 10.4049/jimmunol.174.9.5390
63. Carlsson JA, Wold AE, Sandberg AS, Ostman SM. The polyunsaturated fatty acids arachidonic acid and docosahexaenoic acid induce mouse dendritic cells maturation but reduce T-cell responses *in vitro*. *PLoS ONE* (2015) 10:e0143741. doi: 10.1371/journal.pone.0143741
64. Brix S, Lund P, Kjaer TM, Straarup EM, Hellgren LI, Frokiaer H. CD4(+) T-cell activation is differentially modulated by bacteria-primed dendritic cells, but is generally down-regulated by n-3 polyunsaturated fatty acids. *Immunology* (2010) 129:338–50. doi: 10.1111/j.1365-2567.2009.03163.x
65. McMurray DN, Jolly CA, Chapkin RS. Effects of dietary n-3 fatty acids on T cell activation and T cell receptor-mediated signaling in a murine model. *J Infect Dis.* (2000) 182(Suppl. 1):S103–7. doi: 10.1086/315909
66. Oh DY, Talukdar S, Bae EJ, Imamura T, Morinaga H, Fan W, et al. GPR120 is an omega-3 fatty acid receptor mediating potent anti-inflammatory and insulin-sensitizing effects. *Cell* (2010) 142:687–98. doi: 10.1016/j.cell.2010.07.041
67. Stulnig TM, Huber J, Leitinger N, Imre EM, Angelisova P, Nowotny P, et al. Polyunsaturated eicosapentaenoic acid displaces proteins from membrane rafts by altering raft lipid composition. *J Biol Chem.* (2001) 276:37335–40. doi: 10.1074/jbc.M106193200
68. Fan YY, Ly LH, Barhoumi R, McMurray DN, Chapkin RS. Dietary docosahexaenoic acid suppresses T cell protein kinase C theta lipid raft recruitment and IL-2 production. *J Immunol.* (2004) 173:6151–60. doi: 10.4049/jimmunol.173.10.6151
69. Chapkin RS, Arrington JL, Apanasovich TV, Carroll RJ, McMurray DN. Dietary n-3 PUFA affect TcR-mediated activation of purified murine T cells and accessory cell function in co-cultures. *Clin Exp Immunol.* (2002) 130:12–8. doi: 10.1046/j.1365-2249.2002.01951.x
70. Zurier RB, Rossetti RG, Seiler CM, Laposata M. Human peripheral blood T lymphocyte proliferation after activation of the T cell receptor: effects of unsaturated fatty acids. *Prostaglandins Leukot Essent Fatty Acids* (1999) 60:371–5. doi: 10.1016/S0952-3278(99)80015-5
71. Shaikh SR, Boyle S, Edidin M. A high fat diet containing saturated but not unsaturated fatty acids enhances T cell receptor clustering on the nanoscale. *Prostaglandins Leukot Essent Fatty Acids* (2015) 100:1–4. doi: 10.1016/j.plefa.2015.05.001
72. Lee J, Walsh MC, Hoehn KL, James DE, Wherry EJ, Choi Y. Regulator of fatty acid metabolism, acetyl coenzyme a carboxylase 1, controls T cell immunity. *J Immunol.* (2014) 192:3190–9. doi: 10.4049/jimmunol.1302985
73. Shaikh SR, Mitchell D, Carroll E, Li M, Schneck J, Edidin M. Differential effects of a saturated and a monounsaturated fatty acid on MHC class I antigen presentation. *Scand J Immunol.* (2008) 68:30–42. doi: 10.1111/j.1365-3083.2008.02113.x
74. Pearce EL, Walsh MC, Cejas PJ, Harms GM, Shen H, Wang LS, et al. Enhancing CD8 T-cell memory by modulating fatty acid metabolism. *Nature* (2009) 460:103–7. doi: 10.1038/nature08097
75. Raulien N, Friedrich K, Strobel S, Rubner S, Baumann S, von Bergen M, et al. Fatty acid oxidation compensates for lipopolysaccharide-induced warburg effect in glucose-deprived monocytes. *Front Immunol.* (2017) 8:609. doi: 10.3389/fimmu.2017.00609
76. Zhang Y, Kurupati R, Liu L, Zhou XY, Zhang G, Hudaihed A, et al. Enhancing CD8+ T cell fatty acid catabolism within a metabolically challenging tumor microenvironment increases the efficacy of melanoma immunotherapy. *Cancer Cell* (2017) 32:377–91.e9. doi: 10.1016/j.ccell.2017.08.004
77. Byersdorfer CA, Tkachev V, Opipari AW, Goodell S, Swanson J, Sandquist S, et al. Effector T cells require fatty acid metabolism during murine graft-versus-host disease. *Blood* (2013) 122:3230–7. doi: 10.1182/blood-2013-04-495515
78. Desmet CJ, Ishii KJ. Nucleic acid sensing at the interface between innate and adaptive immunity in vaccination. *Nat Rev Immunol.* (2012) 12:479–91. doi: 10.1038/nri3247
79. Gowda NM, Wu X, Gowda DC. TLR9 and MyD88 are crucial for the development of protective immunity to malaria. *J Immunol.* (2012) 188:5073–85. doi: 10.4049/jimmunol.1102143
80. Ives A, Masina S, Castiglioni P, Prevel F, Revaz-Breton M, Hartley MA, et al. MyD88 and TLR9 dependent immune responses mediate resistance to Leishmania guyanensis infections, irrespective of Leishmania RNA virus burden. *PLoS ONE* (2014) 9:e96766. doi: 10.1371/journal.pone.0096766
81. Scheiermann J, Klinman DM. Clinical evaluation of CpG oligonucleotides as adjuvants for vaccines targeting infectious diseases and cancer. *Vaccine* (2014) 32:6377–89. doi: 10.1016/j.vaccine.2014.06.065
82. Tudor D, Dubuquoy C, Gaboriau V, Lefevre F, Charley B, Riffault S. TLR9 pathway is involved in adjuvant effects of plasmid DNA-based vaccines. *Vaccine* (2005) 23:1258–64. doi: 10.1016/j.vaccine.2004.09.001
83. Fallarino F, Volpi C, Zelante T, Vacca C, Calvitti M, Fioretti MC, et al. IDO mediates TLR9-driven protection from experimental autoimmune diabetes. *J Immunol.* (2009) 183:6303–12. doi: 10.4049/jimmunol.0901577
84. Ciorba MA, Bettonville EE, McDonald KG, Metz R, Prendergast GC, Newberry RD, et al. Induction of IDO-1 by immunostimulatory DNA limits severity of experimental colitis. *J Immunol.* (2010) 184:3907–16. doi: 10.4049/jimmunol.0900291
85. Wang YZ, Lv H, Hao YL, Zhang HQ, Li L, Cai GM, et al. Suppressive oligodeoxynucleotides induced tolerogenic plasmacytoid dendritic cells and ameliorated the experimental autoimmune neuritis. *Immunol Lett.* (2015) 166:13–8. doi: 10.1016/j.imlet.2015.04.007
86. Wingender G, Garbi N, Schumak B, Jungerkes F, Endl E, von Bubnoff D, et al. Systemic application of CpG-rich DNA suppresses adaptive T

cell immunity via induction of IDO. *Eur J Immunol.* (2006) 36:12–20. doi: 10.1002/eji.200535602
87. Xin L, Shelite TR, Gong B, Mendell NL, Soong L, Fang R, et al. Systemic treatment with CpG-B after sublethal rickettsial infection induces mouse death through indoleamine 2,3-dioxygenase (IDO). *PLoS ONE* (2012) 7:e34062. doi: 10.1371/journal.pone.0034062
88. Mellor AL, Baban B, Chandler PR, Manlapat A, Kahler DJ, Munn DH. Cutting edge: CpG oligonucleotides induce splenic CD19+ dendritic cells to acquire potent indoleamine 2,3-dioxygenase-dependent T cell regulatory functions via IFN Type 1 signaling. *J Immunol.* (2005) 175:5601–5. doi: 10.4049/jimmunol.175.9.5601
89. Baban B, Chandler PR, Sharma MD, Pihkala J, Koni PA, Munn DH, et al. IDO activates regulatory T cells and blocks their conversion into Th17-like T cells. *J Immunol.* (2009) 183:2475–83. doi: 10.4049/jimmunol.0900986
90. Ehrlich AK, Fernandez OL, Rodriguez-Pinto D, Castilho TM, Corral Caridad MJ, Goldsmith-Pestana K, et al. Local delivery of the toll-like receptor 9 ligand CpG downregulates host immune and inflammatory responses, ameliorating established *Leishmania* (viannia) panamensis chronic infection. *Infect Immun.* (2017) 85:e00981-16. doi: 10.1128/IAI.00981-16
91. Chen YB, Li SD, He YP, Shi XJ, Chen Y, Gong JP. Immunosuppressive effect of IDO on T cells in patients with chronic hepatitis B*. *Hepatol Res.* (2009) 39:463–8. doi: 10.1111/j.1872-034X.2008.00476.x
92. Schmidt SV, Schultze JL. New Insights into IDO biology in bacterial and viral infections. *Front Immunol.* (2014) 5:384. doi: 10.3389/fimmu.2014.00384
93. Routy JP, Routy B, Graziani GM, Mehraj V. The kynurenine pathway is a double-edged sword in immune-privileged sites and in cancer: implications for immunotherapy. *Int J Tryptophan Res.* (2016) 9:67–77. doi: 10.4137/IJTR.S38355
94. Munn DH, Shafizadeh E, Attwood JT, Bondarev I, Pashine A, Mellor AL. Inhibition of T cell proliferation by macrophage tryptophan catabolism. *J Exp Med.* (1999) 189:1363–72. doi: 10.1084/jem.189.9.1363
95. Chung DJ, Rossi M, Romano E, Ghith J, Yuan J, Munn DH, et al. Indoleamine 2,3-dioxygenase-expressing mature human monocyte-derived dendritic cells expand potent autologous regulatory T cells. *Blood* (2009) 114:555–63. doi: 10.1182/blood-2008-11-191197
96. Lippens C, Duraes FV, Dubrot J, Brighouse D, Lacroix M, Irla M, et al. IDO-orchestrated crosstalk between pDCs and Tregs inhibits autoimmunity. *J Autoimmun.* (2016) 75:39–49. doi: 10.1016/j.jaut.2016.07.004
97. Sharma MD, Hou DY, Baban B, Koni PA, He Y, Chandler PR, et al. Reprogrammed foxp3(+) regulatory T cells provide essential help to support cross-presentation and CD8(+) T cell priming in naive mice. *Immunity* (2010) 33:942–54. doi: 10.1016/j.immuni.2010.11.022
98. Fox JM, Sage LK, Huang L, Barber J, Klonowski KD, Mellor AL, et al. Inhibition of indoleamine 2,3-dioxygenase enhances the T-cell response to influenza virus infection. *J Gen Virol.* (2013) 94:1451–61. doi: 10.1099/vir.0.053124-0
99. Sage LK, Fox JM, Mellor AL, Tompkins SM, Tripp RA. Indoleamine 2,3-dioxygenase (IDO) activity during the primary immune response to influenza infection modifies the memory T cell response to influenza challenge. *Viral Immunol.* (2014) 27:112–23. doi: 10.1089/vim.2013.0105
100. Barber GN. STING: infection, inflammation and cancer. *Nat Rev Immunol.* (2015) 15:760–70. doi: 10.1038/nri3921
101. Chen Q, Sun L, Chen ZJ. Regulation and function of the cGAS-STING pathway of cytosolic DNA sensing. *Nat Immunol.* (2016) 17:1142–9. doi: 10.1038/ni.3558
102. Iurescia S, Fioretti D, Rinaldi M. Nucleic acid sensing machinery: targeting innate immune system for cancer therapy. *Recent Pat Anticancer Drug Discov.* (2018) 13:2–17. doi: 10.2174/1574892812666171030163804
103. Christensen MH, Paludan SR. Viral evasion of DNA-stimulated innate immune responses. *Cell Mol Immunol.* (2017) 14:4–13. doi: 10.1038/cmi.2016.06
104. Junt T, Barchet W. Translating nucleic acid-sensing pathways into therapies. *Nat Rev Immunol.* (2015) 15:529–44. doi: 10.1038/nri3875
105. Dey B, Dey RJ, Cheung LS, Pokkali S, Guo H, Lee JH, et al. A bacterial cyclic dinucleotide activates the cytosolic surveillance pathway and mediates innate resistance to tuberculosis. *Nat Med.* (2015) 21:401–6. doi: 10.1038/nm.3813
106. Collins AC, Cai H, Li T, Franco LH, Li XD, Nair VR, et al. Cyclic GMP-AMP synthase is an innate immune DNA sensor for *Mycobacterium tuberculosis*. *Cell Host Microbe* (2015) 17:820–8. doi: 10.1016/j.chom.2015.05.005
107. Rasmussen SB, Horan KA, Holm CK, Stranks AJ, Mettenleiter TC, Simon AK, et al. Activation of autophagy by alpha-herpesviruses in myeloid cells is mediated by cytoplasmic viral DNA through a mechanism dependent on stimulator of IFN genes. *J Immunol.* (2011) 187:5268–76. doi: 10.4049/jimmunol.1100949
108. Saitoh T, Fujita N, Hayashi T, Takahara K, Satoh T, Lee H, et al. Atg9a controls dsDNA-driven dynamic translocation of STING and the innate immune response. *Proc Natl Acad Sci USA.* (2009) 106:20842–6. doi: 10.1073/pnas.0911267106
109. Li Y, Wilson HL, Kiss-Toth E. Regulating STING in health and disease. *J Inflamm.* (2017) 14:11. doi: 10.1186/s12950-017-0159-2
110. Konno H, Konno K, Barber GN. Cyclic dinucleotides trigger ULK1 (ATG1) phosphorylation of STING to prevent sustained innate immune signaling. *Cell* (2013) 155:688–98. doi: 10.1016/j.cell.2013.09.049
111. Stjepanovic G, Baskaran S, Lin MG, Hurley JH. Vps34 kinase domain dynamics regulate the autophagic PI 3-kinase complex. *Mol Cell* (2017) 67:528–34.e3. doi: 10.1016/j.molcel.2017.07.003
112. Liang Q, Seo GJ, Choi YJ, Kwak MJ, Ge J, Rodgers MA, et al. Crosstalk between the cGAS DNA sensor and Beclin-1 autophagy protein shapes innate antimicrobial immune responses. *Cell Host Microbe* (2014) 15:228–38. doi: 10.1016/j.chom.2014.01.009
113. Prabakaran T, Bodda C, Krapp C, Zhang BC, Christensen MH, Sun C, et al. Attenuation of cGAS-STING signaling is mediated by a p62/SQSTM1-dependent autophagy pathway activated by TBK1. *EMBO J.* (2018) 37:e97858. doi: 10.15252/embj.201797858
114. Criollo A, Chereau F, Malik SA, Niso-Santano M, Marino G, Galluzzi L, et al. Autophagy is required for the activation of NFkappaB. *Cell Cycle* (2012) 11:194–9. doi: 10.4161/cc.11.1.18669
115. Paul S, Kashyap AK, Jia W, He YW, Schaefer BC. Selective autophagy of the adaptor protein Bcl10 modulates T cell receptor activation of NF-kappaB. *Immunity* (2012) 36:947–58. doi: 10.1016/j.immuni.2012.04.008
116. Whang MI, Tavares RM, Benjamin DI, Kattah MG, Advincula R, Nomura DK, et al. The ubiquitin binding protein TAX1BP1 mediates autophagasome induction and the metabolic transition of activated T cells. *Immunity* (2017) 46:405–20. doi: 10.1016/j.immuni.2017.02.018
117. Botbol Y, Guerrero-Ros I, Macian F. Key roles of autophagy in regulating T-cell function. *Eur J Immunol.* (2016) 46:1326–34. doi: 10.1002/eji.201545955
118. Puleston DJ, Zhang H, Powell TJ, Lipina E, Sims S, Panse I, et al. Autophagy is a critical regulator of memory CD8(+) T cell formation. *Elife* (2014) 3:1–21. doi: 10.7554/eLife.03706
119. Xu X, Araki K, Li S, Han JH, Ye L, Tan WG, et al. Autophagy is essential for effector CD8(+) T cell survival and memory formation. *Nat Immunol.* (2014) 15:1152–61. doi: 10.1038/ni.3025
120. Prantner D, Perkins DJ, Vogel SN. AMP-activated Kinase (AMPK) promotes innate immunity and antiviral defense through modulation of stimulator of interferon genes (STING) signaling. *J Biol Chem.* (2017) 292:292–304. doi: 10.1074/jbc.M116.763268
121. Ma EH, Poffenberger MC, Wong AH, Jones RG. The role of AMPK in T cell metabolism and function. *Curr Opin Immunol.* (2017) 46:45–52. doi: 10.1016/j.coi.2017.04.004
122. Blagih J, Coulombe F, Vincent EE, Dupuy F, Galicia-Vazquez G, Yurchenko E, et al. The energy sensor AMPK regulates T cell metabolic adaptation and effector responses *in vivo*. *Immunity* (2015) 42:41–54. doi: 10.1016/j.immuni.2014.12.030
123. Eikawa S, Nishida M, Mizukami S, Yamazaki C, Nakayama E, Udono H. Immune-mediated antitumor effect by type 2 diabetes drug, metformin. *Proc Natl Acad Sci USA.* (2015) 112:1809–14. doi: 10.1073/pnas.1417636112

Conflict of Interest Statement: The authors declare that the research was conducted in the absence of any commercial or financial relationships that could be construed as a potential conflict of interest.

Copyright © 2018 Nicoli, Paul and Appay. This is an open-access article distributed under the terms of the Creative Commons Attribution License (CC BY). The use, distribution or reproduction in other forums is permitted, provided the original author(s) and the copyright owner(s) are credited and that the original publication in this journal is cited, in accordance with accepted academic practice. No use, distribution or reproduction is permitted which does not comply with these terms.

frontiers in Immunology

ORIGINAL RESEARCH
published: 05 November 2018
doi: 10.3389/fimmu.2018.02555

Limited Foxp3$^+$ Regulatory T Cells Response During Acute *Trypanosoma cruzi* Infection Is Required to Allow the Emergence of Robust Parasite-Specific CD8$^+$ T Cell Immunity

*Cintia L. Araujo Furlan[1,2], Jimena Tosello Boari[1,2], Constanza Rodriguez[1,2], Fernando P. Canale[1,2], Facundo Fiocca Vernengo[1,2], Santiago Boccardo[1,2], Cristian G. Beccaria[1,2], Véronique Adoue[3,4,5], Olivier Joffre[3,4,5], Adriana Gruppi[1,2], Carolina L. Montes[1,2] and Eva V. Acosta Rodriguez[1,2]**

[1] Departamento de Bioquímica Clínica, Facultad de Ciencias Químicas, Universidad Nacional de Córdoba, Córdoba, Argentina, [2] Centro de Investigaciones en Bioquímica Clínica e Inmunología, CONICET, Córdoba, Argentina, [3] Institut National de la Santé et de la Recherche Médicale, Toulouse, France, [4] Centre National de la Recherche Scientifique, Toulouse, France, [5] Centre de Physiopathologie de Toulouse Purpan, Université de Toulouse, Université Paul Sabatier, Toulouse, France

While it is now acknowledged that CD4$^+$ T cells expressing CD25 and Foxp3 (Treg cells) regulate immune responses and, consequently, influence the pathogenesis of infectious diseases, the regulatory response mediated by Treg cells upon infection by *Trypanosoma cruzi* was still poorly characterized. In order to understand the role of Treg cells during infection by this protozoan parasite, we determined in time and space the magnitude of the regulatory response and the phenotypic, functional and transcriptional features of the Treg cell population in infected mice. Contrary to the accumulation of Treg cells reported in most chronic infections in mice and humans, experimental *T. cruzi* infection was characterized by sustained numbers but decreased relative frequency of Treg cells. The reduction in Treg cell frequency resulted from a massive accumulation of effector immune cells, and inversely correlated with the magnitude of the effector immune response as well as with emergence of acute immunopathology. In order to understand the causes underlying the marked reduction in Treg cell frequency, we evaluated the dynamics of the Treg cell population and found a low proliferation rate and limited accrual of peripheral Treg cells during infection. We also observed that Treg cells became activated and acquired a phenotypic and transcriptional profile consistent with suppression of type 1 inflammatory responses. To assess the biological relevance of the relative reduction in Treg cells frequency observed during *T. cruzi* infection, we transferred *in vitro* differentiated Treg cells at early moments, when the deregulation of the ratio between regulatory and conventional T cells becomes significant.

OPEN ACCESS

Edited by:
María Fernanda Pascutti, Sanquin Diagnostic Services, Netherlands

Reviewed by:
Ana Rosa Pérez, Consejo Nacional de Investigaciones Científicas y Técnicas (CONICET), Argentina
Derk Amsen, Sanquin Research, Netherlands
Jose M. Alvarez, Universidade de São Paulo, Brazil

***Correspondence:**
Eva V. Acosta Rodriguez
eacosta@fcq.unc.edu.ar

Specialty section:
This article was submitted to T Cell Biology, a section of the journal Frontiers in Immunology

Received: *06 July 2018*
Accepted: *17 October 2018*
Published: *05 November 2018*

Citation:
Araujo Furlan CL, Tosello Boari J, Rodriguez C, Canale FP, Fiocca Vernengo F, Boccardo S, Beccaria CG, Adoue V, Joffre O, Gruppi A, Montes CL and Acosta Rodriguez EV (2018) Limited Foxp3$^+$ Regulatory T Cells Response During Acute Trypanosoma cruzi Infection Is Required to Allow the Emergence of Robust Parasite-Specific CD8$^+$ T Cell Immunity. Front. Immunol. 9:2555. doi: 10.3389/fimmu.2018.02555

Intravenous injection of Treg cells dampened parasite-specific CD8$^+$ T cell immunity and affected parasite control in blood and tissues. Altogether, our results show that limited Treg cell response during the acute phase of *T. cruzi* infection enables the emergence of protective anti-parasite CD8$^+$ T cell immunity and critically influences host resistance.

Keywords: regulatory T (Treg) cells, *Trypanosoma cruzi*, immunity, CD8 cytotoxic T cells$^+$, pathogenesis

INTRODUCTION

Regulatory T (Treg) cells, defined by the expression of the lineage transcription factor forkhead box P3 (Foxp3), are able to suppress most immune cells (1) and their suppressive function is crucial for immune homeostasis and prevention of autoimmunity (2). In addition, Treg cells were shown to be critical mediators in the modulation of host-microbe interaction during infections and to play beneficial or deleterious roles in host resistance (3). Several chronic bacterial infections, such as tuberculosis (4) and leprosy (5) promote the accumulation and preferential migration of Treg cells to target tissues, where these cells exert regulatory effects that compromise protective responses and favor bacterial persistence (6). During viral infections, the role of this cell subset appears to be different between acute and chronic infections and even to change during the same infection with the transition from acute to chronic stages. In this way, Treg cells have been shown to coordinate early protective immunity to mucosal Herpes Simplex Virus (7, 8) and pulmonary Respiratory Syncytial Virus (9, 10), and to sustain memory CD8$^+$ T cell immunity to West Nile virus (11). In contrast, there is by far more evidence that Treg cells accumulate during certain viral infections and dampen adaptive immune responses, specially CD8$^+$ T cell immunity, promoting virus establishment and infection chronicity (12, 13). Thus, Treg cells seem to exert a general beneficial role by limiting exuberant immune responses and the consequent excessive inflammation and immunopathology even at the expense of reducing viral control (12, 14, 15). Similar scenarios have been reported in the course of parasitic infections (16). During leishmaniasis (17) and malaria (18), Treg cells have been shown to limit the magnitude of effector responses, resulting in failure to adequately control infection (19–21). In contrast, these cells favor host resistance during infections with *S. mansoni* and *T. gondii* by restraining collateral tissue damage caused by vigorous anti-parasite immune responses (22–24). In addition, relative or absolute reduction in Treg cell numbers during acute infections with *T. gondii* (23, 25), *L. monocitogenes* (25), vaccinia virus (25) and LCMV clone Armstrong (26) supports the emergence of CD4$^+$ and CD8$^+$ T cell immunity. Therefore, the impact of Treg cells in the outcome of an infection is expected to be different depending on the pathogen, timing and affected tissues, while their manipulation may open up new avenues for therapeutic strategies.

Chagas disease (American Trypanosomiasis) is a life-threatening illness caused by the protozoan parasite *T. cruzi* (27). Last estimates calculated an infected population of about 6 million in endemic areas of Latin America and several hundred thousand worldwide, with more than 70 million people living at risk of infection and 40,000 new cases diagnosed per year (28). Host resistance to *T. cruzi* depends on both innate and adaptive immune responses which are triggered early during infection (29–31). Macrophages, dendritic cells, natural killer cells and B and T lymphocytes act in concert to control parasite replication but are not able to completely eradicate the pathogen (32). In particular, parasite-specific antibodies and CD8$^+$ T cells together with a type I response with production of IFN-γ and TNF are critical for host resistance (32). Nevertheless, exuberant production of these inflammatory cytokines has been associated with tissue damage, immunopathology and disease severity in mice and humans (33–36), supporting the notion that regulatory responses greatly impact in the final outcome of *T. cruzi* infection. In this context, many studies aimed to understand the role of Treg cells during the progression of this parasitic infection, reporting often contradictory results. The frequency and functionality of Treg cells were shown to be increased in the peripheral blood of infected patients that presented less severe chronic disease (37–40), suggesting a beneficial role for this cell subset during human Chagas disease. On the other hand, experimental models reported protective (41, 42), limited (43, 44) and also deleterious (45) effects for Treg cells during *T. cruzi* infection. However, none of these studies addressed the kinetics or the phenotypical and functional features of the regulatory response, and more importantly, all of them targeted Treg cells by non-specific approaches. These technical limitations have delayed an accurate characterization of Treg cell responses during *T. cruzi* infection and, therefore, prevented any rational manipulation of this subset in order to modulate the outcome of the chronic disease.

In this manuscript, we took advantage of Foxp3-EGFP reporter mice to comprehensively determine the magnitude and quality of the Treg cell response triggered by *T. cruzi* infection. In addition, adoptive transfer experiments of *in vitro* differentiated Treg cells allowed us to establish the biological role of this subset in the regulation of protective immunity and parasite control.

MATERIALS AND METHODS

Mice

Mice used for experiments were sex- and age-matched. C57BL/6 and BALB/c wild type mice were obtained from School of Veterinary, La Plata National University (La Plata, Argentina). CD45.1 C57BL/6 mice (B6.SJL-Ptprc^a Pepc^b/BoyJ), Foxp3-EGFP reporter mice (B6.Cg-Foxp3^{tm2Tch}/J), IL-6 deficient mice (B6.129S2-Il6^{tm1Kopf}/J) and Caspase-1/11 deficient mice (B6N.129S2-Casp1^{tm1Flv}/J) were obtained from The Jackson Laboratories (USA). IFNAR deficient mice (Ifnar1^{tm1Ag}) were

obtained from Pasteur Institute (Paris, France) (46). Animals were bred in the animal facility of the Facultad de Ciencias Químicas, Universidad Nacional de Córdoba, and housed under a 12 h: 12 h light-dark cycle with food and water *ad libitum*.

Parasites and Experimental Infection

Bloodstream trypomastigotes of the Tulahuén strain of *T. cruzi* were maintained in BALB/c mice by serial passages each 10–11 days. For experimental infection, 7–10 weeks-old mice were inoculated intraperitoneally with 0.2 ml PBS containing 5×10^3 trypomastigotes. Alternatively, doses of 500 and 5×10^4 trypomastigotes were used as indicated.

Live *T. cruzi* trypomastigotes (Tulahuén) were obtained from the extracellular medium of infected monolayers of Vero cells, as previously described (47).

Quantification of Parasite Numbers in Blood and Parasite Burden in Tissues

Parasitemia was monitored by counting the number of viable trypomastigotes in blood after lysis with a 0.87% ammonium chloride buffer. Abundance of *T. cruzi* satellite DNA in tissues was used to determine parasite burden. Genomic DNA was purified from 50 μg of tissue (spleen and liver) using TRIzol Reagent (Life Technologies) following manufacturer's instructions. Satellite DNA from *T. cruzi* (GenBank AY520036) was quantified by real time PCR using specific Custom Taqman Gene Expression Assay (Applied Biosystem). Primers and probes sequences were previously described by Piron et al (48). A sample was considered positive for *T. cruzi* target when $C_T < 45$. Abundance of satellite DNA from *T. cruzi* was normalized to GAPDH abundance (Taqman Rodent GAPDH Control Reagent, Applied Biosystem), quantified through the comparative C_T method and expressed as arbitrary units.

Cell Preparation, Purification, and Culture

Blood was collected using heparin as anticoagulant. Spleens, thymi, livers and mesenteric and inguinal lymph nodes were obtained and pressed through a tissue strainer to obtain cell suspensions. Bone marrow cells were isolated by flushing femurs and tibias with PBS 2% FBS. Liver infiltrating cells were obtained after 25 min centrifugation (600 g) in a 35 and 70% bilayer of Percoll (GE Healthcare) gradient. Erythrocytes in bone marrow, spleen, thymus and liver cell suspensions were lysed for 3 min in ammonium chloride-potassium phosphate buffer. Cell numbers were counted in Turk's solution using a Neubauer chamber.

$CD4^+$ and $CD8^+$ T cells were isolated from pooled splenic suspensions by magnetic negative selection using EasySep™ Mouse $CD4^+$ or $CD8^+$ T Cell Isolation Kits, respectively (StemCell Technologies). After surface staining, Treg, Tconv and naïve $CD4^+$ T cells were further purified from $CD4^+$ T cell suspensions by cell sorting with a FACSAria II (BD Biosciences) using the following gating strategy: Treg cells: $CD4^+$ Foxp3-GFP^+ CD25int/hi; Tconv cells: $CD4^+$ Foxp3-GFP^- $CD25^{-/+}$; and naïve $CD4^+$ T cells: $CD4^+$ Foxp3-GFP^- $CD25^-$ CD62Lhi CD44lo. Cells were cultured in RPMI 1640 medium (Gibco, Invitrogen) supplemented with 2 mM glutamine (Gibco, Invitrogen), 55 μM 2-ME (Gibco, Invitrogen), and 40 μg/ml gentamicin (Veinfar Laboratories) containing 10% heat inactivated FBS (Gibco or Natocor).

For *in vitro* Treg cell differentiation, naïve $CD4^+$ T cells or total splenocytes were stimulated at a cell density of 2×10^5/well during 3–4 days in 96-well cell culture plates coated with 2 μg/mL anti-CD3 (eBioscience) and 1 μg/mL anti-CD28 (BD Biosciences), in presence or absence of a Treg cell differentiation cocktail containing 100 U/mL mrIL-2 (RandD), 5 ng/mL rTGF-β1 (eBioscence) and 13.3 nM all trans-Retinoic Acid (Sigma). In the experiments aimed to evaluate the inhibition of Treg cell induction, live *T. cruzi* parasites were added in different ratios as described in the corresponding legend for figure.

Biochemical Determinations and Quantification of Cytokines in Plasma

Blood was centrifuged for 8 min at 3,000 rpm and plasma was collected. Plasma samples were sent to Biocon Laboratory (Córdoba, Argentina) for quantification of GOT, GPT, LDH and CPK by UV kinetic methods, and glucose by kinetic/colorimetric method in a Dimension RXL Siemens analyzer. Plasma levels of different cytokines were determined in our laboratory using LEGENDplex™ Multi-Analyte Flow Assay Kit (Biolegend) for Mouse Th Cytokine and Inflammation Panels according to manufacturer's instructions.

Antibodies and Flow Cytometry

For surface staining, cell suspensions were incubated with fluorochrome labeled-antibodies in PBS 2% FBS for 20 min at 4°C. Flow cytometry and/or cell sorting were performed with a combination of the following antibodies: anti-CD4 APC, APC-eFluor-780 or PerCP-eFluor 710 (all clone GK1.5), anti-CD25 PE-Cy7 (P61.5), anti-CD3 PerCP-Cy5.5 (145-2C11), anti-CD8a FITC, PE, PE-Cy7 or PerCP-Cy5.5 (53-6.7), anti-CCR7 PerCP-Cy5.5 (4B2), anti-CD103 PE (2-E7), anti-CD127 PerCP-eFluor-710 (eBioSB/199), anti-CD39 eFluor-660 (24DMS1), anti-CD44 APC-Cy7 (IM7), anti-CD45.2 PerCP-Cy5.5 (104), anti-CD62L PerCP-Cy5.5 (MEL-14), anti-CD73 biotin (eBioTY/11-8), anti-CTLA-4 PE (UC10.4B9), anti-CXCR3 PE (CXCR3-173), anti-FR4 PE (eBio12a5), anti-GARP APC (YGIC86), anti-OX40 APC (OX-86) and anti-PD-1 PE (RMP1-30) from eBioscience; anti-CD4 AlexaFluor700 (GK1.5), anti-CD45.1 APC-Cy7 (A20), anti-GITR PE-Cy7 (DTA-1), anti-LAG-3 PerCP-Cy5.5 (C9B7W), anti-KLRG1 PE (2F1/KLRG) and anti-LAP PE (TW7-20B9) from Biolegend; and anti-CD127 biotin (B12-1) from BD Biosciences. To detect biotinilated antibodies, Streptavidin APC (Biolegend) or PerCP-Cy5.5 (eBioscience) were used. To identify *T. cruzi* specific $CD8^+$ T cells, cell suspensions were incubated with an H-$2K^b$ *T. cruzi* trans-sialidase amino acids 569-576 ANYKFTLV (TSKB20) APC-labeled Tetramer (NIH Tetramer Core Facility) for 20 min at 4°C before further surface staining with additional antibodies. Blood was directly incubated with the indicated antibodies and erythrocytes were lysed with a 0.87% NH_4Cl buffer previously to acquisition. To assess apoptosis, cells were stained for Annexin V PE (Biolegend)

and 7-AAD (BD Biosciences) according to the manufacturer's specifications.

For detection of transcription factors, cells were first stained on surface, washed and then fixed, permeabilized and stained with Foxp3/Transcription Factor Staining Buffers (eBioscience) according to eBioscience One-step protocol for intracellular (nuclear) proteins. The following antibodies were used for intracellular staining: anti-Foxp3 PE, PerCP-Cy5.5 or APC (FJK-16s), anti-T-bet PerCP-Cy5.5 or PE-Cy7 (eBio4B10), and anti-Ki-67 APC (SolA15) from eBioscience.

For intracellular cytokine staining, 2×10^6 cells per well were cultured in 200 μL supplemented RPMI 1640 medium and stimulated during 2–5 h at 37°C with 50 ng/mL PMA and 1 μg/mL ionomycin (Sigma-Aldrich) in the presence of Brefeldin A and/or Monensin (eBioscience). After surface staining, cells were fixed and permeabilized with Intracellular Fixation & Permeabilization Buffer Set (eBioscience) or BD Cytofix/Cytoperm and Perm/Wash (BD Biosciences) following manufacturers' indications. Cells were then labeled with anti-IL-10 APC (JES5-16E3), anti-IFN-γ APC or PE (XMG1.2) and anti-IL-17A PE (eBio17B7) from eBioscience; anti-IL-10 PE (JES5-16B3) and anti-TNF PerCP-Cy5.5 (MP6-XT22) from Biolegend.

All samples were acquired on a FACSCanto II (BD Biosciences) and data were analyzed with FlowJo software.

Adoptive Cell Transfer

For *in vivo* pTreg cells induction experiments, Tconv cells were purified from non-infected Foxp3-EGFP CD45.2 donors as described above. Two millions cells were then intravenously injected in the retro-orbital sinus of CD45.1 recipient mice, which were simultaneously infected with the usual dose of *T. cruzi*. Non-infected and/or non-transferred mice were used as controls. Conversion of injected cells (Foxp3-GFP$^-$) into Treg cells (Foxp3-GFP$^+$) was assessed by flow cytometry in different organs 19 days after treatment.

To assess the biological relevance of reduced Treg cells frequency, 1×10^6 *in vitro* differentiated Treg cells generated from Foxp3-EGFP mice were intravenously transferred into CD45.1 recipient mice at 11 days post-infection (dpi). The effect of Treg cell adoptive transfer was evaluated 7 days later.

RNAseq

Treg cells were purified as described above from the spleens of non-infected and 22-days infected Foxp3-EGFP mice and immediately lysed with QIAzol reagent (Qiagen). Total RNA was extracted by using the RNeasy Micro Kit (Qiagen) and its quality was assessed on a 2100 Bioanalyzer (Agilent Technologies). RNA-seq libraries were then prepared according to the TruSeq Stranded Total RNA Sample protocol (Illumina). Quality controls of the libraries were performed by standard methods, including quantification by Qubit (Thermo Fisher Scientific) and assessment of size distribution using a 2100 Bioanalyzer. Samples were indexed and sequenced on an Illumina HiSeq 3000 (paired-end reads of 150 bp). Bioinformatic analysis of sequenced Reads was performed as described elsewhere (49). *P*-values <0.1 (adjusted for multiple testing by Benjamini–Hochberg procedure) were considered as the cutoff for significantly differentially expressed genes. Gene Set Enrichment Analyses (GSEA) for Th1, Th2, and Th17 signature were performed using specific gene sets selected from several publications as indicated in **Supplementary Table 1** and depicted in heat maps of **Figure 4E**. NCBI Sequence Read Archive accession code: SRP145339.

Statistics

Statistical significance of mean values comparisons was analyzed by *t*-test, Mann Whitney test, One-way ANOVA or Kruskal-Wallis test as indicated. According to the absolute values of r, the Spearman correlation was interpreted as strong ($r = 0.7$–0.9), good ($r = 0.50$–0.70), moderate ($r = 0.30$–0.50), and poor ($r < 0.30$) (50–52). Statistical analysis was performed using GraphPad Prism 7.0 software. *P*-values ≤0.05 were considered significant.

RESULTS

Treg Cell Frequency Is Decreased During the Progression of *T. cruzi* Infection

As an initial step to characterize Treg cell responses, we evaluated how *T. cruzi* infection affected the frequency and absolute numbers of Treg cells and other immune cell subsets. Using Foxp3 reporter mice, we determined that acute *T. cruzi* infection resulted in a significant decrease in the percentage of Treg cells (CD4$^+$ Foxp3-GFP$^+$) in the spleen (**Figure 1A**). This decrease in the frequency of splenic Treg cells was statistically significant after 12 days post-infection (dpi) and remained low even at the end of the acute phase (76 dpi; **Figure 1B**, left panel). Of note, the absolute numbers of Treg cells remained unchanged or were transiently increased at low extent while the numbers of CD4$^+$ Foxp3-GFP (Tconv) cells and total spleen leukocytes were augmented by several orders of magnitude (**Figure 1B**, middle panel). Consequently, the ratios between the numbers of Treg cells and Tconv cells or total cells were significantly decreased along the infection (**Figure 1B**, right panel). A similar picture was observed in secondary lymphoid organs, such as inguinal lymph nodes (iLN) (**Figure 1C**) as well as in the liver, a target tissue with intense parasite replication and immune cell infiltration during the acute phase of *T. cruzi* infection (53) (**Figure 1D**). This reduction in the frequency of Treg cells and/or the ratio of Treg cell numbers to Tconv and total cell numbers were also detected in blood and bone marrow (**Supplementary Figures 1A,B**). Altogether, these results indicate that, in contrast to most chronic infections (6), Treg cells do not significantly accumulate in secondary lymphoid organs or liver during *T. cruzi* infection.

Next, we evaluated Treg cells frequencies and numbers in organs associated with the development of this subset, e.g., thymus and gut-associated mesenteric lymph nodes (mLN) (54). We determined that the percentage of Treg cells as well as the ratio between the numbers of this population and other cell subsets in the thymus were significantly increased during *T. cruzi* infection (**Supplementary Figure 1C**, left and right panels), likely as consequence of conserved Treg cells numbers together with a marked reduction in the number of total

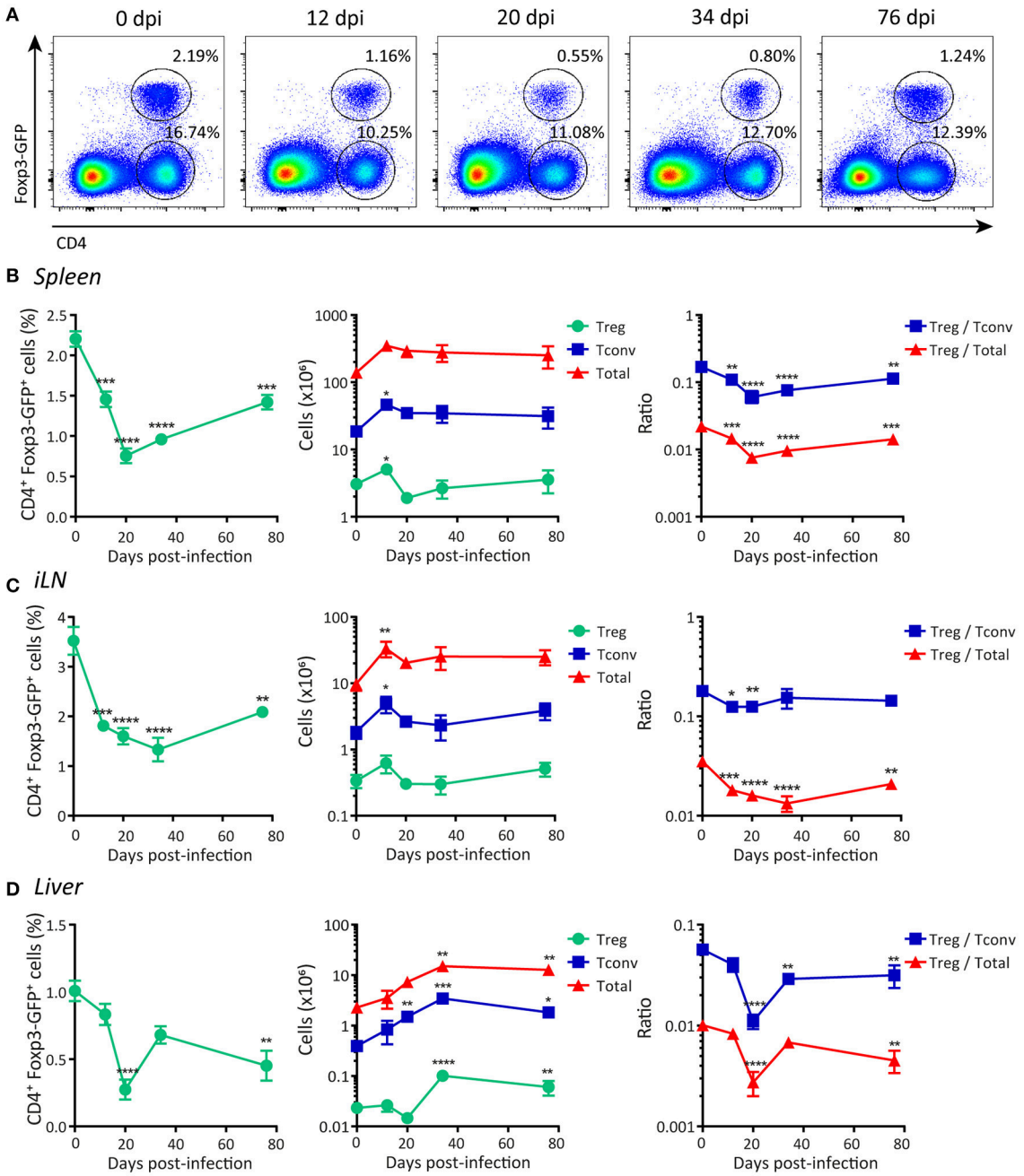

FIGURE 1 | Frequency of Foxp3^{+} regulatory T cells is reduced in peripheral organs during acute *T. cruzi* infection. **(A)** Flow cytometry representative dot plots showing Foxp3-GFP expression and CD4 staining in the spleen of *T. cruzi* infected Foxp3-EGFP mice at different days post-infection (dpi). **(B–D)** Graphs showing CD4^{+} Foxp3-GFP^{+} Treg cell frequencies (left panel), absolute numbers of Treg cells, CD4^{+} Foxp3-GFP^{-} (Tconv) cells and total leukocytes (middle panel), and the ratios of Treg cells to Tconv and to total cells in the spleens **(B)**, inguinal lymph nodes **(C)**, and liver infiltrating leucocytes **(D)** of *T. cruzi* infected Foxp3-EGFP mice at different dpi. Data are presented as mean ± SEM, $n = 3$–11 animals per dpi. Data are representative of at least three independent experiments. *P*-values were calculated by One way ANOVA with Dunnett's multiple comparisons test or Kruskal-Wallis with Dunn's correction (Tconv and total cells absolute numbers in liver only). $^{*}P \leq 0.05$, $^{**}P \leq 0.01$, $^{***}P \leq 0.001$ and $^{****}P \leq 0.0001$.

thymocytes (**Supplementary Figure 1C**, middle panel). In mLN, the numbers of Treg cells showed an initial oscillation (increase followed by decrease) after infection while the frequency and the ratio of Treg cells to Tconv numbers exhibited an early increase, but all these parameters remained unaltered afterwards (**Supplementary Figure 1D**).

The Frequency of Treg Cells Is Negatively Correlated With Markers of Infection Progression and the Development of Effector Immune Responses

We next aimed at studying whether the changes in the frequency of Treg cells during *T. cruzi* infection showed any correlation with disease progression and/or the magnitude of effector immune responses. As markers of progression in the infection by *T. cruzi* we evaluated parasitemia and the levels of different biochemical parameters used to assess general health and tissue damage. As depicted in **Figure 2A**, parasite numbers in blood were low but detectable at 12 dpi, peaked around 20 dpi, diminished by 34 dpi and became undetectable later on. Similar kinetics was observed when measuring the activity of enzymes that reflect tissue damage (i.e., GPT, LDH, GOT, and CPK; **Figure 2A**, middle panel; **Supplementary Figure 2A**). In contrast, the concentration of plasma glucose, whose decrease is generally associated with acute infection (55), was reduced alongside the progression of infection, showing the lowest level around 20 dpi and reaching normal levels afterwards (**Figure 2A**, right panel). Remarkably, changes in the levels of all these parameters showed statistically significant strong, good or moderate correlations with the frequencies of Treg cells in the spleen (**Figure 2B**; **Supplementary Figure 2B**). These correlations were direct for glucose concentration and inverse for parasitemia and enzymatic activity in plasma.

To assess the effector immune response, we quantified the plasma concentration of effector cytokines known to be protective during *T. cruzi* infection, such as IFN-γ and TNF (32). The concentration of IFN-γ showed a marked increase by 12 dpi and diminished later on, while the kinetics of TNF production was slower, showing the peak of plasma concentration at 20 dpi (**Figure 2C**). In addition, we quantified other effector cytokines, such as IL-6, IL-1β, and IL-2. The concentration of IL-6 was significantly increased by 12 dpi, peaked at 20 dpi and decreased afterwards whereas the concentrations of IL-1β and IL-2 remained unchanged along the infection (**Supplementary Figure 2C**). The concentrations of IFN-γ, TNF and IL-6, but not those of IL-1β and IL-2, showed significant strong, good or moderate inverse correlations with the frequency of Treg cells in spleen (**Figure 2D**; **Supplementary Figure 2D**). We also evaluated the presence of parasite-specific $CD8^+$ T cell immunity as a component of the cellular effector immune response known to be critical for parasite control (31). $CD8^+$ T cells specific for the immunodominant *T. cruzi* peptide TSKB20 were identified in the spleen of *T. cruzi* infected mice using tetramers (**Figure 2E**). We found that the frequency and absolute numbers of TSKB20-specific $CD8^+$ T cells increased between 12 and 48 dpi (**Figures 2E,F**). Similar to effector cytokines, the frequency of TSKB20-specific $CD8^+$ T cells showed a good inverse correlation with the frequency of Treg cells (**Figure 2G**).

Limited Expansion and Reduced Accrual of Peripheral Treg Cells During Acute *T. cruzi* Infection

In steady state conditions, the size of the Treg cell population is maintained by a dynamic process, through a balance among development, proliferation and apoptosis (56). During infections, these events may be altered leading to the accumulation, constriction or dysfunction of Treg cells and consequently, modulating the effector immune response and the host-microbe interaction (57). In this context, we aimed to evaluate whether the reduction of Treg cell frequency during *T. cruzi* infection was a consequence of alterations in the mechanisms that sustain Treg cell homeostasis.

We first evaluated the proliferation of splenic Treg cells, Tconv and total leukocytes along *T. cruzi* infection by determining *ex vivo* the expression of the proliferation marker Ki-67. As depicted in the histograms in **Figure 3A**, the frequency of Treg cells expressing Ki-67 showed a moderate increase around 20–34 dpi that persisted at least until 76 dpi. In contrast, the frequencies of Ki-67^+ Tconv and total cells were markedly augmented along the infection with a peak at 20 dpi, returning to the level of non-infected mice by 76 dpi. Thus, Treg cells showed a significantly lower proliferation rate than Tconv and total cells (**Figure 3B**). These differences in proliferation may account for the reduced frequency of Treg cells during the early acute phase of *T. cruzi* infection. Next, we evaluated whether differential cell death within each cell subset may also be involved in Treg cell frequency reduction during *T. cruzi* infection. Determination of the frequency of apoptotic cells by Annexin V and 7-AAD staining, and calculation of the apoptosis rate, revealed that *T. cruzi* infection increased cell death particularly within the Tconv population (**Figures 3C,D**), as previously reported (58). Therefore, an increased cell death within Treg cells was ruled out as a mechanism underlying the decrease in the frequency of this cell subset during *T. cruzi* infection.

We next investigated whether infection with *T. cruzi* restrained Treg cell development and consequently, reduced Treg cell frequency in the periphery. Considering that the numbers of Treg cells are conserved in the thymus of infected mice (**Supplementary Figure 1C**), we speculated that thymic Treg cell development was not significantly altered during *T. cruzi* infection. Then, we focused on the development of peripheral Treg (pTreg) cells through an *in vivo* approach in order to evidence alterations triggered by *T. cruzi* infection. To this end, $CD25^-$ GFP^- $CD4^+$ cells were purified from the spleen of non-infected $CD45.2^+$ Foxp3-GFP reporter mice and injected into CD45.1 WT hosts that were immediately infected. Adoptively transferred non-infected hosts were examined in parallel and used as controls. Twenty days after injection, transferred cells were identified by CD45.2 expression within different organs and the frequency of pTreg was determined according to the up-regulation of Foxp3 and CD25 expression. As illustrated in **Figure 3E**, mLN from non-infected and infected hosts contained a small percentage of injected cells. A high percentage (around 60%) of the injected cells within mLN from non-infected mice

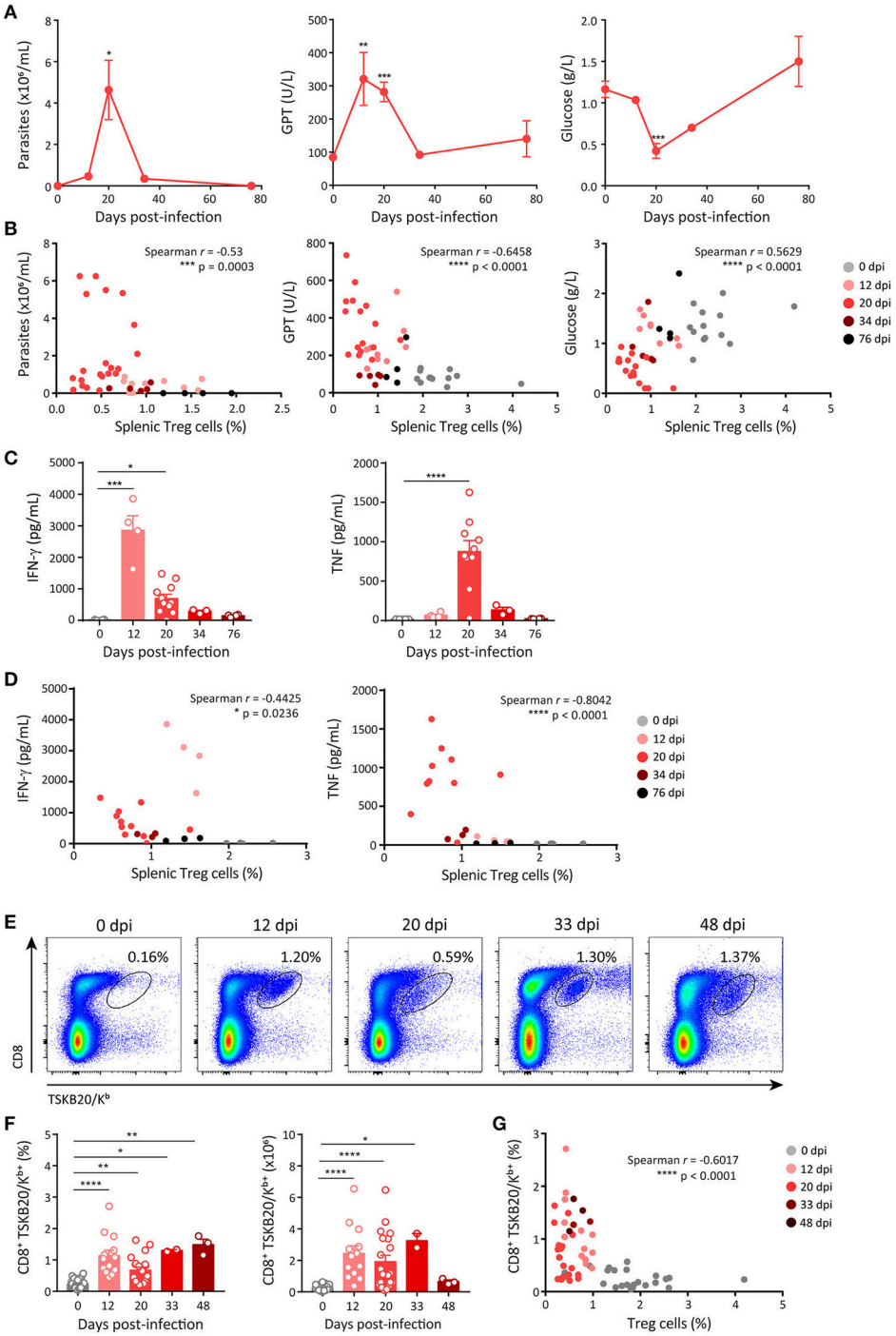

FIGURE 2 | Frequency of Treg cells inversely correlates with markers of acute disease progression and the emergence of effector immune responses. **(A)** Parasitemia (left panel) in blood, activity of glutamate-pyruvate transaminase (GPT) (middle panel) and glucose concentration (right panel) in plasma of *T. cruzi* infected Foxp3-EGFP mice at different dpi. **(B)** Scatter plots showing the relation between splenic Treg cell frequencies and each of the parameters shown in **(A)**. **(C)** Concentration of effector cytokines in plasma of *T. cruzi* infected Foxp3-EGFP mice at different dpi. **(D)** Scatter plots showing the relation between Treg cell frequencies in the spleen and plasma level of effector cytokines. **(E)** Representative dot plots for CD8 and TSKB20/K^b staining in the spleen of *T. cruzi* infected Foxp3-EGFP mice at different dpi. **(F)** Percentage (left) and absolute numbers (right) of parasite-specific $CD8^+$ T cells in the spleen *T. cruzi* infected Foxp3-EGFP mice at different dpi. **(G)** Scatter plots showing the relation between frequencies of Treg cells and parasite-specific $CD8^+$ T cells in the spleen of mice shown in **(F)**. In **(A)** data are presented as mean ± SEM of $n = 3$–11 animals. In **(B–D,F,G)** each circle or dot represents one animal. In **(C,F)** the bars show the mean + SEM of each parameter. Spearman *r* correlation coefficient and significance of the correlation are indicated inside the corresponding graphs. Data were pooled from 1 to 6 experiments according to the dpi and the determination. *P*-values were calculated by One way ANOVA with Dunnett's multiple comparisons test in **(A)** and Kruskal-Wallis with Dunn's correction in **(C,F)**. $^*P \leq 0.05$, $^{**}P \leq 0.01$, $^{***}P \leq 0.001$ and $^{****}P \leq 0.0001$.

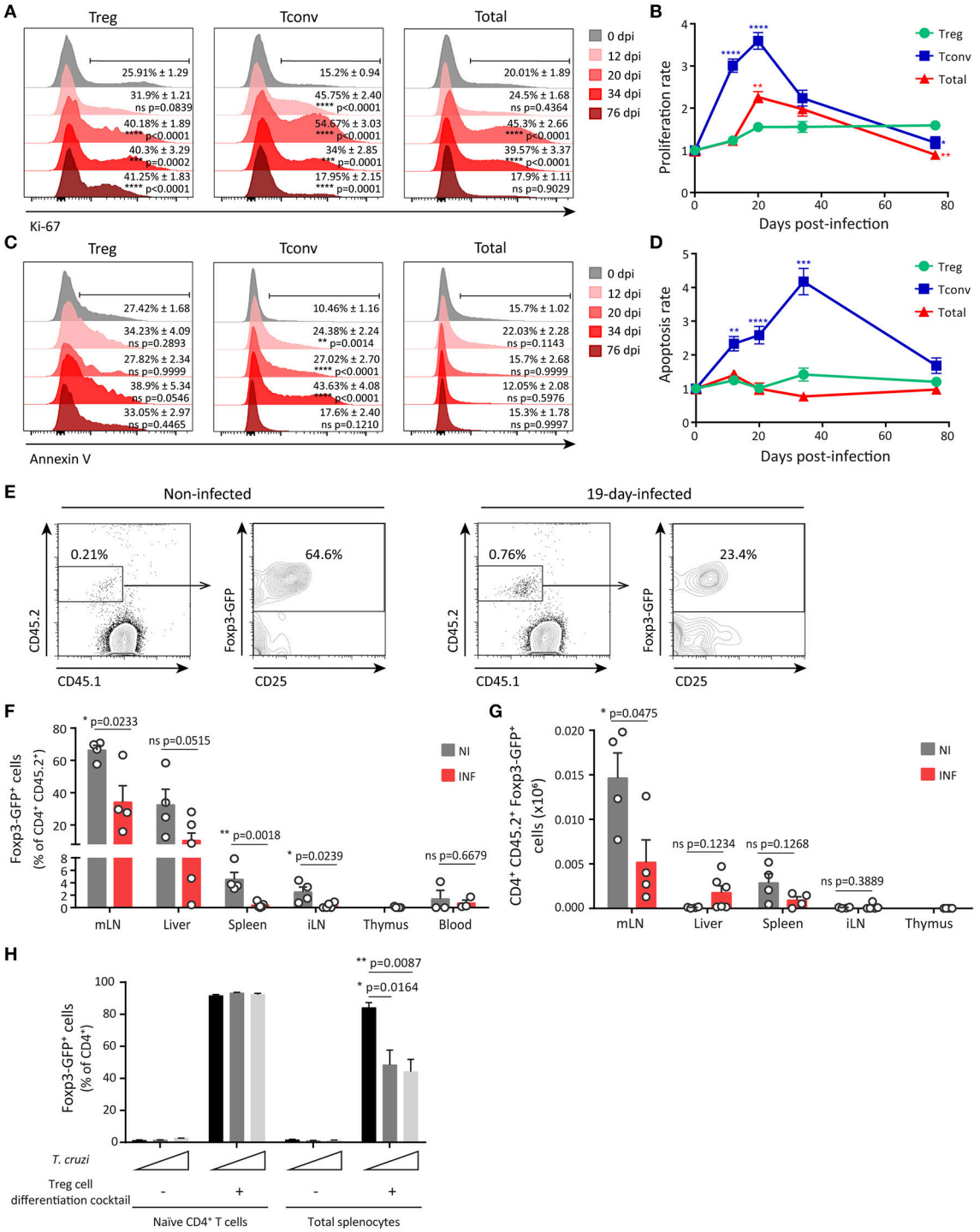

FIGURE 3 | Limited expansion and reduced peripheral differentiation of Treg cells during acute *T. cruzi* infection. **(A)** Histograms for Ki-67 expression in Treg ($CD4^+$ $Foxp3^+$), Tconv ($CD4^+$ $Foxp3^-$) and total cells from the spleen of Foxp3-EGFP mice infected with *T. cruzi* at different dpi. Percentage of positive cells mean ± SEM (n = 3–6 animals) and p-values are indicated for each dpi in comparison to 0 dpi. **(B)** Proliferation rate of cell populations at different dpi calculated as the relation between % of Ki-67^+ cells at 0 dpi and the other time points according to **(A)**. **(C)** Histograms for Annexin V staining in 7-AAD^- gated Treg, Tconv and total cells from the spleen of *T. cruzi* infected Foxp3-EGFP mice at different dpi. Percentage of positive cells mean ± SEM (n = 3–6 animals) and p-values are indicated for each dpi. **(D)** Apoptosis rate of cell populations at different dpi calculated as the relation between % of Annexin V^+ cells at 0 dpi and the other time points according to **(C)**. In **(B,D)** statistics were performed by One Way ANOVA comparing Tconv and total cells rates to Treg cells rate at each dpi (Sidak's multiple comparisons test). $^*P \leq 0.05$, $^{**}P \leq 0.01$, $^{***}P \leq 0.001$, $^{****}P \leq 0.0001$ and *ns* = not significant. **(E–H)** Tconv cells ($CD4^+$ $CD25^-$ Foxp3-GFP^-) from non-infected Foxp3-EGFP CD45.2 donors

(Continued)

FIGURE 3 | were transferred into CD45.1 recipient mice, which were simultaneously infected with *T. cruzi*. Nineteen days after transfer, conversion of transferred cells (GFP-) into Treg cells (GFP^+) was assessed in different organs. Representative dot plots showing donor and host $CD4^+$ cells according to CD45.2 and CD45.1 staining and Foxp3-GFP expression in $CD45.2^+$ $CD4^+$ donor cells in mLN from non-infected (NI) or infected (INF) hosts **(E)**. Bar graphs depicting percentage **(F)** and absolute numbers **(G)** of Treg cells within the population of transferred cells in different organs. Each circle represents one animal. Data were pooled from two independent experiments. *P*-values were calculated by unpaired *t*-test. **(H)** Frequency of Treg cells (GFP^+) determined within the $CD4^+$ gate in cultures of purified naïve $CD4^+$ T cells or total splenocytes stimulated with coated anti-CD3 and anti-CD28 in the presence or absence of the Treg cell differentiation cocktail and live parasites (at a cell:parasite ratio of 1:1 and 2:1) for 3 days. Data were pooled from two independent experiments with two technical replicates. *P*-values were calculated by unpaired *t*-test.

consisted of pTreg cells while most of the exogenous cells in mLN from infected mice were Tconv. The significant reduction in the frequency of pTreg cells originated from the injected Tconv during *T. cruzi* infection was observed not only in mLN that have an environment prone for pTreg cell differentiation, but also in the spleen and iLN (**Figure 3F**). To confirm that induction of pTreg cells was inhibited during *T. cruzi* infection, we calculated the absolute numbers of newly differentiated pTreg cells in the different organs. In agreement with the frequency data, the highest absolute numbers of induced pTreg cells were found in mLN in comparison to other organs (**Figure 3G**). Of note, the numbers of pTreg cells were significantly reduced in mLN from infected mice in comparison to non-infected controls but not in other organs. These data further support the notion that differentiation of pTreg cells is reduced during *T. cruzi* infection.

In order to identify mediators involved in the relative decrease of Treg cells during *T. cruzi* infection, we focused on particular inflammatory cytokines that are increased in the course of this parasitic infection and/or have been reported to modulate peripheral Treg cell proliferation and differentiation. Among these mediators, we selected cytokines, such as IL-6 and IL-1β that are produced during *T. cruzi* infection [**Supplementary Figure 2C** and references (59, 60)] and have been reported to restrain pTreg cell development by favoring a Th17 fate (61, 62). Also, type I interferons increase early during *T. cruzi* infection (63) and have been shown to limit regulatory responses by reducing Treg cell proliferation (26) and peripheral induction (64) in viral infection settings. We determined that mice with deficient production of IL-6 due to deletion of the *Il6* gene ($Il6^{-/-}$) or reduced IL-1β/IL-18 due to the lack of Caspase1/11 ($Casp1/11^{-/-}$) exhibited a similar decrease in Treg cell frequency at 20 dpi when compared to WT mice. Similarly, infected mice deficient in IFNAR, the specific receptor for type I IFNs, also showed a relative reduction of Treg cell responses (**Supplementary Figure 3A**). These results highlight that IL-6, IL-1β, and type I IFN signaling were not responsible of the relative Treg cell reduction triggered by *T. cruzi* infection.

As the frequency of Treg cells inversely correlated with parasitemia (**Figure 2B**), we next speculated that parasites could influence the size of the Treg cell pool during *T. cruzi* infection. To gain further insights in this direction, we evaluated whether changes in parasite levels as consequence of inoculation with different parasite doses have any impact in the frequency of Treg cells in periphery. We determined that 10-fold changes in the parasite dose used for infection resulted in significant dose-dependent differences in parasitemia at 11 dpi but not at 20 dpi, when parasitemia reached a maximum that was independent on the initial infective dose (**Supplementary Figure 3B**). Of note, the frequency of splenic Treg cells at 11 dpi was inversely associated with parasitemia and therefore remained unchanged in mice infected with the lowest dose, that showed barely detectable parasites in blood, but were significantly and dose-dependently reduced in mice infected with the intermediate and highest infective doses. These differences in Treg cell frequency were no longer observed at 20 dpi, when all mouse groups showed the same parasitemia (**Supplementary Figure 3C**). In this context, we designed *in vitro* experiments aimed to evaluate whether *T. cruzi* parasites are capable of inhibiting pTreg cell induction. As shown in **Figure 3H**, most naïve $CD4^+$ T cells differentiated into iTreg cells when activated in the presence of a Treg cell differentiation cocktail containing TFG-β, IL-2, and *all trans* retinoic acid (atRA). Of note, live trypomastigotes were unable to inhibit this differentiation. Similarly, more than 90% of the $CD4^+$ T cells became iTreg cells when total splenocytes were activated in the presence of the Treg cell differentiation cocktail. In contrast to the lack of effect on purified $CD4^+$ T cells, parasites significantly inhibited induction of iTreg cells in cultures of total splenocytes. These results strongly suggest that *T. cruzi* itself is able to actively inhibit Treg cell induction by an indirect mechanism that may depend on accessory cells present within the splenocytes rather than by a direct effect on naïve $CD4^+$ T cells.

Phenotypical and Transcriptional Characterization of Treg Cells During *T. cruzi* Infection Underscore a Specialization in the Regulation of Type 1 Effector Responses

The relative deficiency in the magnitude of Treg cell responses during the course of *T. cruzi* infection may be compensated by the activation and enhancement of the immunosuppressive function of this subset as reported previously (65–67). To address this, we performed a comprehensive evaluation of Treg cell phenotype by flow cytometry, determining the expression of proteins associated with Treg cell activation and suppressive function, such as CD25, CTLA-4, GITR, CD39, CD73, LAG-3, OX40, PD-1, FR4, GARP, TGF-β, and IL-10 together with molecules involved in migration and effector/memory subset classification like CD103, CD127, CCR7, CD44, and CD62L. We also assessed markers of Th1 specialization including T-bet, CXCR3 and IFN-γ in these cells. In order to broadly interpret the phenotypic changes occurring in Treg cells during

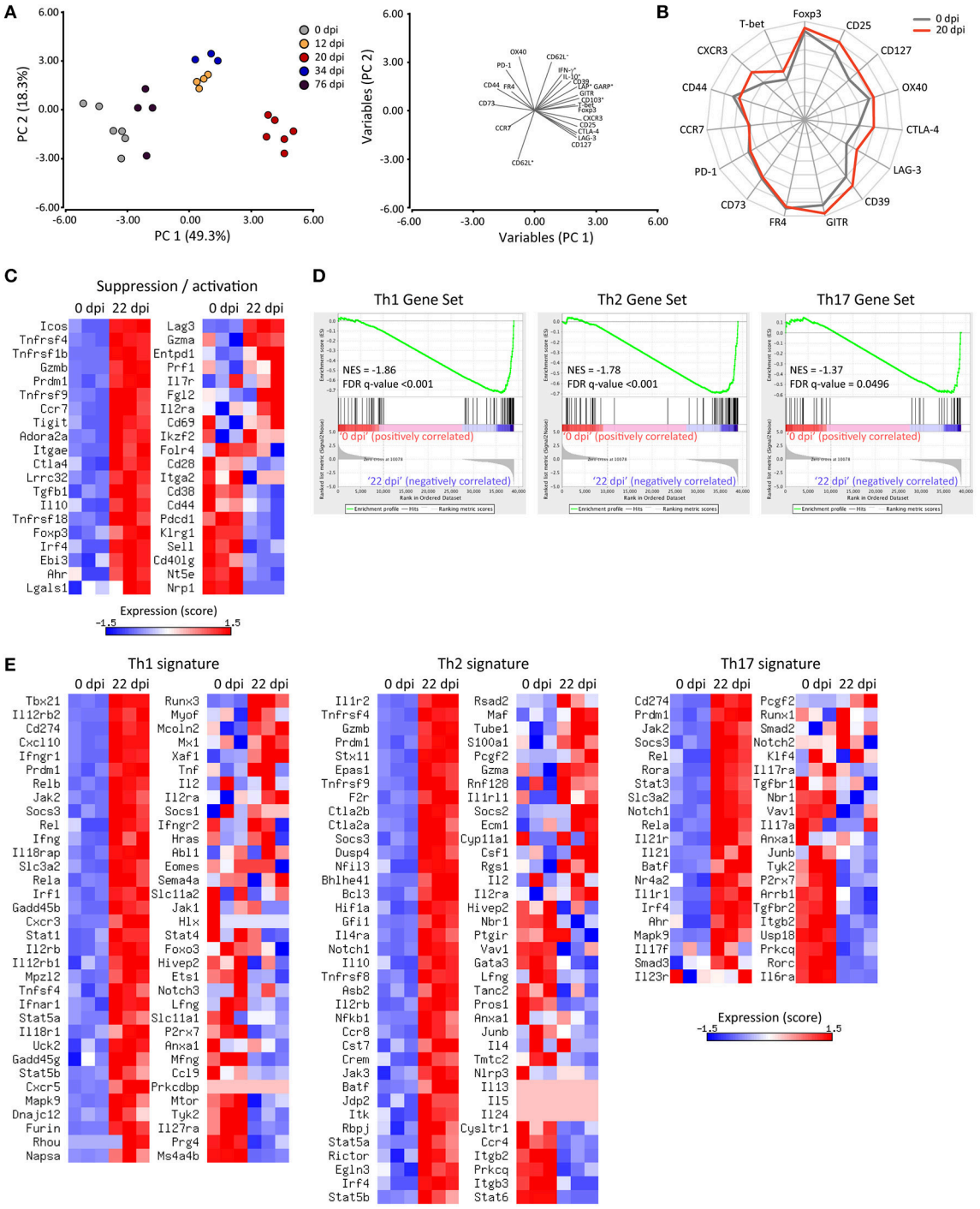

FIGURE 4 | Treg cells show an activated phenotype and acquire a Th1-like profile during *T. cruzi* infection. **(A)** Plots of principal component analysis (PCA) for surface and intracellular markers of Treg cells from the spleens of Foxp3-EGFP mice at the indicated dpi (left panel) and the variables included in PC1 and PC2 (right panel). Each circle represents one animal. **(B)** Star plot displaying the expression of the indicated markers in Treg cells from non-infected (0 dpi, gray line) or infected (20 dpi, red line) mice. Each spoke of the star represents the geometric mean of fluorescence intensity for the indicated marker in a log2 scale from 1 to 16,384. The data length of a spoke is proportional to the MFI of expression of that marker in the corresponding sample. **(C)** Heat maps for the normalized expression scores (row mean values of 0 and variance of 1) of genes encoding suppression and/or activation markers in Treg cells ($CD4^+$ $CD25^+$ Foxp3-GFP^+) purified from the spleen of non-infected (0 dpi) or 22-days-infected (22 dpi) Foxp3-EGFP mice. **(D)** Gene set enrichment analysis of the Treg cell transcriptome for Th1, Th2 and Th17 signatures using selected gene sets. **(E)** Heat maps for the normalized expression scores (row mean values of 0 and variance of 1) of the selected genes used in **(D)**. RNAseq data are from one experiment with three biological replicates. The PCA plot, star plot and heat maps were created using InfoStat software, Microsoft Excel spreadsheet and Matrix2png online tool, respectively.

the progression of *T. cruzi* infection, we focused on changes occuring in spleen and performed multivariate analysis of all the markers evaluated. Principal component analysis (PCA) defined two principal components (PC) that accounted for around 70% of the total variance and allowed to evidence the phenotypic changes suffered by Treg cells along the different dpi (**Figure 4A**, left pannel). The variables included in PC1 and PC2 as well as the direction of their changes are also depicted (**Figure 4A**, right pannel). Interpretation of the PCA plots indicated that the phenotype of Treg cells changed progressively from 0 dpi (non-infected) until 20 dpi (maximal difference) by modifications in the variables included mainly in PC1 and at a lower extent in PC2. This analysis also established that Treg cells at 12 and 34 dpi showed a similar phenotype that is intermediate between those of cells from 0 and 20 dpi while Treg cells at 76 dpi showed features more related to the phenotype of Treg cells from non-infected mice (0 dpi).

The kinetics of expression of each marker highlighted that Treg cells from *T. cruzi* infected mice exhibited phenotypic changes as early as 12 dpi, with a maximum between 20 and 34 dpi (**Supplementary Figure 4A**). Of note, Treg cells from 20-days infected mice showed an evident activated phenotype as demonstrated by the upregulation of activation and memory markers, such as Foxp3, CD25, OX40, CD103, and CD127 in comparison to Treg cells from non-infected mice (68). In addition, Treg cells at 20 dpi showed increased expression of molecules associated with their suppressive function including CTLA-4, GITR, CD39, and LAG-3 but not CD73, PD-1, and FR4. We also established that Treg cells increased their capacity to produce regulatory cytokines, such as TGF-β (as indicated by co-expression of GARP and LAP) and IL-10 (**Supplementary Figure 4B**) after 20 days of infection. Finally, we determined that Treg cells at 20 dpi upregulated CXCR3 and slightly T-bet, and increased IFN-γ production in comparison to counterparts from non-infected mice (0 dpi; **Supplementary Figures 4C,D**). Remarkably, T-bet and CXCR3 expression levels in Treg cells from 20 dpi were comparable and higher than those observed in Tconv cells at the same time point, respectively (**Supplementary Figure 4C**). The expression of several markers studied were represented in a star plot that allowed to evidence differences in the phenotypic profile of Treg cells at 0 and 20 dpi, showing that *T. cruzi* infection induced the up-regulation of activation and Th1-associated markers as well as immunosuppressive mediators (**Figure 4B**).

In order to determine the global impact of *T. cruzi* infection on the transcriptional program of Treg cells, we compared by RNAseq the gene expression profiles of Treg cells purified from the spleen at 0 and 20 dpi. A total of 5,175 genes were differentially expressed in Treg cells as a consequence of *T. cruzi* infection (data not shown). As illustrated by the heat maps in **Figure 4C**, Treg cells from infected mice exhibited a global increase in the levels of many transcripts encoding activation markers and suppressive mediators. In addition to those noticed by flow cytometry (CD25, CD127, CD103, GITR, CTLA-4, TGF-β, and IL-10 among others), we also detected an up-regulation of genes encoding ICOS, Granzyme B, CD137, TIGIT, Adenosin A2a receptor, EBI3, Galectin-1, among others. In agreement with their phenotypic profile, Treg cells from infected mice showed reduced amounts of transcripts encoding CD44, PD-1, CD62L, and CD73. Of note, Treg cells from infected mice showed augmented levels in the expression of Blimp-1 and IRF4, transcription factors that drive effector Treg cell differentiation (67). Altogether, this transcriptional profile reflected a clear activation of Treg cells along *T. cruzi* infection. Next, we aimed to determine whether Treg cells from infected mice exhibit programs that denote any functional specialization (69). To this end, we performed Gene Set Enrichment Analysis of the Treg cell transcriptome for Th1, Th2, and Th17 signatures. As shown in the enrichment plots, the transcriptome of Treg cells from infected mice are significantly enriched in the Th1, Th2, and Th17 gene sets (**Figure 4D**). Interestingly, Treg cells from *T. cruzi* infected mice up-regulated most of the genes classically associated with a Th1 specialization including *Tbx21, Ifng*, and *Cxcr3* and also the two subunits of the IL-12 receptor (*Il12rb2* and *Il12rb1*), *Stat1, Ifngr1*, and *Cxcl10* while they down-regulated *Il27ra* (**Figure 4E**). Of note, Treg cells from infected mice showed increased levels of some transcripts associated with a Th2 signature, such as *Il1r2, Il4ra, Il10*, and *Irf4* but not of other prototypical Th2 genes, such as *Gata3, Il4, Il5*, or *Il13*. Similarly, this cell subset showed increased expression of certain genes associated with a Th17 fate like *Rora, Stat3, Il21r*, and *Ahr* but not of others tightly linked to Th17 cells like *Rorc* and *Il17a*.

Adoptive Transfer of Treg Cells Suppresses Anti-Parasite Effector Response and Diminishes Parasite Control During *T. cruzi* Infection

Once established the features acquired by Treg cells after *T. cruzi* infection, we aimed at evaluating the biological role of this cell subset in the progression of the infection. Considering the results from **Figure 2**, we were particularly interested in addressing the relevance of the limited Treg cell response for the induction/maintenance of effector responses and immunopathology. To this end, we designed an experiment in which Treg cell numbers were increased by the injection of Treg cells differentiated *in vitro* (iTreg cells). iTreg cells were obtained by sorting Foxp3-GFP$^+$ cells from cultures in which CD4$^+$ T cells obtained from Foxp3-EGFP reporter mice were stimulated with anti-CD3 and anti-CD28 in the presence of the Treg cell differentiation cocktail (**Supplementary Figure 5A**). In agreement with data showing that this cocktail induced stable human iTreg cells (70), we determined that iTreg cells generated in these conditions showed immunosuppressive capacity *in vitro* (**Supplementary Figure 5B**), and failed to produce effector cytokines, such as IFN-γ and IL-17 (**Supplementary Figure 5C**).

As schematized in **Figure 5A**, adoptive transfer experiments were designed to inject iTreg cells into infected hosts at 11 dpi, the time point in which the reduction of Treg cell frequency becomes significant. Remarkably, infected hosts that received iTreg cells showed significantly augmented levels of parasites

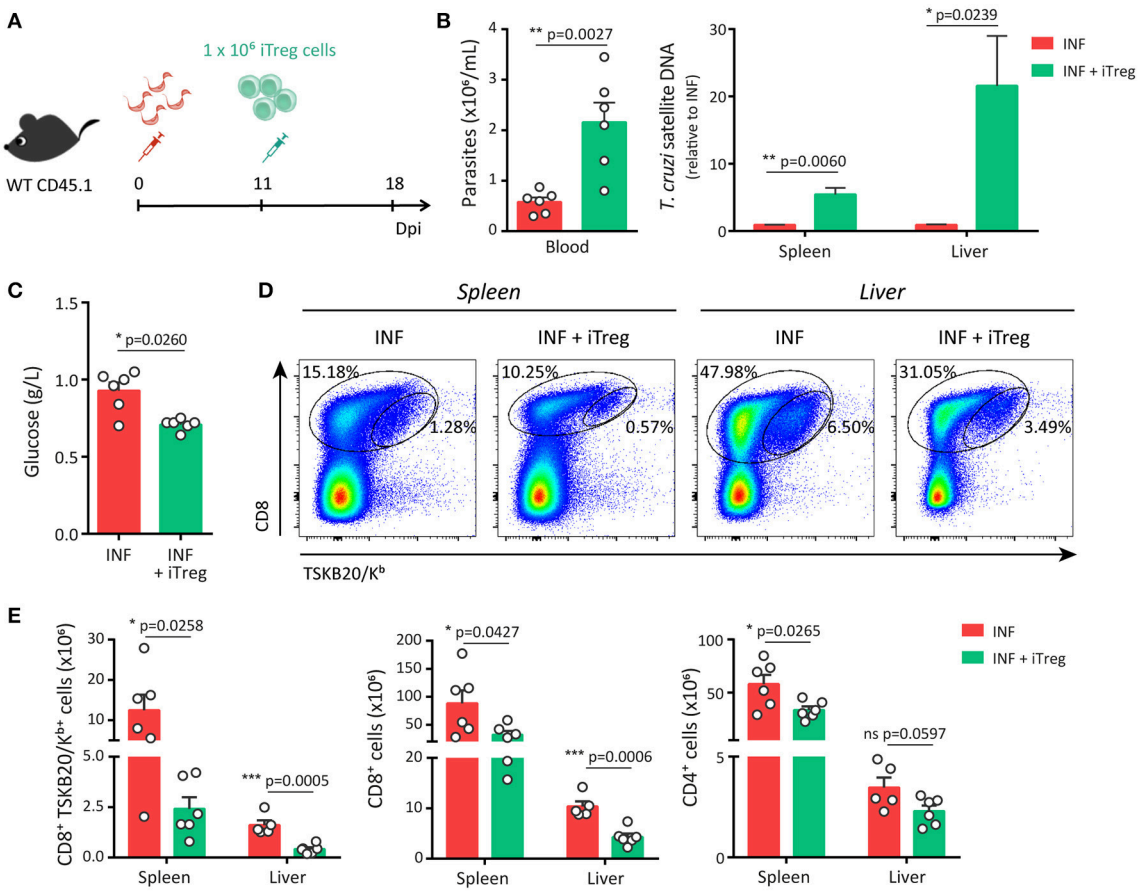

FIGURE 5 | Adoptive transfer of Treg cells restricts the development of a robust parasite-specific CD8$^+$ T cell response during acute *T. cruzi* infection. **(A)** CD45.1 WT mice were infected with *T. cruzi* and 11 days later were transferred with 1 × 10^6 iTreg cells differentiated from Foxp3-EGFP mice. **(B–C)** Parasitemia [**(B)**, left], parasite load by real time PCR in the spleen and liver [**(B)**, right] and glucose concentration in the plasma **(C)** of non-transferred control (INF) and transferred (INF + iTreg) infected mice. **(D–F)** Dot plots **(D)** and graphs showing absolute numbers **(E)** of total and parasite-specific T cells responses in the spleen and liver of transferred and control mice. Data are presented as mean + SEM and are pooled from two independent experiments. *P*-values were calculated by unpaired *t*-test **(B,E)** or Mann Whitney test **(C)**.

in blood and tissues in comparison to control counterparts at 18 dpi (**Figure 5B**). In addition, and likely as consequence of the uncontrolled parasite replication, mice injected with iTreg cells presented reduced blood glucose concentration but biochemical markers of tissue damage were not affected (**Figure 5C** and data not shown). In order to establish the causes of the reduced parasite control, we evaluated the magnitude of the effector immune response. Adoptive transfer of iTreg cells significantly diminished the frequency of parasite-specific CD8$^+$ T cells in spleen and liver of infected mice (**Figure 5D**). Furthermore, the absolute numbers of parasite-specific CD8$^+$ T cells and total CD8$^+$ and CD4$^+$ T cells were also reduced after the injection of iTreg cells in infected hosts (**Figure 5E**). Altogether, these results indicate that increasing Treg cell numbers during *T. cruzi* infection severely compromises the magnitude of protective immune responses including parasite-specific CD8$^+$ T cell immunity and consequently, limits the control of parasite replication and host resistance to the infection.

DISCUSSION

The role played by Treg cells in the progression of *T. cruzi* infection remains controversial likely because any rational mechanistic evaluation is precluded by the limited characterization of the triggered Treg cell response. Considering this, we studied in detail the kinetics of Treg cell responses using Foxp3-EGFP reporter mice and demonstrated that frequency of Treg cells is reduced along *T. cruzi* infection in most peripheral organs including spleen, liver and inguinal lymph nodes. Furthermore, we showed that this relative decrease is not caused by a reduction in Treg cell absolute numbers but rather by a significant expansion of effector cells that affect the ratio of Treg cells to other immune subsets in different tissues. Thus, our results further expand and complement a recent work reporting that frequency of splenic Treg cells is significantly reduced during acute experimental *T. cruzi* infection likely as result of a neuroendocrine dysbalance (41). Altogether, this report and our data underscore that, differently from most chronic infections of

viral, bacterial and parasitic origin which are characterized by a Treg cell accrual, *T. cruzi* infection associates with a significant decrease in the magnitude of the Treg cell response that is prolonged even until the early chronic phase of the infection.

After evaluating recognized mechanisms that regulate Treg cell pool size in periphery, we established that Treg cells exhibited significantly lower proliferation rate in comparison to effector immune subsets during *T. cruzi* infection, confirming a previous report in this direction (41). Although not surprising considering the current views on pTreg cell induction (71), we also demonstrated that the inflammatory environment triggered by *T. cruzi* limits the peripheral induction of Treg cells. Remarkable, infections characterized by Treg cell accumulation triggered a marked proliferation of Treg cells but not peripheral induction of this cell subset. Thus, influenza infection was shown to induce peripheral proliferation and accumulation of Ag-specific thymically derived Treg cells whereas conventional $CD4^+$ T cells with identical specificity for the pathogen underwent little or no peripheral conversion in infected mice (72). Similarly, Treg cells expressing a pathogen-specific transgenic TCR were found to expand in response to *M. tuberculosis* without *de novo* induction of pTreg cells (73). Of note, proliferation of Ag-specific Treg cells was detected during *M. tuberculosis* but not *L. monocytogenes* infection indicating that only certain microbes are able to induce an inflammatory milieu that is conducive to the expansion of Ag-specific Treg cells (74). In this context, the results presented in our manuscript support the notion that *T. cruzi* infection triggers a relatively deficient Treg cell response by inducing an inflammatory context that does not support pTreg cell induction (somehow expected as discussed) but also limits Treg cell proliferation. Given that Treg cells have a high dependence on exogenous IL-2 for differentiation and proliferation, it is likely that Treg cell homeostasis may be affected by the suppressed production or increased consumption of IL-2 that occurs during *T. cruzi* infection (75–77). Indeed, IL-2 consumption by proliferating effector cells resulted in reduced Treg numbers in infections with *Toxoplasma gondii, Listeria monocytogenes*, and vaccinia virus (25). In this regard, we demonstrated that the systemic concentration of IL-2 remained unchanged during the acute phase of *T. cruzi* infection and that it showed no correlation with the frequency of splenic Treg cells. In addition, Gonzalez et al (41) reported that treatment with recombinant IL-2 was not sufficient to increase Treg cell frequency during this parasitic infection. These data suggest that regulation of the Treg cell pool size during *T. cruzi* infection is independent from IL-2 levels.

Several pro-inflammatory mediators have been reported to modulate Treg cell homeostasis during inflammatory conditions (78). Among them, IL-1β and IL-6 emerged as possible candidates to mediate the limited Treg cell response during *T. cruzi* infection, given their largely known function to promote a Th17 over a Treg cell fate (61, 62). We previously demonstrated that Th17 and other IL-17^+ cell subsets are induced early during *T. cruzi* infection (79, 80) and when compared, the kinetics of the increment in Th17 cell frequencies and the relative decrease of Treg cells showed a reciprocal behavior (data not shown). Also, type I IFNs may be involved in the limited proliferation and induction of Treg cells as reported in viral infections (26, 64). However, evaluation of the magnitude of Treg cell responses in infected mice that lacked IL-6, IL-1β, and type I IFNs signaling due to genetic deletions in *Il6*, *Caspase1/11*, and *Ifnar* genes, respectively, ruled out a main role for these pro-inflammatory cytokines in the regulation of the Treg cell size during *T. cruzi* infection. Considering other possible inflammatory mediators involved in this phenomenon; we established that frequency of Treg cells showed a strong inverse correlation with the levels of parasite in blood along the infection. Furthermore, *in vitro* experiments indicated that live parasites are able to inhibit the induction of Treg cells by a mechanism that depends on cell populations other than $CD4^+$ T cells themselves. Altogether, these findings strongly suggest that the *T. cruzi* load affects Treg cell peripheral induction and/or proliferation by indirect mechanisms that are currently under investigation in our laboratory.

Previous studies aimed at addressing the biological relevance of Treg cells in the course of *T. cruzi* infection reported contradictory results regarding the role of this subset in the regulation of the magnitude and functionality of effector immune responses, parasite control and development of immunopathology. Thus, Treg cell depletion by treatment with anti-CD25 depleting antibodies was reported to have a limited role in the induction of parasite-specific $CD8^+$ T cells, and therefore, parasite control and host survival (43), but also to slightly increase host resistance to infection by favoring activation of $CD4^+$ T cells (44). In contrast, combined injection of anti-CD25 and anti-GITR evidenced that Treg cells may be important to prevent exuberant inflammation, particularly at the heart, and increased mortality during this parasitic infection (42). More recently, early and sustained Treg cell depletion with anti-CD25 was reported to modulate Th1 and Th17 responses during *T. cruzi* infection, reducing cardiac parasitosis and inflammation (45). The reasons underlying these controversial data have not yet been determined but may be related to the variability in parasite and host strains, timing of Treg manipulation and the use of non-specific Treg cell depletion strategies. Considering these data and our results demonstrating a limited Treg cell response during *T. cruzi* infection, we reasoned that increasing Treg cell numbers may be a more rational strategy to define the role of Treg cells in this infection setting. Accordingly, we designed adoptive transfer experiments in which Treg cell numbers were manipulated by injection of *in vitro* differentiated Treg cells. This approach has been widely used to modulate the outcome of several pathological conditions including autoimmunity and GVHD (81). We determined that increasing Treg cells at the time when infected mice exhibited a significant reduction in the frequency of this cell subset, limited the accumulation of parasite-specific $CD8^+$ T cells, severely compromising the control of parasite replication in tissues and host resistance to *T. cruzi*. These data are significant though they should be interpreted with caution as the activation status of *in vitro* generated Treg cells may enhance their suppressive function in comparison to endogenous Treg cells as previously reported (82). Even considering these limitations, our findings demonstrate that activated Treg cells are able to dampen specific $CD8^+$

T cell immunity during *T. cruzi* infection. Furthermore, these data suggest that the natural contraction of Treg cell responses observed during the acute phase of *T. cruzi* infection may be critical to allow the emergence of a robust effector response aimed at controlling pathogen replication as previously reported for acute infections (25). Thus, timing and other features of the Treg cell response during this parasitic infection may evidence a particular mechanism of a chronic *T. cruzi*-host adaptation that allows the emergence of effector responses able to sustain partial parasite control and host resistance but preventing complete pathogen elimination. Within this conceptual framework, further research will be required to address the mechanisms involved and to determine if a precise Treg cell manipulation may represent an opportunity to potentiate anti-parasite immunity and parasite control.

It is currently known that Treg cells exert their regulatory function by deploying a plethora of immunosuppressive mechanisms that target different immune cell populations. Treg cells have been reported to modulate the activation, proliferation and/or function of $CD8^+$ and $CD4^+$ T cells, B cells, NK cells, monocytes and dendritic cells, among others (1). Altogether, the phenotypic, transcriptional and functional profiles of Treg cells activated during *T. cruzi* infection highlight the global activation of this cell subset and also evidence a marked heterogeneity in the Treg cell compartment from infected mice. Of note, even though GSEA suggests that *T. cruzi* infection elicit Treg cell subsets that acquire specialized programs for the regulation of Th1, Th2, and Th17 responses, these cells showed a global up-regulation of most of the genes classically associated to the Th1 signature but not of those critical for Th2 and Th17 fates, such as Gata-3 and Rorγt. Therefore, this specialized program may tailor Treg cells with a particular ability to suppress *in vivo* type 1 effector responses guiding Treg cells to Th1 inflammatory sites. Further studies including single-cell RNA-seq may be very helpful to precisely unravel the complexities of Treg cell responses during this infection. By potentiating the regulatory response through iTreg cell adoptive transfer, we established that Treg cells activated in the context of *T. cruzi* infection have the ability to suppress total and parasite-specific $CD8^+$ T cell immunity and, at a minor extent, the polyclonal $CD4^+$ T cell response. Whether Treg cells also influence other immune cell populations in these infectious setting remains unexplored. Although not previously reported for *T. cruzi* infection, Treg cell mediated suppression of $CD8^+$ T cell immunity has been widely described during infections, particularly of viral origin (13). Treg cells are able to regulate many steps of the $CD8^+$ T cell response through mechanisms that remain partially elucidated and involve not only the $CD8^+$ T cells themselves but also antigen presenting cells. In this way, antigen-specific and polyclonal Treg cells impaired $CD8^+$ T cell priming by inhibiting the early expansion of antigen-specific cells (83) and preventing the activation of antigen-presenting cells through CTLA-4 mediated inhibitory signals (84). Even more, Treg cells have been reported to directly limit $CD8^+$ T cell proliferation (85), differentiation into effector cells (86), cytotoxic effector function (87, 88) and to sustain $CD8^+$ T cell exhaustion (89) by mechanisms that involve IL-2 consumption, TGF-β and IL-10 production, PD-1 and CD39 expression, and many others. According to this, Treg cells activated in the context of *T. cruzi* infection acquired a phenotypic profile that would allow direct and indirect regulation of $CD8^+$ T cell immunity. In this regard, a direct suppressive function is supported by the increased expression of CXCR3 in Treg cells activated during *T. cruzi* infection that would allow migration to inflammatory sites. In addition, a direct suppressive mechanism may be responsible for the reduction in the magnitude of the specific $CD8^+$ T cell immunity that occur following iTreg cell adoptive transfer at 11 dpi, a time point after the emergence of the parasite-specific $CD8^+$ T cell response. On the other hand, the fact that Treg cells activated during *T. cruzi* infection expressed remarkably high levels of CTLA-4 may indicate that these cells are particularly prepared for *in vivo* regulation of antigen-presenting cells. A detailed comprehension of the mechanisms underlying the Treg cell-mediated inhibition of $CD8^+$ T cell immunity during this parasitic infection will be essential to design possible immune-intervention strategies aimed at improving parasite-specific immunity without enhancing infection-associated pathology.

Altogether, our data delineate a model in which infection with *T. cruzi* promotes activation but limits proliferation and peripheral induction of Treg cells during the acute phase. Whether these events are mediated by active mechanisms remains to be clearly established as passive pathways are not completely ruled out by our study. In any case, the Treg cell mediated regulatory response seems to exhibit a putatively improved quality but reduced quantity during *T. cruzi* infection. This weakened Treg cell response allows the emergence of a robust parasite-specific effector immunity, particularly of $CD8^+$ T cells, which partially controls parasite replication favoring host resistance. Although these findings support a deleterious role for Treg cells during the acute phase of *T. cruzi* infection, a special attention needs to be given to timing. Indeed, we also determined that during the chronic phase, when parasite replication is limited and inflammation goes down, the frequency and phenotypic profile of Treg cells tended to return to normal conditions. This finding together with reported data in which increased Treg cell frequency and function in chagasic patients correlate with better clinical outcomes, likely as consequence of a limited chronic inflammation, proposes that Treg cell role may switch during *T. cruzi* infection from deleterious in the acute phase to protective during chronic Chagas disease. Further research will be required to definitively address this point in order to establish a rational framework for the design of novel treatment strategies to differentially manipulate Treg cells during different stages of *T. cruzi* infection.

ETHICS STATEMENT

This study was carried out in accordance with the recommendations of Guide to the care and use of experimental animals (Canadian Council on Animal Care, 1993) and Institutional Animal Care and Use Committee Guidebook (ARENA/OLAW IACUC Guidebook, National Institutes of Health, 2002). The protocol was approved by the Institutional Animal Care and Use Committee (IACUC) Facultad de

Ciencias Químicas, Universidad Nacional de Córdoba (Approval Number 565/15 and 731/18) (OLAW Assurance number F16-00193-A5802-01).

AUTHOR CONTRIBUTIONS

CA designed and performed most of the experiments, analyzed data, and wrote/commented on the manuscript. JT, CR, FC, FF, SB, and CB performed experiments and commented on the manuscript. VA and OJ participated in the execution and analysis of the RNAseq experiment and provided funding [Fondation pour la Recherche Médicale (AJE201212 to OJ), the Région Midi-Pyrénées (OJ)]. CM and AG participated in data analysis, commented on the manuscript and provided funding. EA supervised the research, designed experiments, wrote the manuscript, and provided funding.

FUNDING

Research reported in this publication was supported by: Agencia Nacional de Promoción Científica y Técnica (PICT 2013-0070 and PICT 2015-0127), Secretaría de Ciencia y Técnica-Universidad Nacional de Córdoba, Fundación Florencio Fiorini and the National Institute of Allergy and Infectious Diseases of the National Institutes of Health under Award Number R01AI110340. The content is solely the responsibility of the authors and does not necessarily represent the official views of the funding agencies.

ACKNOWLEDGMENTS

We thank M. P. Abadie, M. P. Crespo, F. Navarro, D. Lutti, V. Blanco, R. Villarreal, W. Requena, C. Noriega, A. Romero, L. Gatica, G. Furlán (Centro de Investigaciones en Bioquímica Clínica e Inmunología) and J. Fourquet (Centre de Physiopathologie de Toulouse Purpan) for their excellent technical assistance. We acknowledge the NIH Tetramer Core Facility for provision of the APC-labeled TSKB20/Kb tetramers. We thank the GeT-PlaGe and GenoToul bioinformatics platforms Toulouse Midi-Pyrénées for sequencing and computing resources.

SUPPLEMENTARY MATERIAL

The Supplementary Material for this article can be found online at: https://www.frontiersin.org/articles/10.3389/fimmu.2018.02555/full#supplementary-material

REFERENCES

1. Shevach EM. Mechanisms of foxp3$^+$ T regulatory cell-mediated suppression. *Immunity* (2009) 30:636–45. doi: 10.1016/j.immuni.2009.04.010
2. Sakaguchi S, Yamaguchi T, Nomura T, Ono M. Regulatory T cells and immune tolerance. *Cell* (2008) 133:775–87. doi: 10.1016/j.cell.2008.05.009
3. Stephen-Victor E, Bosschem I, Haesebrouck F, Bayry J. The Yin and Yang of regulatory T cells in infectious diseases and avenues to target them. *Cell Microbiol.* (2017) 19:e12746. doi: 10.1111/cmi.12746
4. Parkash O, Agrawal S, Madhan Kumar M. T regulatory cells: Achilles' heel of Mycobacterium tuberculosis infection? *Immunol Res.* (2015) 62:386–98. doi: 10.1007/s12026-015-8654-0
5. Saini C, Tarique M, Rai R, Siddiqui A, Khanna N, Sharma A. T helper cells in leprosy: an update. *Immunol Lett.* (2017) 184:61–6. doi: 10.1016/j.imlet.2017.02.013
6. Boer MC, Joosten SA, Ottenhoff TH. Regulatory T-cells at the interface between human host and pathogens in infectious diseases and vaccination. *Front Immunol.* (2015) 6:217. doi: 10.3389/fimmu.2015.00217
7. Lund JM, Hsing L, Pham TT, Rudensky AY. Coordination of early protective immunity to viral infection by regulatory T cells. *Science* (2008) 320:1220–4. doi: 10.1126/science.1155209
8. Soerens AG, Da Costa A, Lund JM. Regulatory T cells are essential to promote proper CD4 T-cell priming upon mucosal infection. *Mucosal Immunol.* (2016) 9:1395–406. doi: 10.1038/mi.2016.19
9. Fulton RB, Meyerholz DK, Varga SM. Foxp3$^+$ CD4 regulatory T cells limit pulmonary immunopathology by modulating the CD8 T cell response during respiratory syncytial virus infection. *J Immunol.* (2010) 185:2382–92. doi: 10.4049/jimmunol.1000423
10. Ruckwardt TJ, Bonaparte KL, Nason MC, Graham BS. Regulatory T cells promote early influx of CD8$^+$ T cells in the lungs of respiratory syncytial virus-infected mice and diminish immunodominance disparities. *J Virol.* (2009) 83:3019–28. doi: 10.1128/JVI.00036-09
11. Graham JB, Da Costa A, Lund JM. Regulatory T cells shape the resident memory T cell response to virus infection in the tissues. *J Immunol.* (2014) 192:683–90. doi: 10.4049/jimmunol.1202153
12. Veiga-Parga T, Sehrawat S, Rouse BT. Role of regulatory T cells during virus infection. *Immunol Rev.* (2013) 255:182–96. doi: 10.1111/imr.12085
13. Hasenkrug KJ, Chougnet CA, Dittmer U. Regulatory T cells in retroviral infections. *PLoS Pathog.* (2018) 14:e1006776. doi: 10.1371/journal.ppat.1006776
14. Luhn K, Simmons CP, Moran E, Dung NT, Chau TN, Quyen NT, et al. Increased frequencies of CD4$^+$ CD25(high) regulatory T cells in acute dengue infection. *J Exp Med.* (2007) 204:979–85. doi: 10.1084/jem.20061381
15. Stross L, Gunther J, Gasteiger G, Asen T, Graf S, Aichler M, et al. Foxp3$^+$ regulatory T cells protect the liver from immune damage and compromise virus control during acute experimental hepatitis B virus infection in mice. *Hepatology* (2012) 56:873–83. doi: 10.1002/hep.25765
16. Belkaid Y, Sun CM, Bouladoux N. Parasites and immunoregulatory T cells. *Curr Opin Immunol.* (2006) 18:406–12. doi: 10.1016/j.coi.2006.05.014
17. Peters N, Sacks D. Immune privilege in sites of chronic infection: Leishmania and regulatory T cells. *Immunol Rev.* (2006) 213:159–79. doi: 10.1111/j.1600-065X.2006.00432.x
18. Scholzen A, Minigo G, Plebanski M. Heroes or villains? T regulatory cells in malaria infection. *Trends Parasitol.* (2009) 26:16–25. doi: 10.1016/j.pt.2009.10.004
19. Belkaid Y, Piccirillo CA, Mendez S, Shevach EM, Sacks DL. CD4$^+$CD25$^+$ regulatory T cells control Leishmania major persistence and immunity. *Nature* (2002) 420:502–7. doi: 10.1038/nature01152
20. Hisaeda H, Maekawa Y, Iwakawa D, Okada H, Himeno K, Kishihara K, et al. Escape of malaria parasites from host immunity requires CD4$^+$ CD25$^+$ regulatory T cells. *Nat Med.* (2004) 10:29–30. doi: 10.1038/nm975
21. Abel S, Luckheide N, Westendorf AM, Geffers R, Roers A, Muller W, et al. Strong impact of CD4$^+$ Foxp3$^+$ regulatory T cells and limited effect of T cell-derived IL-10 on pathogen clearance during *Plasmodium yoelii* infection. *J Immunol.* (2012) 188:5467–77. doi: 10.4049/jimmunol.1102223
22. Hesse M, Piccirillo CA, Belkaid Y, Prufer J, Mentink-Kane M, Leusink M, et al. The pathogenesis of schistosomiasis is controlled by cooperating IL-10-producing innate effector and regulatory T cells. *J Immunol.* (2004) 172:3157–66. doi: 10.4049/jimmunol.172.5.3157
23. Oldenhove G, Bouladoux N, Wohlfert EA, Hall JA, Chou D, Dos Santos L, et al. Decrease of Foxp3$^+$ Treg cell number and acquisition of

effector cell phenotype during lethal infection. *Immunity* (2009) 31:772–86. doi: 10.1016/j.immuni.2009.10.001
24. Olguin JE, Fernandez J, Salinas N, Juarez I, Rodriguez-Sosa M, Campuzano J, et al. Adoptive transfer of CD4(+)Foxp3(+) regulatory T cells to C57BL/6J mice during acute infection with Toxoplasma gondii down modulates the exacerbated Th1 immune response. *Microbes Infect.* (2015) 17:586–95. doi: 10.1016/j.micinf.2015.04.002
25. Benson A, Murray S, Divakar P, Burnaevskiy N, Pifer R, Forman J, et al. Microbial infection-induced expansion of effector T cells overcomes the suppressive effects of regulatory T cells via an IL-2 deprivation mechanism. *J Immunol.* (2012) 188:800–10. doi: 10.4049/jimmunol.1100769
26. Srivastava S, Koch MA, Pepper M, Campbell DJ. Type I interferons directly inhibit regulatory T cells to allow optimal antiviral T cell responses during acute LCMV infection. *J Exp Med.* (2014) 211:961–74. doi: 10.1084/jem.20131556
27. Perez-Molina JA, Molina I. Chagas disease. *Lancet* (2018) 391:82–94. doi: 10.1016/S0140-6736(17)31612-4
28. Pan American Health Organization. *Estimación Cuantitativa de la Enfermedad de Chagas en las Americas. OPS/HDM/CD/425-06*. Washington, DC: OMS/OPS (2006).
29. Kayama H, Takeda K. The innate immune response to *Trypanosoma cruzi* infection. *Microbes Infect.* (2010) 12:511–7. doi: 10.1016/j.micinf.2010.03.005
30. Junqueira C, Caetano B, Bartholomeu DC, Melo MB, Ropert C, Rodrigues MM, et al. The endless race between *Trypanosoma cruzi* and host immunity: lessons for and beyond Chagas disease. *Expert Rev Mol Med.* (2010) 12:e29. doi: 10.1017/S1462399410001560
31. Tarleton RL. $CD8^+$ T cells in *Trypanosoma cruzi* infection. *Semin Immunopathol.* (2015) 37:233–8. doi: 10.1007/s00281-015-0481-9
32. Cardillo F, de Pinho RT, Antas PR, Mengel J. Immunity and immune modulation in *Trypanosoma cruzi* infection. *Pathog Dis.* (2015) 73:ftv082. doi: 10.1093/femspd/ftv082
33. Savino W, Villa-Verde DM, Mendes-da-Cruz DA, Silva-Monteiro E, Perez AR, Aoki Mdel P, et al. Cytokines and cell adhesion receptors in the regulation of immunity to *Trypanosoma cruzi*. *Cytokine Growth Factor Rev.* (2007) 18:107–24. doi: 10.1016/j.cytogfr.2007.01.010
34. Holscher C, Mohrs M, Dai WJ, Kohler G, Ryffel B, Schaub GA, et al. Tumor necrosis factor alpha-mediated toxic shock in *Trypanosoma cruzi*-infected interleukin 10-deficient mice. *Infect Immun.* (2000) 68:4075–83. doi: 10.1128/IAI.68.7.4075-4083.2000
35. Hunter CA, Ellis-Neyes LA, Slifer T, Kanaly S, Grunig G, Fort M, et al. IL-10 is required to prevent immune hyperactivity during infection with *Trypanosoma cruzi*. *J Immunol.* (1997) 158:3311–6.
36. Abel LC, Rizzo LV, Ianni B, Albuquerque F, Bacal F, Carrara D, et al. Chronic Chagas' disease cardiomyopathy patients display an increased IFN-gamma response to *Trypanosoma cruzi* infection. *J Autoimmun.* (2001) 17:99–107. doi: 10.1006/jaut.2001.0523
37. Guedes PM, Gutierrez FR, Silva GK, Dellalibera-Joviliano R, Rodrigues GJ, Bendhack LM, et al. Deficient regulatory T cell activity and low frequency of IL-17-producing T cells correlate with the extent of cardiomyopathy in human Chagas' disease. *PLoS Negl Trop Dis.* (2012) 6:e1630. doi: 10.1371/journal.pntd.0001630
38. de Araujo FF, Correa-Oliveira R, Rocha MO, Chaves AT, Fiuza JA, Fares RC, et al. $Foxp3^+CD25$(high) $CD4^+$ regulatory T cells from indeterminate patients with Chagas disease can suppress the effector cells and cytokines and reveal altered correlations with disease severity. *Immunobiology* (2012) 217:768–77. doi: 10.1016/j.imbio.2012.04.008
39. de Araujo FF, Vitelli-Avelar DM, Teixeira-Carvalho A, Antas PR, Assis Silva Gomes J, Sathler-Avelar R, et al. Regulatory T cells phenotype in different clinical forms of Chagas' disease. *PLoS Negl Trop Dis.* (2011) 5:e992. doi: 10.1371/journal.pntd.0000992
40. Vitelli-Avelar DM, Sathler-Avelar R, Dias JC, Pascoal VP, Teixeira-Carvalho A, Lage PS, et al. Chagasic patients with indeterminate clinical form of the disease have high frequencies of circulating $CD3^+CD16$-$CD56^+$ natural killer T cells and $CD4^+CD25$High regulatory T lymphocytes. *Scand J Immunol.* (2005) 62:297–308. doi: 10.1111/j.1365-3083.2005.01668.x
41. Gonzalez FB, Villar SR, Fernandez Bussy R, Martin GH, Perol L, Manarin R, et al. Immunoendocrine dysbalance during uncontrolled *T. cruzi* infection is associated with the acquisition of a Th-1-like phenotype by Foxp3(+) T cells. *Brain Behav Immun.* (2015) 45:219–32. doi: 10.1016/j.bbi.2014.11.016
42. Mariano FS, Gutierrez FR, Pavanelli WR, Milanezi CM, Cavassani KA, Moreira AP, et al. The involvement of $CD4^+CD25^+$ T cells in the acute phase of *Trypanosoma cruzi* infection. *Microbes Infect.* (2008) 10:825–33. doi: 10.1016/j.micinf.2008.04.009
43. Kotner J, Tarleton R. Endogenous CD4(+) CD25(+) regulatory T cells have a limited role in the control of *Trypanosoma cruzi* infection in mice. *Infect Immun.* (2007) 75:861–9. doi: 10.1128/IAI.01500-06
44. Sales PA, Jr., Golgher D, Oliveira RV, Vieira V, Arantes RM, Lannes-Vieira J, et al. The regulatory $CD4^+CD25^+$ T cells have a limited role on pathogenesis of infection with *Trypanosoma cruzi*. *Microbes Infect.* (2008) 10:680–8. doi: 10.1016/j.micinf.2008.03.008
45. Bonney KM, Taylor JM, Thorp EB, Epting CL, Engman DM. Depletion of regulatory T cells decreases cardiac parasitosis and inflammation in experimental Chagas disease. *Parasitol Res.* (2015) 114:1167–78. doi: 10.1007/s00436-014-4300-3
46. Muller U, Steinhoff U, Reis LF, Hemmi S, Pavlovic J, Zinkernagel RM, et al. Functional role of type I and type II interferons in antiviral defense. *Science* (1994) 264:1918–21. doi: 10.1126/science.8009221
47. Stempin CC, Rojas Marquez JD, Ana Y, Cerban FM. GRAIL and Otubain-1 are Related to T Cell Hyporesponsiveness during *Trypanosoma cruzi* Infection. *PLoS Negl Trop Dis.* (2017) 11:e0005307. doi: 10.1371/journal.pntd.0005307
48. Piron M, Fisa R, Casamitjana N, Lopez-Chejade P, Puig L, Verges M, et al. Development of a real-time PCR assay for *Trypanosoma cruzi* detection in blood samples. *Acta Trop.* (2007) 103:195–200. doi: 10.1016/j.actatropica.2007.05.019
49. Thiault N, Darrigues J, Adoue V, Gros M, Binet B, Perals C, et al. Peripheral regulatory T lymphocytes recirculating to the thymus suppress the development of their precursors. *Nat Immunol.* (2015) 16:628–34. doi: 10.1038/ni.3150
50. Mukaka MM. A guide to appropriate use of Correlation coefficient in medical research. *Malawi Med J.* (2012) 24:69–71.
51. Hazra A, Gogtay N. Biostatistics series module 6: correlation and linear regression. *Indian J Dermatol.* (2016) 61:593–601. doi: 10.4103/0019-5154.193662
52. Schober P, Boer C, Schwarte LA. Correlation coefficients: appropriate use and interpretation. *Anesth Analg.* (2018) 126:1763–8. doi: 10.1213/ANE.0000000000002864
53. Sardinha LR, Mosca T, Elias RM, do Nascimento RS, Goncalves LA, Bucci DZ, et al. The liver plays a major role in clearance and destruction of blood trypomastigotes in *Trypanosoma cruzi* chronically infected mice. *PLoS Negl Trop Dis.* (2010) 4:e578. doi: 10.1371/journal.pntd.0000578
54. Lee HM, Bautista JL, Hsieh CS. Thymic and peripheral differentiation of regulatory T cells. *Adv Immunol.* (2011) 112:25–71. doi: 10.1016/B978-0-12-387827-4.00002-4
55. Nagajyothi F, Kuliawat R, Kusminski CM, Machado FS, Desruisseaux MS, Zhao D, et al. Alterations in glucose homeostasis in a murine model of Chagas disease. *Am J Pathol.* (2013) 182:886–94. doi: 10.1016/j.ajpath.2012.11.027
56. Liston A, Gray DH. Homeostatic control of regulatory T cell diversity. *Nat Rev Immunol.* (2014) 14:154–65. doi: 10.1038/nri3605
57. Belkaid Y, Tarbell K. Regulatory T cells in the control of host-microorganism interactions. *Annu Rev Immunol.* (2009) 27:551–89. doi: 10.1146/annurev.immunol.021908.132723
58. Lopes MF, da Veiga VF, Santos AR, Fonseca ME, DosReis GA. Activation-induced $CD4^+$ T cell death by apoptosis in experimental Chagas' disease. *J Immunol.* (1995) 154:744–52.
59. Gao W, Pereira MA. Interleukin-6 is required for parasite specific response and host resistance to *Trypanosoma cruzi*. *Int J Parasitol.* (2002) 32:167–70. doi: 10.1016/S0020-7519(01)00322-8
60. Paroli AF, Gonzalez PV, Diaz-Lujan C, Onofrio LI, Arocena A, Cano RC, et al. NLRP3 inflammasome and caspase-1/11 pathway orchestrate different outcomes in the host protection against *Trypanosoma cruzi* Acute infection. *Front Immunol.* (2018) 9:913. doi: 10.3389/fimmu.2018.00913
61. Korn T, Mitsdoerffer M, Croxford AL, Awasthi A, Dardalhon VA, Galileos G, et al. IL-6 controls Th17 immunity *in vivo* by inhibiting the conversion of conventional T cells into $Foxp3^+$ regulatory T cells. *Proc Natl Acad Sci USA.* (2008) 105:18460–5. doi: 10.1073/pnas.0809850105

62. Basu R, Whitley S, Bhaumik S, Zindl C, Schoeb T, Benveniste E, et al. IL-1 signaling modulates activation of STAT transcription factors to antagonize retinoic acid signaling and control the TH17 cell-iTreg cell balance. *Nat Immunol.* (2015) 16:286–95. doi: 10.1038/ni.3099
63. Vaena de Avalos S, Blader IJ, Fisher M, Boothroyd JC, Burleigh BA. Immediate/early response to *Trypanosoma cruzi* infection involves minimal modulation of host cell transcription. *J Biol Chem.* (2002) 277:639–44. doi: 10.1074/jbc.M109037200
64. Bouziat R, Hinterleitner R, Brown JJ, Stencel-Baerenwald JE, Ikizler M, Mayassi T, et al. Reovirus infection triggers inflammatory responses to dietary antigens and development of celiac disease. *Science* (2017) 356:44–50. doi: 10.1126/science.aah5298
65. Huehn J, Siegmund K, Lehmann JC, Siewert C, Haubold U, Feuerer M, et al. Developmental stage, phenotype, and migration distinguish naive- and effector/memory-like CD4$^+$ regulatory T cells. *J Exp Med.* (2004) 199:303–13. doi: 10.1084/jem.20031562
66. Tomura M, Honda T, Tanizaki H, Otsuka A, Egawa G, Tokura Y, et al. Activated regulatory T cells are the major T cell type emigrating from the skin during a cutaneous immune response in mice. *J Clin Invest.* (2010) 120:883–93. doi: 10.1172/JCI40926
67. Cretney E, Kallies A, Nutt SL. Differentiation and function of Foxp3(+) effector regulatory T cells. *Trends Immunol.* (2013) 34:74–80. doi: 10.1016/j.it.2012.11.002
68. Rosenblum MD, Way SS, Abbas AK. Regulatory T cell memory. *Nat Rev Immunol.* (2016) 16:90–101. doi: 10.1038/nri.2015.1
69. Campbell DJ, Koch MA. Phenotypical and functional specialization of FOXP3$^+$ regulatory T cells. *Nat Rev Immunol.* (2011) 11:119–30. doi: 10.1038/nri2916
70. Wang J, Huizinga TW, Toes RE. De novo generation and enhanced suppression of human CD4$^+$CD25$^+$ regulatory T cells by retinoic acid. *J Immunol.* (2009) 183:4119–26. doi: 10.4049/jimmunol.0901065
71. Lee W, Lee GR. Transcriptional regulation and development of regulatory T cells. *Exp Mol Med.* (2018) 50:e456. doi: 10.1038/emm.2017.313
72. Bedoya F, Cheng GS, Leibow A, Zakhary N, Weissler K, Garcia V, et al. Viral antigen induces differentiation of Foxp3$^+$ natural regulatory T cells in influenza virus-infected mice. *J Immunol.* (2013) 190:6115–25. doi: 10.4049/jimmunol.1203302
73. Shafiani S, Tucker-Heard G, Kariyone A, Takatsu K, Urdahl KB. Pathogen-specific regulatory T cells delay the arrival of effector T cells in the lung during early tuberculosis. *J Exp Med.* (2010) 207:1409–20. doi: 10.1084/jem.20091885
74. Shafiani S, Dinh C, Ertelt JM, Moguche AO, Siddiqui I, Smigiel KS, et al. Pathogen-specific Treg cells expand early during mycobacterium tuberculosis infection but are later eliminated in response to Interleukin-12. *Immunity* (2013) 38:1261–70. doi: 10.1016/j.immuni.2013.06.003
75. Tarleton RL. *Trypanosoma cruzi*-induced suppression of IL-2 production. II. Evidence for a role for suppressor cells. *J Immunol.* (1988) 140:2769–73.
76. Tarleton RL. *Trypanosoma cruzi*-induced suppression of IL-2 production. I. Evidence for the presence of IL-2-producing cells. *J Immunol.* (1988) 140:2763–8.
77. Briceno L, Mosca W. Defective production of interleukin 2 in patients with Chagas' disease. Purified IL-2 augments *in vitro* response in patients with chagasic cardiomyopathy. *Mem Inst Oswaldo Cruz* (1996) 91:601–7. doi: 10.1590/S0074-02761996000500011
78. Smigiel KS, Srivastava S, Stolley JM, Campbell DJ. Regulatory T-cell homeostasis: steady-state maintenance and modulation during inflammation. *Immunol Rev.* (2014) 259:40–59. doi: 10.1111/imr.12170
79. Tosello Boari J, Amezcua Vesely MC, Bermejo DA, Ramello MC, Montes CL, Cejas H, et al. IL-17RA Signaling reduces inflammationand mortality during *Trypanosoma cruzi* infection by recruiting suppressive IL-10-producing neutrophils. *PLoS Pathog.* (2012) 8:e1002658. doi: 10.1371/journal.ppat.1002658
80. Bermejo DA, Jackson SW, Gorosito-Serran M, Acosta-Rodriguez EV, Amezcua-Vesely MC, Sather BD, et al. *Trypanosoma cruzi* trans-sialidase initiates a program independent of the transcription factors RORgammat and Ahr that leads to IL-17 production by activated B cells. *Nat Immunol.* (2013) 14:514–22. doi: 10.1038/ni.2569
81. Singer BD, King LS, D'Alessio FR. Regulatory T cells as immunotherapy. *Front Immunol.* (2014) 5:46. doi: 10.3389/fimmu.2014.00046
82. Nguyen TL, Makhlouf NT, Anthony BA, Teague RM, DiPaolo RJ. *In vitro* induced regulatory T cells are unique from endogenous regulatory T cells and effective at suppressing late stages of ongoing autoimmunity. *PLoS ONE* (2014) 9:e104698. doi: 10.1371/journal.pone.0104698
83. Chappert P, Leboeuf M, Rameau P, Lalfer M, Desbois S, Liblau RS, et al. Antigen-specific Treg impair CD8(+) T-cell priming by blocking early T-cell expansion. *Eur J Immunol.* (2010) 40:339–50. doi: 10.1002/eji.200839107
84. Matheu MP, Othy S, Greenberg ML, Dong TX, Schuijs M, Deswarte K, et al. Imaging regulatory T cell dynamics and CTLA4-mediated suppression of T cell priming. *Nat Commun.* (2015) 6:6219. doi: 10.1038/ncomms7219
85. Zelinskyy G, Dietze KK, Husecken YP, Schimmer S, Nair S, Werner T, et al. The regulatory T-cell response during acute retroviral infection is locally defined and controls the magnitude and duration of the virus-specific cytotoxic T-cell response. *Blood* (2009) 114:3199–207. doi: 10.1182/blood-2009-03-208736
86. McNally A, Hill GR, Sparwasser T, Thomas R, Steptoe RJ. CD4$^+$CD25$^+$ regulatory T cells control CD8$^+$ T-cell effector differentiation by modulating IL-2 homeostasis. *Proc Natl Acad Sci USA.* (2011) 108:7529–34. doi: 10.1073/pnas.1103782108
87. Chen ML, Pittet MJ, Gorelik L, Flavell RA, Weissleder R, von Boehmer H, et al. Regulatory T cells suppress tumor-specific CD8 T cell cytotoxicity through TGF-beta signals *in vivo*. *Proc Natl Acad Sci USA.* (2005) 102:419–24. doi: 10.1073/pnas.0408197102
88. Zelinskyy G, Werner T, Dittmer U. Natural regulatory T cells inhibit production of cytotoxic molecules in CD8(+) T cells during low-level Friend retrovirus infection. *Retrovirology* (2013) 10:109. doi: 10.1186/1742-4690-10-109
89. Penaloza-MacMaster P, Kamphorst AO, Wieland A, Araki K, Iyer SS, West EE, et al. Interplay between regulatory T cells and PD-1 in modulating T cell exhaustion and viral control during chronic LCMV infection. *J Exp Med.* (2014) 211:1905–18. doi: 10.1084/jem.20132577

Conflict of Interest Statement: The authors declare that the research was conducted in the absence of any commercial or financial relationships that could be construed as a potential conflict of interest.

The reviewer DA and handling editor declared their shared affiliation at time of review.

Copyright © 2018 Araujo Furlan, Tosello Boari, Rodriguez, Canale, Fiocca Vernengo, Boccardo, Beccaria, Adoue, Joffre, Gruppi, Montes and Acosta Rodriguez. This is an open-access article distributed under the terms of the Creative Commons Attribution License (CC BY). The use, distribution or reproduction in other forums is permitted, provided the original author(s) and the copyright owner(s) are credited and that the original publication in this journal is cited, in accordance with accepted academic practice. No use, distribution or reproduction is permitted which does not comply with these terms.

frontiers in Immunology

ORIGINAL RESEARCH
published: 08 November 2018
doi: 10.3389/fimmu.2018.02594

CCL22-Producing Resident Macrophages Enhance T Cell Response in Sjögren's Syndrome

*Aya Ushio[1], Rieko Arakaki[1], Kunihiro Otsuka[1], Akiko Yamada[1], Takaaki Tsunematsu[2], Yasusei Kudo[1], Keiko Aota[3], Masayuki Azuma[3] and Naozumi Ishimaru[1]**

[1] Department of Oral Molecular Pathology, Tokushima University Graduate School of Biomedical Sciences, Tokushima, Japan, [2] Department of Pathology and Laboratory Medicine, Tokushima University Graduate School of Biomedical Sciences, Tokushima, Japan, [3] Department of Oral Medicine, Tokushima University Graduate School of Biomedical Sciences, Tokushima, Japan

Macrophages (MΦs) are critical regulators of immune response and serve as a link between innate and acquired immunity. The precise mechanism of involvement of tissue-resident MΦs in the pathogenesis of autoimmune diseases is not clear. Here, using a murine model for Sjögren's syndrome (SS), we investigated the role of tissue-resident MΦs in the onset and development of autoimmunity. Two unique populations of $CD11b^{high}$ and $CD11b^{low}$ resident MΦs were observed in the target tissue of the SS model. Comprehensive gene expression analysis of chemokines revealed effective production of CCL22 by the $CD11b^{high}$ MΦs. CCL22 upregulated the migratory activity of $CD4^+$ T cells by increasing CCR4, a receptor of CCL22, on T cells in the SS model. In addition, CCL22 enhanced IFN-γ production of T cells of the SS model, thereby suggesting that CCL22 may impair the local immune tolerance in the target organ of the SS model. Moreover, administration of anti-CCL22 antibody suppressed autoimmune lesions in the SS model. Finally, histopathological analysis revealed numerous CCL22-producing MΦs in the minor salivary gland tissue specimens of the SS patients. CCL22-producing tissue-resident MΦs may control autoimmune lesions by enhancing T cell response in the SS model. These results suggest that specific chemokines and their receptors may serve as novel therapeutic or diagnostic targets for SS.

Keywords: autoimmunity, tissue-resident macrophage, chemokine, salivary gland, Sjögren's syndrome, T cell response

OPEN ACCESS

Edited by:
Maria Florencia Quiroga, Consejo Nacional de Investigaciones Científicas y Técnicas (CONICET), Argentina

Reviewed by:
Nathalie Arbour, Université de Montréal, Canada
Ruben Dario Motrich, Consejo Nacional de Investigaciones Científicas y Técnicas (CONICET), Argentina

***Correspondence:**
Naozumi Ishimaru
ishimaru.n@tokushima-u.ac.jp

Specialty section:
This article was submitted to Autoimmune and Autoinflammatory Disorders, a section of the journal Frontiers in Immunology

Received: *18 June 2018*
Accepted: *22 October 2018*
Published: *08 November 2018*

Citation:
Ushio A, Arakaki R, Otsuka K, Yamada A, Tsunematsu T, Kudo Y, Aota K, Azuma M and Ishimaru N (2018) CCL22-Producing Resident Macrophages Enhance T Cell Response in Sjögren's Syndrome. Front. Immunol. 9:2594. doi: 10.3389/fimmu.2018.02594

INTRODUCTION

Macrophages (MΦs) differentiate from bone marrow-derived monocytes or tissue-resident cells derived from yolk sac or fetal liver. These cells tend to exhibit distinct tissue-specific phenotypes, such as histiocytes in connective tissues, Kupffer cells in the liver, microglia in the central nervous system and various specialized macrophages in the alveolar, peritoneal, and synovial tissues (1, 2). Tissue-resident MΦs represent a vital component of the innate immunity system and function as phagocytic cells that engulf and digest cellular debris, foreign substances, microbes, and pathogens (3). They also secrete cytokines and chemokines that modulate the activities of other immune cells in inflammatory lesions (3). Besides phagocytosis and immune signaling, in conjunction with DCs, MΦs present antigens to T cells: this acts as a link between innate and acquired immunity (3).

MΦs also contribute to the recovery or remodeling of injured tissues via promotion of angiogenesis or fibrosis (4, 5). However, the multilateral roles of tissue-resident MΦs in various inflammatory disorders are unclear.

Classically activated (M1) MΦs produce pro-inflammatory cytokines, such as interleukin (IL)-1β, interferon (IFN)-γ, and tumor necrosis factor (TNF)-α (1, 6). Alternatively activated (M2) MΦs produce anti-inflammatory cytokines, such as IL-10 and IL-4, with a specific profile that depends on the M2 MΦ subset (M2a, b, and c) (1, 7). MΦs are involved in inflammatory tissue damage associated with autoimmune response (8). In addition, MΦs also support tissue repair and restoration of immune homeostasis (9, 10). Thus, MΦs play a key role in various physiological and pathological responses as classically activated MΦs, wound-healing MΦs, and regulatory MΦs. Although tissue-resident MΦs are also considered as immune cells and have a variety of functions, the precise role of tissue-resident MΦs in autoimmune response is obscure.

Sjögren's syndrome (SS) is a chronic autoimmune disease that affects exocrine glands, such as salivary and lacrimal glands; SS also causes systemic autoimmune lesions (11, 12). A variety of mononuclear cell populations that infiltrate the salivary gland tissues were observed in patients with SS (13, 14). Among these, infiltration of T cells, B cells, DCs, and MΦs is correlated with lesion severity (15). SS is triggered by T cell-mediated autoimmune response; however, other immune cells also contribute to the onset or development of SS, including MΦs (16–18). MΦs are observed in the autoimmune lesions of salivary gland tissues of patients with SS (19). Moreover, elevated expression of MΦ-derived molecules, such as chitinase-3-like protein 1 and chitinase 1, is associated with increased severity of SS lesions, thereby indicating the involvement of MΦ in the pathogenesis of SS (20). Furthermore, several chemokines secreted from MΦs in the salivary glands of patients and animal models with SS contribute to the onset or development of SS (21, 22). However, the molecular or cellular mechanism of the pathogenesis of SS through the tissue-resident MΦs in the target organ has not been defined.

Here, using a mouse model of SS, we investigated the association of resident MΦs in the target organs of SS with the onset and development of autoimmune lesions. In particular, we evaluated the precise contribution of MΦs to T cell response in a SS model and patients with SS. The findings of the current study may help us comprehend a novel pathogenic mechanism of autoimmunity and may also help establish potential new treatments for autoimmunity.

MATERIALS AND METHODS

Mice

Female NFS/N mice carrying the mutant *sld* were bred and maintained in a specific pathogen-free mouse colony in the animal facility at Tokushima University (Tokushima, Japan). Neonatal thymectomy was performed on day 3 after birth to generate the SS model mice. Control mice used in this study were sham (non)-thymectomized NFS/*sld* mice that exhibit no inflammatory lesions in the salivary and lacrimal glands. In addition, we confirmed that the phenotypes and functions of immune cells of control mice showed no abnormality, compared with those of age- and sex-matched C57BL/6 mice. This study was conducted according to the Fundamental Guidelines for Proper Conduct of Animal Experiment and Related Activities in Academic Research Institutions under the jurisdiction of the Ministry of Education, Culture, Sports, Science and Technology of Japan. The protocol was approved by the Committee on Animal Experiments of Tokushima University and Biological Safety Research Center, Japan (Permit Number: T-27-7). All experiments were performed after administration of anesthesia, and all efforts were made to minimize suffering.

Cell Isolation

For the isolation of MΦ from the salivary gland, bilateral whole salivary gland lobes were minced into 1–3 mm pieces and were digested with collagenase (1 mg/mL, Wako), hyarulonidase (1 mg/mL, SIGMA-ALDRICH), and DNase (10 ng/mL, Roche) in Dulbecco's modified Eagle's medium (DMEM) containing 10% fetal calf serum at 37°C for 40 min using gentleMACS Dissociators (Miltenyi Biotec). Subsequently, mononuclear cells were enriched using a Histopaque-1083 (Merck) from a single-cell suspension of salivary gland tissue. Mononuclear cells were labeled with anti-CD45.2, F4/80, CD11b, CD3, and CD19 antibodies (eBioscience); subsequently, $CD11b^{high}$ $F4/80^{+}$ MΦs and $CD11b^{low}$ $F4/80^{+}$ MΦs were isolated using a cell sorter (JSAN JR Swift, Bay Bioscience). Splenocytes and cervical lymph node (cLN) cells were homogenated in DMEM containing 2% FBS using gentleMACS Dissociators (Miltenyi Biotec). Using 0.83% ammonium chloride, red blood cells were removed from the spleen cells. Splenic $CD4^{+}$ T cells were obtained by negative selection using the EasySep mouse $CD4^{+}$ T cell Isolation Kit (STEMCELL Technologies). Flow cytometric analysis showed that $CD4^{+}$ cells accounted for >90% of the isolated cells. In addition, the viability of the isolated cells was checked by cell counter (CYTORECON, GE Healthcare) using trypan blue staining. The cell number was determined as the total absolute number of lymphocytes per each organ by cell counter (CYTORECON) using trypan blue staining; subsequently, the proportion of the suspended cells was analyzed by flow cytometry. The absolute number of T cells or macrophages was calculated using the data pertaining to total cell number and the proportion. As for the salivary gland, we used bilateral lobes to determine the cell number and the proportion of immune cells. As for splenocytes and cervical lymph node cells, the whole spleen and bilateral cervical lymph nodes per mouse were used to determine the cell number and the proportion.

Flow Cytometric Analysis

Immune cells were stained using antibodies against FITC-conjugated anti-mouse CD206 (BioLegend, C068C2) and CD11c (eBioscience, N418) mAbs, PE-conjugated anti-mouse MHC class II (Miltenyi Biotec, REA478), CD86 (BD Bioscience, GL1), CD204 (eBioscience, M204PA), CCR2, CX3CR1, CCR4 (BioLegend, SA203G11, SA011F11, and 2G12), PE-Cy5.5-conjugated anti-mouse CD3 and CD19 (TONBO Biosciences, 145-2C11, and 6D5) and 7-Aminoactinomycin D (7-AAD)

staining solution (TOMBO Biosciences), PE-Cy7-conjugated anti-mouse CD11b (TONBO Biosciences, M1/70), APC-conjugated anti-mouse F4/80 and CD36 (BioLegend, BM8 and HM36), and APC-Cy7-conjugated anti-mouse CD45.2 (TOMBO, 104) mAbs. For detecting intracellular CCL22 expression, rabbit anti-CCL22/MDC (abcam, rabbit monoclonal IgG, EPR1362) Ab, and Alexa Fluor 568 goat anti-rabbit IgG (Invitrogen) were used. A FACScant flow cytometer (BD Biosciences) was used to identify the cell populations according to expression profile. Viable cells were checked by gating on side scatter (SSC)/forward scatter (FSC), FSC-H/FSC-A, 7AAD, CD45.2, and CD4. We used 5×10^5 cells as a sample for the analysis. Data were analyzed using the FlowJo FACS Analysis software (Tree Star Inc.).

Phagocytosis Assay

Phagocytosis was assessed for using the Phagocytosis Assay Kit (IgG FITC, Cayman Chemical). Mononuclear cells from the salivary glands provided as previously described were cultured in DMEM containing 10% FBS at 37°C and were washed with PBS 24 h later to remove unbounded cells. Adherent cells were incubated with the opsonized beads for 2 h at 37°C or at 4°C for controls; this was followed by washing with PBS. The phagocytic activity of F4/80$^+$ CD11b^{high} and F4/80$^+$ CD11b^{low} MΦs was analyzed using flow cytometry.

RNA Extraction

Total RNA was isolated from the purified macrophages and cultured cells using the RNeasy Plus Mini Kit (Qiagen) with a gDNA eliminator column treatment step. Total RNA was extracted from the salivary glands, lung, spleen, and liver tissues using Isogen (FUJIFILM Wako Pure Chemical). Total RNA was then reverse-transcribed into cDNA using the PrimeScript II reverse transcriptase (Takara Bio Inc).

Quantitative Reverse Transcription-Polymerase Chain Reaction (qRT-PCR)

Expression levels of mRNAs encoding CCL22, CCR4, IFN-γ, IL-4, IL-17, and β-actin were determined using a 7300 real time PCR system (Applied Biosystems) with TB Green Premix Ex Taq II (Takara Bio). PCR was performed followed by 40 cycles for 10s at 95°C and for 15 s at 60°C. The primer sequences used were as follows: CCL22: forward, 5′-TCATGGCTACCCTGC GTGTC-3′, and reverse, 5′-CCTTCACTAAACGTGGCAGAG-3′, CCR4: forward, 5′-GGCTACTACGCCGCCGAC-3′, and reverse, 5′-TACCAAAACAGCATGATGCC-3′, IFN-γ: forward, 5′-AGCGGCTGACTGAACTCAGATTGTA-3′, and reverse, 5′-GTCACAGTTTTCAGCTGTATAGGG-3′, IL-4: forward, 5′-TCTCATGGAGCTGCAGAGACTCT-3′, and reverse, 5′-TCC AGGAAGTCTTTCAGTGATGTG-3′, IL-17: forward, 5′-AGT GTTTCCTCTACCCAGCAC-3′, and reverse, 5′-GAAAACCGC CACCGCTTAC-3′, β-actin: forward, 5′-GTGGGCCGCTCT AGGCACCA-3′, and reverse, 5′-CGGTTGGCCTTAGGGTTC AGGGGG-3′. Relative mRNA expression of each transcript was normalized against β-actin mRNA.

Histological Analysis

Salivary gland tissues were fixed with 10% phosphate-buffered formaldehyde (pH 7.2), and were prepared for histological examination. Sections (4 μm) were stained with hematoxylin and eosin (H&E).

Immunohistochemistry

Tissue sections (6 μm) were deparaffinized in xylenes and were rehydrated by passage through serial dilutions of ethanol in distilled water. Heat-induced antigen retrieval was performed in Immunoactive (Matsunami Glass Ind. Ltd) with microwave thrice for 5 min. Anti-mouse F4/80 antibody (eBioscience), anti-human CCL22 (abcam), and anti-mouse CCL22 (abcam) antibody were applied to the sections; the sections were then incubated overnight at 4°C. After washing with PBS, the sections were incubated with biotinylated second antibody and horseradish peroxidase (HRP)-conjugated streptavidin solution (DAKO). HRP reacted with the 3,3′-diaminobenzidine (DAB) substrate using the Histofine DAB substrate kit (Nichirei Biosciences Inc.). The sections were counterstained with hematoxylin.

Confocal Analysis

Frozen sections (6 μm) of salivary gland tissues were fixed with cold acetone, blocked with 10% goat serum (DAKO), and then stained with a rabbit monoclonal antibody against CCL22/MDC (abcam), FITC-conjugated anti-mouse F4/80 (BioRad), rat monoclonal antibody against anti-EpCAM (eBioscience, G8.8), anti-CD3 (eBioscience, 1.45-2C11), anti-CD19 (eBioscience, eBio1D3), and biotinylated anti-CD11c (Biolegend, N418) antibodies. After washing with PBS, Alexa Fluor 568-conjugated anti-rabbit IgG (Invitrogen) and Alexa Fluor 488-conjugated anti-fluorescein Green goat IgG fraction (Invitrogen), or Alexa Fluor 488-conjugated anti-rat IgG (Invitrogen), or Alexa Fluor 488-conjugated streptavidin (Invitrogen) were used as secondary antibodies. Nuclear DNA was stained with 4′,6-Diamdino-2-phenylindole dihydrochloride (DAPI) (Invitrogen). In addition, the paraffin-embedded sections from SS patients and controls were stained with anti-CD68 (DAKO, Klon EBM11), anti-Keratin (DAKO, AE1/AE3), anti-CD3 (DAKO, F7.2.38), anti-CD19 (DAKO, LE-CD19), anti-S100 (abcam, 4C4.9), and anti-CCL22 Abs (abcam). The sections were examined using a PASCAL confocal laser-scanning microscope (LSM: Carl Zeiss) at 400× magnification. LSM image browser version 3.5 (Carl Zeiss) was used for image acquisition.

Gene-Expression Analysis With PCR Array

Chemokine-related gene expression of sorted CD11b^{low} and CD11b^{high} sMΦs were analyzed using PCR array. Total RNA was reverse-transcribed to cDNAs using the RT^2 First Strand Kit (Qiagen). The cDNA was applied to RT2 Profiler PCR array (PAMM-022ZE-1) plates to detect the expression of genes related to chemokines. Real-time PCR reactions were performed on a 7900HT Real-Time PCR System. (Applied Biosystems). Raw data were extracted and analyzed according to the Qiagen RT^2 Profiler PCR Array Data Analysis web

portal. Gene expression levels were calculated using the ΔΔCt method; the relative gene expression levels were normalized using four house-keeping genes (*Actb, B2m, Gapdh,* and *Gusb*).

Chemotactic Migration Assay and *in vitro* Culture of CD4$^+$ T Cell With CCL22

Splenic CD4$^+$ T cell were cultured for 5 days in RPMI 1640 containing 10% FBS with Dynabeads mouse T-activator CD3/CD28 (Invitrogen) at bead/cells ratio of 1:1 and 30 U/mL of rIL-2 (eBioscience). After serum starvation in RPMI 1640 medium for 3 h , splenic CD4$^+$ T cells were seeded (1.0×10^6 cells in 400 μL) in Millicell Culture Plates Inserts (5.0-μm pore size, Merck Millipore). 600 μl of RPMI 1640 containing 0.1% BSA containing CCL22 (200 ng/mL; R&D Systems Inc.) was added to the lower chamber. The cells were cultured for 3 h at 37°C and then the numbers of migrated cells were counted by cell counter (CYTORECON, GE Healthcare UK).

CD4$^+$ T cells purified from the spleen, cLNs, and salivary glands in SS model mice were cultured with CCL22 for 6 h. Then the mRNA of the T cells was purified for analysis of cytokine gene expression.

Analysis of Intracellular Cytokine Expression

CD4$^+$ T cells (1×10^6/well) isolated form spleen of control and SS model mice, or T cells (2×10^5/well) isolated form salivary gland tissues of SS model mice were stimulated with Dynabeads mouse T-activator CD3/CD28 (Invitrogen) at bead/cell ratio of 1:4 and CCL22 (200 ng/mL) for 48 h, and were then cultured with phorbol myristate acetate (PMA; 50 ng/mL, Sigma-Aldrich, St. Louis, MO) and ionomycin (IM; 1 μg/mL, Sigma-Aldrich) in the presence of Brefeldin A (eBioscience) for the last 6 h. After washing, cells were stained with an anti-CD4 mAb, fixed in fixation/permeabilization solution (eBioscience); permeabilized in permeabilization buffer (eBioscience); and stained with anti-IFN-γ (eBioscience, XMC1.2), IL-4 (TONBO, 11B11), and IL-17A (eBioscience, TC11-18H10.1).

Analysis of Cytokine Levels

CD4$^+$ T cells isolated from salivary gland tissues of SS model mice were cultured with or without CCL22 (200 ng/mL) in the presence of Dynabeads mouse T-activator CD3/CD28 (Invitrogen) at bead/cell ratio of 1:4 for 48 h and subsequently cultured with PMA (50 ng/mL, Sigma-Aldrich) and IM (1 μg/mL, Sigma-Aldrich) for the last 6 h. Cytokine levels, including IFN-γ, IL-4, and IL-17, in the supernatant were measured using a Cytokine 20-Plex Mouse Panel Luminex assay kit (Invitrogen) according to the manufacturer's instructions.

Administration of Anti-CCL22 Antibody

Four μg of goat anti-CCL22 polyclonal Ab (R&D System) or control polyclonal goat IgG Ab (Santa Cruz Biotechnology, sc-3887) was intravenously injected into the SS model mice aged 8 weeks on alternate days for 2 weeks. The mice were examined at 10 weeks of age.

Human Subjects

This study was approved by the Institutional Review Board of the Tokushima University Hospital, Japan (No. 2802). All patients with SS were diagnosed according the criteria for diagnosis of SS by the Japanese Ministry of Health and the American College of Rheumatology. Labial salivary gland (LSG) samples were obtained from patients with SS and controls. The degree of lymphocytic infiltration in the specimens was determined using a modification of the system originally introduced by Greenspan (23). The results are classified into five grades in a blind manner by three pathologists: Grade 0 = the absence of lymphocytes and plasma cells per 4 mm^2 in LSGs, Grade 1 = mild infiltration of lymphocytes and plasma cells per 4 mm^2 in LSGs, Grade 2 = a moderate infiltration or less than one focus per 4 mm^2 in LSGs, Grade 3 = a single focus per 4 mm^2 in LSGs, and Grade 4 = more than one focus per 4 mm^2 in LSGs. One focus refers to an aggregate of ≧50 mononuclear cells, including lymphocytes, histiocytes, and plasma cells around the ductal structure. Five to seven samples per group were used for analysis. Control samples were collected from non-inflamed tissues of patients with mucous cyst or other oral disorders.

Statistical Analysis

Differences between individual groups were determined using two-tailed Student's *t*-test or between more than two groups using one-way ANOVA with Turkey's multiple comparison post-test. $p < 0.05$ was considered statistically significant. Power calculations were performed before the beginning of the experiments to determine the sample size for experiments using human samples or animals. Data are presented as mean ± standard error of mean (SEM).

Data Availability

The PCR array data are available from the Gene Expression Omnibus database under accession number GSE110816.

RESULTS

MΦs in the Salivary Gland of the SS Model Mouse

We have established a mouse model of SS wherein NFS/*sld* mice are thymectomized on day 3 after birth (24, 25). The autoimmune lesions in the salivary and lacrimal glands are observed from 6 weeks of age (24). The main subset of immune cells infiltrated in the target organ of the SS model mice at 6 weeks of age is CD4$^+$ T cells; small populations of CD8$^+$ T cells, B cells, macrophages (MΦs), and dendritic cells are also observed (26). The proportion of infiltrated immune cells in the target organ changes with age. At 8 weeks of age, the autoimmune lesions are observed in almost 100% of the SS model mice (24). Female mice exhibit faster onset of disease and more severe inflammatory lesions compared with male mice. In addition, autoantibodies such as anti-SSA, anti-SSB, and anti-α-fodrin were detected in the SS model (24, 25). We compared the distribution of MΦs in the salivary glands (sMΦs) of control and SS model mice. Immunohistochemical analysis revealed sporadic F4/80$^+$ MΦs around ductal, acinar cells and small vessels in the control mice

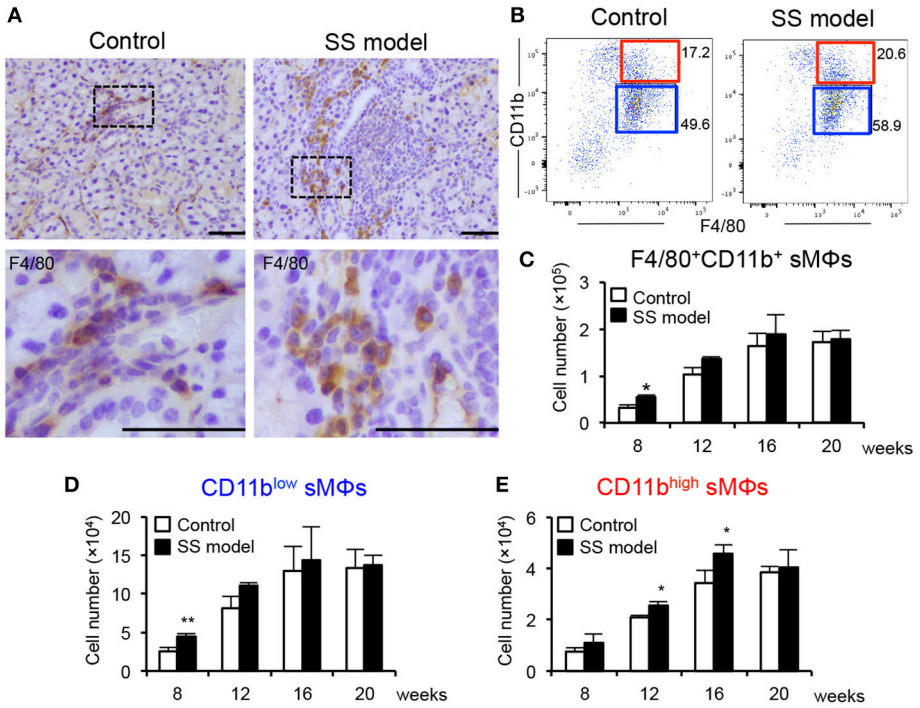

FIGURE 1 | Salivary gland macrophages (sMΦs) of the SS model mice. **(A)** Immunohistochemical analysis of F4/80$^+$ macrophages in the salivary gland sections obtained from the controls and SS models at 8 weeks of age. Photos are representative of 5 mice in each group. Scale bar: 50 μm **(B)** CD11b^{high} and CD11b^{low} F4/80$^+$ sMΦs in the controls and SS models. **(C)** Total number of F4/80$^+$ sMΦs in the controls and SS models from 8 to 20 weeks of age. Bilateral whole salivary gland lobes per mouse were minced and enzymatically digested. Mononuclear cells were enriched using a Histopaque-1083. Cell number was determined by cell counter using trypan blue staining and flow cytometer with antibodies for specific markers. **(D)** Number of CD11b^{low} F4/80$^+$ sMΦs in the controls and SS models from 8 to 20 weeks of age. $^{**}p < 0.005$ by Student's *t*-test. **(E)** CD11b^{high} F4/80$^+$ sMΦs in the controls and SS models from 8 to 20 weeks of age. Data are presented as the mean ± SEM. $^{*}p < 0.05$ by Student's *t*-test. $n = 5$–10 **(C–E)**.

(**Figure 1A**). By contrast, many F4/80$^+$ MΦs were observed surrounding the autoimmune lesions in the SS model mice at 8 weeks of age (**Figure 1A**).

Next, the surface markers on sMΦs were analyzed using flow cytometry. CD45.2$^+$ CD3$^-$ CD19$^-$-gated monocytes (**Supplemental Figure 1**) were examined for CD11b and F4/80 expression (**Figure 1B**). Two subsets that displayed CD11b^{high} F4/80$^+$ and CD11b^{low} F4/80$^+$ MΦs were detected in the salivary glands (**Figure 1B**). These two subsets were evaluated using control and SS model mice from 8 to 20 weeks of age. At 8 weeks of age, the number of F4/80$^+$ CD11b$^+$ sMΦs in the SS model mice was significantly higher than that in control mice (**Figure 1C**). Although the cell numbers in both the control and SS model mice increased with age, there was no difference in the number between control and SS model from 12 to 20 weeks of age (**Figure 1C**). At 8 weeks of age, the number of CD11b^{low} F4/80$^+$ sMΦs in the SS model mice was significantly higher than that in the control mice; however, no changes were observed between the control and SS model mice from 12 to 20 weeks of age (**Figure 1D**). In contrast, the number of CD11b^{high} F4/80$^+$ sMΦs in the SS model mice aged between 12 and 16 weeks was significantly higher than that in the control mice (**Figure 1E**). At 20 weeks, there was no difference in the number of CD11b^{high} F4/80$^+$ sMΦs between control and SS model mice (**Figure 1E**). These findings indicate the existence of CD11b^{high} and CD11b^{low} F4/80$^+$ sMΦ subsets; these two subsets may play a role in the onset or development of autoimmune lesions in the target organs of SS model mice.

Phenotype and Function of Two MΦ Subsets in Salivary Glands

To define the difference between the cell surface phenotypes of the two subsets in the salivary glands, key MΦ markers were analyzed using flow cytometry. No significant differences were observed between the control and SS model mice at 12 weeks of age with respect to any of the markers of two subsets (**Figure 2A**). Among M1 MΦ markers, including CCR2, MHC class II, CD11c, and CD86, the expressions of MHC class II, CD11c, and CD86 on CD11b^{high} F4/80$^+$ sMΦs were higher than those on CD11b^{low} F4/80$^+$ sMΦs (**Figure 2A**). The expression pattern of CCR2 and CX3CR1 expression on CD11b^{high} F4/80$^+$ sMΦs suggested that a fraction of these cells carried the chemokine receptor including CCR2 or CX3CR1, whereas the other fraction did not (**Figures 2A,B**). Expression of CD206 (a M2 and tissue-resident MΦ marker) on CD11b^{high}F4/80$^+$ sMΦs was enhanced compared with that on CD11b^{low}F4/80$^+$ sMΦs (**Figure 2B**). In addition, the expressions of CD204 and CD36 (scavenger receptors) on CD11b^{high} F4/80$^+$ sMΦs in the SS

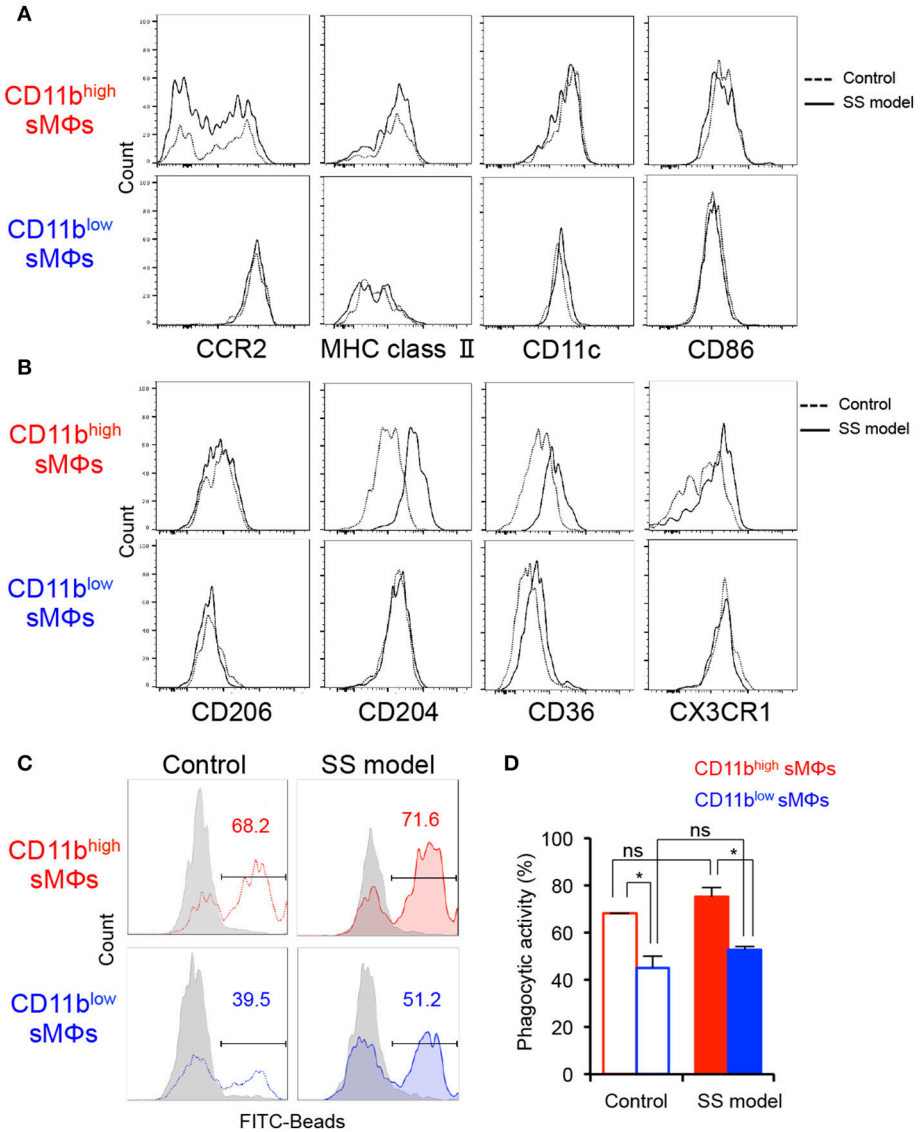

FIGURE 2 | Phenotypes and functionality of tissue-resident MΦs in salivary glands of controls and SS models. **(A,B)** Key surface markers on CD11b^{high} and CD11b^{low} sMΦs of control and SS model mice were detected using flow cytometry. Data are representative of 5 mice in each group at 12 weeks of age. **(C)** Phagocytic activity of CD11b^{high} and CD11b^{low} sMΦs of control and SS model mice at 12 weeks of age was determined by *in vitro* assay with FITC-conjugated beads. Data are representative of three independent experiments. Gray shadow: 4°C culture. **(D)** Phagocytic activity is shown as mean ± SEM. $n = 4$–6 per group. $^*p < 0.05$ by Student's *t*-test.

model were higher than the control mice (**Figure 2B**). These findings indicate that CD11b^{low} F4/80$^+$ sMΦs are M1-like MΦ whereas CD11b^{high} F4/80$^+$ sMΦs are similar to the phenotype of M2-like and tissue resident-like MΦs. However, it is possible that the sMΦs may differentiate into the phenotype or function independent of their differentiation into M1 and M2 MΦs.

To evaluate the *in vitro* phagocytic activity of the two subsets, sMΦs of the control and SS model mice were analyzed using FITC-labeled latex beads. With respect to the phagocytic activity of CD11^{high} F4/80$^+$ sMΦs, no significant differences were observed between the control and SS model mice (**Figures 2C,D**). There was no difference in the phagocytic activity of CD11b^{low} F4/80$^+$ sMΦs between the SS model and control mice (**Figures 2C,D**). Contrarily, in both control and SS model mice, the phagocytic activity of CD11^{high} F4/80$^+$ sMΦs was significantly higher than that of the CD11b^{low} F4/80$^+$ sMΦs (**Figures 2C,D**). These findings indicate that the two subsets of MΦs in the salivary gland are functionally distinct.

Chemokine Expression of CD11b^{high} F4/80$^+$ sMΦs in the SS Model Mice

Next, to define the role of the two subsets of sMΦs in the formation of autoimmune lesions, we focused on chemokine

gene expression of sMΦs of the SS model mice. Using PCR-array, we comprehensively compared chemokine mRNA gene expression between CD11b^{high} and CD11b^{low} F4/80^{+} sMΦs in the SS model mice (**Figure 3A**). Relative to that of CD11b^{low} sMΦs, over 50-fold increase was observed in the mRNA expression of CD11b^{high} sMΦs; this increase was observed in several genes, such as *CCL7*, *CXCL2*, *CCL6*, *CCL8*, *CXCL13*, and *CCL22* (**Figure 3B**). Among these, *CCL22* mRNA expression level of CD11b^{high} sMΦs was over 150-times higher than that of CD11b^{low} sMΦs (**Figure 3B**). In addition, quantitative RT-PCR assay revealed that *CCL22* mRNA level was significantly higher in salivary gland tissues of the SS model mice than of the control mice (**Figure 3C**). Moreover, the *CCL22* mRNA level was also significantly higher in lung tissues of the SS model mice than of the control mice (**Figure 3C**). In addition, intracellular flow cytometric analysis revealed significantly higher expression of CCL22 in the sMΦs in the SS model mice than in the control mice (**Figure 3D**). Furthermore, CD11b^{high} F4/80^{+} but not CD11b^{low} F4/80^{+} sMΦs strongly expressed CCL22 in the SS model mice (**Figure 3E**). Moreover, CCL22-producing F4/80^{+} sMΦs were observed in the SS model mice by confocal microscopic analysis (**Figure 3F**). By contrast, confocal microscopic analysis indicated that EpCAM^{+} epithelial cells, CD3^{+} T cells, CD19^{+} B cells, and CD11c^{+} DCs did not express CCL22 (**Figure 3G**). Immunohistochemical analysis showed that interstitial cells such as fibroblasts, endothelial cells, and nerve cells did not also express CCL22 (**Figure 3H**). The results suggest that CCL22-producing sMΦs may play a potent role in the pathogenesis of SS.

Contribution of CCL22 to Migration and Cytokine Production of T Cells

We evaluated the expression of CCR4 (a receptor of CCL22) in the lymphoid organs and the target organs of control and the SS model mice. The expression level of *CCR4* mRNA was significantly higher in the salivary glands of the SS model mice than of the control mice (**Figure 4A**). The expression in the salivary glands of SS model mice was considerably higher than that of the spleen (Sp), lung, and liver (**Figure 4A**). Furthermore, the expression of CCR4 on CD4^{+} T cells in spleen, cervical lymph node (cLN), and salivary glands was assessed using flow cytometry. The proportion of CCR4^{+} CD4^{+} T cells was significantly higher in the salivary glands than in the spleen and cLN of the SS model mice (**Figure 4B**). There was no significant difference in the proportion of CCR4^{+} CD4^{+} T cells between spleen and cLN in control mice (**Figure 4B**). We analyzed the mRNA expressions of the other chemokine receptors, such as *CXCR3A*, *CCR3*, and *CX3CR1* mRNA in the salivary gland tissues of control and SS model mice. *CXCR3A* mRNA expression in the salivary gland tissues from SS model mice was significantly higher than that in the salivary gland tissues from control mice (**Supplemental Figure 2A**). In addition to CXCR4, other chemokine receptors may affect the pathogenesis of SS. Next, an *in vitro* migration assay was performed using CD4^{+} T cells purified from spleen cells to evaluate the migratory activity of T cells toward CCL22. The migratory activity of CD4^{+} T cells purified from the spleen of the SS model mice was significantly higher than that of CD4^{+} T cells purified from the spleen of the control mice (**Figure 4C**, **Supplemental Figure 2B**). These findings indicate that T cell migration is controlled by CCL22 in the SS model mice.

CCL22 also plays a key role in T cell differentiation in addition to T cell migratory activity (27). In this SS mouse model, Th1 cells that produce IFN-γ contribute to the pathogenesis of autoimmune lesions in the target organ (24) (**Supplemental Figure 3A**). Splenic CD4^{+} T cells from the control and SS model mice were cultured with CCL22 for 6 h; mRNA expression of cytokines, including *IFN-γ*, *IL-4*, and *IL-17*, was then determined by qRT-PCR. IFN-γ mRNA expression of CD4^{+} T cells purified from the spleen of the SS model mice was significantly enhanced in response to CCL22 (**Figure 4D**). *IL-17* mRNA of splenic CD4^{+} T cells in the control mice was significantly enhanced in response to CCL22, whereas no change was observed in *IFN-γ* and *IL-4* mRNA (**Supplemental Figure 3B**). Further, besides up-regulated *IFN-γ* mRNA, *IL-17* mRNA of CD4^{+} T cells from the cLN in the SS model mice was significantly increased in response to CCL22 (**Figure 4D**). Finally, mRNA expressions of all cytokines in CD4^{+} T cells obtained from the salivary glands of the SS model mice were significantly increased in response to CCL22 (**Figure 4D**). Moreover, to examine whether CCL22 influences the cytokine secretion by T cells, concentrations of IFN-γ, IL-4, and IL-17 were analyzed using the culture supernatant of anti-CD3/CD28-stimulated CD4^{+} T cells isolated from the salivary gland tissues of SS model mice. Concentrations of IFN-γ and IL-4 were significantly enhanced by CCL22, whereas no changes were observed in IL-17 level (**Figure 4E**). In addition, to examine the protein level of cytokine production by CCL22, intracellular expressions of IFN-γ, IL-4, and IL-17 in the presence of CCL22 were analyzed using anti-CD3/CD28-stimulated CD4^{+} T cells from spleen of control and SS model mice. IFN-γ expression in CD4^{+} T cells of SS model mice was significantly enhanced by CCL22, whereas there were no changes in IL-4 and IL-17 expressions (**Supplemental Figures 3C,D**). These findings indicate that CCL22 may disturb the regulation of IFN-γ production by T cells in the target organ.

Therapeutic Effect of Anti-CCL22 Antibody (Ab) Administration on Autoimmune Lesions in the SS Model

SS model mice were administered with anti-CCL22 Ab from 8 to 10 weeks of age to determine the effect of CCL22 inhibition on autoimmune lesions. Anti-CCL22 Ab (4 μg) was intravenously injected into a mouse on alternate days for 2 weeks (**Figure 5A**). After treatment with anti-CCL22 Ab, the number of F4/80^{+} CD11b^{+} total sMΦs in salivary glands of SS model mice was significantly decreased compared with that of SS model mice treated with control IgG (**Figure 5B**). Furthermore, the number of both macrophages, CD11b^{high} and CD11b^{low} F4/80^{+} sMΦs, in salivary glands of anti-CCL22-treated mice was significantly decreased compared with that of control IgG-treated SS model

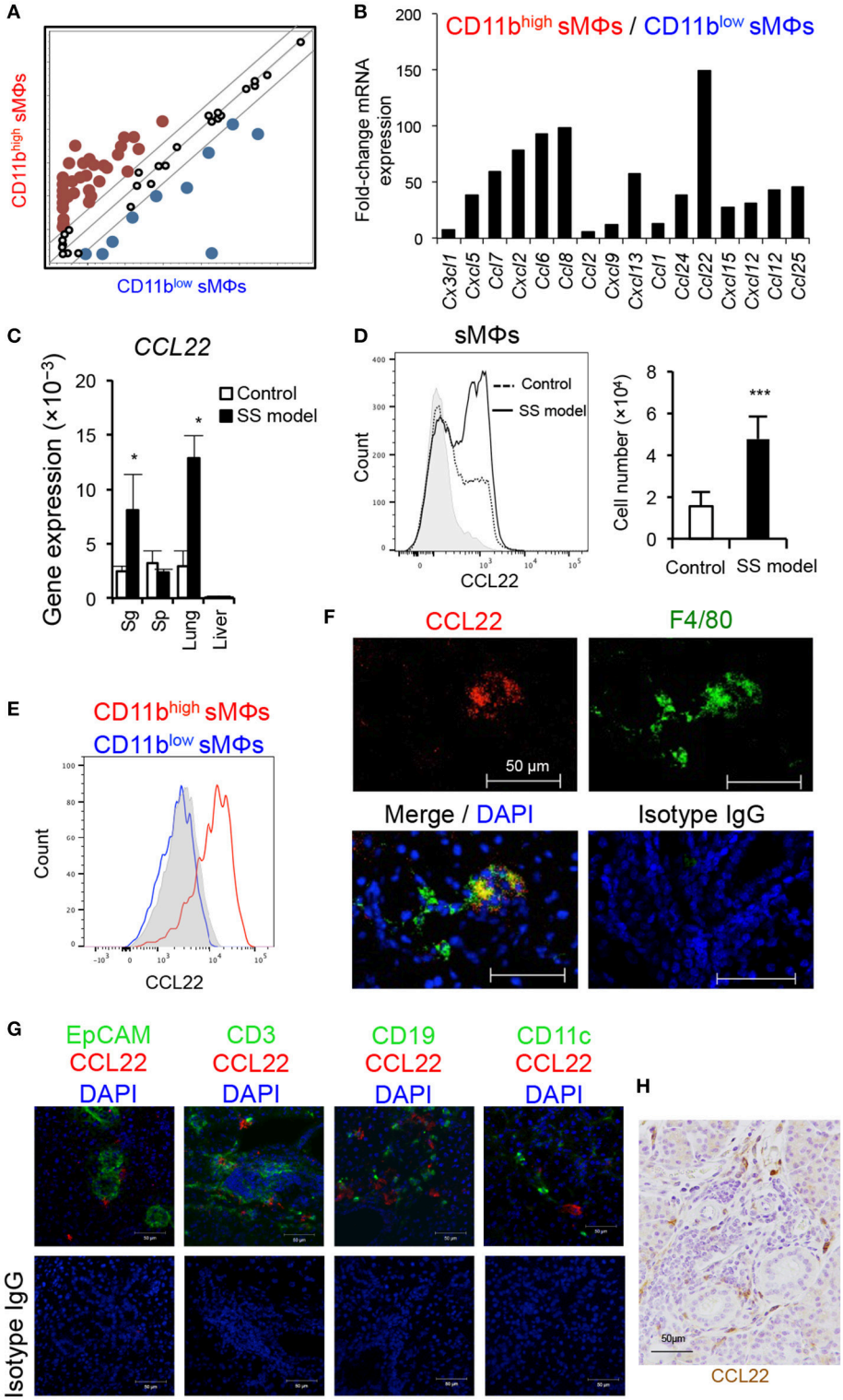

FIGURE 3 | Comprehensive analysis of chemokine genes of sMΦs. **(A,B)** Chemokine mRNA expressions of isolated CD11b^{high} and CD11b^{low} sMΦs of the SS model mice at 12 weeks of age were analyzed using PCR-array. Up-and downregulated genes of CD11b^{high} sMΦs compared with CD11b^{low} sMΦs of the SS model mice. The lines indicate 5-fold change in the gene expression. Red dots are upregulated genes, and blue dots are downregulated genes. Data are representative of three independent experiments. **(C)** CCL22 mRNA expression levels of various tissues of the SS model and control mice at 12 weeks of age were determined using qRT-PCR. Data are presented as mean ± SEM. *$p < 0.05$ by Student's *t*-test. $n = 5$. **(D)** CCL22 expression of sMΦs in salivary glands of control and SS model mice *(Continued)*.

FIGURE 3 | (left). CCL22 positive cell number (right). Data are representative of five mice in each group and are presented as mean ± SEM. ***$p < 0.0005$ by Student's *t*-test. $n = 5$. Gray shadow is isotype control. **(E)** Comparison of CCL22 expression between CD11b^{high} and CD11b^{low} sMΦs of the SS model mice at 12 weeks of age. Data are representative of five mice. Gray shadow is isotype control. **(F)** CCL22-producing sMΦs of the SS model mice were detected by confocal microscopic analysis. Data are representative of five mice. **(G)** Confocal microscopic analysis of CCL22 expression of EpCAM$^+$ epithelial cells, CD3$^+$ T cells, CD19$^+$ B cells, and CD11c$^+$ DCs in the salivary gland tissues form SS model mice. Data are representative of three mice. Nuclei were stained with DAPI. **(H)** Immunohistochenical analysis of CCL22 expression using the salivary gland tissues from SS model mice. The result is representative of three mice. Nuclei were stained with hematoxylin.

mice (**Figure 5C**), suggesting that other cells would be activated by secreting CCL22. Pathological examination revealed that when compared with the effect of isotype control Ab on SS model mice, anti-CCL22 Ab considerably suppressed the inflammatory lesions in the salivary glands of the SS model mice (**Figure 5D**). The number of lymphocytes infiltrated in the salivary gland tissue (/4 mm^2) was significantly lower in the anti-CCL22 Ab-treated mice than in the control isotype antibody-treated mice (**Figure 5E**). In addition, flow cytometric analysis revealed that the number of CD4$^+$ cells that had infiltrated in the salivary glands was significantly lower in the SS model mice injected with anti-CCL22 Ab was significantly decreased compared with that of SS model mice injected with isotype control Ab (**Figures 5F,G**). As for CD8$^+$ T cells, the decrease of the proportion and the cell number was observed in anti-CCL22 Ab-treated mice (**Figures 5F,G**). These results suggest that CCL22-producing sMΦs may serve as a target for treating SS.

Detection of CCL22-Producing sMΦs in Patients With SS

To determine whether the CCL22-producing sMΦs contribute to autoimmune lesions in patients with SS, immunohistochemical analysis was performed with anti-CCL22 Ab using minor salivary gland tissues obtained from controls and patients with SS. Based on the degree of lymphocyte infiltration, tissue sections of lip biopsy specimens were divided into four grades (23, 28). Numerous CCL22-producing cells were detected in the high-grade biopsy sections (**Figure 6A**). Pathological grade and the number of CCL22-producing cells were significantly correlated (**Figure 6B**). The histopathological criterion of SS diagnosis was a focus score $\geqq$1 which includes Grade 3 and 4 (23). Compared with patients with a focus score < 1, the number of CCL22$^+$ cells was significantly higher in the salivary gland tissues from patients with SS with a focus score $\geqq$1 (**Figure 6C**). In addition, confocal microscopy revealed many CCL22-producing CD68$^+$ sMΦs in the minor salivary gland tissues from patients with SS (Grade 4); however, only few CCL22$^+$ sMΦs were detected in controls (**Figure 6D**). In addition, CCL22 was not expressed in stromal cells, such as fibroblasts, endothelial cells, and nerve cells (**Supplemental Figure 4A**). Furthermore, confocal microscopic analysis confirme that Keratin$^+$ epithelial cells (**Supplemental Figure 4B**), CD3$^+$ T cells (**Supplemental Figure 4C**), CD19$^+$ B cells (**Supplemental Figure 4D**), and S100$^+$ DCs (**Supplemental Figure 4E**) did not express CCL22. A previous report indicated that CCL22 is secreted by macrophages or DCs *in vitro* and *in vivo* (29). This result indicates that CCL22-producing sMΦs play a key role in the formation of autoimmune lesions in the target organ of patients with SS.

DISCUSSION

In the current study, we investigated the relationship between autoimmunity and MΦs in the target organs in the SS mouse model and the patient with SS. Resident MΦs were divided into two subsets that displayed low and high expression levels of CD11b in the SS model mice. Via the control of T cell migration and cytokine production, CCL22-producing CD11b^{high} macrophages play a key role in the development of autoimmune lesions in the salivary glands.

The number of MΦs in the salivary glands was significantly higher in the SS model mice than in the control mice at 8 weeks of age; however, no difference was observed in the respect at the subsequent time-point. The number of CD11b^{low} sMΦs also significantly increased at 8 weeks of age, which is the stage of onset of autoimmune lesions in the model. In contrast, the number of CD11b^{high} sMΦs was significantly higher in the SS model mice than in the control mice between 12 and 16 weeks of age, which corresponds to the stage wherein development of autoimmune lesions occurs in the SS model mice. These results suggest that the phenotypic change to CD11b^{high} sMΦs within the target organ may be induced during the development of autoimmune lesions. In addition, it is possible that bone marrow-derived myeloid cells may accumulate to become MΦs in the target organ.

During various inflammatory processes, naïve monocytes differentiate into pro-inflammatory M1 and anti-inflammatory M2 MΦs (30, 31). The diverse phenotypes and functionality of resident MΦ in different organs is well-documented (32, 33). It is difficult to differentiate between the M1 and M2 subsets based on the surface markers (34). No differences were observed between the control mice and SS model mice with respect to M1/M2 markers. However, expressions of scavenger receptors (CD36 and CD204) on CD11b^{low} sMΦs of the SS model mice were clearly enhanced. Phagocytic activity of both CD11b^{low} and CD11b^{high} sMΦs in the SS model mice was also upregulated. These results indicate that the phenotypic difference between CD11b^{low} and CD11b^{high} does not contribute to the differentiation into M1/M2 MΦ subsets and the phagocytic function of MΦ. On the other hand, it is possible that CD11b^{low} sMΦs may play a role in the pathogenesis of the SS model mice. As shown in **Figure 1**, the number of CD11b^{low} sMΦs in SS model mice at 8 weeks of age was significantly higher than that in control mice; therefore, the CD11b^{low} sMΦs may contribute to the onset or early stage of the disease. However, further study is required for a detailed analysis of this population in detail in the next project.

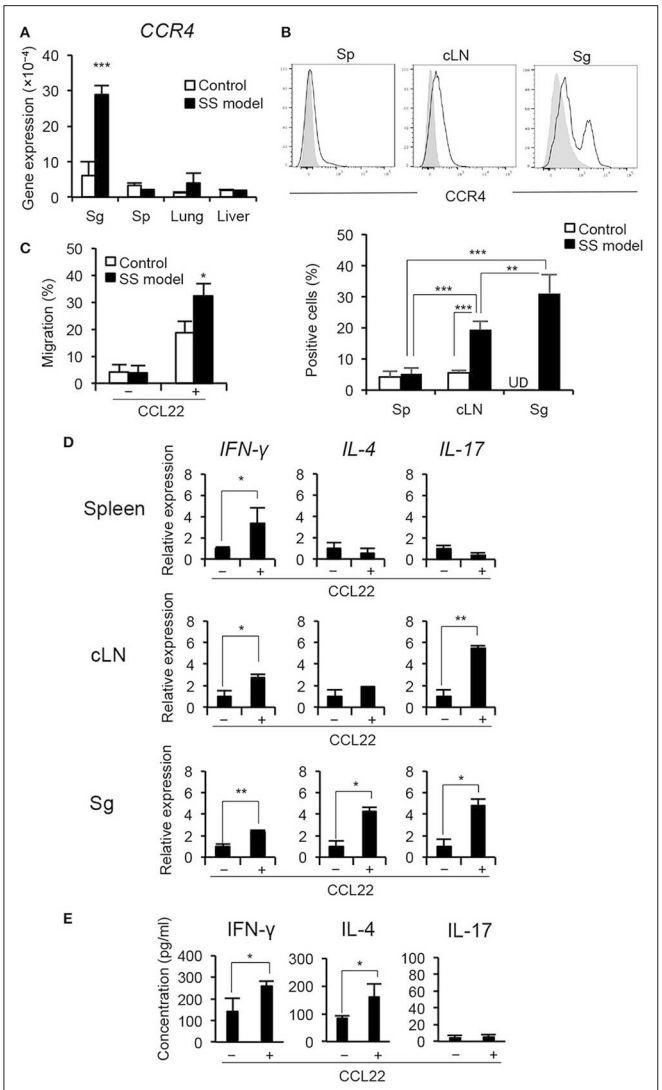

FIGURE 4 | CCR4 expression on peripheral T cells and migratory activity of T cell by CCL22. **(A)** CCR4 mRNA expression levels in tissues were determined by qRT-PCR. Data are presented as mean ± SEM. n = 5. **(B)** CCR4 expression on $CD4^+$ T cells purified form the spleen (Sp), cLN, and salivary glands (Sg) of SS model mice at 12 weeks of age was determined by flow cytometric analysis. Data are representative of five mice, and mean ± SEM of $CCR4^+$ cells (%) of $CD4^+$ T cells. Gray shadow is isotype control. $^{**}p < 0.005$, $^{***}p < 0.0005$ by one-way ANOVA with Turkey's multiple comparison post-test. UD, undetermined. **(C)** Migratory activity of $CD4^+$ T cells from SS model mice to CCL22 (200 ng/mL) was analyzed by *in vitro* migration assay using trans-well. Data are representative of three independent experiments. $^*p < 0.05$ by Student's *t*-test. **(D)** $CD4^+$ T cells purified from the spleen, cLNs, and salivary glands in SS model mice at 12 weeks of age were cultured with CCL22 for 6 h. The mRNA expressions of IFN-γ, IL-4, and IL-17 were detected by qRT-PCR. Data are presented as mean ± SEM relative to that without CCL22 and are representative of three independent experiments. $^*p < 0.05$, $^{**}p < 0.005$ by Student's *t*-test. **(E)** $CD4^+$ T cells isolated from salivary gland tissues of SS model mice were cultured with or without CCL22 (200 ng/mL) in the presence of anti-CD3/CD28 mAb-beads for 48 h, and subsequently cultured with PMA (50 ng/mL) and iomomycin (IM) (1 μg/mL) for the last 6 h. Cytokine levels, including IFN-γ, IL-4, and IL-17, in the supernatant were measured using a Cytokine 20-Plex Mouse Panel Luminex assay kit. Data are expressed as the mean concentration pg/mL) ± SEM, n = 4 per group. $^*p < 0.05$ by Student's *t*-test.

We have checked many markers of macrophage in preliminary experiments before focusing on CD11b expression. Among these, we found that CD11b expression in the target tissue of SS model mice changed with disease progression in the SS model mice. Therefore, we decided to focus on the analysis of the role or function of $CD11b^{low/high}$ sMΦs in the target tissues at the onset or development of the disease.

To determine a key molecule for the development of autoimmune disease in the SS model mice, experiments were conducted in two steps. The first step was comprehensive gene analysis limiting chemokine genes to compare the gene expression of $CD11b^{high}$ sMΦs with that of $CD11b^{low}$ sMΦs in the SS model mice. In the second step, several genes among the upregulated genes that showed a significant difference between the control and SS model mice were picked up. Among these, the CCL22 gene of $CD11b^{high}$ sMΦs was selected as a potential candidate that plays a key role in the development of autoimmune lesions. Alongside the development of autoimmune lesions, CCL22-producing $CD11b^{high}$ sMΦs were increased in SS model mice. M2a, a subset of M2 MΦ, induced by IL-4 and IL-13 exposure expresses arginase I and produces CCL22, IL-10, TGF-β, IL-1Ra, CCL17, and CCL24 to promote Th2 cells, eosinophils, and basophils (1–4, 6). The CCL22-producing sMΦs seem to differ from the M2a MΦ subset.

CCL22 is one of the C-C motif chemokines and is termed as MΦ-derived chemokine (MDC) in humans and mice. CCL22 and CCL17 bind to CCR4, and both chemokines are 39% identical at the amino acid level (34). Both CCL22 and CCL17 are highly expressed in the thymus (35, 36). The role of CCL22 in peripheral T cells is not clear. IFN-γ-producing Th1 cells were shown to contribute to the onset of autoimmune lesions in the SS model mice (24). In the present study, cytokine production in $CD4^+$ T cell response to CCL22 showed differences between the spleen, cLN, and target tissue in the SS model mice. It is possible that the differences regarding receptor expression may be related to the cytokine production through different signaling of the T cells. Hence, CCL22 may play a key role in the breakdown of local immune tolerance in the target organ to induce autoimmune lesions in SS. In addition, our hypothesis is that CCL22 from $CD11b^{high}$ sMΦs may enhance the migration of effector T cells into the target organ through CCR4 on T cells and also the cytokine production, such as IFN-γ, by T cells. In addition, the mRNA expressions of *IFN-γ*, *IL-4*, and *IL-17* in T cells isolated from the salivary gland tissues of SS model mice were enhanced by CCL22. IFN-γ and IL-4 protein secretion was also enhanced by CCL22. As for the discrepancy in IL-17 between the mRNA and protein expressions of IL-17, protein secretion of IL-17 may be influenced by any other factor. Previous reports demonstrate that CCR4 is predominantly expressed by Th2 cells, cutaneous lymphocyte antigen-positive skin-homing T cells, and Treg cells (36, 37). Therefore, CCL22 is considered one of the Th2-associated chemokines (38, 39). Our result was consistent with the elevated CCL22 in salivary gland tissues from patients with SS as described previously (40). The high expression level of CCR4 on $CD4^+$ T cells that infiltrate the target organ is a novel finding that highlights the

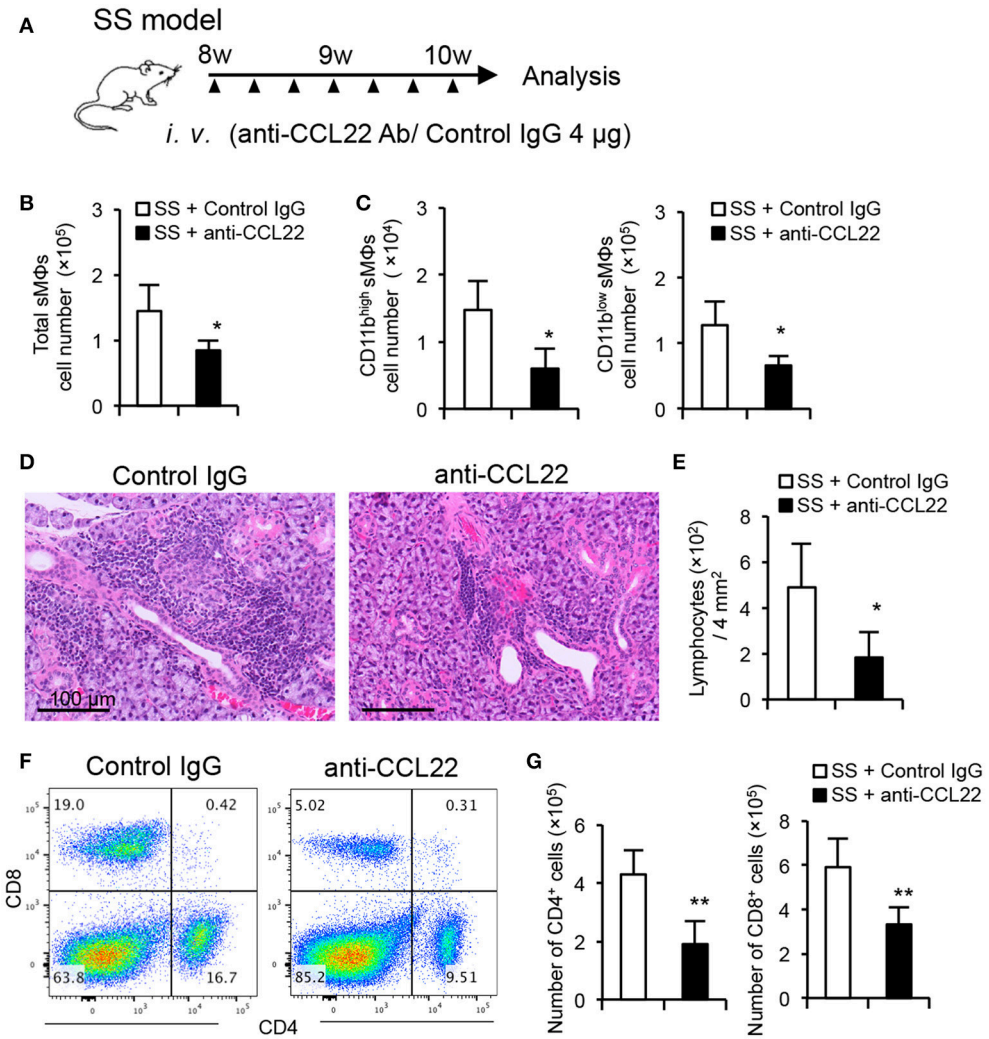

FIGURE 5 | Therapeutic effect of anti-CCL22 Ab administration on autoimmune lesions in SS model mice. **(A)** Experimental schedule. Anti-CCL22 Ab (4 μg) was intravenously injected into a mouse on alternate days for 2 weeks. **(B)** Total number of sMΦs infiltrated in the salivary gland tissues from control IgG and anti-CCL22 Ab treatment was determined by cell counter and flow cytometry. **(C)** The number of CD11b$^{low/high}$ sMΦs in the salivary gland tissues was determined using cell counter and flow cytometry. **(D)** Pathological analysis was performed using H&E-stained sections of salivary gland tissues from the SS model mice administered with anti-CCL22 Ab and isotype control antibody. Data are representative of five mice in each group. **(E)** Number of lymphocytes infiltrated into salivary gland tissues within 2 × 2 mm^2 was counted using H&E-stained sections. **(F)** CD4/CD8 T cell phenotype in the salivary gland tissues was analyzed by flow cytometry. Data are representative of five mice in each group. **(G)** The number of CD4$^+$ (left) and CD8$^+$ T cells in the salivary gland tissues was determined using cell counter and flow cytometry. Data are presented as mean ± SEM of five mice (B, C, E, and G). *$p < 0.05$ **$p < 0.005$ by Student's *t*-test.

key role of the CCL22-CCR4 axis in the autoimmune reaction in the target organ. Previously, CCL22 was detected around the ductal epithelial cells, whereas CCR4 was detected on infiltrating lymphocytes in the minor salivary glands of patients with SS. From our study, any subset of sMΦs may be the source of CCL22 in the target organ of SS. Th1 and Th17 cells may be involved in the initiation of SS, and Th2 cells may contribute to disease progression through the interaction between chemokines and chemokine receptors, such as CCL22 and CCR4. In contrast, although it was reported that CCL22 gene expression of minor salivary glands of patients with SS was less pronounced (20), our study demonstrated that a part of macrophage subsets highly produces CCL22 in the target tissue in SS. Therefore, it is possible that the increased gene expression of CCL22 in the whole tissue cannot be observed. We determined the concentration of CCL22 for *in vitro* migration assay based on a previous report (41) and our preliminary experiment (**Supplemental Figure 2**). Indeed, 200 ng/mL of CCL22 may be much higher than the physiological concentration. However, it is difficult to determine the physiological or pathological concentration *in vivo*, and the concentration gradient may change with disease progression in the SS model mice.

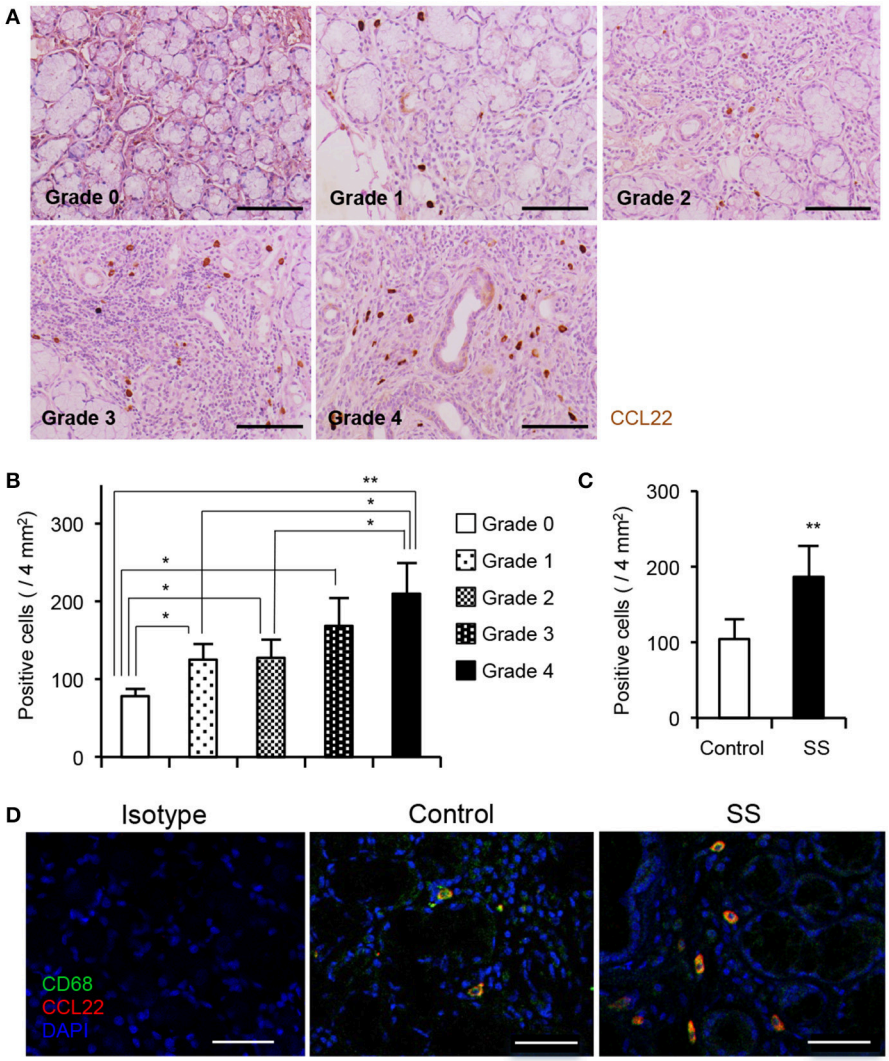

FIGURE 6 | CCL22-producing sMΦs of minor salivary gland tissue from patients with SS. **(A)** CCL22$^+$ cells from the minor salivary gland tissues from controls and patients with SS were detected by immunohistochemical analysis. Sections of controls and patients with SS (Grade 1 to 4) were used for analysis. Photos are representative of 5–7 samples in each group. **(B)** The number of CCL22$^+$ cells was determined, and data are presented as mean ± SEM of five samples. $^*p < 0.05$, $^{**}p < 0.005$ by one-way ANOVA with Turkey's multiple comparison post-test. **(C)** Correlation in CCL22$^+$ cells between focus score 1 < and 1 ≧ patients. The number of CCL22$^+$ cells was determined, and data are presented as mean ± SEM of five samples. $^*p < 0.05$, $^{**}p < 0.005$ by Student's *t*-test. **(D)** CCL22-producing CD68$^+$ sMΦs were detected by confocal analysis using the section of controls and SS patients (Grade 4). Photos are representative of 5 samples in each group. Bar: 50 μm.

In the current study, anti-CCL22 Ab has a therapeutic effect on the autoimmune lesions in the SS model mice. A previous report demonstrated that CCL22 regulates experimental autoimmune encephalaomyelitis (EAE) via the control of MΦ chemoattraction and effector function (27, 42, 43). CCR4 is also known to play a potent role in the development of EAE (44, 45). Furthermore, a CCR4 antagonist was shown to ameliorate EAE via the inhibition of Th1 and Th17 polarization of antigen-induced T cell response (46, 47). In contrast, CCL22-mediated recruitment of Treg cells to the pancreas protects against autoimmune diabetes in a murine type 1 diabetes model (48, 49). CCL22 has also been implicated in various diseases, including allergic disease, and lymphoma (50–54). CCL22 and its receptor contribute to the onset or development of immune disorders by inducing changes in the expression and contribution or the functions (55, 56). In our model, CD11b^{high} sMΦs intensively produced CCL22 to influence T cell responses in the target tissue. In addition, as the infiltration of CD8$^+$ T cells in the salivary gland tissues was also suppressed by the injection of anti-CCL22 Ab, the same mechanism may apply for CD8$^+$ T cell migration to the target organ. A large number of CD8$^+$ T cells were accumulated in the salivary gland tissue of SS model mice (**Figure 5D**). As mentioned, CD4$^+$ T cells are

the main subset of immune cells infiltrated in the salivary gland in this model in the early stage. As shown in **Figure 5**, we analyzed the mice at 10 weeks of age, when $CD8^+$ T cells also are infiltrated in addition to the other immune cell populations.

We analyzed the cytokine mRNA expression of cultured T cells *in vitro* to examine the direct effect of CCL22 on T cells. It is important to detect cytokine expression directly in the target tissues. However, it is difficult to assess the effect of CCL22 on the cytokine expression of T cells *in vivo*. Analysis of CD11b-conditional CCL22 gene knockout mouse in the next study will help define the *in vivo* function of CCL22 in autoimmunity.

In this study, in addition to CCL22 gene, several chemokine genes of $CD11b^{high}$ sMΦs were upregulated, suggesting that complicated chemokine network by resident MΦs with phenotypic change affects the pathogenesis of autoimmune lesions. Moreover, CCL22 gene expression of lung in the SS model mice was significantly higher than that of control mice. As slight inflammatory lesions of the lung in the SS model mice are observed with age, CCL22 may play a key role in the pulmonary lesions.

To summarize, a phenotypic change in the resident sMΦs of SS model mice was observed during the development of autoimmune lesions. CCL22-producing resident MΦs influence T cell migration and cytokine production in the target organ of the SS model mice. Interventions that target MΦs may serve as a potential novel treatment for autoimmune diseases.

ETHICS STATEMENT

All animal experiments were reviewed and approved by he Committee on Animal Experiments of Tokushima University and Biological Safety Research Center, Japan (Permit Number: T29-115). Labial salivary gland (LSG) samples were obtained from patients with SS and controls. The study was approved by the Institutional Review Board of the Tokushima University Hospital, Japan (No. 2802). Written informed consent was received from participants prior to inclusion in the study in accordance with the Declaration of Helsinki.

AUTHOR CONTRIBUTIONS

AU designed and performed the experiments, analyzed the data, and prepared the manuscript. RA designed the experiments and provided intellectual assistance. KO, AY, and TT performed the experiments. YK designed the experiments. KA and MA prepared human samples. NI provided broad guidance in experimental design, data analysis, and manuscript preparation. All authors read, reviewed, and approved the final manuscript.

FUNDING

This research was supported by the JSPS KAKENHI grant (#16H02690 and #16H05511) and the Bristol-Myers Squibb research grant.

ACKNOWLEDGMENTS

We thank Michiko Kino, and Hitomi Fukui for technical assistance with the support of the mouse colony.

SUPPLEMENTARY MATERIAL

The Supplementary Material for this article can be found online at: https://www.frontiersin.org/articles/10.3389/fimmu.2018.02594/full#supplementary-material

Supplemental Figure 1 | Gating strategy and representative gating of immune cells obtained from salivary gland tissues in the SS models. FSC-A/SSC-A, FSC-A/FSC-H, and FSC/CD45.2 panels are shown. After gating single cells and $CD45.2^+$ cells among live cells, $7\text{-}AAD^-CD3^-CD19^-$ cells were gated for obtaining MΦ population.

Supplemental Figure 2 | (A) mRNA expressions of CXCR3A, CCR3, and CX3CR1 in salivary gland tissues from control and SS model mice at 12 weeks of age were determined by qRT-PCR. Data are presented as mean ± SEM. $n = 5$. The primer sequences used were as follows: CXCR3A: forward, 5′-TGCTAGATGCCTCGGACTTT-3′, and reverse, 5′- CGCTGACTCAGT AGCACAGC-3′, CCR3: forward, 5′-TTGATCCTCATAAAGTACAGGAAGC-3′, and reverse, 5′- CAATGCTGCCAGTCCTGCAA-3′, CX3CR1: forward, 5′-CACCATTAGTCTGGGCGTCT-3′, and reverse, 5′- GATGCGGAAGTAG CAAAAGC-3′. Relative mRNA expression of each transcript was normalized against β-actin mRNA. **(B)** Migratory activity of $CD4^+$ T cells from SS model mice to CCL22 (0, 50, 100, and 200 ng/mL) was analyzed by *in vitro* migration assay using trans-well. Data are representative of three independent experiments. $^*p < 0.05$ by Student's *t*-test.

Supplemental Figure 3 | (A) Intracellular expressions of IFN-γ, IL-4, and IL-17 of activated splenic $CD4^+$ T cells. $CD4^+$ T cells purified from spleen of the control and SS model mice were stimulated with PMA (50 ng/mL) and ionomycin (1 μg/ml) for 6 h with Golgi-stop. Data are representative of three independent experiments. **(B)** $CD4^+$ T cells purified from the spleen in control mice were cultured with CCL22 (200 ng/mL) for 6 h. The mRNA expressions of IFN-γ, IL-4, and IL-17 were detected by qRT-PCR. Data are presented as mean ± SEM relative to that without CCL22 and are representative of three independent experiments. $^*p < 0.05$ by Student's *t*-test. **(C)** Intracellular IFN-γ expression in $CD4^+$ T cells of SS model mice. $CD4^+$ T cells were stimulated with or without CCL22 (200 ng/mL) in the presence of anti-CD3/CD28 mAb for 48 h, and were subsequently cultured with PMA (50 ng/mL) and IM (1 μg/mL) in the presence of Brefeldin A for the last 6 h. The results are representative of five samples in each group. **(D)** Intracellular cytokine expressions of IFN-γ, IL-4, and IL-17 in splenic $CD4^+$ T cells of control and SS model mice were analyzed by flow cytometer. Data are presented as mean ± SEM relative to that without CCL22. $n = 5$. $^*p < 0.05$ by Student's *t*-test, $^{**}p < 0.005$ by Student's *t*-test.

Supplemental Figure 4 | (A) Stromal cells did not express CCL22. CCL22 was detected by immunohistochemical analysis. Bar: 500 and 50 μm. **(B–E)** Confocal microscopic analysis of CCL22 expression of $Keratin^+$ epithelial cells **(B)**, $CD3^+$ T cells **(C)**, $CD19^+$ B cells **(D)**, and $S100^+$ DCs **(E)** using the sections of SS patients (Grade 4). Photos are representative of five samples in each group. Bar: 50 μm.

REFERENCES

1. Arango Duque G, Descoteaux A. Macrophage cytokines: involvement in immunity and infectious diseases. *Front Immunol.* (2014) 5:e491. doi: 10.3389/fimmu.2014.00491
2. Wynn TA, Chawla A, Pollard JW. Macrophage biology in development, homeostasis and disease. *Nature* (2013) 496:445–55. doi: 10.1038/nature12034
3. Shi C, Pamer EG. Monocyte recruitment during infection and inflammation. *Nat Rev Immunol.* (2011) 11:762–74. doi: 10.1038/nri3070
4. Murray PJ, Wynn TA. Protective and pathogenic functions of macrophage subsets. *Nat Rev Immunol.* (2011) 11:723–37. doi: 10.1038/nri3073
5. Hams E, Bermingham R, Fallon PG. Macrophage and innate lymphoid cell interplay in the genesis of fibrosis. *Front Immunol.* (2015) 6:e597. doi: 10.3389/fimmu.2015.00597
6. Biswas SK, Mantovani A. Macrophage plasticity and interaction with lymphocyte subsets: cancer as a paradigm. *Nat Immunol.* (2010) 11:889–96. doi: 10.1038/ni.1937
7. Vasiliadou I, Holen I. The role of macrophages in bone metastasis. *J Bone Oncol.* (2013) 2:158–66. doi: 10.1016/j.jbo.2013.07.002
8. Laskin DL, Pendino KJ. Macrophages and inflammatory mediators in tissue injury. *Annu Rev Pharmacol Toxicol.* (1995) 35:655–77. doi: 10.1146/annurev.pa.35.040195.003255
9. Wynn TA, Vannella KM. Macrophages in tissue repair, regeneration, and fibrosis. *Immunity* (2016) 44:450–62. doi: 10.1016/j.immuni.2016.02.015
10. Das A, Sinha M, Datta S, Abas M, Chaffee Ss, Sen CK, Roy S. Monocyte and macrophage plasticity in tissue repair and regeneration. *Am J Pathol.* (2015) 185:2596–606. doi: 10.1016/j.ajpath.2015.06.001
11. Fox RI. Sjögren's syndrome. *Lancet* (2005) 366:321–31. doi: 10.1016/s0140-6736(05)66990-5
12. Qin B, Wang J, Yang Z, Yang M, Ma N, Huang F, Zhong R. Epidemiology of primary Sjogren's syndrome: a systematic review and meta-analysis. *Ann Rheum Dis.* (2015) 74:1983–89. doi: 10.1136/annrheumdis-2014-205375
13. Fox RI, Robinson CA, Curd JG, Kozin F, Howell FV. Sjogren's syndrome. Proposed criteria for classification. *Arthritis Rheum.* (1986) 29:577–85.
14. Christodoulou MI, Kapsogeorgou EK, Moutsopoulos NM, Moutsopoulos HM. Foxp3+ T-regulatory cells in Sjogren's syndrome: correlation with the grade of the autoimmune lesion and certain adverse prognostic factors. *Am J Pathol.* (2008) 173:1389–96. doi: 10.2353/ajpath.2008.080246
15. Katsifis GE, Moutsopoulos NM, Wahl SM. T lymphocytes in Sjogren's syndrome: contributors to and regulators of pathophysiology. *Clin Rev Allergy Immunol.* (2007) 32:252–64. doi: 10.1007/s12016-007-8011-8
16. Moriyama M, Tanaka A, Maehara T, Furukawa S, Nakashima H, Nakamura S. T helper subsets in Sjogren's syndrome and IgG4-related dacryoadenitis and sialoadenitis: a critical review. *J Autoimmun.* (2014) 51:81–88. doi: 10.1016/j.jaut.2013.07.007
17. Nocturne G, Mariette X. B cells in the pathogenesis of primary Sjogren syndrome. *Nat Rev Rheumatol.* (2018) 14:133–45. doi: 10.1038/nrrheum.2018.1
18. Ambrus JL, Suresh L, Peck A. Multiple Roles for B-Lymphocytes in Sjogren's Syndrome. *J Clin Med.* (2016) 5:e87. doi: 10.3390/jcm5100087
19. Ushio A, Arakaki R, Yamada A, Saito M, Tsunematsu T, Kudo Y, Ishimaru N. Crucial roles of macrophages in the pathogenesis of autoimmune disease. *World J Immunol.* (2017) 7:e1. doi: 10.5411/wji.v7.i1.1
20. Greenwell-Wild T, Moutsopoulos NM, Gliozzi M, Kapsogeorgou E, Rangel Z, Munson PJ, et al. Chitinases in the salivary glands and circulation of patients with Sjogren's syndrome: macrophage harbingers of disease severity. *Arthritis Rheum.* (2011) 63:3103–15. doi: 10.1002/art.30465
21. Lee YJ, Scofield RH, Hyon JY, Yun PY, Lee HJ, Lee EY, et al. Salivary chemokine levels in patients with primary Sjogren's syndrome. *Rheumatology* (2010) 49:1747–52. doi: 10.1093/rheumatology/keq121
22. Ogawa N, Ping L, Zhenjun L, Takada Y, Sugai S. Involvement of the interferon-gamma-induced T cell-attracting chemokines, interferon-gamma-inducible 10-kd protein (CXCL10) and monokine induced by interferon-gamma (CXCL9), in the salivary gland lesions of patients with Sjogren's syndrome. *Arthritis Rheum.* (2002) 46:2730–41. doi: 10.1002/art.10577
23. Greenspan JS, Daniels TE, Talal N, Sylvester RA. The histopathology of Sjogren's syndrome in labial salivary gland biopsies. *Oral Surg Oral Med Oral Pathol.* (1974) 37:217–29.
24. Haneji N, Hamano H, Yanagi K, Hayashi Y. A new animal model for primary Sjogren's syndrome in NFS/sld mutant mice. *J Immunol.* (1994) 153:2769–77.
25. Haneji N, Nakamura T, Takio K, Yanagi K, Higashiyama H, Saito I, et al. Identification of alpha-fodrin as a candidate autoantigen in primary Sjogren's syndrome. *Science* (1997) 276:604–7.
26. Ushio A, Arakaki R, Eguchi H, Hotta F, Yamada A, Kudo Y, et al. Pathological analysis of ocular lesions in a murine model of Sjogren's Syndrome. *Int J Mol Sci.* (2017) 18:e1209. doi: 10.3390/ijms18061209
27. Dogan RN, Long N, Forde E, Dennis K, Kohm AP, Miller SD, et al. CCL22 regulates experimental autoimmune encephalomyelitis by controlling inflammatory macrophage accumulation and effector function. *J Leukoc Biol.* (2011) 89:93–104. doi: 10.1189/jlb.0810442
28. Segerberg-Konttinen M, Konttinen YT, Bergroth V. Focus score in the diagnosis of Sjogren's syndrome. *Scand J Rheumatol Suppl.* (1986) 61:47–51.
29. Vulcano M, Albanesi C, Stoppacciaro A, Bagnati R, D'Amico G, Struyf S, et al. Dendritic cells as a major source of macrophage-derived chemokine/CCL22 in vitro and *in vivo*. *Eur J Immunol.* (2001) 31:812–822. doi: 10.1002/1521-4141(200103)31:3<812::AID-IMMU812>3.0.CO;2-L
30. Martinez FO, Sica A, Mantovani A, Locati M. Macrophage activation and polarization. *Front Biosci.* (2008) 13:453–61. doi: 10.2741/2692
31. Galli SJ, Borregaard N, Wynn TA. Phenotypic and functional plasticity of cells of innate immunity: macrophages, mast cells and neutrophils. *Nat Immunol.* (2011) 12:1035–44. doi: 10.1038/ni.2109
32. Lavin Y, Mortha A, Rahman A, Merad M. Regulation of macrophage development and function in peripheral tissues. *Nat Rev Immunol.* (2015) 15:731–44. doi: 10.1038/nri3920
33. Takata K, Kozaki T, Lee CZW, Thion MS, Otsuka M, et al. Induced-pluripotent-stem-cell-derived primitive macrophages provide a platform for modeling tissue-resident macrophage differentiation and function. *Immunity* (2017) 47:183–98. doi: 10.1016/j.immuni.2017.06.017
34. Greter M, Lelios I, Croxford AL. Microglia Versus Myeloid Cell Nomenclature during Brain Inflammation. *Front Immunol.* (2015) 6:e249. doi: 10.3389/fimmu.2015.00249
35. Yoshie O, Matsushima K. CCR4 and its ligands: from bench to bedside. *Int Immunol.* (2015) 27:11–20. doi: 10.1093/intimm/dxu079
36. Horikawa T, Nakayama T, Hikita I, Yamada H, Fujisawa R, Bito T, et al. IFN-γ-inducible expression of thymus and activation-regulated chemokine/CCL17 and macrophage-derived chemokine/CCL22 in epidermal keratinocytes and their roles in atopic dermatitis. *Int Immunol.* (2002) 14:767–73. doi: 10.1093/intimm/dxf044
37. Sigmundsdottir H, Butcher EC. Environmental cues, dendritic cells and the programming of tissue-selective lymphocyte trafficking. *Nat Immunol.* (2008) 9:981–7. doi: 10.1038/ni.f.208
38. Wynn TA. Type 2 cytokines: mechanisms and therapeutic strategies. *Nat Rev Immunol.* (2015) 15:271–82. doi: 10.1038/nri3831
39. Gieseck RL III, Wilson MS, Wynn TA. Type 2 immunity in tissue repair and fibrosis. *Nat Rev Immunol.* (2018) 18:62–76. doi: 10.1038/nri.2017.90
40. Moriyama M, Hayashida JN, Toyoshima T, Ohyama Y, Shinozaki S, Tanaka A, et al. Cytokine/chemokine profiles contribute to understanding the pathogenesis and diagnosis of primary Sjögren's syndrome. *Clin Exp Immunol.* (2012) 169:17–26. doi: 10.1111/j.1365-2249.2012.04587.x.
41. Mailloux AW, Young R. NK-dependent increases in CCL22 secretion selectively recruits regulatory T cells to the tumor microenvironment. *J Immunol.* (2009) 182:2753–65. doi: 10.4049/jimmunol.0801124
42. Saederup N, Cardona AE, Croft K, Mizutani M, Cotleur AC, Tsou CL, et al. Selective chemokine receptor usage by central nervous system myeloid cells in CCR2-red fluorescent protein knock-in mice. *PLoS ONE* (2010) 5:e13693. doi: 10.1371/journal.pone.0013693
43. Jiang Z, Jiang JX, Zhang GX. Macrophages: a double-edged sword in experimental autoimmune encephalomyelitis. *Immunol Lett.* (2014) 160:17–22. doi: 10.1016/j.imlet.2014.03.006
44. Columba-Cabezas S, Serafini B, Ambrosini E, Sanchez M, Penna G, Adorini L, et al. Induction of macrophage-derived chemokine/CCL22 expression in experimental autoimmune encephalomyelitis and cultured microglia: implications for disease regulation. *J Neuroimmunol.* (2002) 130:10–21. doi: 10.1016/S0165-5728(02)00170-4

45. Forde EA, Dogan RN, Karpus WJ. CCR4 contributes to the pathogenesis of experimental autoimmune encephalomyelitis by regulating inflammatory macrophage function. *J Neuroimmunol.* (2011) 236:17–26. doi: 10.1016/j.jneuroim.2011.04.008
46. Jiang HR, Milovanovic M, Allan D, Niedbala W, Besnard AG, Fukada SY, et al. IL-33 attenuates EAE by suppressing IL-17 and IFN-gamma production and inducing alternatively activated macrophages. *Eur J Immunol.* (2012) 42:1804–14. doi: 10.1002/eji.201141947
47. Scheu S, Ali S, Ruland C, Arolt V, Alferink J. The C-C Chemokines CCL17 and CCL22 and Their Receptor CCR4 in CNS Autoimmunity. *Int J Mol Sci.* (2017) 18:e2306. doi: 10.3390/ijms18112306
48. Bischoff L, Alvarez S, Dai DL, Soukhatcheva G, Orban PC, Verchere CB. Cellular mechanisms of CCL22-mediated attenuation of autoimmune diabetes. *J Immunol.* (2015) 194:3054–64. doi: 10.4049/jimmunol.1400567
49. Sarkar SA, Lee CE, Victorino F, Nguyen TT, Walters JA, Burrack A, et al. Expression and regulation of chemokines in murine and human type 1 diabetes. *Diabetes* (2012) 61:436–46. doi: 10.2337/db11-0853
50. Nakazato J, Kishida M, Kuroiwa R, Fujiwara J, Shimoda M, Shinomiya N. Serum levels of Th2 chemokines, CCL17, CCL22, and CCL27, were the important markers of severity in infantile atopic dermatitis. *Pediatr Allergy Immunol.* (2008) 19:605–13. doi: 10.1111/j.1399-3038.2007.00692.x
51. Niens M, Visser L, Nolte IM, van der Steege G, Diepstra A, Cordano P, et al. Serum chemokine levels in Hodgkin lymphoma patients: highly increased levels of CCL17 and CCL22. *Br J Haematol.* (2008) 140:527–36. doi: 10.1111/j.1365-2141.2007.06964.x
52. Toulza F, Nosaka K, Tanaka Y, Schioppa T, Balkwill F, Taylor GP, et al. Human T-lymphotropic virus type 1-induced CC chemokine ligand 22 maintains a high frequency of functional FoxP3+ regulatory T cells. *J Immunol.* (2010) 185:183–9. doi: 10.4049/jimmunol.0903846
53. Gobert M, Treilleux I, Bendriss-Vermare N, Bachelot T, Goddard-Leon S, Arfi V, et al. Regulatory T cells recruited through CCL22/CCR4 are selectively activated in lymphoid infiltrates surrounding primary breast tumors and lead to an adverse clinical outcome. *Cancer Res.* (2009) 69:2000–9. doi: 10.1158/0008-5472.CAN-08-2360
54. Anz D, Rapp M, Eiber S, Koelzer VH, Thaler R, Haubner S, et al. Suppression of intratumoral CCL22 by type i interferon inhibits migration of regulatory T cells and blocks cancer progression. *Cancer Res.* (2015) 75:4483–93. doi: 10.1158/0008-5472.CAN-14-3499
55. Thompson SD, Luyrink LK, Graham TB, Tsoras M, Ryan M, Passo MH, et al. Chemokine receptor CCR4 on CD4+ T cells in juvenile rheumatoid arthritis synovial fluid defines a subset of cells with increased IL-4:IFN-gamma mRNA ratios. *J Immunol.* (2001) 166:6899-906. doi: 10.4049/jimmunol.166.11.6899
56. Flytlie HA, Hvid M, Lindgreen E, Kofod-Olsen E, Petersen EL, Jorgensen A, et al. Expression of MDC/CCL22 and its receptor CCR4 in rheumatoid arthritis, psoriatic arthritis and osteoarthritis. *Cytokine* (2010) 49:24–29. doi: 10.1016/j.cyto.2009.10.005

Conflict of Interest Statement: The authors declare that the research was conducted in the absence of any commercial or financial relationships that could be construed as a potential conflict of interest.

Copyright © 2018 Ushio, Arakaki, Otsuka, Yamada, Tsunematsu, Kudo, Aota, Azuma and Ishimaru. This is an open-access article distributed under the terms of the Creative Commons Attribution License (CC BY). The use, distribution or reproduction in other forums is permitted, provided the original author(s) and the copyright owner(s) are credited and that the original publication in this journal is cited, in accordance with accepted academic practice. No use, distribution or reproduction is permitted which does not comply with these terms.

frontiers in Immunology

ORIGINAL RESEARCH
published: 14 November 2018
doi: 10.3389/fimmu.2018.02584

Sulforaphane Inhibits Inflammatory Responses of Primary Human T-Cells by Increasing ROS and Depleting Glutathione

*Jie Liang[1], Beate Jahraus[1], Emre Balta[1], Jacqueline D. Ziegler[1], Katrin Hübner[1], Norbert Blank[2], Beate Niesler[3,4], Guido H. Wabnitz[1] and Yvonne Samstag[1]**

[1] Section Molecular Immunology, Institute of Immunology, Heidelberg University, Heidelberg, Germany, [2] Division of Rheumatology, Department of Internal Medicine V, Heidelberg University, Heidelberg, Germany, [3] Department of Human Molecular Genetics, Heidelberg University, Heidelberg, Germany, [4] nCounter Core Facility, Department of Human Molecular Genetics, Heidelberg University, Heidelberg, Germany

OPEN ACCESS

Edited by:
Gustavo Javier Martinez, Rosalind Franklin University of Medicine and Science, United States

Reviewed by:
Ruoning Wang, The Research Institute at Nationwide Children's Hospital, United States
Heitor Affonso Paula Neto, Universidade Federal do Rio de Janeiro, Brazil

***Correspondence:**
Yvonne Samstag
yvonne.samstag@urz.uni-heidelberg.de

Specialty section:
This article was submitted to T Cell Biology, a section of the journal Frontiers in Immunology

Received: 18 June 2018
Accepted: 19 October 2018
Published: 14 November 2018

Citation:
Liang J, Jahraus B, Balta E, Ziegler JD, Hübner K, Blank N, Niesler B, Wabnitz GH and Samstag Y (2018) Sulforaphane Inhibits Inflammatory Responses of Primary Human T-Cells by Increasing ROS and Depleting Glutathione. Front. Immunol. 9:2584. doi: 10.3389/fimmu.2018.02584

The activity and function of T-cells are influenced by the intra- and extracellular redox milieu. Oxidative stress induces hypo responsiveness of untransformed T-cells. Vice versa increased glutathione (GSH) levels or decreased levels of reactive oxygen species (ROS) prime T-cell metabolism for inflammation, e.g., in rheumatoid arthritis. Therefore, balancing the T-cell redox milieu may represent a promising new option for therapeutic immune modulation. Here we show that sulforaphane (SFN), a compound derived from plants of the Brassicaceae family, e.g., broccoli, induces a pro-oxidative state in untransformed human T-cells of healthy donors or RA patients. This manifested as an increase of intracellular ROS and a marked decrease of GSH. Consistently, increased global cysteine sulfenylation was detected. Importantly, a major target for SFN-mediated protein oxidation was STAT3, a transcription factor involved in the regulation of T_H17-related genes. Accordingly, SFN significantly inhibited the activation of untransformed human T-cells derived from healthy donors or RA patients, and downregulated the expression of the transcription factor RORγt, and the T_H17-related cytokines IL-17A, IL-17F, and IL-22, which play a major role within the pathophysiology of many chronic inflammatory/autoimmune diseases. The inhibitory effects of SFN could be abolished by exogenously supplied GSH and by the GSH replenishing antioxidant N-acetylcysteine (NAC). Together, our study provides mechanistic insights into the mode of action of the natural substance SFN. It specifically exerts T_H17 prone immunosuppressive effects on untransformed human T-cells by decreasing GSH and accumulation of ROS. Thus, SFN may offer novel clinical options for the treatment of T_H17 related chronic inflammatory/autoimmune diseases such as rheumatoid arthritis.

Keywords: sulforaphane, primary human T-cells, reactive oxygen species, glutathione, T_H17, rheumatoid arthritis

INTRODUCTION

Sulforaphane (SFN) is a natural compound obtained from cruciferous vegetables like broccoli, watercress, brussels sprouts, cabbage, and cauliflower. It has the ability to induce phase II anti-oxidant enzymes and exerts anti-proliferative effects on cancer cells *in vitro* (1–3). Reactive oxygen species (ROS) promote tumor development and progression, which was the rationale of the hypothesis that the ROS-detoxification process induced by SFN might be useful as an adjuvant during anti-cancer therapy. In several phase I and II clinical trials, the therapeutic benefit of SFN has been evaluated for healthy individuals and cancer patients (4, 5). However, a beneficial effect for cancer patients could not be documented in these studies. One possible explanation that has been discussed is a limited SFN concentration or pharmacokinetics in the patients (5). It is also known that the control of tumors is highly dependent on the immune system. Thus, if immune cells would be inhibited by SFN, this immunosuppression could outweigh the anti-tumor effects. However, effects of SFN on the immune system of cancer patients were not considered.

Recently, some studies have provided first hints that SFN is indeed able to modulate the immune system. Kumar et al. demonstrated that *in vitro* the development of human myeloid-derived suppressor cells (MDSCs) from CD14+ monocytes cultured in glioma conditioned medium was inhibited by SFN, which may enhance T-cell proliferation (6). On the other hand, the study by Pal et al. suggested that effects induced by SFN eventually shifted human monocyte polarization to a direction specific to M2 macrophages, promoting an anti-inflammatory phenotype (7). Geisel et al. reported that in a murine system, SFN led to diminished IL-12 and IL-23 expression by dendritic cells (DCs) eventually interfering with pro-inflammatory immune responses (8). Yet, a direct effect of SFN on mouse T-cells was not observed. In line with these latter findings, SFN was found to ameliorate murine experimental arthritis (9) and experimental autoimmune encephalomyelitis (EAE) (8, 10). In contrast to the murine system, SFN also seemed to have a direct inhibitory effect on synovial T-cells derived from rheumatoid arthritis (RA) patients (9). However, the effect of SFN on primary human T-cells from healthy donors was so far not investigated. Given enormous species differences, this aspect is critical for estimating its potential clinical effects.

The molecular principle of how SFN acts in different cell types is as yet only partly understood. Nuclear factor erythroid 2 (NFE2)-related factor 2 (NRF-2) was identified as one target of SFN in murine lymphocytes, murine DCs and cancer cells (11–13). NRF-2 is a leucine-zipper protein that is activated by oxidative stress and induces transcription of genes coding for anti oxidant proteins. Consistent with this, SFN treatment has been shown to boost the ROS-scavenger glutathione (GSH) in murine DCs, and also to result in high expression of the antioxidant protein heme oxygenase-1 (HO-1) (12). In contrast, another study using murine spleen lymphocytes demonstrated that 20 μM SFN rather increased the basal levels of intracellular ROS in murine spleen lymphocytes (11).

Taken together, the existing data create a confusing picture of the effects of SFN on the intracellular redox homeostasis, which might be due to the different systems used, i.e., murine vs. human cells, adaptive vs. innate immune cells or tumor cells vs. primary cells. However, an exact knowledge of the SFN effect on the redox-regulation in human T-cells is crucial to estimate its clinical relevance in T-cell related diseases, since the redox balance strongly modulates T-cell functions (14). In this regards, we have shown earlier that reducing conditions favor activation of primary human T-cells (15), whereas oxidative stress leads to hyporesponsiveness or even cell death of primary human T-cells (16, 17). In line with these findings, it has recently been postulated that low ROS levels in RA patient derived T-cells connects cellular metabolism with auto-aggressive T-cell immunity including biased differentiation of T-cells into IFN-γ and IL-17-producing inflammatory cells (18). Thus, the main purpose of our current study was to investigate whether SFN may serve as a novel means to influence the redox-balance and thereby the function of primary human T-cells.

Here, we show that SFN suppressed costimulation-induced activation and proliferation of primary human T-cells without having cytotoxic effects. In particular, expression of T_H17-related proinflammatory genes were significantly diminished. These effects are attributable to redox regulation by SFN, since (i) SFN induced ROS and in parallel GSH depletion in primary human T-cells and (ii) thiol-containing antioxidants abolished the immunosuppressive effect of SFN. Taken together, our data imply that SFN may act as an immunosuppressive agent for primary human T-cells by regulating the T-cell redox equilibrium. This suppression of T-cell functions by SFN may be beneficial to control auto-inflammatory diseases such as RA.

MATERIALS AND METHODS

Reagents and Antibodies

SFN was purchased from LKT Laboratories (St. Paul, MN). The following chemicals were obtained from Sigma-Aldrich: N-acetylcysteine (NAC), Tiron, Trolox, N-ethyl maleimide (NEM) and 4′,6-Diamidino-2-phenylindole (DAPI). GSH, 5-(and-6)-chloromethyl-2′, 7′-dichlorodihydro-fluorescein diacetate, acetyl ester (CM-H_2DCFDA), ThiolTracker™ Violet and RPMI 1640 were purchased from Thermo Fisher Scientific. The cellular ROS/Superoxide detection assay kit was purchased from Abcam and carboxyfluorescein diacetate succinimidyl ester (CFSE) was from Invitrogen. SiR-actin was ordered from Cytoskeleton Inc. Fetal bovine serum (FBS) was bought from PAN-Biotech and BD FACS™ lysing solution from BD Bioscience. IL-2 was purchased from Peprotech. Human CD8/NK and T_H cytokines panel were from BioLegend. Direct-zol™ RNA MiniPrep kit was purchased from QIAGEN and nCounter® GX Human Immunology v2 panel from nanoString Technologies. Vivaspin 6 (10,000 MWCO) columns were bought from Sartorius.

Antibodies employed in this study were specific for the following molecules: CD3 (clone OKT3 mouse mAb), CD28 (clone 28.2, BD Pharmingen), isotype control antibodies IgG1 and IgG2a (mouse mAb, BD Biosciences), cysteine sulfenic

acid (rabbit polyclonal antibody, Merck), Prx1 (peroxiredoxin1, rabbit polyclonal antibody, Invitrogen), Trx (thioredoxin, Clone 2G11, mouse mAb, BD Bioscience), phospho-STAT3 (pSTAT3, #9131, Cell Signaling Technology), STAT3 (#9139, Cell Signaling Technology), and GAPDH (clone 6C5, mouse mAb, Invitrogen). For the secondary antibodies, donkey anti-rabbit IgG (H+L)-AF488 antibody was purchased from Dianova. IRDye® 800CW donkey anti-rabbit and IRDye® 680CW donkey anti-mouse were purchased from LICOR Biosciences. 7-AAD, Annexin-V and all fluorescently labeled antibodies were bought from BD Bioscience.

Primary Human T-Cell Preparation and Cell Culture

Human peripheral blood mononuclear cells (PBMCs) were obtained by Ficoll–Hypaque (Linaris, Wertheim-Bettingen, Germany) density-gradient centrifugation of heparinized blood from healthy volunteers. T-cells were isolated using the pan T-cell isolation kit purchased from Miltenyi Biotec (Bergisch Gladbach, Germany) as per the manufacturer's instructions. The human T-leukemia cell line Jurkat ACC282 and B-leukemia cell line Raji were grown in RPMI 1640 complete medium containing 10% FBS at 37°C and 5% CO_2. This study was approved by the Ethics Committee of the Heidelberg University (S-269/2015).

Sampling of Blood From RA Patients

Heparinized peripheral blood was collected under aseptic conditions from patients with RA. Informed consent for use of the cells was obtained from all RA patients included in this study. This study was approved by the Ethics Committee of the Heidelberg University (S-119/2017).

T-Cell Costimulation

To co stimulate human peripheral T-cells, microplates (Nunc, Wiesbaden, Germany) were pre-coated with goat anti-mouse IgG+M antibody followed by blocking with complete RPMI medium (RPMI+10% FBS), coating with anti-CD3 (20 ng/mL), and anti-CD28 (5 μg/mL) antibodies or the respective isotype controls. T-cells were spun down on the antibodies and incubated at 37°C for the indicated time points.

Cell Viability Assay

Primary human T-cells or Jurkat T-leukemia cells were cultured in 200 μl complete RPMI medium for the indicated time points with or without SFN (5% CO_2 and 37°C). For viability assays, cells were washed with pre-warmed phosphate-buffered saline (PBS), resuspended in Annexin-V binding buffer containing 7-AAD and Annexin-V and incubated 15 min at room temperature (RT). After washing once with Annexin-V binding buffer, cells were acquired via flow cytometry (LSRII, BD Bioscience, Heidelberg, Germany) and data were analyzed with FlowJo X (FlowJo LLC, Ashland, OR, USA).

T-Cell/APC Conjugate Formation

Conjugates were formed between T-cells and staphylococcus aureus enterotoxin B (SEB) loaded Raji cells as described previously (19). Briefly, T-cells were pre-incubated in the absence or presence of 10 μM SFN for 1 h and Raji cells were loaded with 5 μg/ml SEB or kept unloaded. Then, T-cells and Raji cells were coincubated at a ratio of 1:1 for 45 min at 37°C. Cells were fixed using 1.5% PFA and stained with anti-CD3-APC and anti-CD19-PerCP-Cy5.5 antibodies. Cell couple formation was determined by flow cytometry. Double positive events ($CD3^+CD19^+$) were counted as cell couples.

Analysis of Immune Synapses (IS) by Multispectral Imaging Flow Cytometry (MIFC)

Conjugates were formed between T-cells and SEB loaded Raji cells as described above. Briefly, T-cells were incubated in the absence or presence of 10 μM SFN for 1 or 24 h at 37°C. Then 1×10^6 T-cells/sample were mixed at a 1:1 ratio with Raji cells that were either loaded with 5 μg/ml SEB or kept unloaded, and the cells mixture was incubated for 45 min at 37°C to allow for IS formation. Then cells were fixed in 1.5% PFA, and stained with anti-CD3-PE-TxR, anti-LFA-1-FITC, and DAPI. Thereafter, cells were subjected to MIFC (IS100, Amnis Corp., Seattle, WA, USA) and as many as 15,000 images per sample were acquired. Subcellular localization of proteins was analyzed with IDEAS 6.0 software (Amnis, Seattle, WA, USA) as described previously (20).

Detection of T-Cell Activation

T-cells were kept untreated or treated with SFN and co-stimulated with plate bound anti-CD3/CD28 antibodies (for details see above). Activation of T-cells was evaluated by the expression of CD25 and CD69. Briefly, T-cells were washed once with FACS wash (FW) buffer (0.5% BSA, 0.5% FBS, and 0.07% NaN_3 in 1 X PBS) to remove the culture medium. The cell pellet was resuspended in FW containing anti-CD25-APC and anti-CD69-PE antibodies and incubated for 20 min at RT. Thereafter, cells were washed and analyzed by flow cytometry. To determine the total amount of CD25 and CD69 (cell surface plus intracellular), cells were fixed with 1.5% PFA and permeabilized with FWS (FW containing 0.1% saponin) prior to antibody staining.

Assessment of T-Cell Proliferation

T-cells were washed with pre-warmed PBS, resuspended in PBS, loaded with 1 μM CFSE and incubated for 15 min at 37°C. After washing once with PBS to remove unbound CFSE, SFN was added for 30 min and the cells were seeded on 96-well microplates coated with anti-CD3/CD28 antibodies for co-stimulation as described above. Proliferation was determined after 3 days of incubation using flow cytometry. The proliferation index was calculated according to the instruction of FlowJo documentation. Briefly, the number of cells at the beginning of cell culture (Ns = G0 + G1/2 + G2/4 + G3/8), the total number of divisions (Nt = (G1/2)*1 + (G2/4)*2 + (G3/8)*3) and the number of cells that subjected to division (Nd = Ns–G0) were calculated first. The proliferation index results from the ratio of Nt and Nd.

Cytokine Assay

Human CD8/NK and T_H cytokine panels were used to detect secreted cytokines. To this end, SFN treated T-cells or untreated T-cells (1×10^5 T-cells/100 μl), concentrations as indicated, were co-stimulated with crosslinked anti-CD3/CD28 antibodies.

After 2 days of incubation, the samples were centrifuged, cell-free supernatants were collected and immediately aliquoted and stored at −80°C. The cytokine assay was performed using undiluted samples and 96-well U-bottom microplates as per the manufacturer's instructions.

Detection of Intracellular ROS Levels

Intracellular ROS levels were detected by using the ROS detection reagent CM-H_2DCFDA. T-cells (1×10^6 T-cells/ml) or Jurkat T-leukemia cells were washed with PBS and the cell pellet was re-suspended in PBS. CM-H_2DCFDA was added to a final concentration of 5 μM, and the cell suspension was incubated for 15 min at 37°C in the dark. After washing twice with PBS, the cell pellet was re-suspended in RPMI 1640 complete medium and SFN was added as indicated in the respective figures. As control, we used H2O2 (50 μM for PBTs and 50 μM to 200 μM for Jurkat T-leukemia cells). The fluorescence intensity was immediately determined by flow cytometry and analyzed with FlowJo X.

For detecting of the intracellular ROS level of lymphocytes in whole blood, heparinized peripheral blood from RA patients was pre-treated with 10 μM SFN or left untreated for 5 min (Fresh blood was used up to 2 h after blood donation) at RT. Alexa Fluor® 700-CD45 antibody was used to stain leukocytes, and CM-H_2DCFDA was used to stain intracellular ROS. After staining for 15 min, blood samples were proceeded to erythrocyte lysis with FACS™ lysing solution, washed twice with FW, and measured by flow cytometry and analyzed with FlowJo X.

Detection of Intracellular GSH Levels

The intracellular GSH levels were detected using ThiolTracker™ violet dye according to manufacturer's instructions. Briefly, T-cells or Jurkat T-leukemia cells were kept untreated or treated with the indicated concentration of SFN in RPMI 1640 complete medium. After SFN treatment for the indicated time points, cells were spun down and the supernatant was removed. Cells were rinsed twice with pre-warmed PBS and re-suspended in 100 μl PBS containing 2 μM ThiolTracker™ violet dye and incubated for 15 min at 37°C. After washing and resuspending in 100 μl PBS, cells were immediately measured using flow cytometry and analyzed with FlowJo X.

Assessment of Cysteine Sulfenylation

For assessment of global sulfenylation on cysteine thiols, a dimedone specific antibody was used. Quantification of dimedone signal was performed using flow cytometry and super-resolution microscopy (Structured illumination microscopy, SIM using N-SIM, Nikon). For flow cytometric analysis, 2×10^5 T-cells were treated with 10 μM SFN or kept untreated for 10 min at 37°C. Thereafter, samples were washed and fixed for 10 min with 1.5% PFA containing 0.25% DMSO and 5 mM dimedone, and permeabilized with FWS. Rabbit anti-dimedone serum (1:1,500) and anti-rabbit AF488 (1:1,200) were used to detect the dimedone signal, and data were analyzed with FlowJo X. For microscopic analysis, 2×10^5 T-cells were initially allowed to adhere on coated coverslips and immunocytochemistry protocols were performed as described (21). After adherence on the coverslips, SFN treatment, fixation, and permeabilization were performed as described above. Thereafter, the samples were stained with rabbit anti-dimedone serum (1:1,500) and anti-rabbit AF488 (1:1,200) sequentially. During the process of secondary antibody staining, nuclei were stained with DAPI (1:5,000), and F-actin was detected by incubation with SiR-actin (500 nM). Images of the cells were acquired using an N-SIM microscope equipped with a 100x objective (NA 1.49).

Kinetic Trapping by Trx1

The Trx1 trapping mutant (Trx1 C35S) was purified and loaded on streptavidin beads as described (22). Briefly, T-cells from healthy donors were treated with the indicated concentrations of SFN or H_2O_2 for 10 min at RT. Thiols within the cells were alkylated using 100 mM NEM for 5 min. Excess amount of NEM was removed by extensive washing with PBS. Thereafter, the cells were lysed in TBS with 1% Triton X-100 and protease inhibitor cocktail for 30 min on ice. The cytoplasmic fraction was collected by centrifugation at 10,000 × g for 10 min. The postnuclear lysates were loaded on streptavidin beads that had been preloaded with Trx1 trapping mutant (Trx1 C35S SBP 6x His). The Trx1 loaded beads and lysates were incubated for 3 h on a rotator at 4°C, then the reaction was stopped by adding NEM to a final concentration of 20 mM and incubating on ice for 5 min. Unbound proteins were washed out extensively with the following buffers stepwise: 1% Triton X-100, 500 mM NaCI, 1 mM NEM, 1 M Urea in 1x TBS, 1% Triton X-100, 1 mM NEM in 1x TBS, and 1% Triton X-100 in 1x TBS. The Trx1 C35S and kinetically trapped proteins were released from the streptavidin beads using excess amount of biotin in the elution step. Next, the eluted proteins were concentrated using protein concentrator vivaspin 6 (10,000 MWCO) columns. Finally, the samples were divided into two and mixed with 1x reducing (DTT) or nonreducing (without DTT) sample buffer. The preparates were loaded on SDS-PAGE and immunoblotted for the indicated proteins.

Gene Expression Profiling

The nCounter® Nanostring GX Human Immunology v2 panel designed for the expression analysis of 579 immune and inflammation associated target genes and 15 internal reference control genes, was used for expression profiling. In brief, total RNA was extracted from all samples (1×10^6 T-cells/sample) by Trizol per the manufacturer's instructions. Subsequently, nCounter® Nanostring based gene expression profiling was performed on 25 ng total RNA from each sample. All RNA samples were quantified by using Qubit™ RNA assay kits and quality control was performed on the Agilent 2100 Bioanalyzer system. Qualified samples were subjected to overnight hybridization reaction at 65°C, where 5 μl of total RNA samples were combined with 3 μl of nCounter® reporter CodeSet in 5 μl of hybridization buffer and 2 μl of nCounter® capture ProbeSet for a total reaction volume of 15 μl and incubated for 20 h. Ramp reactions down to 4°C. Afterwards, samples were purified and immobilized on a cartridge and data assessed on the nCounter® *SPRINT* Profiler. During sample processing, the instrument performs a number of tasks including liquid transfers, magnetic bead separation, and immobilization

of molecular labels on the sample surface. This is followed by data collection with an automated fluorescence microscope and digital analysis system. The results then are exported as a comma separated values (CSV) file and analyzed using NanoString's analysis software nSolver 4.0 and R statistical software.

Western Blotting

For total lysate preparation, T-cells (1×10^6 T-cells/ml) were washed with PBS and lysed using PBS with 1x reducing or non-reducing sample buffer. Then the total lysates were run on polyacrylamide gels, proteins were blotted on PVDF-membranes and the membranes were blocked in blocking buffer for 1 h. Afterwards, membranes were stained with primary antibodies against pSTAT3 (1:1,000), STAT3 (1:1,000), GAPDH (1:10,000), Prx1 (1:1,000), Trx1 (1:1,000), and respective secondary antibodies. The membranes were scanned by a Licor infrared scanner (LI-COR Biosciences).

Statistical Analysis

The statistical analysis was performed with GraphPad Prism version 6.00 (STATCON, Witzenhausen, Germany). Two groups were compared using *t*-test or paired *t*-test for matched observations. Multiple groups were compared using ANOVA. Heat maps were generated with R statistical software.

RESULTS

SFN Is Not Toxic to Untransformed Human T-Cells but to Jurkat T-Leukemia Cells

To elucidate the influence of SFN on untransformed human T-cells, we prepared freshly isolated peripheral blood T-cells and incubated these cells with SFN. In previous studies, concentrations of SFN up to 80 μM were used for different *in vitro* experiments. However, since a maximum concentration of 2.5 μM SFN was detected in human plasma after broccoli sprout consumption (23), we did not exceed 20 μM SFN in our current study.

To investigate whether SFN is toxic to primary human T-cells, we first assessed T-cell viability after 1 day of SFN treatment. To this end, we used Annexin-V to specifically identify apoptotic cells, and 7-AAD to evaluate cells with progressive loss of membrane permeability, i.e., dead cells. Dual staining with 7-AAD and Annexin-V-PE showed that SFN had no cytotoxic effect on primary human T-cells up to the maximal concentration of 10 μM (**Figures 1A,B**). To substantiate our finding, we also measured the mitochondrial membrane potential of SFN treated T-cells using TMRM (**Supplementary Figure 1**). In line with the former assay, the mitochondrial membrane potential was not disturbed by SFN. Since cytotoxic effects of SFN were described for tumor cells such as breast cancer cells and prostate cancer cells (24, 25), and especially also for acute lymphoblastic leukemia cells (3), we also measured the effects of SFN on the viability of the Jurkat T-leukemia cell in parallel. Notably, although primary human T-cells did not show any increased levels of apoptosis (**Figures 1A,B**), there was a concentration-dependent increase in toxicity toward Jurkat T-leukemia cells (**Figure 1C**). This clearly shows that in physiologically relevant concentrations SFN negatively influences the survival of malignant T-cells but not of untransformed primary human T-cells.

SFN Does Not Impair T-Cell/APC Conjugate and Immune Synapse Formation

To evaluate the effects of SFN on T-cell activation, we analyzed early and late activation events. Crucial initial steps in that regard are the T-cell/APC (antigen-presenting cell) conjugate formation and maturation of an immune synapse (IS). To investigate this, T-cells were pre-treated with 10 μM SFN or kept untreated for 1 h, then incubated with SEB loaded Raji cells that served as APCs. T-cell/APC couples were identified by a flow cytometry-based conjugate assay (**Figure 2A**). Single CD3 or CD19 positive events represented solitaire T-cells or solitaire Raji cells, respectively, whereas CD3/CD19 double positive events arose from T-cell/APC conjugates. As expected, in the absence of SEB, only 1.65% T-cell/APC conjugates were found (**Figure 2A**, left part). In the presence of SEB, both the untreated and SFN treated group showed a clear formation of T-cell/APC conjugates, i.e., 9.49 or 9.05%, respectively (**Figure 2A**, middle and right part). To quantify the percentage of T-cell/APC conjugates, we acquired up to 10,000 T-cells in three independent experiments and found that T-cell/APC conjugate formation was not significantly influenced by SFN treatment (**Figure 2B**).

Although T-cell/APC conjugate formation can be measured using flow cytometry, this technique is limited for evaluating spatial informations which are important for analysing the formation of the immune synapse. We, therefore, took advantage of MIFC, which combines fluorescence microscopy and flow cytometry and is a suitable means for the analysis of immune synapse formation (26). By defining regions of interest, MIFC allows the spatial quantification of fluorescence signals within T-cells, and thus of the accumulation of receptors at the T-cell/APC interface. In brief, T-cell/APC couples were identified according to DAPI staining and CD3 expression. Then, the accumulation of the TCR/CD3 complex and LFA-1 in the T-cell/APC contact zone was used as measure for the formation of a mature immune synapse. As expected, while most T-cells showed no enrichment of TCR/CD3 and LFA-1 in the contact zone without SEB treatment, a clear receptor enrichment—and thus immune synapse maturation—was observed in the presence of SEB (**Figures 2C,D**). Consistent with the contact formation analysis by flow cytometry, SFN treatment did not impair the immune synapse formation.

SFN Inhibits CD25/CD69 Expression and Proliferation of Primary Human T-Cells

Early T-cell activation events such as T-cell/APC conjugate and immune synapse formation were seemingly not changed by SFN. We, therefore, continued to investigate the T-cell activation process at later stages. To this end, we first analyzed the surface T-cell activation markers, CD25 and CD69. After 12 h of T-cell costimulation with anti-CD3/CD28 antibodies in the absence of SFN, CD25 and CD69 were strongly expressed, while their

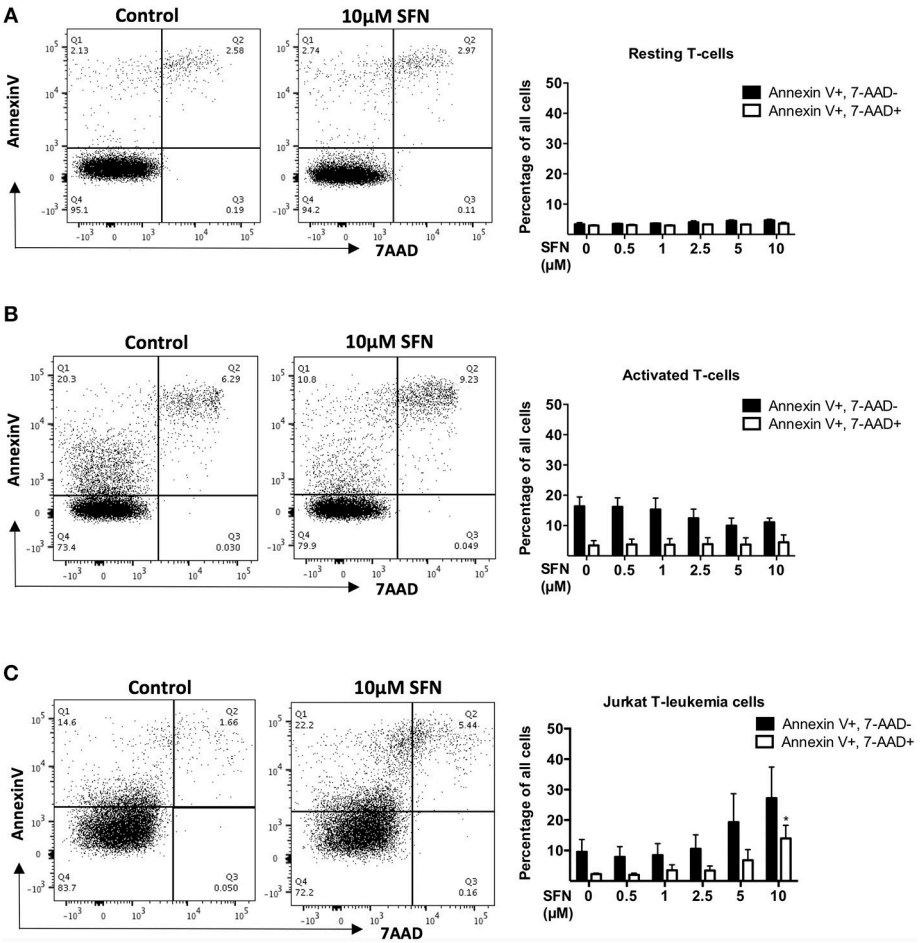

FIGURE 1 | SFN is not cytotoxic to untransformed human T-cells but to Jurkat T-leukemia cells. **(A,B)** Flow cytometry analysis of T-cell viability, resting T-cells were treated with SFN as indicated and **(A)** kept unstimulated (resting T-cells) or **(B)** co-stimulated with anti-CD3(20 ng/ml)/CD28 (5 μg/ml) antibodies for 1 day (activated T-cells), thereafter stained with 7-AAD and Annexin-V. **(C)** Flow cytometry analysis of Jurkat T-leukemia cell viability. Cells were treated with SFN as indicated for 1 day, thereafter stained with 7-AAD and Annexin-V. Shown are representative flow cytometry dot plots (left panel) from three experiments and the corresponding quantification (right panel; $n = 3$; mean; SE; $^*p < 0.05$).

expression was diminished in a dose-dependent manner in the presence of SFN (**Figure 3A**). Notably, even 2.5 μM SFN, a concentration that can be found in human serum after broccoli sprout consumption, was sufficient to dampen the expression of CD25 (and slightly CD69) on the surface of T-cells. We have previously shown that not only the expression, but also the transport of CD25 and CD69 to the T-cell surface requires costimulation (19). To clarify whether the decreased level of CD25 and CD69 was due to impaired functioning of the surface transport or overall expression, we stained the total amount of these proteins within the cells, i.e., after permeabilization with FWS. The results were similar compared to the cell surface staining (**Supplementary Figure 2**), which indicates that SFN inhibited the expression of both proteins, CD25 and CD69. Next, we quantified the expression of the T-cell growth factor IL-2 in the supernatants of T-cells that were treated with various concentrations of SFN and then costimulated for 2 days. **Figure 3B** shows that the level of IL-2 in the supernatant of T-cells significantly decreased with increasing SFN concentrations.

T-cell activation initiates intracellular signaling cascades that ultimately result in T-cell proliferation. Labeling of T-cells with CFSE allows to monitor T-cell division over time. Thus, we pre-treated CFSE-labeled T-cells with SFN and detected the proliferation after 3 days of costimulation using flow cytometry. In line with the finding that expression of IL-2 and the IL-2 receptor CD25 were dampened by SFN, treatment with SFN significantly diminished T-cell proliferation compared to the control cells (**Figure 3C**, left panel). Again, even low SFN concentrations (2.5 μM) were sufficient to hamper T-cell proliferation. Notably, this phenotype could not be rescued by adding exogenous IL-2 (40 U/ml) to costimulated T-cells (**Figure 3C**, right panel). Moreover, the SFN-mediated decrease in CD25 and CD69 expression was not restored by addition of IL-2 (**Supplementary Figure 3**). Collectively, these results show that SFN interfered with T-cell activation events.

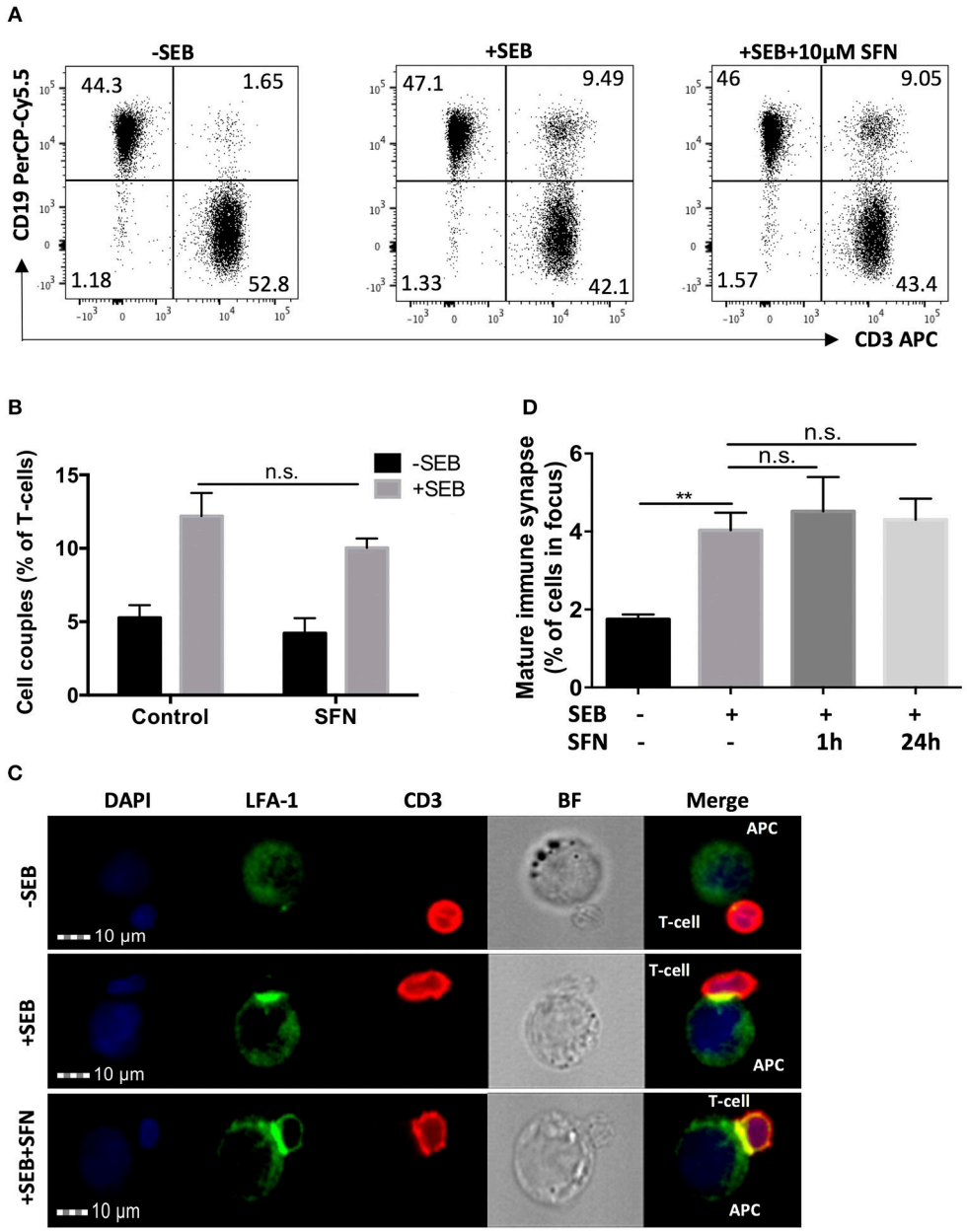

FIGURE 2 | Intact immune synapse formation of SFN treated T-cells. **(A)** Dot plots of T-cell/APC couple formation were identified by flow cytometry-based conjugate assay via CD3 and CD19 expression. T-cells were treated without (left and middle panel) or with (right panel) 10 μM SFN prior to incubation with APCs in the absence (left panel) or presence (middle and right panel) of SEB. Dot plots are representative for three experiments. **(B)** Quantification of the couple formation between T-cells and APCs ($n = 3$; mean; SE). **(C)** Multispectral imaging flow cytometry analysis of mature synapse formation. T-cells were treated without (upper and middle panels) or with (lower panel) 10 μM SFN prior to incubation with APCs in absence (upper panel) or presence (middle and lower panels) of SEB. Cells were stained for nuclei (DAPI, blue), LFA-1 (green) and CD3 (red). The merged image represents the digital overlay of all three colors. Bright field (BF) and fluorescence images are representative for three experiments. **(D)** Quantification of the mature immune synapse between T-cells and APCs. At least 15,000 cells were acquired by imaging flow cytometry for each condition ($n = 3$; mean; SE; $^{**}p < 0.01$).

SFN Induces a Pro-Oxidative Milieu in Untransformed Human T-Cells

ROS are ubiquitously generated and recognized as important signaling molecules for T-cell activation, but excessive ROS generation or prolonged exposure to high ROS concentrations impair T-cell functions (27). SFN was previously reported to have mostly antioxidative effects by promoting Nrf-2 activation (13). Since the effect of SFN on the redox system of primary human T-cells remained unclear, we sought to evaluate the intracellular ROS level in untransformed human T-cells after SFN treatment.

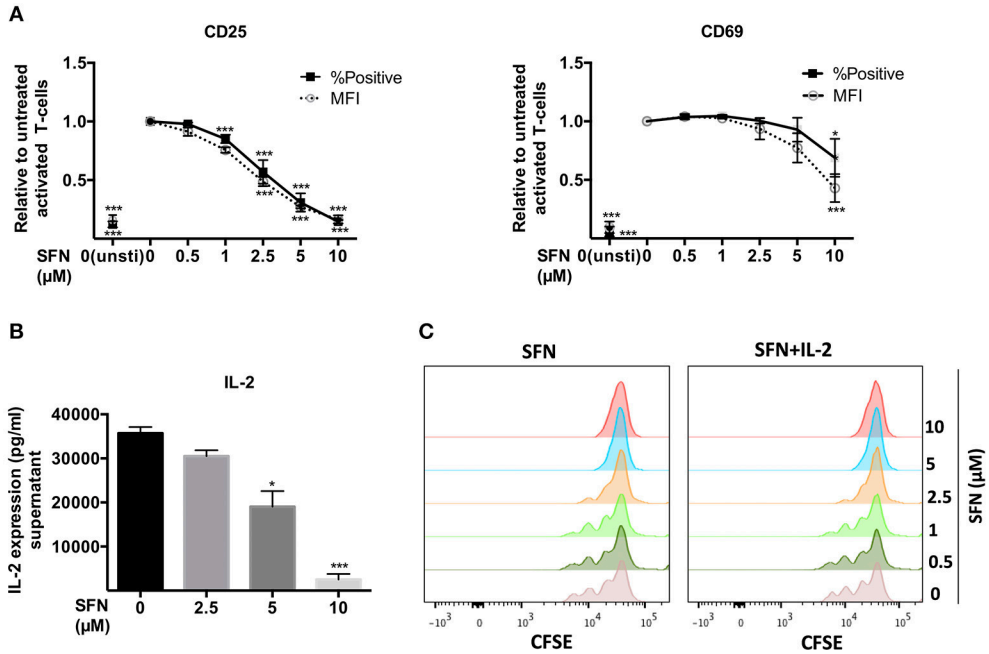

FIGURE 3 | SFN inhibits activation of untransformed human T-cells. **(A)** Flow cytometry analysis of CD25 and CD69 surface expression in T-cells post 12 h stimulation with anti-CD3(20 ng/ml)/CD28(5 μg/ml) antibodies or unstimulated T-cells (unsti). Given are expression levels relative to the stimulated control (no SFN treatment) in terms of %positive cells (black square, solid line) and mean fluorescence intensities (MFI, open circle, dashed line) ($n = 3$; mean; SE; $^{*}p < 0.05$, $^{***}p < 0.001$). **(B)** Quantification of IL-2 production in the supernatant of T-cells without (black histogram) or with SFN (gray histograms) treatment as indicated ($n = 3$; mean; SE; $^{*}p < 0.05$, $^{***}p < 0.001$). **(C)** T-cell proliferation detected via staining of CFSE. T-cells were co-stimulated in the absence/presence of SFN without /with addition of exogenous IL-2. CFSE signals were measured by flow cytometry after 3 days of co-stimulation. Histograms are representative for three experiments.

To this end, T-cells were loaded with the ROS-sensitive probe CM-H_2DCFDA and treated with SFN prior to flow cytometric analysis. SFN treatment induced a significant accumulation of ROS in untransformed human T-cells in a concentration dependent manner (**Figure 4A**). At a concentration of 10 μM SFN, the intracellular ROS levels were comparable to those observed after treatment of 50 μM H_2O_2. The increased intracellular ROS levels after SFN treatment were also confirmed by another assay (cellular ROS/Superoxide detection kit, Abcam, data not shown).

We next examined the intracellular levels of the important ROS-scavenger GSH in T-cells using ThiolTracker^{TM} violet dye and flow cytometry. These experiments showed that SFN decreased the intracellular GSH levels in SFN treated T-cells compared to untreated T-cells (**Figure 4B**). Notably, whereas higher SFN doses were needed to diminish the GSH levels after 1 h, very low SFN concentrations (e.g., 1 μM) were sufficient to significantly interfere with the amount of GSH in T-cells after 1 day. Taken together, these data suggest that SFN has a pro-oxidative effect on untransformed human T-cells leading to an increase of ROS levels and depletion of the ROS-scavenger GSH. Interestingly, in Jurkat T-leukemia cells, SFN also increased the ROS levels (**Figure 4C**). However, in contrast to untransformed human T-cells, in which SFN treatment led to a decrease of GSH, the GSH level in Jurkat T-leukemia cells showed a significant increase after 1 day of SFN treatment (**Figure 4D**). This difference was also confirmed by another GSH specific reagent, namely thiol green dye (**Supplementary Figure 4**). This underpins our previous observation regarding cell viability (**Figure 1**) that SFN affects tumor cells and primary cells differently.

To further elucidate the pro-oxidative effect of SFN on untransformed human T-cells, we next investigated whether SFN promotes oxidation of cellular proteins. The first state of oxidation of thiols (sulfenylation) is reversible and transient. Sulfenylated cysteines are protected from further oxidation either by glutathionylation (S-glutathionylation) or by reduction, e.g., via the Trx1 system. If not protected, the oxidation into disulphide bridge formation or higher oxidation states, namely sulfinylation or sulfonylation will take place. To investigate protein sulfenylation, we treated the cells with 10 μM SFN for up to 10 min and monitored protein sulfenylation by dimedone. Dimedone is a cell-permeable reagent that exclusively recognizes and binds to cysteines at their sulfenylated form (28). **Figure 4E** shows representative N-SIM images of T-cells which revealed a slightly increased global dimedone signal in the cytoplasm and on the cell surface upon SFN treatment. To better quantify the dimedone signal, we, in addition, performed flow cytometric analysis. Similarly, flow cytometry results revealed a significant increase in sulfenylated cysteines after treatment with SFN, as depicted by an increase of the dimedone MFI (**Figure 4F**). These results imply that SFN increases protein oxidation in primary human T-cells.

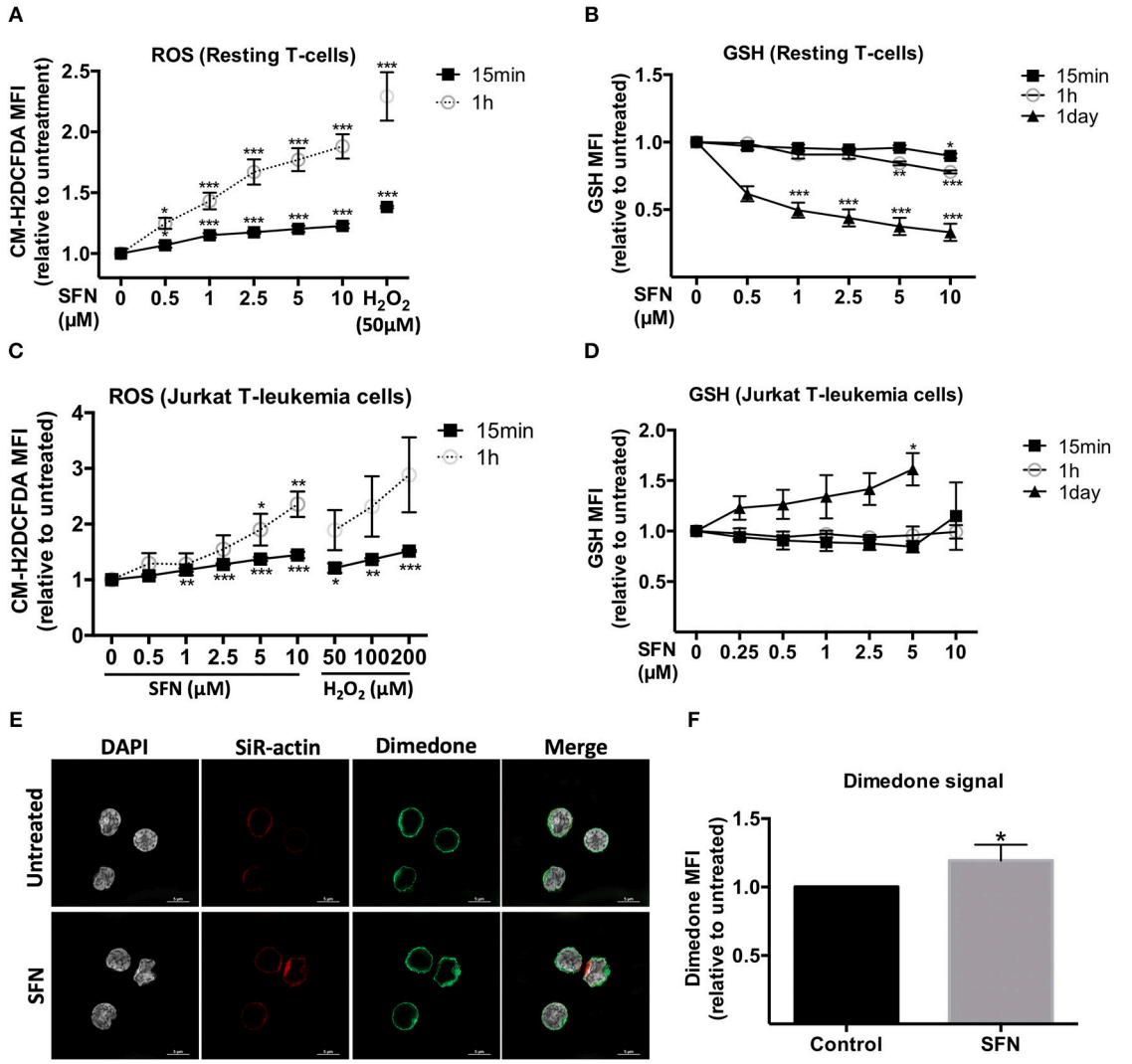

FIGURE 4 | Influence of SFN on the redox state of untransformed human T-cells and Jurkat T- leukemia cells. **(A,C)** Intracellular ROS levels in T-cells and Jurkat T-leukemia cells, respectively, were assessed by flow cytometry. Cells were pre-loaded with CM-H_2DCFDA and, thereafter, treated without or with SFN as indicated for different time points ($n = 3$; mean; SE; $^*p < 0.05$, $^{**}p < 0.01$, $^{***}p < 0.001$). **(B,D)** Intracellular GSH levels of T-cells and Jurkat T-leukemia cells, respectively, were assessed by flow cytometry. Cells were treated with SFN as indicated for different time points and stained with ThiolTracker^{TM} violet dye for 15 min ($n = 3$; mean; SE; $^*p < 0.05$, $^{**}p < 0.01$, $^{***}p < 0.001$). **(E)** Sulfenylated cysteines in T-cells were detected by microscopy. SFN treated T-cells were fixed and permeabilized, stained with DAPI (white), a dimedone specific antibody (green), and SiR-actin (blue). The merged image represents the digital overlay of all four colors. Images are representative for three experiments. **(F)** Quantititive analysis of cysteine sulfenylation by flow cytometry. Histogram shows the MFI relative to control of three independent experiments ($n = 3$; mean; SE; $^*p < 0.05$).

Inhibitory Effects of SFN on T-Cell Activation Are Abrogated by Thiol-Containing Antioxidants

We next aimed to clarify whether the immunosuppressive effect of SFN on T-cells is due to the pro-oxidative capacity of this substance. To this end, we made use of the antioxidants N-acetyl-cysteine (NAC), Tiron and Trolox. Of those only NAC treatment can lead to replenishment of GSH stores (29), while Tiron and Trolox do not. Notably, we observed that only NAC (2 mM), not Tiron or Trolox, reversed the SFN-induced downregulation of CD25 and CD69 (**Figure 5A**). Moreover, NAC abolished the inhibitory effect of SFN on T-cell proliferation (**Figure 5B**). This suggested that SFN mainly exerts its inhibitory effects on T-cell functions via oxidation of cysteine residues through depleted GSH stores. To further substantiate this hypothesis, we tested the effects of SFN on T-cell activation in the presence and absence of exogenously added GSH. Indeed, GSH completely prevented the SFN-induced defect in the costimulation-dependent upregulation of CD25 and CD69, and T-cell proliferation (**Figures 5C,D**). Taken together, these results show that SFN mediates immunosuppressive effects on untransformed human T-cells via depletion of intracellular GSH.

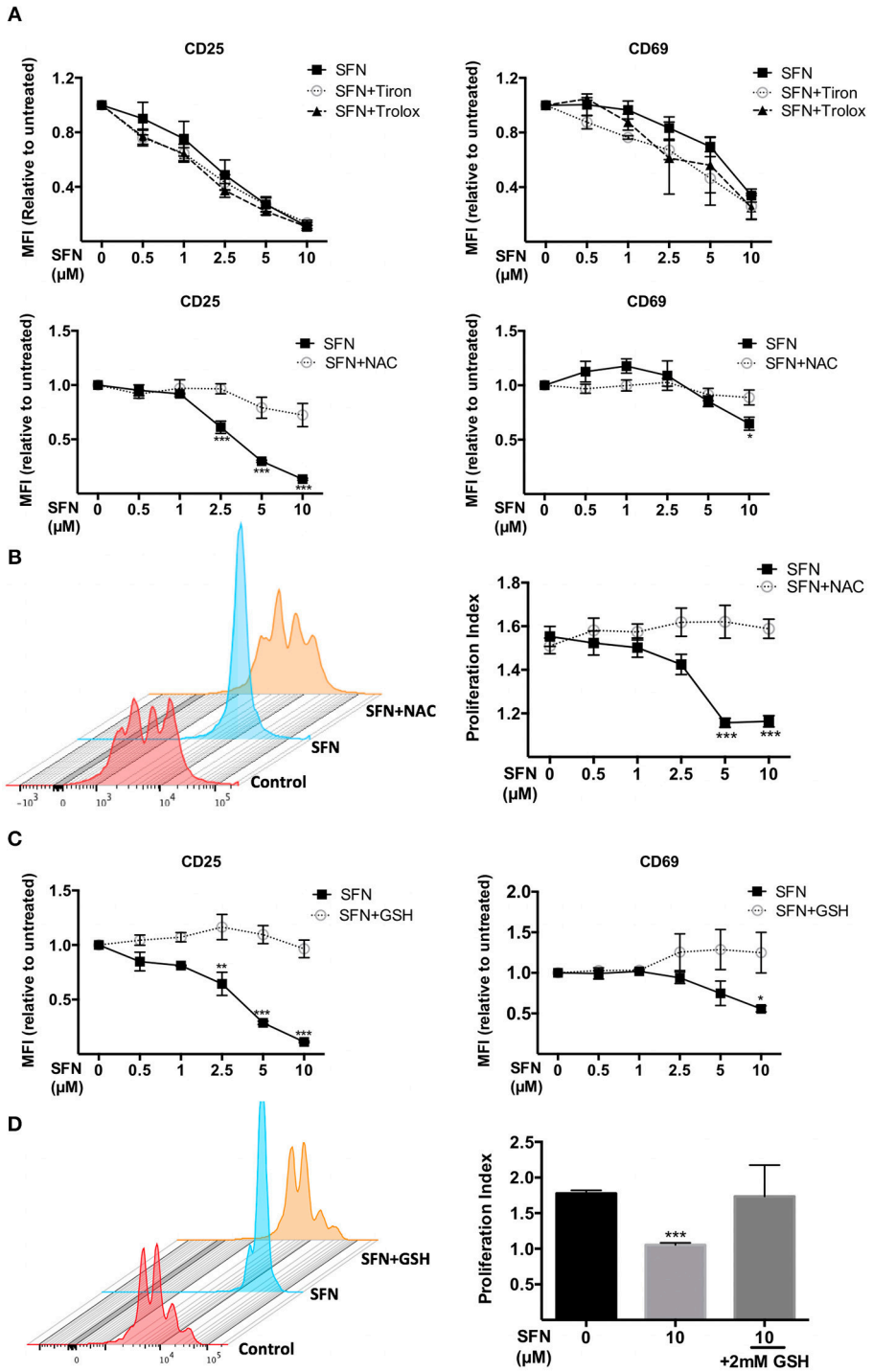

FIGURE 5 | Immunosuppressive effects of SFN were abrogated by thiol-containing antioxidants. **(A,C)** Expression of CD25 (left) and CD69 (right) in T-cells were analyzed by flow cytometry under the indicated conditions. T-cells in the presence/absence of SFN and **(A)** Tiron, Trolox (upper graphs), NAC (lower graphs) or **(C)** GSH were co-stimulated with anti-CD3(20 ng/ml) /CD28(5 μg/ml) antibodies for 1 day. Shown are the MFI ratios of SFN treated to untreated samples ($n = 3$; mean; SE; $^{*}p < 0.05$, $^{**}p < 0.01$, $^{***}p < 0.001$). **(B,D)** T-cell proliferation was detected via staining of CFSE. T-cells were loaded with CFSE, thereafter co-stimulated with anti-CD3 (20 ng/ml)/CD28 (5 μg/ml) antibodies in the absence/presence of SFN without and with addition of exogenous NAC **(B)** or GSH **(D)**. CFSE signals were measured after 3 days of co-stimulation by flow cytometry. Shown are representative histograms (left) and the proliferation index (right) from three independent experiments ($n = 3$; mean; SE; $^{***}p < 0.001$).

Gene Expression Analysis Revealed That T_H17-Related Genes Are Highly Sensitive to SFN

To get an unbiased view on differential mRNA expression profiles in untransformed T-cells after co-stimulation in the presence vs. absence of SFN, we compared the expression of 594 immune relevant genes using the NanoString GX Human Immunology v2 panel. The evaluated genes were associated with leukocyte functions including major classes of cytokines and their receptors. After normalization of the raw counts based on the six housekeeping genes, datasets from three experiments were visualized by hierarchical clustering (**Figure 6A**). Upon SFN treatment, we found that 39 genes were downregulated and 13 genes were upregulated (fold change >2, $p < 0.05$) as compared to untreated cells. Notably, consistent with our findings that SFN inhibited CD25 and IL-2 protein expression, the mRNA levels of CD25 (*IL-2RA*) and IL-2 were substantially decreased by SFN treatment (**Figure 6B**). Moreover, the expression of signal transducer and activator of transcription 5A (*STAT5A)*, an essential mediator of IL-2 signaling in T-cells (30), also decreased with SFN treatment, which may, together with the diminished CD25 expression, explain why the addition of exogenous IL-2 was not sufficient to rescue proliferation of SFN treated T-cells (see above).

Most intriguingly, the expression of T_H17-related genes such as *IL17A, IL17F, IL22,* and B-cell activating transcription factor (BATF) was strongly decreased by SFN, while T_H1, T_H2 or Treg related genes, i.e., *STAT4*, *IL-4,* and *FOXP3* were no major targets of SFN (**Figure 6C**). To substantiate the finding that T_H17-related genes are highly sensitive to SFN-treatment, we measured the amount of IL-17A at the protein level in the supernatants of T-cells pre-incubated in the presence or absence of SFN and costimulated for 2 days. In accordance with the mRNA data, SFN significantly diminished the amount of IL-17A (**Figure 6D**). Note that supplementary treatment with NAC could rescue the decrease in IL-17A production upon SFN treatment. These data show that SFN strongly affects T_H17 polarization.

SFN Induces Thiol Oxidation on STAT3 and Inhibits STAT3 Phosphorylation

Since T_H17 related genes were suppressed by SFN on both mRNA and protein level, we next aimed to clarify how SFN affects T_H17 cells. STAT3 is essential for the differentiation of T_H17 cells (31, 32). We, therefore, analyzed the regulation of STAT3 at the posttranslational level by means of thiol oxidation on cysteines and phosphorylation upon SFN treatment in primary human T-cells. To this end, a Trx1 kinetic trapping mutant was used to analyze whether SFN induces oxidation of STAT3. Trx1 is an oxidoreductase that resolves oxidized proteins by thiol-disulfide exchange reactions. Mutating the catalytic cysteine (C35S) of Trx1 results in formation of long-lived disulphide bridges with its specific targets, enabling trapping of oxidized Trx substrates (33). Since we intended to trap proteins that were oxidized (before reversal) after a very short time, a bolus of high SFN (mM) or H_2O_2 (mM) was chosen to increase the likelihood of oxidized protein detection (34, 35). Using this system, we found that Prx1 [a known target for oxidation that can be trapped by Trx1 (33)] and STAT3 could be trapped with Trx1 following SFN treatment (**Figure 7A**). The amount of trapped STAT3 as well as Prx1 increased in a dose-dependent manner. This result reveals that SFN leads to oxidation of STAT3 and Prx1 in primary human T-cells.

We next scrutinized whether the SFN-mediated increased ROS/decreased GSH levels in T-cells could affect the costimulation-induced phosphorylation of STAT3. To this end, T-cells were pre-treated with SFN with the indicated concentrations in the presence or absence of 2 mM NAC and were costimulated with crosslinked anti-CD3/CD28 antibodies. The intracellular levels of pSTAT3 were analyzed by flow cytometry (data not shown) or western blot (**Figures 7B,C**). STAT3 phosphorylation decreased significantly in the presence of SFN. The inhibitory effect was dose-dependent and started already at 2.5 μM SFN. Importantly, this inhibition was significantly reversed by NAC treatment. These data provide strong evidence that oxidative stress/GSH depletion induced by SFN inhibits STAT3 activation in primary human T-cells connecting SFN treatment to T_H17-skewing of T-cell responses. This notion was further supported by the finding that the expression of RORγt, a master regulator of T_H17-associated gene transcription (36), was also inhibited by SFN (**Figure 7D**). Moreover, this inhibition was also reversed by NAC treatment.

SFN Displays an Immunosuppressive Effect on *ex vivo* T-Cells From RA Patients and Provokes ROS Production in Whole Blood Lymphocytes

Low ROS levels in RA patient-derived T-cells were linked to biased differentiation of T-cells into IFN-γ and IL-17-producing inflammatory cells (18). IL-17A, as the major inflammatory mediator (37), increases bone resorption during RA. We have shown here that SFN increased the intracellular ROS levels in untransformed human T-cells and downregulated T_H17 related genes. Therefore, it was tempting to speculate that an increase of the ROS content in T-cells induced by treatment with SFN should be beneficial for RA patients due to a dampening effect on T_H17 effector functions. We, therefore, investigated the effect of SFN on purified peripheral blood T-cells from RA patients *ex vivo*. These cells were costimulated for 2 days in the absence or presence of 2.5 μM SFN and cytokines in the supernatant were measured by LEGENDplex™. **Figure 8A** shows that IL-17A, IL-17F, and IL-22, three important cytokines produced by T_H17-cells, were significantly decreased when RA T-cells were costimulated in the presence of 2.5 μM SFN. In contrast, TNF-α, IL-2, and IL-21 protein levels were not significantly changed under these conditions. Costimulation-induced proliferation of *ex vivo* RA T-cells was also inhibited by SFN under these conditions (**Figure 8B**).

Our analyses so far were performed with purified human T-cells. Since there are many buffer systems in the whole blood that could interfere with the effects of SFN observed in purified human T-cells, we next analyzed whole blood samples from RA patients. 10 μM SFN were added to the whole blood samples

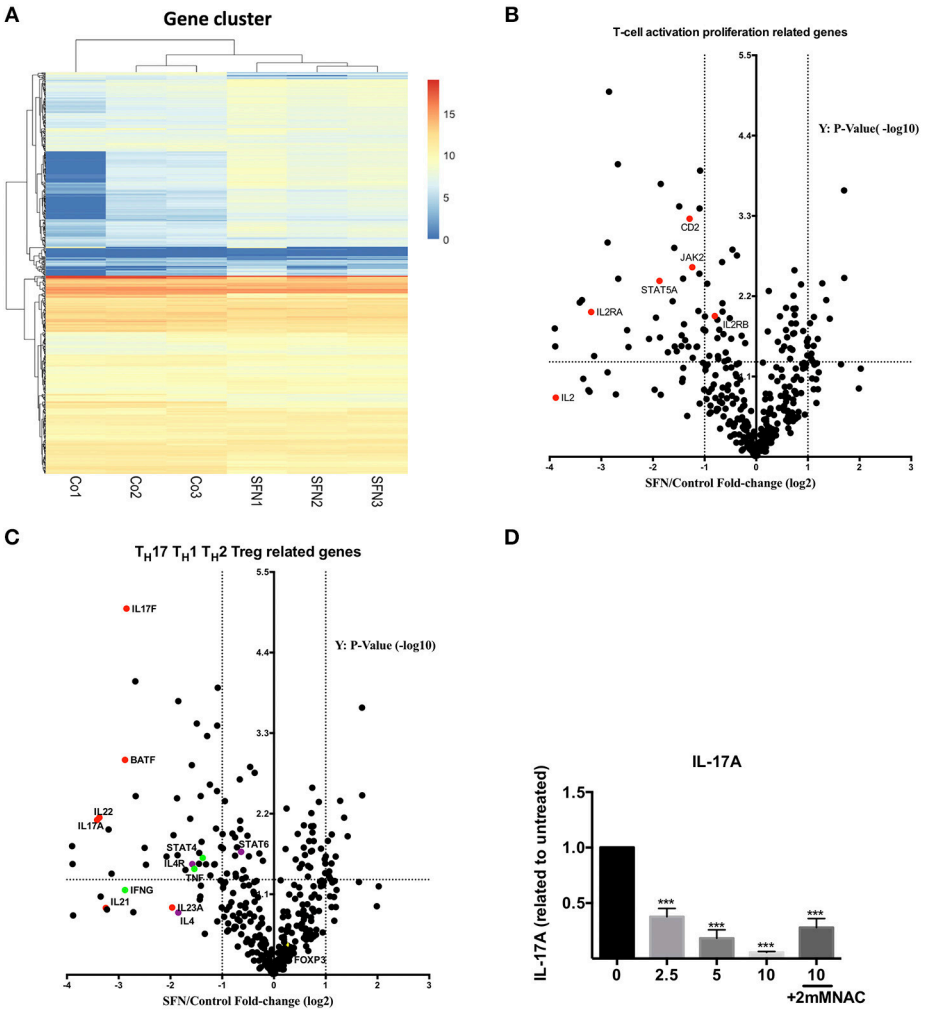

FIGURE 6 | Gene expression analysis (nCounter®). **(A)** Hierarchical clustering of differentially expressed mRNAs in untreated (Co, $n = 3$) and SFN treated (SFN, $n = 3$) T-cells of three different donors. Each column represents an individual sample. Relative fold change is indicated by the color scale (red: high; blue: low). **(B,C)** Volcano plots show the differentially expressed genes important for T-cell activation and proliferation **(B)** and related to T_H1, T_H2, Treg, and T_H17 cells **(C)**. Log2 transformed fold change in expression (SFN vs. control) on the x-axis is plotted against significance (–log10 adjusted *p*-value) on the y-axis. The horizontal dashed lines indicate cutoff for significance $p < 0.05$ (–log10 *p*-value >1.3) and the vertical lines for fold change ≥2/≤-2. **(D)** Quantification of IL-17A in the supernatant of T-cells co-stimulated with anti-CD3 (20 ng/ml)//CD28 (5 μg/ml) antibodies for 2 days in the absence/presence of SFN, with or without NAC supplementary treatment as indicated. IL-17A was measured by a human T_H cytokine panel ($n = 3$; mean; SE; $^*p < 0.05$ $^{***}p < 0.001$).

and the ROS production was analyzed in lymphocytes without a purification step using flow cytometry. These experiments revealed that also in whole blood SFN treatment evoked a significant increase in the intracellular ROS levels in the lymphocyte population (**Figure 8C**). Taken together, these results show that SFN inhibits the production of T_H17 related cytokines from RA T-cells and enhances the ROS levels in whole blood lymphocytes of RA patients.

DISCUSSION

SFN has extensively been studied as an anti-cancer agent, while its impact on untransformed human immune cells remained largely unknown. In our study, the effects of SFN on primary human T-cells were addressed. We demonstrate that SFN does not change immune synapse maturation as determined by clustering of CD3 and the adhesion molecule LFA-1, but it inhibits the activation of untransformed human T-cells, in particular their proliferation and the production of T_H17-related cytokines. As a major finding, we show that SFN induces a pro-oxidative state in untransformed human peripheral blood T-cells. This manifests as an increased general ROS amount, severely depleted intracellular GSH pools, and oxidation of redox sensitive proteins including the T_H17-regulating transcription factor STAT3. Seemingly contradictory, various previous studies on tumor cell lines (38, 39) or murine DCs (8, 12) showed that SFN enhanced the cellular antioxidant capacity by increasing KEAP1/NRF2/ARE-dependent expression

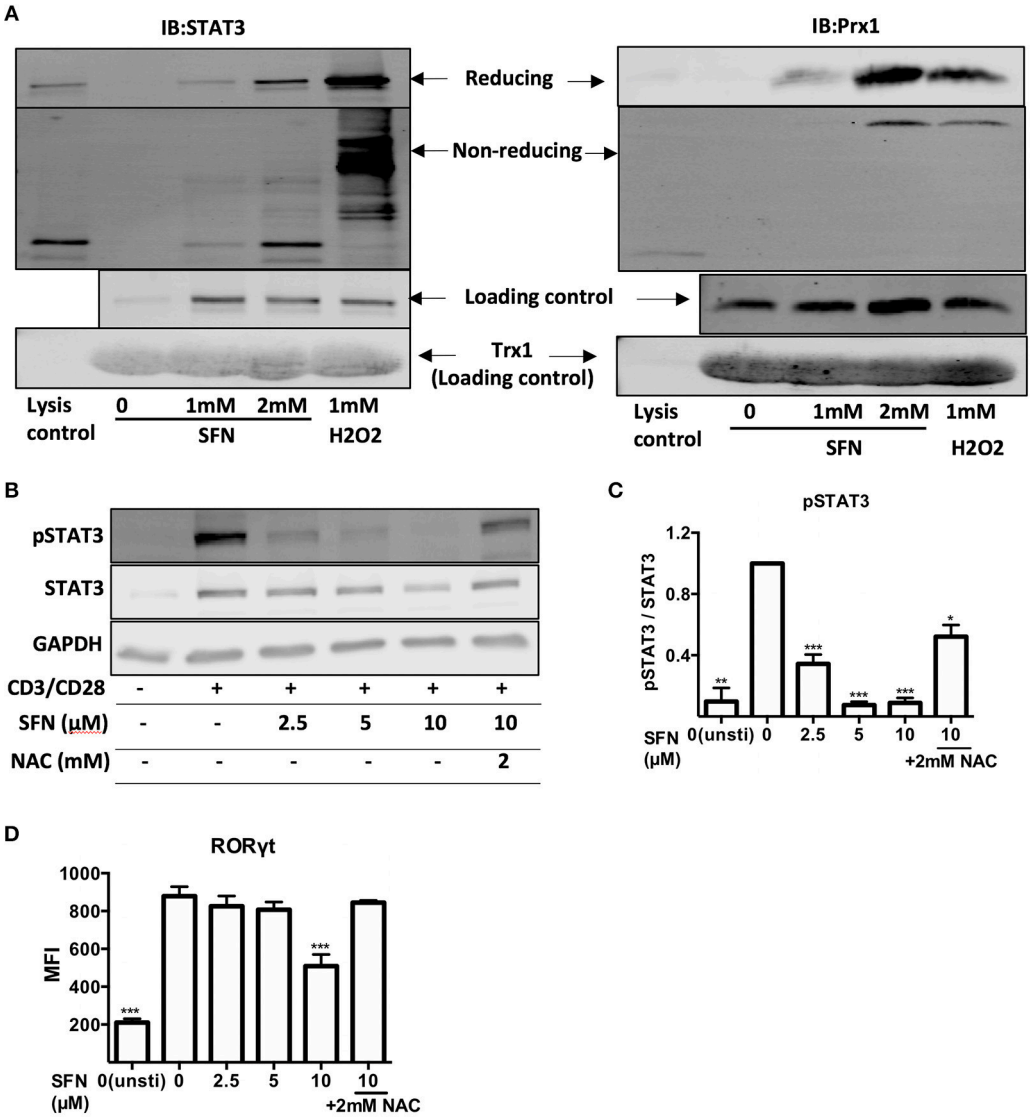

FIGURE 7 | SFN induces thiol oxidation on STAT3 and inhibits STAT3 phosphorylation. **(A)** Oxidized proteins were delineated by Trx1 kinetic trapping. T-cells were treated without or with SFN or H_2O_2 as indicated. Cell lysates were incubated with Trx1 trapping mutant loaded streptavidin beads, eluted proteins were concentrated and loaded on SDS-PAGE gel. Shown immunoblots are representative for three experiments. **(B)** Phosphorylation of STAT3 was detected by western blot. T-cells were treated without or with SFN as indicated under stimulated (+) or unstimulated (−) conditions for 1 day. Cell lysate was loaded on SDS-PAGE gel and immunoblotted for pSTAT3, STAT3, and GAPDH. **(C)** Quantification of pSTAT3 to STAT3 ($n = 3$; mean; SE; $^{*}p < 0.05$, $^{**}p < 0.01$ $^{***}p < 0.001$). **(D)** Quantification of RORγt expression by flow cytometry. T-cells were treated with or without SFN as indicated under stimulated or unstimulated conditions for 2 days and then stained with RORγt specific antibody. Given are expression levels relative to control (no SFN treatment) in terms of MFI ($n = 3$; mean; SE; $^{***}p < 0.001$).

of phase II antioxidant enzymes, e.g., HO-1. This led to the conviction that SFN generally acts as an antioxidative substance. In this regard, we also observed increased levels of *NRF2* and *HO-1* upon SFN treatment in both untransformed human T-cells (**Supplementary Figure 5A**) and prostate cancer PC-3 cells (**Supplementary Figure 5B**). However, the redox regulation within the cells depends on the activity of all ROS producing and eliminating processes (e.g., antioxidant systems) that may vary in different cell types. It is, therefore, crucial to analyze the intracellular net ROS level and its functional consequences, e.g., direct protein oxidation in a time dependent manner.

Mechanistically, depletion of GSH stores in untransformed human T-cells cells was indeed accompanied by increased oxidation of proteins at redox active cysteine residues. Thus, immunostaining against dimedone, a cell permeable cysteine sulfenylation specific reagent, revealed a global increase in oxidation on various proteins. Consistently, our kinetic trapping approach using the Trx1 C35S mutant revealed that well-known redox regulated proteins, such as Prx1, were trapped upon SFN treatment. Interestingly, the thiol antioxidant NAC, which is a precursor for GSH biosynthesis and GSH *per se* could restore T-cell functions in the presence of SFN. Therefore, the SFN effects

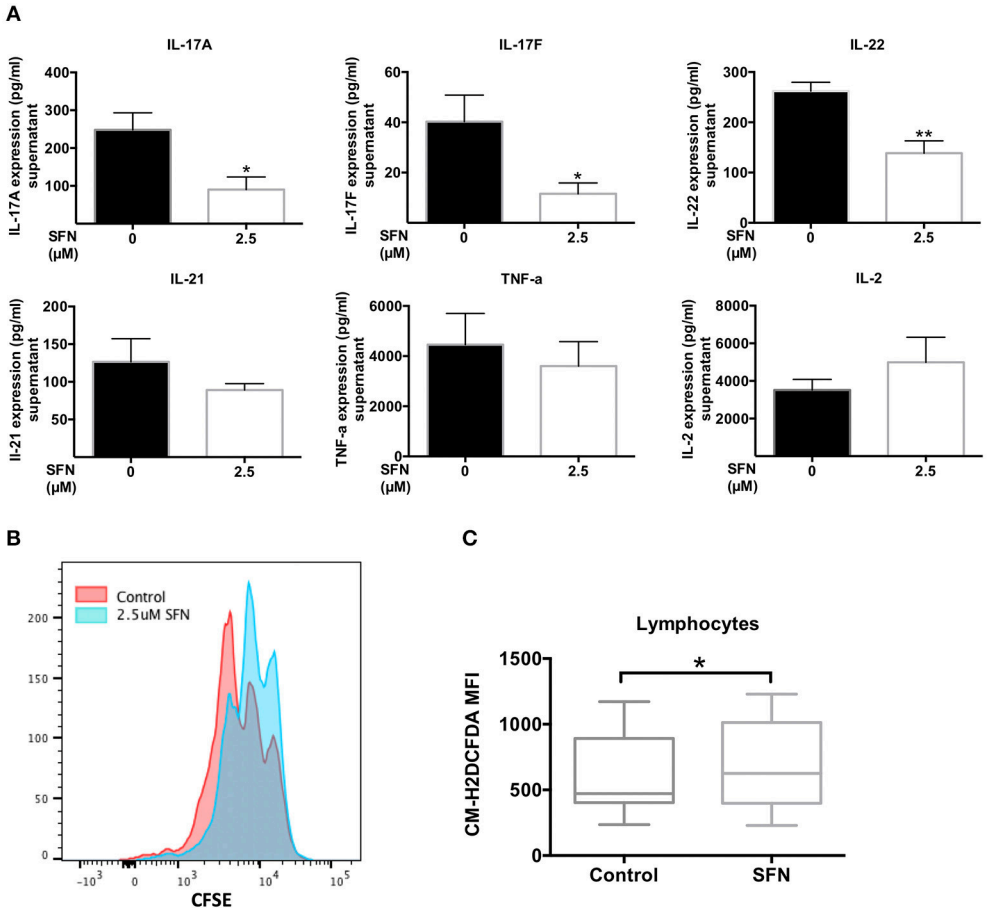

FIGURE 8 | SFN displays an immunosuppressive effect on RA T-cells *ex vivo*. **(A)** Quantification of cytokines in the supernatant of RA T-cells by bead-based immunoassay using the human T_H cytokine panel. RA T-cells were purified and co-stimulated with anti-CD3 (20 ng/ml)/CD28 (5 μg/ml) antibodies for 2 days in the absence/presence of SFN. Shown are the cytokine levels in the supernatant in pg/ml ($n = 4$; mean; SE; $^*p < 0.05$, $^{**}p < 0.01$). **(B)** RA T-cell proliferation was assessed via CFSE staining. RA T-cells were co-stimulated with anti-CD3 (20 ng/ml)/CD28 (20 ng/ml) antibodies in the absence/presence of SFN for 3 days. CFSE signals were detected by flow cytometry. Shown is the representative histogram. **(C)** Intracellular ROS levels of RA blood cells were assessed via staining of CM-H_2DCFDA. Whole blood was stained with AF700-CD45 and CM-H_2DCFDA in the absence/presence of SFN. Shown are ROS levels in terms of MFI in both untreated and SFN treated blood lymphocytes ($n = 17$; medium; SE; $^*p < 0.05$).

on T-cell functions can at least partly be explained by depletion of GSH and accumulation of oxidized proteins. In support of this assumption, GSH has been shown to be essential for maintaining T-cell inflammatory responses (40). Note that since GSH binds to several proteins that control cellular processes such as cell proliferation, apoptosis, and survival, it is not only important to mount a proper anti oxidant response, but also important for many cellular functions that are independent of its anti oxidant activity (41, 42). Depletion of GSH by SFN may, thus, further challenge the cells through inhibiting such functions.

To further characterize the effects of SFN on untransformed human T-cells, immune specific gene analysis was used to get an unbiased view on mRNA expression profiles after T-cell co-stimulation in the presence vs. absence of SFN. Intriguingly, it revealed that SFN especially dampened the expression of the T_H17-related genes *IL17A, IL17F, IL22,* and *BATF*. Importantly, using a Trx1-trapping mutant we found that the T_H17-skewing protein STAT3 is oxidized upon treatment with SFN. It was previously shown that ROS can lead to oxidation of STAT3 (43), but the effect of oxidative stress on STAT3 signaling was reported divergently. On the one hand, ROS in higher concentration, are likely to influence STAT3 signaling indirectly by inhibiting protein tyrosine phosphatases and activating protein kinases, which in turn increases STAT3 phosphorylation (44, 45). On the other hand, Halvorsen et al. reported that oxidative stress blocks tyrosine phosphorylation of STAT3 and the activation of JAK/STAT signaling in neurons (46, 47). According to this, the STAT3 phosphorylation and the STAT3 oxidation state are likely to be dependent on cell type and context. As revealed in our study, in untransformed human T-cells SFN led to STAT3 oxidation and inhibited STAT3 phosphorylation. Notably, this inhibition could be rescued by NAC. Fu et al. have demonstrated that ROS activated Mink1 inhibits phosphorylation of T324 in Smad2 and its nuclear localization, thereby preventing the

induction of T_H17-associated genes (48), e.g., STAT3. Whether this pathway is involved in SFN induced dephosphorylation of STAT3 remains to be elucidated, but the ROS-mediated regulation of STAT3 may partially connect SFN-treatment to the strongly inhibited T_H17 cell responses on the molecular level. Note that Chaudhry et al. have shown that the activation of STAT3 in Tregs endows them with the ability to suppress T_H17 responses through increasing the expression of a subset of suppressor molecules (49). Therefore, STAT3 activation in Treg vs. T_H17 cells seems to lead to a different outcome regarding the net activation of T_H17 cells. In our study, the inhibited STAT3 activity seems to play more a role in T_H17 cells, since the T_H17 cell response was clearly inhibited. Yet, to clarify the specificity of the effects of SFN on STAT3 in different cell populations, further experiments need to be performed in the future.

T_H17 cells have been involved in the progression of many common autoimmune diseases, including psoriasis (50), inflammatory bowel disease (IBD) (51), multiple sclerosis (MS) (52), and rheumatoid arthritis (RA) (53). Although IL-17, as a hallmark cytokine of T_H17 cells, plays critical roles in the pathogenesis of autoimmune diseases, targeting IL-17 alone with anti-IL-17 antibodies was not sufficient to improve clinical end points (54). Recently, the regulatory effects of ROS in autoimmune inflammation have received more and more attention. While the role of ROS in the pathogenesis of psoriasis is still controversially discussed (55–57), it plays a major role in the pathogenesis of IBD and MS. Moreover, Weyand et al. recently reported that RA T-cells are distinguished from healthy T-cells based on diminished ROS production thereby undergoing "reductive stress" (18). It shunts glucose away from pyruvate and ATP production toward the pentose phosphate pathway, where NADPH is generated and cellular ROS are consumed (58). These ROS^{low} RA T-cells are spontaneously biased to develop into IFN-γ and IL-17 producing pro-inflammatory T-cells, which play a central role for disease progression (58, 59). Therefore, strategies that are able to upregulate ROS concentrations in RA T-cells and to re-balance the ROS signaling systems may be promising for therapeutic purposes. In light of these findings, we extended our studies to T-cells derived from RA patients. *Ex vivo* experiments showed that SFN indeed enhanced the ROS levels in lymphocytes within whole blood of RA patients and inhibited production of the pro-inflammatory cytokines IL-17A, IL-17F, and IL-22. These results suggest that SFN may act as a promising substance to control RA in patients. Supporting this assumption, it was demonstrated in mice that SFN dampened the clinical severity of experimental arthritis by inhibiting the production of cartilage destructive metalloproteinases and the expression of IL-17 and TNF-α (9, 60).

Also, of high clinical importance may be our second finding, namely that SFN has differential effects on untransformed human T-cells (decrease of GSH and immunosuppression) and Jurkat T-leukemia cells—prototypical immature transformed T-cells (increase of GSH and cytotoxicity). This finding may be explained by the different anti oxidant capacity of tumor cells vs. untransformed cells. Tumor cells are usually equipped with stronger anti oxidant systems (e.g., GSH and Trx1 systems) and can keep their redox balance more stable (61). For example, the cystine/glutamate antiporter SLC7A11, the main route of cysteine acquisition, and the glutamate cysteine ligase modifier subunit (GCLM), which is necessary for the efficient synthesis of GSH, are upregulated in the tumor cells during oxidant stress to increase the GSH synthesis. Aside from the biosynthesis, tumor cells can regenerate GSH by upregulating the production of NADPH as well. Collectively, ROS induction in tumor cells leads to a positive feedback on their antioxidant capacities. It is, therefore, also expected to observe an increased GSH in Jurkat T-leukemia cells over time with SFN treatment (62). Not only death of malignant cells but also a functional immune response is crucial for tumor rejection. Therefore, our finding that SFN has an immunosuppressive effect on untransformed human T-cells may explain why treatment with SFN did not lead to amelioration of cancer severity in patients as demonstrated in a number of clinical trials (4), although *in vitro* experiments on tumor cells such as breast cancer cell and hepatocellular carcinoma cell strongly suggested that SFN has anti-tumor properties (2, 63).

Together, in our current study, we uncovered a so far unknown molecular mechanism of how SFN controls activation of human T-cells and, notably, its strong effects on T_H17-related genes: SFN is able to create a pro-oxidative ROS enriched milieu in primary human T-cells. It inhibits costimulation-initiated T-cell activation and proliferation by depletion of GSH and oxidation of proteins at redox active cysteine residues. Importantly, SFN also enhanced the ROS levels in lymphocytes within whole blood of RA patients and inhibited the production of pro-inflammatory T_H17 related cytokines. This suggests that SFN may offer a new therapeutic option for the treatment of chronic T_H17 related diseases, e.g., rheumatoid arthritis, due to its redox-related immunosuppressive effects. At the same time, it may be potentially harmful in cancer settings, in which the T-cell mediated defense of tumors plays a decisive role.

AUTHOR CONTRIBUTIONS

JL and YS: conceptualization; JL, BJ, EB, GW, and BN: methodology; JL, BJ, JZ, and EB: investigation; YS and NB: resources; JL, EB, GW, KH, and YS: writing; YS: supervision; YS: funding acquisition; All authors have given approval to the final version of the manuscript.

FUNDING

This study was supported by the Ministry of Science, Research and the Arts Baden-Württemberg to YS (AZKIM, www.azkim.de); German Research Foundation Grant to YS (SA393/3-4). JL was financially supported by the Chinese Scholarship Council (No. 201408370079).

ACKNOWLEDGMENTS

We thank Ralph Röth for experimental support, Tobias P. Dick for providing the Trx1 trapping mutant construct,

and Jan-Christoph Schumacher for collecting clinical samples. We acknowledge financial support by the German Research Foundation within the funding programme Open Access Publishing, by the Baden-Württemberg Ministry of Science, Research and the Arts and by Heidelberg University.

SUPPLEMENTARY MATERIAL

The Supplementary Material for this article can be found online at: https://www.frontiersin.org/articles/10.3389/fimmu.2018.02584/full#supplementary-material

REFERENCES

1. Singh SV, Herman-Antosiewicz A, Singh AV, Lew KL, Srivastava SK, Kamath R, et al. Sulforaphane-induced G2/M phase cell cycle arrest involves checkpoint kinase 2-mediated phosphorylation of cell division cycle 25C. *J Biol Chem.* (2004) 279:25813–22. doi: 10.1074/jbc.M313538200
2. Lewinska A, Adamczyk-Grochala J, Deregowska A Wnuk M. Sulforaphane-induced cell cycle arrest and senescence are accompanied by DNA hypomethylation and changes in microRNA profile in breast cancer cells. *Theranostics* (2017) 7:3461–77. doi: 10.7150/thno.20657
3. Suppipat K, Park CS, Shen Y, Zhu X Lacorazza HD. Sulforaphane induces cell cycle arrest and apoptosis in acute lymphoblastic leukemia cells. *PLoS ONE* (2012) 7:e51251. doi: 10.1371/journal.pone.0051251
4. Atwell LL, Zhang Z, Mori M, Farris PE, Vetto JT, Naik AM, et al. Sulforaphane bioavailability and chemopreventive activity in women scheduled for breast biopsy. *Cancer Prevent Res.* (2015) 8:1184–91. doi: 10.1158/1940-6207.CAPR-15-0119
5. Alumkal JJ, Slottke R, Schwartzman J, Cherala G, Munar M, Graff JN, et al. A phase II study of sulforaphane-rich broccoli sprout extracts in men with recurrent prostate cancer. *Invest New Drugs* (2015) 33:480–9. doi: 10.1007/s10637-014-0189-z
6. Kumar R, de Mooij T, Peterson TE, Kaptzan T, Johnson AJ, Daniels DJ, et al. Modulating glioma-mediated myeloid-derived suppressor cell development with sulforaphane. *PLoS ONE* (2017) 12:e0179012. doi: 10.1371/journal.pone.0179012
7. Pal S, Konkimalla VB. Sulforaphane regulates phenotypic and functional switching of both induced and spontaneously differentiating human monocytes. *Int Immunopharmacol.* (2016) 35:85–98. doi: 10.1016/j.intimp.2016.03.008
8. Geisel J, Bruck J, Glocova I, Dengler K, Sinnberg T, Rothfuss O, et al. Sulforaphane protects from T cell-mediated autoimmune disease by inhibition of IL-23 and IL-12 in dendritic cells. *J Immunol.* (2014) 192:3530–9. doi: 10.4049/jimmunol.1300556
9. Kong JS, Yoo SA, Kim HS, Kim HA, Yea K, Ryu SH, et al. Inhibition of synovial hyperplasia, rheumatoid T cell activation, and experimental arthritis in mice by sulforaphane, a naturally occurring isothiocyanate. *Arthritis Rheum.* (2010) 62:159–70. doi: 10.1002/art.25017
10. Li B, Cui W, Liu J, Li R, Liu Q, Xie XH, et al. Sulforaphane ameliorates the development of experimental autoimmune encephalomyelitis by antagonizing oxidative stress and Th17-related inflammation in mice. *Exp Neurol.* (2013) 250:239–49. doi: 10.1016/j.expneurol.2013.10.002
11. Checker R, Gambhir L, Thoh M, Sharma D, Sandur SK. Sulforaphane, a naturally occurring isothiocyanate, exhibits anti-inflammatory effects by targeting GSK3β/Nrf-2 and NF-κB pathways in T cells. *J Funct Foods* (2015) 19:426–38. doi: 10.1016/j.jff.2015.08.030
12. Kim H-J, Barajas B, Wang M, Nel AE. Nrf2 activation by sulforaphane restores the age-related decrease of TH1 immunity: Role of dendritic cells. *J Allergy Clin Immunol.* (2008) 121:1255–61. e7. doi: 10.1016/j.jaci.2008.01.016
13. Thimmulappa RK, Mai KH, Srisuma S, Kensler TW, Yamamoto M, Biswal S. Identification of Nrf2-regulated genes induced by the chemopreventive agent sulforaphane by oligonucleotide microarray. *Cancer Res.* (2002) 62:5196–203. http://cancerres.aacrjournals.org/content/62/18/5196
14. Samstag Y, John I, Wabnitz GH. Cofilin: a redox sensitive mediator of actin dynamics during T-cell activation and migration. *Immunol Rev.* (2013) 256:30–47. doi: 10.1111/imr.12115
15. Schulte B, John I, Simon B, Brockmann C, Oelmeier SA, Jahraus B, et al. A reducing milieu renders cofilin insensitive to phosphatidylinositol 4,5-bisphosphate (PIP2) inhibition. *J Biol Chem.* (2013) 288:29430–9. doi: 10.1074/jbc.M113.479766
16. Klemke M, Wabnitz GH, Funke F, Funk B, Kirchgessner H, Samstag Y. Oxidation of cofilin mediates T cell hyporesponsiveness under oxidative stress conditions. *Immunity* (2008) 29:404–13. doi: 10.1016/j.immuni.2008.06.016
17. Wabnitz GH, Goursot C, Jahraus B, Kirchgessner H, Hellwig A, Klemke M, et al. Mitochondrial translocation of oxidized cofilin induces caspase-independent necrotic-like programmed cell death of T cells. *Cell Death Dis.* (2010) 1:e58. doi: 10.1038/cddis.2010.36
18. Weyand CM, Shen Y, Goronzy JJ. Redox-sensitive signaling in inflammatory T cells and in autoimmune disease. *Free Radic Biol Med.* (2018) 125:36–43. doi: 10.1016/j.freeradbiomed.2018.03.004
19. Wabnitz GH, Kocher T, Lohneis P, Stober C, Konstandin MH, Funk B, et al. Costimulation induced phosphorylation of L-plastin facilitates surface transport of the T cell activation molecules CD69 and CD25. *Eur J Immunol.* (2007) 37:649–62. doi: 10.1002/eji.200636320
20. Wabnitz GH, Nessmann A, Kirchgessner H, Samstag Y. InFlow microscopy of human leukocytes: a tool for quantitative analysis of actin rearrangements in the immune synapse. *J Immunol Methods* (2015) 423:29–39. doi: 10.1016/j.jim.2015.03.003
21. Balta E, Stopp J, Castelletti L, Kirchgessner H, Samstag Y, Wabnitz GH. Qualitative and quantitative analysis of PMN/T-cell interactions by InFlow and super-resolution microscopy. *Methods* (2017) 112:25–38. doi: 10.1016/j.ymeth.2016.09.013
22. Schwertassek U, Haque A, Krishnan N, Greiner R, Weingarten L, Dick TP, et al. Reactivation of oxidized PTP1B and PTEN by thioredoxin 1. *FEBS J.* (2014) 281:3545–58. doi: 10.1111/febs.12898
23. Clarke JD, Hsu A, Riedl K, Bella D, Schwartz SJ, Stevens JF, et al. Bioavailability and inter-conversion of sulforaphane and erucin in human subjects consuming broccoli sprouts or broccoli supplement in a cross-over study design. *Pharmacol Res.* (2011) 64:456–63. doi: 10.1016/j.phrs.2011.07.005
24. Li Y, Zhang T, Korkaya H, Liu S, Lee H-F, Newman B, et al. Sulforaphane, a dietary component of broccoli/broccoli sprouts, inhibits breast cancer stem cells. *Clin Cancer Res.* (2010) 16:2580–90. doi: 10.1158/1078-0432.CCR-09-2937
25. Singh AV, Xiao D, Lew KL, Dhir R, Singh SV. Sulforaphane induces caspase-mediated apoptosis in cultured PC-3 human prostate cancer cells and retards growth of PC-3 xenografts *in vivo*. *Carcinogenesis* (2004) 25:83–90. doi: 10.1093/carcin/bgg178
26. Wabnitz GH, Kirchgessner H, Samstag Y. Imaging flow cytometry for multiparametric analysis of molecular mechanism involved in the cytotoxicity of human CD8(+) T-cells. *J Cell Biochem.* (2017) 118:2528–33. doi: 10.1002/jcb.25963
27. Thoren FB, Betten A, Romero AI, Hellstrand K. Cutting edge: antioxidative properties of myeloid dendritic cells: protection of T cells and NK cells from oxygen radical-induced inactivation and apoptosis. *J Immunol.* (2007) 179:21–5. doi: 10.4049/jimmunol.179.1.21
28. Seo YH, Carroll KS: Profiling protein thiol oxidation in tumor cells using sulfenic acid-specific antibodies. *Proc Natl Acad Sci.* (2009) 106:16163–8. doi: 10.1073/pnas.0903015106
29. Zafarullah M, Li WQ, Sylvester J, Ahmad M. Molecular mechanisms of N-acetylcysteine actions. *Cell Mol Life Sci.* (2003) 60:6–20. doi: 10.1007/s000180300001
30. Moriggl R, Topham DJ, Teglund S, Sexl V, McKay C, Wang D, et al. Stat5 is required for IL-2-induced cell cycle progression of peripheral T cells. *Immunity* (1999) 10:249–59. doi: 10.1016/S1074-7613(00)80025-4

31. Harris TJ, Grosso JF, Yen H-R, Xin H, Kortylewski M, Albesiano E, et al. Cutting edge: an *in vivo* requirement for STAT3 signaling in TH17 development and TH17-dependent autoimmunity. *J Immunol.* (2007) 179:4313–7. doi: 10.4049/jimmunol.179.7.4313
32. Moon Y-M, Lee S-Y, Kwok S-K, Lee SH, Kim D, Kim WK, et al. The Fos-related antigen 1–JUNB/activator protein 1 transcription complex, a downstream target of signal transducer and activator of transcription 3, induces T helper 17 differentiation and promotes experimental autoimmune arthritis. *Front Immunol.* (2017) 8:1793. doi: 10.3389/fimmu.2017.01793
33. Schwertassek U, Balmer Y, Gutscher M, Weingarten L, Preuss M, Engelhard J, et al. Selective redox regulation of cytokine receptor signaling by extracellular thioredoxin-1. *EMBO J.* (2007) 26:3086–97. doi: 10.1038/sj.emboj.7601746
34. Sobotta MC, Barata AG, Schmidt U, Mueller S, Millonig G, Dick TP. Exposing cells to H2O2: a quantitative comparison between continuous low-dose and one-time high-dose treatments. *Free Radical Biol Med.* (2013) 60:325–35. doi: 10.1016/j.freeradbiomed.2013.02.017
35. Espinosa-Diez C, Miguel V, Mennerich D, Kietzmann T, Sánchez-Pérez P, Cadenas S, et al. Antioxidant responses and cellular adjustments to oxidative stress. *Redox Biol.* (2015) 6:183–97. doi: 10.1016/j.redox.2015.07.008
36. Ciofani M, Madar A, Galan C, Sellars M, Mace K, Pauli F, et al. A validated regulatory network for Th17 cell specification. *Cell* (2012) 151:289–303. doi: 10.1016/j.cell.2012.09.016
37. Qian Y, Kang Z, Liu C, Li X. IL-17 signaling in host defense and inflammatory diseases. *Cell Mol Immunol.* (2010) 7:328–33. doi: 10.1038/cmi.2010.27
38. de Figueiredo MS, Binda SN, Nogueira-Machado AJ, Vieira-Filho AS, Caligiorne BR. The antioxidant properties of organosulfur compounds (sulforaphane). *Recent Patents Endocr Metabol Immune Drug Discov.* (2015) 9:24–39. doi: 10.2174/1872214809666150505164138
39. Keum YS, Yu S, Chang PP, Yuan X, Kim JH, Xu C, et al. Mechanism of action of sulforaphane: inhibition of p38 mitogen-activated protein kinase isoforms contributing to the induction of antioxidant response element-mediated heme oxygenase-1 in human hepatoma HepG2 cells. *Cancer Res.* (2006) 66:8804–13. doi: 10.1158/0008-5472.CAN-05-3513
40. Mak TW, Grusdat M, Duncan GS, Dostert C, Nonnenmacher Y, Cox M, et al. Glutathione primes T cell metabolism for inflammation. *Immunity* (2017) 46:675–89. doi: 10.1016/j.immuni.2017.03.019
41. Franco R, Schoneveld O, Pappa A, Panayiotidis M. The central role of glutathione in the pathophysiology of human diseases. *Arch Physiol Biochem.* (2007) 113:234–58. doi: 10.1080/13813450701661198
42. Aquilano K, Baldelli S, Ciriolo MR. Glutathione: new roles in redox signaling for an old antioxidant. *Front Pharmacol.* (2014) 5:196. doi: 10.3389/fphar.2014.00196
43. Sobotta MC, Liou W, Stocker S, Talwar D, Oehler M, Ruppert T, et al. Peroxiredoxin-2 and STAT3 form a redox relay for H2O2 signaling. *Nat Chem Biol.* (2015) 11:64–70. doi: 10.1038/nchembio.1695
44. Carballo M, Conde M, El Bekay R, Martin-Nieto J, Camacho MJ, Monteseirin J, et al. Oxidative stress triggers STAT3 tyrosine phosphorylation and nuclear translocation in human lymphocytes. *J Biol Chem.* (1999) 274:17580–6. doi: 10.1074/jbc.274.25.17580
45. Myers MP, Andersen JN, Cheng A, Tremblay ML, Horvath CM, Parisien JP, et al. TYK2 and JAK2 are substrates of protein-tyrosine phosphatase 1B. *J Biol Chem.* (2001) 276:47771–4. doi: 10.1074/jbc.C100583200
46. Kaur N, Lu B, Monroe RK, Ward SM, Halvorsen SW. Inducers of oxidative stress block ciliary neurotrophic factor activation of Jak/STAT signaling in neurons. *J Neurochem.* (2005) 92:1521–30. doi: 10.1111/j.1471-4159.2004.02990.x
47. Monroe RK, Halvorsen SW. Cadmium blocks receptor-mediated Jak/STAT signaling in neurons by oxidative stress. *Free Radic Biol Med.* (2006) 41:493–502. doi: 10.1016/j.freeradbiomed.2006.04.023
48. Fu G, Xu Q, Qiu Y, Jin X, Xu T, Dong S, et al. Suppression of Th17 cell differentiation by misshapen/NIK-related kinase MINK1. *J Exp Med.* (2017) 214:1453–69. doi: 10.1084/jem.20161120
49. Chaudhry A, Rudra D, Treuting P, Samstein RM, Liang Y, Kas A, et al. CD4+ regulatory T cells control TH17 responses in a Stat3-dependent manner. *Science* (2009) 326:986–91. doi: 10.1126/science.1172702
50. Di Cesare A, Di Meglio P, Nestle FO. The IL-23/Th17 axis in the immunopathogenesis of psoriasis. *J Invest Dermatol.* (2009) 129:1339–50. doi: 10.1038/jid.2009.59
51. Ueno A, Jeffery L, Kobayashi T, Hibi T, Ghosh S, Jijon H. Th17 plasticity and its relevance to inflammatory bowel disease. *J Autoimmun.* (2018) 87:38–49. doi: 10.1016/j.jaut.2017.12.004
52. Jadidi-Niaragh F, Mirshafiey A. Th17 cell, the new player of neuroinflammatory process in multiple sclerosis. *Scand J Immunol.* (2011) 74:1–13. doi: 10.1111/j.1365-3083.2011.02536.x
53. van Hamburg JP, Tas SW. Molecular mechanisms underpinning T helper 17 cell heterogeneity and functions in rheumatoid arthritis. *J Autoimmun.* (2018) 87:69–81. doi: 10.1016/j.jaut.2017.12.006
54. Yang J, Sundrud MS, Skepner J, Yamagata T. Targeting Th17 cells in autoimmune diseases. *Trends Pharmacol Sci.* (2014) 35:493–500. doi: 10.1016/j.tips.2014.07.006
55. Zhou Q, Mrowietz U, Rostami-Yazdi M. Oxidative stress in the pathogenesis of psoriasis. *Free Radic Biol Med.* (2009) 47:891–905. doi: 10.1016/j.freeradbiomed.2009.06.033
56. Khmaladze I, Kelkka T, Guerard S, Wing K, Pizzolla A, Saxena A, et al. Mannan induces ROS-regulated, IL-17A-dependent psoriasis arthritis-like disease in mice. *Proc Natl Acad Sci USA.* (2014) 111:E3669–78. doi: 10.1073/pnas.1405798111
57. Hagert C, Sareila O, Kelkka T, Jalkanen S, Holmdahl R. The macrophage mannose receptor regulate mannan induced psoriasis, psoriatic arthritis and rheumatoid arthritis-like disease models. *Front Immunol.* (2018) 9:114. doi: 10.3389/fimmu.2018.00114
58. Yang Z, Shen Y, Oishi H, Matteson EL, Tian L, Goronzy JJ, et al. Restoring oxidant signaling suppresses proarthritogenic T cell effector functions in rheumatoid arthritis. *Sci Transl Med.* (2016) 8:331ra38. doi: 10.1126/scitranslmed.aad7151
59. Abimannan T, Peroumal D, Parida JR, Barik PK, Padhan P, Devadas S. Oxidative stress modulates the cytokine response of differentiated Th17 and Th1 cells. *Free Radic Biol Med.* (2016) 99:352–63. doi: 10.1016/j.freeradbiomed.2016.08.026
60. Davidson RK, Jupp O, de Ferrars R, Kay CD, Culley KL, Norton R, et al. Sulforaphane represses matrix-degrading proteases and protects cartilage from destruction *in vitro* and *in vivo*. *Arthritis Rheum.* (2013) 65:3130–40. doi: 10.1002/art.38133
61. Gostner JM, Becker K, Fuchs D, Sucher R. Redox regulation of the immune response. *Redox Rep.* (2013) 18:88–94. doi: 10.1179/1351000213Y.0000000044
62. Kong H, Chandel NS. Regulation of redox balance in cancer and T cells. *J Biol Chem.* (2018) 293:7499–507. doi: 10.1074/jbc.TM117.000257
63. Liu P, Atkinson SJ, Akbareian SE, Zhou Z, Munsterberg A, Robinson SD, et al. Sulforaphane exerts anti-angiogenesis effects against hepatocellular carcinoma through inhibition of STAT3/HIF-1α/VEGF signalling. *Sci Rep.* (2017) 7:12651. doi: 10.1038/s41598-017-12855-w

Conflict of Interest Statement: The authors declare that the research was conducted in the absence of any commercial or financial relationships that could be construed as a potential conflict of interest.

Copyright © 2018 Liang, Jahraus, Balta, Ziegler, Hübner, Blank, Niesler, Wabnitz and Samstag. This is an open-access article distributed under the terms of the Creative Commons Attribution License (CC BY). The use, distribution or reproduction in other forums is permitted, provided the original author(s) and the copyright owner(s) are credited and that the original publication in this journal is cited, in accordance with accepted academic practice. No use, distribution or reproduction is permitted which does not comply with these terms.

frontiers in Immunology

ORIGINAL RESEARCH
published: 30 November 2018
doi: 10.3389/fimmu.2018.02814

CD32 Ligation Promotes the Activation of CD4$^+$ T Cells

María Pía Holgado[1], *Inés Sananez*[1], *Silvina Raiden*[2,3], *Jorge R. Geffner*[1,3] *and Lourdes Arruvito*[1,3]*

[1] Instituto de Investigaciones Biomédicas en Retrovirus y SIDA, Universidad de Buenos Aires, CONICET, Buenos Aires, Argentina, [2] Unidad I, Departamento de Clínica Médica, Hospital de Niños Pedro de Elizalde, Buenos Aires, Argentina, [3] Departamento de Microbiología, Parasitología e Inmunología, Facultad de Medicina, Universidad de Buenos Aires, Buenos Aires, Argentina

Low affinity receptors for the Fc portion of IgG (FcγRs) represent a critical link between innate and adaptive immunity. Immune complexes (ICs) are the natural ligands for low affinity FcγRs, and high levels of ICs are usually detected in both, chronic viral infections and autoimmune diseases. The expression and function of FcγRs in myeloid cells, NK cells and B cells have been well characterized. By contrast, there are controversial reports about the expression and function of FcγRs in T cells. Here, we demonstrated that ∼2% of resting CD4+ T cells express cell surface FcγRII (CD32). Analysis of CD32 expression in permeabilized cells revealed an increased proportion of CD4+CD32+ T cells (∼9%), indicating that CD4+ T cells store a CD32 cytoplasmic pool. Activation of CD4+ T cells markedly increased the expression of CD32 either at the cell surface or intracellularly. Analysis of CD32 mRNA transcripts in activated CD4+ T cells revealed the presence of both, the stimulatory FcγRIIa (CD32a) and the inhibitory FcγRIIb (CD32b) isoforms of CD32, being the CD32a:CD32b mRNA ratio ∼5:1. Consistent with this finding, we found not only that CD4+ T cells bind aggregated IgG, used as an IC model, but also that CD32 ligation by specific mAb induced a strong calcium transient in CD4+ T cells. Moreover, we found that pretreatment of CD4+ T cells with immobilized IgG as well as cross-linking of CD32 by specific antibodies increased both, the proliferative response of CD4+ T cells and the release of a wide pattern of cytokines (IL-2, IL-5, IL-10, IL-17, IFN-γ, and TNF-α) triggered by either PHA or anti-CD3 mAb. Collectively, our results indicate that ligation of CD32 promotes the activation of CD4+ T cells. These findings suggest that ICs might contribute to the perpetuation of chronic inflammatory responses by virtue of its ability to directly interact with CD4+ T cells through CD32a, promoting the activation of T cells into different inflammatory profiles.

Keywords: T cells, FcγR, IgG, cytokines, proliferation, activation

OPEN ACCESS

Edited by:
María Fernanda Pascutti, Sanquin Diagnostic Services, Netherlands

Reviewed by:
Pleun Hombrink, Sanquin Research, Netherlands
Augusto Vaglio, Università degli Studi di Parma, Italy

***Correspondence:**
Lourdes Arruvito
arruvitol@gmail.com

Specialty section:
This article was submitted to T Cell Biology, a section of the journal Frontiers in Immunology

Received: *20 June 2018*
Accepted: *14 November 2018*
Published: *30 November 2018*

Citation:
Holgado MP, Sananez I, Raiden S, Geffner JR and Arruvito L (2018) CD32 Ligation Promotes the Activation of CD4$^+$ T Cells. Front. Immunol. 9:2814. doi: 10.3389/fimmu.2018.02814

INTRODUCTION

Receptors for the Fc portion of IgG (FcγRs) are widely express in immune cells and mediate a large array of effector and immunomodulatory mechanisms that influence both innate and adaptive responses (1). FcγRs are classified into two main types that include different members. Type I FcRs belong to the immunoglobulin receptor superfamily and are represented by the canonical Fcγ receptors, including FcγRI, FcγRII, and FcγRIII. Type II FcRs belong to the family of C-type lectin receptors, and include CD209 (DC-SIGN) and CD23 (2). Based on the signaling motifs expressed

in the cytoplasmic domains, type I FcγRs are classified as stimulatory or inhibitory receptors, which are associated with immunoreceptor tyrosine activation motifs (ITAM) or immunoreceptor tyrosine inhibition motifs (ITIM), respectively (1, 3, 4). Stimulatory type I receptors include FcγRI (CD64), FcγRIIa (CD32a), FcγRIIc (CD32c), and FcγRIIIa (CD16), while inhibitory type I receptors only include FcγRIIb (CD32b) (5). Activating FcγRs signal through an ITAM motif that is either present in their intracytoplasmic domain or in associated signaling subunits, such as the FcRγ chain. These ITAM-containing structures allow FcγRs, once aggregated by multimeric ligands, to stimulate signaling cascades via SRC and SYK kinases promoting cell activation. The inhibitory receptor FcγRIIb possesses instead an ITIM motif in its intracytoplasmic domain, which allows this receptor to recruit the SHIP1 phosphatase that counteracts the signaling cascades initiated by activating FcγRs. Therefore, the co-expression of these divergent receptors, which share almost identical ligand-binding domains, establishes a threshold of cell activation (3, 6–8).

The expression pattern and the function of type I FcγR have been well characterized in innate immune cells and B cells (2, 8, 9). By contrast, the expression and function of CD32 in CD4+ T cells remain controversial. The most cited reviews in the field assume that CD4+ T cells do not express FcγRs (1, 10, 11), however, contrasting observations have been published. It has been reported that resting CD4+ T cells do not express CD32 (12–14), while other studies have shown that a minor fraction of resting CD4+ T cells (1–5%) actually expresses CD32 (15, 16). It has also been reported that activation of CD4+ T cells promotes an increased expression of CD32 (17, 18). Moreover, early studies have claimed that more than 80% of resting CD4+ T cells expresses high amounts of CD32 as an intracellular pool (18–20). Interestingly, recent observations suggested that CD32 is a marker of a CD4+ T cell population that contains an HIV reservoir harboring replication-competent proviruses (14), however this finding remains controversial (16, 21).

Immune complexes (ICs) are the natural ligands of low affinity FcγRs (1). High levels of ICs are found in chronic viral infections and autoimmune diseases (22). Moreover, a large body of evidence suggest that ICs play a key role not only in the induction of tissue injury, but also in the promotion of T cell responses (23–28). The mechanisms underlying the ability of ICs to promote the stimulation of T cells have not been clearly defined yet. However, it is usually assumed that they are related to the ability of ICs to interact with FcγRs expressed by macrophages and dendritic cells improving antigen presentation to both CD4+ and CD8+ T cells (27, 28). Interestingly, the enhanced antigen immunogenicity conferred by ICs has been adopted as strategy to improve the therapeutic efficiency of vaccines in experimental models of viral infectious diseases (27, 29, 30).

Here, we showed that a minor fraction of resting CD4+ T cells express cell surface CD32. Activation of CD4+ T cells promoted a marked increase in the expression of CD32 either at the cell surface or intracellularly. Analysis by qRT-PCR on activated CD4+ T cells revealed the presence of mRNA transcripts for both, the stimulatory FcγRIIa (CD32a) and the inhibitory FcγRIIb (CD32b) isoforms, being the CD32a:CD32b mRNA ratio ∼5:1. Consistent with this finding, we found that cross-linking of CD32 by immobilized IgG or specific mAb directed to CD32 enhanced both, the proliferative response and a wide pattern of cytokines by CD4+ T cells stimulated by PHA or anti-CD3 mAb. Overall, our observations suggest that ICs might perpetuate the chronic inflammatory response in patients with autoimmunity and/or chronic viral infections, not only by stimulating innate immune cells, but also by directly interacting with CD4+ T cells via CD32a.

Abbreviations: aCD3/aCD28, anti-CD3 and anti-CD28 stimulation; aIgG, aggregated IgG; ART, antiretroviral treatment; cIgG, coated IgG; Fab'2, F(ab')2 fragment goat anti mouse IgG; FBS, Fetal Bovine Serum; FcγRs, Fc γ receptors; ICs, Immune Complexes; ITAM, immunoreceptor tyrosine activation motifs; ITIM, immunoreceptor tyrosine inhibition motifs; mAb, monoclonal antibody; PBMCs, Peripheral Blood Mononuclear Cells; PBS, Phosphate Buffered Saline; PHA, phytohemagglutinin; STAT, Signal transducer and activator of transcription; TCR, T cell receptor.

MATERIALS AND METHODS

Subjects

Buffy coat was obtained from 1 unit of blood collected from 45 donors (average 34 years, range 25–42 years), and processed immediately after volunteer's donations. None of the donors had any hereditary disorders, hematologic abnormalities, or infectious diseases. The local ethics committee has approved this study and informed consent was obtained from all donors.

Peripheral Blood Mononuclear Cell (PBMCs) Isolation

PBMCs were obtained from buffy coats by Ficoll-Hypaque gradient centrifugation (GE Healthcare Life Sciences).

Monocytes and CD4+ T Cell Isolation

Monocytes and/or CD4+ T cells were enriched from buffy coats by using the RosetteSep human monocyte and/or CD4+ T cells enrichment cocktails (Stem Cell Technologies) respectively, following the manufacturer's protocols. The purity determined by flow cytometry was always >97%.

Cell Sorting

Both CD32+CD4+ and CD32-CD4+ T cell subsets were purified by cell sorting with a FACSAria Fusion flow cytometer (BD Biosciences). Briefly, previously activated PBMCs were stained with anti-CD3 PerCP, anti-CD4 APC, and CD32 PE-Cy7 monoclonal antibodies (mAbs, all from Biolegend) and sorted yielding the following subpopulations CD4+CD32+ T cells and CD4+CD32- T cells. Cells were collected into RPMI 1640 medium containing 50% FBS and washed twice prior to further studies. The purity determined by flow cytometry was always >99% for each subset. Cells were resuspended in TRIzol reagent (Thermo Fisher) and used for qRT-PCR.

Flow Cytometry

Freshly isolated or *in vitro*-cultured cells were stained with anti-CD3, CD4, CD8, CD14, CD19, CD25, HLA-DR, PD-1, and Tim-3 mAb (all from Biolegend). Staining of CD32 was performed by using two different anti-human CD32 mAb: FUN.2 clone (mouse anti-human CD32 PE or PECy7 conjugated, Biolegend) and IV.3 clone (mouse anti-human CD32 purified antibody, Stem Cell Technologies) that was revealed with a secondary PE goat Fab2 anti-mouse IgG (DAKO). Intracellular detection of Ki-67 antigen with anti-Ki-67 antibody was performed using fixed and permeabilized cells following the manufacturer's instructions (BD Biosciences). Control samples were incubated with an isotype-matched antibody. For the determination of CD32 expression, PE and/or PE-Cy7 mouse IgG2b kappa (Biolegend) were included as isotype controls, using a threshold value ≤ 0.2 in all cases. When CD32 was determined by using unconjugated IV.3 clone, a purified mouse IgG2b kappa (Biolegend) was used as isotype control followed by a secondary PE anti-mouse antibody. Dead cells were excluded by forward and side scatter characteristics. Statistical analyses were based on at least 100,000 events gated on the population of interest. The data were acquired using a FACSCanto II (Becton Dickinson) and analyzed with FlowJo software.

Fluorescence Microscopy

Briefly, purified cells were incubated with monoclonal anti-CD32 Alexa Fluor 647 and anti-CD4 Alexa Fluor 488 or anti-CD14 Alexa Fluor 488 as indicated (all from Biolegend). Then, cells were washed twice and allowed to adhere on polylysine-coated coverslips. After which, cells were fixed with 4% paraformaldehyde in Phosphate Buffered Saline (PBS) for 12 m at 4°C, washed twice and treated with 10 mM glycine for 10 m at room temperature. The coverslips mounted with DAPI Fluoromount-G (SouthernBiotech) were studied in a Nikon Eclipse Ti-S L100 fluorescence microscope using a Plan Apochromat 100 × 1.40 NA oil immersion objective.

PBMCs Culture

PBMCs (1×10^6/ml) were stimulated with IL-2 (20 ng/ml, Peprotech), coated anti-CD3 (aCD3, 10 μg/ml, Beckman Coulter) plus soluble anti-CD28 (aCD28, 1 mg/ml, BD Biosciences), or unstimulated, and cultured for 36 h in medium RPMI 1640 (Gibco) supplemented with 10% heat-inactivated fetal bovine serum (FBS, Natocor), 2 mM L-glutamine (Gibco), 100 U/ml penicillin (Gibco), and 0.1 mg/ml streptomycin (Gibco). In some experiments, cells were treated with phytohemagglutinin (PHA, 4 μg/ml; Sigma-Aldrich) and cultured for 36 h. After that, cells were washed twice and analyzed by flow cytometry.

Real-Time Quantitative RT-PCR

Total RNA was extracted using TRIzol reagent following manufacturer's instructions. Subsequently, RNA was treated with RQ1 RNAse-free DNAse (Promega) and reverse transcripted using M-MLV Reverse Transcriptase (Sigma-Aldrich). PCR analysis for both, CD32a (FcγRIIa) and CD32b (FcγRIIb) isoforms was performed with a real-time PCR detection system (StepONE-Plus Applied Biosystems) using 5 × HOT FIREPol® EvaGreen® qPCR Mix Plus (ROX) (Solis BioDyne Corp) as a fluorescent DNA-binding dye. GAPDH was used as housekeeping gene. The amplification protocol was as follows: 1 cicle at 95°C for 10 m and 40 cycles of denaturation at 95°C for 15 s, annealing at 56°C for 15 s and extension at 72°C for 1 m. The melting curve was also performed. Each sample was evaluated by triplicate.

The following primer sets were used: FcγRIIa forward primer, 5′-ATCATTGTGGCTGTGGTCATTGC-3′ and reverse primer, 5′- TCAGGTAGATGTTTTTATCATCG-3′; and FcγRIIb forward primer, 5′- GGGATCATTGTGGCTGTG-3′ and FcγRIIb reverse primer, 5′-ATTAGTGGGATTGGCTG-3′. GAPDH forward primer, 5′-GAGTCAACGGATTTGGTCGT-3′ and reverse primer 5′-TTGATTTTGGAGGGATCTCG-3′. Primer sets yielded a single product of the correct size.

As a source of cDNA for standard curves to which all samples were normalized (calibrator), monocytes were isolated as previously described. Standard curves and relative quantification was performed as previously published (31). In short, the threshold cycle (C_T) values, determined by the StepONE Plus software v2.3, were used to calculate and plot a linear regression curve to evaluate the quality of the standard curve. The slope of this line was used to determine the efficiency of the reaction *(E)*. From the C_T's and the efficiencies obtained, the normalized value was calculated with the following formula: $E_T^{\,CpT(C)-CpT(S)}$:$E_R^{\,CpR(C)-CpR(S)}$, in which E_T is the efficiency of the PCR of the target gene (FcγRIIa or FcγRIIb2); E_R, the efficiency of the PCR of the reference gene (GAPDH); CpT(C), the measured C_T of the target gene determined for standard or calibrator (FcγRIIa or FcγRIIb of one selected monocyte sample for all measurements); CpT(S), the measured C_T of the target gene determined for the sample (donor of interest); CpR(C), the measured C_T of the reference gene of the calibrator or standard; and CpR(S), the measured C_T of the reference gene of the sample.

Ligation of CD32

CD32 was cross-linked in purified CD4+ T cells by using two different approaches:

1- Ligation with coated IgG (cIgG): We immobilized IgG on plastic plates, as described (32). Human IgG (500 μg/ml, Sigma-Aldrich) was added to each well of a 48 multiwell plate (GBO). After overnight incubation, plates were washed 3 times with PBS to yield immobilized IgG. Purified CD4+ T cells (1×10^6/ml) were seeded on cIgG overnight.

2- Ligation with specific anti-CD32 mAb: Purified CD4+ T cells (1×10^6/ml) were preincubated for 30 m with anti-CD32 mAb (30 μg/ml, clone IV.3; Stem Cell Technologies) and then stimulated by the addition of F(ab′)2 fragment goat anti mouse IgG (Fab'2, 50 μg/ml; Jackson ImmunoResearch) for additional 30 min. Afterwards, cells were seeded on uncoated plates overnight.

After CD32 ligation by one of the two aforementioned approaches, cells were stimulated with suboptimal doses of PHA (0.5 μg/ml) or anti-CD3 coated beads (0.025 μg/ml, Miltenyi Biotec) and cultured during 5 d. As controls, CD4+ T cells

were added to uncoated plates and stimulated with PHA or anti-CD3 coated beads, according to the experiment. The proliferative response and the cytokine levels were analyzed by flow cytometry and ELISA, respectively.

Neutralization Assay

To block the CD32 receptor expressed by CD4+ T cells, cells were incubated with a blocking anti-CD32 mAb (30 μg/ml, clone IV.3) before being exposed to cIgG (IV.3 plus cIgG). An isotype-matched antibody was used as a control.

Binding of Heat-Aggregated IgG (aIgG)

IgG aggregates (aIgG) were prepared by heating human IgG (25 mg/ml) for 12 m at 63°C. Then, aIgG was centrifuged at 10,000 g for 5 m and the precipitate was discarded. Resting or activated purified CD4+ T cells were incubated with different doses of aIgG (50, 100, or 400 μg/ml, as indicated), or serum free-medium for 2 h at 37°C. Then, cells were washed three times and stained with biotinylated anti-human IgG Fc (Biolegend) for 30 m at 4°C followed by streptavidin PerCP and anti-CD4 V500. Binding of aIgG was analyzed by flow cytometry. In blocking experiments, cells were pretreated with the blocking antibody IV.3 clone (30 μg/ml) for 30 m at 4°C, before the addition of aIgG (IV.3 plus aIgG).

Calcium Mobilization Assay

CD32-triggered calcium transients were analyzed by flow cytometry on purified CD4+ T cells using Fluo-3,AM probe (Molecular Probes, Thermo Fisher). Briefly, 1×10^6 resting CD4+ T cells were stained with anti-CD4 mAb APC. After washing twice, cells were treated with 5 μM Fluo-3,AM for 20 m at 37°C. Then, the sample was immediately loaded onto the flow cytometer for calcium baseline measurement during 30 s. Afterward, the purified anti-CD32 mAb (IV.3 clone, 30 μg/ml) was added and calcium measurement was performed for other 30 s. Subsequently, the cells were incubated at 37°C for 15 m. After this time, Fab′2 (50 μg/ml) was added and calcium mobilization was measured immediately and incubated at 37°C for another 60 s. Finally, the fluorescence was recorded during an additional period of 60 s. As a positive control, we treated cells with ionomycin (Sigma-Aldrich). A time-based gate was used for the analysis in gated CD4+ T cells.

STAT5 and STAT6 Phosphorylation

Purified CD4+ T cells (1×10^6) were cultured in the presence of cIgG (500 μg/ml) or IV.3 (30 μg/ml) plus cIgG for 18 h. Then, cells were re-stimulated with PHA (0.5 μg/ml) and cultured for 3 d. After this period, cells were fixed and permeabilized (BD Biosciences) according to the manufacturer's protocols. Cells were washed twice with PBS and stained with anti-CD3 FITC and anti-STAT 5 (pY694) Alexa Fluor 647 or anti-STAT6 (pTyr641) Alexa Fluor 647, for 30 m at room temperature. Cells were then analyzed on a BD FACS Canto II flow cytometer.

ELISA

Levels of IL-2, IL-5, IL-10, IFN-γ, TNF-α (BD Biosciences), and IL-17 (Biolegend) were quantified in cells supernatants by ELISA following manufacturer's recommendations.

Statistical Analysis

Statistical analysis was performed using GraphPad Prism 6 software. Two groups were compared using the Wilcoxon signed-rank test or Mann–Whitney *t*-test as appropriated. Three or more groups were compared using the Kruskall–Wallis test followed by Dunn's multiple comparison tests. A $p < 0.05$ was considered statistically significant.

RESULTS

Resting CD4+ T Cells Express CD32

In a first set of experiments, we explored the expression of CD32 in resting CD4+ T cells by using two different anti-CD32 mAbs (FUN.2 and IV.3 clones). CD32 expression was also analyzed on monocytes, B cells, and CD8+ T cells. As described (33–35), monocytes and B cells showed a high expression of CD32, by contrast only a minor fraction of CD8+ T cells and CD4+ T cells expressed CD32. In fact, we found that ∼2.4% ± 0.4 of CD4+ T cells were shown to be positive for the expression of CD32 ($n = 18$; **Figures 1A–C**). We then analyzed the cytoplasmic expression of CD32 in CD4+ T cells. Results in **Figures 1D,E** show that ∼8.5% ± 1.9 of permeabilized cells expressed CD32 ($n = 9$), indicating that CD4+ T cells store an intracellular pool of this receptor.

Increased Expression of CD32 in Activated CD4+ T Cells

Next, we examined whether T cell activation was able to modulate CD32 expression. PBMCs were stimulated with IL-2 or with antibodies directed to CD3 and CD28 for 18 or 36 h. Then, the expression of CD32 was analyzed. Treatment with aCD3/aCD28 antibodies markedly increased cell surface expression of CD32 at either 18 or 36 h of culture while IL-2 induced no increase of CD32 expression (**Figures 2A,B**). We also observed that activation of CD4+ T cells by aCD3/aCD28 antibodies resulted in an increased pool of cytoplasmic CD32 (**Figures 2C,D**).

Activation of CD4+ T cells by PHA also promoted an increased expression of CD32 (**Figures 2E,F**). Because the expression of CD32 was increased during CD4+ T cell activation, we analyzed whether CD32 expression was associated with the induction of T cell activation markers. Results in **Figure 2G** show that the subpopulation of CD32+ CD4+ T cells was enriched not only in the expression of activation markers such as CD25 and HLA-DR, but also in the expression of the inhibitory receptors PD-1 and Tim-3, which are usually associated with an exhausted CD4+ T cell phenotype (36). Further experiments were performed to evaluate the relative expression of CD32 isoforms (CD32a and CD32b) by qRT-PCR in sorted CD32+CD4+ and CD32-CD4+ T cell subsets, after activation with aCD3/aCD28 antibodies. We found that the mRNA levels for CD32a were significantly higher compared with CD32b, being the CD32a:CD32b mRNA ratio ∼5:1 in both cell subsets ($n = 7$, **Figure 2H**). On the other hand, and consistent with the higher expression of CD32 observed in activated cells, we found that cell activation also resulted in an increased ability of CD4+ T cells to bind aIgG, in a dose-dependent mode (**Figures 3A,B**). As expected, binding of aIgG was prevented by

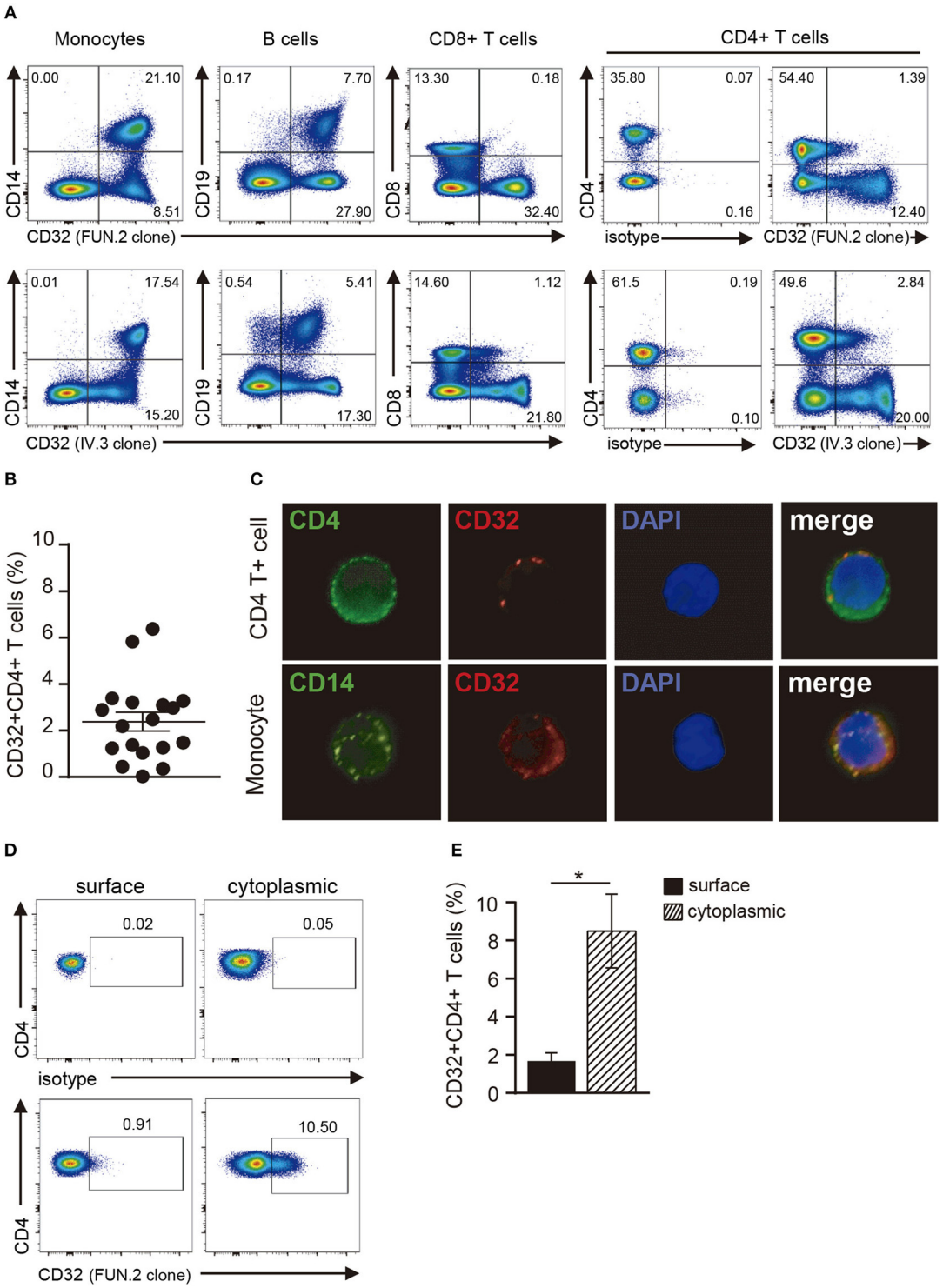

FIGURE 1 | Analysis of CD32 expression in resting CD4+ T cells. **(A)** Representative dot plot of CD32 cell surface expression in monocytes (CD14+), B cells (CD19+), CD8+ and CD4+ T cells from a healthy adult donor using two different anti-CD32 mAb (FUN.2 and IV.3 clones) analyzed by flow cytometry. Surface isotype control labeling was set to stringent criteria. Results are expressed as percentages on PBMCs. **(B)** Frequency of CD32+ cells on gated CD4+ T cells from healthy adults using the FUN.2 clone mAb by flow cytometry. **(C)** Fluorescence microscopy of CD32 expression in purified CD4+ T cells and monocytes (green: CD4 or CD14, red: CD32). Nuclear counterstain with DAPI was used. Representative images are shown at x300. **(D)** Representative dot plot of cell surface and cytoplasmic CD32 expression in permeabilized resting CD4+ T cells. Surface and cytoplasmic isotype controls are shown. **(E)** Frequency of cell surface and cytoplasmic CD32 expression on resting CD4+ T cells. Results are expressed as percentages on CD4+ T cells. Representative experiments are shown in **(A,C,D)**. Mean ± SEM of n donors are shown in **(B)** ($n = 18$) and **(E)** ($n = 9$). *$p < 0.05$. Wilcoxon matched-pairs signed rank test was used for analysis in **(E)**.

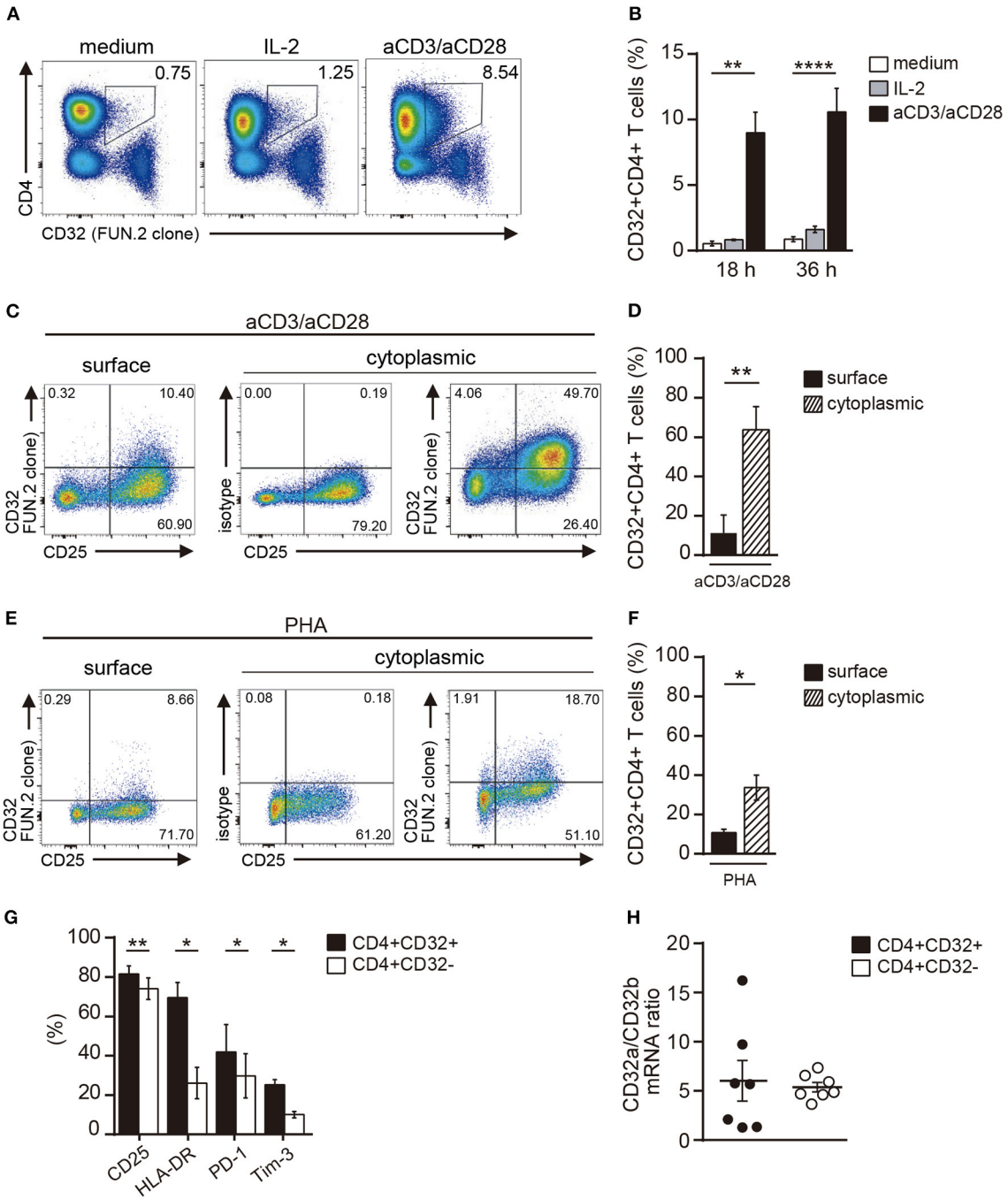

FIGURE 2 | Activation of CD4+ T cells results in an increased expression of CD32. **(A,B)** PBMCs were cultured with medium (controls), IL-2 (20 ng/ml) or immobilized anti-CD3 (10 μg/ml) plus soluble anti-CD28 (1 mg/ml) (aCD3/aCD28) antibodies, during 18 or 36 h. The frequency of CD32+CD4+ T cells was analyzed by flow cytometry. **(A)** Representative dot plots of cell surface expression of CD32 in CD4+ T cells analyzed at 36 h of culture. Results are expressed as percentages on total lymphocytes. **(B)** Frequency of CD32+ cells on gated CD4+ T cells at 18 and 36 h of culture. **(C–F)** PBMCs were activated with either aCD3/aCD28 antibodies **(C,D)** or PHA (4 μg/ml, **E,F**) for 36 h. Then, cell surface or intracellular expression of CD32 was analyzed. Cell surface expression of CD25 was also assessed. Cytoplasmic isotype control is shown in **(C,E)**. **(G)** Cell frequency of the different markers analyzed in CD32+CD4+ and CD32-CD4+ T cells. Results are expressed as percentage on each CD4+ T cell subset analyzed. **(H)** CD32a/CD32b mRNA ratio in activated CD32-CD4+ and CD32+CD4+ T cell subsets analyzed by qRT-PCR. Representative experiments are shown in **(A,C,E)**. Mean ± SEM of *n* donors are shown in **(B)** ($n = 7$), **(D)** ($n = 7$), **(F)** ($n = 7$), **(G)** ($n = 8$), and **(H)** ($n = 7$). $^{*}p < 0.05$, $^{**}p < 0.01$, $^{****}p < 0.0001$. Kruskal–Wallis test followed by Dunn's multiple comparison was used for analysis in **(B)**. Wilcoxon matched-pairs signed rank test was used for analysis in **(D,F,G,H)**.

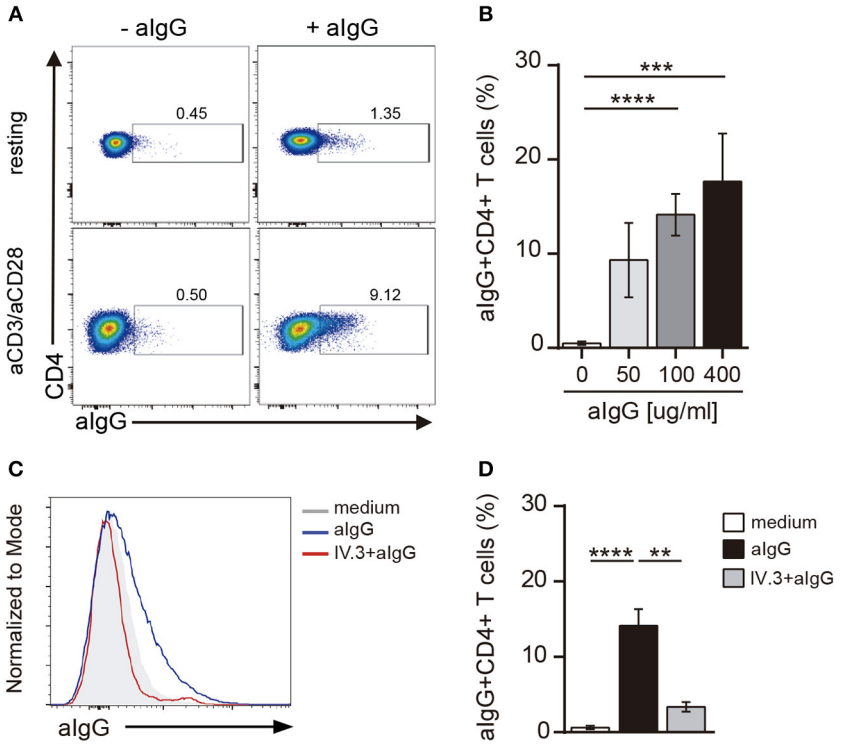

FIGURE 3 | CD4+ T cells bind aIgG. **(A)** Resting or activated purified CD4+ T cells were incubated with aIgG (400 μg/ml) or serum-free medium for 2 h. Then, cells were washed and the binding of aIgG was analyzed by flow cytometry. **(B)** Activated CD4+ T cells were incubated with increasing concentrations of aIgG (50, 100, and 400 μg/ml) or serum-free medium. Data show the percentage of aIgG+CD4+ T cells. **(C,D)** Activated CD4+ T cells were treated with or without an anti-CD32 blocking antibody (IV.3 clone, 30 μg/ml) during 30 m. After washing, cells were incubated with 100 μg/ml of aIgG or serum-free medium. **(C)** Representative histograms of aIgG percentage are shown. **(D)** Percentage of aIgG+CD4+ T cells is shown. Representative experiments are shown in **(A,C)**. Mean ± SEM of *n* donors are shown in **(B)** ($n = 8$) and **(D)** ($n = 8$). $^{**}p < 0.01$, $^{***}p < 0.001$, $^{****}p < 0.0001$. Kruskal–Wallis test followed by Dunn's multiple comparison was used for analysis in **(B)**. Mann–Whitney test was used for analysis in **(D)**.

the anti-CD32 blocking IV.3 mAb (14.1% ± 2.2 vs. 3.4% ± 0.6, for aIgG and IV.3 plus aIgG, respectively, $p < 0.01$, $n = 8$; **Figures 3C,D**).

Ligation of CD32 Promotes the Activation of CD4+ T Cells

Ligation of CD32 has shown to induce calcium signaling in myeloid cells and platelets (37, 38). To analyze the functionality of CD32, we first analyzed its ability to induce calcium transient in CD4+ T cells. In these experiments, cells were preincubated with the IV.3 mAb and then treated with a Fab'2 polyclonal goat anti-mouse IgG (39). Results in **Figure 4A** (upper panel) show that CD32 ligation caused the induction of a strong calcium transient.

We then analyzed whether CD32 ligation was able to promote the proliferation of CD4+ T cells. In these experiments, isolated CD4+ T cells were stimulated, or not, with cIgG or IV.3 plus a Fab′2 polyclonal goat anti-mouse IgG (IV.3 plus Fab′2) for 18 h. Then, cells were re-stimulated with a suboptimal dose of PHA (0.5 μg/ml) and cultured during 5 d. The proliferative response was analyzed by studying the expression of the Ki-67 antigen as a proliferation marker. We found that ligation of CD32 does not induce proliferation of CD4+ T cells (data not shown), but significantly increased the proliferative response induced by PHA. As expected, pretreatment of CD4+ T cells with the blocking IV.3 mAb significantly prevented the enhancing effect induced by cIgG on the proliferation of CD4+ T cells (**Figures 4B,C**). No proliferation was observed in cells treated only with IV.3 or a secondary goat Fab2 anti-mouse IgG, compared with those cells cultured in medium alone (data not shown). Consistent with these findings, we found that CD32 ligation also stimulated the proliferative response of CD4+ T cells triggered by beads coated with anti-CD3 mAb (28.2% ± 7.1 and 3.5% ± 0.9, for CD4+ T cells pretreated, or not, with cIgG, respectively, $p < 0.01$; $n = 6$). Moreover, this enhancing effect was significantly inhibited in presence of the mAb IV.3 (**Figures 4D,E**).

Not only the proliferation, but also the production of a wide pattern of cytokines was stimulated by CD32 ligation in CD4+ T cells cultured with suboptimal doses of PHA. However, the two different approaches for CD32 ligation displayed a different stimulating ability (**Figure 5A**). Cross-linking of IV.3 with a Fab′2 goat anti-mouse IgG (IV.3 plus Fab′2) resulted in a strong enhancement in the production of IL-2 (1738.0 pg/ml ± 490.6 vs. 10.6 pg/ml ± 3.8, $p < 0.001$), IL-5 (267.9 pg/ml ± 57.9 vs. 17.9 pg/ml ± 11.0, $p < 0.001$), IL-10 (793.1 pg/ml ± 15.8 vs. 36.7

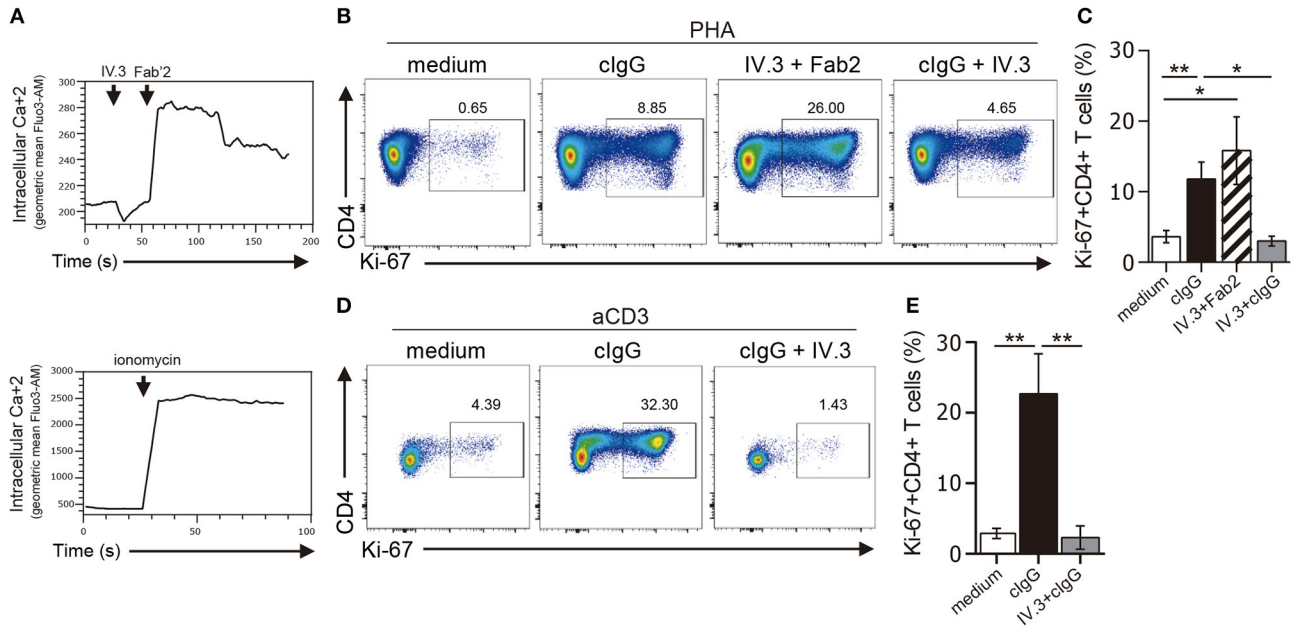

FIGURE 4 | Stimulation through CD32 promotes the expansion of CD4+ T cells activated by suboptimal doses of different stimuli. **(A)** Purified CD4+ T cells labeled with fluo-3,AM fluorescent probe were treated with an anti-CD32 mAb (IV.3 clone) for 15 m. Then a F(ab′)2 fragment goat anti mouse IgG was added to induce the cross-linking of bound IV.3 mAb. Induction of cytosolic calcium transients was analyzed by flow cytometry at three different times: before and after addition of IV.3 and after stimulation with Fab′2 (upper panel). Cells were treated with ionomycin as a positive control (lower panel). A representative experiment is shown (n =5). Geometric mean of fluo-3,AM vs. time is depicted. **(B–E)** Purified CD4+ T cells (1×10^6) were cultured in the presence of medium (control), cIgG or IV.3 plus a Fab′2 antibody directed to mouse IgG, for 18 h. When IV.3 was used as blocking mAb, cells were pretreated with IV.3 clone, before being exposed to cIgG. Then, cells were stimulated with a suboptimal concentration of PHA (0.5 μg/ml, **B,C**) or anti-CD3 coated beads (0.025 μg/ml, **D,E**) and cultured for 5 d. Proliferative response was evaluated by using Ki-67 staining. **(B–D)** Representative dot plots of CD4 and Ki-67 staining are shown. Results are expressed as cell percentages on gated CD4+ T cells. **(C–E)** Percentage of Ki-67+CD4+ T cells analyzed by flow cytometry. Representative experiments are shown in **(B,D)**. Mean ± SEM of n donors are shown in **(C)** (n = 10) and **(E)** (n = 6). *p < 0.05, **p < 0.01. Kruskal–Wallis test followed by Dunn's multiple comparison was used for analysis in **(C,E)**.

pg/ml ± 11.8, $p < 0.0001$), IFN-γ (4443.0 pg/ml ± 1218 vs. 1132.0 pg/ml ± 591.1, $p < 0.05$), and TNF-α (414.6 pg/ml ± 147.0 vs. 12.3 pg/ml ± 4.0, $p < 0.001$), compared with control cells (n = 10). There was also a non-significant increase in the production of IL-17. No cytokine secretion was detected in cells treated only with IV.3 or a secondary goat Fab2 anti-mouse IgG (data not shown). On the other hand, exposure of CD4+ T cells to cIgG did not increase IL-2 levels, but significantly enhanced the secretion of IL-5 (77.9 pg/ml ± 25.3; $p < 0.01$), IL-10 (142.9 pg/ml ± 33.6; $p < 0.05$), IFN-γ (4954.0 pg/ml ± 772.8; $p < 0.001$), and TNF-α (59.1 pg/ml ± 16.9; $p < 0.01$), compared with control cells. Pretreatment of CD4+ T cells with the IV.3 mAb significantly inhibited the stimulatory effect of cIgG on the production of IL5, IFN-γ, and TNF-α (**Figure 5A**).

Similar findings were observed in CD4+ T cells upon stimulation with anti-CD3 coated beads. Exposure of CD4+ T cells to cIgG significantly increased the secretion of IL-5 (338.1 pg/ml ± 90 vs. 75.7 pg/ml ± 37.4; $p < 0.01$), IL-17 (59.1 pg/ml ± 16.4 vs. 13.2 pg/ml ± 7.0; $p < 0.01$), compared with control cells. It also promoted the secretion of IL-2 (208.5 pg/ml ± 93.8 vs. 35.8 pg/ml ± 18.6), IL-10 (329.2 pg/ml ± 69.4 vs. 130.4 pg/ml ± 46.2), IFN-γ (27,323 pg/ml ± 8285 vs. 10,126 pg/ml ± 5704), and TNF-α (360.2 pg/ml ± 123.3 vs. 130.8 pg/ml ± 36.2) compared with control cells, even this enhancing effect did not reach statistical significance (n = 6). As expected, pretreatment of CD4+ T cells with the IV.3 mAb significantly inhibited the stimulatory effect of cIgG on the production of IL5, IL-10, IL-17, IFN-γ, and TNF-α (**Figure 5B**).

IL-2 supports the proliferation of CD4+ T cells being the activation of STAT5 one of the earliest events in IL-2 signaling through the high affinity IL-2 receptor (40). Results in **Figures 5C,D** show that cIgG promoted STAT5 phosphorylation in CD4+ T cells cultured with suboptimal concentrations of PHA (9.4% ± 3.2 vs. 4.4% ± 1.3, for cIgG treated vs. untreated cells, $p < 0.05$). Moreover, we found that cIgG also enhanced the phosphorylation of STAT6, which is the main transcription factor responsible for the development of Th2 cells (41) (38.6% ± 14.5 vs. 10.5% ± 4.6, for cIgG treated vs. untreated cells, $p < 0.05$). As expected, pretreatment with the blocking IV.3 mAb significantly prevented the stimulatory effect induced by cIgG on the phosphorylation of both, STAT5 and STAT6 (**Figure 5E,F**, n = 5).

DISCUSSION

The expression and function of FcγRs in innate immune cells and B cells have been clearly defined (2, 9, 10). Although it is generally assumed that T cells do not express FcγRs (8, 12, 42) a more detailed analysis of early published studies shows

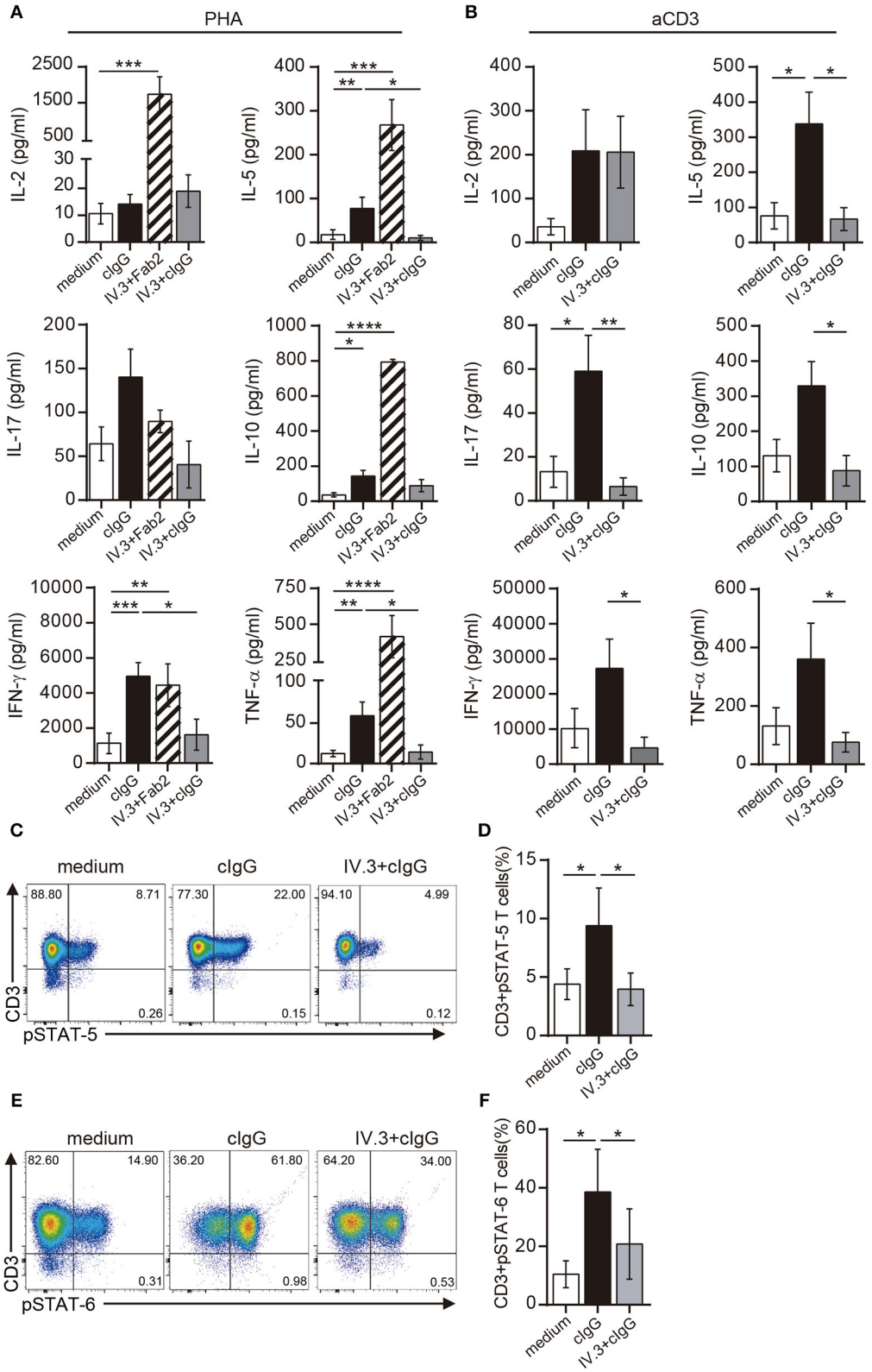

FIGURE 5 | Stimulation through CD32 promotes the release of cytokines in CD4+ T cells activated by suboptimal doses of different stimuli. **(A,B)** Purified CD4+ T cells (1×10^6) were cultured in the presence of medium (control, white bar), cIgG (black bar) or IV.3 plus a Fab′2 antibody directed to mouse IgG (striped bar), for

(Continued)

FIGURE 5 | 18 h. When IV.3 was used as blocking mAb, cells were pretreated with IV.3 clone, before being exposed to cIgG (gray bar). Then, cells were stimulated with a suboptimal concentration of PHA (0.5 μg/ml, **A**) or anti-CD3 (0.025 μg/ml, **B**) and cultured for 5 d. Levels of cytokines were quantified in the culture supernatant by ELISA. **(C–F)** Purified CD4+ T cells (1×10^6) were cultured in the presence of medium or cIgG for 18 h. When IV.3 was used as blocking mAb, cells were pretreated with IV.3 clone, before being exposed to cIgG. Then, cells were stimulated with a suboptimal concentration of PHA (0.5 μg/ml) and cultured for 3 d. STAT5 **(C,D)** and STAT6 **(E,F)** phosphorylation was analyzed by flow cytometry. Results are expressed as percentage on CD4+ T cells. Representative experiments are shown in **(C,E)**. The mean ± SEM of n experiments is shown in **(A)** ($n = 10$), **(B)** ($n = 6$), **(D)** ($n = 5$), and **(F)** ($n = 5$). $^*p < 0.05$, $^{**}p < 0.01$, $^{***}p < 0.001$, $^{****}p < 0.0001$. Mann–Whitney test was used for analysis in **(A,B)**. Kruskal–Wallis test followed by Dunn's multiple comparison was used for analysis in **(D,F)**.

contradictory findings (17–19). In this study, we found not only that a minor fraction of resting CD4+ T cells expresses CD32, but also that T cell activation induces a marked up-regulation of CD32 expression in either the cell surface or the cytoplasmic compartment. The role of CD32, if any, in determining the function of CD4+ T cells remains undefined. Here we reported that, contrasting with the inhibitory effect of CD32 in B cell responses (3, 43), it promotes the activation of CD4+ T cells.

Our observations indicating that a small percentage of resting CD4+ T cells expresses cell surface CD32 are in agreement with those data recently reported by Martin et al. (16) in studies directed to analyze the role of CD32+CD4+ T cells as viral reservoirs in HIV-infected patients. Moreover, in accordance with Sandilands et al. (19), we also found that resting CD4+ T cells express a cytoplasmic pool of CD32. However, while these authors reported that more than 90% of resting CD4+ T cells stores an intracellular pool of CD32, we found that only ∼9% of resting CD4+ T cells contain a cytoplasmic pool of CD32. The reasons underlying this discrepancy are unclear. On the other hand, and in agreement with early works (17, 18), we detected that activation of CD4+ T cells increases cell surface expression of CD32, reaching a peak at 36 h of culture. We also found that CD32 expressing CD4+ T cells displayed an activated phenotype characterized by the expression of activation markers such as CD25 and HLA-DR as well as by the expression of the inhibitory receptors PD-1 and Tim-3, which are usually associated with an exhausted CD4+ T cell phenotype. Accordingly, with these findings, we observed that activated CD4+ T cells bind higher amounts of aIgG compared with resting cell. Our results showing that concentrations of aIgG as high as 100 μg/ml were unable to saturate CD32 binding capacity are consistent with the fact that CD32 is a low- affinity FcγR.

It has long been known that IgG ICs suppress humoral immunity. This effect is mediated through the interaction of the Fc fragment of IgG antibodies with the only FcγR isoform expressed by B cells, FcγRIIb. In fact, cross-linking of FcγRIIb with the B cell receptor has shown to increase the threshold for B cell activation, inhibiting antibody production (3, 43, 44). Interestingly, our findings revealed for the first time that cross-linking of CD32 efficiently promoted the activation of CD4+ T cells stimulated by either suboptimal doses of PHA or anti-CD3 mAb. Our results showing that ligation of CD32 promotes the activation of CD4+ T cells suggest that CD32a is the predominant type of FcγRII expressed in this cell population. The similarity of the extracellular domains of CD32b and CD32a does not enable the differentiation of these receptors by flow cytometry because there are no commercially available antibodies that can distinguish between them. The present study provides evidence indicating the presence of both CD32 mRNA isoforms in activated CD4+ T cells, being CD32a the predominant one. In fact, we found that activation of CD4+ T cells resulted in the expression of both CD32a and CD32b transcripts in a ratio of 5:1, respectively.

Ligation of CD32 induced by seeding CD4+ T cells on immobilized IgG or by treatment with anti-CD32 mAbs promoted neither cell proliferation nor cytokine production by CD4+ T cells. However, both stimuli significantly enhanced the proliferative response and the production of a wide array of cytokines by CD4+ T cells treated with suboptimal doses of PHA or anti-CD3 mAb. We found a higher production of cytokines associated with the development of Th1 (IL-2, IFN-γ, and TNF-α), Th2 (IL-5), and Th17 (IL-17) profiles, suggesting that CD32 ligation does not promote a particular signature in CD4+ T cells. Because ICs are the most important ligands for FcγRs, our observations might be relevant in those disorders associated with the presence of high levels of circulating ICs, such as chronic infections (45–47), autoimmune diseases (48–51) and cancer (52–54). Our results suggest that ICs might promote the development of inflammatory responses, by acting directly on CD4+ T cells via CD32a. Moreover, our results could contribute to better explain why antigens contained in ICs promote a stronger T cell responses compared with non-complexed antigens, a phenomenon usually attributed to the ability of ICs to stimulate antigen presentation through major histocompatibility complex class II and class I molecules (27–30). Further studies are required to confirm both, the ability of ICs to activate CD32 in presence of the high concentrations of monomeric IgG found in plasma and the *in vivo* relevance of our observations.

It should be note that the ability of ICs to modulate the function of CD4+ T cells could be related not only to the expression of CD32, but also to the expression of CD16 (FcγRIII). Early studies showed the expression of CD16 in a small number of peripheral T cells in healthy individuals (12, 55). Moreover, more recent studies performed by Chauhan and coworkers (13, 56–58) reported that CD4+ T cell activation leads to the up-regulation of CD16 expression. In a first paper, the authors showed that ligation of CD16 in CD4+ T cells by ICs induces a co-stimulatory signal promoting IFN-γ production (56). In a second study, they reported that ICs isolated from systemic lupus erythematosus patients interact with CD16 expressed by CD4+ T cells and induce Syk phosphorylation, providing a co-stimulatory signal to T cells in the absence of CD28 signal. This mechanism was shown to be able to promote the development of Th1 and Th17 cells (57). Finally, the authors reported that stimulation of CD4+ T cells by ICs induced, not only the up-regulation of endosomal toll-like receptors (TLRs), but also the accumulation of TLR9 on the cell surface (13).

Overall, our results suggest that CD32 ligation promoted CD4+ T cell activation. Whether CD16 might acts in concert with CD32 to induce the activation of CD4+ T cells remains to be addressed. Because autoimmune diseases are usually associated with the formation and tissue deposition of immune complexes (42), we hypothesize that they might contribute to tissue damage, not only by activating inflammatory mechanisms mediated by innate immune cells, but also by stimulating the chronic activation of CD4+ T cells. Finally, the fact that CD32 ligation can influence CD4+ T cell activation may have another important clinical implication. Modulating the ability of a therapeutic IgG antibody to bind to activating or inhibitory CD32 could promote the balance in favor of CD4+ T cell activation or suppression. Cellular activation is a desired characteristic in immunotherapies directed to cancer or in vaccine generation against infectious diseases. However, when it comes to chronic inflammation or autoimmune diseases, the contrary effect is sought, being the suppression of the immune response a requirement for the induction of immune tolerance. Thus, therapeutic strategies based on monoclonal IgG antibodies must take into account the potential modulation on CD4+ T cell function through their Fc portion as a novel key player.

ETHICS STATEMENT

This study was approved by the Ethics Committee of the University of Buenos Aires, Buenos Aires, Argentina, in accordance with the Declaration of Helsinki (Fortaleza, 2013). Written informed consent was obtained from all donors.

AUTHOR CONTRIBUTIONS

MH designed and performed the experiments, analyzed data, and wrote the manuscript. IS performed some experiments and analyzed data. SR analyzed data. JG contributed to experimental design, data analysis, and revised the manuscript. LA designed the experiments, analyzed data, and wrote the manuscript.

FUNDING

This work was supported by grants from the National Agency for Promotion of Science and Technology, Argentina (PIDC 0010-2015 to JG, and PMO BID PICT 2016-0444 to LA), and CONICET (PIP 2015-2017, 0223 to LA).

ACKNOWLEDGMENTS

We are indebted to Dr. Monica Vermeulen for her technical assistance and for kindly supplied reagents. We also thank to Dr. Carla Pascuale and Dr. Virginia Polo from Flow Cytometry team at INBIRS, Facultad de Medicina, Universidad de Buenos Aires, for their assistance with cell sorting. We thank all the team members of Blood Bank at Servicio de Hemoterapia, Sanatorio Méndez, Buenos Aires, Argentina.

REFERENCES

1. Bournazos S, Chow SK, Abboud N, Casadevall A, Ravetch JV. Human IgG Fc domain engineering enhances antitoxin neutralizing antibody activity. *J Clin Invest.* (2014) 124:725–9. doi: 10.1172/JCI72676
2. Pincetic A, Bournazos S, DiLillo DJ, Maamary J, Wang TT, Dahan R, et al. Type I and type II Fc receptors regulate innate and adaptive immunity. *Nat Immunol.* (2014) 15:707–16. doi: 10.1038/ni.2939
3. Amigorena S, Bonnerot C, Drake JR, Choquet D, Hunziker W, Guillet JG, et al. Cytoplasmic domain heterogeneity and functions of IgG Fc receptors in B lymphocytes. *Science* (1992) 256:1808–12.
4. Swanson JA, Hoppe AD. The coordination of signaling during Fc receptor-mediated phagocytosis. *J Leukoc Biol.* (2004) 76:1093–103. doi: 10.1189/jlb.0804439
5. Muta T, Kurosaki T, Misulovin Z, Sanchez M, Nussenzweig MC, Ravetch JV. A 13-amino-acid motif in the cytoplasmic domain of Fc gamma RIIB modulates B-cell receptor signalling. *Nature* (1994) 369:340. doi: 10.1038/369340a0
6. Ono M, Bolland S, Tempst P, Ravetch JV. Role of the inositol phosphatase SHIP in negative regulation of the immune system by the receptor Fc(gamma)RIIB. *Nature* (1996) 383:263–6. doi: 10.1038/383263a0
7. Ravetch JV, Lanier LL. Immune inhibitory receptors. *Science* (2000) 290:84–9. doi: 10.1126/science.290.5489.84
8. Nimmerjahn F, Ravetch JV. Fcgamma receptors as regulators of immune responses. *Nat Rev Immunol.* (2008) 8:34–47. doi: 10.1038/nri2206
9. Guilliams M, Bruhns P, Saeys Y, Hammad H, Lambrecht BN. The function of Fcgamma receptors in dendritic cells and macrophages. *Nat Rev Immunol.* (2014) 14:94–108. doi: 10.1038/nri3582
10. Ravetch JV, Bolland S. IgG Fc receptors. *Annu Rev Immunol.* (2001) 19:275–90. doi: 10.1146/annurev.immunol.19.1.275
11. Hogarth PM. Fc receptors are major mediators of antibody based inflammation in autoimmunity. *Curr Opin Immunol.* (2002) 14:798–802. doi: 10.1016/s0952-7915(02)00409-0
12. Sandor M, Lynch RG. Lymphocyte Fc receptors: the special case of T cells. *Immunol Today* (1993) 14:227–31.
13. Chauhan AK. Human CD4(+) T-cells: a role for low-affinity fc receptors. *Front Immunol.* (2016) 7:215. doi: 10.3389/fimmu.2016.00215
14. Descours B, Petitjean G, Lopez-Zaragoza JL, Bruel T, Raffel R, Psomas C, et al. CD32a is a marker of a CD4 T-cell HIV reservoir harbouring replication-competent proviruses. *Nature* (2017) 543:564–7. doi: 10.1038/nature21710
15. Mantzioris BX, Berger MF, Sewell W, Zola H. Expression of the Fc receptor for IgG (Fc gamma RII/CDw32) by human circulating T and B lymphocytes. *J Immunol.* (1993) 150:5175–84.
16. Martin GE, Pace M, Thornhill JP, Phetsouphanh C, Meyerowitz J, Gossez M, et al. CD32-expressing CD4 T cells are phenotypically diverse and can contain proviral HIV DNA. *Front Immunol.* (2018) 9:928. doi: 10.3389/fimmu.2018.00928
17. Engelhardt W, Matzke J, Schmidt RE. Activation-dependent expression of low affinity IgG receptors Fc gamma RII(CD32) and Fc gamma RIII(CD16) in subpopulations of human T lymphocytes. *Immunobiology* (1995) 192:297–320.
18. Sandilands GP, MacPherson SA, Burnett ER, Russell AJ, Downie I, MacSween RN. Differential expression of CD32 isoforms following alloactivation of human T cells. *Immunology* (1997) 91:204–11.
19. Sandilands GP, McLaren AP, Howie D, MacSween RN. Occult expression of CD32 (Fc gamma RII) in normal human peripheral blood mononuclear cells. *Immunology* (1995) 86:525–32.
20. Sandilands GP, Burnett ER, MacPherson SA, Downie I, More IA, MacSween RN. Demonstration of cytoplasmic CD32 (Fc gamma RII) within human lymphocytes following microwave treatment. *Immunology* (1997) 90:427–34.
21. Abdel-Mohsen M, Kuri-Cervantes L, Grau-Exposito J, Spivak AM, Nell RA, Tomescu C, et al. CD32 is expressed on cells with transcriptionally active HIV but does not enrich for HIV DNA in resting T cells. *Sci Transl Med.* (2018) 10:eaar6759. doi: 10.1126/scitranslmed.aar6759
22. Theofilopoulos AN, Dixon FJ. Immune complexes in human diseases: a review. *Am J Pathol.* (1980) 100:529–94.

23. Celis E, Chang TW. HBsAg-serum protein complexes stimulate immune T lymphocytes more efficiently than do pure HBsAg. *Hepatology* (1984) 4:1116–23.
24. Xu DZ, Huang KL, Zhao K, Xu LF, Shi N, Yuan ZH, et al. Vaccination with recombinant HBsAg-HBIG complex in healthy adults. *Vaccine* (2005) 23:2658–64. doi: 10.1016/j.vaccine.2004.10.040
25. Heyman B. Antibodies as natural adjuvants. *Curr Top Microbiol Immunol.* (2014) 382:201–19. doi: 10.1007/978-3-319-07911-0_9
26. Pelegrin M, Naranjo-Gomez M, Piechaczyk M. Antiviral monoclonal antibodies: can they be more than simple neutralizing agents? *Trends Microbiol.* (2015) 23:653–65. doi: 10.1016/j.tim.2015.07.005
27. Lambour J, Naranjo-Gomez M, Piechaczyk M, Pelegrin M. Converting monoclonal antibody-based immunotherapies from passive to active: bringing immune complexes into play. *Emerg Microbes Infect.* (2016) 5:e92. doi: 10.1038/emi.2016.97
28. Wen YM, Mu L, Shi Y. Immunoregulatory functions of immune complexes in vaccine and therapy. *EMBO Mol Med.* (2016) 8:1120–33. doi: 10.15252/emmm.201606593
29. Bournazos S, Wang TT, Dahan R, Maamary J, Ravetch JV. Signaling by antibodies: recent progress. *Annu Rev Immunol.* (2017) 35:285–311. doi: 10.1146/annurev-immunol-051116-052433
30. Maamary J, Wang TT, Tan GS, Palese P, Ravetch JV. Increasing the breadth and potency of response to the seasonal influenza virus vaccine by immune complex immunization. *Proc Natl Acad Sci USA.* (2017) 114:10172–7. doi: 10.1073/pnas.1707950114
31. van Mirre E, Breunis WB, Geissler J, Hack CE, de Boer M, Roos D, et al. Neutrophil responsiveness to IgG, as determined by fixed ratios of mRNA levels for activating and inhibitory FcgammaRII (CD32), is stable over time and unaffected by cytokines. *Blood* (2006) 108:584–90. doi: 10.1182/blood-2005-12-4997
32. Banki Z, Kacani L, Mullauer B, Wilflingseder D, Obermoser G, Niederegger H, et al. Cross-linking of CD32 induces maturation of human monocyte-derived dendritic cells via NF-kappa B signaling pathway. *J Immunol.* (2003) 170:3963–70. doi: 10.4049/jimmunol.170.8.3963
33. Brooks DG, Qiu WQ, Luster AD, Ravetch JV. Structure and expression of human IgG FcRII(CD32). Functional heterogeneity is encoded by the alternatively spliced products of multiple genes. *J Exp Med.* (1989) 170:1369–85.
34. de Andres B, Mueller AL, Verbeek S, Sandor M, Lynch RG. A regulatory role for Fcgamma receptors CD16 and CD32 in the development of murine B cells. *Blood* (1998) 92:2823–9.
35. Boruchov AM, Heller G, Veri MC, Bonvini E, Ravetch JV, Young JW. Activating and inhibitory IgG Fc receptors on human DCs mediate opposing functions. *J Clin Invest.* (2005) 115:2914–23. doi: 10.1172/JCI24772
36. Avery L, Filderman J, Szymczak-Workman AL, Kane LP. Tim-3 co-stimulation promotes short-lived effector T cells, restricts memory precursors, and is dispensable for T cell exhaustion. *Proc Natl Acad Sci USA.* (2018) 115:2455–60. doi: 10.1073/pnas.1712107115
37. Roberts GM, Davies EV, Pettit EJ, Hallett MB. The timing and magnitude of Ca2+ signaling by CD32 depends on its redistribution on the cell surface. *Exp Cell Res.* (1997) 230:303–9. doi: 10.1006/excr.1996.3416
38. Arman M, Krauel K. Human platelet IgG Fc receptor FcgammaRIIA in immunity and thrombosis. *J Thromb Haemost.* (2015) 13:893–908. doi: 10.1111/jth.12905
39. Ghazizadeh S, Bolen JB, Fleit HB. Tyrosine phosphorylation and association of Syk with Fc gamma RII in monocytic THP-1 cells. *Biochem J.* (1995) 305(Pt 2):669–74.
40. Burchill MA, Yang J, Vogtenhuber C, Blazar BR, Farrar MA. IL-2 receptor beta-dependent STAT5 activation is required for the development of Foxp3+ regulatory T cells. *J Immunol.* (2007) 178:280–90. doi: 10.4049/jimmunol.178.1.280
41. O'Shea JJ, Paul WE. Mechanisms underlying lineage commitment and plasticity of helper CD4+ T cells. *Science* (2010) 327:1098–02. doi: 10.1126/science.1178334
42. Takai T. Roles of Fc receptors in autoimmunity. *Nat Rev Immunol.* (2002) 2:580–92. doi: 10.1038/nri856
43. Muta T, Kurosaki T, Misulovin Z, Sanchez M, Nussenzweig MC, Ravetch JV. A 13-amino-acid motif in the cytoplasmic domain of Fc gamma RIIB modulates B-cell receptor signalling. *Nature* (1994) 368:70–3. doi: 10.1038/368070a0
44. Xiang Z, Cutler AJ, Brownlie RJ, Fairfax K, Lawlor KE, Severinson E, et al. FcgammaRIIb controls bone marrow plasma cell persistence and apoptosis. *Nat Immunol.* (2007) 8:419–29. doi: 10.1038/ni1440
45. Kliks S. Antibody-enhanced infection of monocytes as the pathogenetic mechanism for severe dengue illness. *AIDS Res Hum Retroviruses* (1990) 6:993–8. doi: 10.1089/aid.1990.6.993
46. Hessell AJ, Hangartner L, Hunter M, Havenith CE, Beurskens FJ, Bakker JM, et al. Fc receptor but not complement binding is important in antibody protection against HIV. *Nature* (2007) 449:101–4. doi: 10.1038/nature06106
47. Monsalvo AC, Batalle JP, Lopez MF, Krause JC, Klemenc J, Hernandez JZ, et al. Severe pandemic 2009 H1N1 influenza disease due to pathogenic immune complexes. *Nat Med.* (2011) 17:195–9. doi: 10.1038/nm.2262
48. Ohyama K, Ueki Y, Kawakami A, Kishikawa N, Tamai M, Osaki M, et al. Immune complexome analysis of serum and its application in screening for immune complex antigens in rheumatoid arthritis. *Clin Chem.* (2011) 57:905–9. doi: 10.1373/clinchem.2010.157776
49. Moore TL. Immune complexes in juvenile idiopathic arthritis. *Front Immunol.* (2016) 7:177. doi: 10.3389/fimmu.2016.00177
50. Mancini I, Ferrari B, Valsecchi C, Pontiggia S, Fornili M, Biganzoli E, et al. ADAMTS13-specific circulating immune complexes as potential predictors of relapse in patients with acquired thrombotic thrombocytopenic purpura. *Eur J Intern Med.* (2017) 39:79–83. doi: 10.1016/j.ejim.2016.11.003
51. Olaru F, Dobel T, Lonsdorf AS, Oehrl S, Maas M, Enk AH, et al. Intracapillary immune complexes recruit and activate slan-expressing CD16+ monocytes in human lupus nephritis. *JCI Insight* (2018) 3:96492. doi: 10.1172/jci.insight.96492
52. Gamberale R, Geffner JR, Giordano M. Immune complexes and apoptosis in B-cell chronic lymphocytic leukemia. *Leuk Lymphoma* (2002) 43:251–5. doi: 10.1080/10428190290006008
53. Dhodapkar KM, Kaufman JL, Ehlers M, Banerjee DK, Bonvini E, Koenig S, et al. Selective blockade of inhibitory Fcgamma receptor enables human dendritic cell maturation with IL-12p70 production and immunity to antibody-coated tumor cells. *Proc Natl Acad Sci USA.* (2005) 102:2910–5. doi: 10.1073/pnas.0500014102
54. Cramer DW, O'Rourke DJ, Vitonis AF, Matulonis UA, Dijohnson DA, Sluss PM, et al. CA125 immune complexes in ovarian cancer patients with low CA125 concentrations. *Clin Chem.* (2010) 56:1889–92. doi: 10.1373/clinchem.2010.153122
55. Lanier LL, Kipps TJ, Phillips JH. Functional properties of a unique subset of cytotoxic CD3+ T lymphocytes that express Fc receptors for IgG (CD16/Leu-11 antigen). *J Exp Med.* (1985) 162:2089–106.
56. Chauhan AK, Chen C, Moore TL, DiPaolo RJ. Induced expression of FcgammaRIIIa (CD16a) on CD4+ T cells triggers generation of IFN-gammahigh subset. *J Biol Chem.* (2015) 290:5127–40. doi: 10.1074/jbc.M114.599266
57. Chauhan AK, Moore TL, Bi Y, Chen C. FcgammaRIIIa-Syk Co-signal modulates CD4+ T-cell response and up-regulates Toll-like Receptor (TLR) expression. *J Biol Chem.* (2016) 291:1368–86. doi: 10.1074/jbc.M115.684795
58. Chauhan AK. A contribution of FcγRIIIa cosignaling in T_{FH} subset development in Systemic Lupus Erythematosus. *bioRxiv* (2018) 256198:1–31. doi: 10.1101/256198

Conflict of Interest Statement: The authors declare that the research was conducted in the absence of any commercial or financial relationships that could be construed as a potential conflict of interest.

Copyright © 2018 Holgado, Sananez, Raiden, Geffner and Arruvito. This is an open-access article distributed under the terms of the Creative Commons Attribution License (CC BY). The use, distribution or reproduction in other forums is permitted, provided the original author(s) and the copyright owner(s) are credited and that the original publication in this journal is cited, in accordance with accepted academic practice. No use, distribution or reproduction is permitted which does not comply with these terms.

frontiers in Immunology

REVIEW
published: 14 December 2018
doi: 10.3389/fimmu.2018.02914

Modulating T Cell Responses via Autophagy: The Intrinsic Influence Controlling the Function of Both Antigen-Presenting Cells and T Cells

Seth D. Merkley[1], *Cameron J. Chock*[2], *Xuexian O. Yang*[2,3], *James Harris*[4] and *Eliseo F. Castillo*[1,3,5]*

[1] Clinical and Translational Science Center, University of New Mexico Health Sciences, Albuquerque, NM, United States, [2] Department of Molecular Genetics and Microbiology, University of New Mexico Health Sciences, Albuquerque, NM, United States, [3] Autophagy Inflammation and Metabolism Center of Biomedical Research Excellence, University of New Mexico Health Sciences, Albuquerque, NM, United States, [4] Rheumatology Group, Centre for Inflammatory Diseases, Department of Medicine, School of Clinical Sciences at Monash Health, Faculty of Medicine, Nursing and Health Sciences, Monash University, Clayton, VIC, Australia, [5] Division of Gastroenterology and Hepatology, Department of Internal Medicine, University of New Mexico School of Medicine, Albuquerque, NM, United States

OPEN ACCESS

Edited by:
Pierre Guermonprez, King's College London, United Kingdom

Reviewed by:
Stephanie Hugues, Université de Genève, Switzerland
Josef Mautner, Technische Universität München, Germany

***Correspondence:**
Eliseo F. Castillo
ecastillo@salud.unm.edu

Specialty section:
This article was submitted to Antigen Presenting Cell Biology, a section of the journal Frontiers in Immunology

Received: *16 August 2018*
Accepted: *28 November 2018*
Published: *14 December 2018*

Citation:
Merkley SD, Chock CJ, Yang XO, Harris J and Castillo EF (2018) Modulating T Cell Responses via Autophagy: The Intrinsic Influence Controlling the Function of Both Antigen-Presenting Cells and T Cells. Front. Immunol. 9:2914. doi: 10.3389/fimmu.2018.02914

Autophagy is a homeostatic and inducible process affecting multiple aspects of the immune system. This intrinsic cellular process is involved in MHC-antigen (Ag) presentation, inflammatory signaling, cytokine regulation, and cellular metabolism. In the context of T cell responses, autophagy has an influential hand in dictating responses to self and non-self by controlling extrinsic factors (e.g., MHC-Ag, cytokine production) in antigen-presenting cells (APC) and intrinsic factors (e.g., cell signaling, survival, cytokine production, and metabolism) in T cells. These attributes make autophagy an attractive therapeutic target to modulate T cell responses. In this review, we examine the impact autophagy has on T cell responses by modulating multiple aspects of APC function; the importance of autophagy in the activation, differentiation and homeostasis of T cells; and discuss how the modulation of autophagy could influence T cell responses.

Keywords: autophagy, T cells, macrophages, inflammation, immunometabolism, immunotherapy

INTRODUCTION

Autophagy is an evolutionarily conserved cellular response that can selectively or non-selectively direct cargo to the lysosome where cargo is degraded for subsequent recycling (1). Autophagy is upregulated under conditions of physiological stress, particularly amino acid starvation, during which it acts as a cell survival mechanism, recycling cytoplasmic macromolecules. The term "autophagy" encompasses three complementary processes; microautophagy, chaperone-mediated autophagy (CMA) and macroautophagy. Each form of autophagy involves the delivery of cytoplasmic substrates to lysosomes for degradation. Microautophagy involves the direct engulfment of cytoplasmic cargo by lysosomes (or the vacuole in plants and fungi) and can either be non-selective, or selective, as in the cases of micropexophagy (degradation of peroxisomes), micromitophagy (degradation of mitochondria), and piecemeal microautophagy of the nucleus (PMN) (2). CMA involves the selective targeting of soluble cytosolic proteins to lysosomes for degradation. Proteins targeted by CMA have a common pentapeptide motif (KFERQ) which is recognized by the chaperone protein Hsc70 (heat shock cognate protein of 70 KDa) (3).

Macroautophagy involves the formation of double-membrane vesicles, termed autophagosomes, around a portion of cytoplasm, including organelles such as damaged/leaky mitochondria (e.g., mitophagy), misfolded or aggregated proteins (e.g., aggrephagy) or microbes (e.g., xenophagy) (4). Autophagosomes are then able to fuse with functional lysosomes ("maturation" or "flux") for degradation of the luminal contents.

Macroautophagy (herein, called autophagy) is a fundamental, homeostatic process integrated into both the innate and adaptive arms of the immune system (4, 5). The immunological functions of autophagy appear to interact and modify "classical" innate immune pathways including (i) direct microbial elimination; (ii) cooperation with pattern recognition receptors (PRR); (iii) inflammasome regulation; (iv) secretion of biomolecules; and (v) major histocompatibility complexes (MHC) and antigen processing (4–6). In addition, autophagy plays a major role in B and T cell activation, proliferation and survival as well as affects positive and negative thymic selection of naïve T cells (7, 8). This integration points to autophagy as an important cellular process that safeguards the host with a functional innate and adaptive immune system. It also highlights how perturbations in autophagy, either because of genetics or environmental factors, might influence health and disease. Notwithstanding, autophagy is an attractive therapeutic target to modulate T cell responses directly in T cells or indirectly through APC like dendritic cells (DC) and macrophages. This network of communication between autophagy with the immunological pathways as well as cellular metabolism is discussed in the following few sections with an emphasis on how it affects T cell responses.

CROSSTALK BETWEEN AUTOPHAGY AND INNATE PATHWAYS TO INFLUENCE T CELL RESPONSES

The above immunological functions of autophagy represent the interplay and interaction of this cellular process within a single cell (e.g., pathogen elimination in APC; proliferation through clearance of cell cycle proteins in T cells). This section seeks to discuss the physiological and immunological relevance of autophagy and how it interacts at a systemic level—whereby autophagy in innate immune cells (e.g., DC and macrophages) affects $CD8^+$ and $CD4^+$ T helper (TH) cell responses. This type of crosstalk may play a critical role in the pathogenesis of various diseases such as Crohn's disease (CD), rheumatoid arthritis (RA) and multiple sclerosis (MS) as well as chronic infections like tuberculosis (TB).

Autophagy and Antigen Presentation

MHC-restricted antigen presentation is key to the specificity of immunity and marks an important intersection between innate and adaptive immune pathways. Processed antigenic peptides are loaded on Class I or II MHC molecules and presented by professional APC to T cells for priming and activation. MHC class I-restricted antigens, which stimulate primed $CD8^+$ T cells, originate mostly from endogenous proteins, processed by proteasomes and transported to the ER for loading (9). MHC Class II-restricted antigens, on the other hand, are recognized by $CD4^+$ T cells and were originally thought to be almost exclusively of extracellular origin, taken up by endocytosis, micropinocytosis, or phagocytosis and processed by specialized endosomal and lysosomal enzymes. However, some exogenous antigens can be cross-presented by MHC Class I (MHC I) molecules, while MHC Class II (MHC II) molecules can also present endogenous proteins (9).

Autophagy is an intricate pathway involving numerous proteins to execute several steps that lead to the degradation of biomolecules, organelles and pathogens (**Figure 1**). A number of studies indicate that autophagy represents an important factor in the presentation of endogenous antigens via MHC II (10). Particularly, autophagosomes have been shown to fuse directly with MHC II loading compartments (11, 12). Moreover, fusion of viral and tumor antigens to the ATG8 (autophagy-related-gene 8) family protein LC3-II, which localizes to autophagosomal membranes, increases presentation to $CD4^+$ T cells (12–14). Interestingly, an unbiased study of the MHC II ligandome by mass spectrometry, revealed nutrient starvation (a mechanism to induce autophagy) leads to a 50% increase in the presentation of nuclear and cytosolic antigens (15). Many MHC II ligands express Atg8-binding domains (LC3-interacting regions; LIR) that may target them to autophagosomes (15). As it is, functional autophagy has been shown to facilitate presentation of several pathogen-derived antigens, including nuclear antigen 1 of the Epstein-Barr virus, the mycobacterial antigen Ag85B and modified vaccinia virus Ankara encoded antigens (16–18).

Autophagy also appears to play an important role in thymic selection of T cells, mediated by thymic epithelial cells (TEC). TEC express low levels of peripheral tissue-specific antigens under the transcriptional regulation of the autoimmune regulator (AIRE), which requires loading of endogenous antigens onto MHC II molecules for positive and negative selection (19). Nedjic and colleagues revealed TEC use autophagy to load endogenous molecules to MHC II molecules and interference of autophagy in TEC results in colitis and multi-organ inflammation (20). They further show positive selection of some, but not all, transgenic $CD4^+$ thymocytes is inhibited in $Atg5^{-/-}$ thymi (20). In addition, targeting of cognate antigens to autophagosomes by fusing them with either LC3B or mitochondria results in negative selection of the respective TCR transgenic $CD4^+$ T cells (21).

A role for autophagy in MHC I presentation has been controversial. MHC I presentation is dependent on proteasomal processing of antigenic peptides and is dependent on the transport of peptides from endosomal compartments to the cytosol, the very opposite of autophagy, which transports cytosolic components to endocytic compartments. Nevertheless, studies have indicated roles for autophagy in this antigen presenting pathway. Loss of autophagy can redirect autophagy substrates to proteasomes for processing and MHC I-restricted presentation (22). Furthermore, autophagosomes have been shown to target proteasome components for degradation (23, 24). Conversely, inhibition of normal MHC I processing pathways, which can occur in some viral infections, may result in increased endosomal/autophagosomal involvement (10). Autophagy has also been implicated in cross-presentation of exogenous antigens.

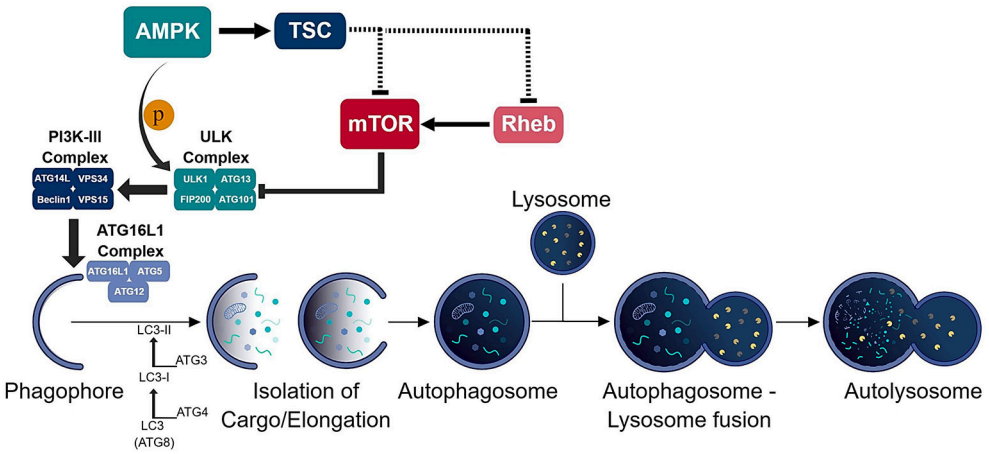

FIGURE 1 | Schematic of the autophagic process. The consecutive activation of the ULK (ULK1/ATG13/FIP200/ATG101) and PI3K-III (ATG14L/VPS34/Beclin-1/VPS15) complexes results in the generation of the phagophore and recruitment of the ATG16L1 (ATG16L1-ATG5-ATG12) conjugation complex to the phagophore. ATG16L1 complex initiates the elongation of the phagophore to become an autophagosome. The formation of the autophagosome and isolation of cargo is assisted by the LC3 (ATG8) conjugation system. The isolated cargo is then degraded in the autolysosome which is formed via autophagosome-lysosome fusion.

Of note, mouse $CD8^+$ DC, which are the predominant cross-presenters *in vivo* (25, 26), have higher basal autophagy rates than $CD8^-$ DC, which are not capable of cross-presentation (27). Similarly, both mouse and human DC more adept at cross-presentation of accumulated large ubiquitinated aggregates, also termed dendritic cell aggresome-like structures (DALIS), that can function as reservoirs for MHC I antigens (22), and these structures were also positive for the autophagy receptor p62/SQSTM1. Additionally, LC3 was recruited to zymosan-containing phagosomes in these cells, indicating that the autophagy machinery intersects with phagosomes containing exogenous antigens. This study went on to demonstrate that the contribution of autophagy was dependent on the form of antigen, being required for cross-presentation of soluble antigen (ovalbumin, OVA), but not OVA targeted to apoptotic bodies or the receptor DEC-205 (cell-associated antigen) (27). How autophagy regulates the cross-presentation of soluble antigens is not yet clear and requires further elucidation. Nonetheless, these studies support an underappreciated role for autophagy in MHC I presentation; however, the effect it has on $CD8^+$ T cell responses remains unclear.

The intersection of autophagy with both MHC I and II pathways reiterate the importance of autophagy in innate cells in controlling T cell responses. Interestingly, MHC II molecules show the strongest linkage to inflammatory and autoimmune diseases like CD, MS, RA, systemic lupus erythematosus (SLE) and type 1 diabetes (T1D) (28, 29). Genome-wide association studies have also implicated autophagy genes *Atg5* and *Atg16l1* in the susceptibility of SLE and CD, respectively (30–34). It is unclear if this genetic linkage is tied to direct autophagy-MHC crosstalk, defects in autophagy, or hyperactive autophagy. However, it was recently shown in animal model of MS that the autophagy gene *Atg5* was required in DC to present endogenous self-peptides to autoreactive $CD4^+$ T cells (35). ATG5 assisted in the fusion of phagosomes containing injured oligodendroglial cells with MHC II compartments. In the absence of ATG5, there was a decrease in autoreactive $CD4^+$ T cells which delayed the onset of disease and reduced clinical severity compared to mice expressing ATG5 in DC (35). Given the apparent role of autophagy in central tolerance, a mechanism to limit autoreactive T cells (20, 21), it is plausible to link autophagy to autoreactive T cells. Thus, while full mechanistic understanding of autophagy/autophagy genes and MHC I and II pathways remains elusive, it is evident autophagy in APC can greatly influence T cell responses via both MHC I and II pathways.

Autophagy and IL-1 Family Cytokines

Numerous studies have shown autophagy intersects with the production, processing and release of IL-1 family cytokines (36, 37). Loss of autophagy in macrophages and DC results in the increased release of IL-1β and IL-18 in response to Toll like receptor (TLR)3 and TLR4 ligation. This is dependent on Toll/IL-1 receptor domain-containing adaptor inducing IFN-β (TRIF), caspase-1 activation, potassium efflux and mitochondria-derived reactive oxygen species (ROS) and DNA (38–41). Moreover, this effect appears to be largely dependent on the NLRP3 inflammasome (38, 40).

Inflammasomes are multi-protein complexes which activate caspase-1 (and in certain cases caspase-4/5) in response to pathogen-associated molecular patterns (PAMPs) and damage-associated molecular patterns (DAMPs) (42–45). The secretion of IL-1β and IL-18 is typically a two-stage process. First, transcription and translation of inactive pro-forms of the cytokines are induced following ligation of pattern recognition receptors, such as TLRs. Second, inflammasome activation occurs in response to ligation or activation of a NOD-like receptor (NLR), such as NLRP1, NLRP3, or NLRC4, or an AIM2-like receptor (ALR) (46). In most cases, the NLR or ALR forms a

complex with apoptosis-associated speck-like protein containing a caspase activation and recruitment domain (ASC) to engage and activate caspase-1, which in turn leads to the cleavage and release of pro-IL-1β or pro-IL-18 into mature, bioactive cytokines (**Figure 2**). The NLRP3 inflammasomes is activated in response to multiple stimuli, including particulates, such as uric acid crystals, vaccine adjuvants and silica (47–49), as well as reactive oxygen species (ROS) and mitochondrial DNA (39, 41).

Thus, loss of autophagy, and more specifically mitophagy (a form of autophagy that sequesters and degrades mitochondria) (50), in macrophages and DC, combined with inflammatory stimulation, can lead to the accumulation of damaged/dysfunctional mitochondria. This chain of events leads to the release of mitochondrial ROS and DNA into the cytosol, which in turns activates the NLRP3 inflammasome, leading to increased caspase-1-dependent processing and release of IL-1β and IL-18. However, the link between autophagy and inflammasome regulation does not end there (**Figure 2**).

Many studies suggest direct links between autophagy, inflammasomes, and inflammatory signaling pathways, although the complexity of this subject is considerable, due to the numerous means autophagy can regulate the same pathways. For example, regulation of inflammasome activation and release of IL-1 family members by autophagy has an indirect effect on nuclear factor kappa-light-chain-enhancer of activated B cells (NF-κB) pathway, as these cytokines (IL-1, IL-18) all signal through NF-κB- dependent pathways. NF-κB is an evolutionary conserved transcription factor that regulates an ever-expanding network of genes with a wide range of functions in cell survival, differentiation, proliferation, and immunity, acting downstream TLRs and cytokine receptors. Studies have demonstrated that, following activation of NF-κB, autophagy plays a role in the degradation of the NF-κB inhibitor family IκB, leading to persistent activation and inflammation (51). Additionally, autophagy inhibits inflammasome activation and IL-1β release by stimulated macrophages through elimination of mitochondrial products, pro-IL-1β and inflammasome components, which in turns leads to reduced NF-κB activation by IL-1β (38, 52, 53). Conversely, loss of autophagy in macrophages and DC leads to increased IL-1β release which activates NF-κB in an autocrine manner (54). Accordingly, autophagy and NF-κB-dependent inflammation and cytokine release converge on multiple levels in APC, with significant impact on cell function and subsequent modulation of immune responses.

Another important function of autophagy is to clear protein complexes that are too large for proteasomal degradation. One study suggests that active inflammasomes may be targeted for lysosomal degradation by autophagosomes (53). These data would suggest that autophagy might represent an important checkpoint for controlling excessive inflammasome activation, which can lead to inflammatory pathologies. Autophagosomes have also been shown to specifically target IL-1β following activation with TLR agonists (38). However, the fate of this autophagosomal IL-1β is potentially more complex than that suggested for inflammasomes. Induction of autophagy during or after priming of cells with a TLR agonist results in a reduction of intracellular pro-IL-1β (38), but it is unclear whether it is degraded in the autophagosomes, or whether it is transported elsewhere for proteasomal degradation, which appears to be the more common route of degradation for this cytokine (55). However, autophagy may also have a role to play in the secretion of IL-1β. While most secreted proteins have an N-terminal signal peptide that allows them to traffic through the classical secretion pathway, a number of secreted proteins, including IL-1β and IL-1α, lack such a signal peptide and are released by largely undefined mechanisms, termed unconventional secretion. Two studies have demonstrated that autophagy may play a role in the unconventional secretion of IL-1β (56, 57). Together, these studies may indicate that autophagosomes act as temporary repository for IL-1β, which can either be directed to a degradative or secretory pathway, depending on the context and specific stimuli. It is not clear whether IL-18 is also targeted to autophagosomes. While the biological effects of IL-1α are similar to those of IL-1β, its release is independent of inflammasome activation *per se*. IL-1α's biological activity does not require proteolytic cleavage, although it can be cleaved by both the calcium-dependent cysteine protease calpain and by the cytotoxic lymphocyte-derived protease granzyme B (58, 59). Nevertheless, inflammasome activation does enhance IL-1α release, possibly due to increased cell death. As with IL-1β and IL-18, autophagic defects in APC increases the release of IL-1α in response to inflammatory stimuli, including TLR agonists and allergens (38, 60, 61). However, unlike IL-1β, this release is independent of NLRP3, caspase-1 and TRIF (38, 60), but dependent on ROS and calpain (60). It is not yet clear whether autophagy is involved in the unconventional secretion of IL-1α, or whether IL-1α associates with autophagosomes.

APC Autophagy and the TH17 Connection

A large and ever-growing body of evidence has established multiple roles for autophagy in the regulation of proinflammatory cytokines (IL-1, IL-18) secreted by APC. A disruption in the autophagy pathway has also been shown to impact the secretion of other proinflammatory cytokines (IL-17, IL-23) and chemokines (CXCL1) (54, 60). For example, IL-1β released from macrophages can stimulate IL-23 secretion in an autocrine manner (62) and this occurs in LPS-stimulated macrophages and DC in which autophagy is inhibited (54). Secretion of IL-23 under these circumstances can be inhibited with an IL-1 receptor antagonist or neutralizing antibody against IL-1β. Similarly, autophagy-deficient macrophages that secrete excess IL-1α have increased CXCL1 output that can be curbed by an IL-1 receptor antagonist (60). Conversely, inducing autophagy after *in vitro* APC stimulation reduces IL-1α, IL-1β, IL-23, and CXCL1 secretion (54, 60). Additionally, treating mice with the autophagy inducer rapamycin inhibits both IL-1β and IL-23 in response to intraperitoneal injection of LPS (38, 54).

Whether directly or indirectly, autophagy appears to regulate cytokines and chemokines that promote IL-17-mediated immune responses. The combination of IL-23 with IL-1α/IL-1β, promotes TH17 cellular differentiation and stimulates the secretion of IL-17 from innate-like γδ T cells (63–65). IL-1, IL-17, and CXCL1 can cause neutrophilic tissue infiltration (66–68).

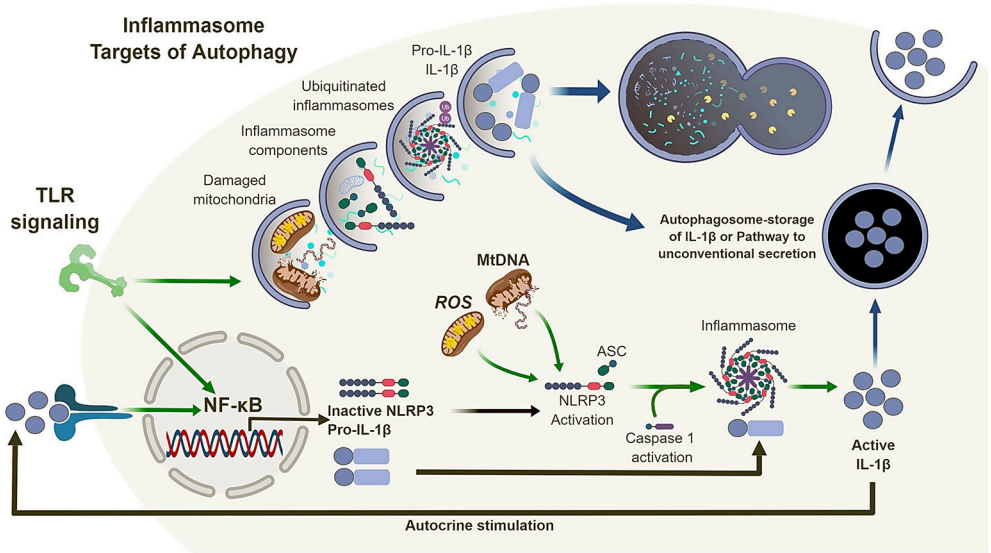

FIGURE 2 | Autophagy and the inflammasome. TLR signaling results in the activation of NF-κB which in turn regulates the expression of NLRP3 and pro-IL-1β. Mitochondrial reactive oxygen species (ROS) and DNA can lead to the activation and oligomerization of NLRP3 and recruitment of the adaptor protein ASC. This complex recruit and activates caspase 1 subsequently, recruiting, and activating IL-1β. Autophagy is also induced by TLR signaling which in turn can regulate the inflammasome pathway via direct clearance of activators (mitochondria), inflammasomes and subunits (NLRP3, ASC) as well as its substrates (pro-IL-1β). In the absence of autophagy, damaged mitochondria can accumulate and activate the inflammasome pathway leading to the dysregulation of IL-1β production and secretion.

Furthermore, *in vitro* treatment of naïve murine $CD3^+$ T cells with supernatants from LPS and 3-MA-treated dendritic cells (high in IL-1α, IL-1β, and IL-23), enhances secretion of IL-17A, IL-17F, IFN-γ, and IL-22 (54).

Regarding TH17 cells, these $CD4^+$ T cells play an important role in controlling extracellular bacteria and fungi by producing the cytokines IL-17A and IL-17F that act on epithelial cells to recruit neutrophils. TH17 cells and cytokines associated with TH17 responses have also been implicated in numerous autoimmune and infectious diseases (69, 70). In fact, several studies confirm that autophagy disruption in APC during infection leads to excessive inflammation which is associated with upregulated levels of IL-1 and IL-17 (**Figure 3**) (60, 61, 71, 72). Given the loss of autophagy in APC leads to increased secretion of IL-1 family cytokines and IL-23 upon inflammatory stimulation, it is perhaps not surprising that mice with autophagy-deficient myeloid cells (*Atg5*$^{fl/fl}$-LysM Cre mice) show elevated serum IL-17 in response to infection with *Mycobacterium tuberculosis* (60). Similarly, mice deficient in the autophagy protein LC3B (MAP1-LC3B) exhibit increased IL-17-induced lung pathology upon infection with respiratory syncytial virus (RSV) and *Map1lc3b*$^{-/-}$ $CD11b^+$ DC infected with RSV induce IL-17 secretion from $CD4^+$ T cells in an IL-1-dependent manner (72). Moreover, *Atg5*$^{fl/fl}$-CD11c Cre mice develop spontaneous airway hyperreactivity and severe neutrophilic lung inflammation, with elevated IL-1 and IL-17 levels in the lungs (61). Together, this points to autophagy as a key regulator of TH17 immune responses.

Autophagy and APC-Derived MIF

Similar to IL-1 family cytokines, loss of autophagy in human and mouse macrophages leads to increased secretion of macrophage migration inhibitory factor (MIF) in response to LPS (73). MIF is expressed in multiple immune cell types, including macrophages, DC, T, and B cells, neutrophils, eosinophils, and mast cells. MIF is critical in the innate immune response to different bacteria, including *Salmonella* and *Mycobacterium* species. MIF can also upregulate TLR4 and increase the release of other pro-inflammatory cytokines, including TNF-α, IL-1, and IFN-γ (74). Interestingly, MIF also directly regulates NLRP3 inflammasome activation, facilitating the processing and release of IL-1β and IL-18 (75). The regulation of MIF by autophagy is dependent on mitochondrial ROS, which accumulates in the cytosol of autophagy-deficient cells. Amino acid starvation, an inducer of autophagy, also results in increased MIF secretion (73, 76). Given that amino starvation is a strong inducer of autophagy, these results may seem contradictory. However, MIF release is unaffected by other autophagy inducers (mammalian target of rapamycin; mTOR inhibitors) (73), suggesting that autophagy induction through mTOR inhibition is not responsible for MIF release. Concerning MIF and T cell activation, MIF has also been shown to induce IL-17 expression and secretion in mouse lymph nodes (77). Moreover, in a mouse model of gout, MIF levels are raised, and MIF deficiency or blockade lowers levels of IL-1β and reduces neutrophil infiltration and pathology (78). Thus, MIF might represent another connection between autophagy, inflammasome activation, and TH17 responses.

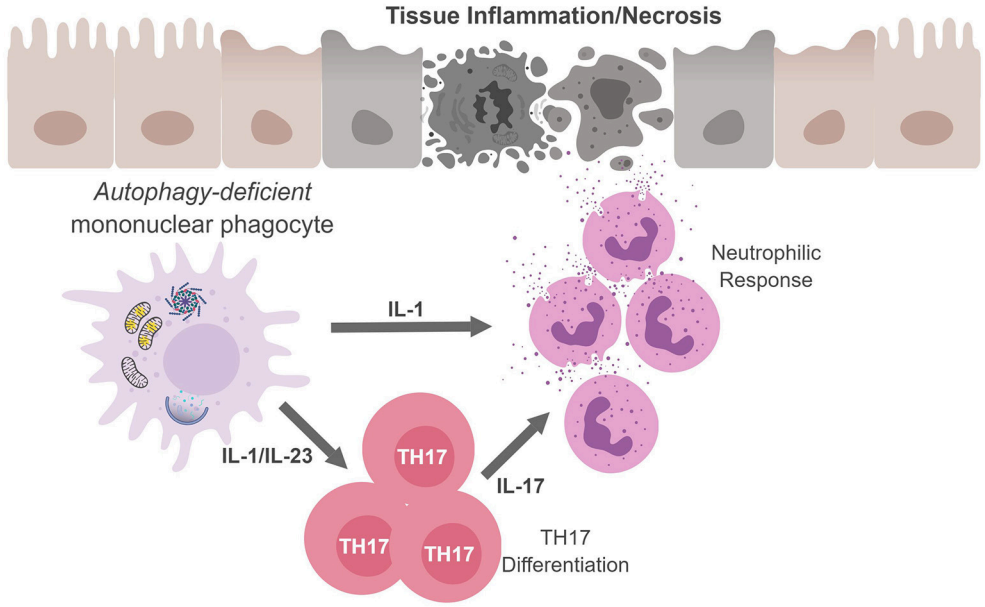

FIGURE 3 | Mononuclear phagocytes cell-autonomous autophagy curbs TH17 responses. Autophagic defects in mononuclear phagocytes results in the accumulation of damaged/dysfunctional mitochondria. Inflammatory activation of mononuclear phagocytes can increase mitochondrial dysfunction and the release of mitochondrial ROS and DNA that activates the inflammasome. Inflammasome activation results in excess IL-1β production and secretion. IL-1β can have (i) autocrine effects and induce IL-23, (ii) IL-1β and IL-23 can drive TH17 differentiation; and (iii) along with IL-17, IL-1β can recruit neutrophils. The inability to curb inflammasome activation due to an autophagic defect can result in continuous inflammation and tissue damage.

Autophagy and a Possible Role in Controlling TH1 Responses

The above observations suggest functional autophagy may curb detrimental IL-17-mediated inflammatory disorders. Nonetheless, it needs to be pointed out that the exacerbated IL-17 response observed in autophagy-deficient APC animal models could be due to compartmentalization of the infection to the lung. In the intestine, autophagy, specifically in epithelial cells, has proven to be important to maintain intestinal homeostasis (79–83). Additionally, an underappreciated role for autophagy in intestinal mononuclear phagocytes has been established. Saitoh et al. first showed hematopoietic cells lacking *Atg16l1* (through the generation of bone marrow chimeras) succumbed to colitis induction demonstrating autophagy in hematopoietic cells controls intestinal inflammation (40). More recently, mice with autophagy-deficient myeloid cells ($Atg7^{fl/fl}$-LysM Cre and $Atg16l1^{fl/fl}$ -LysM Cre mice) but not CD11c-expressing innate cells ($Atg16l1f^{fl/fl}$-CD11c Cre mice) displayed enhanced inflammation of the colon after colitis induction with heightened IL-1β levels found in the serum and being produced by macrophages (84–86). Interestingly, Lee et al. found colonic lamina propria T cells from $Atg7^{fl/fl}$-LysM Cre mice displayed robust TH1 skewing (IFN-γ production) with no difference in TH17 cells (IL-17 production) after colitis induction (84). IL-12p70, a potent inducer of IFN-γ, was not assessed by either group; however, IL-1β can synergize with IL-12p70 to induce IFN-γ (87–90). Interestingly, enhanced IL-12p70 secretion was reported in macrophages deficient in *Atg5* as was serum IL-12p70 during TB infection in $Atg5^{fl/fl}$-LysM Cre mice (60). But it remains unclear if autophagy directly regulates IL-12p70 production or if this an IL-1 autocrine effect as seen with IL-23 (54). And while cytokines involved in TH1 responses (IFN-γ and TNF-α) can affect the autophagy pathway, the intersection of autophagy and APC-derived cytokines driving TH1 (IL-12p70) responses need to be investigated further (91–96).

Past studies have revealed the importance of IFN-γ responses in enteric infections. Specifically, IFN-γ-deficient mice were shown to be susceptible to *Citrobacter rodentium* infection as were IL-12p40-deficient mice both demonstrating IFN-γ responses are critical for *C. rodentium* infections (97, 98). IL-12p40 is a protein subunit that dimerizes with IL-12p35 to form the heterodimeric cytokine, IL-12p70 or IL-23p19 to form IL-23 (90). Regarding enteric infections and autophagy, the Cadwell lab revealed ATG16L1 hypomorph mice were resistant to *C. rodentium* infection albeit in the absence of $CD4^+$ T cells (99). It is unclear if this resistance is due to an exacerbated IFN-γ response by innate lymphocytes. Several studies have shown the influence of lamina propria IFN-γ-producing innate lymphocytes in intestinal infections and IBD (100–102). If IL-12p70 production is dysregulated in autophagy-deficient APC this could lead to enhanced IFN-γ response by T cells and innate lymphoid cells and resistance to *C. rodentium* infection. It could also explain human diseases associated with autophagy defects and strong TH1 and TH17 responses such as IBD, MS, and RA (103–105). Collectively, these studies highlight the impact autophagy may have on skewing immune responses and

suggest the microenvironment could ultimately determine how autophagy controls TH cell polarization.

CELL-AUTONOMOUS AUTOPHAGY GOVERNS T CELL BIOLOGY

As discussed above, autophagy affects APC function in a way that can modulate T cell responses. Similarly, autophagy is quite functional in both $CD8^+$ and $CD4^+$ T cells from naïve to memory cellular states. Mature naïve T cells display a very small, but detectable, level of basal autophagy but are also capable of up-regulating autophagy in response to multiple stimuli. This autophagic program appears to regulate survival and proliferation as well as organelle quality control. Effector and memory T cells both utilize an autophagic program that interacts with intracellular metabolic pathways. This intersection of autophagy and metabolic pathways assists in T cell differentiation and functional capabilities. Through extensive work in genetics, various groups have shown autophagy is an active pathway involved in numerous aspects in T cell biology (**Figure 4**) as discussed below.

Autophagy Regulates T Cell Survival and Proliferation

Over the last decade, several groups have confirmed autophagy as an active cellular process in T cells (106–112). Initially, the confirmation of this pathway, detection of autophagosomes and up-regulation of autophagy proteins, was only observable in T cells after T cell receptor (TCR) stimulation. It was further substantiated to be an active process in naïve T cells due to the expression of numerous autophagy genes (*Atg5*, *Atg7*, *Atg8*, and *Beclin-1*) found prior to stimulation. To further understand the role of autophagy in T cells, several groups generated numerous T cell-specific conditional knockout mice to delete various autophagy genes (i.e. *Atg3, Atg5, Atg7, Atg16L1, Beclin-1, Vps34*) involved at difference steps of the autophagy pathway (**Figure 1**) (106–113). Nevertheless, no matter the autophagy gene deleted, the results were similar between the conditional knockout mice: a reduction in the frequencies of thymocytes as well as peripheral $CD8^+$ and $CD4^+$ T cells. Also, the T cells present in the periphery of these mice displayed a memory-like phenotype likely due to lymphopenia-induced proliferation (114–117). Additionally, autophagy-deficient T cells showed enhanced apoptosis which was linked to enhanced expression of pro-apoptotic molecules pro-caspase-3, caspase-8, and -9 as well as Bim (106, 113). These early studies pointed to autophagy as a key regulator of T cell homeostasis.

The survival of peripheral T cells is an active and involved process for both naïve and memory T cells. Naïve T cells require continuous MHC-TCR interaction as well as cytokine signals from the tissue microenvironment whereas memory T cells require only the latter (118). IL-7 and IL-15 are two common γ-chain (γc) receptor cytokines important for both naïve and memory T cell homeostasis (119). Interestingly, both IL-7 and IL-15 activate autophagy in T cells along with γc cytokines, IL-2, and IL-4, highlighting an emerging role for the JAK-STAT pathway in regulating autophagy (120). Nevertheless, autophagy appears to be important in long-term T cell homeostasis as IL-7 can maintain autophagy-deficient naive T cells in short-term cultures. In long-term cultures (over 24 days), $Atg3^{-/-}$ $CD4^+$ and $CD8^+$ T cells exhibited a higher rate of apoptosis compared to autophagy-proficient T cells (110). Supporting these findings, another study revealed mature T cells lacking *Atg7* quickly undergo apoptosis despite being in conditions with high levels of pro-survival homeostatic cytokines (121). These $Atg7^{-/-}$ T cells also failed to efficiently proliferate in response to TCR stimulation (121). T cells lacking *Atg3*, *Atg5,* or *Vps34* also exhibit proliferation defects (107, 112, 122) which appear to be dependent on the accumulation of Cyclin-dependent kinase inhibitor 1B (CDKN1B/p27/Kip1) which controls the cell cycle progression at G1 by inhibiting the activation of cyclin E-CDK2 and cyclin D-CDK4 complexes. Consequently,

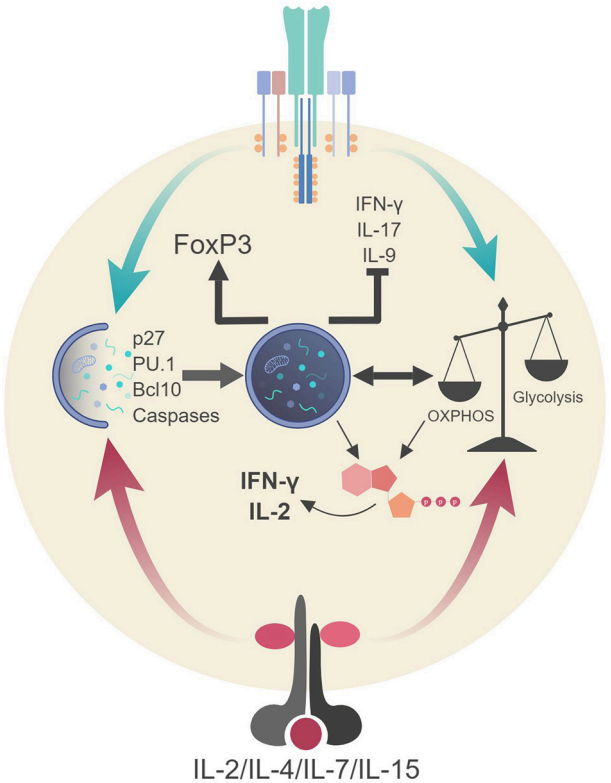

FIGURE 4 | Autophagic regulation of T cell function and metabolism. Autophagy activation via TCR stimulation (and possibly IL-2 production) assists in the proliferation and survival of T cells through direct targeting of p27 (cell cycle inhibitor) and pro-apoptotic factors (i.e., caspases, Bim). Autophagy also targets Bcl10 for degradation to limit NF-κB activation. Additionally, autophagy and metabolic pathways are activated via TCR stimulation and γc-cytokine signaling. These pathways can communicate to generate ATP in TH1 cells which assists in the production of IL-2 and IFN-γ. Autophagy in Tregs impedes glycolysis which stabilizes the regulatory phenotype by maintaining FoxP3 expression and inhibiting the transcriptional network of effector T cells. Lastly, autophagy inhibits TH9 differentiation and subsequent effector function (IL-9 production) via selective targeting of the TH9 lineage specific transcription factor, PU.1.

demonstrating autophagy provides numerous non-redundant mechanisms to ensure the survival and proliferation of T cells beyond homeostatic cytokine signaling and constant TCR-to-MHC contact that is required for both naive and memory T cell homeostasis.

Autophagy Is Essential for CD4$^+$ T Cell Differentiation

Naïve CD4$^+$ T cell differentiation is an intricate process involving interaction with professional APC. T cell activation and differentiation is driven by two simultaneous events—signal (1) MHC II-Ag/TCR interaction and signal (2) co-stimulation (e.g., CD80/CD86–CD28). In addition, APC-derived cytokine signaling assists in lineage commitment. These events trigger a signaling cascade that induces proliferation as well as differentiation that is mediated by the expression of lineage-specific transcription factors (123). This differentiation process grants CD4$^+$ TH cell subsets with specific effector functions. In fact, the differentiation of each TH subset is driven by a specific cytokine like IL-12 for TH1 cells, IL-4 for TH2 cells and TGFβ for regulatory CD4$^+$ T cells (Treg) (123). Other TH subsets require a combination of cytokines as is the case for TH17 cells which require TGF-β, IL-1, and IL-6 whereas TGF-β and IL-4 drives TH9 differentiation (123). The outcome allows each CD4$^+$ T cell effector subset (TH1, TH2, TH9, TH17) to play an important role in activating both innate and adaptive arms of the immune system to specific pathogens. In addition, differentiation can lead to immunosuppressive functions as is the case for Tregs. Both effector and regulatory CD4$^+$ T cells play an important role in host immunity, and a defect in these pathways are linked to numerous inflammatory and autoimmune diseases (123).

Given that TCR and cytokine stimulation can activate autophagy it is easy to speculate autophagy has a hand in CD4$^+$ T cell differentiation and function. However, autophagy's influence on T cell differentiation and function has remained unclear for many years due to autophagy's critical role in T cell survival (107, 112, 124, 125). Moreover, it appears there is a varying degree to which each subset of CD4$^+$ T cells utilize autophagy for differentiation and function. For example, autophagy appears to have an inhibitory effect in the expansion and differentiation of both TH2 and TH9 cells (126–128). Whereas, TH1 and Treg cells appear to rely heavily on autophagy for differentiation and function (121, 126). This discrepancy could be due to cytokine signaling pathways utilized by each CD4$^+$ T cell subset as well as their respective metabolic phenotype (discussed in the next section).

In CD4$^+$ T cells, cytokine signaling plays a major role in regulating both T cell differentiation and function. For instance, IL-2 is secreted immediately after TCR engagement and acts in autocrine fashion. This is crucial for sustained proliferation, survival and effector differentiation. As mentioned above, IL-2 can induce autophagy, thus, there is a high probability CD4$^+$ T cell differentiation and function may stem from cytokine-induced autophagy activation (120, 129). Interestingly, TH1 differentiated T cells lacking autophagy display defects in IL-2 and IFN-γ production (121). Moreover, there were no reported defects in TCR signaling suggesting autophagy may be required for T cell function (i.e., cytokine production). It is unclear if this functional defect is due to inaccessibility of the cytokine loci(s) for optimal transcription following activation (130) or the inability to generate ATP in autophagy-deficient cells which is required for optimal cytokine production (121). *Il2*$^{-/-}$ naïve T cells also produce low levels IFN-γ upon stimulation in TH1 differentiating conditions demonstrating IFN-γ production is partially dependent on both IL-2 and IL-12 signals (131, 132). Therefore, this phenotype in autophagy-deficient TH1 cells regarding IFN-γ production may be like the one observed in autophagy-deficient APC regarding the overexpression of IL-1 and its influence on IL-23 production (54, 60). It would be interesting to determine the level and function of autophagy and ATP generation occurring in TCR-stimulated *Il2*$^{-/-}$ T cells, specifically, whether IL-2 is required for ATP generation through mitophagy.

Harris (91) reviewed evidence suggesting that pro-inflammatory cytokines including IFN-γ, TNF-α, IL-1, IL-2, and IL-6 induce autophagy, while anti-inflammatory cytokines IL-4, IL-10, and IL-13 inhibit autophagy (5, 36, 133, 134). Recent reports, however, suggest that autophagy may be induced by various components of antagonistic immune signaling pathways. For example, IL-10 has been shown to promote mitophagy in macrophages (135) and IL-4 promotes autophagy during DC differentiation (136). Cytokine-induced autophagy is therefore likely to be cell- and context-dependent. IL-4, a potent inducer of TH2 differentiation, induces autophagy in DC; however, autophagy appears to hamper TH2 differentiation. Another example is with TH9 cells, whereby autophagy activation is not required for differentiation and in fact inhibits lineage commitment (128). TH9 cells are a subset of CD4$^+$ T cells that secrete the proinflammatory cytokine IL-9 and can contribute to antitumor immunity. Additionally, TH9 cells (IL-9 expression) increase during chronic inflammatory diseases like CD (123). TH9 lineage commitment and IL-9 expression are controlled by the transcription factor and master regulator of TH9 cell differentiation, PU.1. Interestingly, PU.1 is selectively targeted for autophagic degradation upon TH9 differentiation (128). A combination of TGF-β and IL-6 stimulation is required for TH9 differentiation and both cytokines can induce autophagy (91, 133). It is still unclear how PU.1 expression/TH9 cells are maintained but autophagy clearly impacts the stability of this subset of CD4$^+$ T cells.

Recently, new targeted deletion of autophagy genes in T cell subsets (i.e., CD4-Cre, FoxP3-Cre), has provided clues into autophagy role in the stability of other TH lineages (126, 137, 138). Genetic deletion of *Atg5, Atg7, or Atg16l1* in Foxp3-expressing T cells results in multi-organ inflammation in mice. There was still a dramatic decrease in Treg cells due to enhanced apoptosis. However, one study found a defective autophagic pathway in Tregs leads to destabilization of the Treg phenotype and loss of suppressive function (137). It was suggested the Treg phenotype was in peril due to a decrease in expression of the lineage-specific transcription factor Foxp3 and enhanced TH1/TH17 effector function (IFN-γ/IL-17 production). It is unclear if this is a direct effect of autophagic function or

systemic inflammation as inflammatory stimuli destabilizes FoxP3 expression in Tregs (139). Moreover, whether FoxP3 is a target for autophagic degradation like PU.1 is unclear but these studies suggest autophagy may play a role in lineage stabilization. Nevertheless, further investigation is necessary to definitively demonstrate that autophagy is required for Foxp3 stabilization and Treg function independent of autophagy's impact on Treg survival.

To conclude, these studies shed new light on the autophagic pathway in T cell differentiation. But they also emphasize new possibilities with regards to how autophagy is induced especially along with other signaling pathways. For instance, TCR signaling can activate both autophagy and mammalian target of rapamycin (mTOR) complex nutrient sensing pathways (121, 131). So how does a differentiating T cell deal with these opposing pathways on top of cytokine stimulation? Additionally, are specific autophagic functions being induced by various TH-differentiating cytokines, and do these functions differ from the canonical degradative autophagic pathway? Similar to TH9 cells and possibly Treg cells, does autophagy degrade other TH lineage specific transcription factors? To decipher the numerous autophagic functions in T cells, new sophisticated genetic models are required to understand the complexity of TH differentiation. To add further complexity to these questions, we are finding metabolism is influential in T cell function and that autophagy and metabolism are interconnected as we discuss below. A complete understanding of these intricate details could provide clues to the next therapeutic agents to modulate T cell responses via autophagy.

TABLE 1 | Active and steady state metabolic profiles of immune cells.

	Active state	Steady state
Metabolic polarization axis	M1 macrophages	M2 or quiescent macrophages
	Activated DC	Quiescent or Naïve DC
	TH1	Naïve mature $CD4^+$ T-cells, $CD4^+$ Memory T cells
	TH2	TH2, Naïve mature $CD4^+$ T cells, $CD4^+$ memory T cells
	TH17	$CD4^+$ Treg, $CD4^+$ memory T cells
	Activated $CD8^+$ T cells	Naïve mature $CD8^+$ T cells, $CD8^+$ memory T cells
Bias of metabolic profile	Anabolism: aerobic glycolysis, glutaminolysis, fatty acid synthesis, pentose phosphate pathway	Catabolism: oxidative phosphorylation, fatty acid oxidation
Upstream activated nutrient sensing pathway	mTOR	AMPK
Nutrient sensing pathway's effect on autophagic profile	mTOR: inhibits autophagy via inhibiting ULK1 activity	AMPK: stimulates autophagy via activating ULK1 and inhibiting mTOR

This table provides a general overview of immunometabolism in various immune subsets including APC and $CD4^+$ and $CD8^+$ T cells.

CONVERGENCE OF AUTOPHAGY AND METABOLISM TO CONTROL IMMUNE FUNCTION

Recent evidence has highlighted the importance of intracellular metabolic programming in immune cells (140, 141). This metabolic change between aerobic glycolysis and oxidative phosphorylation (OXPHOS) impacts both the innate and adaptive arms of the immune system, particularly the function and differentiation of cells. These metabolic pathways are triggered by environmental cues such as nutrients, O_2 levels, and activation state, which are each modulated by numerous stimuli. Moreover, autophagy has been shown to affect these metabolic pathways (142).

A functional autophagic pathway is frequently required for successful metabolic reprogramming during differentiation states of immune cells. For competent immunogenic (or homeostatic) cellular differentiation, both metabolism and autophagy must accurately sense nutrient levels and respond such that nutrients and biomolecules are appropriately utilized, stored, or recycled (5, 7, 143). For instance, induced shifts between different metabolic and autophagic profiles in immune cells are often regulated by shared networks of nutrient-sensing pathways, such as the mammalian target of rapamycin complex 1 (mTORC1) and AMP-activated protein kinase (AMPK) axes (144–146).

Evidence from various immune cells converges around two distinct inducible profiles of metabolic signaling and function: one for an "active-state" and another for the "steady-state" (140, 144–146). This evidence is summarized in **Table 1**. The kinase mTOR is a potent negative regulator of autophagy, and its associated mTORC1 complex is known to play a role in inducing a metabolic active-state (145–147). AMPK, conversely, triggers ATP generation via fatty acid oxidation (FAO), promoting a metabolic steady-state. Additionally, AMPK indirectly and directly facilitates autophagy by suppressing mTORC1 activity and activating autophagy-initiating kinase ULK1 (148).

An active-state metabolic profil*e* is generally anabolic, relying on aerobic glycolysis, glutaminolysis, fatty acid synthesis (FAS), and/or the Pentose-5 Phosphate Pathway (PPP) to generate amino acids, nucleotide precursors, redox co-enzymes, and membrane lipids to facilitate immunogenic functions (149–151). The steady-state metabolic profile, on the other hand, relies on the more sustainable and efficient ATP-generation capacity of catabolic pathways such as OXPHOS and FAO (140, 148, 149, 151). A growing literature suggests many hallmarks for active- versus steady-states are conserved across hematopoietic and non-hematopoietic cell-types (7, 140, 146, 149).

Autophagy plays numerous roles in basic cellular function during both "active" and "steady" metabolic states across immune cell-types, including for immunogenic function during antigen presentation, cytokine secretion, and regulation of inflammation

(152–155). Surprisingly, autophagy is induced by various components of antagonistic immune and metabolic signaling pathways. For example, anti-inflammatory cytokines such as IL-10 and IL-4 appear to promote both steady-state metabolism and autophagy (135, 156–158), while IL-2, TGF-β, and IFN-γ promote the metabolic active-state as well as induce autophagy (133, 134). Nevertheless, the influence autophagy and these metabolic pathways have on immune cell function highlights potential therapeutic targets to modulate T cell responses. Below we discuss the interconnection between autophagy and metabolism in both APC and T cells.

Cross-Talk Between Autophagic and Metabolic Pathways in Antigen-Presenting Cells

Studies have shown that macrophages and DC undergo profound metabolic changes in response to activation. For instance, stimulation of macrophages with lipopolysaccharide (LPS) leads to a shift in metabolism toward increased glycolysis, while IL-4 promotes OXPHOS (156–158), suggesting that metabolic profiles may influence, or are influenced by, macrophage polarization. More recently, Ip et al. reported the loss of IL-10-responsiveness in macrophages increased glycolysis and lowered OXPHOS in response to LPS treatment which promoted a proinflammatory phenotype (135). They went on to show that IL-10 inhibits glycolysis by reducing LPS-induced glucose uptake and downregulating glycolytic gene expression. Moreover, the reduced OXPHOS in LPS-treated *Il10*$^{-/-}$ macrophages was accompanied by an increase in dysfunctional mitochondria, suggesting that IL-10 is required for mitophagy during activation to limit proinflammatory responses in macrophages (135).

The mechanism by which IL-10 induces autophagy is not fully understood, but IL-10 was shown to regulate mTOR through STAT3-dependent upregulation of the mTOR inhibitor DDIT (135). IL-10 may simultaneously regulate autophagy/ mitophagy through activation of AMPK (135, 159). Another study has shown that LPS induces the expression of interferon regulatory factor-1 (IRF-1), which increases mitochondrial damage (160) and inhibits macrophage mitophagy (161, 162). It is not fully clear whether IRF-1 directly regulates IL-10, or vice versa, but one study has demonstrated that *Irf1*$^{-/-}$ DC express higher levels of IL-10 (163), suggesting a possible connection. Other studies have suggested that IL-10 inhibits autophagy in response to starvation, rapamycin and IL-17 via both STAT3 and Akt signaling pathways (164–166). Whether IL-10 can exert different effects on autophagy depending of stimulus or context, or whether it specifically regulates mitophagy, rather than other forms of autophagy, remains to be elucidated.

Interestingly, *Il10* polymorphisms confer increased risk for CD as well as autoimmune diseases SLE, RA and MS (167–170). Additionally, defects in IL-10 signaling specifically in intestinal macrophages disrupt an educational process that differentiate macrophages to become anti-inflammatory and tolerant (i.e., limiting proinflammatory cytokine secretion) to microbial stimulation; and a loss of this educational process leads to colitis in mice (171–173). Moreover, studies have indicated that autophagy may influence the polarization of other tissue macrophages. Notably, autophagy promotes cell survival during monocyte-macrophage differentiation (174, 175) and loss of autophagy appears to promote differentiation of M1 macrophages and decreases their potential to differentiate into M2 macrophages (176–178). This, in turn, will greatly affect the response of those macrophages to stimuli, particularly their cytokine profile, which has the potential to change the resulting T cell response. In the most simplistic terms, M1 polarization of macrophages will favor TH1 polarization of T cells, while M2 macrophages (particularly M2a and M2b) promote TH2 responses (179). Nevertheless, as discussed above, defects in the autophagy pathway in macrophages or DC tend to drive a hyperresponsive IL-17/TH17 response (**Figure 3**).

Autophagy and T Cell Metabolism

Initial stimulation of TCR leads to the activation of both mTOR and mTOR-independent autophagy nutrient sensing pathways. Autophagy is possibly induced by a JAK/STAT pathway downstream of IL-2 and IL-4 signaling (120). Induction of autophagy in CD4$^+$ T cells by other common γc cytokines such as IL-7 and IL-15 may act through the same pathway. These signals initiate complete metabolic reprogramming in activated T cells. This reprogramming is also associated with a global change in the metabolic transcriptome, with induction of endogenous myelocytomatosis oncogene (c-Myc) and hypoxia inducible factor 1, alpha subunit (HIF1α). The mTORC1-c-Myc pathway has been demonstrated to directly regulate T cell proliferation through transcriptional control of cell cycle regulators (180, 181), and has been implicated as an essential coordinator of T cell activation-induced cell growth and proliferation (182). HIF1α and c-Myc are both critical for the upregulation of glucose transporters and glycolytic enzymes, and at least some of mTOR's pro-glycolytic actions are mediated by its upregulation of HIF1α (183, 184).

Interestingly, autophagy-deficient CD4$^+$ T cells show increased expression of c-Myc and a glycolytic phenotype suggesting autophagy inhibits glycolysis. In Tregs, this loss of autophagy and subsequent enhanced glycolytic metabolism results in lineage destabilization and loss of effector function (126, 137). Although this an extreme scenario, these studies demonstrate (i) metabolism dictates effector function in T cells and (ii) autophagy is a major regulator of metabolic profiles. T cells generally conform to the "active" and "steady-state" metabolic profile dichotomy, though the unique demands of T cell immunogenic functions give rise to distinct metabolic trajectories between subsets (7, 149, 185). For example, Lunt and Vander Heiden (149) report that the shift toward glycolytic anabolism during the active state supports the needs of proliferation across cell types by generating the materials required to produce new daughter cells (149). Activated T cells have been shown to rely on OXPHOS to support early proliferation and cytokine production. Glycolytic-incompetent T cells can proliferate upon activation whereas OXPHOS-incompetent T cells fail to do so (144). Consequently, activated T cells appear to maintain mitochondrial ATP generation via OXPHOS for between 1 and 2 days after activation in part to

support the metabolic demands of proliferation (144, 185). ATP generation via OXPHOS is also required for efficient IFN-γ production by TH1 cells. A disruption in autophagy (a catabolic process) diminishes ATP and IFN-γ output from TH1 cells (121). Furthermore, glycolytic-incompetent differentiated $CD4^+$ T cells, while able to proliferate, exhibit a diminished effector response, mediated in part by GAPDH's competitive role as a negative regulator of IFN-γ mRNA in the absence of glycolytic metabolism (144).

An overview of active and steady state profiles of T cells are provided in **Table 1**. Activated and differentiated T cells are highly anabolic, while naïve and memory T cells are overall more catabolic. Evidence also supports further nuance in metabolic phenotypes of other TH subsets. For example, TH17 cells appear to rely more heavily on fatty acid synthesis than do other effector T cell subsets (186), and TH2 cells are more dependent on glycolysis for effector function than are Tregs, TH1, or TH17 cells (126). In fact, autophagy (and its inhibitory role in glycolysis) appear to restrict TH2 expansion. Several of TH2 effector functions are also in part dependent on FAO and OXPHOS (187, 188). This dual nature of TH2 metabolism is represented by its placement in both "active" and "steady" states. Additionally, AMPK has been shown to support $CD8^+$ T cell effector function in glucose-starved conditions while FAO is needed for the transition from effector to memory CD8 T cell (145, 148, 151, 185–187, 189).

Discerning the degree to which different autophagic pathways coincide with, negatively regulate, or enhance polarization toward active- or steady-state metabolic pathways remains a considerable challenge. Still, evidence suggests that some major autophagic pathways may more readily co-occur with the catabolic steady-state, an effect in part mediated by AMPK (145, 146, 148). Future therapeutic and research programs will benefit from the consideration of the substantial cross-talk between metabolic and autophagic signaling pathways. Additionally, treatments targeting autophagy should include holistic consideration of the treatment's effect on the metabolic and profile of the target cell-type compared to the known profile for cells with the desired therapeutic effector or suppressor function.

THERAPEUTIC TARGETING OF AUTOPHAGY TO MODULATE T CELL RESPONSES

Recently, there has been surge of interest in examining the therapeutic potential of autophagy in various human diseases (190). In fact, numerous clinical trials are on-going with autophagy modulating agents for both neurodegenerative diseases and various cancers (190, 191). This tremendous attention is supported by both animal models and clinical conditions demonstrating alterations in the autophagic pathway is linked to these human pathological conditions. Besides neurological diseases and cancer, autoimmune diseases and metabolic disorders have also been linked to autophagy (192, 193). Additionally, there has been considerable interest in discovering novel agents as well as repurposing FDA-approved pharmaceuticals to modulate autophagy (194–196). Below we discuss potential T cell-linked diseases that may benefit from autophagy modulation.

Inflammatory Bowel Disease

Inflammatory bowel disease (IBD) is a chronic relapsing inflammatory response of the gastrointestinal tract, and CD and ulcerative colitis (UC) are its major forms (197, 198). There are several underlying causes of IBD including immune dysregulation, intestinal barrier defects and dysbiosis, which all pose a significant barrier for clinicians. Dysregulated T cell responses including TH1 (IFN-γ) and TH17 (IL-17) cells also appear to contribute to IBD pathogenesis (103); however, an elusive goal in the field of IBD is to identify the causative factors initiating and maintaining chronic inflammation. Furthermore, this diversity of physiological defects along with the numerous cell-types (T cells, APC and epithelial cells) and cytokines (IL-1, IL-2, IL-6, IL-12, IL-13, IL-17, IL-23, IFN-γ, and TNF-α) involved in inflammation make treating IBD a daunting task (199, 200).

Currently, there are five main categories of therapeutics utilized to treat IBD patients: aminosalicylates, corticosteroids, immunomodulators (e.g., azathioprine), antibiotics (e.g., ciprofloxacin and metronidazole), and biological therapeutics (201). Biologics currently show the most potential for patients with moderate to severe CD and UC (202, 203). As mentioned above proinflammatory cytokines are highly expressed during IBD and are a current target for biological therapeutics. One biologic, infliximab, an antibody targeting TNF-α, a cytokine highly elevated in IBD patients, has had some clinical success (204, 205). At least 40% of CD patients and 25% of UC patients go into clinical remission when treated with infliximab alone. When used in combination with the immunomodulator drug azathioprine up to 56% of CD patients go into clinical remission (205). Regarding T cells, vedolizumab, a monoclonal antibody against α4β7 integrin which should prevent T cell binding to MAdCAM-1 and entry into the intestinal mucosa has had some clinical success in patients with moderate to severe CD and UC with clinical remission rates up to 39% and 41.8% at week 52, respectively (206, 207). Overall, the best treatment affects a little more than 50% of the subjects, which at best gives patients a 2-3-year period of remission before relapsing and left with no other option but surgery. Therefore, novel therapeutics are urgently needed to offer better and longer-lasting treatment options for IBD patients.

Through the work of many, autophagy appears to be vital for immune regulation, the intestinal barrier and host-bacteria interaction. Not surprisingly, there have been numerous genes identified that are within IBD risk loci that contribute to the autophagic pathway [reviewed in (208)]. The most well-known and studied is the autophagy gene *ATG16L1* which in Crohn's patients is encoded as a missense variant *ATG16L1* T300A (30–33). ATG16L1 functions as a core autophagy factor (**Figure 1**) and individuals carrying the variant *ATG16L1* T300A display immune dysregulation and intestinal barrier defects (79, 80, 82, 209). Other identified IBD risk loci involved in autophagy include *ULK1* and *MTMR3* or specifically, in xenophagy (a form of

autophagy utilized to degrade pathogens) include *IRGM* and *SMURF1* (210–216). Recently, several animal models of colitis that mimic IBD have demonstrated targeting autophagy can prevent intestinal inflammation (217, 218). These autophagy-inducing agents reduced the expression of proinflammatory cytokines and $CD4^+$ T cell infiltration into the mucosa *in vivo*. It is likely autophagy induction is also acting on numerous other cells and pathways that contribute to intestinal inflammation. For example, autophagy induction in colonic intestinal epithelial cells enhances barrier function (81, 82, 209, 219). Some of the autophagy modulators utilized in these studies include sirolimus (rapamycin), everolimus (a derivative of sirolimus), and trehalose (a disaccharide). The mode of autophagy induction for sirolimus and everolimus is through mTORC1 inhibition (220). Trehalose induces autophagy through AMPK activation independent of mTORC1 (221). Interestingly, dietary trehalose (commonly used as a food additive) has been shown to exacerbate another intestinal disease caused by the nosocomial bacterium *Clostridioides difficile* by increasing its virulence (222). Nevertheless, these studies provide a proof-of-concept that autophagy can dampen inflammatory responses. Lastly, a recent clinical trial reported targeting the IL-12p70 and IL-23 shared subunit IL-12p40 with the monoclonal antibody ustekinumab induced remission in patients with moderate to severe active Crohn's disease (223). Given the data autophagy may curb both IL-12p70 and IL-23 (via IL-1) production (54, 60), autophagy modulation rather than biological therapy could prove beneficial on many fronts of IBD treatment. This includes dampening inflammation by turning off IL-12p70 and IL-23 that would promote TH1 and TH17 cell differentiation as well as induce xenophagy and enhance the intestinal barrier. Moreover, it would allow the avoidance of issues associated with biologics like immunogenicity and loss of function over time, and the cost associated with maintenance therapy (224).

Autoimmune and Infectious Diseases

Concerning autoimmune diseases (e.g., RA and MS) and chronic infectious diseases like TB, can autophagy modulation ameliorate disease progression? Targeting autophagy in several animal models of neurodegenerative diseases and TB supports a role for autophagy in ameliorating disease (225). However, these models are assessing autophagy's degradative role in clearing pathogen or disease-causing proteins. Thus, it remains unclear if these therapeutic agents are impacting immune responses, i.e., TH and APC effector and metabolic profiles.

Rheumatoid arthritis (RA) is an autoimmune disease and like IBD is a chronic inflammatory disease except it primary site of inflammation is in the joints (105). IL-17 and TH17 cells have been implicated in early- and disease-onset phase of RA (69, 105) along with T cell plasticity (TH17 to TH1 conversion) and the ability to produce both IFN-γ and IL-17 (226, 227). In addition, unique metabolic profiles of both T cells and macrophages are associated with disease severity reviewed in (228). Furthermore, a variant of the autophagy-related gene *ATG5* has been identified in group of RA patients and protein levels of ATG7 and BECN1 that are involved in autophagy are upregulated in RA patients (34, 229, 230). It is unclear if this variant contributes to the enhancement or inhibition of autophagy as evidence is suggested for both (231, 232) but chloroquine and hydroxychloroquine (inhibitors of autophagy) have shown efficacy in patients with mild to moderate RA (233). Other evidence to support active autophagy in RA pathogenesis comes from the role of autophagy in generating citrullinated peptides which are targeted by autoantibodies and a cause of bone loss (234, 235). Thus, autophagy may act at several levels of disease including the generation and presentation of citrullinated peptides, increased T cell survival, and manipulation of T cell and macrophage metabolism.

MS, a chronic autoimmune disease that attacks the central nervous system is also characterized by potent TH1 and TH17 responses (104). TH17 and IL-17 appear to be involved in both the initiation and maintenance phase of disease for MS (69, 236) and $CD4^+$ T cells capable of producing both IFN-γ and IL-17 are present in the disease tissue (104). Similar to RA, autophagy and autophagy genes maybe upregulated in inflammatory cells that contributes to disease pathogenesis. As mentioned above, the autophagy gene *Atg5* was critical in the processing and presentation of self-peptides by dendritic cells to autoreactive T cells suggesting autophagy factors contribute to disease (35, 237). In T cells, enhanced Atg5 levels have been found in patients with MS possibly leading to enhanced survival and an active metabolic state (238, 239). Further evidence for a role of autophagy activation in MS pathogenesis was the identification of a single nucleotide polymorphism in the *CLEC16A* gene (240). CLEC16A regulates MHC II presentation in APC and can regulate autophagy through the modulation of mTOR activity (241, 242). So unlike in IBD (autophagy defects leads to inflammation), hyperactive autophagy appears to contribute to the pathogenesis observed in both RA and MS through T cell survival and metabolism as well as APC antigen presentation.

M. tuberculosis infection is the quintessential bacterial model that have been utilized to understand xenophagy (243–247). Additionally, autophagy's role in immune function during TB infection appears to be extremely important for host protection (60, 71). As discussed above, autophagic defects in APC affects cytokine secretion and subsequently promotes an exacerbated TH17-mediated immune response in animal models of TB infection (54, 60, 61, 72). Moreover, polymorphisms in the autophagy-related genes *IRGM*, *ULK1,* and *P2RX7* are associated with susceptibility to TB infection (243, 248–251). It is unclear if autophagy acts as a double-edge sword controlling TB and the immune response but animal models show the gene *Atg5* in myeloid cells appear to be the most critical for both functions (60, 71, 252).

TH17 cells and TH17-related cytokines are beneficial in the initial phase of TB infections; however, continuous IL-17-mediated inflammation (i.e., neutrophilic infiltration) contributes to TB pathogenesis (70). Thus, curbing TH17-mediated immune responses through autophagy could prove beneficial in TB (60, 70, 252). Furthermore, numerous autophagy inducing agents have been utilized *in vivo* to induce xenophagy to control *M. tuberculosis* infection (225). It could be that the induction of autophagy also limits APC-derived TH17-promoting cytokines (IL-1, IL-23, MIF) and neutrophil recruiting

factors (IL-1, CXCL1) as well as influencing TH17 cells toward the catabolic "steady" state. Additionally, whether autophagy has a role in IL-12-TH1/IFN-γ responses remains to be seen but tipping the TH1/TH17/Treg balance could have serious implications in disease progression.

In conclusion, it is clear the complex interconnections between autophagy, immune function and metabolism highlight vital intracellular events that must be coordinated in both T cells and APC to provide protection against pathogens. The last decade has provided novel results demonstrating the importance of autophagy in immune cells with recent research elucidating the interrelationship between autophagy and cellular metabolism. These recent findings highlight how autophagic and metabolic pathways are profoundly intertwined and help determine the balance between health and disease. Autophagy is an attainable therapeutic target; however, numerous details that surround autophagy, metabolism, and immune function as well as the full extent of their crosstalk are still unclear. Therefore, future research must further dissect and understand the many roles autophagy has in immune function and metabolism. Understanding these biological events will have an influential impact on future therapeutic treatments for both autoimmune and infectious diseases.

AUTHOR CONTRIBUTIONS

SDM, CJC, XOY, JH, and EFC wrote the manuscript. JH and EFC edited the manuscript.

ACKNOWLEDGMENTS

Supported in part by the National Center for Research Resources and the National Center for Advancing Translational Sciences of the National Institutes of Health (NIH) through grant no. UL1TR001449 (EFC) and in part by NIH grant P20GM121176 (EFC and XOY). Figures were created with BioRender.io (Toronto, Ontario, Canada).

REFERENCES

1. Gatica D, Lahiri V, Klionsky DJ. Cargo recognition and degradation by selective autophagy. *Nat Cell Biol.* (2018) 20:233–42. doi: 10.1038/s41556-018-0037-z
2. Li WW, Li J, Bao JK. Microautophagy: lesser-known self-eating. *Cell Mol Life Sci* (2012) 69:1125–36. doi: 10.1007/s00018-011-0865-5
3. Kaushik S, Cuervo AM. Chaperone-mediated autophagy: a unique way to enter the lysosome world. *Trends Cell Biol.* (2012) 22:407–17. doi: 10.1016/j.tcb.2012.05.006
4. Deretic V, Levine B. Autophagy balances inflammation in innate immunity. *Autophagy* (2018) 14:243–51. doi: 10.1080/15548627.2017.1402992
5. Deretic V, Saitoh T, Akira S. Autophagy in infection, inflammation and immunity. *Nat Rev Immunol.* (2013) 13:722–37. doi: 10.1038/nri3532
6. Valecka J, Almeida CR, Su B, Pierre P, Gatti E. Autophagy and MHC-restricted antigen presentation. *Mol Immunol.* (2018) 99:163–70. doi: 10.1016/j.molimm.2018.05.009
7. Dowling SD, Macian F. Autophagy and T cell metabolism. *Can Lett.* (2018) 419:20–6. doi: 10.1016/j.canlet.2018.01.033
8. Jacquin E, Apetoh L. Cell-intrinsic roles for autophagy in modulating CD4 T cell functions. *Front Immunol.* (2018) 9:1023. doi: 10.3389/fimmu.2018.01023
9. Blum JS, Wearsch PA, Cresswell P. Pathways of antigen processing. *Annu Rev Immunol.* (2013) 31:443–73. doi: 10.1146/annurev-immunol-032712-095910
10. Munz C. Autophagy proteins in antigen processing for presentation on MHC molecules. *Immunol Rev.* (2016) 272:17–27. doi: 10.1111/imr.12422
11. Kasai M, Tanida I, Ueno T, Kominami E, Seki S, Ikeda T, et al. Autophagic compartments gain access to the MHC class II compartments in thymic epithelium. *J Immunol.* (2009) 183:7278–85. doi: 10.4049/jimmunol.0804087
12. Schmid D, Pypaert M, Munz C. Antigen-loading compartments for major histocompatibility complex class II molecules continuously receive input from autophagosomes. *Immunity* (2007) 26:79–92. doi: 10.1016/j.immuni.2006.10.018
13. Fonteneau JF, Brilot F, Munz C, Gannage M. The tumor antigen NY-ESO-1 mediates direct recognition of melanoma cells by CD4+ T cells after intercellular antigen transfer. *J Immunol.* (2016) 196:64–71. doi: 10.4049/jimmunol.1402664
14. Jin Y, Sun C, Feng L, Li P, Xiao L, Ren Y, et al. Regulation of SIV antigen-specific CD4+ T cellular immunity via autophagosome-mediated MHC II molecule-targeting antigen presentation in mice. *PLoS ONE* (2014) 9:e93143. doi: 10.1371/journal.pone.0093143
15. Dengjel J, Schoor O, Fischer R, Reich M, Kraus M, Muller M, et al. Autophagy promotes MHC class II presentation of peptides from intracellular source proteins. *Proc Natl Acad Sci USA.* (2005) 102:7922–7. doi: 10.1073/pnas.0501190102
16. Jagannath C, Lindsey DR, Dhandayuthapani S, Xu Y, Hunter RL Jr, Eissa NT. Autophagy enhances the efficacy of BCG vaccine by increasing peptide presentation in mouse dendritic cells. *Nat Med.* (2009) 15:267–76. doi: 10.1038/nm.1928
17. Paludan C, Schmid D, Landthaler M, Vockerodt M, Kube D, Tuschl T, et al. Endogenous MHC class II processing of a viral nuclear antigen after autophagy. *Science* (2005) 307:593–6. doi: 10.1126/science.1104904
18. Thiele F, Tao S, Zhang Y, Muschaweckh A, Zollmann T, Protzer U, et al. Modified vaccinia virus Ankara-infected dendritic cells present CD4+ T-cell epitopes by endogenous major histocompatibility complex class II presentation pathways. *J Virol.* (2015) 89:2698–709. doi: 10.1128/JVI.03244-14
19. Anderson MS, Venanzi ES, Klein L, Chen Z, Berzins SP, Turley SJ, et al. Projection of an immunological self shadow within the thymus by the aire protein. *Science* (2002) 298:1395–401. doi: 10.1126/science.1075958
20. Nedjic J, Aichinger M, Emmerich J, Mizushima N, Klein L. Autophagy in thymic epithelium shapes the T-cell repertoire and is essential for tolerance. *Nature* (2008) 455:396–400. doi: 10.1038/nature07208
21. Aichinger M, Wu C, Nedjic J, Klein L. Macroautophagy substrates are loaded onto MHC class II of medullary thymic epithelial cells for central tolerance. *J Exp Med.* (2013) 210:287–300. doi: 10.1084/jem.20122149
22. Wenger T, Terawaki S, Camosseto V, Abdelrassoul R, Mies A, Catalan N, et al. Autophagy inhibition promotes defective neosynthesized proteins storage in ALIS, and induces redirection toward proteasome processing and MHCI-restricted presentation. *Autophagy* (2012) 8:350–63. doi: 10.4161/auto.18806
23. Dengjel J, Hoyer-Hansen M, Nielsen MO, Eisenberg T, Harder LM, Schandorff S, et al. Identification of autophagosome-associated proteins and regulators by quantitative proteomic analysis and genetic screens. *Mol Cell Proteom.* (2012) 11:M111014035. doi: 10.1074/mcp.M111.014035
24. Marshall RS, Li F, Gemperline DC, Book AJ, Vierstra RD. Autophagic degradation of the 26s proteasome is mediated by the dual ATG8/Ubiquitin receptor RPN10 in Arabidopsis. *Mol Cell* (2015) 58:1053–66. doi: 10.1016/j.molcel.2015.04.023
25. Pooley JL, Heath WR, Shortman K. Cutting edge: intravenous soluble antigen is presented to CD4 T cells by CD8- dendritic cells, but cross-presented to CD8 T cells by CD8+ dendritic cells. *J Immunol.* (2001) 166:5327–30. doi: 10.4049/jimmunol.166.9.5327
26. den Haan JM, Bevan MJ. Constitutive versus activation-dependent cross-presentation of immune complexes by CD8(+) and CD8(−) dendritic

cells *in vivo*. *J Exp Med*. (2002) 196:817–27. doi: 10.1084/jem.20020295
27. Mintern JD, Macri C, Chin WJ, Panozza SE, Segura E, Patterson NL, et al. Differential use of autophagy by primary dendritic cells specialized in cross-presentation. *Autophagy* (2015) 11:906–17. doi: 10.1080/15548627.2015.1045178
28. Matzaraki V, Kumar V, Wijmenga C, Zhernakova A. The MHC locus and genetic susceptibility to autoimmune and infectious diseases. *Genome Biol.* (2017) 18:76. doi: 10.1186/s13059-017-1207-1
29. Gianfrani C, Pisapia L, Picascia S, Strazzullo M, Del Pozzo G. Expression level of risk genes of MHC class II is a susceptibility factor for autoimmunity: New insights. *J Autoimmun.* (2018) 89:1–10. doi: 10.1016/j.jaut.2017.12.016
30. Hampe J, Franke A, Rosenstiel P, Till A, Teuber M, Huse K, et al. A genome-wide association scan of nonsynonymous SNPs identifies a susceptibility variant for Crohn disease in ATG16L1. *Nat Genet.* (2007) 39:207–11. doi: 10.1038/ng1954
31. Rioux JD, Xavier RJ, Taylor KD, Silverberg MS, Goyette P, Huett A, et al. Genome-wide association study identifies new susceptibility loci for Crohn disease and implicates autophagy in disease pathogenesis. *Nat Genet.* (2007) 39:596–604. doi: 10.1038/ng2032
32. Roberts RL, Gearry RB, Hollis-Moffatt JE, Miller AL, Reid J, Abkevich V, et al. IL23R R381Q and ATG16L1 T300A are strongly associated with Crohn's disease in a study of New Zealand Caucasians with inflammatory bowel disease. *Am J Gastroenterol.* (2007) 102:2754–61. doi: 10.1111/j.1572-0241.2007.01525.x
33. Yamazaki K, Onouchi Y, Takazoe M, Kubo M, Nakamura Y, Hata A. Association analysis of genetic variants in IL23R, ATG16L1 and 5p13.1 loci with Crohn's disease in Japanese patients. *J Hum Genet.* (2007) 52:575–83. doi: 10.1007/s10038-007-0156-z
34. Zhou XJ, Lu XL, Lv JC, Yang HZ, Qin LX, Zhao MH, et al. Genetic association of PRDM1-ATG5 intergenic region and autophagy with systemic lupus erythematosus in a Chinese population. *Ann Rheum Dis.* (2011) 70:1330–7. doi: 10.1136/ard.2010.140111
35. Keller CW, Sina C, Kotur MB, Ramelli G, Mundt S, Quast I, et al. ATG-dependent phagocytosis in dendritic cells drives myelin-specific CD4(+) T cell pathogenicity during CNS inflammation. *Proc Natl Acad Sci USA*. (2017) 114:E11228–37. doi: 10.1073/pnas.1713664114
36. Harris J. Autophagy and IL-1 family cytokines. *Front Immunol.* (2013) 4:83. doi: 10.3389/fimmu.2013.00083
37. Harris J, Lang T, Thomas JPW, Sukkar MB, Nabar NR, Kehrl JH. Autophagy and inflammasomes. *Mol Immunol.* (2017) 86:10–15. doi: 10.1016/j.molimm.2017.02.013
38. Harris J, Hartman M, Roche C, Zeng SG, O'Shea A, Sharp FA, et al. Autophagy controls IL-1beta secretion by targeting pro-IL-1beta for degradation. *J Biol Chem.* (2011) 286:9587–97. doi: 10.1074/jbc.M110.202911
39. Nakahira K, Haspel JA, Rathinam VA, Lee SJ, Dolinay T, Lam HC, et al. Autophagy proteins regulate innate immune responses by inhibiting the release of mitochondrial DNA mediated by the NALP3 inflammasome. *Nat Immunol.* (2011) 12:222–30. doi: 10.1038/ni.1980
40. Saitoh T, Fujita N, Jang MH, Uematsu S, Yang BG, Satoh T, et al. Loss of the autophagy protein Atg16L1 enhances endotoxin-induced IL-1beta production. *Nature* (2008) 456:264–8. doi: 10.1038/nature07383
41. Zhou R, Yazdi AS, Menu P, Tschopp J. A role for mitochondria in NLRP3 inflammasome activation. *Nature* (2011) 469:221–5. doi: 10.1038/nature09663
42. Vigano E, Diamond CE, Spreafico R, Balachander A, Sobota RM, Mortellaro A. Human caspase-4 and caspase-5 regulate the one-step non-canonical inflammasome activation in monocytes. *Nat Commun.* (2015) 6:8761. doi: 10.1038/ncomms9761
43. Guey B, Bodnar M, Manie SN, Tardivel A, Petrilli V. Caspase-1 autoproteolysis is differentially required for NLRP1b and NLRP3 inflammasome function. *Proc Natl Acad Sci USA*. (2014) 111:17254–9. doi: 10.1073/pnas.1415756111
44. Van Opdenbosch N, Gurung P, Vande Walle L, Fossoul A, Kanneganti TD, Lamkanfi M. Activation of the NLRP1b inflammasome independently of ASC-mediated caspase-1 autoproteolysis and speck formation. *Nat Commun.* (2014) 5:3209. doi: 10.1038/ncomms4209
45. Yu J, Nagasu H, Murakami T, Hoang H, Broderick L, Hoffman HM, et al. Inflammasome activation leads to Caspase-1-dependent mitochondrial damage and block of mitophagy. *Proc Natl Acad Sci USA*. (2014) 111:15514–9. doi: 10.1073/pnas.1414859111
46. Kanneganti TD. The inflammasome: firing up innate immunity. *Immunol Rev.* (2015) 265:1–5. doi: 10.1111/imr.12297
47. Dostert C, Petrilli V, Van Bruggen R, Steele C, Mossman BT, Tschopp J. Innate immune activation through Nalp3 inflammasome sensing of asbestos and silica. *Science* (2008) 320:674–7. doi: 10.1126/science.1156995
48. Martinon F, Petrilli V, Mayor A, Tardivel A, Tschopp J. Gout-associated uric acid crystals activate the NALP3 inflammasome. *Nature* (2006) 440:237–41. doi: 10.1038/nature04516
49. Sharp FA, Ruane D, Claass B, Creagh E, Harris J, Malyala P, et al. Uptake of particulate vaccine adjuvants by dendritic cells activates the NALP3 inflammasome. *Proc Natl Acad Sci USA*. (2009) 106:870–5. doi: 10.1073/pnas.0804897106
50. Harris J, Deen N, Zamani S, Hasnat MA. Mitophagy and the release of inflammatory cytokines. *Mitochondrion* (2017) 41:2–8. doi: 10.1016/j.mito.2017.10.009
51. Colleran A, Ryan A, O'Gorman A, Mureau C, Liptrot C, Dockery P, et al. Autophagosomal IkappaB alpha degradation plays a role in the long term control of tumor necrosis factor-alpha-induced nuclear factor-kappaB (NF-kappaB) activity. *J Biol Chem.* (2011) 286:22886–93. doi: 10.1074/jbc.M110.199950
52. Ko JH, Yoon SO, Lee HJ, Oh JY. Rapamycin regulates macrophage activation by inhibiting NLRP3 inflammasome-p38 MAPK-NFkappaB pathways in autophagy- and p62-dependent manners. *Oncotarget* (2017) 8:40817–831. doi: 10.18632/oncotarget.17256
53. Shi CS, Shenderov K, Huang NN, Kabat J, Abu-Asab M, Fitzgerald KA, et al. Activation of autophagy by inflammatory signals limits IL-1beta production by targeting ubiquitinated inflammasomes for destruction. *Nat Immunol.* (2012) 13:255–63. doi: 10.1038/ni.2215
54. Peral de Castro C, Jones SA, Ni Cheallaigh C, Hearnden CA, Williams L, Winter J, et al. Autophagy regulates IL-23 secretion and innate T cell responses through effects on IL-1 secretion. *J Immunol.* (2012) 189:4144–53. doi: 10.4049/jimmunol.1201946
55. Ainscough JS, Frank Gerberick G, Zahedi-Nejad M, Lopez-Castejon G, Brough D, Kimber I, et al. Dendritic cell IL-1alpha and IL-1beta are polyubiquitinated and degraded by the proteasome. *J Biol Chem.* (2014) 289:35582–92. doi: 10.1074/jbc.M114.595686
56. Dupont N, Jiang S, Pilli M, Ornatowski W, Bhattacharya D, Deretic V. Autophagy-based unconventional secretory pathway for extracellular delivery of IL-1beta. *EMBO J.* (2011) 30:4701–11. doi: 10.1038/emboj.2011.398
57. Zhang M, Kenny SJ, Ge L, Xu K, Schekman R. Translocation of interleukin-1beta into a vesicle intermediate in autophagy-mediated secretion. *Elife* (2015) 4:e11205. doi: 10.7554/eLife.11205
58. Afonina IS, Muller C, Martin SJ, Beyaert R. Proteolytic processing of interleukin-1 family cytokines: variations on a common theme. *Immunity* (2015) 42:991–1004. doi: 10.1016/j.immuni.2015.06.003
59. Afonina IS, Tynan GA, Logue SE, Cullen SP, Bots M, Luthi AU, et al. Granzyme B-dependent proteolysis acts as a switch to enhance the proinflammatory activity of IL-1alpha. *Mol Cell* (2011) 44:265–78. doi: 10.1016/j.molcel.2011.07.037
60. Castillo EF, Dekonenko A, Arko-Mensah J, Mandell MA, Dupont N, Jiang S, et al. Autophagy protects against active tuberculosis by suppressing bacterial burden and inflammation. *Proc Natl Acad Sci USA*. (2012) 109:E3168–76. doi: 10.1073/pnas.1210500109
61. Suzuki Y, Maazi H, Sankaranarayanan I, Lam J, Khoo B, Soroosh P, et al. Lack of autophagy induces steroid-resistant airway inflammation. *J Allergy Clin Immunol.* (2016) 137:1382–1389 e9. doi: 10.1016/j.jaci.2015.09.033
62. Harris KM, Fasano A, Mann DL. Cutting edge: IL-1 controls the IL-23 response induced by gliadin, the etiologic agent in celiac disease. *J Immunol.* (2008) 181:4457–60. doi: 10.4049/jimmunol.181.7.4457
63. Cho ML, Kang JW, Moon YM, Nam HJ, Jhun JY, Heo SB, et al. STAT3 and NF-kappaB signal pathway is required for IL-23-mediated IL-17 production in spontaneous arthritis animal model IL-1 receptor antagonist-deficient mice. *J Immunol.* (2006) 176:5652–61. doi: 10.4049/jimmunol.176.9.5652

64. Sutton C, Brereton C, Keogh B, Mills KH, Lavelle EC. A crucial role for interleukin (IL)-1 in the induction of IL-17-producing T cells that mediate autoimmune encephalomyelitis. *J Exp Med.* (2006) 203:1685–91. doi: 10.1084/jem.20060285
65. Sutton CE, Lalor SJ, Sweeney CM, Brereton CF, Lavelle EC, Mills KH. Interleukin-1 and IL-23 induce innate IL-17 production from gammadelta T cells, amplifying Th17 responses and autoimmunity. *Immunity* (2009) 31:331–41. doi: 10.1016/j.immuni.2009.08.001
66. Sawant KV, Xu R, Cox R, Hawkins H, Sbrana E, Kolli D, et al. Chemokine CXCL1-Mediated Neutrophil Trafficking in the Lung: Role of CXCR2 Activation. *J Innate Immun.* (2015) 7:647–58. doi: 10.1159/000430914
67. Rider P, Carmi Y, Guttman O, Braiman A, Cohen I, Voronov E, et al. IL-1alpha and IL-1beta recruit different myeloid cells and promote different stages of sterile inflammation. *J Immunol.* (2011) 187:4835–43. doi: 10.4049/jimmunol.1102048
68. Laan M, Cui ZH, Hoshino H, Lotvall J, Sjostrand M, Gruenert DC, et al. Neutrophil recruitment by human IL-17 via C-X-C chemokine release in the airways. *J Immunol.* (1999) 162:2347–52.
69. Lohr J, Knoechel B, Wang JJ, Villarino AV, Abbas AK. Role of IL-17 and regulatory T lymphocytes in a systemic autoimmune disease. *J Exp Med.* (2006) 203:2785–91. doi: 10.1084/jem.20061341
70. Shen H, Chen ZW. The crucial roles of Th17-related cytokines/signal pathways in M. tuberculosis infection. *Cell Mol Immunol.* (2018) 15:216–25. doi: 10.1038/cmi.2017.128
71. Watson RO, Manzanillo PS, Cox JS. Extracellular M. tuberculosis DNA targets bacteria for autophagy by activating the host DNA-sensing pathway. *Cell* (2012) 150:803–15. doi: 10.1016/j.cell.2012.06.040
72. Reed M, Morris SH, Owczarczyk AB, Lukacs NW. Deficiency of autophagy protein Map1-LC3b mediates IL-17-dependent lung pathology during respiratory viral infection via ER stress-associated IL-1. *Mucosal Immunol.* (2015) 8:1118–30. doi: 10.1038/mi.2015.3
73. Lee JP, Foote A, Fan H, Peral de Castro C, Lang T, Jones SA, et al. Loss of autophagy enhances MIF/macrophage migration inhibitory factor release by macrophages. *Autophagy* (2016) 12:907–16. doi: 10.1080/15548627.2016.1164358
74. Lang T, Foote A, Lee JP, Morand EF, Harris J. MIF: implications in the pathoetiology of systemic lupus erythematosus. *Front Immunol* (2015) 6:577. doi: 10.3389/fimmu.2015.00577
75. Lang T, Lee JPW, Elgass K, Pinar AA, Tate MD, Aitken EH, et al. Macrophage migration inhibitory factor is required for NLRP3 inflammasome activation. *Nat Commun.* (2018) 9:2223. doi: 10.1038/s41467-018-04581-2
76. Chuang YC, Su WH, Lei HY, Lin YS, Liu HS, Chang CP, et al. Macrophage migration inhibitory factor induces autophagy via reactive oxygen species generation. *PLoS ONE* (2012) 7:e37613. doi: 10.1371/journal.pone.0037613
77. Stojanovic I, Cvjeticanin T, Lazaroski S, Stosic-Grujicic S, Miljkovic D. Macrophage migration inhibitory factor stimulates interleukin-17 expression and production in lymph node cells. *Immunology* (2009) 126:74–83. doi: 10.1111/j.1365-2567.2008.02879.x
78. Galvao I, Dias AC, Tavares LD, Rodrigues IP, Queiroz-Junior CM, Costa VV, et al. Macrophage migration inhibitory factor drives neutrophil accumulation by facilitating IL-1beta production in a murine model of acute gout. *J Leukoc Biol.* (2016) 99:1035–43. doi: 10.1189/jlb.3MA0915-418R
79. Cadwell K, Liu JY, Brown SL, Miyoshi H, Loh J, Lennerz JK, et al. A key role for autophagy and the autophagy gene Atg16l1 in mouse and human intestinal Paneth cells. *Nature* (2008) 456:259–63. doi: 10.1038/nature07416
80. Cadwell K, Patel KK, Komatsu M, Virgin HWT, Stappenbeck TS. A common role for Atg16L1, Atg5 and Atg7 in small intestinal Paneth cells and Crohn disease. *Autophagy* (2009) 5:250–2. doi: 10.4161/auto.5.2.7560
81. Patel KK, Miyoshi H, Beatty WL, Head RD, Malvin NP, Cadwell K, et al. Autophagy proteins control goblet cell function by potentiating reactive oxygen species production. *Embo J.* (2013) 32:3130–44. doi: 10.1038/emboj.2013.233
82. Matsuzawa-Ishimoto Y, Shono Y, Gomez LE, Hubbard-Lucey VM, Cammer M, Neil J, et al. Autophagy protein ATG16L1 prevents necroptosis in the intestinal epithelium. *J Exp Med.* (2017) 214:3687–705. doi: 10.1084/jem.20170558
83. Benjamin JL, Sumpter R Jr, Levine B, Hooper LV. Intestinal epithelial autophagy is essential for host defense against invasive bacteria. *Cell Host Microbe* (2013) 13:723–34. doi: 10.1016/j.chom.2013.05.004
84. Lee HY, Kim J, Quan W, Lee JC, Kim MS, Kim SH, et al. Autophagy deficiency in myeloid cells increases susceptibility to obesity-induced diabetes and experimental colitis. *Autophagy* (2016) 12:1390–403. doi: 10.1080/15548627.2016.1184799
85. Zhang H, Zheng L, Chen J, Fukata M, Ichikawa R, Shih DQ, et al. The protection role of Atg16l1 in CD11c(+)dendritic cells in murine colitis. *Immunobiology* (2017) 222:831–41. doi: 10.1016/j.imbio.2017.03.002
86. Zhang H, Zheng L, McGovern DP, Hamill AM, Ichikawa R, Kanazawa Y, et al. Myeloid ATG16L1 facilitates host-bacteria interactions in maintaining intestinal homeostasis. *J Immunol.* (2017) 198:2133–46. doi: 10.4049/jimmunol.1601293
87. Wu CY, Demeure C, Kiniwa M, Gately M, Delespesse G. IL-12 induces the production of IFN-gamma by neonatal human CD4 T cells. *J Immunol.* (1993) 151:1938–49.
88. Cooper MA, Fehniger TA, Ponnappan A, Mehta V, Wewers MD, Caligiuri MA. Interleukin-1beta costimulates interferon-gamma production by human natural killer cells. *Eur J Immunol.* (2001) 31:792–801. doi: 10.1002/1521-4141(200103)31:3<792::AID-IMMU792>3.0.CO;2-U
89. Tominaga K, Yoshimoto T, Torigoe K, Kurimoto M, Matsui K, Hada T, et al. IL-12 synergizes with IL-18 or IL-1beta for IFN-gamma production from human T cells. *Int Immunol.* (2000) 12:151–60. doi: 10.1093/intimm/12.2.151
90. Vignali DA, Kuchroo VK. IL-12 family cytokines: immunological playmakers. *Nat Immunol.* (2012) 13:722–8. doi: 10.1038/ni.2366
91. Harris J. Autophagy and cytokines. *Cytokine* (2011) 56:140–4. doi: 10.1016/j.cyto.2011.08.022
92. Harris J, Master SS, De Haro SA, Delgado M, Roberts EA, Hope JC, et al. Th1-Th2 polarisation and autophagy in the control of intracellular mycobacteria by macrophages. *Vet Immunol Immunopathol.* (2009) 128:37–43. doi: 10.1016/j.vetimm.2008.10.293
93. Yuan Y, Ding D, Zhang N, Xia Z, Wang J, Yang H, et al. TNF-alpha induces autophagy through ERK1/2 pathway to regulate apoptosis in neonatal necrotizing enterocolitis model cells IEC-6. *Cell Cycle* (2018) 17:1390–402. doi: 10.1080/15384101.2018.1482150
94. Feng CG, Zheng L, Lenardo MJ, Sher A. Interferon-inducible immunity-related GTPase Irgm1 regulates IFN gamma-dependent host defense, lymphocyte survival and autophagy. *Autophagy* (2009) 5:232–4. doi: 10.4161/auto.5.2.7445
95. Al-Zeer MA, Al-Younes HM, Braun PR, Zerrahn J, Meyer TF. IFN-gamma-inducible Irga6 mediates host resistance against Chlamydia trachomatis via autophagy. *PLoS ONE* (2009) 4:e4588. doi: 10.1371/journal.pone.0004588
96. Matsuzawa T, Kim BH, Shenoy AR, Kamitani S, Miyake M, Macmicking JD. IFN-gamma elicits macrophage autophagy via the p38 MAPK signaling pathway. *J Immunol.* (2012) 189:813–8. doi: 10.4049/jimmunol.1102041
97. Simmons CP, Goncalves NS, Ghaem-Maghami M, Bajaj-Elliott M, Clare S, Neves B, et al. Impaired resistance and enhanced pathology during infection with a noninvasive, attaching-effacing enteric bacterial pathogen, Citrobacter rodentium, in mice lacking IL-12 or IFN-gamma. *J Immunol.* (2002) 168:1804–12. doi: 10.4049/jimmunol.168.4.1804
98. Shiomi H, Masuda A, Nishiumi S, Nishida M, Takagawa T, Shiomi Y, et al. Gamma interferon produced by antigen-specific CD4+ T cells regulates the mucosal immune responses to Citrobacter rodentium infection. *Infect Immun.* (2010) 78:2653–66. doi: 10.1128/IAI.01343-09
99. Marchiando AM, Ramanan D, Ding Y, Gomez LE, Hubbard-Lucey VM, Maurer K, et al. A deficiency in the autophagy gene Atg16L1 enhances resistance to enteric bacterial infection. *Cell Host Microbe* (2013) 14:216–24. doi: 10.1016/j.chom.2013.07.013
100. Abt MC, Lewis BB, Caballero S, Xiong H, Carter RA, Susac B, et al. Innate immune defenses mediated by two ILC subsets are critical for protection against acute clostridium difficile infection. *Cell Host Microbe* (2015) 18:27–37. doi: 10.1016/j.chom.2015.06.011
101. Bernink JH, Peters CP, Munneke M, te Velde AA, Meijer SL, Weijer K, et al. Human type 1 innate lymphoid cells accumulate in inflamed mucosal tissues. *Nat Immunol.* (2013) 14:221–9. doi: 10.1038/ni.2534
102. Fuchs A, Vermi W, Lee JS, Lonardi S, Gilfillan S, Newberry RD, et al. Intraepithelial type 1 innate lymphoid cells are a unique subset of IL-12- and

IL-15-responsive IFN-gamma-producing cells. *Immunity* (2013) 38:769–81. doi: 10.1016/j.immuni.2013.02.010
103. Imam T, Park S, Kaplan MH, Olson MR. Effector T helper cell subsets in inflammatory bowel diseases. *Front Immunol.* (2018) 9:1212. doi: 10.3389/fimmu.2018.01212
104. Kaskow BJ, Baecher-Allan C. Effector T cells in multiple sclerosis. *Cold Spring Harb Perspect Med.* (2018) 8:a029025. doi: 10.1101/cshperspect.a029025
105. Kotake S, Yago T, Kobashigawa T, Nanke Y. The plasticity of Th17 cells in the pathogenesis of rheumatoid arthritis. *J Clin Med.* (2017) 6:E67. doi: 10.3390/jcm6070067
106. Li C, Capan E, Zhao Y, Zhao J, Stolz D, Watkins SC, et al. Autophagy is induced in CD4+ T cells and important for the growth factor-withdrawal cell death. *J Immunol.* (2006) 177:5163–8. doi: 10.4049/jimmunol.177.8.5163
107. Pua HH, Dzhagalov I, Chuck M, Mizushima N, He YW. A critical role for the autophagy gene Atg5 in T cell survival and proliferation. *J Exp Med.* (2007) 204:25–31. doi: 10.1084/jem.20061303
108. Pua HH, Guo J, Komatsu M, He YW. Autophagy is essential for mitochondrial clearance in mature T lymphocytes. *J Immunol.* (2009) 182:4046–55. doi: 10.4049/jimmunol.0801143
109. Arsov I, Adebayo A, Kucerova-Levisohn M, Haye J, MacNeil M, Papavasiliou FN, et al. A role for autophagic protein beclin 1 early in lymphocyte development. *J Immunol.* (2011) 186:2201–9. doi: 10.4049/jimmunol.1002223
110. Jia W, He YW. Temporal regulation of intracellular organelle homeostasis in T lymphocytes by autophagy. *J Immunol.* (2011) 186:5313–22. doi: 10.4049/jimmunol.1002404
111. Jia W, Pua HH, Li QJ, He YW. Autophagy regulates endoplasmic reticulum homeostasis and calcium mobilization in T lymphocytes. *J Immunol.* (2011) 186:1564–74. doi: 10.4049/jimmunol.1001822
112. McLeod IX, Zhou X, Li QJ, Wang F, He YW. The class III kinase Vps34 promotes T lymphocyte survival through regulating IL-7Ralpha surface expression. *J Immunol.* (2011) 187:5051–61. doi: 10.4049/jimmunol.1100710
113. Kovacs JR, Li C, Yang Q, Li G, Garcia IG, Ju S, et al. Autophagy promotes T-cell survival through degradation of proteins of the cell death machinery. *Cell Death Different.* (2012) 19:144–52. doi: 10.1038/cdd.2011.78
114. Schluns KS, Kieper WC, Jameson SC, Lefrancois L. Interleukin-7 mediates the homeostasis of naive and memory CD8 T cells *in vivo*. *Nat Immunol.* (2000) 1:426–32. doi: 10.1038/80868
115. Hagen KA, Moses CT, Drasler EF, Podetz-Pedersen KM, Jameson SC, Khoruts A. A role for CD28 in lymphopenia-induced proliferation of CD4 T cells. *J Immunol.* (2004) 173:3909–15. doi: 10.4049/jimmunol.173.6.3909
116. Sandau MM, Winstead CJ, Jameson SC. IL-15 is required for sustained lymphopenia-driven proliferation and accumulation of CD8 T cells. *J Immunol.* (2007) 179:120–5. doi: 10.4049/jimmunol.179.1.120
117. Voehringer D, Liang HE, Locksley RM. Homeostasis and effector function of lymphopenia-induced "memory-like" T cells in constitutively T cell-depleted mice. *J Immunol.* (2008) 180:4742–53. doi: 10.4049/jimmunol.180.7.4742
118. Sprent J, Surh CD. Normal T cell homeostasis: the conversion of naive cells into memory-phenotype cells. *Nat Immunol.* (2011) 12:478–84. doi: 10.1038/ni.2018
119. Raeber ME, Zurbuchen Y, Impellizzieri D, Boyman O. The role of cytokines in T-cell memory in health and disease. *Immunol Rev.* (2018) 283:176–93. doi: 10.1111/imr.12644
120. Botbol Y, Patel B, Macian F. Common gamma-chain cytokine signaling is required for macroautophagy induction during CD4+ T-cell activation. *Autophagy* (2015) 11:1864–77. doi: 10.1080/15548627.2015.1089374
121. Hubbard VM, Valdor R, Patel B, Singh R, Cuervo AM, Macian F. Macroautophagy regulates energy metabolism during effector T cell activation. *J Immunol.* (2010) 185:7349–57. doi: 10.4049/jimmunol.1000576
122. Jia W, He MX, McLeod IX, Guo J, Ji D, He YW. Autophagy regulates T lymphocyte proliferation through selective degradation of the cell-cycle inhibitor CDKN1B/p27Kip1. *Autophagy* (2015) 11:2335–45. doi: 10.1080/15548627.2015.1110666
123. Hirahara K, Nakayama T. CD4+ T-cell subsets in inflammatory diseases: beyond the Th1/Th2 paradigm. *Int Immunol.* (2016) 28:163–71. doi: 10.1093/intimm/dxw006
124. Murera D, Arbogast F, Arnold J, Bouis D, Muller S, Gros F. CD4 T cell autophagy is integral to memory maintenance. *Sci Rep.* (2018) 8:5951. doi: 10.1038/s41598-018-23993-0
125. Xu X, Araki K, Li S, Han JH, Ye L, Tan WG, et al. Autophagy is essential for effector CD8(+) T cell survival and memory formation. *Nat Immunol.* (2014) 15:1152–61. doi: 10.1038/ni.3025
126. Kabat AM, Harrison OJ, Riffelmacher T, Moghaddam AE, Pearson CF, Laing A, et al. The autophagy gene Atg16l1 differentially regulates Treg and TH2 cells to control intestinal inflammation. *Elife* (2016) 5:e12444. doi: 10.7554/eLife.12444
127. Benoit-Lizon I, Jacquin E, Apetoh L. Selective autophagy restricts IL-9 secretion from TH9 cells: relevance in cancer growth. *Cell Cycle* (2018) 17:391–2. doi: 10.1080/15384101.2017.1414680
128. Rivera Vargas T, Cai Z, Shen Y, Dosset M, Benoit-Lizon I, Martin T, et al. Selective degradation of PU.1 during autophagy represses the differentiation and antitumour activity of TH9 cells. *Nat Commun.* (2017) 8:559. doi: 10.1038/s41467-017-00468-w
129. Jonchere B, Belanger A, Guette C, Barre B, Coqueret O. STAT3 as a new autophagy regulator. *JAKSTAT* (2013) 2:e24353. doi: 10.4161/jkst.24353
130. Winders BR, Schwartz RH, Bruniquel D. A distinct region of the murine IFN-gamma promoter is hypomethylated from early T cell development through mature naive and Th1 cell differentiation, but is hypermethylated in Th2 cells. *J Immunol.* (2004) 173:7377–84. doi: 10.4049/jimmunol.173.12.7377
131. Powell JD, Bruniquel D, Schwartz RH. TCR engagement in the absence of cell cycle progression leads to T cell anergy independent of p27(Kip1). *Eur J Immunol.* (2001) 31:3737–46. doi: 10.1002/1521-4141(200112)31:12<3737::AID-IMMU3737>3.0.CO;2-G
132. Chang JT, Segal BM, Shevach EM. Role of costimulation in the induction of the IL-12/IL-12 receptor pathway and the development of autoimmunity. *J Immunol.* (2000) 164:100–6. doi: 10.4049/jimmunol.164.1.100
133. Kiyono K, Suzuki HI, Matsuyama H, Morishita Y, Komuro A, Kano MR, et al. Autophagy is activated by TGF-beta and potentiates TGF-beta-mediated growth inhibition in human hepatocellular carcinoma cells. *Cancer Res.* (2009) 69:8844–52. doi: 10.1158/0008-5472.CAN-08-4401
134. Liang X, De Vera ME, Buchser WJ, Romo de Vivar Chavez A, Loughran P, Beer Stolz D, et al. Inhibiting systemic autophagy during interleukin 2 immunotherapy promotes long-term tumor regression. *Cancer Res.* (2012) 72:2791–801. doi: 10.1158/0008-5472.CAN-12-0320
135. W.Ip KE, Hoshi N, Shouval DS, Snapper S, Medzhitov R. Anti-inflammatory effect of IL-10 mediated by metabolic reprogramming of macrophages. *Science* (2017) 356:513–9. doi: 10.1126/science.aal3535
136. Terawaki S, Camosseto V, Prete F, Wenger T, Papadopoulos A, Rondeau C, et al. RUN and FYVE domain-containing protein 4 enhances autophagy and lysosome tethering in response to Interleukin-4. *J Cell Biol.* (2015) 210:1133–52. doi: 10.1083/jcb.201501059
137. Wei J, Long L, Yang K, Guy C, Shrestha S, Chen Z, et al. Autophagy enforces functional integrity of regulatory T cells by coupling environmental cues and metabolic homeostasis. *Nat Immunol.* (2016) 17:277–85. doi: 10.1038/ni.3365
138. Le Texier L, Lineburg KE, Cao B, McDonald-Hyman C, Leveque-El Mouttie L, Nicholls J, et al. Autophagy-dependent regulatory T cells are critical for the control of graft-versus-host disease. *JCI Insight* (2016) 1:e86850. doi: 10.1172/jci.insight.86850
139. Gao Y, Tang J, Chen W, Li Q, Nie J, Lin F, et al. Inflammation negatively regulates FOXP3 and regulatory T-cell function via DBC1. *Proc Natl Acad Sci USA.* (2015) 112:E3246–54. doi: 10.1073/pnas.1421463112
140. O'Neill LA, Pearce EJ. Immunometabolism governs dendritic cell and macrophage function. *J Exp Med.* (2016) 213:15–23. doi: 10.1084/jem.20151570
141. Phan AT, Goldrath AW, Glass CK. Metabolic and epigenetic coordination of T Cell and macrophage immunity. *Immunity* (2017) 46:714–29. doi: 10.1016/j.immuni.2017.04.016
142. White E, Mehnert JM, Chan CS. Autophagy, metabolism, and cancer. *Clin Can Res.* (2015) 21:5037–46. doi: 10.1158/1078-0432.CCR-15-0490
143. Levine B, Mizushima N, Virgin HW. Autophagy in immunity and inflammation. *Nature* (2011) 469:323–35. doi: 10.1038/nature09782

144. Chang CH, Curtis JD, Maggi LB Jr., Faubert B, Villarino AV, O'Sullivan D, et al. Posttranscriptional control of T cell effector function by aerobic glycolysis. *Cell* (2013) 153:1239–51. doi: 10.1016/j.cell.2013.05.016
145. O'Neill LA, Hardie DG. Metabolism of inflammation limited by AMPK and pseudo-starvation. *Nature* (2013) 493:346–55. doi: 10.1038/nature11862
146. Riffelmacher T, Richter FC, Simon AK. Autophagy dictates metabolism and differentiation of inflammatory immune cells. *Autophagy* (2018) 14:199–206. doi: 10.1080/15548627.2017.1362525
147. Dunlop EA, Tee AR. mTOR and autophagy: a dynamic relationship governed by nutrients and energy. *Semin Cell Dev Biol.* (2014) 36:121–9. doi: 10.1016/j.semcdb.2014.08.006
148. Martinez J, Verbist K, Wang R, Green DR. The relationship between metabolism and the autophagy machinery during the innate immune response. *Cell Metab.* (2013) 17:895–900. doi: 10.1016/j.cmet.2013.05.012
149. Lunt SY, Vander Heiden MG. Aerobic glycolysis: meeting the metabolic requirements of cell proliferation. *Annu Rev Cell Dev Biol.* (2011) 27:441–64. doi: 10.1146/annurev-cellbio-092910-154237
150. Amiel E, Everts B, Fritz D, Beauchamp S, Ge B, Pearce EL, et al. Mechanistic target of rapamycin inhibition extends cellular lifespan in dendritic cells by preserving mitochondrial function. *J Immunol.* (2014) 193:2821–30. doi: 10.4049/jimmunol.1302498
151. Everts B, Amiel E, Huang SC, Smith AM, Chang CH, Lam WY, et al. TLR-driven early glycolytic reprogramming via the kinases TBK1-IKKvarepsilon supports the anabolic demands of dendritic cell activation. *Nat Immunol.* (2014) 15:323–32. doi: 10.1038/ni.2833
152. Riffelmacher T, Clarke A, Richter FC, Stranks A, Pandey S, Danielli S, et al. Autophagy-dependent generation of free fatty acids is critical for normal neutrophil differentiation. *Immunity* (2017) 47:466–80.e5. doi: 10.1016/j.immuni.2017.08.005
153. Khan N, Vidyarthi A, Pahari S, Negi S, Aqdas M, Nadeem S, et al. Signaling through NOD-2 and TLR-4 bolsters the T cell priming capability of dendritic cells by inducing autophagy. *Sci Rep.* (2016) 6:19084. doi: 10.1038/srep19084
154. Pollizzi KN, Powell JD. Integrating canonical and metabolic signalling programmes in the regulation of T cell responses. *Nat Rev Immunol.* (2014) 14:435–46. doi: 10.1038/nri3701
155. Wang P, Long M, Zhang S, Cheng Z, Zhao X, He F, et al. Hypoxia inducible factor-1alpha regulates autophagy via the p27-E2F1 signaling pathway. *Mol Med Rep.* (2017) 16:2107–12. doi: 10.3892/mmr.2017.6794
156. Rodriguez-Prados JC, Traves PG, Cuenca J, Rico D, Aragones J, Martin-Sanz P, et al. Substrate fate in activated macrophages: a comparison between innate, classic, and alternative activation. *J Immunol.* (2010) 185:605–14. doi: 10.4049/jimmunol.0901698
157. Krawczyk CM, Holowka T, Sun J, Blagih J, Amiel E, DeBerardinis RJ, et al. Toll-like receptor-induced changes in glycolytic metabolism regulate dendritic cell activation. *Blood* (2010) 115:4742–9. doi: 10.1182/blood-2009-10-249540
158. Vats D, Mukundan L, Odegaard JI, Zhang L, Smith KL, Morel CR, et al. Oxidative metabolism and PGC-1beta attenuate macrophage-mediated inflammation. *Cell Metab.* (2006) 4:13–24. doi: 10.1016/j.cmet.2006.05.011
159. Sag D, Carling D, Stout RD, Suttles J. Adenosine 5'-monophosphate-activated protein kinase promotes macrophage polarization to an anti-inflammatory functional phenotype. *J Immunol.* (2008) 181:8633–41. doi: 10.4049/jimmunol.181.12.8633
160. Deng SY, Zhang LM, Ai YH, Pan PH, Zhao SP, Su XL, et al. Role of interferon regulatory factor-1 in lipopolysaccharide-induced mitochondrial damage and oxidative stress responses in macrophages. *Int J Mol Med.* (2017) 40:1261–9. doi: 10.3892/ijmm.2017.3110
161. Zhang L, Cardinal JS, Bahar R, Evankovich J, Huang H, Nace G, et al. Interferon regulatory factor-1 regulates the autophagic response in LPS-stimulated macrophages through nitric oxide. *Mol Med.* (2012) 18:201–8. doi: 10.2119/molmed.2011.00094
162. Zhang L, Cardinal JS, Pan P, Rosborough BR, Chang Y, Yan W, et al. Splenocyte apoptosis and autophagy is mediated by interferon regulatory factor 1 during murine endotoxemia. *Shock* (2012) 37:511–7. doi: 10.1097/SHK.0b013e318249cfa2
163. Gabriele L, Fragale A, Borghi P, Sestili P, Stellacci E, Venditti M, et al. IRF-1 deficiency skews the differentiation of dendritic cells toward plasmacytoid and tolerogenic features. *J Leukoc Biol.* (2006) 80:1500–11. doi: 10.1189/jlb.0406246
164. Park HJ, Lee SJ, Kim SH, Han J, Bae J, Kim SJ, et al. IL-10 inhibits the starvation induced autophagy in macrophages via class I phosphatidylinositol 3-kinase (PI3K) pathway. *Mol Immunol.* (2011) 48:720–7. doi: 10.1016/j.molimm.2010.10.020
165. Van Grol J, Subauste C, Andrade RM, Fujinaga K, Nelson J, Subauste CS. HIV-1 inhibits autophagy in bystander macrophage/monocytic cells through Src-Akt and STAT3. *PLoS ONE* (2010) 5:e11733. doi: 10.1371/journal.pone.0011733
166. Zhang XW, Mi S, Li Z, Zhou JC, Xie J, Hua F, et al. Antagonism of Interleukin-17A ameliorates experimental hepatic fibrosis by restoring the IL-10/STAT3-suppressed autophagy in hepatocytes. *Oncotarget* (2017) 8:9922–34. doi: 10.18632/oncotarget.14266
167. Lv H, Jiang Y, Li J, Zhang M, Shang Z, Zheng J, et al. Association between polymorphisms in the promoter region of interleukin-10 and susceptibility to inflammatory bowel disease. *Mol Biol Rep.* (2014) 41:1299–310. doi: 10.1007/s11033-013-2975-7
168. Zhang J, Zhang Y, Jin J, Li M, Xie K, Wen C, et al. The−1082A/G polymorphism in the Interleukin-10 gene and the risk of rheumatoid arthritis: a meta-analysis. *Cytokine* (2011) 56:351–5. doi: 10.1016/j.cyto.2011.05.022
169. Lv TT, Wu J, Li J, Zhang TP, Yang XK, Xiang N, et al. Association of interleukin-10 gene single nucleotide polymorphisms with susceptibility to systemic lupus erythematosus in a Chinese population. *Gene* (2018) 642:549–54. doi: 10.1016/j.gene.2017.11.072
170. Ramakrishnan V, Akram Husain RS, Ahmed SS. Genetic predisposition of IL-10 promoter polymorphisms with risk of multiple sclerosis: a meta-analysis. *J Neuroimmunol.* (2017) 306:11–8. doi: 10.1016/j.jneuroim.2017.02.015
171. Bain CC, Mowat AM. Macrophages in intestinal homeostasis and inflammation. *Immunol Rev.* (2014) 260:102–17. doi: 10.1111/imr.12192
172. Zigmond E, Bernshtein B, Friedlander G, Walker CR, Yona S, Kim KW, et al. Macrophage-restricted interleukin-10 receptor deficiency, but not IL-10 deficiency, causes severe spontaneous colitis. *Immunity* (2014) 40:720–33. doi: 10.1016/j.immuni.2014.03.012
173. Shouval DS, Biswas A, Goettel JA, McCann K, Conaway E, Redhu NS, et al. Interleukin-10 receptor signaling in innate immune cells regulates mucosal immune tolerance and anti-inflammatory macrophage function. *Immunity* (2014) 40:706–19. doi: 10.1016/j.immuni.2014.03.011
174. Jacquel A, Obba S, Boyer L, Dufies M, Robert G, Gounon P, et al. Autophagy is required for CSF-1-induced macrophagic differentiation and acquisition of phagocytic functions. *Blood* (2012) 119:4527–31. doi: 10.1182/blood-2011-11-392167
175. Zhang Y, Morgan MJ, Chen K, Choksi S, Liu ZG. Induction of autophagy is essential for monocyte-macrophage differentiation. *Blood* (2012) 119:2895–905. doi: 10.1182/blood-2011-08-372383
176. Kang YH, Cho MH, Kim JY, Kwon MS, Peak JJ, Kang SW, et al. Impaired macrophage autophagy induces systemic insulin resistance in obesity. *Oncotarget* (2016) 7:35577–91. doi: 10.18632/oncotarget.9590
177. Liu K, Zhao E, Ilyas G, Lalazar G, Lin Y, Haseeb M, et al. Impaired macrophage autophagy increases the immune response in obese mice by promoting proinflammatory macrophage polarization. *Autophagy* (2015) 11:271–84. doi: 10.1080/15548627.2015.1009787
178. Stranks AJ, Hansen AL, Panse I, Mortensen M, Ferguson DJ, Puleston DJ, et al. Autophagy controls acquisition of aging features in macrophages. *J Innate Immun.* (2015) 7:375–91. doi: 10.1159/000370112
179. Muraille E, Leo O, Moser M. TH1/TH2 paradigm extended: macrophage polarization as an unappreciated pathogen-driven escape mechanism? *Front Immunol.* (2014) 5:603. doi: 10.3389/fimmu.2014.00603
180. Dose M, Khan I, Guo Z, Kovalovsky D, Krueger A, von Boehmer H, et al. c-Myc mediates pre-TCR-induced proliferation but not developmental progression. *Blood* (2006) 108:2669–77. doi: 10.1182/blood-2006-02-005900
181. Iritani BM, Delrow J, Grandori C, Gomez I, Klacking M, Carlos LS, et al. Modulation of T-lymphocyte development, growth and cell size by the Myc antagonist and transcriptional repressor Mad1. *EMBO J* (2002) 21:4820–30. doi: 10.1093/emboj/cdf492

182. Wang R, Dillon CP, Shi LZ, Milasta S, Carter R, Finkelstein D, et al. The transcription factor Myc controls metabolic reprogramming upon T lymphocyte activation. *Immunity* (2011) 35:871–82. doi: 10.1016/j.immuni.2011.09.021
183. Cheng SC, Quintin J, Cramer RA, Shepardson KM, Saeed S, Kumar V, et al. mTOR- and HIF-1alpha-mediated aerobic glycolysis as metabolic basis for trained immunity. *Science* (2014) 345:1250684. doi: 10.1126/science.1250684
184. Molon B, Cali B, Viola A. T cells and cancer: how metabolism shapes immunity. *Front Immunol.* (2016) 7:20. doi: 10.3389/fimmu.2016.00020
185. Geltink RIK, Kyle RL, Pearce EL. Unraveling the complex interplay between T cell metabolism and function. *Ann Rev Immunol.* (2018) 36:461–88. doi: 10.1146/annurev-immunol-042617-053019
186. Barbi J, Pardoll D, Pan F. Metabolic control of the Treg/Th17 axis. *Immunol Rev.* (2013) 252:52–77. doi: 10.1111/imr.12029
187. Yang K, Shrestha S, Zeng H, Karmaus PW, Neale G, Vogel P, et al. T cell exit from quiescence and differentiation into Th2 cells depend on Raptor-mTORC1-mediated metabolic reprogramming. *Immunity* (2013) 39:1043–56. doi: 10.1016/j.immuni.2013.09.015
188. Pelgrom LR, Everts B. Metabolic control of type 2 immunity. *Eur J Immunol.* (2017) 47:1266–75. doi: 10.1002/eji.201646728
189. Rolf J, Zarrouk M, Finlay DK, Foretz M, Viollet B, Cantrell DA. AMPKalpha1: a glucose sensor that controls CD8 T-cell memory. *Eur J Immunol.* (2013) 43:889–96. doi: 10.1002/eji.201243008
190. Galluzzi L, Bravo-San Pedro JM, Levine B, Green DR, Kroemer G. Pharmacological modulation of autophagy: therapeutic potential and persisting obstacles. *Nat Rev Drug Discov.* (2017) 16:487–511. doi: 10.1038/nrd.2017.22
191. Towers CG, Thorburn A. Therapeutic targeting of autophagy. *EBioMedicine* (2016) 14:15–23. doi: 10.1016/j.ebiom.2016.10.034
192. Gianchecchi E, Delfino DV, Fierabracci A. Recent insights on the putative role of autophagy in autoimmune diseases. *Autoimm Rev.* (2014) 13:231–41. doi: 10.1016/j.autrev.2013.10.007
193. Kim KH, Lee MS. Autophagy–a key player in cellular and body metabolism. *Nat Rev Endocrinol.* (2014) 10:322–37. doi: 10.1038/nrendo.2014.35
194. Chauhan S, Ahmed Z, Bradfute SB, Arko-Mensah J, Mandell MA, Won Choi S, et al. Pharmaceutical screen identifies novel target processes for activation of autophagy with a broad translational potential. *Nat Commun.* (2015) 6:8620. doi: 10.1038/ncomms9620
195. Cho YS, Kwon HJ. Control of autophagy with small molecules. *Arch Pharm Res.* (2010) 33:1881–9. doi: 10.1007/s12272-010-1201-6
196. Iorio F, Isacchi A, di Bernardo D, Brunetti-Pierri N. Identification of small molecules enhancing autophagic function from drug network analysis. *Autophagy* (2010) 6:1204–5. doi: 10.4161/auto.6.8.13551
197. Ungaro R, Mehandru S, Allen PB, Peyrin-Biroulet L, Colombel JF. Ulcerative colitis. *Lancet* (2017) 389:1756–70. doi: 10.1016/S0140-6736(16)32126-2
198. Torres J, Mehandru S, Colombel JF, Peyrin-Biroulet L. Crohn's disease. *Lancet* (2017) 389:1741–55. doi: 10.1016/S0140-6736(12)60026-9
199. Cader MZ, Kaser A. Recent advances in inflammatory bowel disease: mucosal immune cells in intestinal inflammation. *Gut* (2013) 62:1653–64. doi: 10.1136/gutjnl-2012-303955
200. Neurath MF, Cytokines in inflammatory bowel disease. *Nat Rev Immunol.* (2014) 14:329–42. doi: 10.1038/nri3661
201. Neurath MF, Current and emerging therapeutic targets for IBD. *Nat Rev Gastroenterol Hepatol.* (2017) 14:269–78. doi: 10.1038/nrgastro.2016.208
202. Gecse KB, Lakatos PL. IBD in 2016: biologicals and biosimilars in IBD - the road to personalized treatment. *Nat Rev Gastroenterol Hepatol.* (2017) 14:74–6. doi: 10.1038/nrgastro.2016.206
203. Katsanos KH, Papadakis KA. Inflammatory bowel disease: updates on molecular targets for biologics. *Gut Liver* (2017) 11:455–63. doi: 10.5009/gnl16308
204. Panaccione R, Ghosh S, Middleton S, Marquez JR, Scott BB, Flint L, et al. Combination therapy with infliximab and azathioprine is superior to monotherapy with either agent in ulcerative colitis. *Gastroenterology* (2014) 146:392–400.e3. doi: 10.1053/j.gastro.2013.10.052
205. Colombel JF, Sandborn WJ, Reinisch W, Mantzaris GJ, Kornbluth A, Rachmilewitz D, et al. Infliximab, azathioprine, or combination therapy for Crohn's disease. *N Eng J Med.* (2010) 362:1383–95. doi: 10.1056/NEJMoa0904492
206. Feagan BG, Rutgeerts P, Sands BE, Hanauer S, Colombel JF, Sandborn WJ, et al. Vedolizumab as induction and maintenance therapy for ulcerative colitis. *N Eng J Med.* (2013) 369:699–710. doi: 10.1056/NEJMoa1215734
207. Sandborn WJ, Feagan BG, Rutgeerts P, Hanauer S, Colombel JF, Sands BE, et al. Vedolizumab as induction and maintenance therapy for Crohn's disease. *N Eng J Med.* (2013) 369:711–21. doi: 10.1056/NEJMoa1215739
208. Lassen KG, Xavier RJ. Genetic control of autophagy underlies pathogenesis of inflammatory bowel disease. *Mucosal Immunol.* (2017) 10:589–97. doi: 10.1038/mi.2017.18
209. Bel S, Pendse M, Wang Y, Li Y, Ruhn KA, Hassell B, et al. Paneth cells secrete lysozyme via secretory autophagy during bacterial infection of the intestine. *Science* (2017) 357:1047–52. doi: 10.1126/science.aal4677
210. Henckaerts L, Cleynen I, Brinar M, John JM, Van Steen K, Rutgeerts P, et al. Genetic variation in the autophagy gene ULK1 and risk of Crohn's disease. *Inflamm Bowel Dis.* (2011) 17:1392–7. doi: 10.1002/ibd.21486
211. Lahiri A, Hedl M, Abraham C. MTMR3 risk allele enhances innate receptor-induced signaling and cytokines by decreasing autophagy and increasing caspase-1 activation. *Proc Natl Acad Sci USA*. (2015) 112:10461–6. doi: 10.1073/pnas.1501752112
212. Brest P, Lapaquette P, Souidi M, Lebrigand K, Cesaro A, Vouret-Craviari V, et al. A synonymous variant in IRGM alters a binding site for miR-196 and causes deregulation of IRGM-dependent xenophagy in Crohn's disease. *Nat Genet.* (2011) 43:242–5. doi: 10.1038/ng.762
213. McCarroll SA, Huett A, Kuballa P, Chilewski SD, Landry A, Goyette P, et al. Deletion polymorphism upstream of IRGM associated with altered IRGM expression and Crohn's disease. *Nat Genet.* (2008) 40:1107–12. doi: 10.1038/ng.215
214. Parkes M, Barrett JC, Prescott NJ, Tremelling M, Anderson CA, Fisher SA, et al. Sequence variants in the autophagy gene IRGM and multiple other replicating loci contribute to Crohn's disease susceptibility. *Nat Genet.* (2007) 39:830–2. doi: 10.1038/ng2061
215. Barrett JC, Hansoul S, Nicolae DL, Cho JH, Duerr RH, Rioux JD, et al. Genome-wide association defines more than 30 distinct susceptibility loci for Crohn's disease. *Nat Genet.* (2008) 40:955–62. doi: 10.1038/ng.175
216. Franke A, Balschun T, Sina C, Ellinghaus D, Hasler R, Mayr G, et al. Genome-wide association study for ulcerative colitis identifies risk loci at 7q22 and 22q13 (IL17REL). *Nat Genet.* (2010) 42:292–4. doi: 10.1038/ng.553
217. Matsuda C, Ito T, Song J, Mizushima T, Tamagawa H, Kai Y, et al. Therapeutic effect of a new immunosuppressive agent, everolimus, on interleukin-10 gene-deficient mice with colitis. *Clin Exp Immunol.* (2007) 148:348–59. doi: 10.1111/j.1365-2249.2007.03345.x
218. Macias-Ceja DC, Cosin-Roger J, Ortiz-Masia D, Salvador P, Hernandez C, Esplugues JV, et al. Stimulation of autophagy prevents intestinal mucosal inflammation and ameliorates murine colitis. *Br J Pharmacol.* (2017) 174:2501–11. doi: 10.1111/bph.13860
219. Nighot PK, Hu CA, Ma TY. Autophagy enhances intestinal epithelial tight junction barrier function by targeting claudin-2 protein degradation. *J Biol Chem.* (2015) 290:7234–46. doi: 10.1074/jbc.M114.597492
220. Kim YC, Guan KL. mTOR: a pharmacologic target for autophagy regulation. *J Clin Invest.* (2015) 125:25–32. doi: 10.1172/JCI73939
221. Mardones P, Rubinsztein DC, Hetz C. Mystery solved: Trehalose kickstarts autophagy by blocking glucose transport. *Sci Signal.* (2016) 9:fs2. doi: 10.1126/scisignal.aaf1937
222. Collins J, Robinson C, Danhof H, Knetsch CW, van Leeuwen HC, Lawley TD, et al. Dietary trehalose enhances virulence of epidemic Clostridium difficile. *Nature* (2018) 553:291–4. doi: 10.1038/nature25178
223. Feagan BG, Sandborn WJ, Gasink C, Jacobstein D, Lang Y, Friedman JR, et al. Ustekinumab as induction and maintenance therapy for Crohn's disease. *N Eng J Med.* (2016) 375:1946–60. doi: 10.1056/NEJMoa1602773
224. D'Haens G. Risks and benefits of biologic therapy for inflammatory bowel diseases. *Gut* (2007) 56:725–32. doi: 10.1136/gut.2006.103564
225. Rubinsztein DC, Bento CF, Deretic V. Therapeutic targeting of autophagy in neurodegenerative and infectious diseases. *J Exp Med.* (2015) 212:979–90. doi: 10.1084/jem.20150956
226. Nistala K, Adams S, Cambrook H, Ursu S, Olivito B, de Jager W, et al. Th17 plasticity in human autoimmune arthritis is driven by the inflammatory environment. *Proc Natl Acad Sci USA*. (2010) 107:14751–6. doi: 10.1073/pnas.1003852107

227. Kotake S, Nanke Y, Yago T, Kawamoto M, Kobashigawa T, Yamanaka H. Elevated ratio of Th17 cell-derived Th1 cells (CD161(+)Th1 Cells) to CD161(+)Th17 cells in peripheral blood of early-onset rheumatoid arthritis patients. *Biomed Res Int.* (2016) 2016:4186027. doi: 10.1155/2016/4186027
228. Weyand CM, Goronzy JJ. Immunometabolism in early and late stages of rheumatoid arthritis. *Nat Rev Rheumatol.* (2017) 13:291–301. doi: 10.1038/nrrheum.2017.49
229. Lin NY, Beyer C, Giessl A, Kireva T, Scholtysek C, Uderhardt S, et al. Autophagy regulates TNFalpha-mediated joint destruction in experimental arthritis. *Ann Rheum Dis.* (2013) 72:761–8. doi: 10.1136/annrheumdis-2012-201671
230. Orozco G, Eyre S, Hinks A, Bowes J, Morgan AW, Wilson AG, et al. Study of the common genetic background for rheumatoid arthritis and systemic lupus erythematosus. *Ann Rheum Dis.* (2011) 70:463–8. doi: 10.1136/ard.2010.137174
231. Yang Z, Fujii H, Mohan SV, Goronzy JJ, Weyand CM. Phosphofructokinase deficiency impairs ATP generation, autophagy, and redox balance in rheumatoid arthritis T cells. *J Exp Med.* (2013) 210:2119–34. doi: 10.1084/jem.20130252
232. van Loosdregt J, Rossetti M, Spreafico R, Moshref M, Olmer M, Williams GW, et al. Increased autophagy in CD4(+) T cells of rheumatoid arthritis patients results in T-cell hyperactivation and apoptosis resistance. *Eur J Immunol.* (2016) 46:2862–70. doi: 10.1002/eji.201646375
233. Rainsford KD, Parke AL, Clifford-Rashotte M, Kean WF. Therapy and pharmacological properties of hydroxychloroquine and chloroquine in treatment of systemic lupus erythematosus, rheumatoid arthritis and related diseases. *Inflammopharmacology* (2015) 23:231–69. doi: 10.1007/s10787-015-0239-y
234. Sorice M, Iannuccelli C, Manganelli V, Capozzi A, Alessandri C, Lococo E, et al. Autophagy generates citrullinated peptides in human synoviocytes: a possible trigger for anti-citrullinated peptide antibodies. *Rheumatology* (2016) 55:1374–85. doi: 10.1093/rheumatology/kew178
235. Krishnamurthy A, Joshua V, Haj Hensvold A, Jin T, Sun M, Vivar N, et al. Identification of a novel chemokine-dependent molecular mechanism underlying rheumatoid arthritis-associated autoantibody-mediated bone loss. *Ann Rheum Dis.* (2016) 75:721–9. doi: 10.1136/annrheumdis-2015-208093
236. Rostami A, Ciric B. Role of Th17 cells in the pathogenesis of CNS inflammatory demyelination. *J Neurol Sci.* (2013) 333:76–87. doi: 10.1016/j.jns.2013.03.002
237. Keller CW, Lunemann JD. Autophagy and autophagy-related proteins in CNS autoimmunity. *Front Immunol.* (2017) 8:165. doi: 10.3389/fimmu.2017.00165
238. Alirezaei M, Fox HS, Flynn CT, Moore CS, Hebb AL, Frausto RF, et al. Elevated ATG5 expression in autoimmune demyelination and multiple sclerosis. *Autophagy* (2009) 5:152–8. doi: 10.4161/auto.5.2.7348
239. Patergnani S, Castellazzi M, Bonora M, Marchi S, Casetta I, Pugliatti M, et al. Autophagy and mitophagy elements are increased in body fluids of multiple sclerosis-affected individuals. *J Neurol Neurosurg Psychiatry* (2018) 89:439–41. doi: 10.1136/jnnp-2017-316234
240. Berge T, Leikfoss IS, Harbo HF. From identification to characterization of the multiple sclerosis susceptibility gene CLEC16A. *Int J Mol Sci.* (2013) 14:4476–97. doi: 10.3390/ijms14034476
241. Tam RC, Li MW, Gao YP, Pang YT, Yan S, Ge W, et al. Human CLEC16A regulates autophagy through modulating mTOR activity. *Exp Cell Res.* (2017) 352:304–12. doi: 10.1016/j.yexcr.2017.02.017
242. van Luijn MM, Kreft KL, Jongsma ML, Mes SW, Wierenga-Wolf AF, van Meurs M, et al. Multiple sclerosis-associated CLEC16A controls HLA class II expression via late endosome biogenesis. *Brain* (2015) 138:1531–47. doi: 10.1093/brain/awv080
243. Singh SB, Davis AS, Taylor GA, Deretic V. Human IRGM induces autophagy to eliminate intracellular mycobacteria. *Science* (2006) 313:1438–41. doi: 10.1126/science.1129577
244. Ponpuak M, Davis AS, Roberts EA, Delgado MA, Dinkins C, Zhao Z, et al. Delivery of cytosolic components by autophagic adaptor protein p62 endows autophagosomes with unique antimicrobial properties. *Immunity* (2010) 32:329–41. doi: 10.1016/j.immuni.2010.02.009
245. Harris J, De Haro SA, Master SS, Keane J, Roberts EA, Delgado M, et al. T helper 2 cytokines inhibit autophagic control of intracellular Mycobacterium tuberculosis. *Immunity* (2007) 27:505–17. doi: 10.1016/j.immuni.2007.07.022
246. Gutierrez MG, Master SS, Singh SB, Taylor GA, Colombo MI, Deretic V. Autophagy is a defense mechanism inhibiting BCG and Mycobacterium tuberculosis survival in infected macrophages. *Cell* (2004) 119:753–66. doi: 10.1016/j.cell.2004.11.038
247. Bradfute SB, Castillo EF, Arko-Mensah J, Chauhan S, Jiang S, Mandell M, Deretic V. Autophagy as an immune effector against tuberculosis. *Curr Opin Microbiol.* (2013) 16:355–65. doi: 10.1016/j.mib.2013.05.003
248. Xie H, Li C, Zhang M, Zhong N, Chen L. Association between IRGM polymorphisms and tuberculosis risk: a meta-analysis. *Medicine* (2017) 96:e8189. doi: 10.1097/MD.0000000000008189
249. Horne DJ, Graustein AD, Shah JA, Peterson G, Savlov M, Steele S, et al. Human ULK1 Variation and Susceptibility to Mycobacterium tuberculosis Infection. *J Infect Dis.* (2016) 214:1260–7. doi: 10.1093/infdis/jiw347
250. Fernando SL, Saunders BM, Sluyter R, Skarratt KK, Goldberg H, Marks GB, et al. A polymorphism in the P2X7 gene increases susceptibility to extrapulmonary tuberculosis. *Am J Respir Crit Care Med.* (2007) 175:360–6. doi: 10.1164/rccm.200607-970OC
251. Li CM, Campbell SJ, Kumararatne DS, Bellamy R, Ruwende C, McAdam KP, et al. Association of a polymorphism in the P2X7 gene with tuberculosis in a Gambian population. *J Infect Dis.* (2002) 186:1458–62. doi: 10.1086/344351
252. Kimmey JM, Huynh JP, Weiss LA, Park S, Kambal A, Debnath J, et al. Unique role for ATG5 in neutrophil-mediated immunopathology during M. tuberculosis infection. *Nature* (2015) 528:565–9. doi: 10.1038/nature16451

Conflict of Interest Statement: The authors declare that the research was conducted in the absence of any commercial or financial relationships that could be construed as a potential conflict of interest.

Copyright © 2018 Merkley, Chock, Yang, Harris and Castillo. This is an open-access article distributed under the terms of the Creative Commons Attribution License (CC BY). The use, distribution or reproduction in other forums is permitted, provided the original author(s) and the copyright owner(s) are credited and that the original publication in this journal is cited, in accordance with accepted academic practice. No use, distribution or reproduction is permitted which does not comply with these terms.

frontiers in Immunology

ORIGINAL RESEARCH
published: 04 February 2019
doi: 10.3389/fimmu.2019.00115

Differential Regulation of Human Treg and Th17 Cells by Fatty Acid Synthesis and Glycolysis

Deborah Cluxton[1], *Andreea Petrasca*[1], *Barry Moran*[1] *and Jean M. Fletcher*[1,2]*

[1] School of Biochemistry and Immunology, Trinity Biomedical Sciences Institute, Trinity College Dublin, Dublin, Ireland,
[2] School of Medicine, Trinity Biomedical Sciences Institute, Trinity College Dublin, Dublin, Ireland

In this study we examined the metabolic requirements of human T helper cells and the effect of manipulating metabolic pathways in Th17 and Treg cells. The Th17:Treg cell axis is dysregulated in a number of autoimmune or inflammatory diseases and therefore it is of key importance to identify novel strategies to modulate this axis in favor of Treg cells. We investigated the role of carbohydrate and fatty acid metabolism in the regulation of human memory T helper cell subsets, in order to understand how T cells are regulated at the site of inflammation where essential nutrients including oxygen may be limiting. We found that Th17 lineage cells primarily utilize glycolysis, as glucose-deprivation and treatment with rapamycin resulted in a reduction in these cells. On the other hand, Treg cells exhibited increased glycolysis, mitochondrial respiration, and fatty acid oxidation, whereas Th17 cells demonstrated a reliance upon fatty acid synthesis. Treg cells were somewhat reliant on glycolysis, but to a lesser extent than Th17 cells. Here we expose a fundamental difference in the metabolic requirements of human Treg and Th17 cells and a possible mechanism for manipulating the Th17:Treg cell axis.

Keywords: T cells, Th17 cells, Treg cells, immunometabolism, fatty acid synthesis, glycolysis (glycolytic pathway), immune modulation

OPEN ACCESS

Edited by:
Gustavo Javier Martinez, Rosalind Franklin University of Medicine and Science, United States

Reviewed by:
Duncan Howie, University of Oxford, United Kingdom
Giuseppe Matarese, Università degli Studi di Napoli Federico II, Italy

***Correspondence:**
Jean M. Fletcher
jean.fletcher@tcd.ie

Specialty section:
This article was submitted to T Cell Biology, a section of the journal Frontiers in Immunology

Received: *25 June 2018*
Accepted: *15 January 2019*
Published: *04 February 2019*

Citation:
Cluxton D, Petrasca A, Moran B and Fletcher JM (2019) Differential Regulation of Human Treg and Th17 Cells by Fatty Acid Synthesis and Glycolysis. Front. Immunol. 10:115. doi: 10.3389/fimmu.2019.00115

INTRODUCTION

Th17 cells are highly proinflammatory cells which have been implicated in the development and perpetuation of many autoimmune and inflammatory diseases, including rheumatoid arthritis, inflammatory bowel disease, psoriasis, and multiple sclerosis (1–3). In contrast, regulatory T (Treg) cells play a crucial role in maintaining immune tolerance to self-antigen as well as dampening the inflammatory immune response (4). A balance between immune regulation and inflammation is required to maintain optimal immunity and disruption of the Th17:Treg cell axis may contribute to disease. Therefore, skewing the Th17:Treg cell axis in favor of immune regulation by exploiting mechanisms of Th17 cell inhibition may combat inflammation and autoimmunity, and targeting cellular metabolism may be one way to modulate this axis (5, 6).

The carbohydrate metabolism of immune cells shifts between glycolysis and oxidative phosphorylation, depending on their activation state and the availability of surrounding nutrients. The transition from quiescence to activation results in greater metabolic demands. Aerobic glycolysis is induced within minutes after TCR activation via pyruvate dehydrogenase kinase 1 (PDHK1), which diverts pyruvate away from oxidative phosphorylation to lactate production independent of transcription, translation, or increased glucose uptake (7). Following

activation, glycolysis involves increased glucose uptake, mammalian target of rapamycin (mTOR)-dependent pathways and a subsequent increase in the synthesis of essential biomolecules for cell growth (7, 8). Activated T cells can still utilize oxidative phosphorylation (9); however, glycolysis is required for the differentiation of specific effector T cell subsets. In mice, mTOR inhibition with rapamycin results in the decreased differentiation of Th17 cells and a subsequent increase in Treg cell generation (10, 11). Additionally, newly differentiated murine Th17 cells demonstrate increased glucose transporter 1 (Glut1) expression and glucose uptake, whilst Treg cells show a decrease in both, compared with Th1 cells (12). Murine Treg cells have been shown to express less mTOR complex 1 (mTORC1), which is known to promote glycolysis, and subsequently express high levels of AMP-activated protein kinase (AMPK), a protein which promotes oxidative phosphorylation as AMP levels increase (12). Additionally, the mTOR complexes have been shown to be differentially expressed in murine effector T cells, with Th17 and Th1 cells expressing mostly mTORC1, while Th2 cells predominantly express mTORC2 (13). In agreement with these findings, the deletion of the hypoxia-inducible factor 1α (HIF-1α), which is known to increase the expression of glycolytic enzymes (10) and promote glycolysis during low oxygen availability (14), was shown to promote FoxP3 expression and Treg cell differentiation, and conversely decrease Th17 cell differentiation (10, 15).

In addition to carbohydrate metabolism, fatty acid (FA) metabolism has key roles in regulating innate and adaptive immune responses. The enforced expression of carnitine palmitoyltransferase 1 (CPT1; transporter of FAs into the mitochondria in order to promote their oxidation) in macrophage cell lines results in decreased production of proinflammatory cytokines (16). In murine studies, newly differentiated Treg cells demonstrated the highest oxidation of the FA palmitate compared with other effector T cell subsets (12). Additionally, Treg cell differentiation was inhibited following treatment with etomoxir (inhibitor of CPT1), while Th17 cell differentiation was unaffected (12). As previously described, Treg cells have enhanced expression of AMPK, which is known to promote mitochondrial lipid oxidation and therefore could give rise to increased FA oxidation (FAO). Interestingly, the upregulation of fatty acid synthesis (FAS) correlates with a downregulation of FAO, demonstrating that these pathways are reciprocally linked (17). The inhibition of acetyl-CoA carboxylase (ACC) enzymes (involved in the FAS pathway) with soraphen A can decrease IL-17-expressing T cell differentiation, the expression of Th17 cell-specific genes, and IL-17 production by murine T cells under Th17-skewing conditions (18). Following induction of experimental autoimmune encephalomyelitis (EAE), mice with a T cell-specific knockdown of ACC1 showed no signs of disease. Moreover, these mice exhibited a marked reduction and promotion in the percentage of IL-17$^+$ and FoxP3$^+$ T cells respectively in the central nervous system compared with wild-type controls (18). Additionally, ACC1 is required in obesity for the DNA-binding activity of RORγt in differentiating Th17 cells, and therefore can regulate Th17 cell-mediated pathogenesis in disease (19). These studies highlight a requirement by murine Th17 cells for FAS, contrasted with the need for FAO by Treg cells during T cell differentiation. However, the metabolic pathways utilized by differentiated human Th cells at sites of inflammation is as of yet unknown. In this study, we investigated the role of carbohydrate and FA metabolism in the regulation of human memory Th cell subsets, in order to better understand how T cells are regulated.

Abbreviations: 2-NBDG, 2-[*N*-(7-Nitrobenz-2-oxa-1,3-diazol-4-yl)amino]-2-deoxy-D-glucose; ACC, Acetyl-CoA carboxylase; AICAR, 5-Aminoimidazole-4-carboxamide ribonucleotide; AMPK, AMP-activated protein kinase; CPT1, carnitine palmitoyltransferase I; EAE, experimental autoimmune encephalomyelitis; ECAR, extracellular acidification rate; FA, fatty acid; FAO, fatty acid oxidation; FAS, fatty acid synthesis; FASN, fatty acid synthase; HC, healthy control; HIF-1α, hypoxia-inducible factor 1α; Glut1, glucose transporter 1; MFI, median fluorescent intensity; mTOR, mammalian target or rapamycin; PDHK1, pyruvate dehydrogenase kinase 1; pS6, phosphorylated ribosomal protein S6; OCR, oxygen consumption rate.

MATERIALS AND METHODS

Isolation of Human Cells

PBMC were isolated by Ficoll gradient centrifugation from leukocyte-enriched buffy coats from anonymous healthy donors (HC) (obtained with permission from the Irish Blood Transfusion Board, St. James's Hospital, Dublin and ethical approval from the School of Biochemistry and Immunology Research Ethics Committee, Trinity College Dublin). Total or memory (CD45RO$^+$) CD4$^+$ T cells were enriched using magnetic microbeads (Miltenyi Biotec). CD161$^+$ (CD4$^+$ CD45RO$^+$ CD161$^+$), CD161$^-$ (CD4$^+$ CD45RO$^+$ CD161$^-$), conventional T (Tconv; CD4$^+$CD45RO$^+$notCD25$^+$CD127^{Lo}), and Treg (CD4$^+$CD25$^+$CD127^{Lo}) cells were sorted from HC PBMC on a MoFlo Legacy (Dako Cytomation/ Beckman Coulter) or FACSAria Fusion (BD Biosciences) cell sorter, with purities routinely >98%.

T Cell Stimulation and Culture

Memory CD4$^+$ T cells were cultured in complete RPMI (RPMI (Labtech) supplemented with 10% FCS (Sigma Aldrich), 2 mM L-glutamine with 1% penicillin/streptomycin (Sigma Aldrich) with irradiated antigen-presenting cells (irrAPC), anti-CD3 (eBioscience) and, where indicated, in the presence of dichloroacetate (DCA) (10 mM, Sigma Aldrich), rapamycin (20 nM, Sigma Aldrich), 5-(Tetradecyloxy)-2-furoic acid (TOFA) (1.2 μg/ml, Sigma Aldrich), C-75 (0.6 μg/ml, Sigma Aldrich), cerulenin (3.1 μM, Sigma Aldrich), or palmitate (25 μM, Seahorse Biosciences) for 5 days. Isolated CD161$^+$, CD161$^-$, and Tconv cells were cultured with irradiated antigen presenting cells (irrAPC), anti-CD3 and IL-2 (20 u/ml, eBioscience) for 6 days or in some cases with PMA/ionomycin for 18 h prior to Seahorse analysis. Isolated Treg cells were cultured using the Treg cell expansion kit (Miltenyi Biotec) in the presence of IL-2 (500 u/ml) for 6 days prior to Seahorse analysis. During glucose deprivation, memory CD4$^+$ T cells were cultured in glucose-free complete RPMI (RPMI (Biosciences) supplemented with 10% dialysed FCS (Sigma Aldrich), 1% vitamin cocktail (InvivoGen),

and 1% selenium/insulin cocktail (InvivoGen) supplemented with either 10 mM glucose (Sigma Aldrich) or 10 mM galactose (Sigma Aldrich) for 5 days.

Flow Cytometry

Cells were labeled with the Fixable Viability Dye eFluor506 (eBioscience), then stained extracellularly with fluorochrome-conjugated antibodies specific for CD3, CD4, CD69, CD71, CD98, CD161, (BD Biosciences), CD8, CD25, CD127 (eBioscience), CD45RO (BioLegend), Glut1-GFP (5 μg/ml, Metafora Biosystems), MitoTracker Green (4 nM, InvivoGen), pS6 (Cell Signaling), and 2-NBDG (100 μM, InvivoGen). For FoxP3 (eBioscience) and/or pS6 analysis, cells were fixed and permeabilized for intranuclear staining (FoxP3 staining buffer kit, eBioscience). For intracellular cytokine analysis, cells were stimulated with PMA (50 ng/ml) and ionomycin (500 ng/ml) in the presence of brefeldin A (5 μg/ml, Sigma) for 5 h; then surface stained, fixed and permeabilized (Caltag fix and perm kit, Biosciences) and stained intracellularly for IL-17 (eBioscience) and IFN-γ (BD Biosciences). PMA and ionomycin stimulation of human $CD4^+$ T cells down-regulates the expression of CD4, therefore $CD4^+$ T cells were alternatively identified as $CD3^+CD8^-$. For proliferation of cells, the cells were stained intracellularly with Ki67 (BD Biosciences). Cells were acquired on a FACSCanto II or LSRFortessa cytometer (BD Biosciences) and analyzed using FlowJo software (FlowJo LLC). Viable lymphocytes were identified by forward and side scatter, with dead cells (Fixable Viability Dye eFluor506 positive) and doublets subsequently excluded. IrrAPC were stained with CellTrace CSFE and excluded from the analysis. Gates were set using fluorescence minus one (FMO) controls, isotype controls or unstimulated cells as appropriate.

Metabolic Marker Expression and Glucose Uptake

For the examination of Glut1 expression, cells were washed with warmed Glut1 staining buffer A (complete RPMI, 0.2% EDTA, 2% sodium azide) and stained with Glut1-GFP (5 μg/ml, Metafora Biosystems) and surface markers in staining buffer A and incubated for 20 min at 37 °C. The cells were then washed with the Glut1 staining buffer B (PBS, 0.2% EDTA, 2% sodium azide, 2% FCS) and analyzed by flow cytometry.

For investigating glucose uptake, cells were washed twice in glucose-free RPMI and incubated at 37 °C for 15 min. Cells were incubated with 2-NBDG (100 μM) in glucose-free RPMI for 1 h at 37 °C, washed in pre-cooled PBS and stained for surface markers as previously described. Unfixed cells were then analyzed immediately by flow cytometry.

Metabolic Flux Analysis

Extracellular acidification rate (ECAR) and oxygen consumption rate (OCR) were measured with an XF24 or XFe96 extracellular flux analyzer (Seahorse Bioscience). T cells were stimulated with PMA and ionomycin for 24 h prior to analysis by the Seahorse analyzer (6 x 10^5 cells/well) and adhered to the plate with Cell-Tak (1 μg/well, Corning). ECAR and OCR were measured in real time following injections of oligomycin A (1 μg/ml), FCCP (450 nM), antimycin A (2.5 μM) and rotenone (500 nM), and 2-deoxyglucose (25 mM) (Sigma Aldrich).

FAO was measured using the XF Palmitate-BSA FAO Substrate (Seahorse Bioscience) using the manufacturer-recommended protocols. T cells were stimulated with PMA and ionomycin for 24 h prior to analysis by the Seahorse analyzer (6×10^5 cells/well) and adhered to the plate with Cell-Tak. Cells were washed in substrate-limited medium (DMEM supplemented with 0.5 mM glucose, 1 mM L-glutamine, 0.5 mM L-carnitine (Sigma Aldrich), and 1% FCS), counted and then seeded in FAO assay medium [KHB (111 mM NaCl, 4.7 mM KCl, 1.25 mM $CaCl_2$, 2 mM $MgSO_4$, 1.2 mM NaH_2PO_4) supplemented with 2.5 mM glucose, 0.5 mM L-carnitine, and 5 mM HEPES, adjusted to pH 7.4 at 37 °C]. Etomoxir (40 μM) in FAO assay medium was added to control wells 15 min prior to running the assay in the Seahorse analyzer. Finally, BSA or Palmitate-BSA FAO Substrate was added to the appropriate wells immediately before running the assay. OCR was measured in real time following injections of oligomycin A, FCCP, antimycin A and rotenone, and 2-deoxyglucose.

RT qPCR Analysis of Glycolytic Genes

Memory $CD4^+$ T cells (1×10^6 cells per well of 12-well plate) were left unstimulated or stimulated with anti-CD3 and−28 antibodies and treated in the presence or absence of DCA (10 mM) for 4 h. Following incubation, the cells were lysed using Qiazol lysis reagent (Qiagen) and frozen to −80 °C. RNA was isolated according to manufacturer's instructions (miRNeasy kit, Qiagen) and transcribed to cDNA using a high-capacity cDNA binding kit (Bio-Sciences). The cDNA was analyzed by RT-qPCR for the expression of Glut1, hexokinase 2 (HK2), lactate dehydrogenase (LDHa), and glucose 6 phosphate dehydrogenase (G6PD) using forward and reverse primers (Integrated DNA Technologies), relative to the housekeeper gene ribosomal protein lateral stalk subunit p0 (RPLP0). Data was normalized to the unstimulated control.

Statistical Analysis

Statistical analyses were performed using Prism 5 software; 2 groups within a sample were determined by Student's Paired *T*-test with two-tailed *p*-values. *P*-values of < 0.05 were considered significant and denoted as follows: $^*p < 0.05$, $^{**}p < 0.01$, and $^{***}p < 0.001$.

RESULTS

Th17-Lineage Cells Show Increased Expression of Glycolytic Markers Compared With Non-th17 Cells

Initially we sought to examine the presence of metabolic markers that correlate with metabolic pathways in human Th17 cells. Human PBMC were stained with MitoTracker® dye which provides an indication of mitochondrial mass, a correlate of oxidative phosphorylation. Memory $CD4^+CD161^-$ (non-Th17 lineage cells) exhibited significantly higher levels of MitoTracker® dye compared with memory $CD4^+CD161^+$ (Th17-lineage cells) ($p < 0.05$) (**Figure 1A**), suggesting that

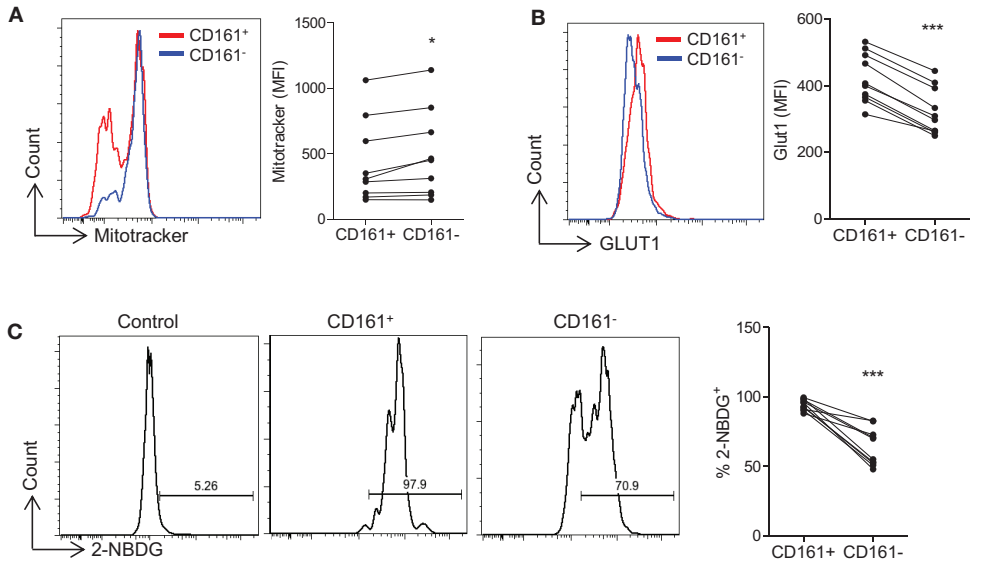

FIGURE 1 | Th17-lineage cells show increased expression of glycolytic markers compared with non-Th17 cells**.** PBMC were isolated from healthy controls and cells were stained *ex vivo* with fluorochrome-conjugated antibodies specific for CD4, CD45RO, CD161, and MitoTracker® Green. The expression of MitoTracker® Green in $CD4^+CD45RO^+CD161^+$ ($CD161^+$) and $CD4^+CD45RO^+CD161^-$ ($CD161^-$) ($n = 9$) **(A)**. Memory $CD4^+$ T cells were isolated from HC by magnetic separation and stimulated in the presence of anti-CD3 and irrAPC. Cells were stained with fluorochrome-conjugated antibodies specific for CD4, CD161, Glut1, and 2-NBDG. The expression of Glut1 in $CD4^+$ $CD161^+$ ($CD161^+$) and $CD4^+$ $CD161^-$ ($CD161^-$) ($n = 10$) at 24 h stimulation **(B)**. The uptake of 2-NBDG in $CD161^+$ and $CD161^-$ cells compared with unstimulated $CD4^+$ T cells (control) ($n = 10$) at 72 h stimulation **(C)**. $^*p < 0.05$, $^{***}p < 0.001$.

Th17-lineage cells may utilize less oxidative phosphorylation than non-Th17 cells. Glycolysis relies on the uptake of glucose via specific cell surface transporters such as Glut1, and the expression of Glut1 has been shown to correlate with glycolytic activity (20, 21). We therefore examined the expression of Glut1 on sorted and activated human memory $CD45RO^+CD4^+$ T cells and demonstrated significantly increased Glut1 expression on Th17 vs. non-Th17 lineage cells ($p < 0.001$) (**Figure 1B**). We also examined the uptake of 2-NBDG, a fluorescent glucose analog, and showed significantly increased uptake of 2-NBDG by Th17-lineage cells compared with non-Th17 lineage cells ($p < 0.001$) (**Figure 1C**). These data suggested that Th17-lineage cells have an increased capacity for glucose uptake, indicative of increased glycolytic activity.

Th17-Lineage Cells Are Dependent on Glycolysis

Having demonstrated that Th17-lineage cells expressed markers consistent with a glycolytic profile, we next determined whether they were dependent on glycolysis for their function. Replacement of glucose with galactose as a fuel source is known to inhibit glycolysis (22) as confirmed in **Figure 2A**, where activated $CD4^+$ T cells cultured in galactose containing medium exhibited reduced ECAR levels compared with those cultured in glucose containing medium, whereas OCR was unchanged except for basal OCR which was relatively increased in galactose containing medium. No differences in cell viability were observed between glucose and galactose conditions (data not shown). Having confirmed that glucose deprivation inhibits glycolysis, human $CD45RO^+CD4^+$ T cells were activated and cultured for 5 days in medium containing either glucose or galactose and their expression of CD161, IL-17, or IFN-γ was examined by flow cytometry. $CD4^+$ T cells cultured in galactose exhibited significantly reduced expression of both CD161 ($p < 0.01$) and IL-17 ($p < 0.01$) by $CD4^+$ T cells (**Figure 2B**). On the other hand, there was no significant change in the expression of IFN-γ by $CD4^+$ T cells (**Figure 2B**). Glycolysis has been shown to be dependent on mTOR signaling (10), therefore sorted $CD45RO^+CD4^+$ T cells were stimulated for 5 d in the presence or absence of the mTOR inhibitor rapamycin. Expression of both CD161 ($p < 0.01$) and IL-17 ($p < 0.05$) by $CD4^+$ T cells was significantly reduced in the presence of rapamycin ($p < 0.05$), whereas IFN-γ was unchanged (**Figure 2C**). As an alternative strategy to inhibit glycolysis, we also treated memory $CD4^+$ T cell cultures with DCA, which directly inhibits pyruvate dehydrogenase kinase in the glycolytic pathway. As shown in **Figure S1**, DCA significantly reduced the frequency of Th17 cells ($p < 0.001$) (**Figure S1A**) in addition to their survival ($p < 0.01$) (**Figure S1B**) and proliferation ($p < 0.05$) (**Figure S1C**). In contrast, DCA had no significant effect on the frequency, viability or proliferation of Th1 cells (**Figures S1A–C**). The efficacy of DCA in inhibiting glycolysis was confirmed in **Figure S2A**, where DCA inhibited the expression of genes associated with glycolysis *HK2*, *LDHa*, *G6PD,* and *GLUT1*. Furthermore, Seahorse analysis showed that DCA reduced the ECAR and ECAR:OCR ratio in memory CD4 T cells, indicating inhibition of glycolysis (**Figures S2B,C**). Taken together, these data indicate that inhibition of glycolysis via glucose removal, inhibition of pyruvate dehydrogenase kinase or mTOR inhibition reduced the frequency of Th17 cells but did not appear to

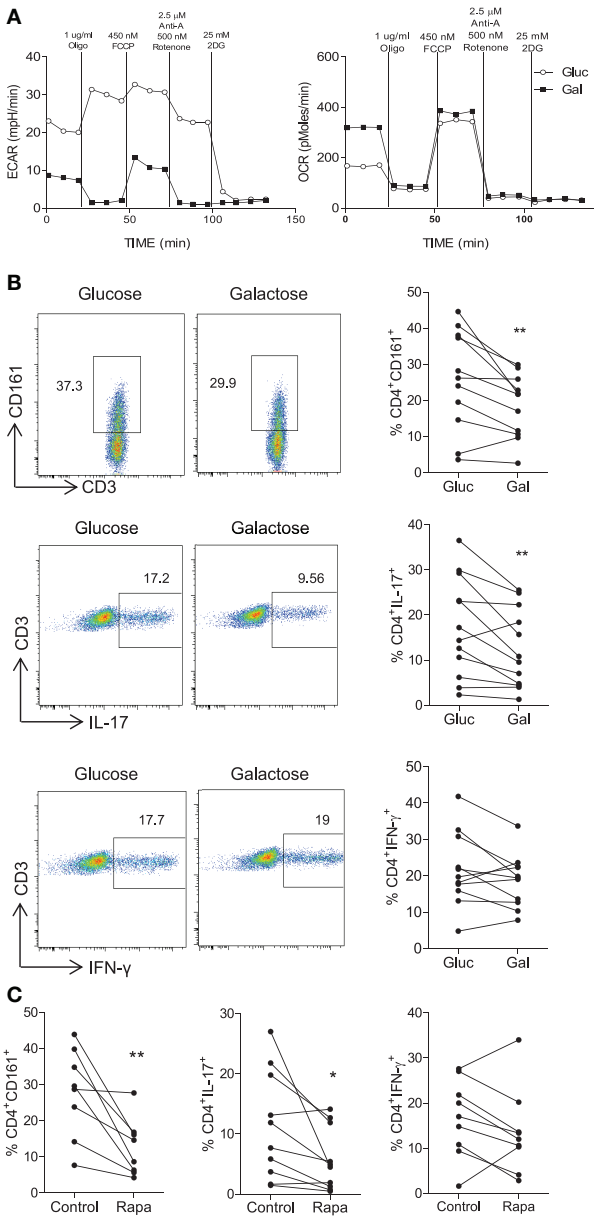

FIGURE 2 | Inhibition of glycolysis constrains Th17-lineage cells**.** PBMC were isolated from healthy donors. $CD4^+$ T cells were isolated by magnetic separation and stimulated for 18 h with PMA and ionomycin in glucose-free RPMI supplemented with glucose (10 mM) (Gluc) or galactose (10 mM) (Gal). Representative plots of ECAR and OCR over time are shown **(A)**. Memory $CD45RO^+CD4^+$ T cells were isolated by magnetic separation and cultured for 5 d in the presence of anti-CD3 and irrAPC in glucose-free medium supplemented with glucose or galactose. Cells were re-stimulated with PMA and ionomycin in the presence of brefeldin A; stained for CD161, IL-17, IFN-γ, CD3, and CD8 and analyzed by flow cytometry. Representative dot plots (gated on single, live, CD4 [$CD3^+CD8^-$] cells), accompanied by the frequencies of $CD4^+$ T cells expressing CD161 and proinflammatory cytokines ($n = 11$) **(B)**. Memory $CD4^+$ T cells were cultured for 5 d with anti-CD3 and irrAPC in the presence or absence of rapamycin (Rapa). Cells were re-stimulated with PMA and ionomycin in the presence of brefeldin A, stained for CD161, IL-17, IFN-γ, CD3, and CD8 and analyzed by flow cytometry. The frequencies of $CD4^+$ T cells (gated on live, single $CD3^+CD8^-$ cells) expressing CD161, IL-17, or IFN-γ ($n = 8$–10) **(C)**. $^*p < 0.05$, $^{**}p < 0.01$.

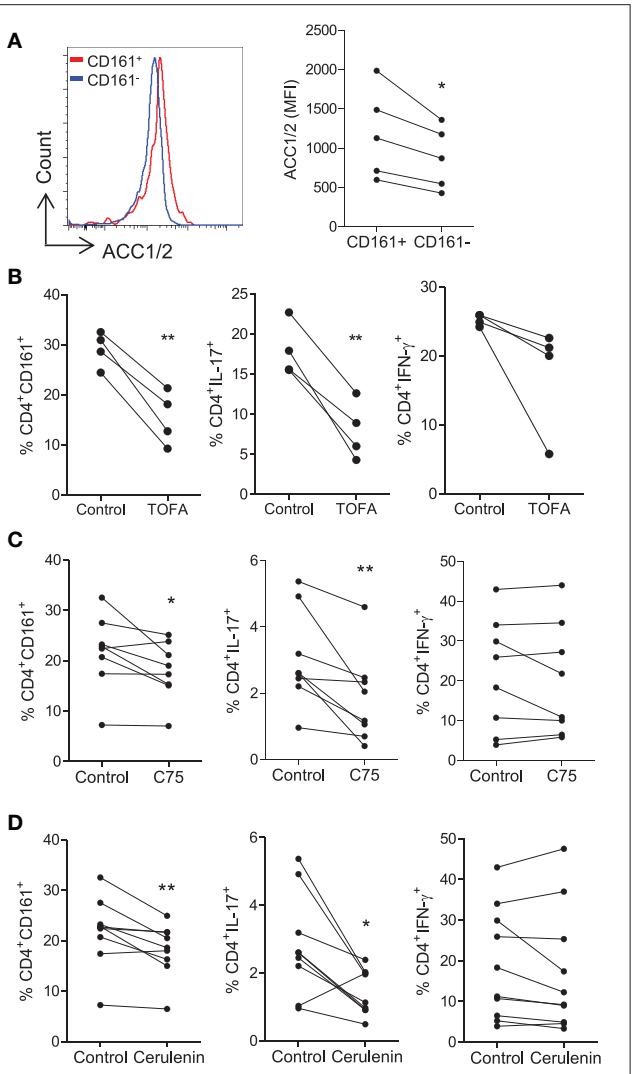

FIGURE 3 | Th17-lineage cells are reduced following the inhibition of fatty acid synthesis**.** Memory $CD45RO^+CD4^+$ T cells were isolated from PBMC of healthy donors, stimulated with anti-CD3 and irrAPC for 5 d and stained for CD4, CD161, and ACC1/2. Representative histograms and MFI of ACC1/2 expression on $CD4^+CD161^+$ ($CD161^+$) and $CD4^+CD161^-$ ($CD161^-$) cells ($n = 5$) **(A)**. Memory $CD45RO^+CD4^+$ T cells were cultured for 5 d with anti-CD3 and irrAPC in the presence or absence of TOFA, C75, or cerulenin. Cells were re-stimulated with PMA and ionomycin in the presence of brefeldin A; stained for CD161, IL-17, IFN-γ, CD3, and CD8 and analyzed by flow cytometry (gated on live, single $CD3^+CD8^-$ cells). The effect of TOFA ($n = 4$) **(B)**, C75 ($n = 8$) **(C)**, or cerulenin ($n = 9$–10) **(D)** on the frequencies of $CD4^+$ T cells expressing CD161, IL-17 and IFN-γ are shown. **(B)** $^*p < 0.05$, $^{**}p < 0.01$.

constrain Th1 cells, suggesting that Th17 cells are dependent on glycolysis.

Th17 Lineage Cells Are Dependent on Fatty Acid Synthesis

We next investigated the role of fatty acid synthesis in fuelling human $CD4^+$ T cells. Initially, the expression of ACC1/2 was determined on $CD161^+$ and $CD161^-$ $CD4^+$ T cells, since ACC1/2 enzymes are involved in the FAS

pathway. Increased expression of ACC1/2 was observed on the $CD4^+CD161^+$ cells when compared with $CD4^+CD161^-$ T cells ($p < 0.05$) (**Figure 3A**). Next, the effect of TOFA, which is an ACC1/2 inhibitor, on $CD4^+$ T cells was investigated. Memory $CD45RO^+CD4^+$ T cells were isolated and stimulated for 5 days in the presence or absence of TOFA. In cells cultured with TOFA we observed a significant decrease in the frequency of $CD4^+CD161^+$ ($p < 0.01$) and $CD4^+$IL-17^+ ($p < 0.01$) T cells (**Figure 3B**). In contrast however, there was no change in the frequency of $CD4^+$IFN-γ^+ T cells (**Figure 3B**). The effect of blocking the FAS pathway downstream of ACC1/2, by using inhibitors of FASN was investigated next. Memory $CD45RO^+CD4^+$ T cells were isolated and stimulated for 5 days in the presence or absence of the fatty acid synthase (FASN) inhibitors C75 or cerulenin. In cells cultured with C75 we observed a significant decrease in the frequency of $CD4^+CD161^+$ ($p < 0.05$) and $CD4^+$IL-17^+ ($p < 0.01$) T cells (**Figure 3C**). In contrast however, there was no change in the frequency of $CD4^+$IFN-γ^+ T cells (**Figure 3C**). As shown in **Figure S3**, C75 significantly inhibited the proliferation of Th17 lineage cells ($p < 0.0001$) with a lesser effect of the proliferation of Th1 cells ($p < 0.05$). Cerulenin exerted a similar effect to that of C75, showing a significant decrease in the frequency of $CD4^+CD161^+$ ($p < 0.01$) and $CD4^+$IL-17^+ ($p < 0.05$) T cells, but had no effect on the frequency of $CD4^+$IFN-γ^+ T cells (**Figure 3D**). Taken together, these data indicate that Th17-lineage cells utilize, and are relatively more dependent on fatty acid synthesis than Th1 cells.

Treg Cells Exhibit Increased Oxidative Phosphorylation and Glycolysis, but Are Not Dependent on Glycolysis

Next the metabolic profile of Treg cells was investigated and compared to that of non-Treg (Tconv) cells. PBMC were stained for the expression of Treg cell markers and MitoTracker® Green as an indicator of mitochondrial mass. Memory Treg cells ($CD4^+CD45RO^+CD25^+CD127^{Lo}$) trended toward higher mitochondrial mass than memory Tconv cells ($CD4^+CD45RO^+$ NOT $CD25^+CD127^{Lo}$) ($p = 0.07$) (**Figure 4A**). We also examined the expression of Glut1, pS6, and uptake of 2-NBDG on Treg vs. Tconv cells. Although no difference in the expression of Glut1 between Treg and Tconv cells was observed, there was a significant increase in the uptake of 2-NBDG by Treg cells ($p < 0.001$) (**Figure 4B**). There was also a significant increase in the expression of pS6 in Treg cells compared with Tconv cells ($p < 0.001$), indicating increased activation of mTOR in Treg cells (**Figure 4B**). These data suggest that indicators of both glycolysis and oxidative phosphorylation were elevated in Treg cells when compared with Tconv cells. In order to investigate the metabolic profile of Treg cells further, we performed Seahorse flux analysis using purified Treg and Tconv cells. As shown in **Figure 4C**, Treg cells exhibited an overall higher ECAR profile, and significantly increased basal glycolysis ($p < 0.05$) and maximal glycolysis ($p < 0.05$) compared with Tconv cells (**Figure 4D**). No difference in glycolytic reserve was observed (**Figure 4D**). In addition, Treg cells exhibited an overall increase in OCR profile compared with Tconv cells (**Figure 4E**). This was reflected in significantly increased basal respiration ($p < 0.05$), maximal respiration ($p < 0.01$), and respiratory reserve ($p < 0.05$) in Treg vs. Tconv cells (**Figure 4F**). These data indicated that activated Treg cells utilize both glycolysis and oxidative phosphorylation to a greater extent than activated Tconv cells. Since it was possible that the expansion protocol used above prior to Seahorse flux analysis may have altered the metabolic profiles of Treg or Tconv, we also performed Seahorse analysis on freshly sorted Treg and Tconv that were stimulated for 18 h. However, as shown in **Figure S4**, Treg cells failed to be fully activated after 18 h stimulation with PMA/Ionomycin. Both OCR (**Figure S4A**) and ECAR (**Figure S4B**) were very low in Treg compared with Tconv. Nonetheless the ECAR:OCR ratio was higher in Treg than Tconv (**Figure S4C**). A relative lack of activation of Treg relative to Tconv cells was indicated by significantly lower expression of the early activation marker CD69 on Treg cells (**Figure S4D**). Furthermore, the fact that similar levels of activation (**Figures S5A–C**) and proliferation (**Figure S5D**) were observed after the 5 day expansion protocol validates this protocol which was used in **Figure 4**. Next we investigated the dependence of Treg cells on glycolysis by inhibiting glycolysis via glucose deprivation or mTOR inhibition. Culture of memory $CD4^+$ T cells in the presence of galactose vs. glucose resulted in an increased frequency of Treg cells relative to Tconv cells ($p < 0.05$) (**Figure 4G**), as did culture with rapamycin ($p < 0.01$) (**Figure 4H**). We also used DCA as an alternative strategy to inhibit glycolysis, and determined the effect on the frequency of Treg cells as well as their viability and proliferation. Culture in the presence of DCA did not significantly alter the overall frequency of Treg cells although there were variable effects in different donors (**Figure S1A**). DCA reduced the viability ($p < 0.05$) and reduced proliferation of Treg cells in the majority of donors (ns), but not to the extent that was seen for Th17 cells (**Figures S1B,C**). Taken together these data indicate that activated Treg cells can utilize both glycolysis and oxidative phosphorylation. Furthermore, Treg cells are somewhat dependent on glycolysis for their proliferation but not to the same extent as Th17 cells. Hence any increased frequency of Treg cells observed when glycolysis was inhibited is the result of a relative advantage for Treg cells.

Treg Cells Exhibit Increased Oxidation of Fatty Acids Compared With Tconv Cells and Are Not Dependent on Fatty Acid Synthesis

Next we investigated the fatty acid metabolism requirements of human Treg cells. In order to measure FAO, the Seahorse XF FAO assay was utilized where palmitate-BSA is provided as a source of FA and uptake of fatty acids is inhibited using etomoxir as an inhibitor of CPT1. In the presence of palmitate, Treg cells exhibited an increased OCR profile and this was inhibited by etomoxir (**Figure 5A**), indicating that Treg cells were taking up and oxidizing FA. On the other hand Tconv cells did not exhibit obviously increased OCR in the presence of palmitate (**Figure 5A**). Overall there was a highly significant increase in

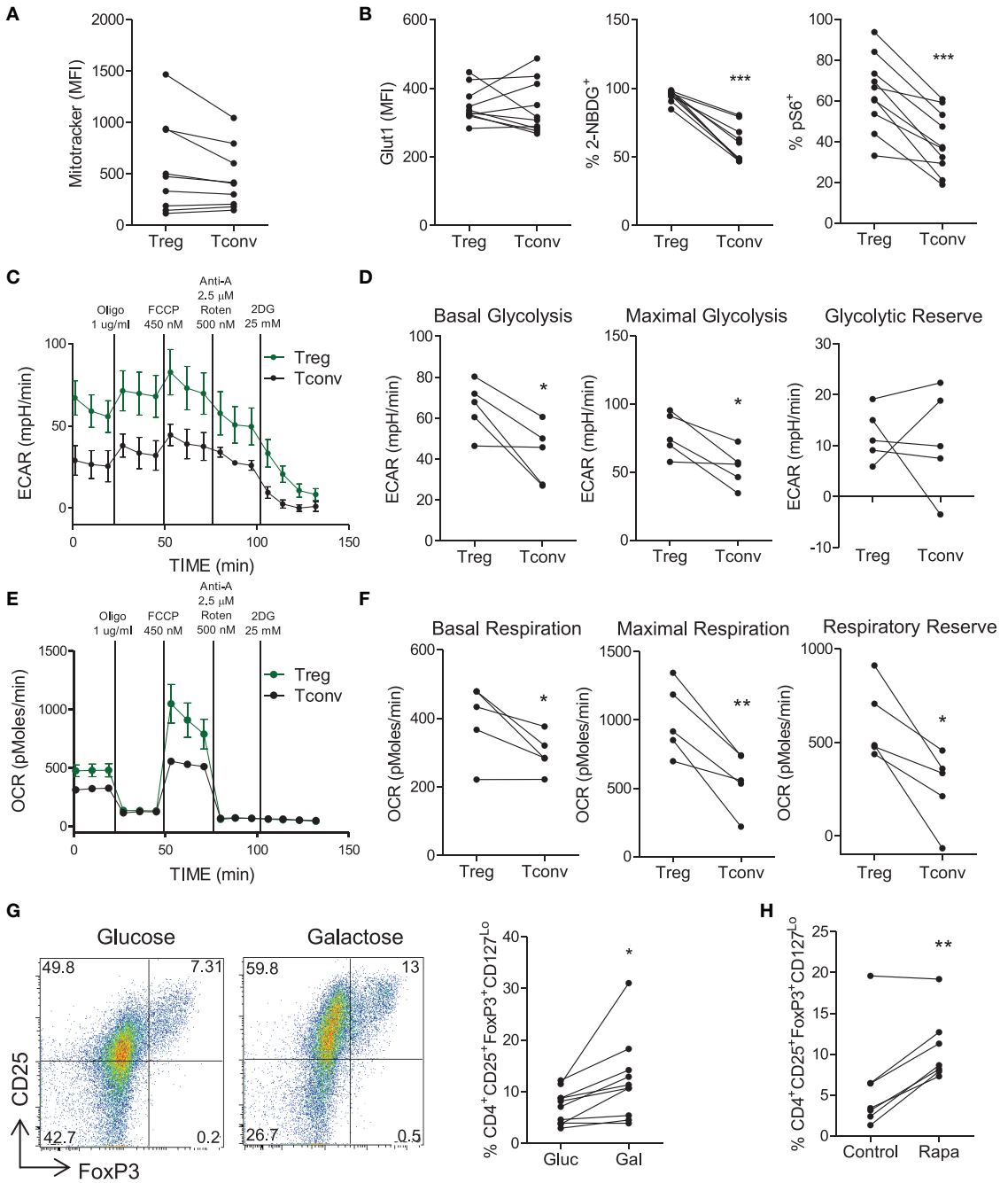

FIGURE 4 | Treg cells demonstrate increased glycolysis and oxidative phosphorylation relative to conventional T cells, but do not depend on glycolysis**.** PBMC were isolated from healthy controls and cells were stained *ex vivo* for CD4, CD25, CD45RO, CD127 and MitoTracker® Green. MitoTracker® Green staining in $CD4^+CD45RO^+CD25^+CD127^{Lo}$ (Treg) and $CD4^+CD45RO^+$NotCD25+CD127Lo (Tconv) ($n = 9$) **(A)**. Memory $CD4^+$ T cells were isolated from PBMC by magnetic separation and stimulated with anti-CD3 and irrAPC. Cells were stained for CD4, CD25, CD127, FoxP3, Glut1, pS6, and 2-NBDG uptake was measured. The expression of Glut1 in Treg and Tconv at 24 h stimulation, 2-NBDG at 72 h, and pS6 at 24 h ($n = 10$) **(B)**. Treg and Tconv cells were cell sorted from PBMC. Cells were cultured for 6 d in the presence of anti-CD3, irrAPC and IL-2. Cells were stimulated for 18 h with PMA and ionomycin prior to Seahorse extracellular flux analysis. Representative plot of ECAR over time for Treg and Tconv **(C)**. Basal glycolysis, maximal glycolytic capacity and glycolytic reserve rates for Treg and Tconv ($n = 5$) **(D)**. Representative plot of OCR over time for Treg and Tconv **(E)**. Basal respiration, maximal respiratory capacity and respiratory reserve rates for Treg and Tconv ($n = 5$) **(F)**. Memory $CD4^+$ T cells were isolated by magnetic separation and cultured for 5 d in the presence of anti-CD3 and irrAPC in glucose-free medium supplemented with glucose (Gluc) or galactose (Gal). Cells were stained for CD4, CD25, CD127, and FoxP3; and analyzed by flow cytometry. Representative dot plots accompanied by the frequencies of Treg cells in glucose or galactose medium ($n = 9$) **(G)**. Memory $CD4^+$ T cells were cultured for 5 d with anti-CD3 and irrAPC in the presence or absence of rapamycin (Rapa). Cells were stained for CD4, CD25, CD127, and FoxP3; and analyzed by flow cytometry. The frequencies of Treg cells following control or Rapa treatment ($n = 6$) **(H)**. $^*p < 0.05$, $^{**}p < 0.01$, $^{***}p < 0.001$.

OCR from Treg cells in the presence of palmitate-BSA vs. the control BSA ($p < 0.001$), while there was a lesser increase in OCR from Tconv cells in the presence of palmitate vs. BSA control ($p < 0.05$) (**Figure 5B**). Having previously shown that Th17 cells relied on the synthesis of fatty acids, we next investigated the effect of promoting FAO on the Th17:Treg cell ratio. In order to exclude the confounding factor of cells utilizing glycolysis as an alternative source, we inhibited glycolysis by using galactose medium. Memory $CD4^+$ T cells were stimulated and cultured in glucose free medium supplemented with galactose in order to inhibit glycolysis, and in the presence or absence of palmitate. Culture with palmitate decreased the ratio of Th17:Treg cells ($p < 0.05$), indicating that promoting FAO in the absence of glycolysis manipulates the Th17:Treg cell ratio in favor of Treg cells (**Figure 5C**). Finally, we investigated the role of FAS in Treg cells by culturing memory T cells in the presence or absence of the ACC1/2 inhibitor TOFA or the FASN inhibitor C75. In contrast to the previously shown dependence on FAS for Th17-lineage cells, inhibition of FASN exerted no overall effect on the frequency of Treg cells compared with control (**Figure 5D**). However, when the ratio of Th17:Treg cells was compared in the presence or absence of C75, there was a significant decrease in the Th17:Treg cell ratio when FASN was inhibited ($p < 0.05$) (**Figure 5D**). Similarly, ACC1/2 inhibition did not affect the frequency of Treg cells, but did significantly decrease the ratio of Th17:Treg cells ($p < 0.05$) (**Figure 5E**). Together these data indicate that inhibition of FAS or promotion of FAO modulates the Th17:Treg axis in favor of Treg cells.

DISCUSSION

In this study we examined the metabolic requirements of human T cell subsets and the effect of manipulating metabolic pathways on Th17 and Treg cells. As the Th17:Treg cell axis is dysregulated in a number of autoimmune or inflammatory diseases, it is therefore of key importance to identify novel strategies to modulate this axis in favor of Treg cells. We investigated the role of carbohydrate and fatty acid metabolism in the regulation of human memory T cell subsets in order to gain insight as to how effector T cells and Treg cells may be regulated at sites of inflammation. We found that Th17-lineage cells were dependent on glycolysis, as glucose-deprivation, inhibition of glycolysis, and treatment with rapamycin resulted in a reduction of these cells. Interestingly, activated Treg cells exhibited increased glycolysis, mitochondrial respiration and FAO; whereas Th17 cells demonstrated a reliance upon FAS for survival. Here we expose a fundamental difference between human Treg and Th17 cells and a possible mechanism for targeting and/or manipulating the Th17:Treg cell axis.

In this project we considered the role of metabolic pathways in regulating differentiated human memory T cells, since these are the cells that would be found at sites of autoimmune inflammation where nutrients are most likely to be limiting, requiring cells to undergo metabolic reprogramming. Murine studies have shown a clear role for metabolism in reciprocally regulating the *de novo* differentiation of Th17 and Treg cells, where differentiation of Th17 cells depended on HIF-1α and glycolysis, while Treg cell differentiation was inhibited by HIF-1α and required oxidative phosphorylation (10, 12, 23). In addition development of Th17 cells was dependent on fatty acid synthesis, whereas Treg cell differentiation required FAO (12, 18). However, recent evidence indicates that there may be important differences in the metabolic requirements for differentiation of Treg cells as opposed to activated Treg cells engaged in suppression (24). Furthermore, in the context of autoimmunity where already differentiated natural/thymically derived Treg cells control pathogenic autoreactive effector T cells, the regulation of activated Treg cell proliferation and suppressive function may be more relevant than that of Treg cell differentiation. Thus, if metabolic pathways are to be targeted to regulate T cell pathogenicity in disease then it will be important to gain a clearer understanding of how metabolic requirements impact on the effector and regulatory functions of differentiated human T cells, where the metabolic requirements are poorly understood.

We demonstrated that activated human Th17 cells required glycolysis since they were inhibited in the absence of glucose and after mTOR or pyruvate dehydrogenase kinase inhibition. Consistent with this, Th17-lineage cells exhibited increased expression of Glut1 and uptake of a glucose analog relative to non-Th17 lineage cells. On the other hand, IFN-γ producing Th1 cells were not inhibited when glycolysis was blocked. Memory $CD161^-$ T helper cells (comprising mostly Th1 cells) exhibited increased mitochondrial mass relative to Th17 lineage cells, suggesting that Th17 cells are less inclined to utilize oxidative phosphorylation than other Th cells. Together these data indicated that Th17 cells utilize glycolysis and are dependent on it. Whilst there is a dearth of directly comparable studies in human T cells, murine studies have demonstrated that activation and differentiation of naïve T cells into various effector T cell subsets in general requires metabolic reprogramming and a switch to aerobic glycolysis (25). Specifically, murine Th17 cell differentiation was shown to be dependent on HIF-1α and glycolysis, with reciprocal effects on Treg cells (10). In contrast to the study by Shi et al. (10) a recent study demonstrated that various conditions that promote cellular stress, including glucose deprivation induced by 2-deoxyglucose, actually promoted Th17 cell differentiation and inhibited Th1, Th2, and Treg cell differentiation (26). It is not yet clear how this disparity can be explained. Another murine study showed that differentiation of murine Th cell subsets including Th1, Th2, and Th17 cells depended on glycolysis, whereas differentiation of Treg cells required FAO (12). The latter findings indicate that differentiation of all effector T cell subsets require glycolysis, whereas we found that committed human Th17 lineage cells depended on glycolysis, but other effector T cell subsets such as IFN-γ producing Th1 cells did not. However, in support of our findings, in a recent study the metabolic requirements of *in vitro* polarized murine Th1, Th17, and Treg cells were compared where Th17 cells exhibited the highest ECAR rate followed by Th1 cells, while Treg cells had substantially lower ECAR (27). Interestingly, PDHK1 which diverts pyruvate away from oxidative phosphorylation toward lactate, was expressed in Th17 cells but not Th1 or Treg cells (27). Thus, it would be

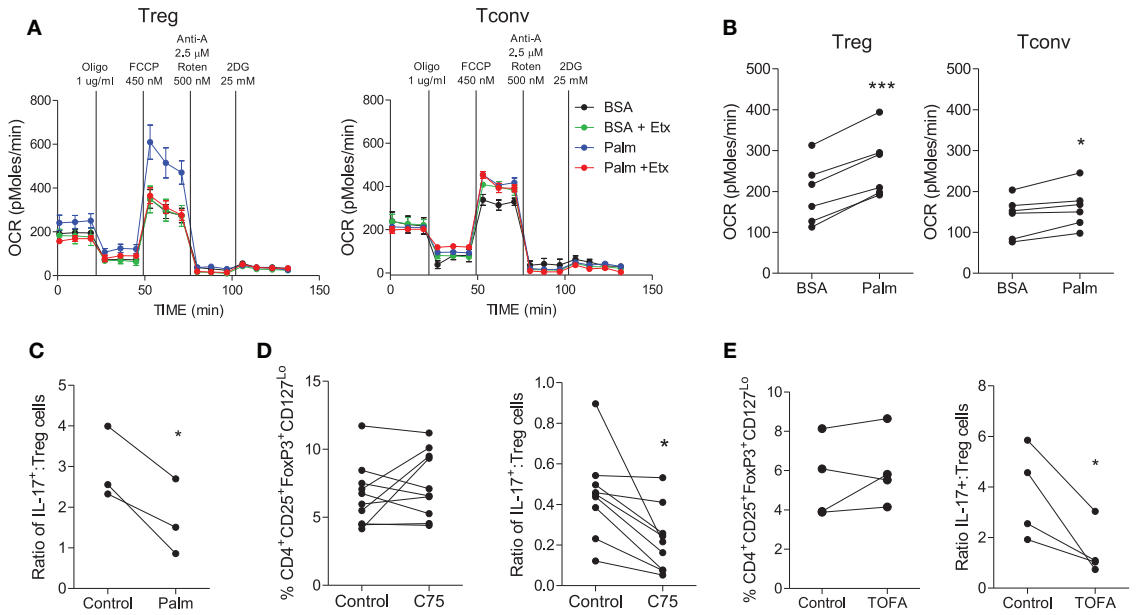

FIGURE 5 | Treg cells demonstrate increased oxidation of fatty acids compared with Tconv cells and are not reliant upon fatty acid synthesis**.** Treg ($CD4^+CD25^+CD127^{Lo}$) and Tconv ($CD4^+CD45RO^+NotCD25^+CD127^{Lo}$) cells were cell sorted from PBMC. Cells were cultured for 6 d in the presence of anti-CD3, irrAPC, and IL-2. Cells were stimulated for 18 h with PMA and ionomycin prior to Seahorse extracellular flux analysis. The Seahorse XF Palmitate-BSA FAO assay was performed to analyse the oxidation of fatty acids to fuel mitochondrial respiration. Representative plot of OCR over time for Treg and Tconv in the presence of BSA (BSA) or palmitate (Palm) and in the presence or absence of etomoxir (Etx) **(A)**. OCR for Treg and Tconv in the presence of BSA control or palmitate ($n = 6$) **(B)**. Memory $CD4^+$ T cells were isolated by magnetic separation and cultured for 5 d in the presence of anti-CD3 and irrAPC in glucose-free medium supplemented with galactose in the presence or absence of palmitate (Palm). The ratio of $IL\text{-}17^+$ to Treg cells is shown **(C)**. Memory $CD45RO^+CD4^+$ T cells were cultured for 5 d with anti-CD3 and irrAPC in the presence or absence of TOFA or C75 and stained directly for Treg markers CD4, CD25, CD127, and FoxP3, or re-stimulated with PMA and ionomycin and stained for IL-17, CD3, and CD8 and analyzed by flow cytometry (gated on live, single $CD3^+CD8^-$ cells). The frequencies of Treg cells, and the ratio of $IL\text{-}17^+$ to Treg cells following culture with TOFA ($n = 4$) **(D)** or C75 ($n = 9$) **(E)**. $^*p < 0.05$, $^{***}p < 0.001$.

of interest to determine whether PDHK1 expression in human Th17 cells promotes their glycolytic profile. It is possible that there may be different requirements for *in vitro* or *in vivo* differentiation, proliferation and effector functions of established T cell subsets. In support of this idea, a surprising recent finding was that differentiated murine Th17 cells generated *in vivo* were dependent on oxidative phosphorylation for their energy and cytokine production (28). Furthermore, inhibition of oxidative phosphorylation using oligomycin ameliorated Th17-driven mouse models of psoriasis and colitis (28).

We also investigated the metabolic requirements of Treg cells. Interestingly, both glycolytic and oxidative phosphorylation profiles were increased in Treg cells compared with Tconv cells, indicating flexibility in the metabolic requirements of activated Treg cells. In contrast to the findings for Th17 cells however, inhibition of glycolysis either enhanced or did not affect the frequency of Treg cells. However, this increased or unaltered Treg frequency observed after inhibition of glycolysis, appeared to result from a relative advantage conferred to Treg cells, since their proliferation was inhibited but to a lesser extent than that of Th17 cells. These data suggest that activated Treg cells utilize glycolysis as well as oxidative phosphorylation, and they are partly dependent on glycolysis. It is possible that this lesser dependence on glycolysis results from their ability to utilize oxidative phosphorylation when glycolysis is blocked. Our finding that mTOR inhibition promoted Treg cells over Tconv cells is consistent with a study which showed that rapamycin treatment favored the expansion of suppressive Treg cells, while proliferation of Tconv cells was inhibited (29). In support of our data showing that activated Treg cells utilized both glycolysis and oxidative phosphorylation, a proteomic signature of both glycolysis and FAO/oxidative phosphorylation in activated human Treg cells has been identified (30). On the other hand activated human Tconv cells exhibited a metabolic signature consistent with glycolysis (30). However, in the Procaccini et al. study, inhibition of either glycolysis or FAO inhibited the expansion of Treg cells (30), whereas we found that inhibition of glycolysis promoted the frequency of Treg cells relative to Tconv cells. This disparity may be accounted for by technical differences between the studies; the previous study used anti-leptin in addition to anti-CD3/28 stimulation in order to overcome Treg cell anergy. It is possible that the stronger stimulation may have rendered the Treg cells more dependent on glycolysis than those in our study which were stimulated with anti-CD3/28 plus IL-2. Another recent study found that human nTreg cells and tumor associated Treg cells utilized glycolysis and depended on it for their suppressive function (31). In further support of a key role for glycolysis in activated

Treg cells, the relative advantage of Treg over Tconv cells in tumors was attributed to their flexibility in responding to the tumor microenvironment by utilizing glycolysis and FAS (32). In these studies (30–32), Treg cells exhibited a greater degree of dependence on glycolysis, whereas in our study Treg cells were partly dependent on glycolysis. Furthermore, the utilization of FAS by tumor Treg cells contrasts with our findings that Treg cells *in vitro* appeared to take up and oxidize FA and were not inhibited by FAS inhibitors, however it is possible that Treg cells exhibited metabolic flexibility in response to the nutrient availability within the tumor (32).

Taken together these findings challenge the dogma that Treg cells favor oxidative phosphorylation over glycolysis; and since the majority of such studies were performed in mice, it is possible that human and murine Treg cells may differ in their metabolic requirements. In addition the metabolic profiles exhibited by T cells are likely to be context specific and dependent on the activation status of the cells and availability of nutrients (33).

Human peripheral blood includes both Treg cells that originated in the thymus (tTreg) as well as those differentiated in the periphery (pTreg/iTreg). However, since it is not possible to distinguish memory tTreg from pTreg, we could not dissect the individual contributions of pTreg and tTreg to the increased glycolytic and FAO activity that we observed in Treg vs. Tconv cells. It has been shown that Treg cells induced *in vitro* by the presence of low tryptophan and high kynurenine exhibited increased glycolysis and oxidative phosphorylation relative to T effector cells and tTreg cells (34). In support of this, another study showed that the induction and function of *in vitro* differentiated pTreg was dependent on glycolysis, and that the glycolytic enzyme enolase regulated *FOXP3* splicing (35). Thus, it is possible that the increased Treg cell glycolysis and oxidative phosphorylation that we observed may be accounted for by the pTreg component of the Treg population and hence will require further investigation. Our data, showing partial dependence of Treg cell proliferation on glycolysis, taken together with other studies, call into question the wisdom of strategies to target glycolysis in Th17 driven inflammatory disease. Although inhibition of glycolysis conferred a relative advantage to Tregs in terms of frequency, an overall reduction in Treg cell proliferation and number could be disadvantageous. It has also not yet been determined how glycolytic inhibition would impact on Treg suppressive function which is an important consideration for future studies.

Lipid metabolism is another important pathway by which immune cells can potentially be modulated. We found that human Th17 cells were dependent on FAS for their lipid requirements since they were inhibited in the presence of an ACC1/2 inhibitor and two different FASN inhibitors. Consistent with this finding, Th17 cells expressed higher levels of the ACC1/2 enzymes involved in the FAS pathway. In contrast however, Treg cells were not inhibited by ACC1/2 or FASN inhibitors. Furthermore, ACC1/2 or FASN inhibition significantly decreased the Th17:Treg ratio, suggesting that FAS could be targeted to modulate this axis in favor of Treg cells. Rather than synthesizing fatty acids, Treg cells oxidized exogenous fatty acids as shown by Seahorse analysis of oxygen consumption, where Treg cells increased their consumption to a greater extent than Tconv cells in the presence of added palmitate. In addition, culturing memory Th cells in the presence of palmitate while blocking glycolysis modulated the Th17:Treg axis in favor of Treg cells. Of interest, a recent study using CPT1a deficient mice, has shown that murine Treg cells *in vivo* did not depend on FAO, since Treg homeostasis and suppressive function were not affected in these mice (36). It is not yet clear whether these findings extrapolate to human Treg cells, since conclusions drawn from previous studies using etomoxir ($>100\,\mu M$) to inhibit CPT1a are likely to be compromised as a result of off-target effects of etomoxir (36). Our study indicates that human Treg cells oxidize fatty acids in a CPT1a dependent manner when exogenous palmitate is provided, but does not provide evidence of Treg dependence on FAO. It is possible that such a dependence on FAO may only be evident in the absence of glycolysis as an alternative energy source.

Thus, our data suggest that human Th17 lineage cells are dependent on FAS, whereas Treg cells are dependent on the uptake and oxidation of fatty acids which feed into oxidative phosphorylation. These findings are broadly consistent with other studies performed using mice, although these mostly examined the role of fatty acid metabolism in the differentiation of Th cells whereas we show effects on $CD4^+$ T cells that have already differentiated into subsets. Inhibition of ACC1, which is required for FAS, inhibited the *in vitro* differentiation of Th17 cells and promoted the differentiation of Treg cells from naïve T cells, in both mice and humans (18). In addition, T cell-specific deletion of ACC1 inhibited Th17-mediated EAE, and since Th17 cells are likely to exert their effects during the induction phase of EAE, these effects were likely mediated by reduced differentiation of Th17 cells as a result of FAS inhibition (18). In addition, blockade of FASN, which is downstream of ACC1, inhibited the development of Th17 cells, and Th17-specific inhibition of FASN ameliorated EAE (37). In another murine study, enhancing FAO via AMPK activation using the AMP analog 5-aminoimidazole-4-carboxamide ribonucleotide (AICAR), promoted the polarization of Treg cells and inhibited Th17 cells both *in vitro* and *in vivo* (38). Interestingly, it was suggested that obesity induces the expression of ACC1 which drives Th17 cell differentiation via RORγt, as shown in mice fed a high fat diet (19). In addition, there was a correlation between expression of ACC1 and the frequency of Th17 cells in obese humans, suggesting that ACC1 also drives Th17 differentiation *in vivo* in humans (19). FAS was also implicated in T cell pathogenicity in RA, where blockade of FAS inhibited the tissue invasiveness of RA T cells *in vivo* (39). Together with our findings, these studies provide further support for the strategy of targeting Th17 cells via the FAS pathway on which they depend, although further investigation will be required to determine whether these findings can be extrapolated to disease settings *in vivo*.

In summary, our data indicates that inhibition of either glycolysis or FAS can tilt the Th17:Treg axis in favor of Treg cells, suggesting that these pathways could be targeted to combat

multiple inflammatory diseases. However, as discussed above, the concept of a clear dichotomy between the requirements for glycolysis vs. oxidative phosphorylation by Treg and Th17 cells may be too simplistic and therefore targeting of the glycolytic pathway in inflammatory disease may not be viable. Fatty acid metabolism however, represents a promising target for the modulation of the human Th17:Treg cell axis, since inhibition of FAS or induction of FAO tips the axis in favor of Treg cells.

AUTHOR CONTRIBUTIONS

DC and JF contributed to the conception and design of the study. DC, AP, and BM designed and performed experiments. DC and JF wrote the first draft of the manuscript. All authors contributed to manuscript revision, read and approved the submitted version.

FUNDING

This publication has emanated from research supported by a research grant from Science Foundation (SFI) under the SFI Strategic Partnership Programme Grant Number 15/SPP/3212 and support from AbbVie Inc., and a Programme for Research in Third Level Institute and Science Foundation Ireland grant 12/RI/2340(7). AP was supported by Irish Higher Research Board grant (HRA-POR-2015-1106). The TBSI Flow Cytometry Facility which was used extensively in this study is funded by the Irish Higher Education Authority.

SUPPLEMENTARY MATERIAL

The Supplementary Material for this article can be found online at: https://www.frontiersin.org/articles/10.3389/fimmu.2019.00115/full#supplementary-material

REFERENCES

1. Sallusto F, Lanzavecchia A. Human Th17 cells in infection and autoimmunity. *Microbes Infect.* (2009) 11:620–4. doi: 10.1016/j.micinf.2009.04.004
2. Fletcher JM, Lalor SJ, Sweeney CM, Tubridy N, Mills KH. T cells in multiple sclerosis and experimental autoimmune encephalomyelitis. *Clin Exp Immunol.* (2010) 162:1–11. doi: 10.1111/j.1365-2249.2010.04143.x
3. Mease PJ. Inhibition of interleukin-17, interleukin-23 and the TH17 cell pathway in the treatment of psoriatic arthritis and psoriasis. *Curr Opin Rheumatol.* (2015) 27:127–33. doi: 10.1097/BOR.0000000000000147
4. Piccirillo CA. Regulatory T cells in health and disease. *Cytokine* (2008) 43:395–401. doi: 10.1016/j.cyto.2008.07.469
5. Barbi J, Pardoll D, Pan F. Metabolic control of the Treg/Th17 axis. *Immunol Rev.* (2013) 252:52–77. doi: 10.1111/imr.12029
6. O'Sullivan D, Pearce EL. Targeting T cell metabolism for therapy. *Trends Immunol.* (2015) 36:71–80. doi: 10.1016/j.it.2014.12.004
7. Menk AV, Scharping NE, Moreci RS, Zeng X, Guy C, Delgoffe GM, et al. Early TCR signaling induces rapid aerobic glycolysis enabling distinct acute T cell effector. *Funct Cell Rep.* (2018) 22:1509–21. doi: 10.1016/j.celrep.2018.01.040
8. Wang R, Green DR. Metabolic checkpoints in activated T cells. *Nat Immunol.* (2012) 13:907–15. doi: 10.1038/ni.2386
9. Chang CH, Curtis JD, Maggi LB Jr, Faubert B, Villarino AV, Pearce EL, et al. Posttranscriptional control of T cell effector function by aerobic glycolysis. *Cell* (2013) 153:1239–51. doi: 10.1016/j.cell.2013.05.016
10. Shi LZ, Wang R, Huang G, Vogel P, Neale G, Green D, et al. HIF1alpha-dependent glycolytic pathway orchestrates a metabolic checkpoint for the differentiation of TH17 and Treg cells. *J Exp Med.* (2011) 208:1367–76. doi: 10.1084/jem.20110278
11. Kopf H, de la Rosa GM, Howard OM, Chen X. Rapamycin inhibits differentiation of Th17 cells and promotes generation of FoxP3+ T regulatory cells. *Int Immunopharmacol.* (2007) 7:1819–24. doi: 10.1016/j.intimp.2007.08.027
12. Michalek RD, Gerriets VA, Jacobs SR, Macintyre AN, MacIver NJ, Rathmell JC, et al. Cutting edge: distinct glycolytic and lipid oxidative metabolic programs are essential for effector and regulatory CD4+ T cell subsets. *J Immunol.* (2011) 186:3299–303. doi: 10.4049/jimmunol.1003613
13. Delgoffe GM, Pollizzi KN, Waickman AT, Heikamp E, Meyers DJ, Powell JD, et al. The kinase mTOR regulates the differentiation of helper T cells through the selective activation of signaling by mTORC1 and mTORC2. *Nat Immunol.* (2011) 12:295–303. doi: 10.1038/ni.2005
14. Majmundar AJ, Wong WJ, Simon MC. Hypoxia-inducible factors and the response to hypoxic stress. *Mol Cell* (2010) 40:294–309. doi: 10.1016/j.molcel.2010.09.022
15. Dang EV, Barbi J, Yang HY, Jinasena D, Yu H, Pan F, et al. Control of T(H)17/T(reg) balance by hypoxia-inducible factor 1. *Cell* (2011) 146:772–84. doi: 10.1016/j.cell.2011.07.033
16. Malandrino MI, Fucho R, Weber M, Calderon-Dominguez M, Mir JF, Herrero L, et al. Enhanced fatty acid oxidation in adipocytes and macrophages reduces lipid-induced triglyceride accumulation and inflammation. *Am J Physiol Endocrinol Metab.* (2015) 308:E756–69. doi: 10.1152/ajpendo.00362.2014
17. Wang R, Dillon CP, Shi LZ, Milasta S, Carter R, Green DR, et al. The transcription factor Myc controls metabolic reprogramming upon T lymphocyte activation. *Immunity* (2011) 35:871–82. doi: 10.1016/j.immuni.2011.09.021
18. Berod L, Friedrich C, Nandan A, Freitag J, Hagemann S, Harmrolfs K, Sparwasser T, et al. *De novo* fatty acid synthesis controls the fate between regulatory T and T helper 17 cells. *Nat Med.* (2014) 20:1327–33. doi: 10.1038/nm.3704
19. Endo Y, Asou HK, Matsugae N, Hirahara K, Shinoda K, Nakayama T, et al. Obesity drives Th17 cell differentiation by inducing the lipid metabolic kinase, ACC1. *Cell Rep.* (2015) 12:1042–55. doi: 10.1016/j.celrep.2015.07.014
20. Gerriets VA, Rathmell JC. Metabolic pathways in T cell fate and function. *Trends Immunol.* (2012) 33:168–73. doi: 10.1016/j.it.2012.01.010
21. Rathmell JC, Fox CJ, Plas DR, Hammerman PS, Cinalli RM, Thompson CB. Akt-directed glucose metabolism can prevent Bax conformation change and promote growth factor-independent survival. *Mol Cell Biol.* (2003) 23:7315–28. doi: 10.1128/MCB.23.20.7315-7328.2003
22. Aguer C, Gambarotta D, Mailloux RJ, Moffat C, Dent R, Harper ME, et al. Galactose enhances oxidative metabolism and reveals mitochondrial dysfunction in human primary muscle cells. *PLoS ONE* (2011) 6:e28536. doi: 10.1371/journal.pone.0028536
23. Bettelli E, Carrier Y, Gao W, Korn T, Strom TB, Kuchroo VK, et al. Reciprocal developmental pathways for the generation of pathogenic effector TH17 and regulatory T cells. *Nature* (2006) 441:235–8. doi: 10.1038/nature04753
24. Gabriel SS, Kallies A. Sugars and fat - a healthy way to generate functional regulatory T cells. *Eur J Immunol.* (2016) 46:2705–9. doi: 10.1002/eji.201646663
25. Buck MD, O'Sullivan D, Pearce EL. T cell metabolism drives immunity. *J Exp Med.* (2015) 212:1345–60. doi: 10.1084/jem.20151159
26. Brucklacher-Waldert V, Ferreira C, Stebegg M, Fesneau O, Innocentin S, Marie J, et al. Cellular stress in the context of an inflammatory environment supports TGF-beta-Independent T Helper-17 differentiation. *Cell Rep.* (2017) 19:2357–70. doi: 10.1016/j.celrep.2017.05.052

27. Gerriets VA, Kishton RJ, Nichols AG, Macintyre AN, Inoue M, Rathmell JC, et al. Metabolic programming and PDHK1 control CD4+ T cell subsets and inflammation. *J Clin Invest.* (2015) 125:194–207. doi: 10.1172/JCI76012
28. Franchi L, Monteleone I, Hao LY, Spahr MA, Zhao W, Glick GD, et al. Inhibiting oxidative phosphorylation *in vivo* restrains Th17 effector responses and ameliorates murine colitis. *J Immunol.* (2017) 198:2735–46. doi: 10.4049/jimmunol.1600810
29. Strauss L, Whiteside TL, Knights A, Bergmann C, Knuth A, Zippelius A. Selective survival of naturally occurring human CD4+CD25+Foxp3+ regulatory T cells cultured with rapamycin. *J Immunol.* (2007) 178:320–9. doi: 10.4049/jimmunol.178.1.320
30. Procaccini C, Carbone F, Di Silvestre D, Brambilla F, De Rosa V, Galgani M, et al. The proteomic landscape of human *ex vivo* regulatory and conventional t cells reveals specific metabolic requirements *Immunity* (2016) 44:406–21. doi: 10.1016/j.immuni.2016.01.028
31. Li L, Liu X, Sanders KL, Edwards JL, Ye J, Peng G, et al. TLR8-mediated metabolic control of human treg function: a mechanistic target for cancer immunotherapy. *Cell Metab*. (2018) 29:103–23. doi: 10.1016/j.cmet.2018.09.020
32. Pacella I, Procaccini C, Focaccetti C, Miacci S, Timperi E, Faicchia D, et al. Fatty acid metabolism complements glycolysis in the selective regulatory T cell expansion during tumor growth. *Proc Natl Acad Sci USA*. (2018) 115:E6546–55. doi: 10.1073/pnas.1720113115
33. Gerriets VA, Kishton RJ, Johnson MO, Cohen S, Siska PJ, Rathmell JC, et al. Foxp3 and Toll-like receptor signaling balance Treg cell anabolic metabolism for suppression. *Nat Immunol.* (2016) 17:1459–66. doi: 10.1038/ni.3577
34. Hippen KL, O'Connor RS, Lemire AM, Saha A, Hanse EA, Blazar BR, et al. *In vitro* induction of human regulatory t cells using conditions of low tryptophan plus kynurenines *Am J Transplant.* (2017) 17:3098–113. doi: 10.1111/ajt.14338
35. De Rosa V, Galgani M, Porcellini A, Colamatteo A, Santopaolo M, Zuchegna C, et al. Glycolysis controls the induction of human regulatory T cells by modulating the expression of FOXP3 exon 2 splicing variants. *Nat Immunol.* (2015) 16:1174–84. doi: 10.1038/ni.3269
36. Raud B, Roy DG, Divakaruni AS, Tarasenko TN, Franke R, Berod L, et al. Etomoxir actions on regulatory and memory T cells are independent of Cpt1a-mediated fatty acid oxidation. *Cell Metab.* (2018) 28:504–15. doi: 10.1016/j.cmet.2018.06.002
37. Young KE, Flaherty S, Woodman KM, Sharma-Walia N, Reynolds JM. Fatty acid synthase regulates the pathogenicity of Th17 cells. *J Leukoc Biol.* (2017) 102:1229–35. doi: 10.1189/jlb.3AB0417-159RR
38. Gualdoni GA, Mayer KA, Goschl L, Boucheron N, Ellmeier W, Zlabinger GJ. The AMP analog AICAR modulates the Treg/Th17 axis through enhancement of fatty acid oxidation. *FASEB J.* (2016) 30:3800–9. doi: 10.1096/fj.201600522R
39. Shen Y, Wen Z, Li Y, Matteson EL, Hong J, Weyand CM, et al. Metabolic control of the scaffold protein TKS5 in tissue-invasive, proinflammatory T cells. *Nat Immunol.* (2017) 18:1025–34. doi: 10.1038/ni.3808

Conflict of Interest Statement: This study was part funded by AbbVie Inc. JF has received honoraria from Novartis.

The remaining authors declare that the research was conducted in the absence of any commercial or financial relationships that could be construed as a potential conflict of interest.

Copyright © 2019 Cluxton, Petrasca, Moran and Fletcher. This is an open-access article distributed under the terms of the Creative Commons Attribution License (CC BY). The use, distribution or reproduction in other forums is permitted, provided the original author(s) and the copyright owner(s) are credited and that the original publication in this journal is cited, in accordance with accepted academic practice. No use, distribution or reproduction is permitted which does not comply with these terms.

Advantages of publishing in Frontiers

OPEN ACCESS
Articles are free to read for greatest visibility and readership

FAST PUBLICATION
Around 90 days from submission to decision

HIGH QUALITY PEER-REVIEW
Rigorous, collaborative, and constructive peer-review

TRANSPARENT PEER-REVIEW
Editors and reviewers acknowledged by name on published articles

Frontiers
Avenue du Tribunal-Fédéral 34
1005 Lausanne | Switzerland

Visit us: www.frontiersin.org
Contact us: info@frontiersin.org | +41 21 510 17 00

REPRODUCIBILITY OF RESEARCH
Support open data and methods to enhance research reproducibility

DIGITAL PUBLISHING
Articles designed for optimal readership across devices

FOLLOW US
@frontiersin

IMPACT METRICS
Advanced article metrics track visibility across digital media

EXTENSIVE PROMOTION
Marketing and promotion of impactful research

LOOP RESEARCH NETWORK
Our network increases your article's readership